THE IMPORTANCE OF MINOR SEQUENCE ALTERATIONS ON THE HYDROLYSIS BEHAVIORS OF DEGRADABLE POLYESTERS

by

Jamie Andrew Nowalk

B.S. Chemistry, Lock Haven University of Pennsylvania, 2014

Submitted to the Graduate Faculty of the

Kenneth P. Dietrich School of Arts and Sciences in partial fulfillment

of the requirements for the degree of

Doctor of Philosophy

University of Pittsburgh

2019

UNIVERSITY OF PITTSBURGH

DIETRICH SCHOOL OF ARTS AND SCIENCES

This dissertation was presented

by

Jamie Andrew Nowalk

It was defended on

May 31, 2019

and approved by

W. Seth Horne, Associate Professor, Department of Chemistry

Peng Liu, Associate Professor, Department of Chemistry, Department of Chemical and Petroleum Engineering

Kacey Marra, Professor and Vice-Chair of Research, Department of Plastic Surgery, Department of Bioengineering, and The McGowan Institute for Regenerative Medicine

Thesis Advisor/Dissertation Director: Tara Y. Meyer, Professor, Department of Chemistry and The McGowan Institute for Regenerative Medicine

Copyright © by Jamie Andrew Nowalk

2019

Abstract

THE IMPORTANCE OF MINOR SEQUENCE ALTERATIONS ON THE HYDROLYSIS BEHAVIORS OF DEGRADABLE POLYESTERS

Jamie Andrew Nowalk, PhD

University of Pittsburgh, 2019

The extent to which small changes in monomer sequence affect the behaviors of biological macromolecules is studied regularly, yet the dependence of bulk properties on small sequence alterations is underexplored for synthetic copolymers. Investigations of this type are limited by the arduous syntheses required, lack of scalability, and scarcity of examples of polymer systems that are known to exhibit sensitive sequence/property dependencies. Our group has previously explored the hydrolysis behaviors of a library of sequenced poly-(lactic-*co*-glycolic acid)s (PLGAs) and found a strong correlation with the L-G sequence. To investigate the degree to which properties are dominated in this system by relatively minor sequence changes, L-G sequences were incorporated into cyclic macromonomers, and these macromonomers were subjected to entropy-driven ring-opening metathesis polymerization. This polymerization method produces polymers with molecular weight control and sequence preservation, both being required for studies in which subtle sequence changes are compared.

Two hydrolysis studies were performed in which a precisely sequenced polymer containing a base alternating sequenced segment, LGLGL, was compared against 1) a copolymer in which the LGLGL segment was randomized, i.e., L_3G_2, thus confining disorder within this short segment,

and 2) the base sequence doped with varying, small quantities of LGGGL “error” segments. In this first hydrolysis study, molecular weight decrease, mass loss, thermal behaviors, and film/surface characteristics were monitored to reveal stark differences in degradation behaviors despite the confinement of errors within a short segment. In the second hydrolysis study, degradation rate proved tolerant to substitutions up to 1% of the monomers but accelerated significantly when the error population was larger.

In instances where copolymer properties are dependent on monomer order, sequence engineering expands the functional capabilities of a given set of monomers. Investigations of how localized, property-dominating sequence segments affect behavior may aid researchers in establishing synthetic methods to either incorporate or eliminate such sequences for the preparation of materials for advanced function.

Table of Contents

Title Page i

Abstract iv

List of Tables ix

List of Figures x

List of Schemes xv

List of Abbreviations xvii

Dedication xix

Acknowledgements xx

1.0 Introduction 1

- **1.1 Overview** 1
- **1.2 Significance** 1
- **1.3 Synthetic Methods Toward Sequence Controlled Polymers** 2
- **1.4 Preparation of Sequenced PLGAs and Similar Copolymers** 5
- **1.5 Bulk Property Sensitivity in Sequence Controlled Polymers** 9
  - **1.5.1 Overview** 9
  - **1.5.2 Bulk Properties of Stereosequenced PLAs** 10
  - **1.5.3 Alternating vs. Random Comonomer Sequences** 12
  - **1.5.4 Reports of Sequence Effects on Bulk Properties** 15
- **1.6 Thesis Overview** 15

2.0 Synthetic Advances toward Sequence-Controlled Polyesters with Molecular Weight Control 18

2.1 Overview 18

2.2 Introduction 19

2.3 Results and Discussion 25

2.3.1 Optimization of SEED-ROMP Block Copolymerizations 25

2.3.2 Macrocyclic Oligomers via Macrolactonization: Linkage Directionality and Scalability 30

2.3.3 Syringic Acid Incorporation to Elevate T_g 33

2.3.4 Establishing Molecular Weight Control 34

2.3.5 Monomer Conversion and Regiochemistry 35

2.3.6 Sequence Characterization 36

2.3.7 Synthesis of N-Carboxyanhydride-Containing Macrocycles 38

2.3.8 Entropy-Driven Ring-Opening Transesterification Polymerization 39

2.4 Conclusion 44

2.5 Experimental Section 45

2.5.1 General Information 45

2.5.2 Experimental Procedures 46

3.0 The Influence of Short-Range Scrambling of Monomer Order on the Hydrolysis Behaviors of Sequenced Degradable Polyesters 85

3.1 Overview 85

3.2 Introduction 85

3.3 Results 89

3.3.1 Synthesis of Sequence Controlled Polymers 89

3.3.2 Sequence Characterization 91

3.3.3 Film Casting 94

3.3.4 Hydrolysis 95

3.3.5 Molecular Weight and Mass Loss 97

3.3.6 Thermal Behavior 98

3.3.7 Film Characteristics 100

3.4 Discussion 101

3.5 Conclusion 104

3.6 Experimental Section 105

3.6.1 General Information 105

3.6.2 Experimental Procedures 106

4.0 The Consequences of Accumulating Critical Monomer Errors on the Hydrolysis Behaviors of Degradable Sequenced Polyesters 118

4.1 Overview 118

4.2 Introduction 118

4.3 Results and Discussion 121

4.4 Conclusions 129

4.5 Experimental Section 130

4.5.1 Experimental Procedures 130

5.0 Prospectus 143

Appendix A: Experimental Spectra and Supporting Data for Chapter 2 145

Appendix B: Experimental Spectra and Supporting Data for Chapter 3 185

Appendix C: Experimental Spectra and Supporting Data for Chapter 4 208

6.0 Bibliography 227

List of Tables

Table 1. Definitions of sequence-controlled polymer terms……………………………..……….3

Table 2. Error-doped polymer molecular weight data………………………..…………..…123

Table 3. Preparation of errormer mixtures…………………………..……………………..…..140

List of Figures

Figure 1. Synthetic overview depicting methods toward sequence-controlled polyesters, including segmer-assembly polymerization (top) and entropy-driven ring-opening metathesis polymerization (bottom). 6

Figure 2. Hydrolysis behaviors of devices prepared from sequenced and random poly-(lactic-co-glycolic acid)s. (A) Photographs of pellets as a function of hydrolysis time. Reproduced with persmission from Elsevier. (B) Internal pH measurements and scanning-electron microscopy images of polymer microparticles during hydrolysis. Reproduced with permission from Elsevier. 8

Figure 3. Classes of sequence-dependent properties. Molecular properties lead to solution- and solid-phase properties as well as complex behaviors. Reproduced with permission from Wiley-VCH Verlag GmbH & Co. 10

Figure 4. Overall synthetic approach involving ring-closing to prepare macrocycles with embedded monomer sequences and sequence-retaining metathesis polymerizations. Reproduced with permission from the American Chemical Society. 21

Figure 5. Living polymerization character as it relates to the relative rates of propagation (k_{pr}) and secondary metathesis (k_{sm}) in entropy-driven ring-opening metathesis polymerization. Reproduced with permission from the American Chemical Society. 22

Figure 6. Representative size exlclusion chromatograms of SEED-ROMP-b-ROMP copolymerizations with norbornene. (A) 5 mol% G2, SEED-ROMP 10 min, ROMP 20 min, RT. (B) 2.5 mol% G2, SEED-ROMP 10 minutes, ROMP 10 minutes, RT. (C) 2.5 mol% G2, SEED-

ROMP 10 minutes, ROMP 2 minutes, 0 °C. Reproduced with permission from the American Chemical Society. 28

Figure 7. (A) ^{1}H NMR spectra for *cis*-Eg(LGLM)$_2$, polymerization to 50 kDa Poly Eg(LGLM)$_2$, and Poly Eg(LGLM)$_2$-*b*-COE. (x denotes CH_2Cl_2) (B) SEC traces of control and block extension using NBE (unpurified), displaying large dispersity due to secondary metathesis. (C) SEC traces of control and block extension with COE (unpurified). Reproduced with permission from the American Chemical Society. 30

Figure 8. Differential scanning calorimetry thermograms of Poly LMLGLGLG and Poly SyLMLGLGL. 34

Figure 9. Molecular weights as a function of catalyst loading from palindromic monomers *trans*-Eg(LLCM)$_2$, *cis*-Eg(LGLM)$_2$, and unsymmetric *trans*-LMLGLGLG. (A) Size exlusion chromatographs of Poly LMLGLGLG at varying catalyst loadings. (B) Plots of molecular weights as a function of catalyst loading. Figure adapted with permission from the American Chemical Society.. 35

Figure 10. ^{1}H NMR spectroscopy and MALDI-TOF mass spectrometry characterization of sequence fidelity. (A)^{1}H NMR spectra of olefin and methylene resonances of *trans*-LMLGLGLG (top) and Poly LMLGLGLG (bottom), displaying head-tail olefin resonances, and MALDI-TOF spectrum of low molecular weight cyclic Poly LMLGLGLG. (B) ^{1}H NMR methylene resonances of *trans*-SyLMLGLGL (top) and Poly SyLMLGLGL (bottom); and MALDI-TOF spectrum of low molecular weight cyclic Poly SyLMLGLGL. Reproduced with permission from the American Chemical Society. 37

Figure 11. ^{1}H NMR spectra overlay of macrolactonization product reaction mixture and the corresponding hexamer and dodecamer... 40

Figure 12. ^{1}H NMR spectral overlays of polymerization timepoints for (A) Cyc-LGLGLGLGLGLG and (B) Cyc-LGLGLG using catalytic stannous octanoate, with perfectly alternating Poly LG for reference. 43

Figure 13. Range of bulk property/sequence tolerance profiles for random and sequence-controlled copolymers where A represents a precisely alternating and B represents a statistically random copolymer. 86

Figure 14. Synthesis of Poly SyLM(L_3G_2): A) Synthesis of Cyc-SyLM(L_3G_2) macrocycle; B) polymerization of macrocycles to produce precisely sequenced and controlled random copolymers of identical composition; and C) size exclusion chromatography traces of both copolymers...... 89

Figure 15. The theoretical and experimental sequence outcomes within the mixture of random L_3G_2-Si pentamers prepared from precursor dimers, and ^{1}H NMR spectroscopy (red labels are theoretical and black are experimental). 91

Figure 16. Sequence characterization of macrocycles: A) ^{1}H NMR spectra of methyne, methylene, and olefin regions of Cyc-SyLM(LGLGL) and Cyc-SyLM(L_3G_2); B) high resolution mass spectrum of Cyc-SyLM(LGLGL); and C) high resolution mass spectrum of Cyc-SyLM(L_3G_2) macrocycle mixture... 92

Figure 17. Cartoon depiction of solution film-casting of polymer discs (left) and photograph of Poly SyLM(LGLGL) and Poly SyLM(L_3G_2) free-standing discs (right). 94

Figure 18. Optical profilometry countours of sliced films of Poly SyLM(LGLGL) and Poly SyLM(L_3G_2) discs.. 95

Figure 19. Molecular weight and mass loss profiles of Poly SyLM(LGLGL) and Poly SyLM(L_3G_2): A) number average molecular weight (M_n) loss over time; B) weight average molecular weight (M_w) loss over time; C) dispersity (Đ) over time; and D) film mass loss over time. Range bars are included for sample sets with significant deviations (> 0.1 on y-axis)....... 97

Figure 20. Size exclusion chromatographs during hydrolysis for Poly SyLM(L_3G_2) (top) and Poly SyLM(LGLGL) (bottom)... 98

Figure 21. Differential scanning calorimetry thermograms for Poly SyLM(LGLGL) (left) and Poly SyLM(L_3G_2) (right) at each time point during hydrolysis... 99

Figure 22. Scanning electron microscopy images (secondary ion detection, 10 kEv) of polymer films over the course of hydrolysis. (A) Poly SyLM(LGLGL) at Week 7, ~50% loss of M_n, 100x. (B) Poly SyLM(L_3G_2) at Week 4, ~50% loss of M_n, 100x. (C) Poly SyLM(LGLGL) at Week 7, 1,000x. (D) Poly SyLM(L_3G_2) at Week 4, 1,000x. (E) Poly SyLM(LGLGL) at Week 10, 3,000x. (F) Poly SyLM(L_3G_2) at Week 6, 3,000x. Note the presence of residual buffer salt crystals in SEM-D.. 100

Figure 23. Photographs of copolymer thick films over the course of hydrolysis...................... 101

Figure 24. Sequence tolerance pathways as a function of errors in a sequence-controlled polymer. 120

Figure 25. (Top) ^1H NMR spectra of G-methylene, L-methyne, and M-olefin protons of Cyc-SyLMLGLGL (top) and Cyc-SyLMLGGGL (bottom) with HRMS spectrum......................... 121

Figure 26. Sequence characterization of the five copolymers, including ^1H NMR spectral region of the diastereotopic G methylene protons, ^{13}C NMR spectra of the central L monomer in the base alternating sequence, MALDI-TOF spectra, and size exlclusion chromatographs. 124

Figure 27. Cartoon depiction of the preparation of macromonomer solution mixtures, solution casting, and photographs of films before and after delamination from aluminum bases. 125

Figure 28. Optical profilometry step-contours of sliced films prepared from each of the five copolymers. 126

Figure 29. (Top) Molecular weight loss during hydrolysis. (Bottom) Photographs of films at given time points during hydrolysis. X denotes particles too small to photograph. 127

Figure 30. Scanning electron microscopy images of thick films at varying time points in hydrolysis. 128

Figure 31. SEC trace of Poly SyLMLGLGL. $M_n = 36$, $M_w = 44$, $Đ = 1.2$, relative to polystyrene standards. 184

Figure 32. SEC trace of Poly SyLMLGLGL. $M_n = 44$, $M_w = 51$, $Đ = 1.2$, relative to polystyrene standards. 184

Figure 33. Low magnification (100x) images of Poly SyLM(LGLGL) and Poly SyLM(L_3G_2) at the six time points over the course of hydrolysis. 185

Figure 34. High magnification (1000x) of Poly SyLM(L_3G_2) (left) after three weeks of hydrolysis and Poly SyLM(LGLGL) (right) after five weeks of hydrolysis. 186

Figure 35. High magnification (3000x) of the porous structure developed within Poly SyLM(L_3G_2) at Week 5 of hydrolysis. 186

Figure 36. EDX characterization of residual buffer salt crystals on the degraded films. 207

Figure 37. Scanning electron microscopy images (100x) of the films over the course of hydrolysis. 208

Figure 38. Scanning electron microscopy images (100x) of the films over the course of hydrolysis. 209

List of Schemes

Scheme 1. Utilizing ED-ROMP to prepare sequence-controlled polyesters with controllable molecular weights. A) Structures of Grubbs Second Generation Catalyst (G2) and Z-Selective Grubbs Nitrato Catalsyt (GN). B) Ring-closing metathesis reactions and subsequent polymerizations. C) Selectivity-enhanced entropy-driven ring-opening metathesis polymerization to produce a block copolymer with norbornene. Figure adapted with permission from the American Chemical Society. 25

Scheme 2. SEED-ROMP-b-ROMP copolymerization with *cis*-cyclooctene. Scheme adapted with permission from the American Chemical Society. 29

Scheme 3. Preparation of alcohol-protected LGLGLG-Si segmer. 31

Scheme 4. Preparation of Poly LMLGLGLG. 32

Scheme 5. Preparation of Poly SyLMLGLGL. 33

Scheme 6. Intended preparation of Poly LGLGL“G” from an N-carboxyanhydride-containing macrocycle. 38

Scheme 7. Macrolactonization of open-chain LGLGLG segmer leading to ring-closed species. 40

Scheme 8. Polymerization of mixtures of macrocycles to prepare a sequenced polyester with varying errormer dopant. 122

Scheme 9. Synthetic steps toward LGGGL-Si. 210

Scheme 10. Steglich esterification to Bn-SyLMLGGGL-Si. 210

Scheme 11. Benzyl and silyl deprotections to yield SyLMLGGGL and subsequent macrolactonization reaction to prepare Cyc-SyLMLGGGL. 211

Preface

The work presented herein was conducted at the University of Pittsburgh. I was the lead researcher whom was responsible for areas of concept formation, data collection and analysis, as well as manuscript composition. Dr. Tara Y. Meyer was the supervisory author and primary investigator on this project and was involved throughout the project in concept formation and manuscript composition. The work presented within this thesis was funded by the National Science Foundation (CHE-1410119, CHE-1709144, and CHE-1625002).

List of Abbreviations

AcOH	Acetic acid
ADMET	Acyclic diene metathesis
Bn	Benzyl
B-THF	Borane-tetrahydrofuran complex
C	6-hydroxy hexanoic acid
CH_2Cl_2	Dichloromethane
Đ	Polydispersity index, PDI
DCC	*N*,*N*′-dicyclohexylcarbodiimide
DCE	1,2-Dichloroethane
DIC	*N*,*N*′-Diisopropylcarbodiimide
DMSO	Dimethyl sulfoxide
DP	Degree of polymerization
DPTS	4-(dimethylamino)pyridinium 4-toluenesulfonate
EI	Electron ionization
ESE	Electrospray ionization
ED-ROMP	Entropy-driven ring-opening metathesis polymerization
Eg	Ethylene glycol
eq.	Equivalent
ESI	Electrospray ionization
Et	Ethyl
EtOAc	Ethyl acetate
EVE	Ethyl vinyl ether
FT	Fourier transform
G	Glycolic acid subunit
GN	Grubbs Nitrato Z-selective Catalyst
GPC	Gel permeation chromatography
G2	Grubbs Second Generation Catalyst
G3	Grubbs Third Generation Catalyst
hr	Hour
IR	Infrared spectroscopy
L	Lactic acid subunit
M	Molar, or Metathesis-active monomer
MALDI-TOF	Matrix-assisted laser desorption ionization – time of flight
MCO	Macrocyclic oligomer
MD	Molecular dynamics
Me	Methyl
Min	Minute

Muc	*Trans*-β-hydromuconic acid
Mucol	Hydroxyacid metathesis-active linker subunit
mL	Milliliter
M_n	Number average molecular weight
MS	Mass spectroscopy
M_w	Weight average molecular weight
Mol	Mole
NEt_3	Triethylamine
NHC	*N*-heterocyclic carbene
NMR	Nuclear magnetic resonance
P	Pentenoic acid subunit
PDI	Polydispersity index, Đ
PEG	Polyethylene glycol
Ph	Phenyl
PLA	Poly-lactic acid
PLGA	Poly-(lactic-*co*-glycolic acid)
PS	Polystyrene
RCM	Ring-closing metathesis
ROMP	Ring-opening metathesis polymerization
ROP	Ring-opening polymerization
ROTEP	Ring-opening transesterification polymerization
rt	Room temperature
SAP	Segmer assembly polymerization
sec	Second
SEC	Size exclusion chromatography
SEED-ROMP	Selectivity-enhanced ED-ROMP
segmer	Sequenced oligomer
Si	Silyl protecting group (TBDPS)
Sy	Syringic acid monomer
TBAF	tetrabutylammonium fluoride
TBDPS	*tert*-Butyl dimethylsilyl
T_g	Glass transition temperature
THF	Tetrahydrofuran

Dedication

To my father,

Cleon Ralph Nowalk,

Who made this all possible with his love, sacrifice, selflessness, kindness, and patience.

For the countless times he said that he wished to have given me more, let this be proof that he provided everything I ever needed to build a wonderful life.

In my best qualities, I see you.

Acknowledgements

First, I would like to thank Prof. Tara Y. Meyer for her mentorship during my PhD studies. Thank you for being such a devoted, enthusiastic, and caring advisor as well as a personal confidant and active ally. Your demand for scientific excellence has allowed me to grow in ways I never could have imagined. Thank you to the members of my thesis committee: Prof. W. Seth Horne, Prof. Peng Liu, and Prof. Kacey G. Marra for the guidance, productive discussions, and encouragement.

I would like to sincerely thank the chemistry faculty at Lock Haven University of Pennsylvania for teaching me the foundations of chemistry: Prof. Brent May, Prof. Troy Dermota, Prof. Kurt Rublein, Prof. Laura Lee, Prof. Jackie Whitling Dumm, Prof. Kevin Range, Prof. Martin Maresch, and Prof. Stephen Coval. I also extend my gratitude to my undergraduate research advisor, Prof. Marian Tzolov, and my high school chemistry teacher, Joanne Perry.

To the friends who became my family at Lock Haven University – Paul Van Auken, Austin Theis, Mackenzie Crafa, Jourdan Strishock, Megan Mishler, and Elizabeth Schultz – I am so privileged to have your unwavering friendship and encouragement.

To all past and present Meyer Group members that I had the pleasure to work with: Michael A. Washington, Amy L. Short, Ryan M. Weiss, Jeffrey T. Auletta, Shaopeng Zhang, Colin D. Ladd, Anneliese Schmidt, Jordan Fitch, Mike Cole, and Emily F. Barker, thank you for the amazing memories and support over the years. To Jordan H. Swisher, I cannot thank you enough for helping me become a better scientist with your never-ending brainstorming, encouragement, honesty, scientific and philosophical discussions, and unyielding enthusiasm.

This would not have been possible without the support of the person I met one week after moving to Pittsburgh to pursue my PhD, my partner, Vincent Ridilla. Your love and support during my moments of anxiety and doubt have seen me through. To Vince's family, who have become my own, I will never be able to fully express how full you have made my heart over the past five years.

To my parents, Cleon and Susan Nowalk, and my brothers Michael Nowalk and Patrick Nowalk, thank you for your support for all my life.

1.0 Introduction

1.1 Overview

Portions of this introduction were adapted from: Swisher, Jordan H.; Nowalk, Jamie A.; Washington, Michael A.; Meyer, Tara Y. Chapter 15: Properties and Applications of Sequence-Controlled Polymers, *Sequence-Controlled Polymers*; Lutz, J.-F., Ed.; Wiley: 2017.

1.2 Significance

Traditional Poly-(lactic-*co*-glycolic acid) (PLGA) is a random sequence, bioresorbable polyester used in biological engineering as degradable sutures, drug delivery platforms, cell scaffolds, and degradable films with property tunability possible by varying monomer composition and molecular weight.[1-10] The Meyer group has previously demonstrated, using polymers prepared by a step-growth synthesis, that the hydrolytic degradation of PLGA is dramatically affected by monomer sequence. While much was learned in prior studies about hydrolytic property dependence as a function of periodic sequence, the employed step-growth mechanism used to prepare sequenced PLGAs provided no molecular weight control, unpredictable yields, and limited scalability. Due to these synthetic limitations, comparisons between only subtle changes in sequences and the effectiveness to which they swayed properties remained challenging.

The extent to which small changes in monomer sequence affect the behaviors of biological macromolecules is studied regularly, yet the dependence of bulk properties on small sequence alterations is underexplored for synthetic copolymers. Investigations of this type are limited by the arduous syntheses required, lack of scalability, and scarcity of examples of polymer systems that are known to exhibit sensitive sequence/property dependencies.[11] In order to perform studies of this type on PLGAs, whose hydrolysis properties are highly sequence dependent, a synthetic method to prepare scalable and reproducible materials with molecular weight control is critical.

The work described herein, along with the founding work of Weiss, et al. and Short, et al., describes a method to prepare precisely-sequenced PLGA-like copolymers that involved the ring-opening polymerization of sequenced macrocycles, a method that provides molecular weight control, the reproducible preparation of materials, and appropriate scalability for bulk studies. This method has made it possible to vary monomer sequence to only a small degree and to combine distinct sequences into a single copolymer while providing identical molecular weights across samples. The prepared materials were subjected to hydrolysis and astoundingly small sequence alterations that interrupted a base alternating sequence were found to significantly affect degradation profiles. As researchers further investigate the property effects of sequence, the combination of a “base sequence” and discrete amounts of a property-dominating sequence segment may expand the range of properties for a given copolymer.

1.3 Synthetic Methods Toward Sequence Controlled Polymers

A decade ago, Lutz and coworkers described sequence-controlled polymerizations as the next “Holy Grail” in polymer science.[12] Since then, increased efforts in controlled syntheses have made it possible both to prepare varying sequence isomers of the same collection of comonomers and to compare polymer properties as a function of sequence. The work described in this thesis involves both sequence/property studies and the synthetic development on which they rely and, therefore, what follows is a general overview of synthetic methods in the field that have aided in the inspiration of this work. Selected terminology commonly used in the field of sequence-controlled polymers is included in Table 1.

Table 1. Definitions of sequence-controlled polymer terms.

Term	Definition
Oligomer	Chain of one or more monomers that comprises a unique periodic sequence with dispersity > 1 and low degree of polymerization
Segmer	Chain of one or more monomers that comprises a unique or periodic sequence with dispersity = 1 and low degree of polymerization
Block length	The degree of polymerization of segmers/oligomers comprising a multiblock copolymer
Block dispersity	A metric that expresses the range of block lengths present in a multiblock copolymer
Microstructure	The arrangement of monomers in a polymer, oligomer, or segmer
Sequence Isomers	A set of polymers, oligomers, or segmers with the same monomer composition but different microstructures
Repeating-Sequence Copolymer	A copolymer containing sequences of 2-10 monomers repeated throughout a chain, or a periodic copolymer

The epitome of a macromolecule in which monomer sequence dictates function can be considered DNA, which Nature prepares by a templated approach to encode unique genetic information for every living being. In synthetic polymer science, our ability to assemble complex sequences is comparatively underdeveloped. The overwhelming majority of non-biological sequenced materials requires at least a moderate degree of iterative synthetic steps to build complex sequences outside the regime of blocky, tapered, or gradient microstructures, which at the most fundamental level limits the efficacy and practicality of syntheses. Researchers have, however, made impressive strides in synthetic chemistry to overcome this challenge to prepare functional sequence-controlled polymers.[12-15]

Mimicking Nature's strategy to encode information, Lutz and coworkers employ iterative phosphoramidite couplings on a solid support to build up sequences from a single monomer at a time.[16, 17] Similar to this approach, high efficiency preparations of biologically-inspired polypeptoids have been developed by Zuckermann and coworkers[18-22] as well as Segalman and coworkers.[23, 24] Recently, work by the Johnson group has developed a similarly efficient method that exploits flow chemistry that they term Iterative Exponential Growth, in which monomers are sequentially coupled to dimers, tetramers, octamers, and so on, while installing switchable sequences and stereocenters.[25, 26] Elegant methods such as these, which often benefit from automation, are able to produce virtually any sequences based on input monomers but suffer from a relatively low molecular weight limit and/or restricted scalability due to the requirements of distinct functional groups for quantitative couplings, excess reagents, and excessive washings.

The synthesis of sequence-controlled polymers is also approached from a different perspective, which commonly sacrifices the ability to prepare any sequence imaginable for coarse control in monomer composition throughout a chain (i.e. statistical, alternating, gradient, blocky) in addition to periodic sequences (i.e. $(ABC)_n$ or $(BAC)_n$). These methods benefit from greater scalability. Polymers with monomer distribution control are commonly prepared using controlled radical polymerizations including atom-transfer radical polymerizations (ATRP)[27] and reversible addition-fragmentation chain transfer polymerizations (RAFT).[28-31] In the preparation of more defined sequences, repeating-sequence copolymers (RSCs) are often prepared using multi-component reactions such as Ugi and Passerini reactions[32, 33] and various step-growth polymerizations.[34] In developing a route toward sequenced copolyesters, or periodic PLGAS, a polymerization method in this latter category of sequence installation was optimal for future bulk property studies.

1.4 Preparation of Sequenced PLGAs and Similar Copolymers

Previous work in the Meyer group has stablished that the hydrolysis properties of PLGAs are sequence-dependent.[35-37] In the current thesis, we explore this sequence dependence further by preparing PLGA-like copolyesters with molecular weight control. PLGAs are a class of Food and Drug Administration (FDA)-approved biodegradable copolymers that have become a staple in biological engineering.[13] Comprising lactic and glycolic acid monomer units, PLGAs are traditionally produced by a metal-catalyzed random-sequence ring-opening copolymerization of the six-membered rings lactide and glycolide. Importantly, this reaction does not allow for sequence control in PLGAs—only the L:G ratio, the absolute stereochemistry of L used in the feed, and molecular weight can be controlled. The most common metal catalyst in this process is tin(II) octanoate, or $Sn(Oct)_2$, which is a food additive approved by the FDA, commercially available, and easy to handle.[14] In industry, PLGAs are named according to the stereochemistry and percent content of lactic acid, two factors affecting the mechanical properties and hydrolysis behavior of the materials.[15] Though PLGAs are rich in application, their function during hydrolysis is limited by sudden loss of mechanical properties, burst releases of guest molecules, acidic pH, and composition drift due to the more facile elimination of glycolic acid monomers from the polymer matrix.[5, 7, 38] Our group hypothesized that sequence control in PLGAs could improve upon these functional shortcomings.

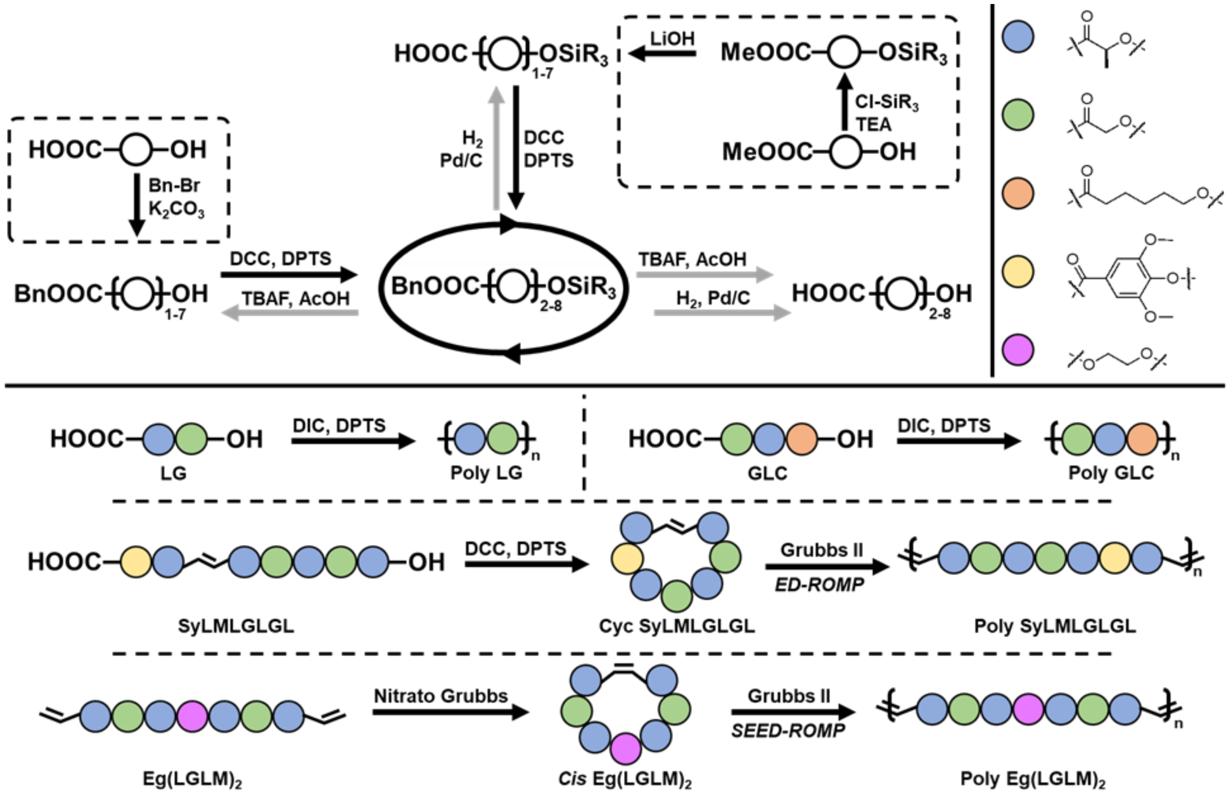
HOOC-OSiR$_3$ 1-7
LiOH
MeOOC-OSiR$_3$
Cl-SiR$_3$
TEA
MeOOC-OH
H$_2$
Pd/C
DCC
DPTS
HOOC-OH
Bn-Br
K$_2$CO$_3$
BnOOC-OH 1-7
DCC, DPTS
TBAF, AcOH
BnOOC-OSiR$_3$ 2-8
TBAF, AcOH
H$_2$, Pd/C
HOOC-OH 2-8
HOOC-OH
LG
DIC, DPTS
Poly LG
HOOC-OH
GLC
DIC, DPTS
Poly GLC
HOOC-OH
SyLMLGLGL
DCC, DPTS
Cyc SyLMLGLGL
Grubbs II
ED-ROMP
Poly SyLMLGLGL
Eg(LGLM)$_2$
Nitrato Grubbs
Cis Eg(LGLM)$_2$
Grubbs II
SEED-ROMP
Poly Eg(LGLM)$_2$

Figure 1. Synthetic overview depicting methods toward sequence-controlled polyesters, including segmer-assembly polymerization (top) and entropy-driven ring-opening metathesis polymerization (bottom).

The Meyer group has used both segmer assembly polymerization (SAP) and entropy-driven ring-opening metathesis polymerization (ED-ROMP) to prepare sequenced PLGAs, as is outlined in Figure 1. Using the SAP methodology the Meyer group has synthesized a family of sequenced PLGAs and polymers containing 6-hydroxyhexanoic acid (C) from 15-36 kDa with various lactic acid content and stereochemistry by utilizing orthogonal protecting groups, and has demonstrated that monomer sequence has a dramatic effect on properties.[9-13,17] The deprotected sequence is first synthesized, and this synthesis is followed by a condensation polymerization with diisopropylcarbodiimide (DIC) and amine catalyst dimethylaminopyridinium 4-toluene sulfonate (DPTS), reagents incapable of inducing transesterification (or sequence scrambling). Prepared in this fashion, the alternating, stereopure copolymer termed **Poly LG** (L = L_S) became of interest due to its largest deviation in behavior when compared to its random-sequence analog during *in vitro* degradation studies – linear molecular weight decrease, a zero order release profile of loaded guest molecule rhodamine-B, minimal swelling and water-uptake, and extended retention of mechanical properties.[9,10,12] Additionally, a brief *in vivo* study indicated that **Poly LG** microparticles both outlast the random PLGA and provoke a lessened inflammatory response when subcutaneously injected into mice samples and allowed to degrade.[37] Highlights of these sequence/property comparisons are shown in Figure 2. The underlying cause of these property deviations was hypothesized to be the complete elimination of G-G linkages, as hydrolysis rates are known to proceed as: G-G > L-G , G-L > LL. Though the SAP method has successfully demonstrated these properties are sequence-dependent, this methodology is limited by low polymerization yields and lack of molecular weight control, so a new polymerization method was pursued.

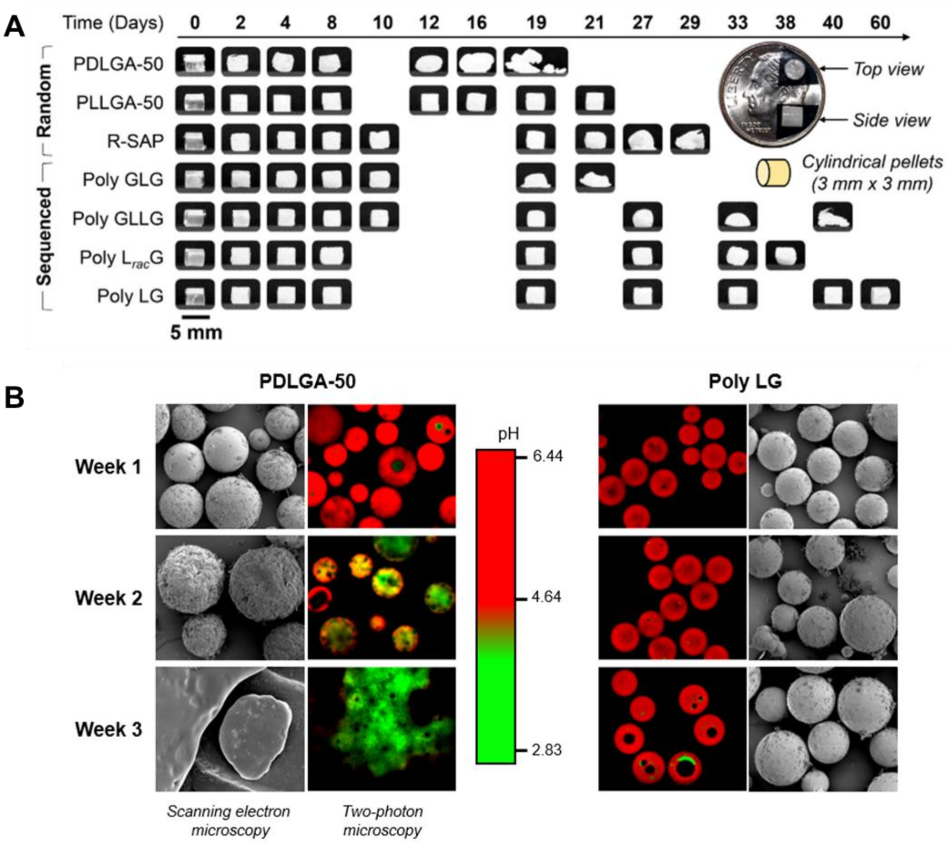
A
Time (Days)
0
2
4
8
10
12
16
19
21
27
29
33
38
40
60
Random
Sequenced
PDLGA-50
PLLGA-50
R-SAP
Poly GLG
Poly GLLG
Poly L$_{rac}$G
Poly LG
5 mm
Top view
Side view
Cylindrical pellets
(3 mm x 3 mm)
B
PDLGA-50
Poly LG
Week 1
Week 2
Week 3
pH
6.44
4.64
2.83
Scanning electron microscopy
Two-photon microscopy

Figure 2. Hydrolysis behaviors of devices prepared from sequenced and random poly-(lactic-co-glycolic acid)s. (A) Photographs of pellets as a function of hydrolysis time. Reproduced with persmission from Elsevier. (B) Internal pH measurements and scanning-electron microscopy images of polymer microparticles during hydrolysis. Reproduced with permission from Elsevier.

More recently, the Meyer group developed a new synthetic approach to sequenced copolymers using ED-ROMP, which involves the ring-opening of strainless macrocycles typically greater than 14 atoms into polymer chains.[22] The polymerization is thermodynamically driven since the conformational flexibility of polymer chains is entropically favored over rings at high concentrations. Additionally, monomer conversion is typically high, limited by ring-chain equilibrium.[23] Resembling a chain polymerization, ED-ROMP allows molecular weights to be predicted from the mole percent of initiator present – i.e., the number of catalyst molecules determines the number of polymer chains initially produced.[24]

Metathesis has led to the efficient syntheses of drugs and plastics by providing a high throughput route to carbon-carbon bonds[19], and has recently been employed in the synthesis of sequenced macromonomers and copolymers.[18] The development of particular Grubbs catalysts such as Grubbs second and third generation catalysts, Hoyveda-Grubbs catalyst, and Z-selective Grubbs catalyst have brought about a wide range of metathesis capabilities, including cross metathesis, ring-closing metathesis (RCM), and metathesis polymerizations. Most notably, Grubbs second generation (G2) is air/moisture stable and is chemically tolerant of functional groups such as acids and alcohols.[19] Additionally, a Z-selective Grubbs (Nitrato Grubbs, GN) catalyst has made it possible to attain primarily *cis*-olefins as products. Both G2 and GN have been employed in the Meyer group for RCM to prepare macrocyclic oligomers bearing LG sequences that undergo ED-ROMP.[20,21]

1.5 Bulk Property Sensitivity in Sequence Controlled Polymers

1.5.1 Overview

The understanding of how monomer sequence affects the properties of synthetic copolymers is underdeveloped when compared to our knowledge of how sequence alterations affect the properties of natural macromolecules such as DNA and proteins. Aside from general sequence alterations such as blocky, gradient, and tapered microstructures, from which the majority of all sequence/property relationships are reported,[11] monomer-by-monomer sequence/property relationships can be categorized into either solution phase or bulk phase studies (Figure 3). In the solution phase categories, studies may typically be grouped into systems that involve either molecular folding, aggregation, or recognition, and these studies represent the majority of work in the field. This volume of work is due to solution-phase studies requiring less material for measurements and, therefore, synthetic scalability is a less limiting factor in experimental design. Despite the demand for more material in more comprehensive bulk-phase studies, there is still a considerable body of work in this category that will be discussed further herein.

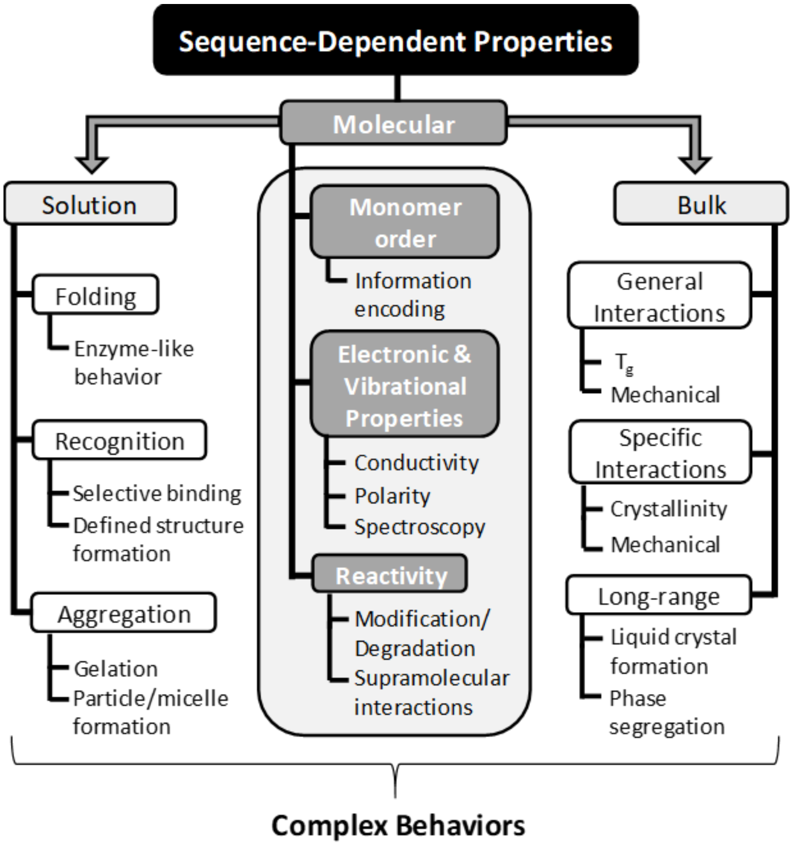
Sequence-Dependent Properties
Molecular
Solution
Folding
Enzyme-like behavior
Recognition
Selective binding
Defined structure formation
Aggregation
Gelation
Particle/micelle formation
Monomer order
Information encoding
Electronic & Vibrational Properties
Conductivity
Polarity
Spectroscopy
Reactivity
Modification/ Degradation
Supramolecular interactions
Bulk
General Interactions
T_g
Mechanical
Specific Interactions
Crystallinity
Mechanical
Long-range
Liquid crystal formation
Phase segregation
Complex Behaviors

Figure 3. Classes of sequence-dependent properties. Molecular properties lead to solution- and solid-phase properties as well as complex behaviors. Reproduced with permission from Wiley-VCH Verlag GmbH & Co.

1.5.2 Bulk Properties of Stereosequenced PLAs

As stereosequence has shown to affect bulk properties for a variety of polymers such as poly(ethylene-*co*-norbornene),[39] poly(1-butene),[40] poly(methyl methacrylate),[41] and polystyrene,[42, 43] it is not surprising that the monomer order in copolymers may affect bulk properties. Homopolymers comprising monomers that are either prochiral or chiral can be regarded as types of sequenced copolymers, even when the repeat units are identical in atomic composition. Moreover, stereosequences in this class have been extensively studied and there exists a body of data that links properties to the control of the tacticity of polymer chains. While detailed tacticity studies have not been performed on the bulk properties of PLGAs, closely-related poly-(lactic acid) (PLA), which involves the chiral lactic acid monomer, has exhibited bulk properties that are significantly sensitive to tacticity.[44-48]

PLA is widely studied because the polymer, which is well-known for biodegradability, can be prepared with a high degree of stereosequence control by the ring-opening polymerization of the various lactide monomers: (*R*,*R*)-lactide and (*S*,*S*)-lactide, *meso*-lactide, and the *rac*-lactide mixture of (*R*,*R*)- and (*S*,*S*)-lactide.[49, 50] Not surprisingly, the degree of order in the bulk polymer affects the thermal properties of PLA and, therefore, tacticity directly affects these properties. Atactic PLA (PDLA) is generally an amorphous solid with glass transition temperature (T_g) = 32 °C, whereas isotactic PLA (PLLA) is a highly-crystalline polymer with T_g = 55 °C and T_m = 175 °C.[51] Catalyst development by Coates and coworkers provided a route to syndiotactic PLA,[52] as well as heterotactic PLA, which contains alternating stereo pairs (...*SSRRSSRR*...). The heterotactic polymer exhibits a higher glass transition but a lower melting temperature than the syndiotactic analogue.[51, 53]

A gradient PDLA-PLLA copolymer prepared by Spassky and coworkers exhibited an elevated melting temperature,[54] while the stereoblock isotactic copolymer prepared by Coates, which alternates between PDLA and PLLA blocks, exhibited a melting point higher than the isotactic analogue, due to the formation of a stereocomplex.[55] Additionally, Ishii and coworkers demonstrated a direct relationship between the isotactic stereoselectivity (P_{meso}) during the polymerization of *rac*-lactide and melting temperature,[56] and Abe and coworkers observed a similar relationship with T_m and isotacticity in alternating copolymers of lactic acid and 4-hydroxybutyrate.[34]

Hatzikiriakos and coworkers recently compared rheological and mechanical properties of PLAs of varying tacticity.[51] Primarily atactic, heterotactic, syndiotactic and isotactic PLAs with high molecular weights were prepared and underwent testing to acquire intrinsic viscosity, zero shear viscosity, elongational viscosity, plateau modulus, linear viscoelastic moduli, decomposition temperatures, and average relaxation times of each polymer. One of the key findings in this study was that the molecular weight between entanglement (M_e) varied substantially as a function of tactiticy: syndiotactic > heterotactic > atactic > isotactic. As M_e increases and aggregate domains increase in size the polymer becomes stiffer and more stable.

Beyond the scope of PLA and degradable polyesters a variety of copolymers have exhibited bulk properties that are sequence-dependent. In the current thesis, a base alternating sequence is manipulated in order investigate the sensitivity of hydrolysis behaviors as LG alternation is interrupted. Similar investigations, which compare alternating sequenced copolymers and random analogs, exist in the literature and will be discussed further.

1.5.3 Alternating vs. Random Comonomer Sequences

Due to the unique synthetic accessibility of alternating copolymers, they represent some of the most commonly reported sequenced copolymers and, not surprisingly, the comparison of alternating copolymers relative to random analogues is the most studied. Fortunately, this comparison is of significant importance, especially when contrasted, as is often done, with the AB block copolymer of the same composition. As these three sequences represent key points on the monomer distribution continuum, it is expected that their properties will define for many polymers the range of behaviors that could be expected for any sequence with the same A:B monomer ratio.

The effects of sequence on the copolymer miscibility have been extensively studied.[57, 58] Galvin and Winey and coworkers, for example, investigated the sequence effects on phase behavior in polymer blends of block, random or alternating poly(styrene-*co*-methyl methacrylate) with corresponding homopolymers.[59, 60] Using both microscopy and thermal characterization they confirmed that the alternating copolymer was more miscible than block and random copolymers in a blend with PMMA.

The degree of sequence control affects the ability of copolymers to exhibit property-directing interchain interactions. Colquhoun and coworkers found that the alternating copolymer of an aromatic sulfone and an aromatic ketone was fully amorphous while the random copolymer was partially crystalline.[61] In a later study, they found the opposite was true in an aromatic poly(ether ketone) system where the introduction of randomness through controlled transetherification led to decreased crystallinity.[62]

Choe and company compared a series of well-defined and random aromatic copolyesters and aromatic copolyesteramides and reported distinct differences in thermal properties in both systems, wherein the random analogues displayed lower and more broad T_gs and higher decomposition temperatures (T_ds).[63] Kricheldorf and coworkers saw similar broad thermal transitions in a random copolyester when compared to an alternating analogue.[64]

Akashi and coworkers investigated sequence effects on the thermal and mechanical properties of alternating and random poly(dimethyl siloxane) – polyamide copolymers.[65] The random polymers showed two T_gs, one each for the hard and soft block, while the alternating polymer showed only one T_g. The random polymer had a Young's modulus 7× that of the alternating polymer, a larger tensile strength, and a lower elongation at break, leading to the conclusion that the random polymer behaves like a thermoplastic elastomer while the sequenced polymer behaves like a soft rubber.

Halary and coworkers compared the properties of random and alternating styrene-methyl methacrylate (SM) copolymers and observed that the alternating copolymer exhibited a higher loss modulus and lower strain softening amplitude at low temperatures, higher strain softening amplitude at high temperatures, lower pseudo-equilibrium modulus of the entanglement network and a lower T_g.[66] They speculate the properties in the copolymers are likely dictated by the ability of acrylate groups to interact, which is facilitated in random copolymers, as well as the distribution of MSM triads throughout the backbone.

The Kim group directly compared random and alternating donor-acceptor conjugated copolymers and found a higher T_d, open-circuit voltage, short-circuit current density, power conversion efficiency and more ideal charge transfer properties for the alternating polymer, due to the consecutive linkages of electron-deficient acceptor units acting as a charge trap.[67] Lee and coworkers, examining a more subtle difference in sequence, compared inherently alternating donor-acceptor thiophene-based copolymers which, while maintaining an overall alternating AD pattern, embedded two different donors in either an alternating or random fashion, i.e., D_1AD_2A vs $D_{1/2}AD_{1/2}A$.[68] The more sequenced polymer shows a higher X_C, a larger optical bandgap and a 500% higher power conversion efficiency than the random analogue.

1.5.4 Reports of Sequence Effects on Bulk Properties

Although uncommon, there have been some relevant reports of small populations of a sequence alteration affecting properties. The most prevalent studies typically involve solution-phase properties, particularly polymer folding,[21, 69-71] aggregation,[22, 72-78] and molecular recognition.[79-82] In the bulk phase, this phenomenon is even less studied but there are some notable examples including the work of Winey and co-workers who determined that small alterations in sidechain spacing can affect morphological order in ionomers,[83-86] Jannasch and co-workers who described the sensitivity of proton conductivity to small deviations in monomer spacing,[87] and Segalman and co-workers who described the dependence of surface structure and hydration of polypeptoids on the positioning of discrete sequences within a chain.[88] Previous work in the Meyer group has indicated that the hydrolytic behaviors of sequenced PLGAs may exhibit this caliber of sequence sensitivity to consecutive glycolic acid units in a chain.

In systems that exhibit a clear sensitivity to sequence, the realm between fully sequenced and random copolymers may be explored to obtain copolymers with combinations of properties that are distinctly unique. The approach of using known monomers to prepare new polymers by diverse monomer arrangements is both economical and practical.

1.6 Thesis Overview

Meyer and coworkers have observed that an alternating PLGA, termed **Poly LG**, exhibited dramatic deviation in hydrolysis behaviors when compared to its random sequence counterpart, and this wide divergence of behavior begs the following question: how tolerant are the hydrolysis properties of PLGAs to deviations in this alternating sequence? In this dissertation, we describe the synthesis of PLGA-like copolymers that is first developed to provide copolyesters with controlled molecular weights on a scale that allows for bulk hydrolysis studies, in addition to two hydrolysis studies that employ this synthetic method – one including the comparisons between a base alternating sequence and a derivative containing a slightly scrambled sequence, and the second including the comparisons between a base alternating sequence and copolymers with varying degrees of a glycolic acid error that interrupts the base sequence.

In Chapter 2 of this dissertation, the preparation of sequence-controlled polymers using ED-ROMP is described. The scalable synthesis of large, sequence-imbedded macrocycles is optimized, followed by studies regarding the establishment of molecular weight control, sequence retention, living polymerization conditions, block copolymerizations, and additional monomer incorporation to elevate the T_g for hydrolysis studies.

In Chapter 3 of this dissertation, the synthesis of an ED-ROMP copolymer containing a repeating LG alternating sequenced pentamer (LGLGL), interrupted by a linker unit, is described alongside the synthesis of a copolymer of identical monomer composition with sequence disorder confined to the pentamer segment (L_3G_2). These two copolymers, the precisely sequenced and "controlled random" copolymers, were cast as thick films and allowed to hydrolyze. Molecular weight loss, mass loss, thermal properties, and surface features were monitored to reveal drastic differences in hydrolysis behaviors despite only a small change in sequence precision.

In Chapter 4 of this dissertation, macrocycles containing the same LGLGL segment as described in Chapter 3 and a macrocyclic "errormer" containing an LGGGL segment are combined in varying quantities to prepare five copolymers of differing error content. The molecular weight and surface features of these polymers were monitored during hydrolysis to establish the tolerance to sequence errors for this PLGA-like system.

2.0 Synthetic Advances toward Sequence-Controlled Polyesters with Molecular Weight Control

2.1 Overview

The majority of content in this chapter was previously published in the Journal of the American Chemical Society, Volume 141, Issue 14, Pages 5741 - 5752, in an article entitled "*Sequence-Controlled Polymers Through Entropy-Driven Ring-Opening Metathesis Polymerization: Theory, Molecular Weight Control, and Monomer Design*." This publication also includes the original work by Ryan M. Weiss, PhD, Amy L. Short, PhD, and Cheng Fang, PhD, who experimentally and computationally investigated the preliminary synthetic routes from which this chapter is built. Ryan M. Weiss investigated the reactivities of varying olefin linkers in addition to performing kinetic experiments and molecular weight control studies using *trans*-macromonomers. Amy L. Short investigated the reactivity of the *cis*-macromonomer variant by performing kinetic experiments, molecular weight control studies, chain extension experiments, and preliminary block copolymerizations with norbornene. Cheng Fang contributed theoretical insight by performing molecular dynamics-density functional theory (MD-DFT) calculations to establish the cause of the heightened reactivity of the *cis*-macromonomer.

My contributions to this polymerization method began with the preparation of unsymmetric monomers prepared via ester ring-closing, molecular weight control studies on this type of monomer, olefin connectivity determination, and the insertion of a syringic acid monomer unit. Additionally, I continued the work of Amy Short in preparing block copolymers using a *cis*-

macromonomer in addition to norbornene and *cis*-cyclooctene. The following chapter particularly highlights these contributions.

In this chapter, the development of scalable and controllable syntheses of sequence-controlled polyesters using ED-ROMP is described in detail. Additionally, this chapter includes the description of alternative synthetic routes toward sequenced polyesters that did not produce material for further studies. These methods include an N-carboxyanhydride polymerization as well as a ring-opening transesterification polymerization.

2.2 Introduction

There exists a clear demand for the development of general, scalable, and controllable synthetic methods for imbedding monomer sequence in synthetic copolymers both to enable the production of novel materials for applications and to define more clearly how sequence controls properties. The effects of monomer sequence on polymer properties are well-established in Nature, wherein precise monomer order can be directly mapped to macromolecular function. In synthetic polymer chemistry, in contrast, sequence control and the derivation of structure/function relationships have been limited to a variety of more easily accessible motifs including alternating, gradient, or blocky structures.[89-91] The attainment of a more detailed understanding has been inhibited by the challenges inherent in preparing precisely sequenced copolymers with molecular weight control. In the few classes of materials for which data have been obtained, the majority of the work has focused on solution phase properties; the most studied systems include peptoids,[24, 92] foldamers,[23, 69, 71] and systems exploiting molecular recognition moieties.[82, 93, 94] Bulk-phase structure/function studies, which typically require gram-scale quantities,[95] are extremely rare.[19, 20, 24, 49, 51, 68, 85, 96-100]

Our group has long been interested in understanding the connections between sequence and properties in non-biological polymers. In the course of that work we have developed synthetic routes to periodically sequenced poly(lactic-*co*-glycolic acid)s (PLGA)s and established that bulk phase behaviors during hydrolysis are extremely dependent on constituent monomer sequence.[35-37] Our interest in this class of polymers and their behavior arose because of their potential for application as degradable sutures, drug delivery vehicles, and cell scaffolds.[3, 5, 7, 9, 38, 101] The random version of this class of polymer, which is widely used and FDA-approved, exhibits a degradation profile that is controlled primarily by molecular weight and the ratio of lactic (L) to glycolic acid (G) monomers.[7] Our work on periodic PLGAs demonstrated that monomer sequence is an even more powerful tool for controlling hydrolysis behavior, facilitating not only rate control, but also affecting the retention of mechanical properties, swelling, internal pH, lactic acid release, and release of guest molecules *in vitro*.[35-37]

Despite our successes in carrying out structure/function studies on sequenced PLGAs, the scalable and controllable syntheses of these polymers remained an ongoing challenge. Our original synthetic efforts relied on materials prepared by a step-growth synthesis in which hydroxy-acid sequenced oligomers (segmers) were first prepared and then polymerized. Using this segmer-assembly polymerization (SAP) method, we were able to prepare a large range of periodic copolymers. Although moderately scalable, SAP provided no molecular weight control, unpredictable yields, poor reproducibility, and relatively large dispersities ($Đ = 1.5 – 1.8$). These issues limited the accuracy and scope of structure/function studies for these materials.

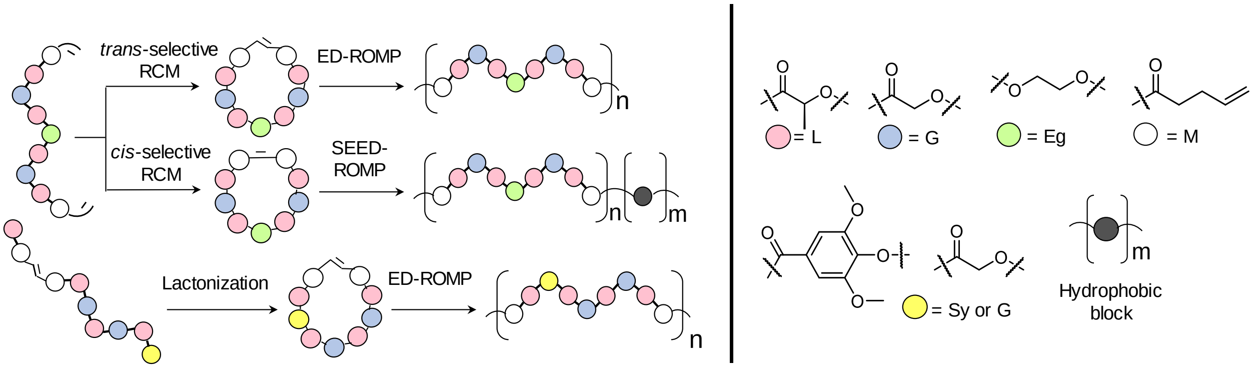

Figure 4. Overall synthetic approach involving ring-closing to prepare macrocycles with embedded monomer sequences and sequence-retaining metathesis polymerizations. Reproduced with permission from the American Chemical Society.

To address these synthetic limitations, we sought to develop a general method of preparing sequence-controlled polymers that proceeded, at least initially, via a chain-mechanism pathway. Specifically, we targeted entropy-driven ring-opening metathesis polymerization (ED-ROMP), which has been used previously to polymerize cyclic macromonomers.[102-111] We sought to prepare sequenced macrocyclic oligomers (MCOs) containing LG segments, a "linker" monomer to connect these segments that would not dominate bulk properties,[112] and an olefin-metathesis site (Figure 4). This new polymerization approach was expected to improve molecular weight control, decrease dispersity, and achieve higher molecular weights than those obtained by the step-growth SAP methodology. In previous publications,[113, 114] we reported our initial successes using this approach, detailing how ED-ROMP functions in this system and how we were able to introduce living character into the polymerization through a simple *trans*- to *cis*-olefin substitution.

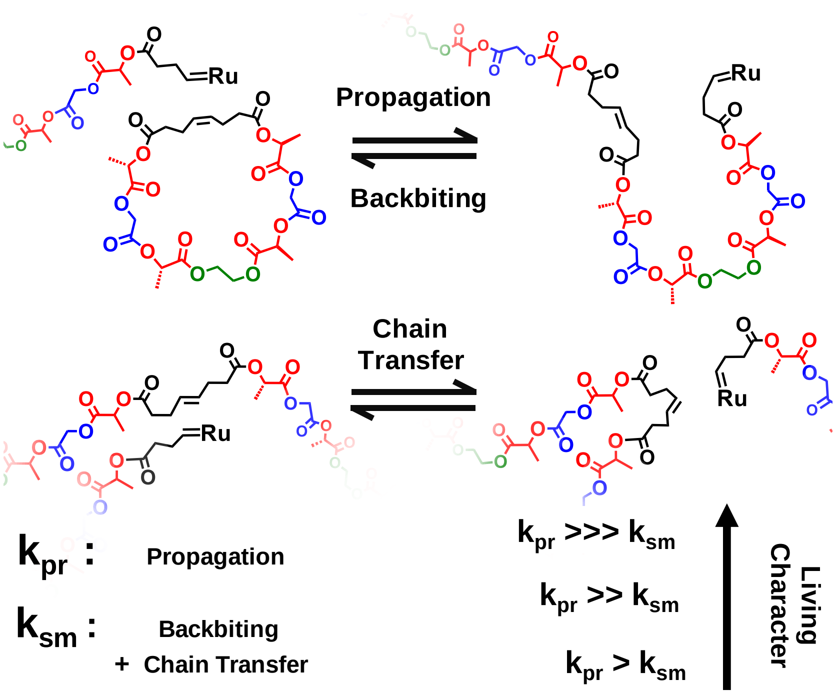
Propagation
Backbiting
Chain Transfer
Ru
k_{pr} : Propagation
k_{sm} : Backbiting
+ Chain Transfer
$k_{pr} >>> k_{sm}$
$k_{pr} >> k_{sm}$
$k_{pr} > k_{sm}$
Living Character

Figure 5. Living polymerization character as it relates to the relative rates of propagation (k_{pr}) and secondary metathesis (k_{sm}) in entropy-driven ring-opening metathesis polymerization. Reproduced with permission from the American Chemical Society.

ED-ROMP has been used previously to polymerize strainless macrocycles, typically containing greater than 14 atoms, with entropy serving as the primary driving force for the reaction (Figure 5).[102] High concentration is used to favor polymer chains over cyclic species. The molecular weight and dispersity observed at any timepoint in the reaction depend on the rate of propagation (k_{pr}) relative to that of secondary metathesis (k_{sm}).[115-117] It should be noted that termination reactions are not typically observed in these systems on the timescale of a normal polymerization. Final molecular weights and dispersities are a function of monomer-to-catalyst loading ([M]/[cat]), ring-chain equilibrium, and overall concentration.[102, 118] ED-ROMP typically results in dispersities greater than 1.1 due to competing secondary metathesis/backbiting (chain-transfer) reactions.

Although unmodified ED-ROMP does allow for molecular weight control, the prevalence of secondary metatheses of the newly produced olefin backbone interferes with the ideal behavior that would be expected for a system in which k_{pr} is much greater than k_{sm}. Such a system would be expected to behave in a more "living" fashion, giving chains that grow steadily and similarly in molecular weight. Knowing that these rates depend on the steric accessibility of the olefin,[119] we have investigated, both theoretically and experimentally, the effects on mechanism and living character of the olefin geometry.[114] Our findings resulted in the description of a new variant that we termed Selectivity-Enhanced ED-ROMP, or SEED-ROMP. Living polymerization character was observed during SEED-ROMP due to the dramatic increase in k_{pr}. Computational analysis suggested that this increase is primarily the result of a greater ensemble of metathesis active *cis*-olefin conformers that result from decreased structural flexibility.

As the polymerizations of metathesis-linker-containing MCOs produced polymers with T_gs of 18 - 20 °C, which are lower than that required for most biomedical applications (~ 40 - 50 °C), we sought to improve upon these synthetic advancements and prepare an MCO without the **Eg** linker, thus breaking the palindromic symmetry of the macrocycles and resulting polymers. This was achieved by ring-closing via macrolactonization of a hydroxy-acid segmer, followed by exploitation of this modular approach to incorporate a biocompatible monomer that would elevate T_g further without dominating other properties such as degradation rates. We were inspired by the Miller group to include syringic acid (Sy), a phenolic acid antioxidant found in grains and plant cell walls.[112, 120] The incorporation of this rigid monomer into the polymer backbone brought about a polymer that can be prepared with the same improved scalability and molecular weight control, along with a similar T_g to pure PLGAs. This copolymer system ultimately became an ideal candidate to study how hydrolysis behaviors are affected by small changes in sequence.

This chapter comprises a progression of synthetic developments that build upon the previous work of Weiss et. al.[113] and Short et. al.[114] (Scheme 1) in utilizing ED-ROMP to polymerize sequenced MCOs. The current work includes optimization of block copolymerizations of MCOs using SEED-ROMP, the synthetic details leading to non-palindromic MCOs, the demonstration of molecular weight control during the polymerization of these novel macromonomers, and the incorporation of syringic acid to elevate T_g. The synthetic developments outlined in this chapter form the basis of the bulk-scale comparisons of minor sequence effects in these polyesters during hydrolysis. Lastly, the scalable, controllable preparation and polymerization of these MCOs sans linkers is desirable yet synthetically challenging. Other, less-successful methods to produce sequenced PLGAs with minimal to no linker incorporation were investigated and are discussed herein, including the N-carboxyanhydride (NCA) polymerizations of sequenced MCOs and ring-opening transesterification polymerizations (ROTEP).

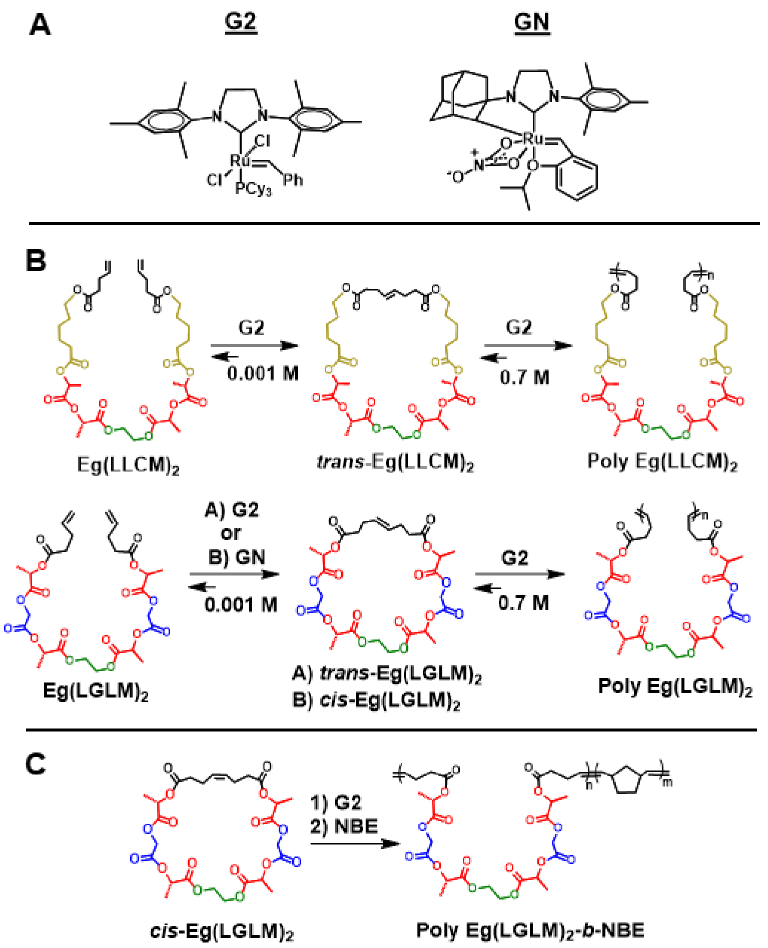
A
G2
GN
N
N
Cl
Ru
Cl
PCy3
Ph
B
G2
0.001 M
G2
0.7 M
Eg(LLCM)2
trans-Eg(LLCM)2
Poly Eg(LLCM)2
A) G2
or
B) GN
0.001 M
G2
0.7 M
Eg(LGLM)2
A) trans-Eg(LGLM)2
B) cis-Eg(LGLM)2
Poly Eg(LGLM)2
C
1) G2
2) NBE
cis-Eg(LGLM)2
Poly Eg(LGLM)2-b-NBE

Scheme 1. Utilizing ED-ROMP to prepare sequence-controlled polyesters with controllable molecular weights. A) Structures of Grubbs Second Generation Catalyst (G2) and Z-Selective Grubbs Nitrato Catalsyt (GN). B) Ring-closing metathesis reactions and subsequent polymerizations. C) Selectivity-enhanced entropy-driven ring-opening metathesis polymerization to produce a block copolymer with norbornene. Figure adapted with permission from the American Chemical Society.

2.3 Results and Discussion

2.3.1 Optimization of SEED-ROMP Block Copolymerizations

In the preparation of palindromic MCOs, synthesis begins with orthogonal protections of L or G monomers—acid moieties with benzyl (Bn) groups and alcohols with tert-butyldiphenylsilyl (TBDPS) groups. Ester couplings with dicyclohexylcarbodiimide (DCC) and nucleophilic amine catalyst DPTS provide di-protected hydroxyacids which are named from the acid-terminus to alcohol-terminus. Removal of the Bn group via hydrogenolysis provides free acids and removal of the TBDPS group with TBAF provides free alcohols that are then available for sequential cycles of couplings and deprotection. Under these reaction conditions little or no transesterification is observed.

MCO ***cis*-Eg(LGLM)$_2$** was prepared as described in the literature by Short et. al.[114] The symmetric coupling of trimer **LGL-Si** to **Eg** was performed to prepare the palindromic, di-protected species **Eg(LGL-Si)$_2$** which then underwent complete silyl deprotection in the presence of TBAF and acetic acid. The resulting diol **Eg(LGL)$_2$** was coupled to 4-pentenoic acid (**M**) to give an acyclic diene, **Eg(LGLM)$_2$**. Ring-closing metathesis (RCM) with Z-selective Grubbs Nitrato catalyst (**GN**) [121] provided the MCO product in excellent yield, with ~90% *cis*-selectivity. The Z-selective RCM is highly reproducible but requires extremely low concentrations (0.001 M), reflux (DCE) under high vacuum, and 10-15 mol% catalyst loadings.[114, 122]

It was previously observed that polymerization of ***cis*-Eg(LGLM)$_2$** with **G2** at high concentration (0.7 M) resulted in polymerization rates and molecular weight control exceeding those observed with the isomer ***trans*-Eg(LGLM)$_2$**. The reaction solution becomes an immobile gel after 2 min, and conversion reaches >90% after only 10 min. In contrast, the *trans*-macromonomer requires 2 h to reach this conversion.

Polymer molecular weights exceeded 60 kDa, and secondary metathesis was significantly reduced as can be seen from the narrow dispersities (Đ = 1.1) throughout the course of the reaction. Consistent with a chain mechanism, monomer conversion was linear with time. Molecular weight was linear over an extended range of catalyst loadings, enabling molecular weights between 40 and 75 kDa to be targeted. These results are consistent with incomplete initiation but a high degree of living character, such that the number of active chain ends is proportional to catalyst loading. The presence of active catalysts on the majority of chains was further demonstrated by successful chain extension experiments. In the first of these experiments, a second aliquot of cis-MCO was added to an already formed SEED-ROMP chain. Coplotting of the size exclusion chromatography (SEC) data demonstrates an increase in M_n with no increase in dispersity.

As we were interested in determining the degree to which these polymerizations could be considered living, we carried out block copolymerizations with ***cis*-Eg(LGLM)$_2$** and hydrophobic monomers (Figure 6). Preliminary data from Short[114] suggested that block copolymerization with the commonly-used, strained ROMP monomer norbornene (NBE) had potential for success, so this was investigated further. To prepare block copolymers, the initial polymerization of the MCO was followed by the addition of ROMP monomer.

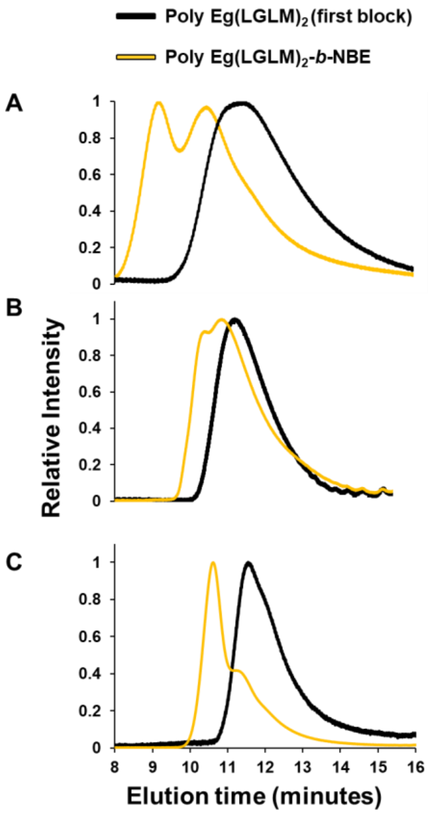

Figure 6. Representative size exlclusion chromatograms of SEED-ROMP-b-ROMP copolymerizations with norbornene. (A) 5 mol% G2, SEED-ROMP 10 min, ROMP 20 min, RT. (B) 2.5 mol% G2, SEED-ROMP 10 minutes, ROMP 10 minutes, RT. (C) 2.5 mol% G2, SEED-ROMP 10 minutes, ROMP 2 minutes, 0 °C. Reproduced with permission from the American Chemical Society.

When the experiment was undertaken with NBE, block copolymers ranging from 60-90 kDa were obtained. These polymers, however, exhibited significant secondary metathesis resulting in unpredictable final molecular weights and considerable increases in dispersities (Figure 6). Attempts to control the block formation by controlling reaction time and temperature resulted in only small improvements. Each time block addition was repeated, a clear increase in molecular weight with minimal increase in dispersity was observed within 1 min, but molecular weight quickly decreased and broadened in dispersity thereafter, eventually leading to bimodal molecular weight distributions. However, ^{1}H NMR spectra remained clean in the G methylene region, indicating that the polyester block did not suffer from significant secondary metathesis and the uncontrollable molecular weights originated from the highly reactive norbornene block. It is worth mentioning that there exist copious variants of functionalized norbornenes that offer more control,[123-125] but these derivatives were not investigated in this current proof of principle study.

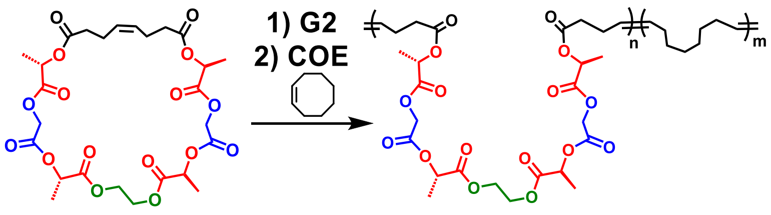

***cis*-Eg(LGLM)$_2$**   **Poly Eg(LGLM)$_2$-*b*-COE**

Scheme 2. SEED-ROMP-b-ROMP copolymerization with *cis*-cyclooctene. Scheme adapted with permission from the American Chemical Society.

The significant increases in dispersities and small increases in molecular weights could also indicate that a significant portion of chain ends were deactivated and unable to undergo block extension. To address this possibility, the experiment was repeated with less-strained *cis*-cyclooctene (COE) (Scheme 2), which is known to have a smaller k_{pr} than NBE during polymerization with **G2**,[123] a feature that can be exploited to allow catalyst quenching before the complete depletion of monomer and, therefore, before significant secondary metathesis reactions can occur.[126-129] In this case, block addition was achieved with no increase in dispersity and molecular weights of ~70 kDa (Figure 7). This result is consistent with the conservation of a high percentage of active chain ends. As the process would not be expected to be purely living, however, some degree of chain transfer is expected.

It is worth noting that ROMP monomers such as NBE and COE may be functionalized to potentially attach deliverable payloads into biological systems for controlled release, or initiate micellar self-assembly.[127, 130, 131] SEED-ROMP is therefore an exceptionally powerful tool in engineering materials for controlled and precise function.

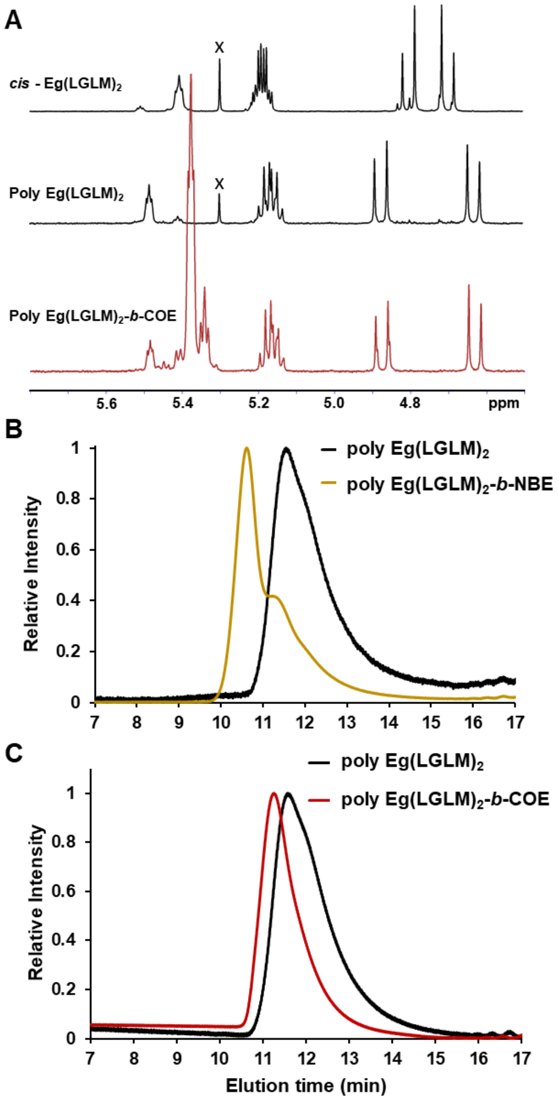

Figure 7. (A) ^{1}H NMR spectra for *cis*-Eg(LGLM)$_2$, polymerization to 50 kDa Poly Eg(LGLM)$_2$, and Poly Eg(LGLM)$_2$-*b*-COE. (x denotes CH_2Cl_2) (B) SEC traces of control and block extension using NBE (unpurified), displaying large dispersity due to secondary metathesis. (C) SEC traces of control and block extension with COE (unpurified). Reproduced with permission from the American Chemical Society.

2.3.2 Macrocyclic Oligomers via Macrolactonization: Linkage Directionality and Scalability

Although the palindromic monomers were moderately scalable, we were able both to improve scalability and remove the **Eg** unit by de-symmetrizing the open-chain oligomer and incorporating the olefin as an intact unit. This method, which exploits macrolactonization[132] to achieve the ring-closing, benefits from eliminating the large ruthenium catalyst loadings required for RCM and can be used to obtain similar yields using 30x less solvent.

Additionally, the nonsymmetrical monomers provide linkage directionality more closely resembling virgin PLGAs with acid and alcohol termini. In this fashion, sequenced precursors **LMLGLGLG** and **SyLMLGLGL** were ring-closed at low concentration at 60 °C in dichloroethane charged with the coupling agent DCC and DPTS catalyst. Slow addition of the oligomer over the course of 16 hr. provided the desired product in yields >85%. Polymerization of these MCOs produced polymers with a conservation of order within each MCO-derived segment but head-tail disorder at the olefin connector as evidenced by ^{1}H NMR spectroscopy (Figure 10).

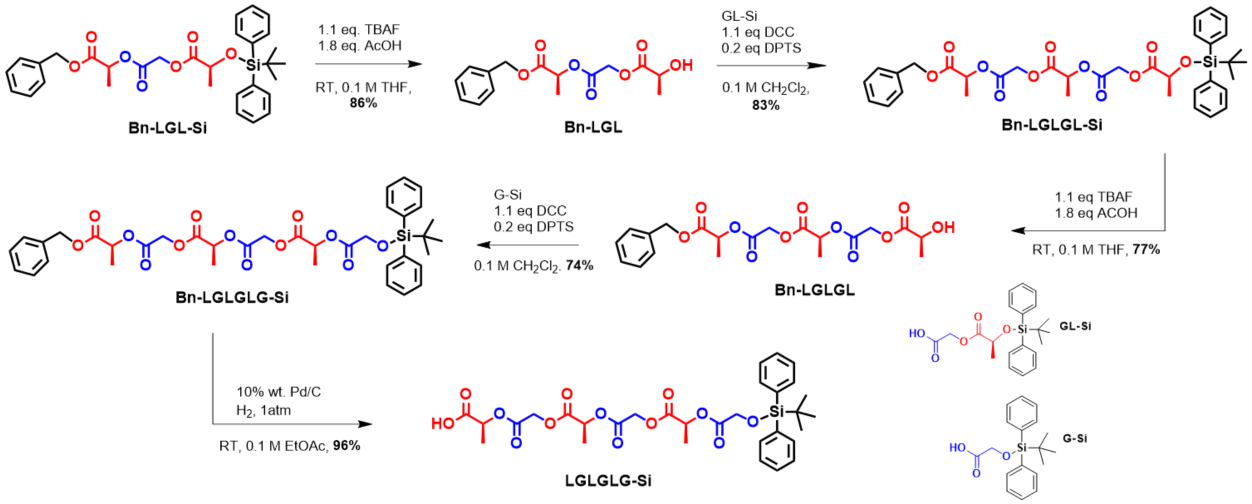
Bn-LGL-Si
1.1 eq. TBAF
1.8 eq. AcOH
RT, 0.1 M THF, 86%
Bn-LGL
GL-Si
1.1 eq DCC
0.2 eq DPTS
0.1 M CH₂Cl₂, 83%
Bn-LGLGL-Si
1.1 eq TBAF
1.8 eq ACOH
RT, 0.1 M THF, 77%
Bn-LGLGL
G-Si
1.1 eq DCC
0.2 eq DPTS
0.1 M CH₂Cl₂. 74%
Bn-LGLGLG-Si
GL-Si
G-Si
10% wt. Pd/C
H₂, 1atm
RT, 0.1 M EtOAc, 96%
LGLGLG-Si

Scheme 3. Preparation of alcohol-protected LGLGLG-Si segmer.

To prepare the octamer **LMLGLGLG**, first the alternating hexameric sequence **LGLGLG-Si** was prepared (Scheme 3) and attached to an olefin-containing segment. The syntheses of the dimer **GL-Si** and trimer **Bn-LGL-Si** were carried out according to Weiss, et al.[17] **Bn-LGL-Si** was silyl deprotected in the presence of tetrabutylammonium fluoride (TBAF) and acetic acid in THF in an 86% yield to obtain **Bn-LGL**, which was then coupled with **GL-Si** via DCC, DPTS in methylene chloride to yield **Bn-LGLGL-Si** in an 83% yield. Another silyl deprotection with 77% yield resulted in **Bn-LGLGL**, which was then coupled to **G-Si** to obtain **Bn-LGLGLG-Si**. A benzyl deprotection with palladium on carbon in the presence of hydrogen gas yielded the hexamer **LGLGLG-Si** with a 96% yield.

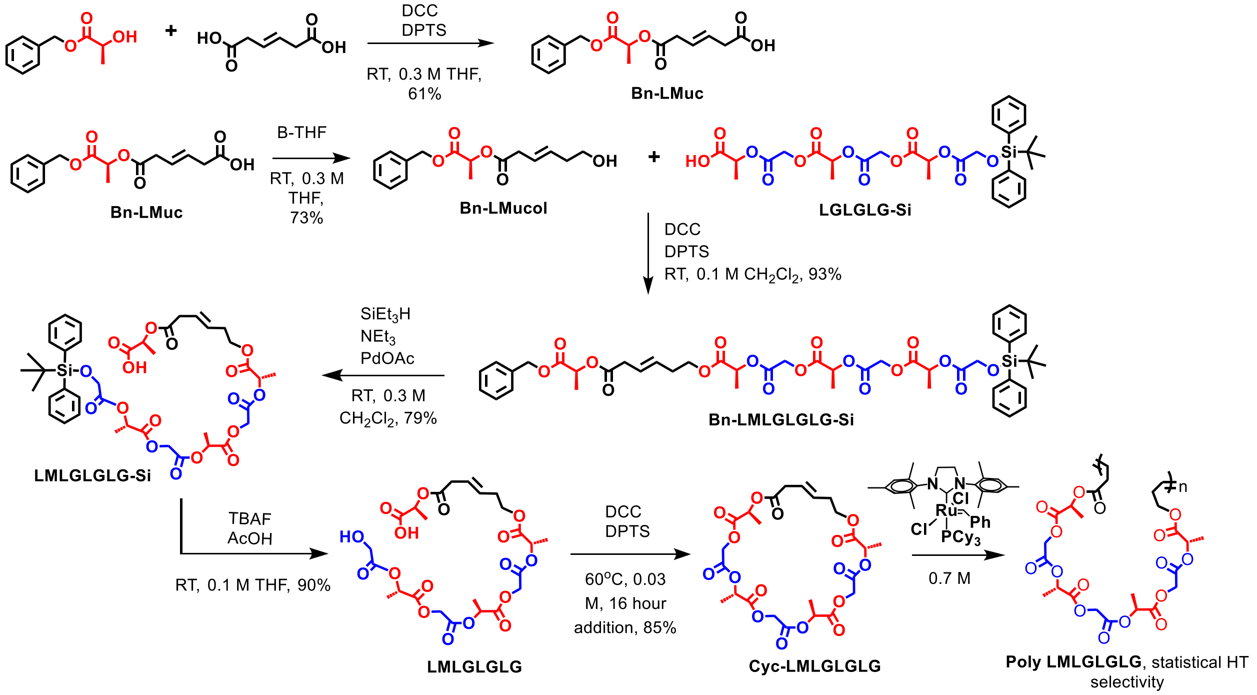

DCC
DPTS
RT, 0.3 M THF, 61%
Bn-LMuc
B-THF
RT, 0.3 M THF, 73%
Bn-LMuc
Bn-LMucol
LGLGLG-Si
DCC
DPTS
RT, 0.1 M CH_2Cl_2, 93%
$SiEt_3H$
NEt_3
PdOAc
RT, 0.3 M CH_2Cl_2, 79%
Bn-LMLGLGLG-Si
LMLGLGLG-Si
TBAF
AcOH
RT, 0.1 M THF, 90%
LMLGLGLG
DCC
DPTS
60°C, 0.03 M, 16 hour addition, 85%
Cyc-LMLGLGLG
PCy_3
0.7 M
Poly LMLGLGLG, statistical HT selectivity

Scheme 4. Preparation of Poly LMLGLGLG.

To undergo ED-ROMP, this sequence was attached to an olefin handle, deprotected, and ring-closed to yield the macrolactone **Cyc-LMLGLGLG** (Scheme 4). **Bn-L** was coupled with excess trans-β-hydromuconic acid (**M**) with DCC and DPTS in THF to give **Bn-LMuc** with a 61% yield. The resulting carboxylic acid was reduced by borane-tetrahydrofuran complex in THF with a 73% yield to obtain the primary alcohol named **Bn-L-Mucol**. Upon coupling with **LGLGLG-Si**, the open-chain di-protected monomer **Bn-LMLGLGLGLG-Si** was prepared with a 93% yield. This compound was then benzyl deprotected with triethylsilane in the presence of triethylamine and catalytic palladium acetate, a reaction selective to benzyl reduction over alkene reduction.[133] Silyl deprotection then yielded **LMLGLGLG**, which was then ring-closed using DCC and DPTS under dilute conditions and a sixteen-hour addition of starting material. The resulting macrocyclic oligomer was obtained in 84% yield. **Cyc-LMLGLGLG** was polymerized at room temperature using **G2** at high concentration (0.7 M) to promote polymerization over non-productive intramolecular ring forming reactions.

2.3.3 Syringic Acid Incorporation to Elevate T_g

As the ED-ROMP of **M**-containing MCOs produced polymers with T_gs of 18 - 20 °C, which are lower than that required for most biomedical applications (~ 40 - 50 °C), we exploited the modular nature of the synthetic method to incorporate a biocompatible monomer that would elevate T_g (Scheme 5). We were inspired by the Miller group to include syringic acid (**Sy**), a phenolic acid antioxidant found in grains and plant cell walls.[112, 120] Thus, the segmer **SyLMLGLGL** was ring-closed via lactonization, and polymerized to prepare **Poly SyLMLGLGL** with M_ns up to 45 kDa. The polymer exhibited the targeted increase in T_g to 50 °C (Figure 8).

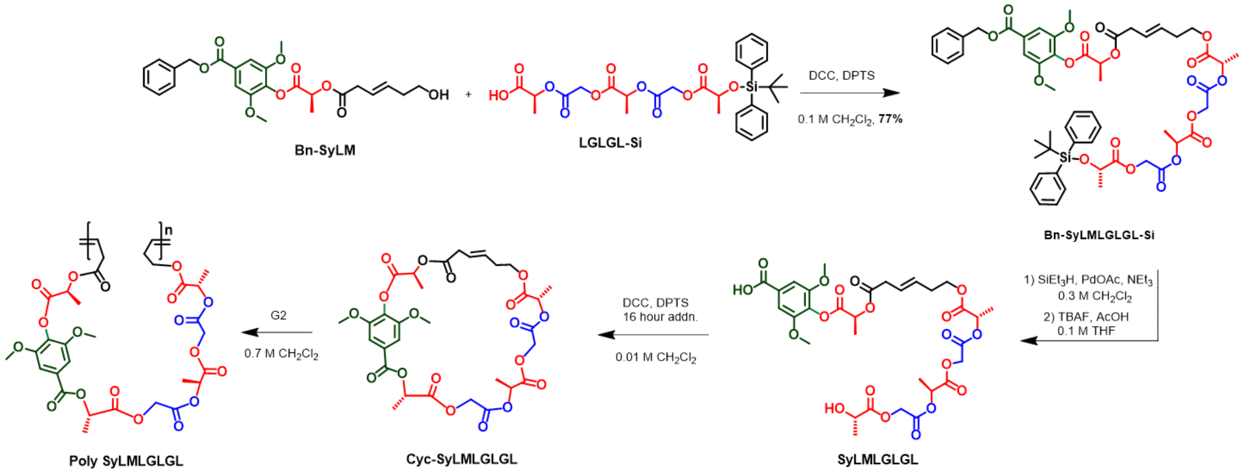
Bn-SyLM
+
LGLGL-Si
DCC, DPTS
0.1 M CH_2Cl_2, 77%
Bn-SyLMLGLGL-Si
1) $SiEt_3H$, PdOAc, NEt_3
0.3 M CH_2Cl_2
2) TBAF, AcOH
0.1 M THF
SyLMLGLGL
DCC, DPTS
16 hour addn.
0.01 M CH_2Cl_2
Cyc-SyLMLGLGL
G2
0.7 M CH_2Cl_2
Poly SyLMLGLGL

Scheme 5. Preparation of Poly SyLMLGLGL.

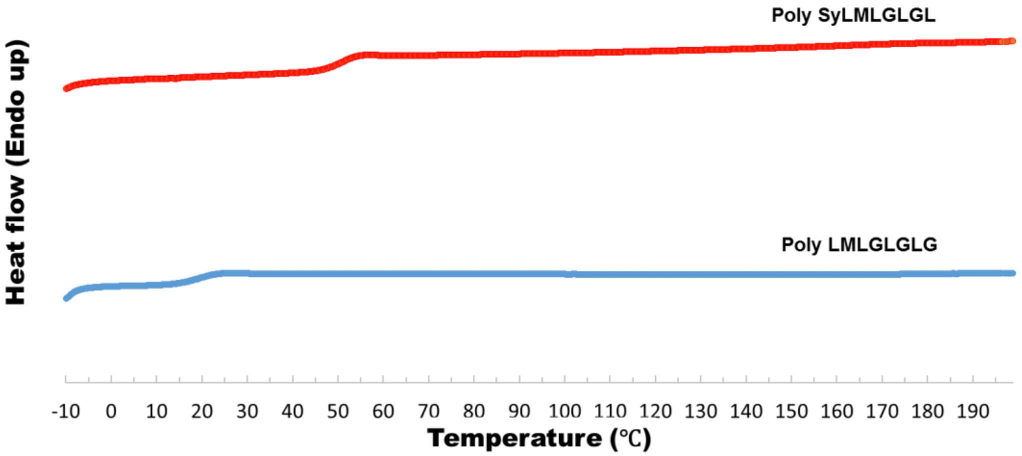

Figure 8. Differential scanning calorimetry thermograms of Poly LMLGLGLG and Poly SyLMLGLGL.

2.3.4 Establishing Molecular Weight Control

The ability to control the molecular weights of polymers prepared from these novel substrates is important for demonstrating that macrolactonization is both a scalable and effective addition to this synthetic method. Molecular weights were varied from 22-43 kDa by varying the percentage of **G2** loading from 1.0 - 3.0%, resulting in dispersities from 1.3 – 1.5. Molecular weights were slightly above theoretical for higher catalyst loadings, and slightly below theoretical below catalyst loadings of 1.25% (Figure 9), an observed feature of ED-ROMP.[25] Though the molecular weight trend is not perfectly linear, the trend is apparent, highly reproducible, and sufficiently similar to those obtained during the polymerizations of the palindromic MCOs (Figure 9B).

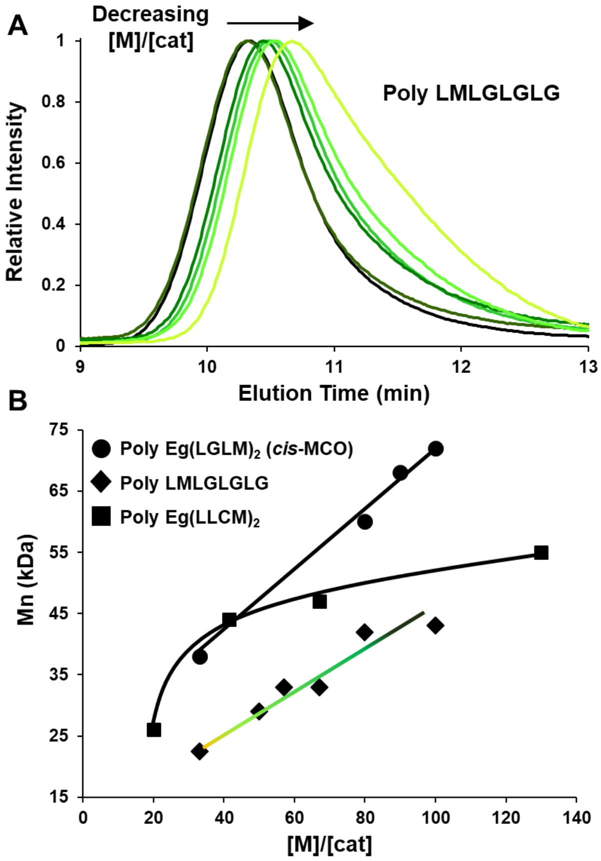

Figure 9. Molecular weights as a function of catalyst loading from palindromic monomers *trans*-Eg(LLCM)$_2$, *cis*-Eg(LGLM)$_2$, and unsymmetric *trans*-LMLGLGLG. (A) Size exlusion chromatographs of Poly LMLGLGLG at varying catalyst loadings. (B) Plots of molecular weights as a function of catalyst loading. Figure adapted with permission from the American Chemical Society.

2.3.5 Monomer Conversion and Regiochemistry

The diastereotopic methylene protons on the glycolic acid units, when adjacent to a chiral lactic acid unit, provide resolved proton resonances due to preferred solution-phase conformations. These resolved signals have confirmed SAP monomeric sequences extensively.[23] In ED-ROMP, the signals are disinct between monomer and polymer and can be integrated to calculate monomer conversion.

Neither ***trans*-LM$_{\text{H-T}}$LGLGLG** nor ***trans*-SyLM$_{\text{H-T}}$LGLGL** polymerized regioselectively. Thus, a statistical distribution of head-tail connectivities of 50% head-tail **M$_{\text{H-T}}$**, 25% head-head **M$_{\text{H-H}}$**, and 25% tail-tail **M$_{\text{T-T}}$** resulted, as evidenced by the distinct ^{1}H NMR olefin signals (Figure 10). This analysis confirms that the selected **M** linker is long enough to eliminate local electronic effects of constituent monomers. We hypothesize that the selectivity could be improved by using a tri-substituted olefin although those experiments were not performed in this study.[107, 134-138] The conversion of ***trans*-SyLMLGLGL** to **Poly SyLMLGLGL** can be similarly followed spectroscopically (Figure 10B).

2.3.6 Sequence Characterization

The exquisite sensitivity of the diastereotopic G methylene protons provide a fingerprint of sequence in ^{1}H NMR spectra. We have previously determined that in some instances the chemical shifts of these protons are affected by sequence differences up to six monomer units away, and as little as 2% sequence error can be easily resolved.[139] As such, we are able to clearly characterize and differentiate copolymers with a range of structures. In addition to general characterization and confirmation of sequence, this sensitivity also makes it possible to monitor quantitatively the progress of the polymerization reaction as a function of time and isomer.

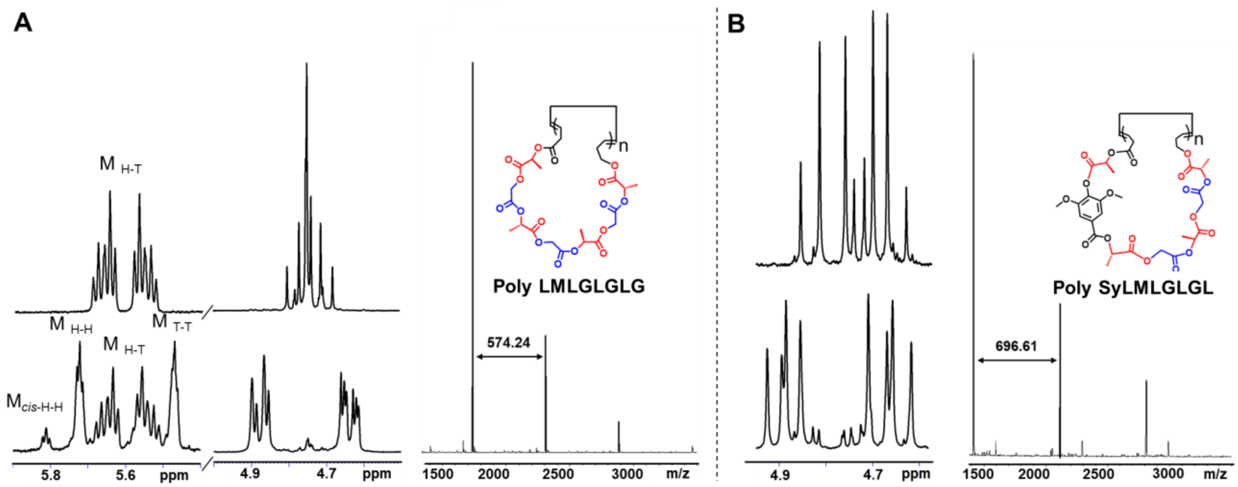

Figure 10. ^{1}H NMR spectroscopy and MALDI-TOF mass spectrometry characterization of sequence fidelity. (A)^{1}H NMR spectra of olefin and methylene resonances of *trans*-LMLGLGLG (top) and Poly LMLGLGLG (bottom), displaying head-tail olefin resonances, and MALDI-TOF spectrum of low molecular weight cyclic Poly LMLGLGLG. (B) ^{1}H NMR methylene resonances of *trans*-SyLMLGLGL (top) and Poly SyLMLGLGL (bottom); and MALDI-TOF spectrum of low molecular weight cyclic Poly SyLMLGLGL. Reproduced with permission from the American Chemical Society.

The palindromic MCOs provided the simplest spectra. Pairs of doublets in which *cis*- and *trans*-olefin composition can be monitored allowed us to monitor RCM conformational selectivity and polymerization kinetics. The unsymmetric MCOs obtained via macrolactonization displayed more complex methylene resonances, yet ring-opened chains could still be fully distinguished from monomer (Figure 10).

In addition to NMR spectroscopy as a sequence characterization tool, we have previously demonstrated the power of MALDI-TOF mass spectrometry to characterize the fidelity of sequenced polyesters, even in cases where only the most volatile shorter chains in the distribution are observed.[140] In the currently reported ED-ROMP copolymers, a similar analysis consists primarily of chains whose molecular weights are multiples of the MCO masses. Peaks for sequence errors that either add, omit or substitute monomers within repeat units are weak or not observed.

2.3.7 Synthesis of N-Carboxyanhydride-Containing Macrocycles

The development of synthetic methods to prepare molecular weight- and sequence-controlled polymers with reaction handles that impart minimal property effects on the resulting copolymers is a non-trivial problem in the field of polymer chemistry.[112] Some of the most notable examples in the literature that demonstrate exceptional polymerization control incorporate bulky, property-dominating linker groups.[16, 135, 141] While our ED-ROMP methodology requires the use of a conformationally-flexible metathesis linker, whose property effects can be counteracted with the addition of other monomers (see section 2.2.3), we still aimed to reduce the linker-incorporation when preparing sequenced polyesters while still maintaining molecular weight control through a chain-growth mechanism.

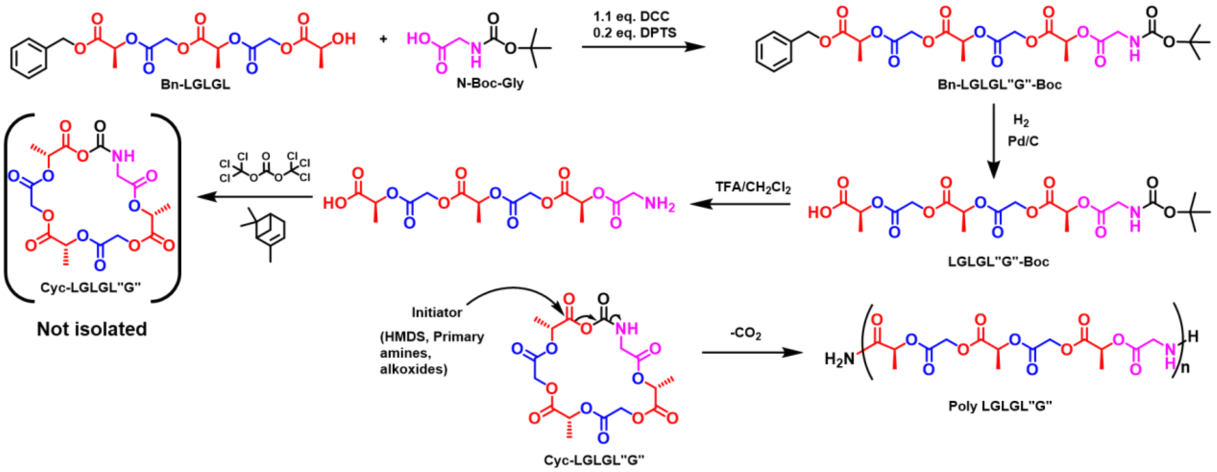
Bn-LGLGL
N-Boc-Gly
1.1 eq. DCC
0.2 eq. DPTS
Bn-LGLGL"G"-Boc
H2
Pd/C
TFA/CH2Cl2
LGLGL"G"-Boc
Cyc-LGLGL"G"
Not isolated
Initiator
(HMDS, Primary amines, alkoxides)
-CO2
Poly LGLGL"G"

Scheme 6. Intended preparation of Poly LGLGL“G” from an N-carboxyanhydride-containing macrocycle.

A reactive functional group, which is used to prepare well-defined polypeptides, is the N-carboxyanhydride (NCA) functionality that is prepared from the coupling of a carboxylic acid and primary amine facilitated with phosgene derivatives. The resulting cycle, traditionally a 5-membered ring, can be ring-opened using appropriate initiators to produce monodisperse polypeptides, driven by the loss of CO_2 (g).[142-145] We sought to imbed an NCA reaction handle into a sequenced MCO by first coupling commercially-available N-Boc-glycine (**N-Boc-"G"**) to **Bn-LGLGL**, followed by a traditional NCA ring-closing reaction with triphosgene (Scheme 6). **Bn-LGLGL"G"-Boc** was prepared in good yield, followed by Bn hydrogenolysis (H_2 (g), Pd/C) and Boc-deprotection (TFA/CH_2Cl_2). Repeated attempts to ring-close the open-chain species **LGLGL"G"** with triphosgene in the presence of proton-scavenger α-pinene or triethylamine resulted in the formation of a new species as evidenced by TLC, which may have been the targeted product. Unfortunately, this species proved unstable, decomposing before isolation.

The repeated inability to isolate pure product in the ring-closing reaction, coupled with the fact that traditional NCAs require rigorous pre-polymerization purification steps that severely limit scalability,[146, 147] led us to no longer pursue this polymerization method. However, ongoing developments in facile NCA synthesis with truncated work-up procedures provide hope for a similar method to be used for the purposes of sequence control in the future.[146]

2.3.8 Entropy-Driven Ring-Opening Transesterification Polymerization

The entropy-driven ring-opening polymerization of large lactones has been achieved previously through enzymatic polymerizations, organocatalyzed polymerizations, and transition-metal catalyzed transesterification reactions, and we sought to polymerize sequenced macrolactones to obtain an alternating copolymer with molecular weight control. This method would not only produce pure PLGAs but would benefit from even greater scalability. The successful execution of polymerization mechanism requires the delicate balance of inducing enough transesterification to open the unstrained rings while minimizing transesterification within the newly-formed polymer chains.

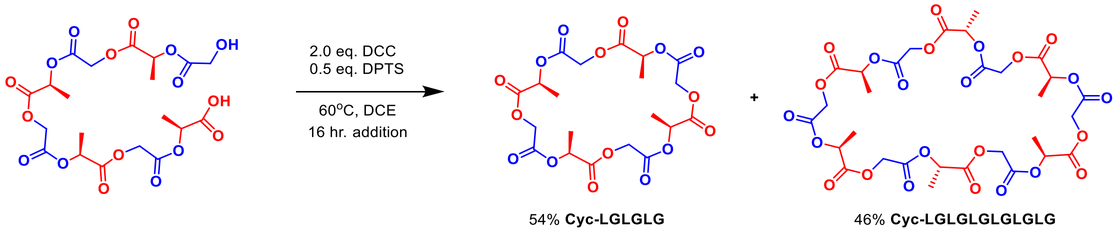

Scheme 7. Macrolactonization of open-chain LGLGLG segmer leading to ring-closed species.

Our synthesis employed with the standard ester coupling techniques described previously to produce the alternating open-chain hexamer **LGLGLG**. Using the identical macrolactonization conditions as described above resulted in a nearly 50:50 mixture of **Cyc-LGLGLG** and its corresponding dimer (a dodecamer) **Cyc-LGLGLGLGLGLG** (Scheme 7). Surprisingly, the two major products were, to an extent, separated by column chromatography (Figure 11) and multiple polymerization techniques were investigated on both MCOs.

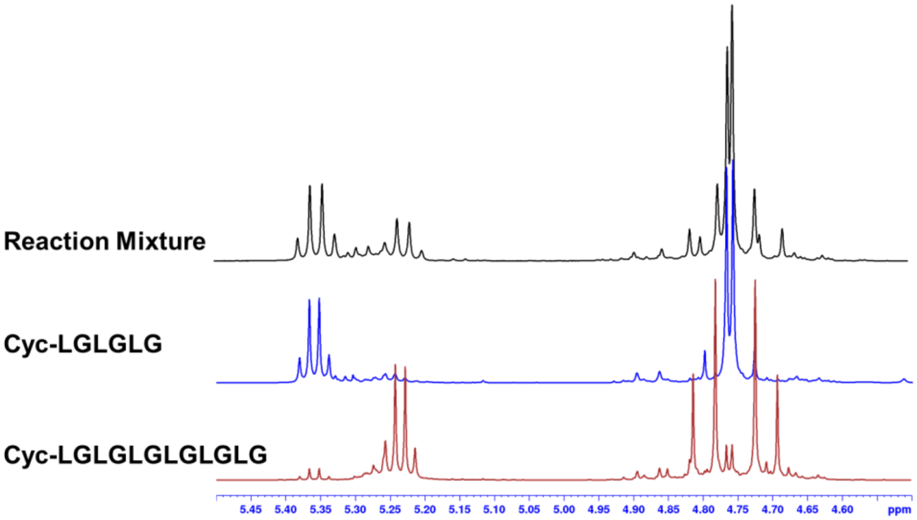

Figure 11. ^{1}H NMR spectra overlay of macrolactonization product reaction mixture and the corresponding hexamer and dodecamer.

Polymerization of these large MCOs via ring-opening transesterification polymerization (ROTEP) proved challenging, with molecular weights generally plateauing at 4 kDa and broad molecular weight distributions (≥ 2.0). The polymerizations were attempted both in bulk and in solution with a range of commonly used ROTEP catalysts (0.001 – 1.00 mol%) including stannous octanoate,[148] aluminum isopropoxide,[50] dibutyl magnesium,[149] titanium isopropoxide,[150] a thiourea moiety,[151] and candida antarctica lipase B.[152] The use of a primary alcohol initiator (0.003 – 3.00 mol% pyrene butanol, butanol, or lauryl alcohol) was investigated and resulted in no additional control over molecular weights.

Bulk reaction progress using catalytic stannous octanoate and lauryl alcohol initiator at 140 °C was monitored by ^{1}H NMR spectroscopy and indicated immediate loss of L:G alternation due to transesterification (Figure 12). Though linkage selectivity in the newly-forming polymer chains was expected to be minimal, the spectra indicated further sequence scrambling, exceeding the 1-in-6 or 1-in-12 random linkages expected for each MCO. The dodecamer MCO, however, retained more alternating character and polymerized more slowly than the 6-mer, most probably due to the lowered gain in translational entropy as the rings open to form polymer. Sequence retention of both monomers worsened at higher monomer conversions, again indicative of an increased rate of interchain transesterification.[149] Interestingly, Hillmyer and coworkers very recently attempted this technique to polymerize MCOs containing four ester units in an alternating sequence. Although molecular weights were moderately controlled and exceeded 50 kDa in some instances with a titanium isopropoxide catalyst, the alternating sequences were not retained during the polymerization.[153]

In our system, the lack of thermodynamic driving force for these reactions paired with the loss of sequence fidelity at moderate MCO conversion makes this polymerization method, as it currently stands, incapable of producing sequence- and molecular weight-controlled polymers with known ROTEP catalysts. Undoubtedly, the use of more sophisticated catalytic systems may increase sequence retention and promote chain propagation over chain transfer reactions,[52, 54, 55, [148, 154, 155] but these limitations led us to study sequence effects by preparing copolymers with our established ED-ROMP methodology.

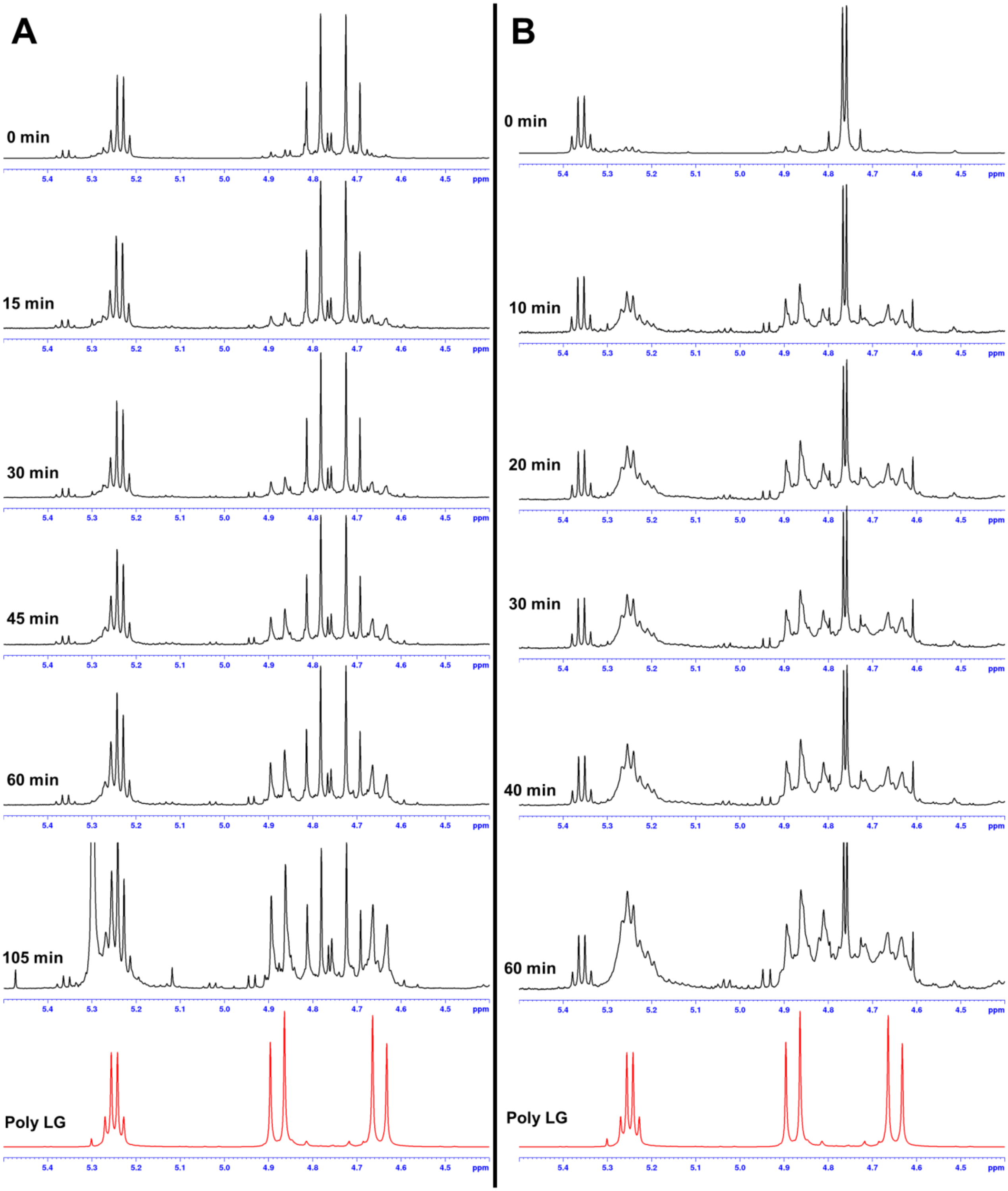

Figure 12. ^{1}**H NMR spectral overlays of polymerization timepoints for (A) Cyc-LGLGLGLGLGLG and (B) Cyc-LGLGLG using catalytic stannous octanoate, with perfectly alternating Poly LG for reference.**

2.4 Conclusion

We have successfully designed a general, modular, and scalable synthetic method for the preparation of copolymers in which sequence is imbedded into a large macrocycle which is then polymerized using ED-ROMP. SEED-ROMP, which exploits a more reactive *cis*-olefin metathesis handle, enhanced the living character of the polymerization, improving molecular weight control, decreasing dispersity, and facilitating the preparation of block copolymers.

We have also established that ring-closing via macrolactonization can be carried out at higher concentrations and less expensively than RCM-based ring-closure in the preparation of the cyclic MCOs. Moreover, the precursor oligomers required for this method do not require an additional linker group (**Eg**) in their construction, meaning that the final polymers more closely resemble the ideal structure for a poly(α-hydroxy acid) and monomers may be incorporated into these polymers specifically to tailor properties. Ideally, linker-free methods may be used to prepare sequence- and molecular weight-controlled polyesters, but these syntheses remain a challenge.

The development of sequence-controlled polymer syntheses is an ongoing effort, in which homogeneity across samples in molecular weight and dispersity is critical to study bulk property relationships. The current approach utilizing ED-ROMP has expanded both the range of materials that can be prepared and our ability to control their characteristics. It seems likely, moreover, that this general approach will be applicable to polymers other than poly(α-hydroxy acid)s; all that is required is that target sequence be incorporated into an MCO with a metathesis-active olefin. With such methods it should be possible to better target sequenced materials for future applications.

2.5 Experimental Section

2.5.1 General Information

All experiments were carried out in oven-dried glassware under an atmosphere of N_2 using standard Schlenk line techniques. N,N’-dicyclohexylcarbodiimide (DCC) was purchased from Oakwood Chemical and used without further purification. 10% Pd/C was purchased from Alfa Aesar. Palladium, 10wt% (dry basis) on activated carbon was purchased from Sigma Aldrich. Ethylene glycol (Eg) was purchased from Mallinckrodt and used as is. Methylene chloride (CH_2Cl_2, Fisher) and ethyl acetate (EtOAc, Sigma Aldrich) were purified by a Solvent Dispensing System by J. C. Meyer. Both were passed over two columns of neutral alumina. Anhydrous, inhibitor-free tetrahydrofuran (THF) and Grubb’s 2nd generation catalyst were purchased from Sigma Aldrich. Column chromatography was performed using Sorbent Technologies 60 Å, 40-63 µm standard grade silica.

^1H (300, 400, 600, and 700 MHz) and ^{13}C were obtained using Bruker spectrometers and are reported as δ values in ppm relative to the reported solvent ($CDCl_3$ referenced to 7.26). Splitting patterns are abbreviated as follows: singlet (s), doublet (d), triplet (t), quartet (q), multiplet (m), broad (br), and combinations thereof. HRMS data were obtained on a LC/Q-TOF instrument. Molecular weights and dispersities were obtained on a Waters GPC (THF) with Jordi 500, 1000, and 10000 Å divinyl benzene columns, and refractive index detector (Waters) was calibrated to polystyrene standards.

2.5.2 Experimental Procedures

It should be noted that characterization data in this section is represented in two different formats, a traditional paragraph style which is the style favored for printed journals and a more easily read chart format that has been adopted by the Meyer group for data that is not subject to the constraints of printing, such as those that appear in supporting information.

SEED-ROMP Fast Catalyst Initiation Experiments (G2 vs. G3)

The *cis*-macromonomer was added to two separate vial charged with a stir bar and pumped into a nitrogen filled glove box. An appropriate amount of dry CH_2Cl_2 (0.7M with respect to monomer final volume) was added to dissolve the monomer. Solutions of Grubbs' 2nd generation catalyst (G2) and Grubbs 3rd generation catalyst (G3) were prepared and added to monomer solution (1.25 cat. mol %) and allowed to stir for 10 min. Both polymerizations gelled after reaction for 2 min. After the 10 min reaction, the polymerizations were quenched with ethyl vinyl ether and allowed to stir for 5 min before concentrating *in vacuo*. Unpurified polymers were analyzed via SEC to determine molecular weights relative to polystyrene standards.

Ruthenium Removal and Inductively-Coupled Plasma- Optical Emission Spectroscopy (ICP-OES)

A 100 mg/mL solution of polymer was prepared in DCM, to which Quadrasil MP (1.0-1.5 mmol/g) was added in a 50:1 scavenger:Ru ratio. The solution was stirred overnight, filtered and concentrated. This process was repeated as necessary.

ICP-OES was performed under argon flow with a PerkinElmer Optima spectrometer. A 5% volume/volume nitric acid matrix was prepared by diluting pure nitric acid (Sigma, >99.999%) with 18.2 MΩ cm water, and all samples were digested in concentrated nitric acid. Ruthenium concentrations were determined by comparison to a seven-point calibration curve (0.10, 0.50, 1.0, 2.5, 5.0, 7.5, and 10 ppm Ru) prepared using a ruthenium standard (Inorganic Ventures). All samples were measured six times and averaged. A seven minute flush time with 5% nitric acid matrix was used between all runs, and a blank was sampled between each run.

Preparation of L-TBDPS.

To a stirring solution of Me-L-Si (37.8 g, 110 mmol) in THF (500 mL) at 0 ^{o}C was slowly added a solution of LiOH (18.5 g, 442 mmol) in H_2O (500 mL). Once the addition was complete, the solution was allowed to warm to rt and stirred for an additional 3 h. The reaction solution was concentrated to half volume, diluted with brine (100 mL) and extracted with Et_2O (3 × 200 mL). The aqueous layer was acidified to pH < 1 with 3 M HCl. The mixture was then extracted with Et_2O (5 × 100 mL), dried over $MgSO_4$, filtered, and concentrated *in vacuo* to provide the crude product as a colorless oil (32.0 g, 88%). ^{1}H NMR (400 MHz, $CDCl_3$) δ 7.68 (m, 4 H), 7.43 (m, 6 H), 4.35 (q, J = 6.8 Hz, 1 H), 1.34 (d, J = 7.2 Hz, 3 H), 1.12 (s, 9 H).

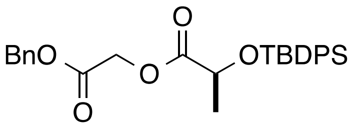

Preparation of Bn-GL-TBDPS.

To a stirring solution of Bn-G (17.8 g, 107 mmol) and L-TBDPS (32.0 g, 97.5 mmol) in CH_2Cl_2 (1000 mL) was added DPTS (5.74 g, 19.5 mmol). Once the DPTS had dissolved, DCC (22.1 g, 107 mmol) was added and the solution stirred overnight. The reaction mixture was then filtered, concentrated to approximately 250 mL, diluted with hexanes, and filtered again. This concentration and filtration cycle was repeated one additional time whereupon the solution was concentrated *in vacuo*. The crude material was purified by flash chromatography (SiO_2, 2.5-10%

EtOAc in hexanes) to provide the product as a colorless oil (46.5 g, 87%); ^{1}H NMR (500 MHz, $CDCl_3$) δ 7.67 (m, 4H), 7.44 (m, 11H), 5.8 (s, 2H), 4.61 (d, *J* = 16.0 Hz, 1H), 4.46 (d, *J* = 15.6 Hz, 1H), 4.39 (q, *J* = 6.8 Hz, 1H), 1.38 (d, *J* = 6.8 Hz, 3H), 1.07 (s, 9H).

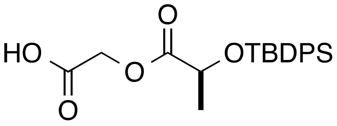

Preparation of GL-TBDPS.

To a stirring solution of **Bn-GL-TBDPS** (34.1 g, 71.4 mmol) in EtOAc (700 mL) under N_2 was added 10% Pd/C (3.41 g, 10% w/w). The reaction vessel was then purged twice with a H_2 balloon and allowed to stir overnight under 1 atm H_2. Once the reaction had completed, the vessel was evacuated and filled with N_2 and the mixture was filtered over celite and concentrated *in vacuo*. The crude material was purified by flash chromatography (SiO_2, 2.5-25% EtOAc in hexanes) to provide the product as a colorless liquid (27.6 g, 88%); ^{1}H NMR (400 MHz, CDCl3) δ 11.03 (br s, 1H), 7.68 (m, 4H), 7.46 (m, 6H), 4.62 (d, *J* = 16.4 Hz, 1H), 4.51 (d, *J* = 16.4 Hz, 1H), 4.42 (q, *J* = 6.8 Hz, 1H), 1.42 (d, *J* = 6.8 Hz, 3H), 1.10 (s, 9H); ^{13}C NMR (100 MHz, CDCl3) δ 173.03, 172.79, 135.89, 135.73, 133.39, 132.89, 129.84, 127.67, 127.61, 68.60, 59.98, 26.77, 21.23, 19.21; HRMS (ESI) [M-H]+ calc mass 385.14713, found 385.14768.

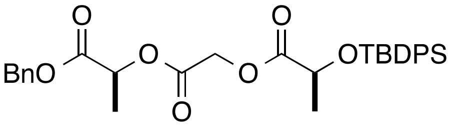

Preparation of Bn-LGL-TBDPS.

To a stirring solution of **Bn-L** (11.6 g, 64.2 mmol) and **GL-TBDPS** (22.6 g, 58.4 mmol), in CH_2Cl_2 (290 mL) was added DPTS (13.3 g, 64.2 mmol). Once the mixture became homogeneous, DCC (13.3 g, 64.2 mmol) was added and the reaction was allowed to stir overnight. The solution was filtered and the filtrate was concentrated *in vacuo*. The crude material was purified by flash chromatography (SiO_2, 2.5-25% EtOAc in hexanes) to provide the product as a colorless liquid (32.0 g, 93%); ^{1}H NMR (400 MHz, $CDCl_3$) δ 7.70 (m, 4H), 7.46 (m, 11H), 5.18 (q, *J* = 7.2 Hz, 1H), 5.18 (d, *J* = 14.0 Hz, 1H), 5.17 (d, *J* = 14.0 Hz, 1H), 4.70 (d, *J* = 16.0 Hz, 1H), 4.47 (d, *J* = 16.0 Hz, 1H), 4.41 (d, *J* = 6.8 Hz, 1H), 1.50 (d, *J* = 6.8 Hz, 3H), 1.44 (d, *J* = 6.8 Hz, 3H), 1.08 (s, 9H); ^{13}C NMR (100 MHz, $CDCl_3$) δ 173.15, 170.06, 167.01, 136.05, 135.88, 135.30, 133.57, 133.11, 129.97, 128.77, 128.60, 128.30, 127.81, 127.76, 69.43, 68.76, 67.32, 60.45, 26.94, 21.43, 19.37, 16.96; HRMS (ESI) $[M+NH_4]^+$ calc mass 566.2574, found 566.2578.

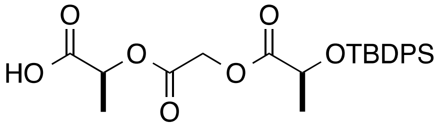

Preparation of LGL-TBDPS.

To a stirring solution of **Bn-LGL-TBDPS** (29.8 g, 54.2 mmol) in EtOAc (540 mL) under N_2 was added 10% Pd/C (10 % w/w, 5.42 g). The reaction vessel was evacuated and purged three times with a 1 atm H_2 balloon. The reaction was allowed to stir 1 day under 1 atm H_2. The vessel was placed under N_2, filtered over celite, and concentrated *in vacuo*. The crude material was purified by flash chromatography (SiO_2, 5-100% EtOAc in hexanes) to provide the product as a colorless liquid (25.0 g, 99%); ^{1}H NMR (400 MHz, CDCl3) δ 11.13 (br s, 1H), 7.66-7.64 (m, 4H), 7.43-7.32 (m, 6H), 5.16 (q, *J* = 7.2 Hz, 1H), 4.65 (d, *J* = 16 Hz, 1H), 4.42 (d, *J* = 16 Hz, 1H), 4.36 (q, *J* = 6.8 Hz, 1H), 1.50 (d, *J* = 7.2 Hz, 3H), 1.40 (d, *J* = 6.8 Hz, 3H), 1.07 (s, 9H); ^{13}C NMR (100 MHz, CDCl3) δ 174.96, 173.08, 166.82, 135.89, 135.72, 133.38, 132.93, 129.82, 127.65, 127.60, 68.70, 68.59, 60.23, 26.77, 21.26, 19.20, 16.67; HRMS (ESI) [M+H]+ calc mass 457.16771, found 457.16838.

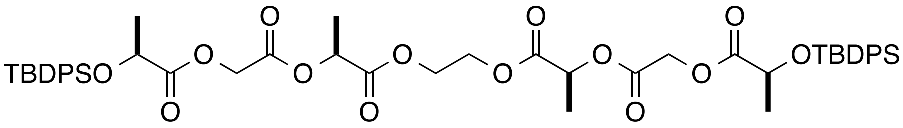

Preparation of Eg-(LGL-Si)$_2$.

To a stirring solution of ethylene glycol (1.84 mL, 32.5) and **LGL-Si** (24.9 g, 54.2) in CH_2Cl_2 (120 mL) was added DPTS (1.43 g, 4.85 mmol). Once the mixture became homogeneous, DCC (5.45 g, 26.4 mmol) was added and the reaction was allowed to stir overnight. The solution was filtered and the filtrate was concentrated *in vacuo*. The crude material was purified by flash chromatography (SiO_2, 7.5-20% EtOAc in hexanes) to provide the product as a colorless liquid (11.3 g, 98.3%); ^{1}H NMR (400 MHz, $CDCl_3$) δ 7.68 (m, 8H), 7.46-7.34 (m, 12H), 5.17 (q, *J* = 6.8 Hz, 2H), 4.68 (d, *J* = 16.0 Hz, 2H), 4.46 (d, *J* =15.6 Hz, 2H), 4.40 (q, *J* = 6.8 Hz, 2H), 4.34 (m, 4H), 1.48 (d, *J* = 7.2 Hz, 6H), 1.40 (d, *J* = 6.8 Hz, 6H), 1.07 (s, 18H); 13C NMR (100 MHz, CDCl3) δ 172.98, 169.75, 166.82, 135.88, 135.71, 133.38, 132.95, 129.81, 127.65, 127.59, 69.09, 68.58, 62.69, 60.24, 26.77, 21.26, 19.20, 16.70; HRMS (ESI) [M+NH4]+ calc mass 960.4022, found 960.4017.

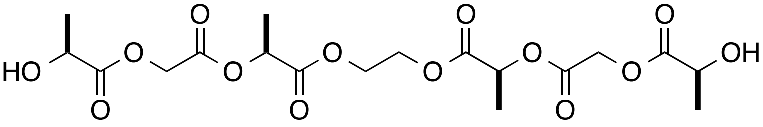

Preparation of Eg-(LGL)$_2$.

To a stirring solution of **Eg-(LGL-TBDPS)₂** (3.16 g, 3.33 mmol) in THF (83 mL) at 0 °C under N_2 was slowly added acetic acid (3.0 mL, 53 mmol) and then TBAF (1.0 M in THF, 10.0 mL). The reaction was stirred at 0 °C overnight, then the ice bath was removed and stirring continued at rt for an additional day. After cooling the reaction mixture to 0 °C, brine (150 mL) was added. The resulting aqueous layer was extracted with CH2Cl2 (3 × 150 mL), the combined organic layers were washed with aqueous saturated sodium bicarbonate solution (150 mL), dried over $MgSO_4$ and then concentrated *in vacuo*. The concentrate was then chromatographed over silica using 25-75% EtOAc in hexanes as the eluent to provide the product as a white solid (1.55 g, quantitative). *Note: although this particular experiment was the highest yielding of all attempts, the conditions described above did not lead to consistent reaction outcomes. An optimized procedure is also included here with a typical yield.* To a stirring solution of **Eg-(LGL-TBDPS)₂** (0.114 g, 0.12 mmol) in THF at 0 °C was added AcOH (55 μL, 0.97 mmol) that had been pre-dried over 3 Å molecular sieves prior to use. TBAF (1.0 M in THF, 363 μL, 0.36 mmol) was added dropwise and the resulting solution was stirred at rt 4 h. The solution was then cooled to 0 °C, diluted with EtOAc (5 mL) and pH 7.4 buffer (5 mL) was added. The aqueous layer was extracted with EtOAc (3 × 5 mL), the combined organic layers were dried over Na_2SO_4, filtered, and concentrated *in vacuo* to give the crude product as a faintly yellow oil. The residue was purified by chromatography on SiO_2 (35−100% EtOAc in hexanes) to provide the product as a colorless liquid (89%; R_f = 0.10, 50% EtOAc in hexanes); 1H NMR (500 MHz, CDCl3) δ 5.22 (q, *J* = 7.0 Hz, 2H), 4.85 (d, *J* = 16.0 Hz, 2H), 4.76 (d, *J* = 16.0 Hz, 2H), 4.44 (m, 6H), 2.89 (s, 1H), 2.88 (s, 1H), 1.54 (d, *J* = 7.0 Hz, 6H), 1.50 (d, *J* = 6.8 Hz, 6H); 13C NMR (125 MHz, CDCl3) δ 175.01, 169.89, 166.90, 69.58, 66.91, 62.96, 61.02, 20.40, 16.87; HRMS (ESI) [M+NH4]+calc mass 484.1666, found 484.1627.

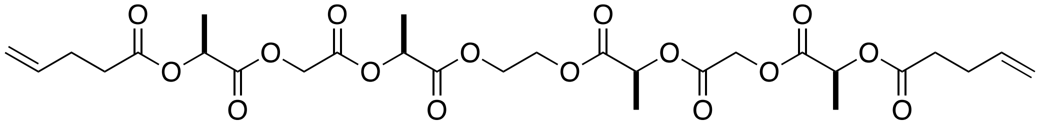

Preparation of Eg-(LGLM)$_2$.

To a stirring solution of **Eg-(LGL)$_2$** (0.980 g, 2.10 mmol), 3-butenoic acid (0.47 mL, 4.62 mmol) in CH_2Cl_2 (42 mL) was added DPTS (0.247 g, 0.840 mmol). Once the mixture became homogeneous, DCC (0.954 g, 4.62 mmol) was added and the reaction was allowed to stir overnight. The reaction was concentrated to half volume and then filtered. The filtrate was washed with 1 M HCl (10 mL), and washed with saturated aqueous $NaHCO_3$ (10 mL). The aqueous layer was then extracted with CH_2Cl_2 (10 mL), the organic layers were combined, washed with brine (15 mL), dried over Na_2SO_4, and concentrated *in vacuo*. The crude material was purified by flash chromatography (SiO_2, 15-20% EtOAc in hexanes) to provide the product as a colorless liquid (1.13 g, 86%); ^{1}H NMR (400 MHz, CDCl3) δ 5.89 (ddt, *J* = 16.8, 10.4, 6.4 Hz, 2H), 5.200 (q, *J* = 7.2 Hz, 2H), 5.197 (q, *J* = 7.2 Hz, 2H), 5.09 (dd, *J* = 16.8, 1.2 Hz, 2H), 5.02 (dd, *J* = 10.4, 1.2 Hz, 2H), 4.89 (d, *J* = 16.0 Hz, 2H), 4.65 (d, *J* = 16.0 Hz, 2H), 4.41 (m, 4H), 2.56 (m, 4H), 2.44 (m, 4H), 1.57 (d, J = 7.2 Hz, 6H), 1.53 (d, *J* = 7.2 Hz, 6H); ^{13}C NMR (100 MHz, CDCl3) δ 172.51, 170.39, 169.87, 166.77, 136.55, 115.78, 69.40, 68.32, 62.90, 60.82, 33.23, 28.78, 17.00, 16.87; HRMS (ESI) [M+H]$^+$ calc mass 631.22326, found 631.2225. $^{156\ 156\ 156\ 156\ 156\ 197\ 196\ 196\ 196\ 164\ 164\ 164}$

164 164 1 1 1

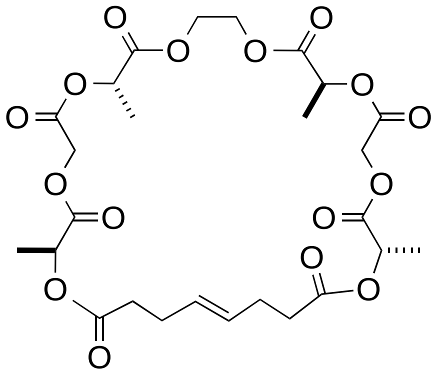

Preparation of *trans-cyclic*-Eg-(LGLM)$_2$.

To a stirring solution of **Eg-(LGLM)$_2$** (17 mg, 27 μmol) in CH_2Cl_2 (27 μL) was added a solution of catalyst **G2** (2.3 mg, 2.7 μmol) in CH_2Cl_2 (1 mL). The resulting solution was stirred for 18 h before being quenched through the addition of ethyl vinyl ether (0.2 mL). Once concentrated, the crude oil was purified by chromatography on SiO_2 (10–20% EtOAc in hexanes) to afford ***trans-cyclic*-Eg-(LGLM)$_2$** (17 mg, 93% yield, 84% *trans*) as a colorless oil. ^{1}H NMR (500 MHz, $CDCl_3$) δ 5.54 (m, *trans*) and 5.41 (m, *cis*) (2H), 5.23 (m, 4H), 4.83 (d, *J* = 16 Hz, 2H), 4.72 (d, *J* = 16 Hz, 2H), 4.41 (m, 4H), 2.47 (m, 4H), 2.36 (m, 4H), 1.55 (d, *J* = 7.0 Hz, 6H), 1.53 (d, *J* = 7.0 Hz); ^{13}C NMR (125 MHz, $CDCl_3$) δ 172.37, 170.35, 169.92, 166.77, 129.49 (*trans*), 129.14 (*cis*), 69.51, 68.26, 62.87, 60.94, 33.79, 27.72, 17.02, 16.85; HRMS (ESI) $[M+H]^+$ calc mass 603.19251, found 603.19028.

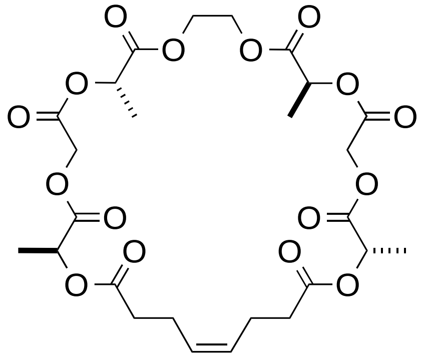

Preparation of *cis-cyclic*-Eg-(LGLM)$_2$.

In the glovebox, a solution of ruthenium catalyst **GN** (69 mg, 0.1094 mmol) in DCE (20 mL) was added to a stirring solution of **Eg-(LGLM)$_2$** (690 mg, 1.094 mmol) in DCE (200 mL). The vessel was immediately removed from the glovebox and stirred at 60 °C under a constant low vacuum (photo of apparatus follows protocol). After 26 h of stirring, the reaction solution was cooled to rt, ethyl vinyl ether (2 mL) was added, and the solution was stirred for an additional 30 min before being concentrated. The crude product was purified by chromatography on SiO$_2$ (10–25% EtOAc in hexanes) to afford ***cis-cyclic*-Eg-(LGLM)$_2$** (0.578 g, 88% yield, 95 % BRSM, 12:88 *E:Z*) as a colorless oil; ^{1}H NMR (500 MHz, CDCl$_3$) δ 5.51 (m, *trans*) and 5.43 (m, *cis*)(2H), 5.23 (m, 4H), 4.83 (d, *J* = 16.0 Hz, 2H, *trans*), 4.81 (d, *J* = 16.0 Hz, 2H, *cis*), 4.40 (m, 4 H), 2.48 (m, 8H), 1.55 (d, *J* = 7.0 Hz, 6H), 1.53 (d, *J* = 7.0 Hz, 6H); ^{13}C NMR (125 MHz, CDCl$_3$) δ 172.44, 170.32, 169.92, 166.77, 129.47 (*trans*), 129.12 (*cis*), 69.52, 68.34, 62.81, 60.96, 33.96, 22.91, 16.94, 16.80; HRMS (ESI) calc. mass 603.1920, found 603.1940.

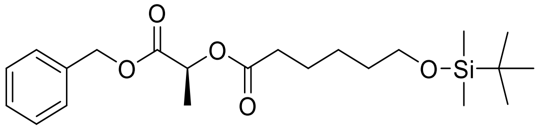

Bn-LC-SiR$_3$.

To a stirring solution of **Bn-L** (6.46 g, 35.8 mmol, 1.1 equiv) and **C-SiR$_3$** (7.72 g, 31.3 mmol, 1 equiv) in CH$_2$Cl$_2$ (325 mL) was added DPTS (1.86 g, 6.32 mmol, 0.2 equiv). Once the mixture became homogeneous, DCC (7.13 g, 34.5 mmol, 1.1 equiv) was added and the reaction was allowed to stir overnight. The solution was filtered and the filtrate was concentrated *in vacuo*. The crude material was purified by flash chromatography (SiO$_2$, 2.5% EtOAc in hexanes) to provide the product as a colorless liquid (12.80 g, 96%). ^{1}H NMR (300 MHz, CDCl$_3$) δ 7.37-7.28

(m, 5H), 5.18 (d, J = 12.3 Hz, 1H), 5.12 (d, J = 12.3 Hz, 1H), 5.12 (q, J = 7.0 Hz, 1H), 3.57 (t, J = 6.3 Hz, 2H), 2.36 (dt, J1 = 15.6 Hz, J2 = 7.8 Hz, 1H), 2.35 (dt, J1 = 15.6 Hz, J2 = 7.4 Hz, 1H), 1.68-1.58 (m, 2H), 1.53-1.46 (m, 2H), 1.47 (d, J = 7.0 Hz, 3H), 1.39-1.29 (m, 2H), 0.87 (s, 9H), 0.02 (s, 6H); ^{13}C NMR (75 MHz, $CDCl_3$) δ 173.04, 170.72, 135.35, 128.56, 128.35, 128.10, 68.38, 66.91, 62.92, 33.94, 32.42, 25.94, 25.33, 24.61, 18.32, 16.89, -5.31; HRMS (M+Na) calc mass 431.2230, found 431.2240.

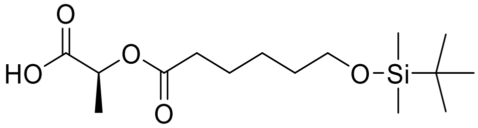

LC-SiR$_3$

Bn-LC-SiR$_3$ (8.74 g, 21.4 mmol) and 10% Pd/C (0.44 g, 5% w/w) were added to a stirring solution of EtOAc (215 mL, 0.1 M in substrate) under N_2. The reaction vessel was then purged twice with a H_2 balloon and allowed to stir overnight under 1 atm H_2. Once the reaction had completed, the vessel was evacuated and filled with N_2 and the mixture was filtered over celite and concentrated *in vacuo*. The crude material was purified by flash chromatography (SiO_2, 2.5% EtOAc in hexanes) to provide the product as a colorless liquid (6.20 g, 91.1%). ^{1}H NMR (300 MHz, $CDCl_3$) δ 9.57 (br s, 1H), 5.08 (q, J = 7.1 Hz, 1H), 3.58 (t, J = 6.5 Hz, 2H), 2.37 (dt, J1 = 15.6 Hz, J2 = 7.7 Hz, 1H), 2.36 (dt, J1 = 15.9 Hz, J2 = 7.5 Hz, 1H), 1.70-1.60 (m, 2H), 1.56- 1.47 (m, 2H), 1.50 (d, J = 7.1 Hz, 3H), 1.40-1.33 (m, 2H), 0.90 (s, 9H), 0.06 (s, 6H); ^{13}C NMR (75 MHz, $CDCl_3$) δ 176.30, 173.09, 67.90, 63.00, 33.86, 32.40, 25.94, 25.31, 24.56, 18.34, 16.80, -5.30; HRMS (M+Na) calc mass 341.1760, found 341.1745.

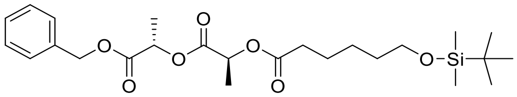

Bn-LLC-SiR₃.

To a stirring solution of **Bn-L** (2.92 g, 16.2 mmol, 1.1 equiv) and **LC-SiR₃** (4.66 g, 14.6 mmol, equiv) in CH_2Cl_2 (150 mL) was added DPTS (0.87 g, 2.94 mmol, 0.2 equiv). Once the mixture became homogeneous, DCC (3.18 g, 15.4 mmol, 1.1 equiv) was added and the reaction was allowed to stir overnight. The solution was filtered and the filtrate was concentrated *in vacuo*. The crude material was purified by flash chromatography (SiO_2, 5% EtOAc in hexanes) to provide the product as a colorless liquid (6.54 g, 93%). ^{1}H NMR (300 MHz, $CDCl_3$) δ 7.38-7.28 (m, 5H), 5.18 (q, J = 7.1 Hz, 1H), 5.17 (d, J = 12.3 Hz, 1H), 5.11 (d, *J* = 12.0 Hz, 1H), 5.07 (q, J = 7 Hz, 1H), 3.58 (t, J = 6.5 Hz, 2H), 2.37 (dt, J1 = 15.6 Hz, J2 = 7.7 Hz, 1H), 2.36 (dt, J1 = 15.9 Hz, J2 = 7.5 Hz, 1H), 1.69-1.59 (m, 2H), 1.55-1.46 (m, 2H), 1.51 (d, J = 7.2 Hz, 3H), 1.47 (d, J = 7.2 Hz, 3H), 1.40-1.30 (m, 2H), 0.86 (s, 9H), 0.02 (s, 6H); ^{13}C NMR (75 MHz, $CDCl_3$) δ 173.12, 170.33, 170.09, 135.10, 128.59, 128.46, 128.22, 69.03, 68.12, 67.13, 62.93, 33.85, 32.42, 25.94, 25.31, 24.57, 18.32, 16.78, 16.69, -5.31; HRMS (M+Na) calc mass 503.2441, found 503.2395.

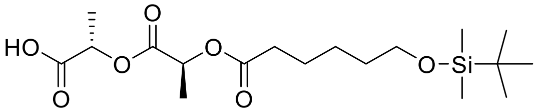

LLC-SiR₃

Bn-LLC-SiR₃ (6.35 g, 13.2 mmol) was combined with 10% Pd/C (0.31 g, 5 % w/w) in EtOAc (135 mL, 0.1 M in substrate) and stirred under N_2. The reaction vessel was evacuated and purged twice with a 1 atm H_2 balloon. The reaction was allowed to stir overnight under 1 atm H_2. The vessel was placed under N_2, filtered over celite, and concentrated *in vacuo*. The concentrate was chromatographed over silica using 10% EtOAc in hexanes as the eluent. The product was a

colorless liquid (4.22 g, 81.8%). ^{1}H NMR (400 MHz, $CDCl_3$) δ 9.59 (br s, 1H), 5.17 (q, J = 7.1 Hz, 1H), 5.09 (q, J = 7.2 Hz, 1H), 3.59 (t, J = 6.4 Hz, 2H), 2.38 (dt, J1 = 15.6 Hz, J2 = 7.6 Hz, 1H), 2.37 (dt, J1 = 15.6 Hz, J2 = 7.4 Hz, 1H), 1.68-1.61 (m, 2H), 1.55-1.47 (m, 2H), 1.54 (d, J = 7.2 Hz, 3H), 1.52 (d, J = 7.2 Hz, 3H), 1.40 (m, 2H), 0.86 (s, 9H), 0.02 (s, 6H); ^{13}C NMR (100 MHz, $CDCl_3$) δ 175.27, 173.21, 170.26, 68.57, 68.15, 63.03, 33.85, 32.36, 25.95, 25.31, 24.58, 18.34, 16.70, 16.68, -.531; HRMS (M-H$^+$) calc mass 389.1996, found 389.2010.

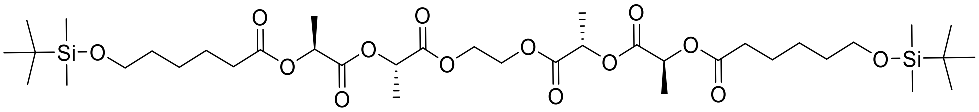

Eg-(LLC-SiR$_3$)$_2$

To a stirring solution of ethylene glycol (0.26 g, 4.15 mmol, 1 equiv) and **LLC-SiR$_3$** (3.96 g, 10.2 mmol, 2.1 equiv) in CH_2Cl_2 (42 mL) was added DPTS (0.24 g, 0.82 mmol, 0.2 equiv). Once the mixture became homogeneous, DCC (1.77 g, 8.57 mmol, 2.1 equiv) was added and the reaction was allowed to stir overnight. The solution was filtered and the filtrate was concentrated *in vacuo*. The crude material was purified by flash chromatography (SiO_2, 10% EtOAc in hexanes) to provide the product as a colorless liquid (2.74 g, 81.8%). ^{1}H NMR (300 MHz, $CDCl_3$) δ 5.13 (q, J = 7.2 Hz, 2H), 5.08 (q, J = 7.2 Hz, 2H), 4.38-4.27 (m, 4H), 3.58 (t, J = 6.5 Hz, 4H), 2.37 (dt, J1 = 15.9 Hz, J2 = 7.8 Hz, 2H), 2.36 (dt, J1 = 15.6 Hz, J2 = 7.5 Hz, 2H), 1.69-1.59 (m, 4H), 1.56-1.40 (m, 4H), 1.53 (d, J = 7.2 Hz, 6H), 1.50 (d, J = 7.2 Hz, 6H), 1.39-1.29 (m 4H), 0.86 (s, 18H), 0.02 (s, 12H); ^{13}C NMR (75 MHz, $CDCl_3$) δ 173.08, 170.27, 169.97, 68.87, 68.10, 62.94, 62.69, 33.88, 32.44, 25.96, 25.36, 24.60, 18.33, 16.75, 16.72, -5.30; HRMS (M+NH4$^+$) calc mass 824.4648, found 824.4626.

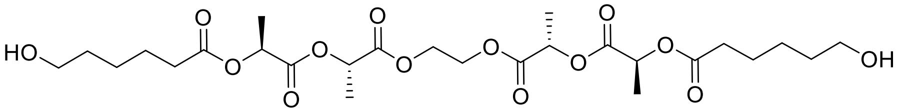

Eg-(LLC)$_2$

To a stirring solution of **Eg-(LLC-SiR$_3$)$_2$** (1.48 g, 1.83 mmol, 1 equiv.) in THF (37 mL) under N_2 was slowly added acetic acid (1.7 mL, 29.3 mmol, 16 equiv) and then tetrabutylammonium fluoride (1.0 M in THF, 5.5 mL, 5.5 mmol at rt. The reaction mixture was poured into brine (50 mL). The resulting aqueous layer was extracted with CH_2Cl_2 (3 x 50 mL), the combined organic layers were washed with aqueous saturated sodium bicarbonate solution (75 mL), dried over $MgSO_4$ and then concentrated *in vacuo*. The concentrate was then chromatographed over silica using 50-60% EtOAc in hexanes as the eluent to provide the product as a colorless liquid (0.90 g, 84.5%). ^{1}H NMR (400 MHz, $CDCl_3$) δ 5.13 (q, J = 7.1 Hz, 2H), 5.08 (q, J = 7.1 Hz, 2H), 4.35-4.28 (m, 4H), 3.61 (t, J = 6.4 Hz, 4H), 2.39 (dt, J1 = 16.0 Hz, J2 = 7.6 Hz, 2H), 2.37 (dt, J1 = 15.6 Hz, J2 = 7.4 Hz, 2H), 1.70-1.62 (m, 4H), 1.59-1.47 (m, 6H),1.52 (d, J = 7.2 Hz, 6H), 1.50 (d, J = 7.2 Hz, 6H), 1.44-1.36 (m, 4H); ^{13}C NMR (100 MHz, $CDCl_3$) δ 173.07, 170.30, 169.95, 68.91, 68.13, 62.66, 62.49, 33.75, 32.21, 25.04, 24.43, 16.71, 16.69; HRMS (M+H+) calc mass 579.2653, found 579.2643.

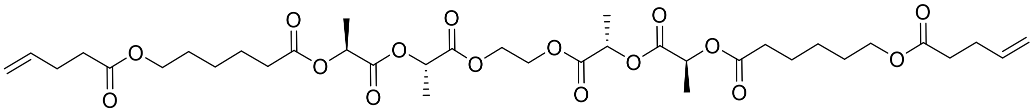

Eg-(LLCM)$_2$

To a stirring solution of **Eg-(LLC)$_2$** (0.65 g, 1.12 mmol, 1 equiv) and 4-pentenoic acid (0.25 mL, 2.45 mmol, 2.2 equiv) in CH_2Cl_2 (23 mL) was added DPTS (0.13 g, 0.45 mmol, 0.4 equiv). Once the mixture became homogeneous, DCC (0.51 g, 2.47 mmol, 2.2 equiv) was added and the reaction was allowed to stir overnight. The reaction was filtered to remove the urea byproduct, the filtrate was diluted with CH_2Cl_2 (25 mL) and washed with sat. $NaHCO_3$ (50 mL). The aqueous layer was then extracted with CH_2Cl_2 (2 × 50 mL), the organic layers were combined, dried over $MgSO_4$, and concentrated *in vacuo*. The crude material was purified by flash chromatography (SiO_2, 15-17.5% EtOAc in hexanes) to provide the product as a colorless liquid (0.77 g, 92.9%). ^1H NMR (400 MHz, $CDCl_3$) δ 5.84-5.74 (m, 2H), 5.13 (q, J = 7.1 Hz, 2H), 5.08 (q, J = 7.2 Hz, 2H), 5.05-5.00 (m, 2H), 4.99-4.96 (m, 2H), 4.36-4.27 (m, 4H), 2.43- 2.31 (m, 12H), 1.69-1.58 (m, 4H), 1.52 (d, J = 7.2 Hz, 6H), 1.50 (d, J = 7.2 Hz, 6H), 1.42-1.34 (m, 4H); ^{13}C-NMR(100 MHz, $CDCl_3$) δ 173.04, 172.85, 170.22, 169.92, 136.69, 115.42, 68.85, 68.13, 64.12, 62.67, 33.65, 33.51, 28.85, 28.87, 25.37, 24.35, 16.71, 16.70; HRMS ($M+H^+$) calc. mass 743.34846, found 743.34834.

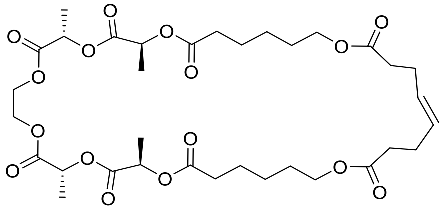

cyclic-Eg-(LLCM)$_2$

A solution of Grubbs' 2nd generation catalyst (94.9 mg, 0.12 mmol) in CH_2Cl_2 (1 mL) was added to a stirring solution of **Eg-(LLCM)$_2$** (0.82 g, 1.11 mmol) in CH_2Cl_2 (815 mL). An additional 1 mL of CH_2Cl_2 was used to rinse the vial that had contained the catalyst solution, and the reaction was allowed to stir at rt overnight. The reaction was quenched by adding 1 mL ethyl vinyl ether, and then concentrated *in vacuo*. The crude material was purified by flash chromatography (SiO_2, 15% EtOAc in hexanes) to provide the product as a colorless liquid with an *E/Z* ratio of 7.3/1 (0.58 g, 73.6%). ^1H NMR (400 MHz, $CDCl_3$) δ 5.48- 5.39 (*trans*) and 5.37-

5.35 (*cis*) (m, 2H), 5.12 (q, J = 7.2 Hz, 2H), 5.08 (q, J = 7.1 Hz, 2H), 4.39- 4.25 (m, 4H), 4.05 (*cis*) and 4.04 (*trans*) (t, J = 6.4 Hz, 4H), ; ^{13}C NMR (100 MHz, $CDCl_3$) □ 173.07, 172.89, 170.11, 170.02, 129.40 (*trans*), 129.03 (*cis*), 68.93, 68.12, 64.06, 62.64, 34.16, 33.66, 28.26, 27.78, 25.40, 24.38, 16.70 (2); HRMS ($M+H^+$) calc mass 603.19251, found 603.19028.

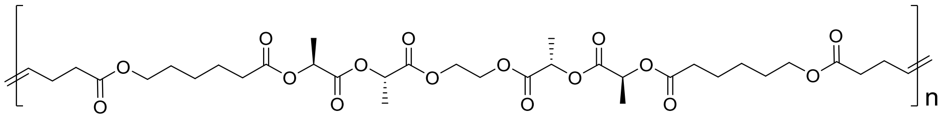

Poly Eg(LLCM)$_2$

G2 (0.76 mg, 8.9x10-4 mmol, 1.33 mol%) was dissolved in CH_2Cl_2 (15 μL), and to a stirring solution of ***cyclic*-Eg-(LLCM)$_2$** (48.0 mg, 0.067 mmol) in CH_2Cl_2 (81 μL). The reaction was allowed to stir at rt for 4 h before being quenched through the addition of ethyl vinyl ether was allowed to stir for 5 min and then was dried under vacuum overnight to yield an off-white solid (quant). ^{1}H NMR (400 MHz, $CDCl_3$) δ 5.48-5.40 (*trans*) and 5.40-5.35 (*cis*) (m, 2H), 5.13 (q, J = 7.2 Hz, 2H), 5.07 (q, J = 7.2 Hz, 2H), 4.37-4.27 (m, 4H), 4.034 (*cis*) and 4.029 (*trans*) (t, J = 6.8 Hz, 4H), 2.37 (dt, J1 = 16 Hz , J2 = 7.6 Hz, 2H), 2.35 (dt, J1 = 16 Hz, J2 = 7.4 Hz, 2H), 2.33-2.23 (m, 8H), 1.69-1.58 (m, 8H), 1.53 (d, J = 7,2 Hz, 6H), 1.50 (d, J = 7.2 Hz, 6H), 1.42-1.34 (m, 4H); ^{13}C NMR (100 MHz, $CDCl_3$) δ 173.09, 172.88, 170.25, 169.93, 129.39 (*trans*), 128.98 (*cis*), 68.85, 68.13, 64.10, 62.69, 34.10, 33.64, 28.27, 27.77, 25.37, 24.35, 16.72, 16.70; DSC: Tg = -11 °C; SEC (THF): Mn = 47 kDa, Mw = 60 kDa, Đ = 1.3.

Bn-L-Muc

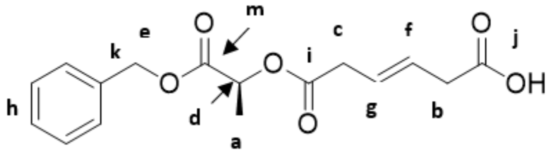

¹H-NMR (500 MHz, $CDCl_3$)

δ (ppm)	Mult. (J)	Int.	Assignment
1.50	d (7.0)	3	**a**
3.12	d (2)	2	**b**
3.18	d (2)	2	**c**
5.16	m	3	**d + e**
5.71	m	2	**f , g**
7.35	m	5	**h**

¹³C-NMR (500 MHz, $CDCl_3$)

δ (ppm) + Assignment	
16.86	**a**
37.384	**b**
37.482	**c**
67.07	**e**
68.89	**d**
125.60	**f**
125.94	**g**
128.15	**h** (ortho, meta)
128.44	**h** (para)
128.62	**h** (ortho, meta)
135.29	**k**
170.55	**i**
170.87	**m**
177.39	**j**

HRMS (ESI)

Calc. Mass
306.11 amu

Calc. $[M-H]^-$
305.10 amu

Found
$[M - H]^-$
305.10312 amu

Composition
$C_{16}H_{18}O_6$

Bn-LM

Bn-L (1.38 g, 7.66 mmol) and *trans*-b-hydromuconic acid (0.735 g, 5.15 mmol) were dissolved in 50 mL dry THF. DPTS (0.301 g, 1.02 mmol) was added and allowed to dissolve, and DCC (1.06 g, 5.15 mmol) was added. The reaction was allowed to stir at room temperature under nitrogen overnight. The mixture was filtered, concentrated *in vacuo*, and diluted with ethyl acetate. Saturated sodium bicarbonate solution was added and extracted 3x. The aqueous layers were combined, acidified with 1 M HCl, and extracted three times with methylene chloride. The combined organics were washed with brine, dried, filtered, and concentrated *in vacuo*, resulting in a yellow oil needing no further purification (0.979 g, 65%).

Bn-L-Mucol

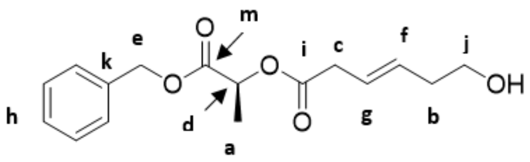

^{1}H-NMR (400 MHz, $CDCl_3$)			
δ (ppm)	Mult. (J)	Int.	Assignment
1.50	d (7.2)	3	**a**
2.30	q (6.4)	2	**b**
3.14	m	2	**c**
3.65	t (6)	2	**j**
5.16	m	3	**d , e**
5.63	m	2	**f , g**
7.26 – 7.38	m	5	**h**

^{13}C-NMR (500 MHz, $CDCl_3$)	
δ (ppm) + Assignment	
16.86	**a**
35.84	**b**
37.64	**c**
61.64	**j**
67.07	**e**
68.76	**d**
124.46	**g**
128.15	**h** (ortho, meta)
128.43	**h** (para)
128.62	**h** (ortho, meta)
131.17	**f**
135.28	**k**
170.63	**i**
171.26	**m**

HRMS (ESI)
Calc. Mass 292.33 amu
Calc. $[M+H]^+$ 293.14 amu
Found $[M + H]^+$ 293.13781 amu
Composition $C_{16}H_{20}O_5$

Bn-LMucol

Bn-L-Muc (1.20 g, 3.92 mmol) was dissolved in 40 mL dry THF under nitrogen and cooled to 0 °C while stirring. Borane-tetrahydrofuran complex solution (1.0 M in THF, 3.92 mL) was added dropwise via syringe, resulting in substantial hydrogen formation, over a period of fifteen min. The reaction mixture was allowed to equilibrate to RT and stir overnight. The mixture was cooled to 0 °C and quenched with 30 mL deionized water. Brine was added and the organics were extracted 3x with ethyl acetate. The combined organics were dried, filtered, and concentrated *in vacuo.* The product was a yellow oil. Column chromatography (100 mL silica, 10% ethyl acetate in hexanes) was used to purify the material (0.802 g, 70%).

Bn-LGLGLG-Si

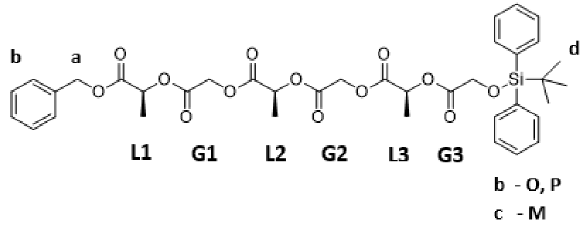

^{1}H-NMR (400 MHz, CDCl$_3$)

δ (ppm)	Mult. (J)	Int.	Assignment
1.11	s	9	**d**
1.54	d (7.2)	6	L2, L3 (CH$_3$)
1.62	d (7.2)	3	L1 (CH$_3$)
4.32	d (16)	1	G3
4.39	d (16)	1	G3
4.65	d (16)	1	G1, G2
4.66	d (16)	1	G1, G2
4.89	d (16)	2	G1, G2
5.17 – 5.28	m	5	**a**, L1,2,3 (CH)
7.29 – 7.48	m	11	**b**
7.70 – 7.72	m	4	**c**

^{13}C-NMR (500 MHz, CDCl$_3$)

δ (ppm) + Assignment			
16.77	L (CH$_3$)	128.52	Arene
16.80	L (CH$_3$)	128.66	Arene
16.84	L (CH$_3$)	129.53	Arene
19.28	**d** (C)	132.73	Arene
26.65	**d** (CH$_3$)	135.58	Arene
60.72	L (CH)	135.61	Arene
60.88	L (CH)	166.50	CO
61.98	L (CH)	168.60	CO
67.26	**a**	169.43	CO
68.45	G (CH$_2$)	169.81	CO
69.15	G (CH$_2$)	169.87	CO
69.53	G (CH$_2$)	170.58	CO
127.82	Arene		
128.19	Arene		

HRMS (ESI)

Calc. Mass
736.26 amu

Calc. [M+Na]$^+$
754.29 amu

Found
[M + Na]$^+$
754.28406 amu

Composition
$C_{38}H_{44}O_{13}Si$

Bn-LGLGLG-Si

Bn-LGLGL (6.24 g, 14.2 mmol) and **G-Si** (4.90 g, 15.6 mmol) were dissolved in 141 mL dry methylene chloride while stirring. DPTS (0.834 g, 2.83 mmol) was added and allowed to dissolve, followed by DCC (3.22 g, 15.6 mmol). The reaction was allowed to stir overnight at RT under N$_2$. The reaction mixture was filtered and concentrated *in vacuo*, resulting in a pale yellow oil. The crude product was purified by column chromatography (500 mL silica, 5% ethyl acetate in hexanes) and began eluting in the fifth 500-mL fraction (8.71 g, 83%).

Bn-LGLGL-Si

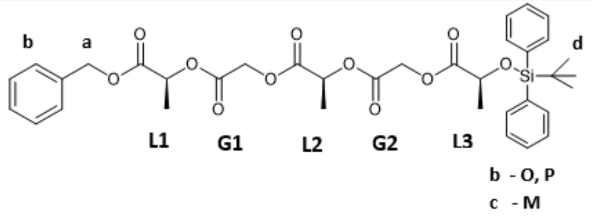

^{1}H-NMR (400 MHz, $CDCl_3$)

δ (ppm)	Mult. (J)	Int.	Assignment
1.09	s	9	**d**
1.42	d (6.8)	3	L3 (CH_3)
1.51	d (7.2)	3	L1 (CH_3)
1.56	d (6.8)	3	L2 (CH_3)
4.12	q (6.8)	1	L1 (CH)
4.45	d (16)	1	G1, G2
4.63	d (16)	1	G1, G2
4.67	d (16)	1	G1, G2
4.85	d (16)	1	G1, G2
5.22	m	4	**a** , L2,3 (CH)
7.32 – 7.44	m	11	**b**
7.65 – 7.69	m	4	**c**

^{13}C-NMR (500 MHz, $CDCl_3$)

δ (ppm)	+ Assignment
16.79	L (CH_3)
19.23	L (CH_3)
21.06	L (CH_3)
21.29	**d** (C)
26.81	**d** (CH_3)
60.40	L (CH)
60.84	L (CH)
67.26	**a**
68.62	L (CH)
68.97	G (CH_2)
69.51	G (CH_2)
127.69	Arene
128.19	Arene
128.52	Arene
129.85	Arene
132.98	Arene
133.42	Arene
135.13	Arene
135.75	Arene
166.52	CO
166.86	CO
169.49	CO
169.81	CO
173.03	CO

HRMS (ESI)

Calc. Mass
678.25 amu

Calc. $[M-H]^-$
677.24 amu

Found
$[M - H]^-$
677.24240 amu

Composition
$C_{36}H_{42}O_{11}Si$

Bn-LGLGL-Si

Bn-LGL (7.86 g, 22.8 mmol) and **GL-Si** (8.02 g, 20.8 mmol) were dissolved in 230 mL dry methylene chloride while stirring. DPTS (1.22 g, 4.15 mmol) was added and allowed to dissolve, followed by DCC (4.71 g, 20.8 mmol). The reaction was allowed to stir overnight at RT under N_2. The reaction mixture was filtered and concentrated *in vacuo*, resulting in a pale yellow oil. The crude product was purified by column chromatography (500 mL silica, 5% ethyl acetate in hexanes) and began eluting in the fourth 500-mL fraction (10.80 g, 77%).

Bn-LGLGL

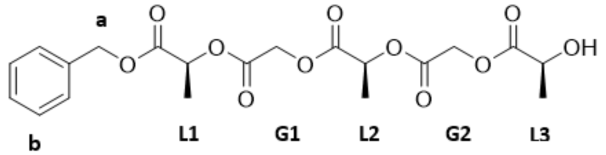

^{1}H-NMR (400 MHz, $CDCl_3$)

δ (ppm)	Mult. (J)	Int.	Assignment
1.48	d (6.8)	3	L3 (CH_3)
1.51	d (7.2)	3	L1 (CH_3)
1.59	d (6.8)	3	L2 (CH_3)
2.78	s	1	L1 (CH)
4.40	q (6.8)	1	L3
4.64	d (16)	1	G1, G2
4.71	d (16)	1	G1, G2
4.86	d (16)	1	G1, G2
5.20	m	4	**a** , L1,2 (CH)
7.32 - 7.44	m	4	**b**

^{13}C-NMR (500 MHz, $CDCl_3$)

δ (ppm)	Assignment
16.78	L (CH_3)
16.79	L (CH_3)
20.35	L (CH_3)
60.88	**a**
60.90	L (CH)
66.74	L (CH)
67.26	L (CH)
69.19	G (CH_2)
69.53	G (CH_2)
128.18	Arene
128.51	Arene
128.64	Arene
135.12	Arene
166.48	CO
166.63	CO
169.37	CO
169.80	CO
174.92	CO

HRMS (ESI)

Calc. Mass
440.13 amu

Found
440 amu parent peak

Composition
$C_{20}H_{24}O_{11}$

Bn-LGLGL

Bn-LGLGL-Si (10.8 g, 15.9 mmol) was dissolved in 160 mL dry THF under nitrogen while stirring. The solution was cooled to 0°C. TBAF solution (1.0 M in THF, 23.8 mL, 23.8 mmol) was mixed with acetic acid (1.70 mL, 28.6 mmol) and added dropwise via syringe to the solution. The reaction was allowed to equilibrate to RT and stir for one hour. The reaction mixture was cooled to 0 °C and quenched with 50 mL brine, and organics were extracted with ethyl acetate 3x. The organic layers were combined, washed with brine, dried, filtered and concentrated *in vacuo* to yield a yellow oil. Column chromatography (200 mL silica gel, 5% ethyl acetate in hexanes) was used to purify the material, and product began to elute in the seventh 500 mL fraction (6.24 g, 89%).

LGLGLG-Si

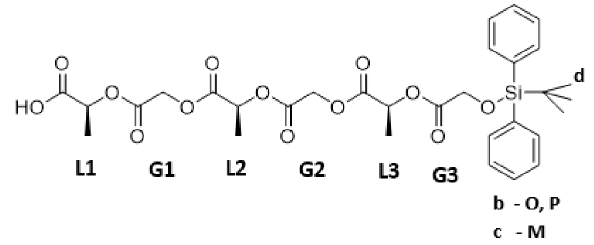

^{1}H-NMR (400 MHz, $CDCl_3$)

δ (ppm)	Mult. (J)	Int.	Assignment
1.09	s	9	**d**
1.51	d (6.8)	3	L1 (CH_3)
1.55	d (6.8)	3	L3 (CH_3)
1.60	d (7.2)	3	L2 (CH_3)
4.29	d (16)	1	G3
4.37	d (16)	1	G3
4.64	d (16)	2	G1, G2
4.86	d (16)	1	G1, G2
4.87	d (16)	1	G1, G2
5.18 – 5.26	m	3	L1,2,3 (CH)
7.36 – 7.45	m	6	**b**
7.67 – 7.70	m	4	**c**

^{13}C-NMR (500 MHz, $CDCl_3$)

δ (ppm) + Assignment	
16.68	L (CH_3)
16.76	L (CH_3)
16.82	L (CH_3)
19.07	**d** (C)
26.63	**d** (CH_3)
60.74	L (CH)
60.84	L (CH)
61.97	L (CH)
68.47	G (CH_2)
69.00	G (CH_2)
127.83	Arene
130.05	Arene
132.70	Arene
135.45	Arene
166.57	CO
169.49	CO
169.88	CO
170.67	CO
174.99	CO

HRMS (ESI)

Calc. Mass
646.21 amu

Calc. $[M+H]^+$
647.22 amu

Found
$[M + H]^+$
647.21713 amu

Composition
$C_{31}H_{38}O_{13}Si$

LGLGLG-Si

Bn-LGLGLG-Si (3.50 g, 4.75 mmol) was dissolved in 50 mL dry ethyl acetate under N_2 while stirring. Pd/C catalyst (0.350 g, 10 wt. %) was added to the flask, and the flask was purged with a hydrogen balloon twice. A third hydrogen balloon served as a static hydrogen source for the reaction, and the reaction mixture was allowed to stir overnight. The mixture was filtered over a bed of celite and concentrated *in vacuo* to obtain pure product, a colorless oil (3.04 g, 99%).

Bn-LMLGLGLG-Si

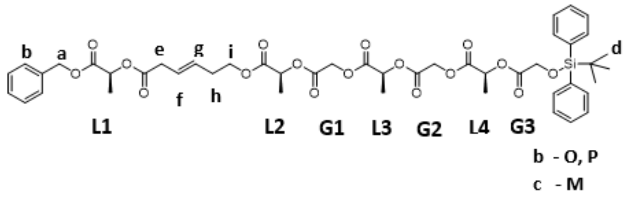

^{1}H-NMR (400 MHz, $CDCl_3$)

δ (ppm)	Mult. (J)	Int.	Assignment
1.08	s	9	**d**
1.49 - 1.52	m	9	L1,3,4 (CH_3)
1.59	d (7.2)	3	L2 (CH_3)
2.37	q (7.2)	2	**h**
3.11	d (2)	2	**e**
4.15 - 4.21	m	2	**i**
4.30	d (16)	1	G3
4.35	d (16)	1	G3
4.61	d (16)	2	G1, G2
4.88	d (16)	2	G1, G2
5.12 - 5.21	m	6	**a,** L 1-4 (CH)
5.55 - 5.69	m	2	**f, g**
7.32 - 7.43	m	11	**b**
7.67 - 7.69	m	4	**c**

^{13}C-NMR (500 MHz, $CDCl_3$)

δ (ppm) + Assignment			
16.77	L (CH_3)	127.81	Arene
16.82	L (CH_3)	128.12	Arene
16.85	L (CH_3)	128.42	Arene
16.87	L (CH_3)	128.61	Arene
19.27	**d** (C)	129.51	Arene
26.63	**d** (CH_3)	129.92	Arene
31.74	**e**	132.71	**f**
37.49	**h**	135.33	Arene
60.38	L (CH)	135.60	Arene
60.86	L (CH)	166.47	CO
61.96	L (CH)	166.59	CO
64.50	G (CH_2)	169.43	CO
67.01	**a**	169.85	CO
68.43	G (CH_2)	170.52	CO
68.78	L1 (CH)	170.56	CO
69.14	G (CH_2)	171.02	CO
69.50	**i**	171.12	CO
124.48	**g**		

HRMS
(ESI)

Calc. Mass
920.33 amu

Calc.
$[M+H]^+$
921.34

Found
$[M + H]^+$
921.33989
amu

Composition
$C_{47}H_{56}O_{17}Si$

Bn-LMLGLGLG-Si

Bn-L-Mucol (1.13 g, 3.87 mmol) and LGLGLG-Si (2.37 g, 3.68 mmol) were dissolved in 40 mL methylene chloride while stirring. DPTS (0.217 g, 0.736 mmol) was added and allowed to dissolve, followed by DCC (0.799 g, 3.87 mmol). The reaction was allowed to stir at RT under N_2 overnight. The reaction mixture was filtered and concentrated *in vacuo*, resulting in a pale yellow oil. The crude product was purified by column chromatography (200 mL silica, 10% ethyl acetate in hexanes) and eluted in the tenth 250-mL fraction (3.14 g, 93%).

LMLGLGLG-Si

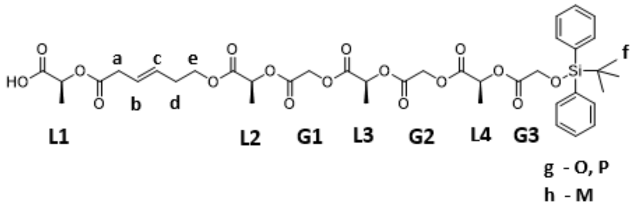

^{1}**H-NMR** (400 MHz, CDCl$_3$)			
δ (ppm)	Mult. (J)	Int.	Assignment
1.08	s	9	**f**
1.43	d	3	L1 (CH$_3$)
1.47 - 1.51	m	6	L3, L4 (CH$_3$)
1.58	d	3	L2 (CH$_3$)
2.36	q	2	**d**
3.10	m	2	**a**
4.17	m	2	**e**
4.29	d (16)	1	G3
4.35	d (16)	1	G3
4.61	d (16)	2	G1, G2
4.88	d (16)	2	G1, G2
4.96	q	1	L1 (CH)
5.12 - 5.21	m	3	L 2-4 (CH)
5.55 - 5.69	m	2	**b** , **c**
7.32 - 7.43	m	6	**g**
7.67 - 7.69	m	4	**h**

^{13}**C-NMR** (500 MHz, CDCl$_3$)			
δ (ppm) + Assignment			
16.77	L (CH$_3$)	127.85	Arene
16.82	L (CH$_3$)	129.93	Arene
16.85	L (CH$_3$)	132.70	**b**
17.02	L (CH$_3$)	135.56	Arene
19.27	**f** (C)	135.59	Arene
26.63	**f** (CH$_3$)	166.55	CO
31.74	**a**	166.62	CO
37.60	**d**	169.43	CO
60.44	L (CH)	169.85	CO
60.72	L (CH)	170.52	CO
60.88	L (CH)	170.56	CO
61.96	L (CH)	171.02	CO
64.57	G (CH$_2$)	171.12	CO
68.45	G (CH$_2$)		
69.14	G (CH$_2$)		
69.47	**e**		
127.83	**c**		

HRMS (ESI)
Calc. Mass
830.28 amu
Calc. [M-H]$^-$
829.27 amu
Found
[M - H]$^-$ 829.27570 amu
Composition
$C_{40}H_{50}O_{17}Si$

LMLGLGLG-Si

A solution of palladium acetate (12.1 mg, 0.0543 mmol), triethylamine (15.1 μL, 0.109 mmol), and triethylsilane (0.263 mL, 1.74 mmol) in 0.75 mL dichloromethane was stirred under nitrogen for 15 min**. Bn-LMLGLGLG-Si** (1.03 g, 1.12 mmol) was dissolved in 0.25 mL dichloromethane and added dropwise into the reaction mixture. The reaction was allowed to stir for fifteen hrs before being quenched with saturated aqueous ammonium chloride solution. The organics were extracted with ethyl acetate, combined, dried with magnesium sulfate, filtered, and concentrated *in vacuo* to yield a yellow oil. Column chromatography (50 mL silica gel, 15% ethyl acetate in hexanes loading) recovered starting material, and a methanol flush then yielded the pure product, a white, tacky solid (0.632 g, 70%).

LMLGLGLG

To a 0.1 M solution of **LMLGLGLG-Si** (1.15 g, 1.42 mmol) in THF, a solution of tetrabutylammonium fluoride (1M in THF, 2.13 mL) and acetic acid (0.15 mL, 2.16 mmol) was added dropwise while stirring. The reaction was allowed to stir for one hour before being quenched with brine. The organics were extracted with ethyl acetate, washed with brine, dried, filtered, and concentrated *in vacuo* to yield a yellow oil. The oil was purified by passage through a silica plug (10 mL silica gel, 100 mL 15% ethyl acetate in hexanes followed by methanol flush). The product was a white solid (0.632 g, 75%).

Cyc-LMLGLGLG

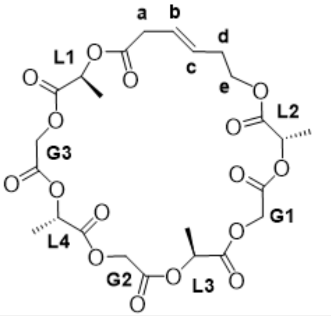

^{1}H-NMR (400 MHz, $CDCl_3$)

δ (ppm)	Mult. (J)	Int.	Assignment
1.50	d (7.2)	3	L2 (CH_3)
1.53	d (7.2)	3	L (CH3)
1.56	d (7.2)	3	L (CH3)
1.59	d (7.2)	3	L (CH3)
2.39	q (5.6)	2	**d**
3.17	m	2	**a**
4.21	m	2	**e**
4.74	m	6	G1, G2, G3
5.12	q (7.2)	1	L2 (CH)
5.24	q (7.2)	1	L (CH)
5.29	q (7.2)	1	L (CH)
5.31	q (7.2)	1	L (CH)

^{13}C-NMR (500 MHz, $CDCl_3$)

δ (ppm)	Assignment
16.61	L (CH_3)
16.68	L (CH_3)
16.71	L (CH_3)
16.77	L (CH_3)
31.79	**d**
37.47	**a**
60.92	L (CH)
61.01	L (CH)
61.11	L (CH)
64.10	L (CH)
68.33	**e**
68.12	G (CH_2)
69.16	G (CH_2)
69.74	G (CH_2)
124.52	**b**
129.75	**c**
166.21	CO
166.25	CO
166.33	CO
169.22	CO
169.29	CO
169.82	CO
169.98	CO

HRMS (ESI)

Calc. Mass
574.15 amu

Calc. $[M+H]^+$
575.16 amu

Found
$[M + H]^+$
575.15975 amu

Composition
$C_{24}H_{30}O_{16}$

Cyc-LMLGLGLG

To 30 mL anhydrous methylene chloride, DCC (0.242 g, 1.17 mmol) and DPTS (0.0628 g, 0.213 mmol) were added while stirring. **LMLGLGLG** (0.632 g, 1.07 mmol) was dissolved in

5 mL of the solvent and added using a syringe pump at a rate of 0.32 mL/hour. The reaction was allowed to stir for sixteen hrs. The mixture was filtered and concentrated to produce a viscous oil. Purification by column chromatography (150 mL silica, 15% ethyl acetate in hexanes) resulted in a white solid (0.410 g, 65%).

Poly LMLGLGLG

G2 (0.76 mg, $8.9\text{x}10^{-4}$ mmol, 1.33 mol%) was dissolved in CH_2Cl_2 (15 µL), and to a stirring solution of **Cyc-LMLGLGLG** (20.0 mg, 0.035 mmol) in CH_2Cl_2 (50 µL). The reaction was allowed to stir at rt for 2 h before being quenched through the addition of ethyl vinyl ether was allowed to stir for 5 min and then was dried under vacuum overnight to yield an off-white solid (quant). ^{1}H NMR (400 MHz, $CDCl_3$) δ 5.48-5.40 (*trans*) and 5.40-5.35 (*cis*) (m, 2H), 5.13 (q, J = 7.2 Hz, 2H), 5.07 (q, J = 7.2 Hz, 2H), 4.37-4.27 (m, 4H), 4.034 (*cis*) and 4.029 (*trans*) (t, J = 6.8 Hz, 4H), 2.37 (dt, J1 = 16 Hz , J2 = 7.6 Hz, 2H), 2.35 (dt, J1 = 16 Hz, J2 = 7.4 Hz, 2H), 2.33-2.23 (m, 8H), 1.69-1.58 (m, 8H), 1.53 (d, J = 7,2 Hz, 6H), 1.50 (d, J = 7.2 Hz, 6H), 1.42-1.34 (m, 4H); ^{13}C NMR (100 MHz, $CDCl_3$) δ 173.09, 172.88, 170.25, 169.93, 129.39 (*trans*), 128.98 (*cis*), 68.85, 68.13, 64.10, 62.69, 34.10, 33.64, 28.27, 27.77, 25.37, 24.35, 16.72, 16.70; DSC: Tg = -11 oC; SEC (THF): Mn = 47 kDa, Mw = 60 kDa, Đ = 1.3.

Bn-Sy

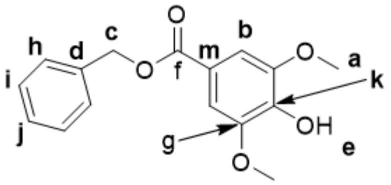

^{1}H-NMR (500 MHz, $CDCl_3$)

δ (ppm)	Mult. (J)	Int.	Assignment
3.93	s	6	**a**
5.36	s	2	**c**
5.91	s	1	**e**
7.39	m	7	**b , d**

^{13}C-NMR (500 MHz, $CDCl_3$)

δ (ppm) + Assignment	
56.66	**a**
66.87	**c**
107.00	**b**
121.26	**j**
128.39	**d**
128.41	**i**
129.80	**h**
136.44	**k**
139.56	**m**
146.84	**g**
166.44	**f**

HRMS (ESI)

Calc. Mass
288.10 amu

Calc. $[M+H]^+$
289.11 amu

Found
$[M + H]^+$
289.10571 amu

Composition
$C_{16}H_{17}O_5$

Bn-Sy

To 15 mL of DMF under nitrogen, syringic acid (3.00 g, 15.1 mmol) was added and dissolved. Sodium carbonate (1.60 g, 15.4 mmol) was added and the reaction was stirred under gentle heating for fifteen min until most of the salt was dissolved. Benzyl bromide (1.80 mL, 15.4 mmol) was added and the reaction was allowed to stir overnight. The reaction mixture was diluted with brine (45 mL) and extracted three times with ethyl ether. The combined organics were washed with brine, dried with magnesium sulfate, filtered, and concentrated to yield a white solid. Purification by column (20% ethyl acetate in hexanes) yielded a fine, white crystalline solid (2.26 g, 51%).

Bn-LMucol-Si

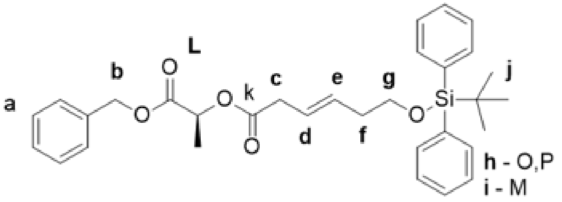

^{1}H-NMR (400 MHz, CDCl$_3$)

δ (ppm)	Mult. (J)	Int.	Assignment
1.05	s	9	**j** (CH$_3$)
1.49	d (7.2)	3	**L** (CH$_3$)
2.31	q (6.0)	2	**f**
3.11	d (4.0)	2	**c**
3.89	t (6.4)	2	**g**
5.15	m	3	**b** , **L** (CH)
5.59	m	2	**d** , **e**
7.35	m	12	**a** , **h**
7.64	m	4	**i**

^{13}C-NMR (400 MHz, CDCl$_3$)

δ (ppm)	Assignment
16.91	**L** (CH$_3$)
19.04	**j** (C)
26.86	**j** (CH$_3$)
35.93	**f**
37.74	**c**
63.61	**g**
67.01	**b**
68.72	**L** (CH)
123.07	**d**
127.63	Arene
128.13	Arene
128.41	Arene
128.62	Arene
129.59	Arene
131.55	**e**
133.94	Arene
134.32	Arene
135.60	Arene
170.65	**k**
171.38	L (CO)

HRMS (ESI)

Calc. Mass
530.25 amu

Calc. [M+H]$^+$
531.26 amu

Found
[M + H]$^+$
531.25634 amu

Composition
C$_{32}$H$_{38}$O$_5$Si

Bn-LMucol-Si

Bn-LMucol (5.77 g, 19.8 mmol) was dissolved in 200 mL dry methylene chloride, followed by addition of triethylamine (5.48 mL, 39.5 mmol) and DMAP (1.34 g, 10.9 mmol). The reaction mixture was placed in an ice bath and tert-butyldiphenylsilyl chloride (5.75 mL, 22.0 mmol) was added dropwise. The reaction was allowed to stir overnight. The solution was filtered, washed three times with 1 M HCl, dried with magnesium sulfate, filtered, and concentrated to yield pure product (10.5 g, 98%).

LMucol-Si

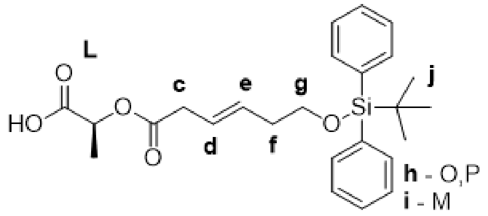

^{1}H-NMR (400 MHz, CDCl$_3$)

δ (ppm)	Mult. (J)	Int.	Assignment
1.04	s	9	**j** (CH$_3$)
1.52	d (7.2)	3	**L** (CH$_3$)
2.30	q (5.6)	2	**f**
3.11	d (4.8)	2	**c**
3.69	t (6.8)	2	**g**
5.10	q (7.2)	1	**L** (CH)
5.58	m	2	**d , e**
7.40	m	6	**h**
7.65	m	4	**i**

^{13}C-NMR (400 MHz, CDCl$_3$)

δ (ppm) + Assignment	
16.80	**L** (CH$_3$)
19.22	**j** (C)
26.85	**j** (CH$_3$)
35.90	**f**
37.62	**c**
63.43	**g**
68.19	**L** (CH)
122.89	**d**
127.63	Arene
129.59	Arene
131.70	**e**
133.92	Arene
135.60	Arene
171.37	**L** (CO)
176.28	Mucol (CO)

HRMS (ESI)

Calc. Mass
440.20 amu

Calc. [M-H]$^-$
439.19 amu

Found
[M - H]$^-$
439.19346 amu

Composition
$C_{25}H_{32}O_5Si$

LMucol-Si

To a solution of triethylamine (0.383 mL, 2.76 mmol), palladium (II) acetate (0.206 g, 0.920 mmol), and triethylsilane (4.56 mL, 28.6 mmol) in 40 mL dry methylene chloride under nitrogen, a solution of **Bn-LMucol-Si** (10.9 g, 20.4 mmol) in 28 mL of methylene chloride was added while stirring. The solution was allowed to stir for 16 hrs and was quenched with saturated aqueous ammonium chloride solution. The organics were extracted with methylene chloride, dried with magnesium sulfate, filtered over a bed of celite, and concentrated to obtain the crude product. A 5" column packed with 5% ethyl acetate in hexanes was used to purify the material, which eluted in fractions 7-8 (250 mL fractions) resulting in a 70% yield. Product was a yellow oil (6.49 g, 72%).

Bn-SyLMucol-Si

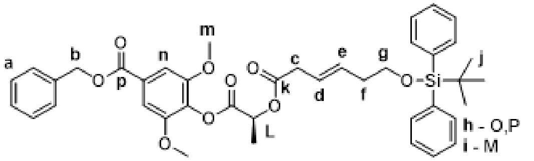

¹H-NMR (400 MHz, $CDCl_3$)

δ (ppm)	Mult. (J)	Int.	Assignment
1.03	s	9	**j** (CH_3)
1.66	d (7.2)	3	**L** (CH_3)
2.29	q (5.6)	2	**f**
3.13	d (4.4)	2	**c**
3.67	t (6.4)	2	**g**
3.83	s	6	**m**
5.37	s	2	**b**
5.44	q (7.2)	1	**L** (CH)
5.59	m	2	**d** , **e**
7.40	m	13	**a** , **h** , **n**
7.63	m	4	**i**

¹³C-NMR (400 MHz, $CDCl_3$)

δ (ppm)	+ Assignment
17.17	**L** (CH_3)
19.21	**j** (C)
26.85	**j** (CH_3)
35.93	**f**
37.72	**c**
56.44	**m**
63.50	**g**
67.05	**b**
68.32	**L** (CH)
106.49	Arene
123.12	**d**
127.62	Arene
128.24	Arene
128.36	Arene
128.66	Arene
129.57	Arene
131.47	**e**
132.18	Arene
133.93	Arene
135.59	Arene
135.92	Arene
152.07	Arene
165.80	**p**
168.17	**k**
171.05	**L** (CO)

HRMS (ESI)
Calc. Mass
710.90 amu

Bn-SyLMucol-Si

Bn-Sy (1.92 g, 6.65 mmol) and **LMucol-Si** (3.07 g, 6.98 mmol) were dissolved in 68 mL dry methylene chloride under N_2. DPTS (0.400 g, 1.13 mmol) was dissolved followed by DCC (1.51 g, 7.32 mmol). The reaction was allowed to stir overnight. The reaction was then filtered and concentrated to obtain the crude product. The material was purified by column loaded with 5% ethyl acetate in hexanes (4.49 g, 95%).

Bn-SyLMucol

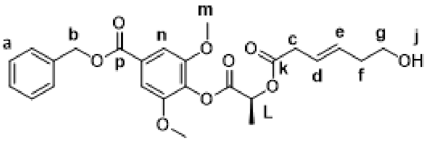

^{1}H-NMR (400 MHz, $CDCl_3$)

δ (ppm)	Mult. (J)	Int.	Assignment
1.61	t (5.6)	1	**j**
1.69	d (6.8)	3	**L** (CH_3)
2.32	q (6)	2	**f**
3.17	m	2	**c**
3.64	q (5.6)	2	**g**
3.85	s	6	**m**
5.37	s	2	**b**
5.45	q (7.2)	1	**L** (CH)
5.63	m	2	**d** , **e**
7.40	m	7	**a** , **n**

^{13}C-NMR (400 MHz, $CDCl_3$)

δ (ppm)	Assignment
17.17	**L** (CH_3)
19.21	**j** (C)
26.85	**j** (CH_3)
35.93	**f**
37.72	**c**
56.44	**m**
63.50	**g**
67.05	**b**
68.32	L (CH)
106.49	Arene
123.12	**d**
127.62	Arene
128.24	Arene
128.36	Arene
128.66	Arene
129.57	Arene
131.47	**e**
132.18	Arene
133.93	Arene
135.59	Arene
135.92	Arene
152.07	Arene
165.80	**p**
168.17	**k**
171.05	**L** (CO)

HRMS (ESI)

Calc. Mass
472.49 amu

Bn-SyLMucol

Bn-SyLMucol-Si (4.49 g, 6.32 mmol) was dissolved in 65 mL dry THF under nitrogen and placed in an ice bath. TBAF solution (1 M in THF, 9.50 mL, 9.50 mmol) and acetic acid (2.89 mL, 50.5 mmol) were combined and added dropwise to the solution. The reaction was stirred for one hour and was quenched with brine. The organics were extracted with ethyl acetate, dried with magnesium sulfate, filtered, and concentrated to obtain the crude product. A column was loaded with 5% ethyl acetate in hexanes to purify the material. Polarity was increased to 50% until all product eluted (2.41 g, 81%).

LGLGL-Si

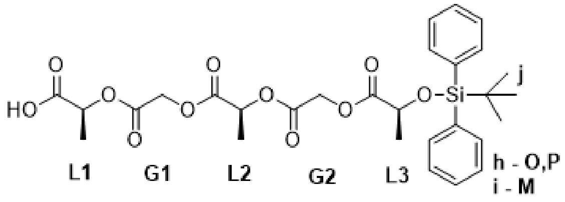

^{1}H-NMR (400 MHz, CDCl$_3$)

δ (ppm)	Mult. (J)	Int.	Assignment
1.08	s	9	**j**
1.41	d (6.4)	3	L3 (CH$_3$)
1.56	m	6	L1 , L3 (CH$_3$)
4.37	q (6.8)	1	L3 (CH)
4.43	d (11)	1	G1, G2
4.63	d (16)	1	G1, G2
4.68	d (16)	1	G1, G2
4.85	d (16)	1	G1, G2
5.26	m	2	L1 , L2 (CH)
7.37	m	6	**h**
7.65	m	4	**i**

^{13}C-NMR (400 MHz, CDCl$_3$)

δ (ppm) + Assignment	
16.70	L (CH$_3$)
16.77	L (CH$_3$)
19.23	**j** (C)
21.30	L (CH$_3$)
26.80	**j** (CH$_3$)
60.29	G (CH$_2$)
60.83	G (CH$_2$)
68.61	L (CH)
69.00	L (CH)
69.13	L (CH)
127.64	Arene
129.86	Arene
133.38	Arene
135.92	Arene
166.57	G (CO)
166.93	G (CO)
169.62	L (CO)
173.12	L (CO)
174.50	L (CO)

HRMS (ESI)

HRMS (ESI)
Calc. Mass 588.20 amu
Calc. [M-H]$^-$ 587.19 amu
Found [M - H]$^-$ 587.19553 amu
Composition $C_{29}H_{36}O_{11}Si$

LGLGL-Si

Bn-LGLGL-Si (7.00 g, 9.51 mmol) was dissolved in 120 mL dry ethyl acetate under N_2 while stirring. Pd/C catalyst (0.700 g, 10 wt. %) was added to the flask, and the flask was purged with a hydrogen balloon twice. A third hydrogen balloon was served as a static hydrogen source for the reaction, and the reaction mixture was allowed to stir overnight. The mixture was filtered over a bed of celite and concentrated *in vacuo* to obtain the product, a colorless oil (5.59 g, Quantitative yield).

Bn-SyLMLGLGL-Si

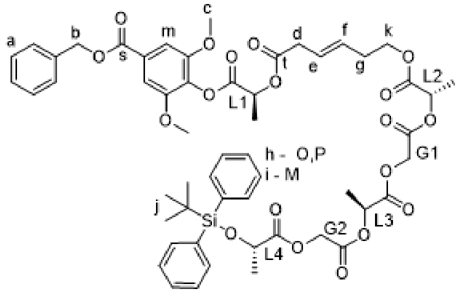

^{1}H-NMR (400 MHz, CDCl$_3$)

δ (ppm)	Mult. (J)	Int.	Assignment
1.09	s	9	**j**
1.41	d (6.4)	3	L4 (CH$_3$)
1.48	d (6.4)	3	L2
1.55	d (6.4)	3	L3
1.68	d (6.4)	3	L1 (CH$_3$)
2.38	q (6.8)	2	**g**
3.13	m	2	**d**
3.85	s	6	**c**
4.15	m	2	**k**
4.37	q (6.4)	1	L4 (CH)
4.44	d (16)	1	G1, G2
4.63	d (16)	1	G1, G2
4.70	d (16)	1	G1, G2
4.85	d (16)	1	G1, G2
5.12	q (6.4)	1	L3 (CH)
5.22	q (6.4)	1	L2 (CH)
5.37	s	2	**b**
5.45	q (6.4)	1	L1 (CH)
5.60	m	2	**d , e**
7.40	m	13	**a , h , m**
7.65	m	4	**i**

^{13}C-NMR (400 MHz, CDCl$_3$)

δ (ppm) + Assignment			
16.80	L (CH$_3$)	127.69	Arene
16.85	L (CH$_3$)	128.36	Arene
17.16	L1(CH$_3$)	128.66	Arene
19.23	**j** (C)	129.46	Arene
21.30	L (CH$_3$)	129.85	Arene
26.80	**j** (CH$_3$)	132.13	**f**
31.75	**g**	132.96	Arene
37.51	**d**	133.40	Arene
56.44	**c**	135.75	Arene
60.27	G (CH$_2$)	135.92	Arene
60.82	G (CH$_2$)	152.05	Arene
64.52	L (CH)	165.78	s
67.06	**b**	166.51	G (CO)
68.39	L (CH)	166.87	G (CO)
68.60	L (CH)	168.12	**t**
68.97	L (CH)	169.52	L (CO)
69.48	**k**	169.90	L (CO)
106.48	Arene	170.75	L (CO)
124.53	**e**	173.04	L (CO)
127.63	Arene		

HRMS
(ESI)

Calc. Mass
1042.37 amu

Calc Mass
N/A

Composition
$C_{54}H_{62}O_{19}Si$

Bn-SyLMLGLGL-Si

Bn-SyLM (2.41 g, 5.10 mmol) and **LGLGL-Si** (2.86 g, 4.85 mmol) were dissolved in 50 mL dry methylene chloride under nitrogen. DPTS (0.286 g, 0.971 mmol) was added and allowed to dissolve, followed by DCC (1.10 g, 5.34 mmol). The reaction was allowed to stir overnight. The reaction was then filtered and concentrated to obtain the crude product. The material was purified by column loaded with 5% ethyl acetate in hexanes (4.29 g, 85%).

SyLMLGLGL-Si

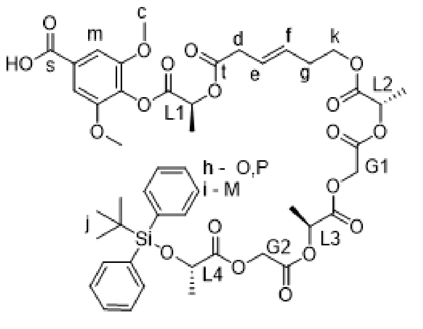

^{1}H-NMR (400 MHz, $CDCl_3$)

δ (ppm)	Mult. (J)	Int.	Assignment
1.09	s	9	**j**
1.41	d (6.8)	3	L4 (CH_3)
1.48	d (6.8)	3	L2
1.55	d (6.8)	3	L3
1.69	d (6.8)	3	L1 (CH_3)
2.38	q (6.4)	2	**g**
3.17	m	2	**d**
3.87	s	6	**c**
4.15	m	2	**k**
4.37	q (6.8)	1	L4 (CH)
4.44	d (16)	1	G1, G2
4.63	d (16)	1	G1, G2
4.70	d (16)	1	G1, G2
4.85	d (16)	1	G1, G2
5.12	q (6.8)	1	L3 (CH)
5.22	q (6.8)	1	L2 (CH)
5.46	q (6.4)	1	L1 (CH)
5.60	m	2	**d** , **e**
7.40	m	8	**h** , **m**
7.65	m	4	**i**

^{13}C-NMR (400 MHz, $CDCl_3$)

δ (ppm) + Assignment

16.85	L (CH_3)	127.69	Arene
17.16	L1(CH_3)	129.48	Arene
19.23	**j** (C)	129.86	Arene
21.30	L (CH_3)	132.13	**f**
26.80	**j** (CH_3)	132.95	Arene
31.75	**g**	133.40	Arene
37.52	**d**	135.74	Arene
56.43	**c**	135.94	Arene
60.28	G (CH_2)	152.12	Arene
60.83	G (CH_2)	161.13	**s**
64.52	L (CH)	166.51	G (CO)
68.39	L (CH)	166.88	G (CO)
68.60	L (CH)	168.12	**t**
68.98	L (CH)	169.52	L (CO)
69.49	**k**	169.90	L (CO)
106.87	Arene	170.75	L (CO)
124.52	**e**	173.04	L (CO)
127.64	Arene		

HRMS
(ESI)

Calc. Mass
952.32 amu

Calc Mass
N/A

Composition
$C_{47}H_{56}O_{19}Si$

SyLMLGLGL-Si

To a solution of triethylamine (0.008 mL, 0.6 mmol), palladium (II) acetate (0.0416 g, 0.0185mmol), and triethylsilane (0.919 mL, 5.77 mmol) in 6 mL dry methylene chloride under nitrogen, a solution of Bn-**SyLMLGLGL-Si** (4.29 g, 4.12 mmol) in 7 mL of methylene chloride was added while stirring. The solution was allowed to stir for 16 hrs and was quenched with saturated aqueous ammonium chloride solution. The organics were extracted with methylene chloride, dried with magnesium sulfate, filtered over a bed of celite, and concentrated to obtain the crude product. A 5” column packed with 10% ethyl acetate in hexanes was used to purify the material (3.927 g, 70%). Product was a white solid.

SyLMLGLGL

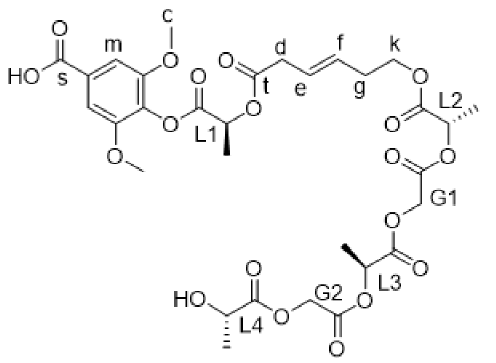

^{1}H-NMR (400 MHz, CDCl$_3$)

δ (ppm)	Mult. (J)	Int.	Assignment
1.49	m	6	L (CH$_3$)
1.59	d (7.2)	3	L (CH$_3$)
1.69	d (7.2)	3	L (CH$_3$)
2.38	q (6.8)	2	**g**
3.17	m	2	**d**
3.87	s	6	**c**
4.17	m	2	**k**
4.40	q (7.2)	1	L4 (CH)
4.64	d (16)	1	G1, G2
4.72	d (16)	1	G1, G2
4.86	d (16)	2	G1, G2
5.12	q (7.2)	1	L3 (CH)
5.22	q (7.2)	1	L2 (CH)
5.46	q (7.2)	1	L1 (CH)
5.60	m	2	**d , e**
7.37	s	2	**m**

^{13}C-NMR (400 MHz, CDCl$_3$)

δ (ppm) + Assignment			
16.80	L (CH$_3$)	127.22	Arene
17.15	L1(CH$_3$)	129.86	Arene
18.00	L (CH$_3$)	132.13	**f**
20.28	L (CH$_3$)	152.08	Arene
31.76	**g**	166.47	**s**
37.54	**d**	166.65	G (CO)
56.43	**c**	166.88	G (CO)
60.28	G (CH$_2$)	168.11	**t**
60.83	G (CH$_2$)	169.52	L (CO)
64.53	L (CH)	169.90	L (CO)
68.41	L (CH)	170.75	L (CO)
68.60	L (CH)	175.06	L (CO)
68.98	L (CH)		
69.49	**k**		
106.87	Arene		
124.52	**e**		

HRMS (ESI)

Calc. Mass
714.20 amu

Calc Mass
N/A

Composition
$C_{31}H_{38}O_{19}$

SyLMLGLGL

SyLMLGLGL-Si (2.71 g, 2.84 mmol) was dissolved in 28 mL dry THF under nitrogen and cooled to 0°C. TBAF solution (1 M in THF, 4.26 mL, 4.26 mmol) and acetic acid (0.351 mL, 4.26 mmol) were combined and added dropwise to the solution. The reaction was stirred for one hour and was quenched with brine. The organics were extracted with ethyl acetate, dried with magnesium sulfate, filtered, and concentrated to obtain the crude product. A column was loaded with 10% ethyl acetate in hexanes to purify the material. Polarity was increased to 90% until all product eluted (1.61 g, 81%).

Cyc-SyLMLGLGL

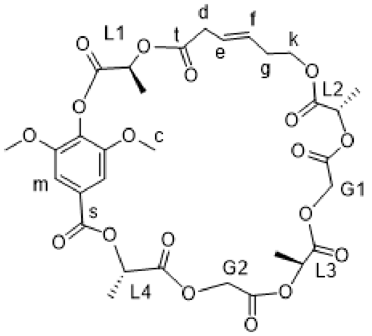

^{1}H-NMR (400 MHz, CDCl$_3$)

δ (ppm)	Mult. (J)	Int.	Assignment
1.36	d (7.2)	3	L (CH$_3$)
1.49	d (7.2)	3	L (CH$_3$)
1.67	m	6	L (CH$_3$)
2.35	q (6.8)	2	**g**
3.16	m	2	**d**
3.85	s	6	**c**
4.11	t (6.8)	2	**k**
4.63	d (16)	1	G1, G2
4.68	d (16)	1	G1, G2
4.72	d (16)	1	G1, G2
4.85	d (16)	1	G1, G2
5.03	q (7.2)	1	L (CH)
5.22	q (7.2)	1	L (CH)
5.46	q (7.2)	1	L (CH)
5.50	q (7.2)	1	L (CH)
7.36	s	2	**m**

^{13}C-NMR (400 MHz, CDCl$_3$)

δ (ppm) + Assignment

δ (ppm)	Assignment	δ (ppm)	Assignment
16.58	L (CH$_3$)	127.73	Arene
16.66	L1(CH$_3$)	129.44	Arene
16.91	L (CH$_3$)	132.38	**f**
17.02	L (CH$_3$)	152.09	Arene
31.69	**g**	165.08	**s**
37.77	**d**	166.19	G (CO)
56.43	**c**	166.30	G (CO)
60.42	G (CH$_2$)	167.90	**t**
60.97	G (CH$_2$)	169.25	L (CO)
64.32	L (CH)	169.82	L (CO)
68.50	L (CH)	170.06	L (CO)
69.07	L (CH)	175.65	L (CO)
69.33	L (CH)		
69.57	**k**		
106.65	Arene		
124.51	**e**		

HRMS
(ESI)

Calc. Mass
696.19 amu

Calc Mass
[M+H]$^+$
697.20 amu

Found
[M+H]$^+$
697.19686

Composition
C$_{31}$H$_{36}$O$_{18}$

Cyc-SyLMLGLGL

SyLMLGLGL (1.61 g, 2.25 mmol) was dissolved in 25 mL dry methylene chloride and injected to a solution of DCC (0.510 g, 2.47 mmol) and DPTS (0.132 g, 0.450 mmol) in 225 mL dichloroethane at 60 °C over a span of 16 hrs. The solution was allowed to stir for an additional 24 hrs before being filtered and concentrated to obtain the crude product. A column loaded with 15% ethyl acetate in hexanes was used to purify the product (1.38 g, 88%), a white solid.

Poly SyLMLGLGL

G2 (0.76 mg, 8.9x10-4 mmol, 1.33 mol%) was dissolved in CH$_2$Cl$_2$ (15 μL), and to a stirring solution of **Cyc-SyLMLGLGL** (20.0 mg, 0.029 mmol) in CH$_2$Cl$_2$ (50 μL). The reaction was allowed to stir at rt for 2 h before being quenched through the addition of ethyl vinyl ether was allowed to stir for 5 min and then was dried under vacuum overnight to yield an off-white solid (quant). ^{1}H NMR (400 MHz, $CDCl_3$) δ 5.48-5.40 (*trans*) and 5.40-5.35 (*cis*) (m, 2H), 5.13 (q, J = 7.2 Hz, 2H), 5.07 (q, J = 7.2 Hz, 2H), 4.37-4.27 (m, 4H), 4.034 (*cis*) and 4.029 (*trans*) (t, J = 6.8 Hz, 4H), 2.37 (dt, J1 = 16 Hz , J2 = 7.6 Hz, 2H), 2.35 (dt, J1 = 16 Hz, J2 = 7.4 Hz, 2H), 2.33-2.23 (m, 8H), 1.69-1.58 (m, 8H), 1.53 (d, J = 7,2 Hz, 6H), 1.50 (d, J = 7.2 Hz, 6H), 1.42-1.34 (m, 4H); ^{13}C NMR (100 MHz, $CDCl_3$) δ 173.09, 172.88, 170.25, 169.93, 129.39 (*trans*), 128.98 (*cis*), 68.85, 68.13, 64.10, 62.69, 34.10, 33.64, 28.27, 27.77, 25.37, 24.35, 16.72, 16.70; DSC: Tg = -11 °C; SEC (THF): Mn = 47 kDa, Mw = 60 kDa, Đ = 1.3.

ED-ROMP competition experiment between *cis* and *trans-cyclic*-Eg-(LGLM)$_2$.

A pre-mixed solution of ***trans-cyclic*-Eg-(LGLM)$_2$** (6.2 mg, 10.2 μmol) and ***cis-cyclic*-Eg-(LGLM)$_2$** (5.8 mg, 9.6 μmol) in $CDCl_3$ (315 μmol) was added to an NMR tube equipped with a controlled atmosphere valve. A solution of **G2** (220 μg, 0.25 μmol) in $CDCl_3$ (160 μL) was then added under N_2 and the tube was inserted into a 600 MHz NMR for further analysis as the reaction progressed. 20 ^{1}H NMR spectra were acquired over the course of 4 hrs, with particular attention being paid to the G-methylene peak region 4.65-4.85 ppm. A final ratio of *cis*:*trans* observed for the quenched solution was 0.20 to 1, corresponding to 17% *cis*-monomer remaining. Data for the remaining time points is shown below.

SEED-ROMP kinetics study.

To a stirring solution of ***cis-cyclic*-Eg-(LGLM)$_2$** (72 mg, 120 μmol) and CH_2Cl_2 (121 μL) was added a solution of catalyst **G2** (1.3 mg, 1.5 μmol) in CH_2Cl_2 (50 μL). Aliquots were removed via pipette at the specified time points over the course of 2 days and added to a GC vial containing a solution of ethyl vinyl ether in order to quench the catalyst. Samples were diluted with CH_2Cl_2, passed through a celite plug and concentrated. The *cis*-to-*trans* ratio of monomer was approximated by comparing peak integrations at 4.85-4.75 ppm. Total conversion was approximated by comparing peak integrations at 4.9-4.75 ppm. The *E:Z* ratio of polymeric materials, as determined by peak integrations at 5.6-5.3 ppm, was 85:15.

Poly Eg(LLCM)$_2$ molecular weight control study.

The LLC-macromonomer was added to a vial charged with a stir bar and pumped into a nitrogen filled glove box. An appropriate amount of dry CH_2Cl_2 (0.7M with respect to monomer final volume) was added to dissolve the monomer. A solution of Grubbs' 2nd generation catalyst (varying catalyst mol %) was prepared and added to monomer solution and allowed to stir for 4h. After 4h, the polymerizations were quenched with ethyl vinyl ether and allowed to stir for 5 min before concentrating *in vacuo*.

Poly Eg(LGLM)$_2$ molecular weight control study.

A solution of catalyst **G2** (1-3 mol%) in CH_2Cl_2 (~0.5 M) was added to a vial containing ***cis-cyclic*-Eg-(LGLM)$_2$** in CH_2Cl_2 (final concentration 0.7 M). Reaction mixtures were shaken for 2 h, quenched with EVE (0.5 mL), and shaken an additional 30 min. The mixture was dissolved in CH_2Cl_2 and concentrated *in vacuo* to yield **poly Eg(LGLP)$_2$** with varying molecular weights.

Chain extension experiment of poly (LGL-Eg-LGL-M).

A solution of catalyst **G2** (0.18 mg, 0.22 μmol) in CH_2Cl_2 (10 μL) was added to a pre-mixed solution of ***cis-cyclic*-Eg-(LGL-M)$_2$** (10.5 mg, 17.4 μmol) in CH_2Cl_2 (15 μL). After shaking for 20 min, a second aliquot of ***cis-cyclic*-Eg-(LGL-M)$_2$** (10.5 mg, 17.4 μmol) in CH_2Cl_2 (25 μL) was added. The polymerization was quenched through the addition of EVE (0.5 mL) and allowed to shake for 30 min. The mixture was dissolved in CH_2Cl_2 and passed through a celite plug before concentrating *in vacuo* to yield a viscous residue (18.4 mg, 90.6% conversion, 31% *cis*-olefin in unreacted starting material). Spectral data matched that previously reported for p**oly (LGL-Eg-LGL-M)**. SEC (THF): molecular weights too high to be determined; Đ ≈ 1.11. *Note: when each phase of polymerization was allowed to stir for only 10 min, polymer was obtained with 68% conversion, adjusted theo.* M_n *= 60.0 kDa, actual* M_n *= 74.3 kDa,* M_w *= 82.5 kDa, Đ = 1.11.*

Sequential SEED-ROMP—ROMP: preparation of poly [(Eg(LGLM)$_2$-*block*-(NBE)].

SEED-ROMP—ROMP reactions were carried out sequentially, with SEED-ROMP occurring for 10 min prior to NBE addition. ROMP was allowed to continue for either 1 min or 5 min. Control experiments were quenched after the SEED-ROMP phase of the reaction. A sample protocol is detailed below:

A solution of **G2** (0.18 mg, 0.218 μmol) in CH_2Cl_2 (10 μL) was added to a pre-mixed solution of ***cis-cyclic*-Eg(LGLM)$_2$** (10.5 mg, 17.4 μmol) in CH_2Cl_2 (15 μL) and allowed to shake for 10 min before a pre-mixed solution of NBE (41 mg, 435 μmol) in CH_2Cl_2 (25 μL) was added at room temperature. The vial was shaken for 1 min, and EVE was added and was shaken for an additional 10 min. The mixture was diluted to a pre-weighed vial after diluting with CH_2Cl_2 (0.3 mL) and concentrated *in vacuo* to provide crude **poly [(LGL-Eg-LGLM)-*block*-(NBE)]** as a solid (18.5 mg, 93% SEED-ROMP monomer conversion, 64% *cis*-olefin incorporation in **poly(NBE)**; based on DP, composition is 46 mol% block A (**poly (LGL-Eg-LGL-M)**, DP 100) and 54 mol% block B (**poly(NBE)**, DP 117). To add clarity to integration numbers presented herein, a 50:50 ratio of A:B has been assigned, and a 50:50 *cis:trans* ratio has been assigned for the NBE block. ^1H NMR (500 MHz, $CDCl_3$) δ 5.51 (m, a_{trans}) and 1.42 (m, a_{cis}) (2H), 5.35 (br s, 1H, j_{trans}) and 5.21 (m, 5H, *dg* & j_{cis}), 4.89 (d, *J* = 16.0 Hz, 2H, *f*), 4.65 (d, *J* = 16.5 Hz, 2H, *f*), 4.41 (m, 4H, *i*), 2.85 (br s, 2H, k_{cis}), 2.50 (m, 5H, *c* and k_{trans}), 2.33 (m, 4H, *b*), 1.87 (m, 1H, m_1), 1.80 (m, 2H, l_1) 1.55 (d, *J* = 6.0 Hz, 6H, *e*), 1.53 (d, *J* = 7.0 Hz, 6H, *h*) 1.35 (m, 2H, l_2), 1.09 (m, 1H, m_2); ^{13}C NMR

(125 MHz, $CDCl_3$) δ 172.49 (*A*), 170.38 (*A*), 169.86 (*A*), 166.78 (*A*), 134.14 (*B*), 134.07 (*B*), 134.03 (*B*), 133.99 (*B*), 133.90 (*B*), 133.28 (*B*), 133.15 (*B*), 133.00 (*B*), 129.49 (*A*), 129.154 (*B*), 129.04 (*B*), 69.41 (*A*), 68.36 (*A*), 68.30 (*A*), 62.92 (*A*), 60.83 (*A*), 43.56 (*B*), 43.27 (*B*), 42.90 (*B*), 42.24 (*B*), 38.81 (*B*), 38.56 (*B*), 33.84 (*A*), 33.25 (*B*), 33.07 (*B*), 32.52 (*B*), 32.36 (*B*), 27.72 (*A*), 17.02 (*A*), 16.88 (*A*); SEC (THF): M_n = 71.4 kDa, M_w = 78.8 kDa, Đ = 1.10.

3.0 The Influence of Short-Range Scrambling of Monomer Order on the Hydrolysis Behaviors of Sequenced Degradable Polyesters

3.1 Overview

The work described in this chapter has been submitted as a journal article entitled "*The Influence of Short-Range Scrambling of Monomer Order on the Hydrolysis Behaviors of Sequenced Degradable Polyesters*" to ACS Macromolecules. Jordan H. Swisher is listed as a contributing author on this publication for his assistance in the preparation of starting materials, experimental design, and scientific discussions. In this chapter, the hydrolysis behaviors of two copolymers containing only a slight difference of sequence precision are compared.

3.2 Introduction

In synthetic polymer science, there are few studies of the sensitivity of bulk properties to discrete changes in monomer sequence in an otherwise sequence-controlled polymer (SCP). The degree to which sequence plays a role in macromolecular function is well established in Nature and most appreciated within the scope of biological chemistry, where it is well understood that for some biopolymers a single monomer sequencing error can dramatically affect function, e.g. DNA, while for others the behavior is controlled by an overall sequence pattern rather than exact monomer identity and placement, e.g. structural proteins like spider silk.[157-159]

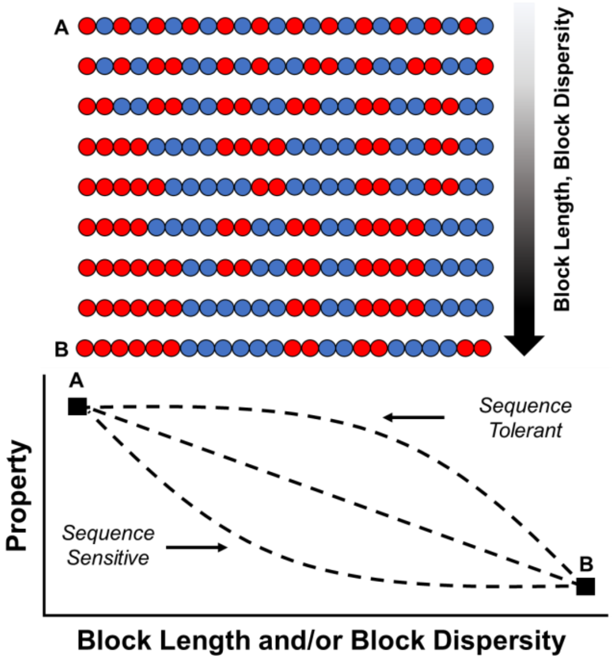
A
B
Block Length, Block Dispersity
A
Sequence Tolerant
Property
Sequence Sensitive
B
Block Length and/or Block Dispersity

Figure 13. Range of bulk property/sequence tolerance profiles for random and sequence-controlled copolymers where A represents a precisely alternating and B represents a statistically random copolymer.

Although there has been an increasing effort in studying structure and function in SCPs,[11, 14, 95] little is known about the sensitivity of properties to sequence errors. Synthetic advances have aided both in the expansion in number and types of SCPs,[13, 15, 29, 107, 135, 138, 160-166] and in the studies of the bulk properties,[51, 70, 167-169] solution properties,[21, 70, 71, 75, 81, 82, 93, 163, 170, 171] and complex behaviors[19, 76, 96, 172-176] of these materials. Still, there has been less effort to date in trying to understand the effects of sequence errors. One way to visualize sequence errors that is applicable to periodic copolymers of the type discussed herein is illustrated in Figure 13. In this model, the introduction of increasing numbers of errors to the base alternating sequence eventually yields a polymer with the block lengths and block dispersities similar to those that would be obtained from a statistical polymerization. Based on this model, a variety of property responses can be envisioned. At one end of the continuum a property could be found to behave like DNA, wherein even small numbers of errors cause dramatic differences in the property (Figure 13, bottom curve).

At the other, a base sequence could be found, as in structural proteins, to be resilient to the introduction of sequence mistakes, retaining the performance of the fully sequenced version despite a significant introduction of errors (Figure 13, top curve). The exact profile and the degree of dependence would, of course, be important both to improve sequence engineering for particular behaviors and to allow more practical syntheses of semi-sequenced copolymers in systems in which errors can be tolerated.[70, 83, 172, 177-180]

In this chapter, the effect of sequence on properties will be studied for a class of degradable polyesters closely related to poly-(lactic-*co*-glycolic acid)s (PLGAs). PLGAs, which are widely used for bioengineering applications including drug delivery and cell growth scaffolding, are almost always random in sequence.[1, 4-7, 9, 10, 38, 101] Random PLGAs such as **PDLGA-50** are traditionally prepared from the ring-opening polymerization of lactide and glycolide, which, due to the reaction's statistical nature, typically results in a polymer with a wide distribution of block lengths. This distribution is important because it is known that G-rich regions degrade more rapidly than mixed or L-rich regions in an aqueous environment. As a result, polymer mass and molecular weight decrease rapidly upon exposure to water.[181] The degree of this hydrolytic susceptibility of fully random PLGAs is commonly controlled by altering the composition of the monomer feed. Average block length and thus degradation rates, however, are not dramatically affected until approximately 80-90% of the monomer feed composition is one monomer.[182-184]

Our group has invested significant effort in establishing hydrolysis behaviors as a function of sequence for PLGAs.[35-37, 113, 114, 139, 140, 185] A library of SCPs comprising the three monomer units, s-lactic acid (**L**), R-lactic acid (**L$_{\mathbf{R}}$**), and glycolic acid (**G**), was previously studied. Hydrolysis was found to be sequence-dependent in all cases, and a dramatic difference was observed relative to random copolymers of the same compositions.[35, 36] We previously reported the property differences between alternating copolymer $(LG)_n$ which we termed **Poly LG**, and its random sequence analog **PDLGA-50** (and the stereopure variant **PLLGA-50**). The dramatic differences in hydrolysis behaviors between the alternating and random sequences presents an opportunity to investigate the degree of property sensitivity to minor sequence alterations.

We sought to design a sequenced polyester with an alternating LG segment and study its degradation behaviors alongside a semi-scrambled, or controlled random, copolymer. This synthetic route was used, as opposed to preparing two precisely-sequenced copolymers, to investigate the realm between sequenced and random. Our goal was to study the property tolerance of this family of polyesters to sequence errors and to search for unexpected, sequence-induced complex behaviors like those observed in our previous works.[35-37, 97, 98, 139] We chose to prepare these polymers using entropy-driven ring-opening metathesis polymerization (ED-ROMP). Using this process, large macrocycles are ring-opened to form entropically-favored linear chains with reproducible, controlled molecular weights.[104, 186, 187] Though these copolymers deviate in structure from pure PLGAs due to the necessary incorporation of the polymerizable olefin functionality, the realized molecular weight control is crucial to effectively make comparisons between polymers containing subtle differences in sequence.[114]

Herein, we describe the synthesis of a precisely sequenced polyester comprising **L**, **G**, syringic acid (**Sy**), and a metathesis-active olefin linker (**M**), and a copolymer of identical monomer composition but with a slightly scrambled LG sequence. Syringic acid was incorporated in these copolymers to elevate the T_g above 37 °C, which is important for future applications.[188] Molecular weight decrease, mass loss, thermal properties, and film characteristics were monitored. Dramatic differences in the degradation behaviors of the two polymers were observed, despite the relatively small differences in sequence.

3.3 Results

3.3.1 Synthesis of Sequence Controlled Polymers

All L monomers denoted in this work are the L-lactic acid isomer. Oligomers are named from the acid-terminus to the alcohol-terminus by listing each unit. The oligomer **SyLM(LGLGL)**, for example, consists of syringic acid - lactic acid - metathesis linker and an alternating sequence of three lactic acid and two glycolic acid units. A prefix of Cyc- is used to indicate the ring-closed macromonomer and Poly is used to indicate the ring-opened polymer.

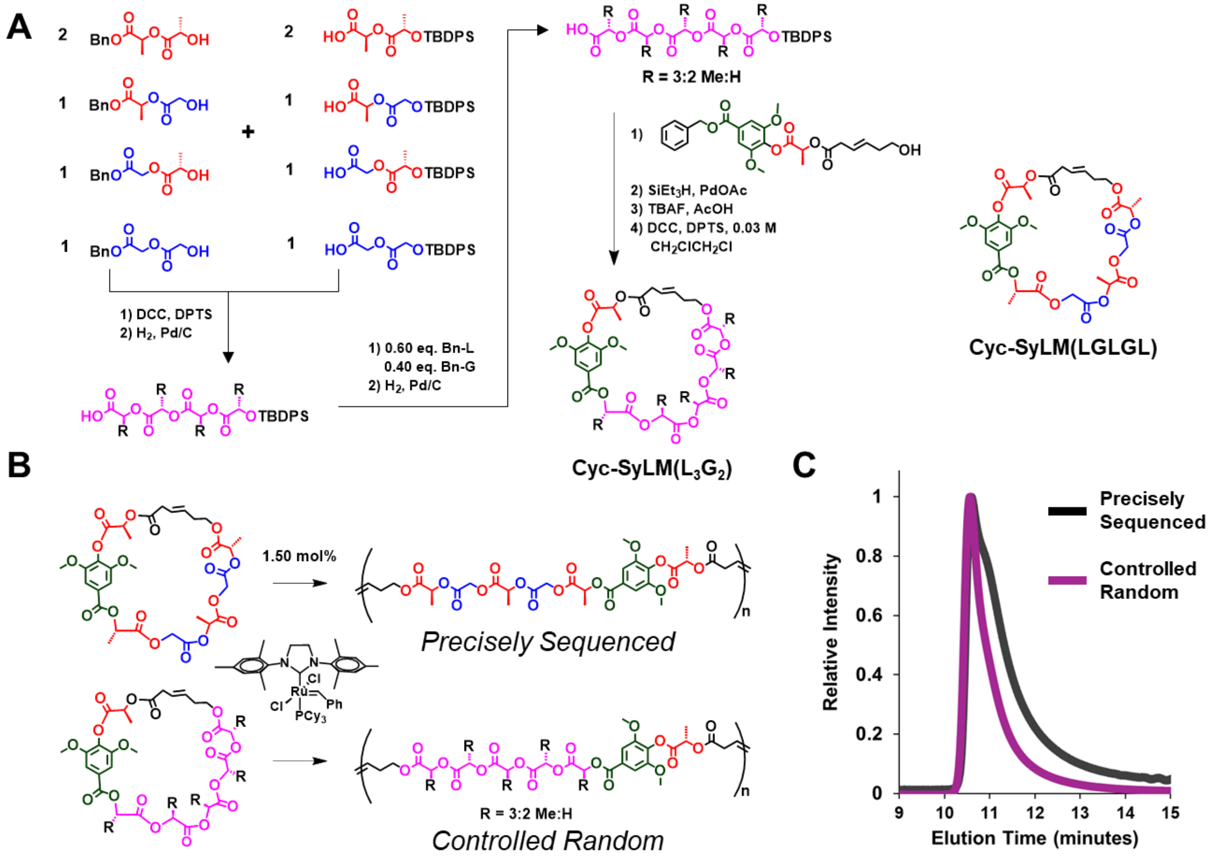

A
2
1
1
1
+
2
1
1
1
TBDPS
1) DCC, DPTS
2) H$_2$, Pd/C
1) 0.60 eq. Bn-L
0.40 eq. Bn-G
2) H$_2$, Pd/C
R = 3:2 Me:H
1)
2) SiEt$_3$H, PdOAc
3) TBAF, AcOH
4) DCC, DPTS, 0.03 M CH$_2$ClCH$_2$Cl
Cyc-SyLM(L$_3$G$_2$)
Cyc-SyLM(LGLGL)
B
1.50 mol%
Precisely Sequenced
R = 3:2 Me:H
Controlled Random
C
Precisely Sequenced
Controlled Random
Relative Intensity
Elution Time (minutes)
0
0.2
0.4
0.6
0.8
1
9
10
11
12
13
14
15

Figure 14. Synthesis of Poly SyLM(L$_3$G$_2$): A) Synthesis of Cyc-SyLM(L$_3$G$_2$) macrocycle; B) polymerization of macrocycles to produce precisely sequenced and controlled random copolymers of identical composition; and C) size exclusion chromatography traces of both copolymers.

The hydroxy-acid sequenced oligomer **SyLM(LGLGL)** was prepared utilizing standard iterative ester coupling techniques described by our group,[139, 185] and the ring-closed species **Cyc-SyLM(LGLGL)** was obtained in good yield upon macrolactonization under dilute conditions as described previously.[188] **Sy**, which introduces the largest structural deviation from a traditional aliphatic polyester such as PLGA, was incorporated as an inert, conformationally-rigid unit to counteract the dramatic lowering of the glass transition temperature that results from the incorporation of the conformationally-flexible metathesis linker **M**.[112, 120, 189]

As the first step in preparing a randomized analog to this macrocycle, **Cyc-SyLM(L_3G_2)**, a mixture of random pentamers comprising 60 mol% **L** and 40 mol% **G** (i.e. **L_3G_2**) was prepared by the ester coupling of a mixture of mono-protected dimers: **Bn-LL**, **Bn-LG**, **Bn-GL**, **Bn-GG**, **LL-Si**, **LG-Si**, **GL-Si**, and **GG-Si** (Si = TBDPS, Bn = benzyl); followed by full benzyl hydrogenolysis and subsequent coupling with additional **Bn-L** (0.60 eq.) and **Bn-G** (0.40 eq.). The resulting **Bn-L_3G_2-Si** was then deprotected once more via hydrogenolysis to yield the free-acid pentamer **L_3G_2-Si** (Figure 14). During the synthesis of these mixtures of compounds, significant differences in polarity of the protected and unprotected species allowed for surprisingly uncomplicated purifications using column chromatography.

Randomized hydroxy-acid oligomer **SyLM(L_3G_2)** was prepared by coupling an acid-protected **Bn-SyLM** to the random alcohol-protected pentamer **L_3G_2-Si** followed by sequential benzyl and silyl deprotection reactions. Macrocyclic oligomer **Cyc-SyLM(L_3G_2)** was then prepared utilizing the same macrolactonization technique described above (Figure 14A). Both cyclic species were then subjected to ED-ROMP at 0.7 M with 1.50 mol% Grubbs second generation catalyst to obtain **Poly SyLM(LGLGL)** (M_n = 44.3 kDa, Đ = 1.15) and **Poly SyLM(L_3G_2)** (M_n = 47.6 kDa, Đ = 1.07) (Figure 14 B,C). This synthetic approach yielded both the perfectly-sequenced copolymer and the scrambled analog wherein the disorder was confined to the LG-pentamer region of the otherwise precise copolymer.

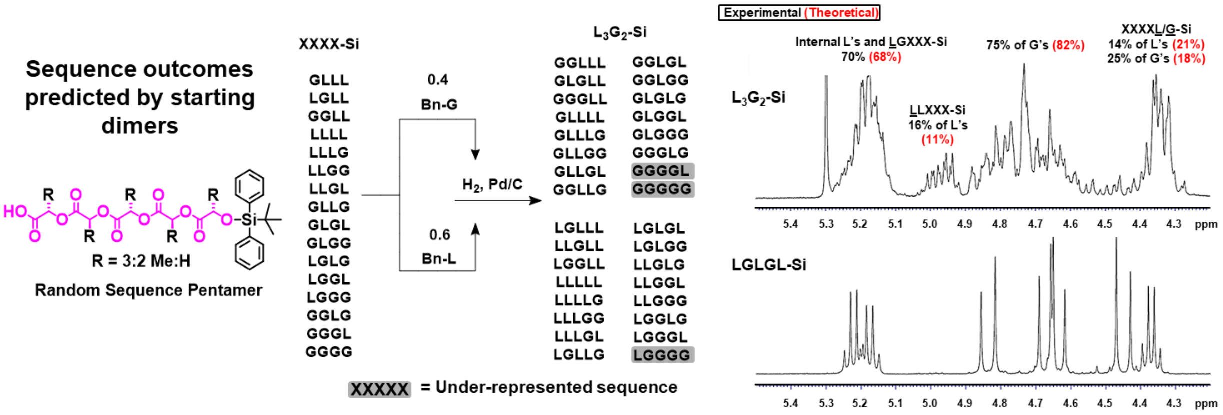
Sequence outcomes predicted by starting dimers
HO
R
O
Si
R = 3:2 Me:H
Random Sequence Pentamer
XXXX-Si
GLLL
LGLL
GGLL
LLLL
LLLG
LLGG
LLGL
GLLG
GLGL
GLGG
LGLG
LGGL
LGGG
GGLG
GGGL
GGGG
0.4
Bn-G
H2, Pd/C
0.6
Bn-L
L3G2-Si
GGLLL
GLGLL
GGGLL
GLLLL
GLLLG
GLLGG
GLLGL
GGLLG
GGLGL
GGLGG
GLGLG
GLGGL
GLGGG
GGGLG
GGGGL
GGGGG
LGLLL
LLGLL
LGGLL
LLLLL
LLLLG
LLLGG
LLLGL
LGLLG
LGLGL
LGLGG
LLGLG
LLGGL
LLGGG
LGGLG
LGGGL
LGGGG
XXXXX = Under-represented sequence
Experimental (Theoretical)
Internal L's and LGXXX-Si 70% (68%)
75% of G's (82%)
XXXXL/G-Si 14% of L's (21%) 25% of G's (18%)
LLXXX-Si 16% of L's (11%)
L3G2-Si
LGLGL-Si
5.4
5.3
5.2
5.1
5.0
4.9
4.8
4.7
4.6
4.5
4.4
4.3
ppm

Figure 15. The theoretical and experimental sequence outcomes within the mixture of random L_3G_2-Si pentamers prepared from precursor dimers, and ^{1}H NMR spectroscopy (red labels are theoretical and black are experimental).

3.3.2 Sequence Characterization

The structure of **Poly SyLM(LGLGL)** was confirmed by comparison with previously-acquired NMR spectroscopy and MALDI-TOF mass spectrometry data.[188] The analysis shows that sequence is preserved throughout all steps of the synthesis.

The structure of the random copolymer is more complex but can be confirmed by first analyzing the composition of the pentamers that are embedded. ^{1}H NMR spectroscopy and mass spectrometry show that the distribution in **L_3G_2-Si** is consistent with the expected 32 sequence outcomes arising from the statistical combination of protected dimers (Figure 15).

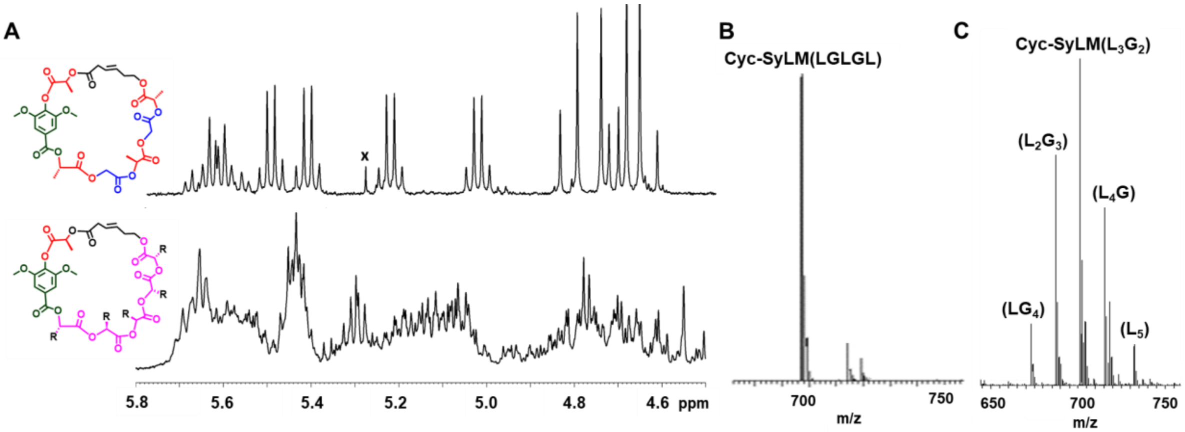

Figure 16. Sequence characterization of macrocycles: A) ^{1}H NMR spectra of methyne, methylene, and olefin regions of Cyc-SyLM(LGLGL) and Cyc-SyLM(L_3G_2); B) high resolution mass spectrum of Cyc-SyLM(LGLGL); and C) high resolution mass spectrum of Cyc-SyLM(L_3G_2) macrocycle mixture.

While the complete assignment of the sequences is not possible, select signals of known monomer units, when compared to our large library of L/G-containing sequenced oligomers, allowed us to quantify to a degree the sequence outcomes. A terminal, deprotected L methyne proton displays a resonance near 5.2 ppm unless the next unit in the sequence is another L, in which case the signal shifts to 5.0 ppm. The theoretical composition of **L**LXXX-Si units is 11% of all L's, whereas the ^{1}H NMR spectrum indicates 16% of L's in this placement. Resonances for both L methyne and G methylene protons that are last in the pentameric sequences, adjacent to the silyl protecting group (XXXX**L**/**G**-Si), appear at 4.35 ppm. Based on the L units already accounted for and the integrations of the L methyl resonances at 1.3 ppm, the signals displayed from L units in this region were calculated to represent 14% of all L's, whereas this theoretical value was 21%. The signals for G units appear in one of two regions – either 4.5 – 4.9 ppm or in the 4.35 region (XXXX**G**-Si). The theoretical values compared to the experimental placements of G's varied by 7%. Overall, these integrations are consistent with those expected. The differences likely correspond to a small degree of oligomer bond cleavage that occurred during the synthesis and isolation steps.

After ring-closing, the sequences and monomer composition of both macrocycles were elucidated using ^{1}H NMR spectroscopy and HRMS. The ^{1}H NMR spectra of the macrocycles are most informative in the 4.5 – 6.0 ppm region, where **G**-methylene, **L**-methyne, and **M**-olefin protons appear (Figure 16A). The sequenced macrocycle clearly displays four distinct quartets corresponding to the **L**-methyne protons, as well as two pairs of doublets from the **G**-methylene protons. Although this spectral region is complex for the controlled random macrocycle, the same subregions of **G**-methylene (4.5 – 4.9 ppm), **L**-methyne (5.0 – 5.5 ppm), and **M**-olefin protons (5.5 – 5.8 ppm) remain distinct. Further structural insights were obtained from the HRMS of both macrocycles. **Cyc-SyLM(LGLGL)** displayed a single major peak matching the theoretical mass (Figure 14B), whereas **Cyc-SyLM(L_3G_2)** displayed five peaks corresponding to the masses of macrocycles containing LG_4 to L_5 pentamers. The peak associated with a **Cyc-SyLM(G_5)** species was not observed, which confirms that this hydrolytically-sensitive species did not survive the final steps in the synthesis (Figure 16C). Even without this sensitive macrocycle in the mixture, the overall monomer composition did not suffer dramatically. A synthetic target of 3:2 L-to-G ratio resulted in an experimental ratio of 3:1.88 according to the ^{1}H NMR spectrum.

3.3.3 Film Casting

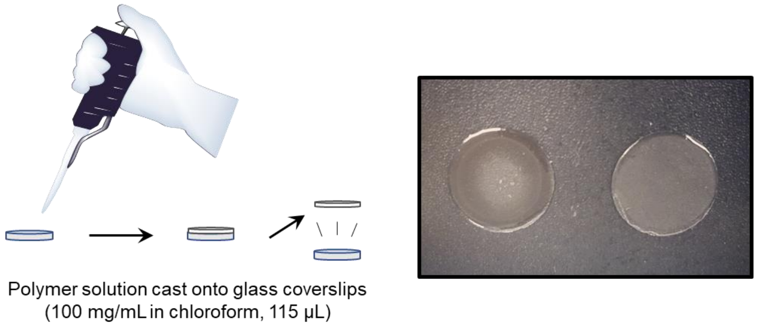
Polymer solution cast onto glass coverslips
(100 mg/mL in chloroform, 115 µL)

Figure 17. Cartoon depiction of solution film-casting of polymer discs (left) and photograph of Poly SyLM(LGLGL) and Poly SyLM(L_3G_2) free-standing discs (right).

PLGAs may be processed into a variety of devices including high surface area scaffolds, microparticles, pellets, and films.[4, 6-10] In our sequence/property investigations we wished to produce uniform devices of small mass with high efficiency, and we found that solution casting of thick polymer films, or discs, was effective in this endeavor.[112] Thick films were cast on 1.25 cm glass coverslips[2] (Figure 17) and thicknesses were measured using optical profilometry (Figure 18). The 120-150 μm films were dried in a vacuum chamber, delaminated from the glass coverslips, and placed in phosphate buffer solution upon the commencement of the hydrolysis study.

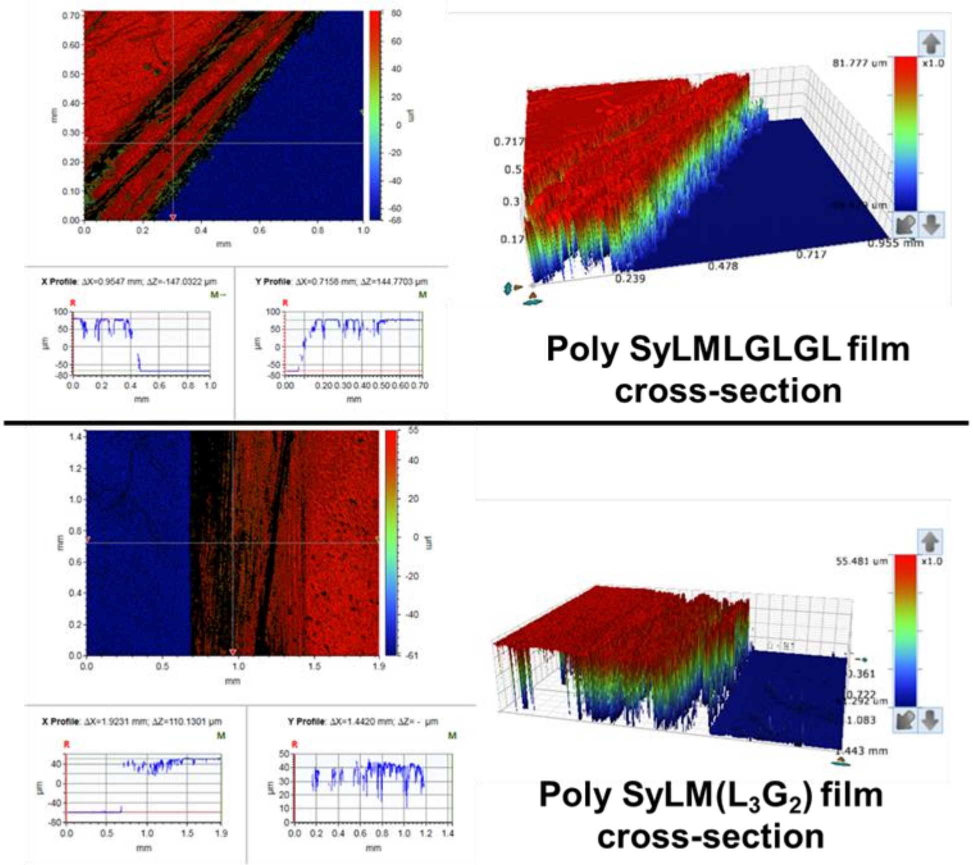

Figure 18. Optical profilometry countours of sliced films of Poly SyLM(LGLGL) and Poly SyLM(L_3G_2) discs.

3.3.4 Hydrolysis

Samples were placed in 10x phosphate buffer solution and incubated at 37 °C for the duration of the study. A preliminary molecular weight loss study was performed on a single film of both samples to determine time points for the full study. In the full study reported herein, three films were used for each molecular weight and mass data point and averages were calculated. A single film was used for DSC measurements and SEM imaging. At a given time point, samples were removed from the buffer solution, blotted dry, frozen in liquid N_2, and lyophilized for three hrs to remove residual water. The pH of the buffer was monitored over time and remained unchanged for the duration of the study.

The ^{1}H NMR spectra of the lyophilized films over the course of the study neither showed significant L:G composition change nor transesterification/sequence-scrambling, similar to the previously-studied sequenced PLGAs. It is notable that in fully random PLGAs, the L:G ratio increases over time as G linkages are cleaved and short-chain oligomers are washed away.[7] ^{1}H NMR spectra of each copolymer in this study did show a decrease in **M** content near the very end of the study, indicating the **L**-**M**-**L** linkages are hydrolysable yet do not limit the lifetimes of these polymers in an aqueous environment. Similarly, the resonance of the syringic acid methoxy protons, initially a singlet at 3.8 ppm, developed a shoulder peak at 3.9 ppm at the very end of the film's lifetime, indicating the **L-Sy-L** linkages are slower to cleave than the pentameric LG sequences.

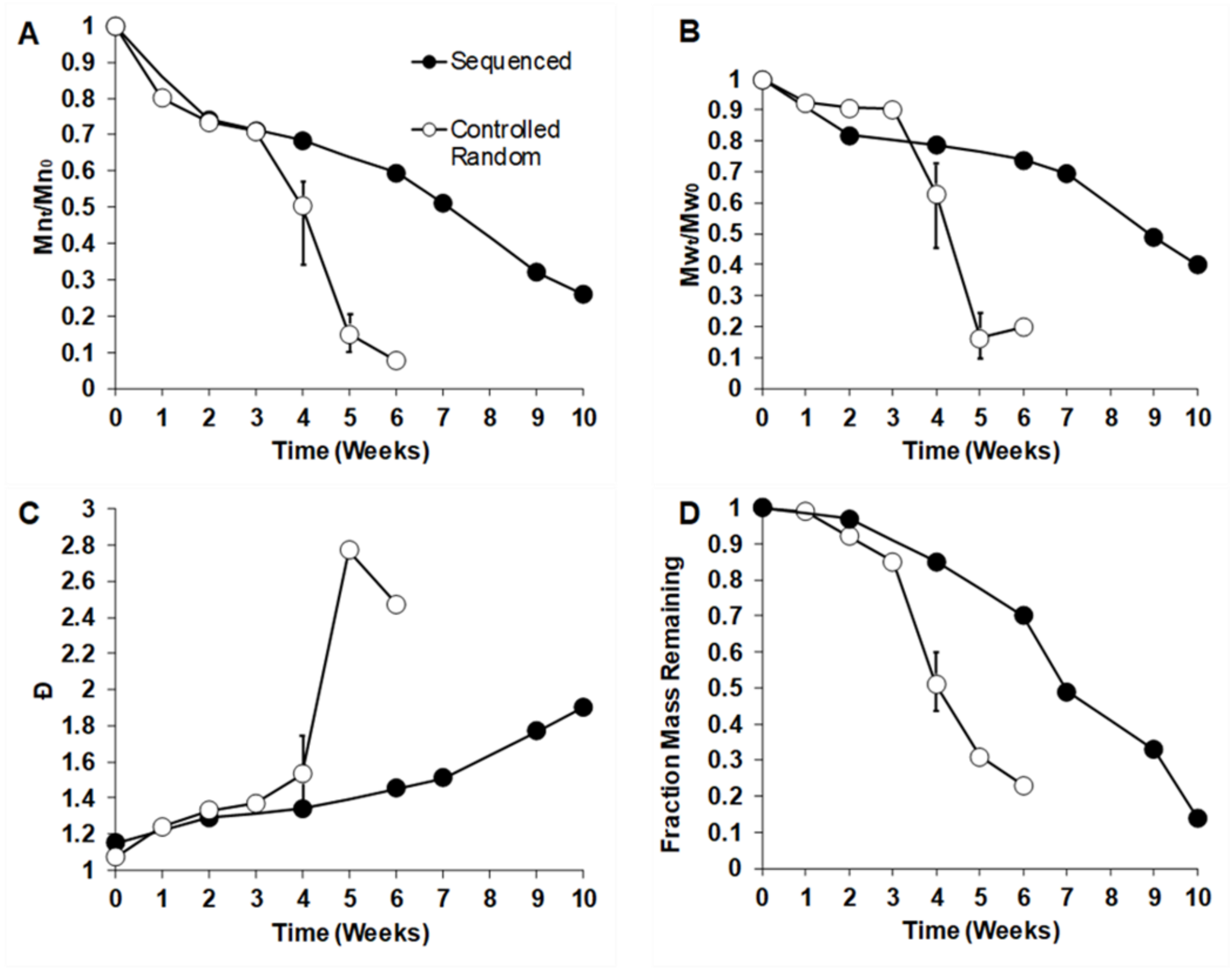

Figure 19. Molecular weight and mass loss profiles of Poly SyLM(LGLGL) and Poly SyLM(L_3G_2): A) number average molecular weight (M_n) loss over time; B) weight average molecular weight (M_w) loss over time; C) dispersity (Đ) over time; and D) film mass loss over time. Range bars are included for sample sets with significant deviations (> 0.1 on y-axis).

3.3.5 Molecular Weight and Mass Loss

In the first three weeks of degradation, the two copolymers behaved similarly in molecular weight loss and mass loss (Figures 19, 20). At Week 4, the degradation profiles become distinct as a sharp drop in the controlled random copolymer's molecular weight results in a larger increase in mass loss, while the precisely sequenced copolymer drops at a more gradual rate. This faster mass loss for the controlled random copolymer is consistent with the formation of a high fraction of short-chain byproducts, similar to the behavior seen in fully random PLGAs.[190]

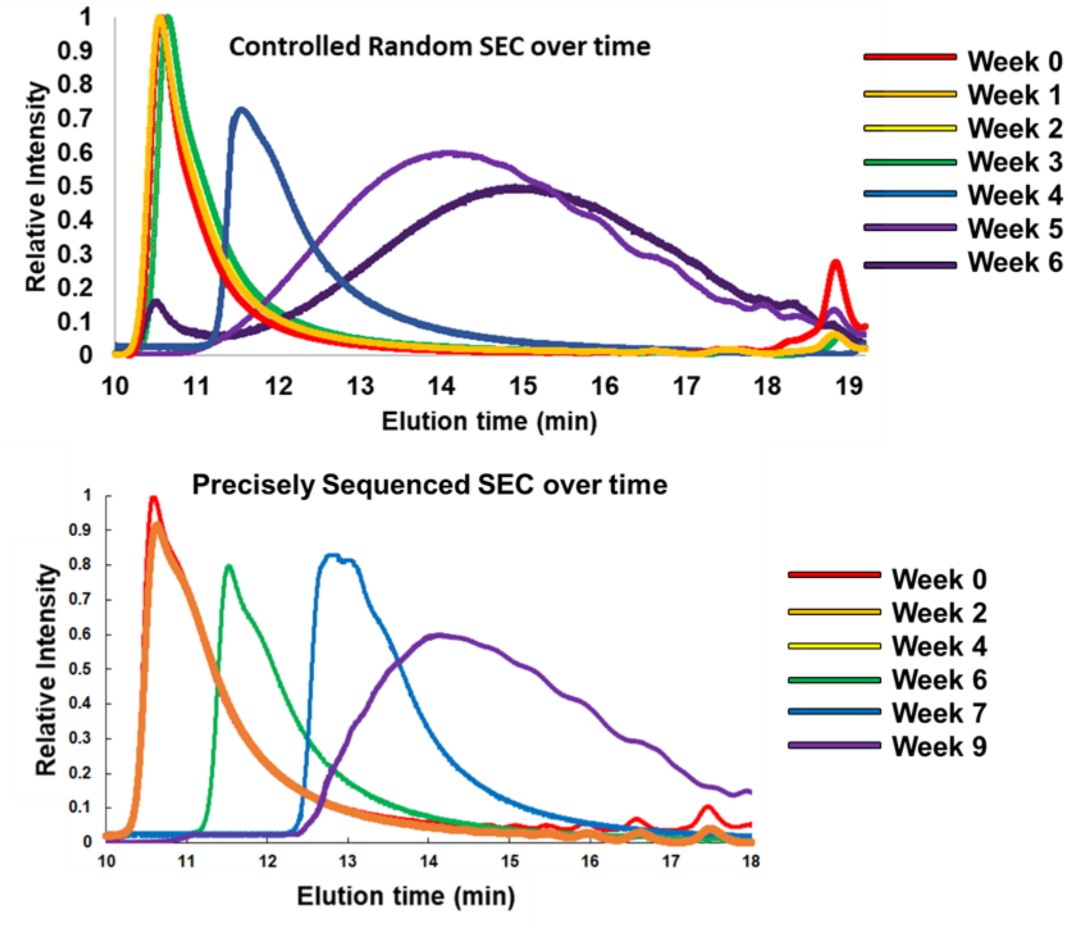

Figure 20. Size exclusion chromatographs during hydrolysis for Poly SyLM(L$_3$G$_2$) (top) and Poly SyLM(LGLGL) (bottom).

3.3.6 Thermal Behavior

The thermal characteristics of the two polymers were monitored by differential scanning calorimetry during the hydrolysis study (Figure 21). Thermograms were collected on the first heating cycle to obtain the native thermal features at a given time point. The initial thermograms of the polymers (Week 0) display identical glass transition temperatures at 50 °C, as expected from the Flory-Fox equation, given their identical monomer composition.[112] Initially, neither displayed crystallization nor melting transitions. Slight degradation of the controlled random copolymer, however, resulted in the development of sharp, low temperature melting transitions near 60 °C. In the sequenced copolymer, no melting transitions are observed and the T_g remains at 50 °C. It should be noted that the unusual shape of the glass transitions is due to an increased short-range ordering of chains upon aging which leads to enthalpic relaxation.[191] The optical transparency of the films correlates well with the thermograms – both films are transparent at Week 0 and the controlled random becomes opaque by Week 1 just as melting transitions appear (Figure 23). The sequenced films remain mostly transparent until approximately Week 7 of hydrolysis.

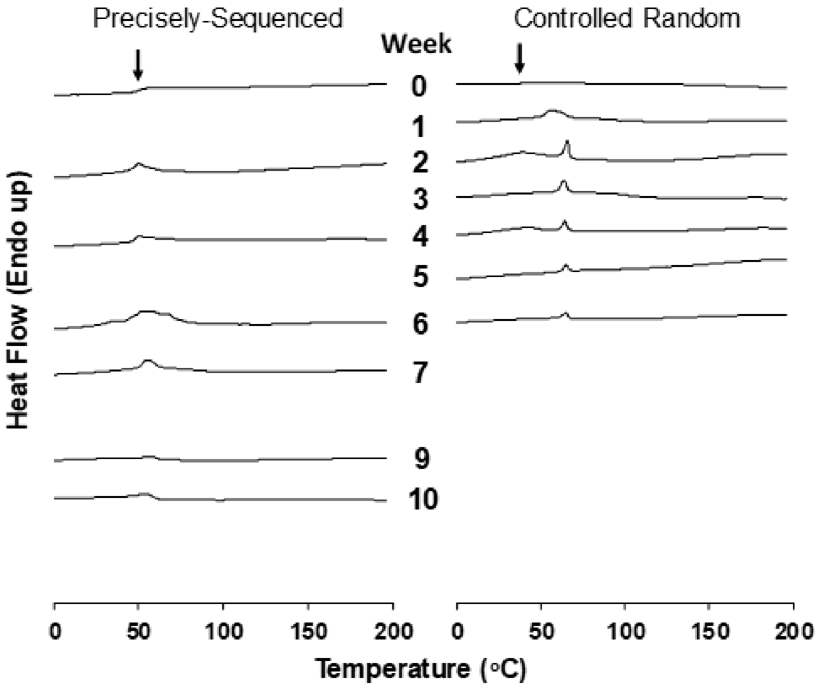

Figure 21. Differential scanning calorimetry thermograms for Poly SyLM(LGLGL) (left) and Poly SyLM(L_3G_2) (right) at each time point during hydrolysis.

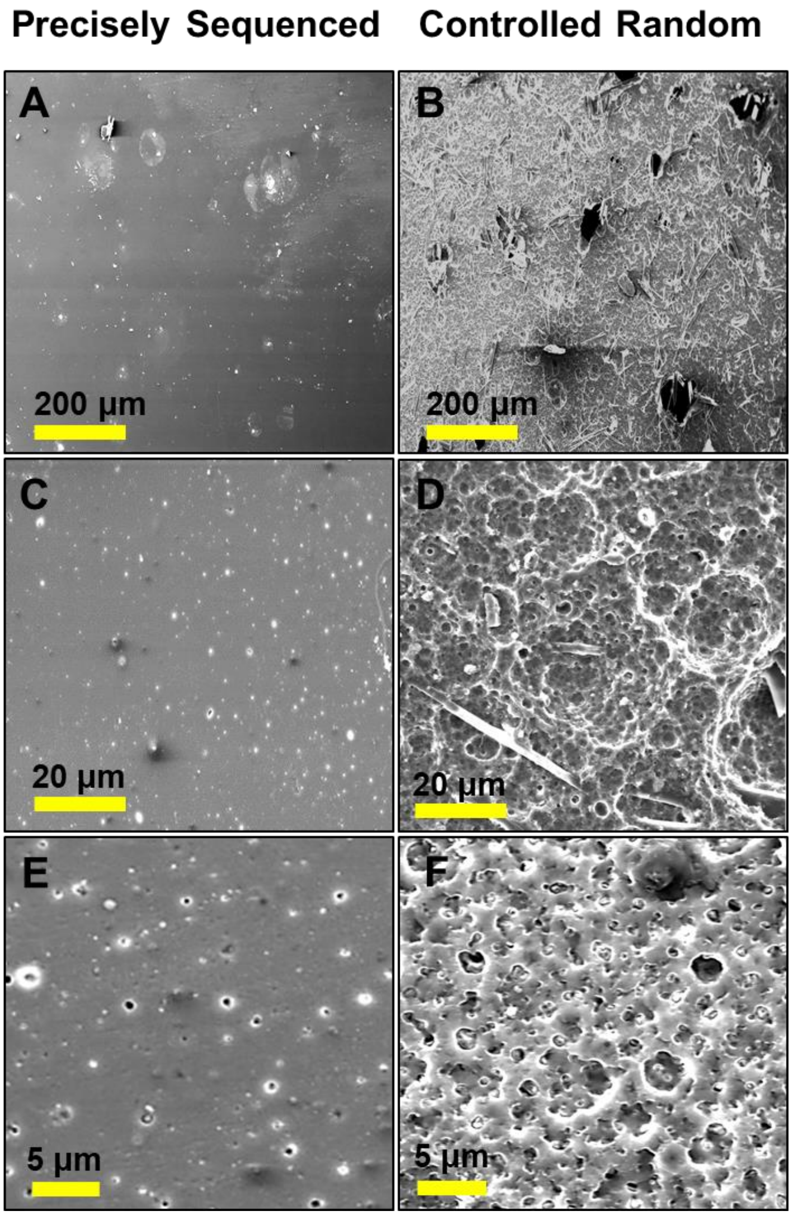
Precisely Sequenced
Controlled Random
A
B
200 µm
200 µm
C
D
20 µm
20 µm
E
F
5 µm
5 µm

Figure 22. Scanning electron microscopy images (secondary ion detection, 10 kEv) of polymer films over the course of hydrolysis. (A) Poly SyLM(LGLGL) at Week 7, ~50% loss of M_n, 100x. (B) Poly SyLM(L_3G_2) at Week 4, ~50% loss of M_n, 100x. (C) Poly SyLM(LGLGL) at Week 7, 1,000x. (D) Poly SyLM(L_3G_2) at Week 4, 1,000x. (E) Poly SyLM(LGLGL) at Week 10, 3,000x. (F) Poly SyLM(L_3G_2) at Week 6, 3,000x. Note the presence of residual buffer salt crystals in SEM-D.

3.3.7 Film Characteristics

The surface features of the thick films were imaged by scanning electron microscopy. Low magnification images (100x) showed the sequenced polymer maintained its native surface uniformity throughout degradation and underwent clean fractures. The controlled random, however, exhibited immediate changes in surface appearance upon hydrolysis and degraded non-uniformly with the development of large voids and micron-sized pores (Figure 22). The bulk portions of films remaining at the end of hydrolysis were flakey and soft, differing from the small, dense particles left for the sequenced copolymer films (Figure 23). The brittle fracture pattern observed for the precisely sequenced copolymer can be explained by the increasing order of the chains during aging.[191] This explanation correlates well with the increased enthalpic relaxation observed in the thermograms.

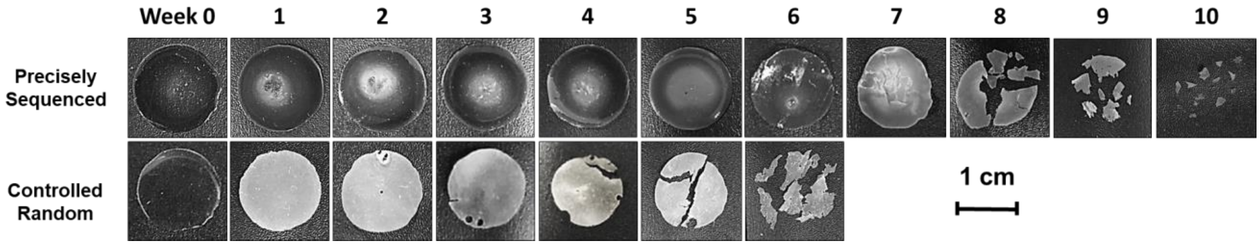

Figure 23. Photographs of copolymer thick films over the course of hydrolysis.

3.4 Discussion

Although we have established previously and have observed in this study that hydrolysis behaviors are extremely sensitive to sequence, we note that not all polymer properties are as sequence-dependent. Specifically, for PLGAs we have found that the pre-hydrolysis bulk and thermal properties are largely independent of monomer sequencing. [113, 139] For instance, while one might expect that the highly ordered structure of a precise polymer could affect the T_g or crystallinity, we have generally observed that polyesters of identical composition but different sequencing display differences in T_g that are so small as to be difficult to differentiate from those that could be attributed to minor variations in molecular weight, thermal history, and plasticization due to humidity.[35, 185] Moreover, despite the high degree of order in the backbone, the periodically sequenced copolymers are often poorly crystalline or amorphous. It is not surprising, therefore, that sequence errors do not result in significant differences in degree of crystallinity.

In contrast with the thermal properties, we have found that the course of hydrolysis is extremely sequence dependent as are the properties of the partially degraded copolymers at each time point. We have shown in our prior studies on related PLGAs that the hydrolytic degradation can be correlated with differences in bond cleavage rates of the monomers, which in turn affect the predominant mechanism of degradation.[35, 36] Bond cleavage in polymer backbones generally proceeds by two mechanisms – intrachain scission, in which a bond is broken in the middle of a chain, and end-chain scission, which most commonly involves back-biting by a reactive end-group.[192] Though both mechanisms act concurrently, the prevalence of one mechanism over the other results in distinctive molecular weight and mass loss profiles.[190] In a primarily chain-end degradation mechanism, molecular weight decreases linearly with accompanying small increases in dispersity. As small molecule byproducts are eliminated, the mass decreases gradually. However, when even a small degree of intrachain scission occurs, rapid molecular weight loss and large increases in dispersity result. Additionally, the fraction of small-chain oligomers that may be eliminated from the polymer matrix rapidly increases, causing a faster mass loss than would be observed for a sample in which chain-end degradation dominates.

We have previously shown, for example, that a simply alternating copolymer, $(LG)_n$, which we name **Poly LG**, exhibits chain-end hydrolysis as its primary mechanism, whereas the random analog of the same composition, **PDLGA-50**, shows significant intrachain cleavage during hydrolysis. This change can be logically correlated with the known kinetic differences in the reactivity with water of the various linkages: G-G > G-L, L-G > L-L.[36] In **PDLGA-50**, the fast-cleaving G-G linkages appear to lead to significant intrachain scission. That being said, it was not clear that G-G cleavage rates were the only factor that affected the hydrolysis profile. A major goal of the current study was, therefore, to isolate short-range monomer connectivity kinetics from other possible contributions, like stereochemistry and micro- or nano-phase separation that could occur in the random copolymer, given the likely presence of longer L-rich and G-rich regions in the statistical chains.

Despite their relatively high degree of homology, differences during hydrolysis between **Poly SyLM(LGLGL)** and **Poly SyLM(L_3G_2)** mimic the scission patterns observed for **Poly LG** and **PDLGA-50**. Based on the rapid increase in dispersity, more rapid mass loss, and the development of low temperature melting transitions, it is clear that the controlled random copolymer produces a larger fraction of small chain oligomers and that the degradation involves significant intrachain scission.[1] For the sequenced copolymer in this work, the lesser and more gradual increase in dispersity and the more gradual mass loss suggest that less intrachain scission occurs during hydrolysis.

We also observe a strong effect of the monomer scrambling in the structure of the films during hydrolysis. In particular, the pore pattern that is observed in the SEM images of the controlled random polymer is consistent with the proposed predominance of intrachain scission cleaving G-G linkages to produce a heterogeneous pattern. Interestingly, however, **PDLGA-50**, which also comprises L- and G-rich regions, does not exhibit an analogous pore structure during degradation but instead plasticizes extensively to give a visually unstructured surface at the 1-10 μm scale.[2] We hypothesize that this difference is a result of the presence of the conformationally-rigid and slower-degrading Sy-L-M linkages after every five monomer units, which limits the population and frequency of hydrolytically-susceptible G-G linkages locally within the chain.

Moreover, when combined with the randomly-occurring L-rich segments, the range of differences in hydrolysis kinetics between regions is accentuated relative to the fully random PLGA. We note that the porous degradation structure observed for the controlled random copolymer could prove useful for applications in which mechanical properties of a scaffolding need to be preserved as long as possible during degradation.

Having previously identified the effectiveness of G-G linkages in altering the hydrolysis behaviors of PLGAs, we originally sought to investigate the magnitude of general sequence sensitivity as a sequenced PLGA becomes slightly randomized. In this study we have observed that PLGA-inspired polyesters are incredibly sensitive to the precision of short-range monomer order, having found that hydrolysis behaviors are changed dramatically by only a small degree of sequence scrambling. The synthetic method we employed effectively capped single monomer repetitions to five units. Therefore, the preparation of a precisely-sequenced and a controlled-random analog represents only a slight shift in the sequenced/randomized continuum (Figure 13, bottom curve).

3.5 Conclusion

To address the tolerance of properties to short range sequence scrambling, we used ED-ROMP to prepare a precisely sequenced polyester comprising lactic, glycolic, and syringic acids along with a copolymer with identical monomer composition but a slightly scrambled monomer sequence. Hydrolysis behaviors were monitored over time to reveal drastic contrasts despite a relatively small difference in precision sequencing. Molecular weight loss was accelerated within the controlled random copolymer and dispersity measurements were consistent with an increased rate of intrachain scission versus the precisely sequenced copolymer. Microscopic pores and larger voids developed within the controlled random copolymer, whereas the precisely sequenced copolymer retained its native surface features to a larger degree throughout the course of degradation.

Lastly, while there exist many comonomer systems to prepare materials with targeted applications, sequence remains an exciting tool for expanding the functional capacity of any given set of comonomers. While synthesis continues to be a bottleneck in the preparation of sequenced materials, semi-sequencing may be used to avoid overly-laborious syntheses. We are continuing our efforts in understanding how sequence errors affect behavior and in identifying properties that depend on sequence but can tolerate error.

3.6 Experimental Section

3.6.1 General Information

All experiments were carried out in oven-dried glassware under N_2 using standard Schlenk line techniques. N,N’-dicyclohexylcarbodiimide (DCC) was purchased from Oakwood Chemical and used without further purification. Palladium, 10wt% (dry basis) on carbon (Pd/C) was purchased from Sigma Aldrich. Methylene chloride (CH_2Cl_2, Fisher) and ethyl acetate (EtOAc, Sigma Aldrich) were purified by a Solvent Dispensing System by J. C. Meyer (neutral alumina columns). Anhydrous, inhibitor-free tetrahydrofuran (THF) and Grubb’s 2nd generation catalyst were purchased from Sigma Aldrich. Syringic acid was purchased from Sigma Aldrich and used with no further purification. Column chromatography was performed using Sorbent Technologies 60 Å, 40-63 µm standard grade silica.

^{1}H (300, 400, 500 MHz) and ^{13}C were obtained using Bruker spectrometers and are reported as δ values in ppm relative to the reported solvent ($CDCl_3$ referenced to 7.26 and 77.16). Splitting patterns are abbreviated as follows: singlet (s), doublet (d), triplet (t), quartet (q), multiplet (m), broad (br), and combinations thereof. HRMS data were obtained on a LC/Q-TOF instrument. Molecular weights and dispersities were obtained on a TOSOH HLC-8320GPC EcoSEC equipped with TSK-3000H and TSK-4000H columns and tetrahydrofuran as mobile phase, relative to polystyrene standards (2.5, 9, 30, 50, 90 kDa).

3.6.2 Experimental Procedures

The preparation of dimers **Bn-LL**, **Bn-GL**, **Bn-GG**, **Bn-LG**, **LL-Si**, **GL-Si**, **GG-Si**, and **LG-Si** were previously reported by our group. The detailed synthesis of **Cyc-SyLMLGLGL** was previously reported.[188]

(L_3G_2)-TBDPS (Tetramer Mixture)

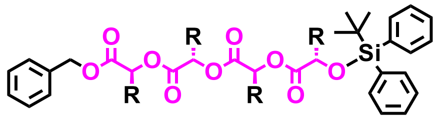

^{1}H-NMR (400 MHz, $CDCl_3$)

δ (ppm)	Mult. (J)	Int.	Assignment
1.09	s	9	TBDPS (tBu)
1.30-1.65	m	9	L (CH_3)
4.25-5.25	m	9	L (CH), G (CH_2), Bn
5.50 – 5.80	m	6	TBDPS
7.35	m	4	TBDPS

^{13}C-NMR (400 MHz, $CDCl_3$)

δ (ppm) + Assignment			
16.58	L (CH_3)	127.73	Arene
16.66	L(CH_3)	128.12	Arene
16.91	L (CH_3)	128.42	Arene
17.02	L (CH_3)	128.61	Arene
19.23	TBDPS (C)	132.96	Arene
26.82	TBDPS (CH_3)	133.40	Arene
60.42	G (CH_2)	135.75	Arene
60.99	G (CH_2)	135.92	Arene
64.28	L (CH)	152.09	Arene
68.50	L (CH)	166.19	G (CO)
69.07	L (CH)	166.30	G (CO)
69.34	L (CH)	169.25	L (CO)
106.65	Arene	170.06	L (CO)
		175.65	L (CO)

Bn-XXXX-Si, X = 3:2 L:G

Bn-LL (2.12 g, 8.40 mmol), Bn-GL (1.00 g, 4.20 mmol), Bn-LG (1.00 g, 4.20 mmol), Bn-GG (3.36 g, 4.20 mmol), LL-Si (3.36 g, 8.40 mmol), GL-Si (1.62 g, 4.20 mmol), LG-Si (1.62 g, 4.20 mmol), and GG-Si (1.56 g, 4.20 mmol) were dissolved in 500 mL DCM. DPTS (1.00 g, 3.40 mmol) was added and allowed to dissolve before the addition of DCC (4.76 g, 23.1 mmol). The reaction was stoppered and allowed to stir at RT overnight. The solution was filtered, concentrated *in vacuo*, and purified by column chromatography using 5% ethyl acetate in hexanes. Product eluted in fractions 3-12 (250 mL fractions). ^{1}H NMR displayed the anticipated 3:2 L:G ratio, 10.03 g yield (65%).

(L_3G_2)-TBDPS (Tetramer Mixture)

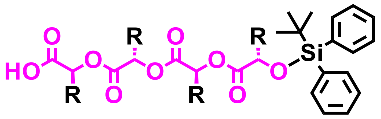

^{1}H-NMR (400 MHz, $CDCl_3$)

δ (ppm)	Mult. (J)	Int.	Assignment
1.09	s	9	TBDPS (tBu)
1.30-1.65	m	9	L (CH_3)
4.25-5.25	m	6	L (CH), G (CH_2)
5.50 – 5.80	m	6	TBDPS
7.35	m	4	TBDPS

^{13}C-NMR (400 MHz, $CDCl_3$)

δ (ppm) + Assignment			
16.58	L (CH_3)	127.73	Arene
16.66	L(CH_3)	132.96	Arene
16.91	L (CH_3)	133.40	Arene
17.02	L (CH_3)	135.75	Arene
19.23	TBDPS (C)	135.92	Arene
26.82	TBDPS (CH_3)	152.09	Arene
60.42	G (CH_2)	166.19	G (CO)
60.99	G (CH_2)	166.30	G (CO)
64.28	L (CH)	169.25	L (CO)
68.50	L (CH)	170.06	L (CO)
69.07	L (CH)	175.65	L (CO)
69.34	L (CH)		
106.65	Arene		

XXXX-Si, X = 3:2 L:G

Bn-XXXX-Si (8.50 g, 13.7 mmol) was dissolved in 140 mL ethyl acetate in a Schlenk flask to prepare a 0.1 M solution. Pd/C (0.850 g, 10% by mass) was added, and two balloons of H_2 (g) were passed through the flask. A third balloon was attached to serve as a source of excess H_2 (g). The reaction was stirred at RT overnight. The solution was then filtered through a thick pad of celite and concentrated to provide the pure product, 8.5 g yield (90%).

Bn-(L_3G_2)-TBDPS (Pentamer Mixture)

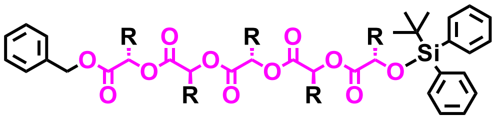

^{1}H-NMR (400 MHz, $CDCl_3$)

δ (ppm)	Mult. (J)	Int.	Assignment
1.09	s	9	TBDPS (tBu)
1.30-1.65	m	9	L (CH_3)
4.25-5.25	m	9	L (CH), G (CH_2), Bn (CH_2)
5.50 – 5.80	m	11	TBDPS, Bn
7.35	m	4	TBDPS

^{13}C-NMR (400 MHz, $CDCl_3$)

δ (ppm) + Assignment			
16.58	L (CH_3)	127.73	Arene
16.66	L(CH_3)	128.12	Arene
16.91	L (CH_3)	128.42	Arene
17.02	L (CH_3)	128.61	Arene
19.23	TBDPS (C)	129.44	Arene
26.82	TBDPS (CH_3)	132.96	Arene
60.42	G (CH_2)	133.40	Arene
60.99	G (CH_2)	135.75	Arene
64.28	L (CH)	135.92	Arene
67.01	Bn (CH_2)	152.09	Arene
68.50	L (CH)	166.19	G (CO)
69.07	L (CH)	166.30	G (CO)
69.34	L (CH)	169.25	L (CO)
106.65	Arene	169.82	L (CO)
		170.06	L (CO)
		175.65	L (CO)

Bn-L_3G_2-Si

Bn-L (1.31 g, 7.32 mmol (0.60 eq.), **Bn-G** (0.815 g, 4.88 mmol, 0.4 eq.), and **XXXX-Si** (8.5 g, 12.2 mmol) were dissolved in 125 mL DCM. DPTS (0.718 g, 2.44 mmol) was added and allowed to dissolve before the addition of DCC (2.75 g, 13.4 mmol). The reaction was stoppered and allowed to stir at RT overnight. The solution was filtered, concentrated *in vacuo*, and purified by column chromatography using 5% ethyl acetate in hexanes. Product eluted in fractions 2-7 (250 mL fractions). ^{1}H NMR displayed the anticipated 3:2 L:G ratio, 9.01 g yield (85%).

(L_3G_2)-TBDPS (Pentamer Mixture)

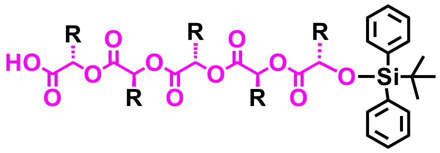

^{1}H-NMR (400 MHz, $CDCl_3$)

δ (ppm)	Mult. (J)	Int.	Assignment
1.09	s	9	TBDPS (tBu)
1.30-1.65	m	9	L (CH_3)
4.25-5.25	m	7	L (CH) and G (CH_2) region
5.50 – 5.80	m	6	TBDPS
7.35	m	4	TBDPS

^{13}C-NMR (400 MHz, $CDCl_3$)

δ (ppm) + Assignment

16.58	L (CH_3)	127.73	Arene
16.66	L(CH_3)	129.44	Arene
16.91	L (CH_3)	132.96	Arene
17.02	L (CH_3)	133.40	Arene
19.23	TBDPS (C)	135.75	Arene
26.82	TBDPS (CH_3)	135.92	Arene
60.42	G (CH_2)	152.09	Arene
60.99	G (CH_2)	166.19	G (CO)
64.28	L (CH)	166.30	G (CO)
68.50	L (CH)	169.25	L (CO)
69.07	L (CH)	169.82	L (CO)
69.34	L (CH)	170.06	L (CO)
106.65	Arene	175.65	L (CO)

L_3G_2-Si

Bn-L_3G_2-Si (9.01 g, 10.4 mmol) was dissolved in 100 mL ethyl acetate in a Schlenk flask to prepare a 0.1 M solution. Pd/C (0.901 g, 10% by mass) was added, and two balloons of H_2 (g) were passed through the flask. A third balloon was attached to serve as a source of excess H_2 (g). The reaction was stirred at RT overnight. The solution was then filtered through a thick pad of celite and concentrated to provide the pure product, 6.05 g yield (88%).

Bn-SyLM(L_3G_2)-TBDPS (Mixture)

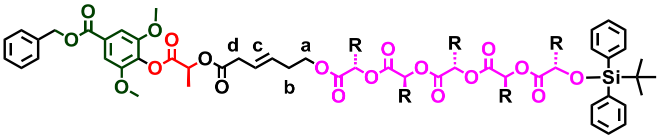

^{1}H-NMR (400 MHz, $CDCl_3$)

δ (ppm)	Mult. (J)	Int.	Assignment
1.09	s	9	TBDPS (tBu)
1.30-1.65	m	12	L (CH_3)
2.35	m	2	**b**
3.16	m	2	**d**
3.87	s	6	Sy (OCH_3)
4.15	m	2	**a**
5.38	s	2	Bn CH_2
4.40 – 5.50		7	L (CH) and G (CH_2) region
5.50 – 5.80	m	2	**c**
7.35	m	13	Sy (arene) + TBDPS + Bn
7.65	m	4	TBDPS

^{13}C-NMR (400 MHz, $CDCl_3$)

δ (ppm) + Assignment			
16.58	L (CH_3)	69.57	**a**
16.66	L(CH_3)	106.65	Arene
16.91	L (CH_3)	124.51	**c**
17.02	L (CH_3)	127.73	Arene
19.23	TBDPS (C)	129.44	Arene
26.82	TBDPS (CH_3)	133.38	**c**
31.69	**b**	132.96	Arene
37.77	**d**	133.40	Arene
56.46	Sy (OCH_3)	135.75	Arene
60.42	G (CH_2)	135.92	Arene
60.99	G (CH_2)	152.05	Arene
64.28	L (CH)	152.09	Arene
68.50	L (CH)	166.08	Sy (CO)
69.07	L (CH)	166.19	G (CO)
69.34	L (CH)	166.30	G (CO)
69.57	**a**	167.90	M (CO)
106.65	Arene	169.25	L (CO)
124.51	**c**	169.82	L (CO)
		170.06	L (CO)
		175.65	L (CO)

Bn-SyLM(L_3G_2)-Si

Bn-SyLM (2.00 g, 4.22 mmol) , and **L_3G_2-Si** (2.37 g, 4.01 mmol) were dissolved in 40 mL DCM. DPTS (0.237 g, 1.1 mmol) was added and allowed to dissolve before the addition of DCC (0.912 g, 5.78 mmol). The reaction was stoppered and allowed to stir at RT overnight. The solution was filtered, concentrated *in vacuo*, and purified by column chromatography using 10% ethyl acetate in hexanes. Product eluted in fractions 7-15 (250 mL fractions). ^{1}H NMR spectrum displayed the anticipated 3:2 L:G ratio, 3.70 g yield (85%).

SyLM(L_3G_2)-TBDPS (Mixture)

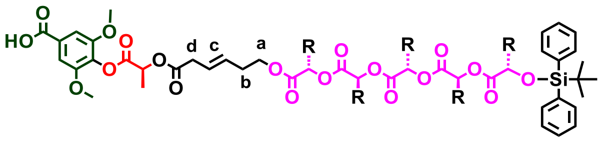

δ (ppm)	Mult. (J)	Int.	Assignment
^{1}H-NMR (400 MHz, $CDCl_3$)			
1.09	s	9	TBDPS (tBu)
1.30-1.65	m	12	L (CH_3)
2.35	m	2	**b**
3.16	m	2	**d**
3.87	s	6	Sy (OCH_3)
4.15	m	2	**a**
4.40 – 5.50	m	7	L (CH) and G (CH_2) region
5.50 – 5.80		2	**c**
7.35	m	2	Sy (arene)

^{13}C-NMR (400 MHz, $CDCl_3$)

δ (ppm) + Assignment			
16.58	L (CH_3)	69.57	**a**
16.66	L(CH_3)	106.65	Arene
16.91	L (CH_3)	124.51	**c**
17.02	L (CH_3)	127.73	Arene
19.23	TBDPS (C)	129.44	Arene
26.82	TBDPS (CH_3)	133.38	**c**
31.69	**b**	152.09	Arene
37.77	**d**	166.08	Sy (CO)
56.46	Sy (OCH_3)	166.19	G (CO)
60.42	G (CH_2)	166.30	G (CO)
60.99	G (CH_2)	167.90	M (CO)
64.28	L (CH)	169.25	L (CO)
68.50	L (CH)	169.82	L (CO)
69.07	L (CH)	170.06	L (CO)
69.34	L (CH)	175.65	L (CO)
69.57	**a**		
106.65	Arene		
124.51	**c**		

SyLM(L_3G_2)-Si

A 0.60 M solution of **Bn-SyLM(L_3G_2-Si)** (3.70 g, 3.40 mmol) was prepared in DCM. A 0.60 M solution of palladium (II) acetate (0.034 g, 0.153 mmol), triethylamine (66 µL, 0.459 mmol), and triethylsilane (758 µL, 4.76 mmol) was prepared and allowed to stir for 30 min. The solution of **Bn-SyLM(L_3G_2)-Si** was then added dropwise over the course of 5 min. The reaction was allowed to stir at RT overnight. The solution was quenched with 20 mL saturated aqueous ammonium chloride solution and the organic layer was extracted 3x with DCM. The organics were dried with magnesium sulfate, filtered, and concentrated *in vacuo* to yield the crude product as a yellow oil. The product was purified by column chromatography using 10% ethyl acetate in hexanes to yield pure product as a white solid (2.26 g, 70%). ^{1}H NMR spectrum displayed a slight alteration of L:G ratio to 3:1.94.

SyLM(L$_3$G$_2$) (Mixture)

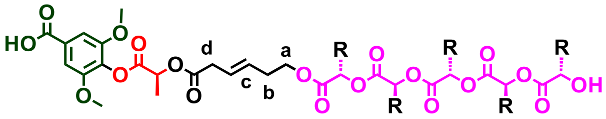

^{1}H-NMR (400 MHz, CDCl$_3$)

δ (ppm)	Mult. (J)	Int.	Assignment
1.30-1.65	m	12	L (CH$_3$)
2.35	m	2	**b**
3.16	m	2	**d**
3.80	s	6	Sy (OCH$_3$)
4.15	m	2	**a**
4.40 – 5.50	m	7	L (CH) and G (CH$_2$) region
5.50 – 5.80		2	**c**
7.35	m	2	Sy (arene)

^{13}C-NMR (400 MHz, CDCl$_3$)

δ (ppm)	Assignment	δ (ppm)	Assignment
16.58	L (CH$_3$)	127.73	Arene
16.66	L(CH$_3$)	129.44	Arene
16.91	L (CH$_3$)	132.38	**c**
17.02	L (CH$_3$)	152.09	Arene
31.69	**b**	165.08	Sy (CO)
37.77	**d**	166.19	G (CO)
56.43	Sy (OCH$_3$)	166.30	G (CO)
60.42	G (CH$_2$)	167.90	M (CO)
60.97	G (CH$_2$)	169.25	L (CO)
64.32	L (CH)	169.82	L (CO)
68.50	L (CH)	170.06	L (CO)
69.07	L (CH)	175.65	L (CO)
69.33	L (CH)		
69.57	**a**		
106.65	Arene		
124.51	**c**		

SyLM(L$_3$G$_2$)

SyLM(L$_3$G$_2$)-Si (2.26 g, 2.38 mmol) was dissolved in 25 mL THF to prepare a 0.1 M solution. The flask was cooled to 0 °C. TBAF (3.57 mL as a 1.0 M solution in THF, 3.57 mmol) was added to a vial and acetic acid (0.25 mL, 4.04 mmol) was added. The vial was vortexed briefly and this solution was added steadily to the solution of starting material. The reaction was warmed to RT over the course of 1 hr and the reaction was quenched with 20 mL brine. The organics were extracted 3x with ethyl acetate, were dried with magnesium sulfate, filtered, and concentrated *in vacuo* to provide the crude product as a yellow oil. The product was purified by column chromatography (25% ethyl acetate in hexanes increased gradually to 90% ethyl acetate in hexanes). The product was a white solid (1.05 g, 60%). ^{1}H NMR spectrum displayed an altered L:G ratio of 3:1.88.

Cyc-SyLM(L_3G_2) (Mixture)

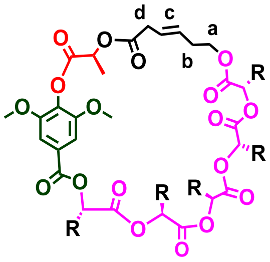

Cyc-SyLM(L_3G_2)
R = 3:2 Me:H

^{1}**H-NMR** (400 MHz, $CDCl_3$)

δ (ppm)	Mult. (J)	Int.	Assignment
1.30-1.65	m	12	L (CH_3)
2.35	m	2	**b**
3.16	m	2	**d**
3.80	s	6	Sy (OCH_3)
4.15	m	2	**a**
4.40 – 5.50	m	7	L (CH) and G (CH_2) region
5.50 – 5.80		2	**c**
7.35	m	2	Sy (arene)

^{13}**C-NMR** (400 MHz, $CDCl_3$)

δ (ppm)	Assignment	δ (ppm)	Assignment
16.58	L (CH_3)	127.73	Arene
16.66	L(CH_3)	129.44	Arene
16.91	L (CH_3)	132.38	**c**
17.02	L (CH_3)	152.09	Arene
31.69	**b**	165.08	Sy (CO)
37.77	**d**	166.19	G (CO)
56.43	Sy (OCH_3)	166.30	G (CO)
60.42	G (CH_2)	167.90	M (CO)
60.97	G (CH_2)	169.25	L (CO)
64.32	L (CH)	169.82	L (CO)
68.50	L (CH)	170.06	L (CO)
69.07	L (CH)	175.65	L (CO)
69.33	L (CH)		
69.57	**a**		
106.65	Arene		
124.51	**c**		

HRMS (ESI)

Calc Mass $[M+H]^+$ (amu)	Found (amu)
655.12	
669.15	669.14
683.17	683.13
697.20	697.20
711.22	711.20
725.25 amu	725.21

Cyc-SyLM(L_3G_2)

SyLM(L_3G_2) (1.05 g, 1.42 mmol) was dissolved in 25 mL dichloroethane and injected to a solution of DCC (0.510 g, 2.80 mmol) and DPTS (0.132 g, 0.450 mmol) in 225 mL dichloroethane at 60 °C over a span of 16 hrs. The solution was allowed to stir for an additional 24 hrs before being filtered and concentrated to obtain the crude product. A column loaded with 15% ethyl acetate in hexanes was used to purify the product (0.824 g, 88%), a white solid. ^{1}H NMR spectrum displayed no alteration in L:G ratio, 3:1.88.

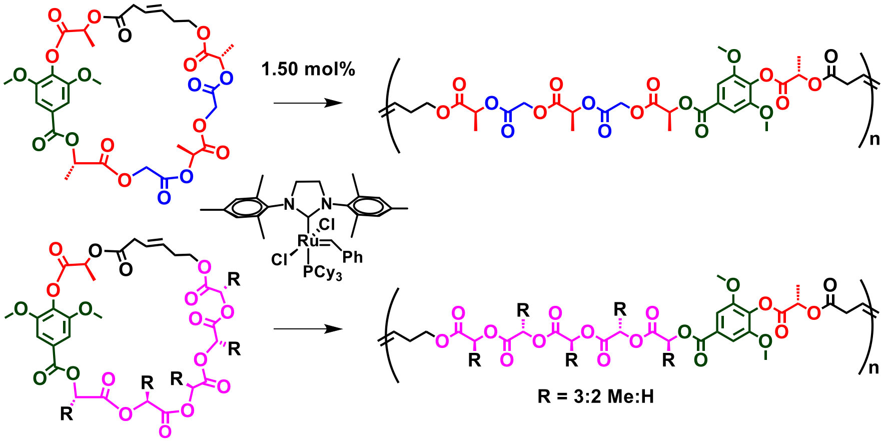

Poly SyLMLGLGL and Poly SyLM(L_3G_2)

The polymerizations were performed in 20 mL vials with dry DCM obtained from the solvent system. The solvent was sparged with nitrogen for 10 min prior to use. Grubbs II was weighed (7.38 mg for sequenced and 9.63 mg for random, 1.50 mol% each) and taken up in 1/2 of the required volume of DCM for each reaction (0.403 g sequenced monomer, 0.526 g random monomer, 0.414 mL for sequenced and 0.504 for the random). The same volume of methylene chloride was used to dissolve each respective monomer before the catalyst solution was added (final volume for sequenced: 0.828 mL and 1.08 mL for random, 0.7 M solutions). The vials were purged with nitrogen and sealed. Within 20 min, both solutions became very viscous. The reactions were left for 4 hrs before quenching with 0.05 mL of ethyl vinyl ether. The vials were then concentrated *in vacuo* and placed in a vacuum chamber overnight. NMR spectra and SEC traces were collected on the following day. The sequenced copolymer showed small amounts of cyclic species. The polymers were reprecipitated in 600 mL methanol (in an ice bath) and allowed to stir for a half hour before filtering.

Solution Casting of Thick Polymer Films

The polymers (200 mg) were dissolved in 2.000 mL of methylene chloride to make a 100 mg/mL solution using a 100-1000 uL micropipettor. On 1.25 cm glass microscope cover slides, 115 uL of this solution was cast onto each (with a 10-200 uL micropipettor), very carefully to create a convex droplet that covered the entire surface. The best films were prepared by first coating the perimeter of the slide and then filling in the middle. The solution was allowed to dry on the slides for 3 hrs before being placed in a vacuum chamber. After 2 days, those films that contained bubbles were removed from the glass slides using a razor blade and re-dissolved to prepare a 100 mg/mL solution. The procedure was repeated on these 8. Films used for the hydrolysis study contained no bubbles, tears, or noticeable defects. The films were tan and transparent.

Film thicknesses were measured on representative films cut through the center using optical profilometry. A Bruker Contour Elite I optical profilometer was used. Samples were sliced to create a step indicative of film thickness and then analyzed.

Hydrolysis Study

Polymer films, removed from glass slides, were placed in scintillation vials followed by the addition of 15 mL 10x phosphate buffer solution, pH = 7.4 The vials were capped and placed in an incubator set at 37 °C. The films were placed on a rotating platform with a slow speed of 8 rpm to promote gentle mixing and to prevent localized concentration of acidic monomer around the films. The pH of the buffer solution was monitored over time and showed no distinguishable change. When timepoints were collected, the appropriate films were removed from the incubator, removed from the buffer solution, and blotted dry with a paper towel. Photographs were taken of each film at this point. The films were then rinsed with deionized water, blotted dry again and placed in new vials. Liquid N_2 was poured over the films and the films were lyophilized for several hrs. The masses of dried films were then collected using an analytical balance and recordings were documented when readings stabilized for at least 15 s. A ¼ pie slice of each film was used for SEC analysis (~3 mg) and DSC analysis.

4.0 The Consequences of Accumulating Critical Monomer Errors on the Hydrolysis Behaviors of Degradable Sequenced Polyesters

4.1 Overview

The work described in this chapter is to be submitted for publication in the Royal Society of Chemistry's journal Polymer Chemistry as a communication entitled "*The Consequences of Accumulating Critical Monomer Errors on the Hydrolysis Behaviors of Degradable Sequenced Polyesters*." Jordan H. Swisher is listed as a contributing author on this publication for his assistance in the preparation of starting materials, experimental design, and scientific discussions. In this chapter, precise quantities of a critical sequence error are doped into a sequenced, primarily alternating polyester and the degree to which hydrolysis behaviors are affected by this distinct and potent sequence-error is quantified. The degradation rate proved tolerant to substitutions up to 1% of the monomers but accelerated significantly when the error population was larger.

4.2 Introduction

Despite the known sensitivity to sequence mutations of biological polymers, little is known about the effects of errors in sequenced synthetic copolymers (Figure 24). The degradation behaviors of copolyesters, for example, are known to depend on monomer-by-monomer order, yet the contribution of isolated monomer substitutions on hydrolysis behaviors has not been studied.

We have developed a synthetic method in which precise quantities of a critical sequence error are doped into a sequenced polyester and studied how hydrolysis behaviors are affected by this distinct and potent sequence-error dopant. Sensitivity was found to be significant with degradation rates increasing with monomer substitution rates as low as 1%.

Single monomer substitution errors in natural biomacromolecules are known to affect function, but synthetic polymer chemists are far behind Nature in synthesizing sequence-controlled polymers (SCPs) to understand the severity to which small populations of monomer sequence errors may dominate a material's performance.[193] An impressive body of work exists in the study of how single site mutations in proteins and foldamers affect structure and function,[194] yet studies of this type relating to synthetic copolymers remain scarce in the literature. In addition to characterizing the negative consequences of error introduction, such studies could also broaden the range of function for a given library of monomers through deliberate error doping with a property-dominating segment.

Several instances have been reported in which extremely small populations of a sequence alteration dominates properties. The extent to which a minor sequence variation may affect properties is studied most regularly in the scope of solution-phase properties, particularly in polymer folding,[21, 69-71] aggregation,[22, 72-78] and molecular recognition.[79-82] In the bulk phase, this phenomenon is less studied, but notable examples include the work of Winey and co-workers who determined that small alterations in sidechain spacing can affect morphological order in ionomers,[83-86] Jannasch and co-workers who described the sensitivity of proton conductivity to small deviations in monomer spacing,[87] and Segalman and co-workers who described the dependence of surface structure and hydration of polypeptoids on the positioning of discrete sequences within a chain.[88]

Our group has established that a wide range of hydrolysis behaviours of poly(lactic-*co*-glycolic acid)s (PLGAs) are highly sequence-dependent, including degradation rates, guest molecule release, internal pH, and water uptake of devices made from this material.[35-37] We have not, however, probed the effects of isolated and accumulating errors on the behaviour of these materials. It is important to note that in bioengineering, bioresorbable polyesters such as PLGAs are rich in application, serving as drug delivery vehicles, cell scaffolds, degradable sutures, and osteofixation devices. The necessity of functional variation for this class of material is limited only by the diversity of biological systems.[2-4, 7, 9, 10, 101] In this endeavour we hope to establish design factors in the engineering of tailored bioresorbable polyesters.

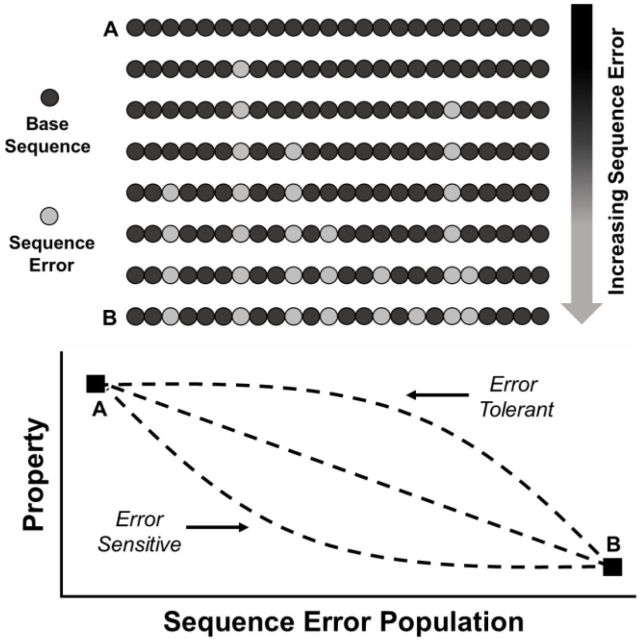
A
B
Base Sequence
Sequence Error
Increasing Sequence Error
A
Error Tolerant
Property
Error Sensitive
B
Sequence Error Population

Figure 24. Sequence tolerance pathways as a function of errors in a sequence-controlled polymer.

4.3 Results and Discussion

For the current studies, we have employed entropy-driven ring-opening metathesis polymerization (ED-ROMP) for the synthesis of the sequenced materials. In prior studies, we have prepared periodic copolymers by step-growth coupling of pre-formed sequenced oligomers. ED-ROMP, which involves the ring-opening of an unstrained macromonomer that includes a sequenced segment, offers important benefits in terms of molecular weight control, reproducibility, dispersity minimization, and scalability.[188] Although ED-ROMP polymers necessarily include linker segments in addition to the sequenced portion, these benefits are crucial to characterizing often subtle property changes connected with introduction of errors.

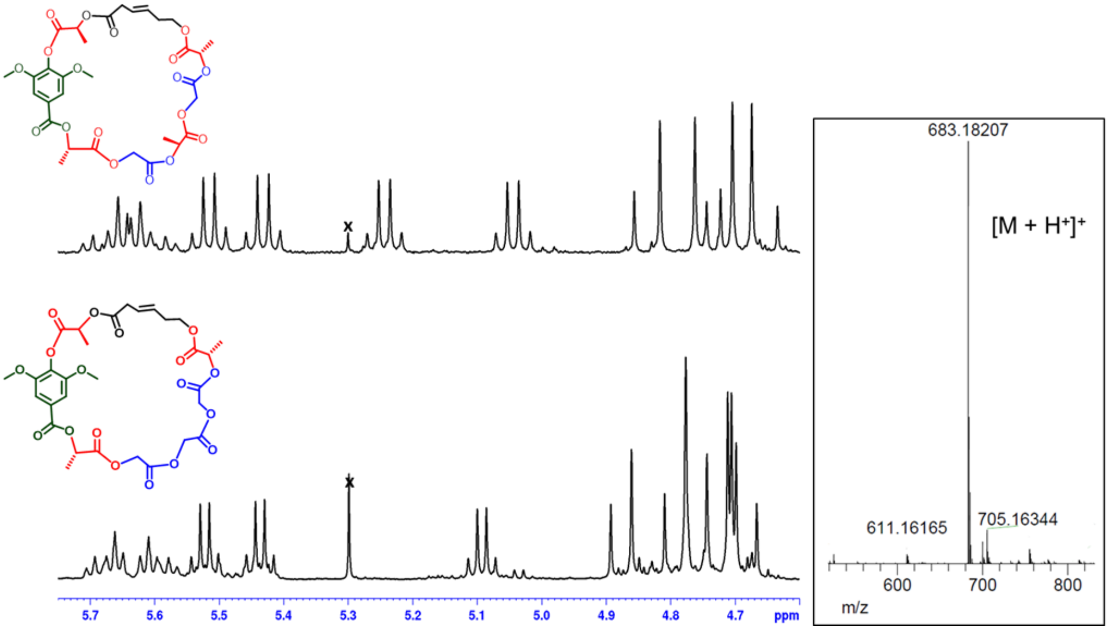

Figure 25. (Top) ^{1}H NMR spectra of G-methylene, L-methyne, and M-olefin protons of Cyc-SyLMLGLGL (top) and Cyc-SyLMLGGGL (bottom) with HRMS spectrum.

In our prior studies on PLGAS, the most dramatic deviation in behaviour during hydrolysis was observed when random-sequence PLGA and the alternating sequence prepared by our group, which we named **Poly LG**, were compared. We identified that glycolic-glycolic (G-G) linkages were a key factor in determining the hydrolytic profile of PLGAs and similar copolymers, but we wished to more precisely quantify this sequence tolerance. In the current study we will address this question by preparing copolymers that consist of a repeating unit bearing a metathesis-active unit (**M**), a syringic acid unit to elevate T_g (**Sy**), and a PLGA pentamer. To introduce errors we vary the proportion of macromonomers that include a perfectly sequenced LGLGL segment and one that includes the dopant LGGGL segment, i.e., the errormer (Figure 25).

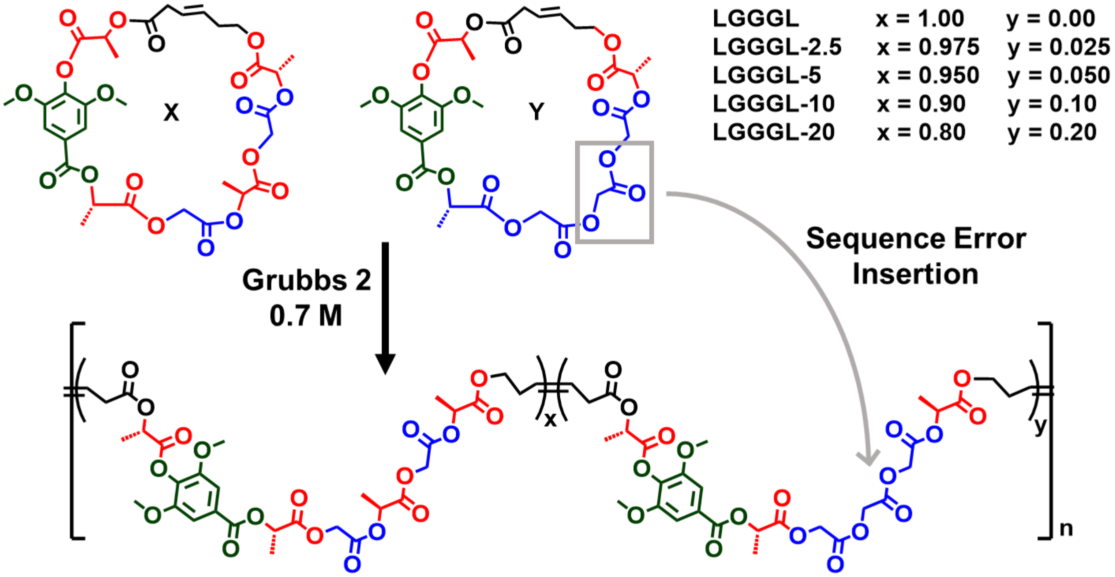
X
Y
LGGGL x = 1.00 y = 0.00
LGGGL-2.5 x = 0.975 y = 0.025
LGGGL-5 x = 0.950 y = 0.050
LGGGL-10 x = 0.90 y = 0.10
LGGGL-20 x = 0.80 y = 0.20
Sequence Error Insertion
Grubbs 2
0.7 M
x
y
n

Scheme 8. Polymerization of mixtures of macrocycles to prepare a sequenced polyester with varying errormer dopant.

The macrocyclic monomers (Scheme 8) were prepared using previously reported methods that include sequential ester couplings, orthogonal protections, and deprotections.[139, 185] Benzyl (Bn) protected oligomer **Bn-SyLM** was coupled to either silyl-protected **LGLGL-Si** or **LGGGL-Si** (Si = TBDPS). Sequential benzyl and silyl deprotections yielded the respective open-chain hydroxy-acid oligomers that were ring-closed under dilute lactonization conditions to yield the cyclic macromonomers. Prior to polymerization, the macromonomers were combined in dichloromethane to prepare mixtures containing 0, 2.5, 5, 10, and 20 mol% of **LGGGL** error dopant. The mixtures were subjected to ED-ROMP with 1.50 mol% Grubbs second generation catalyst (Table 1).

Table 2. Error-doped polymer molecular weight data.

Polymer	M_n (kDa)	M_w (kDa)	Đ
LGLGL	54	66	1.22
LGGGL-2.5	54	66	1.22
LGGGL-5	50	61	1.23
LGGGL-10	50	61	1.24
LGGGL-20	49	60	1.24

The errormer mole percentages correspond to an average of 0, 3.2, 6.3, 12.6, 25.2 substitution errors per chain, where average degree of polymerization is 530 (50 kDa). The five copolymers are named by their error content, e.g. **LGLGL** contains only the base alternating sequence and **LGGGL-5** contains 5 mol% errormer. Due to the unsymmetric design of the macrocyclic monomers, the resulting copolymers contain statistical head-tail disorder at each olefin connectivity as evidenced by the olefin region in the ^{1}H NMR spectra. More importantly, however, the monomer-by-monomer linkages were not affected by the polymerization.[188]

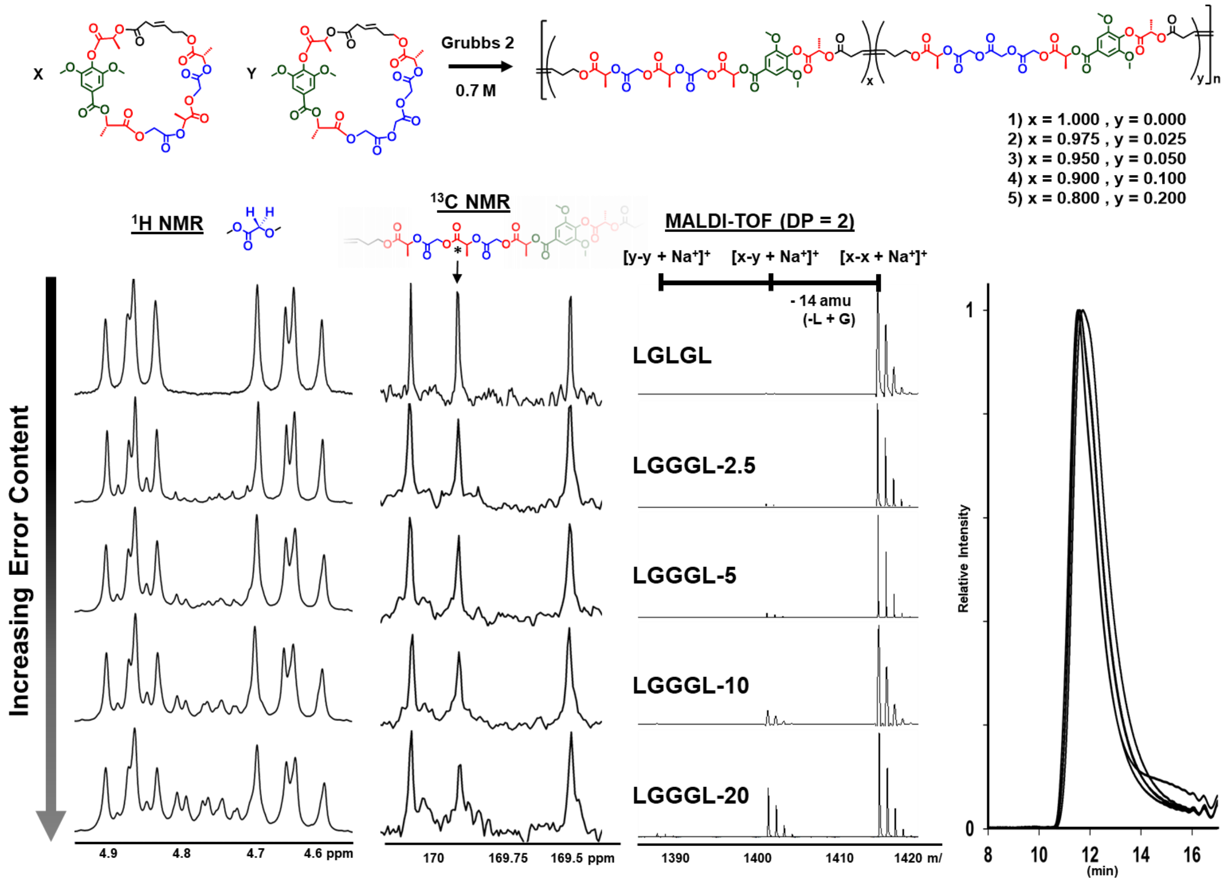

Figure 26. Sequence characterization of the five copolymers, including ^{1}H NMR spectral region of the diastereotopic G methylene protons, ^{13}C NMR spectra of the central L monomer in the base alternating sequence, MALDI-TOF spectra, and size exlclusion chromatographs.

Typically, the degree of sequence fidelity of PLGA-like copolymers can be quantified in the 4.5-5.0 ppm region in ^{1}H NMR spectra, where the signal of the incredibly sensitive, diastereotopic G-methylene protons appears (Figure 26). Additionally, the ^{13}C spectra showed a gradual decrease in the sharpness and intensity of the central L carbonyl carbon in the LGLGL segment. MALDI-TOF mass spectra of the copolymers was consistent with the degree of error incorporation targeted. In particular, low molecular weight dimers showed a clear statistical distribution of errors. Although it is challenging to use mass spectrometry for quantification, in this case the dimeric species are sufficiently similar in composition that their representation in the spectrum should correlate well with the representation in the original sample. Extrapolation of these mass data paired with the ^{1}H NMR spectra indicated that the error dopant was randomly and quantitatively incorporated during the polymerizations.

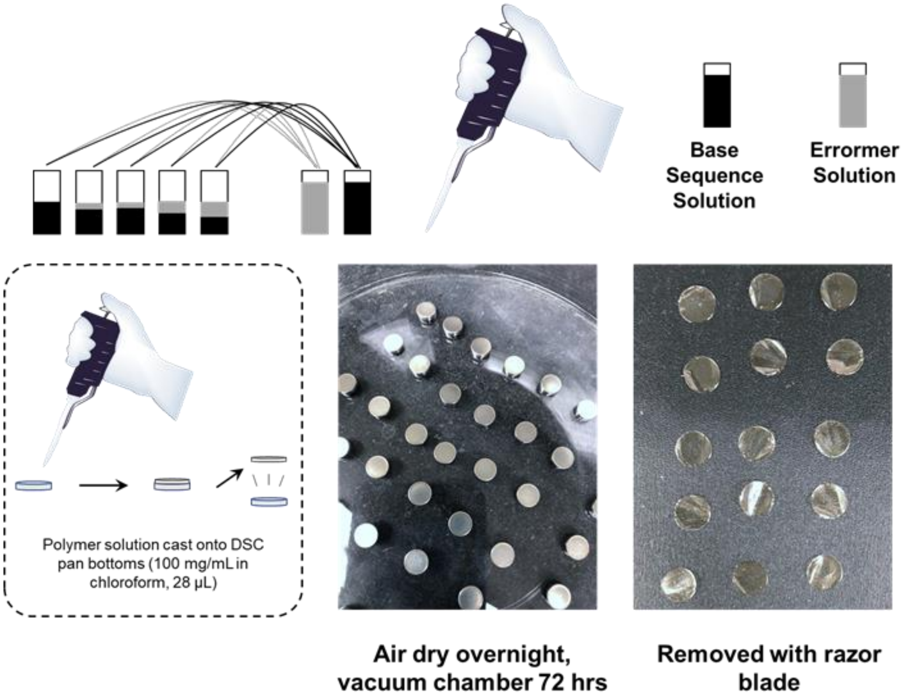
Base Sequence Solution
Errormer Solution
Polymer solution cast onto DSC pan bottoms (100 mg/mL in chloroform, 28 µL)
Air dry overnight, vacuum chamber 72 hrs
Removed with razor blade

Figure 27. Cartoon depiction of the preparation of macromonomer solution mixtures, solution casting, and photographs of films before and after delamination from aluminum bases.

Thick polymer films of 7.5 mm diameter were prepared by solution casting 28 µL of a 100 mg/mL solution onto a circular aluminium base (Figure 27). The solution was air dried for three hrs followed by further drying in a vacuum chamber for 72 hrs. Each film was easily removed from the base to undergo hydrolysis. In our prior work involving the determination of bulk phase sequence/property relationships with limited sample mass, we found that solution casting of thick polymer films was both efficient and reproducible.[112]

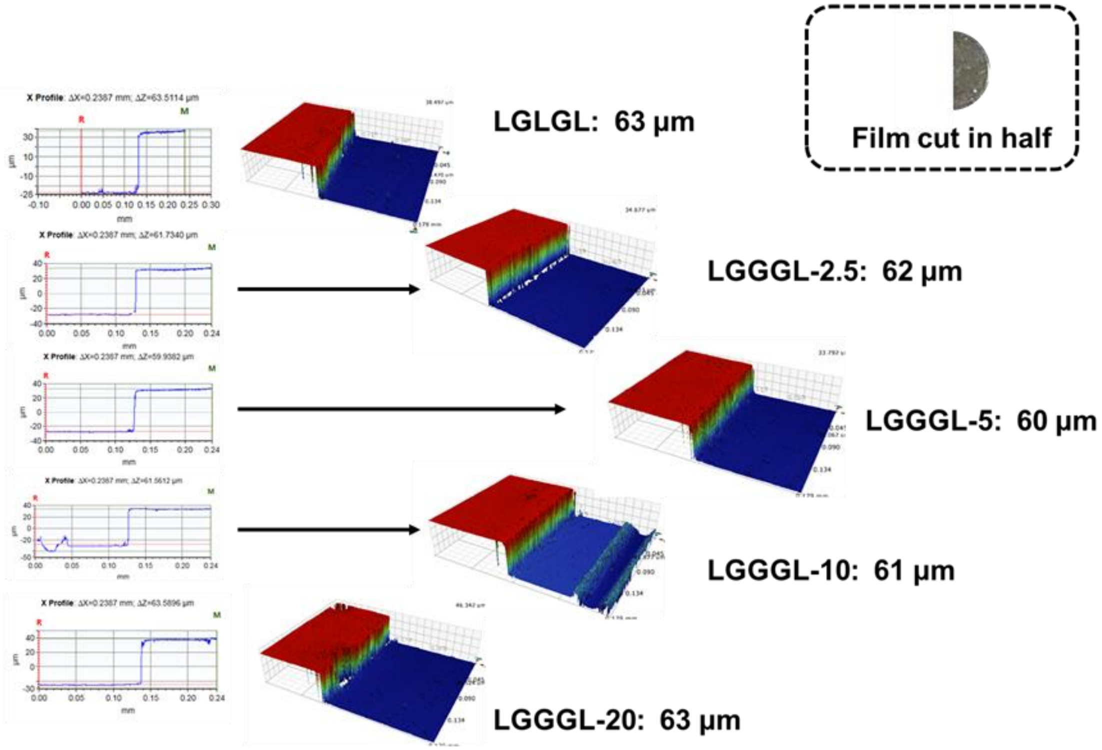

Figure 28. Optical profilometry step-contours of sliced films prepared from each of the five copolymers.

Each film, 60 µm thick (Figure 28) and weighing ~3 mg, was placed in a dram vial with 2 mL of 10x phosphate buffer solution (PBS, pH = 7.4) and placed in an incubator at 37 °C on a rotating platform (8 rpm). Each week for ten weeks, three films of each sample were removed for SEC analysis and the reported molecular weights are an average of these three samples. The copolymers degraded uniformly with extremely little variation in molecular weights in a given set of three. Over time, as can be seen in Figure 29A, the copolymers behave similarly until 10% error incorporation. **LGGGL-10** degraded identically to the others until week 7; thereafter, a more rapid degradation was observed. **LGGGL-20** degraded more rapidly beginning after week 2.

The site of polyester chain cleavage may dramatically affect the rate of molecular weight loss. When significant intrachain scission occurs, molecular weight drops rapidly. When the primary cleavage mechanism is end-chain scission, however, molecular weight decreases gradually as short segments near chain ends are cleaved and eliminated. We previously observed that the alternating LG sequence is resistant to significant amounts of intrachain scission.[36] We found that G-G linkages increased the prevalence of intrachain scission events that lead to an accelerated molecular weight loss.[190, 192, 195] The extent of this enhancement, which is studied herein, indicates that the base alternating sequence in this copolyester system is able to withstand an average of 6.3 monomer substitution errors per chain of 530 monomers before significant intrachain scission occurs and, therefore, degradation rates are affected.

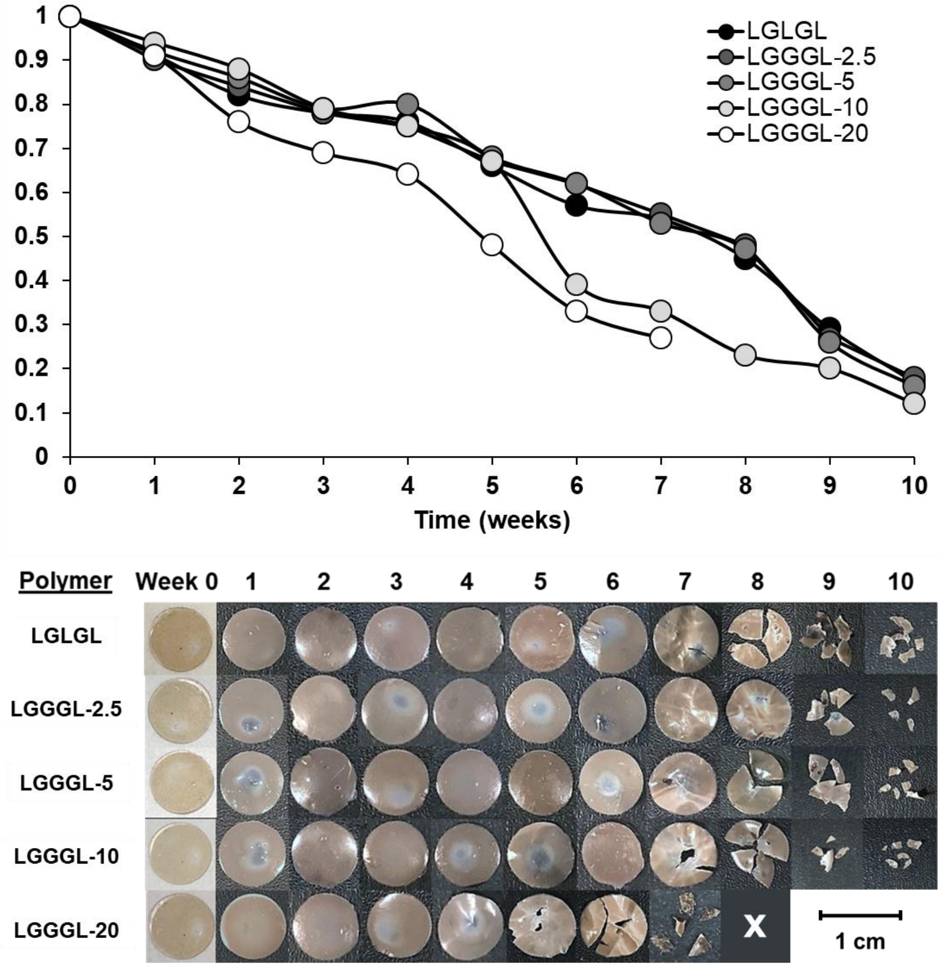

Figure 29. (Top) Molecular weight loss during hydrolysis. (Bottom) Photographs of films at given time points during hydrolysis. X denotes particles too small to photograph.

When significant degradation occurred, the films became brittle and fractured neatly into pieces (Figure 29B). It became difficult to remove the films from vials without damaging them. The extent of this fracturing seemed to depend on error content. Above 10% error-doping, the film masses and particle size decreased quickly after initial fracturing. Fractures were also observed in the SEM images of each film. Additionally, high magnification images (1,000x) showed an increase in surface roughening as more error was introduced (Figure 30).

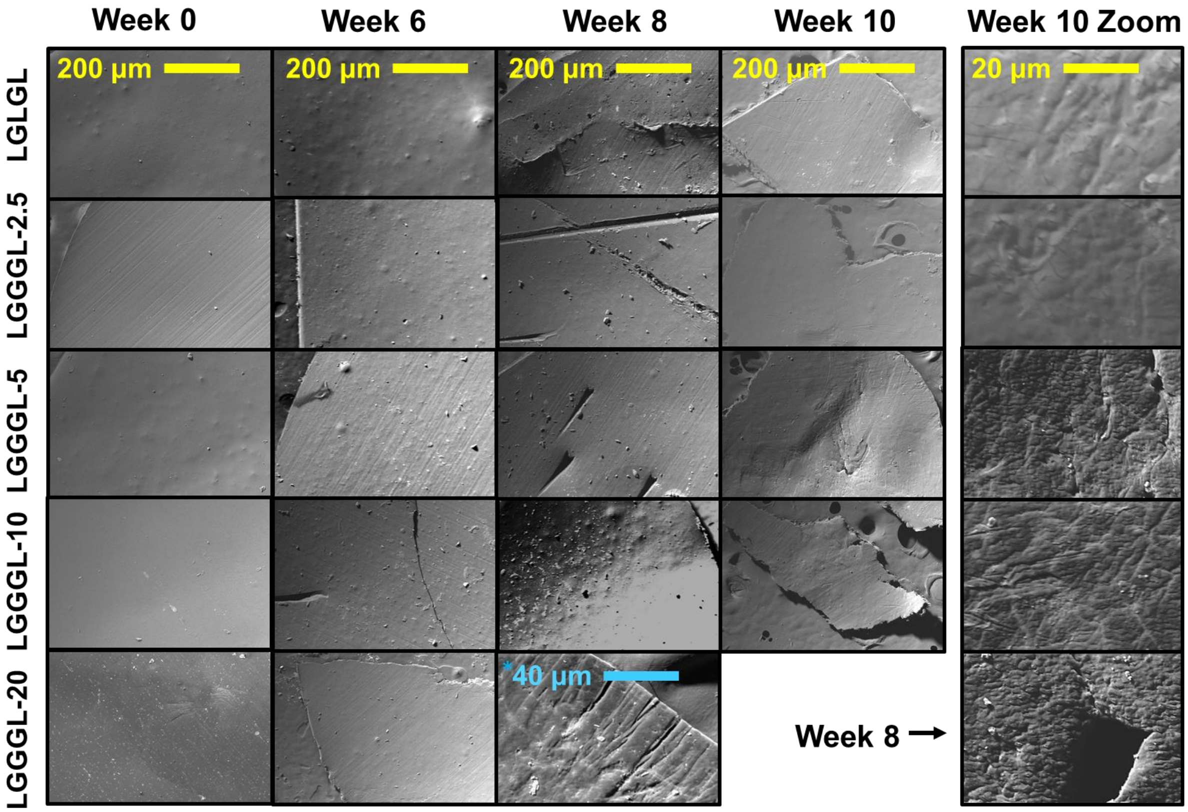
Week 0
Week 6
Week 8
Week 10
Week 10 Zoom
LGLGL
LGGGL-2.5
LGGGL-5
LGGGL-10
LGGGL-20
200 µm
200 µm
200 µm
200 µm
20 µm
*40 µm
Week 8 →

Figure 30. Scanning electron microscopy images of thick films at varying time points in hydrolysis.

4.4 Conclusions

We have embedded varying quantities of a glycolic acid monomer sequence error to disrupt a primarily alternating base sequence within degradable polyesters and subjected the polymers to hydrolysis. Hydrolysis rates and surface features were monitored over time. Molecular weight loss was largely unaffected up to the incorporation of 10 mol% cyclic macromonomer, which translates to an average of 6.3 monomer sequence errors per chain of ~530 monomers or approximately 1%.

We anticipate that the knowledge gained from the current study can aid in the engineering of PLGA-type polymers with specific properties. One approach would be to exploit potent error dopants to tune one property with a minimal impact on another. We could, for example, tune degradation times by adding a small number of G-G linkage errors without dramatically affecting other properties like swelling or loading capacities. We are continuing our investigations into semi-sequencing techniques to manipulate behaviours.

4.5 Experimental Section

4.5.1 Experimental Procedures

Bn-GGL-Si

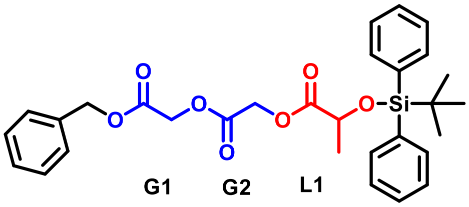

^{1}H-NMR (500 MHz, CDCl$_3$)

δ (ppm)	Mult. (J)	Int.	Assignment
1.11	s	9	TBDPS - tBu
1.42	d (6.5)	3	L1 (CH$_3$)
4.40	q (6.5)	1	L1 (CH)
4.53	d (16)	1	G
4.73	d (16)	1	G
4.71	s	2	G
5.20	s	2	Bn (CH$_2$)
7.37	m	11	TBDPS – o, p + Bn
7.65	m	4	TBDPS - m

^{13}C-NMR (400 MHz, CDCl$_3$)

δ (ppm)	Assignment
19.90	TBDPS (C)
21.92	L1 (CH$_3$)
27.47	TBDPS (CH$_3$)
60.89	G (CH$_2$)
61.71	G (CH$_2$)
67.94	Bn (CH$_2$)
69.34	L1 (CH)
127.79	Arene
127.82	Arene
128.29	Arene
128.34	Arene
129.99	Arene
133.58	Arene
133.61	Arene
135.28	Arene
136.07	Arene
167.59	G1, G2 (CO)
173.62	L (CO)

HRMS (ESI)

Calc. Mass
534.21 amu

Calc. [M+Na$^+$]$^+$
557.20 amu

Found [M+Na$^+$]$^+$
557.19766 amu

Composition
$C_{30}H_{34}O_7Si$

Bn-GGL-Si

Bn-G (5.12 g, 30.8 mmol) and **GL-Si** (11.4 g, 31.9 mmol) were dissolved in 290 mL DCM. DPTS (1.71 g, 5.8 mmol) was added and allowed to dissolve before the addition of DCC (6.58 g, 31.9 mmol). The reaction was stoppered and allowed to stir at RT overnight. The solution was filtered, concentrated *in vacuo*, and purified by column chromatography using 5% ethyl acetate in hexanes. Product eluted in fractions 5-11 (250 mL fractions). 10.3 g (66%)

GGL-Si

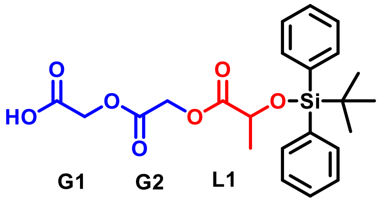

^{1}H-NMR (500 MHz, $CDCl_3$)

δ (ppm)	Mult. (J)	Int.	Assignment
1.09	s	9	TBDPS - tBu
1.42	d (6.5)	3	L1 (CH_3)
4.40	q (6.5)	1	L1 (CH)
4.53	d (16)	1	G
4.73	d (16)	1	G
4.71	s	2	G
7.37	m	6	TBDPS – o, p
7.65	m	4	TBDPS - m

^{13}C-NMR (400 MHz, $CDCl_3$)

δ (ppm)	+ Assignment
19.38	TBDPS (C)
21.40	TBDPS (CH_3)
21.93	L1 (CH_3)
60.32	G (CH_2)
61.34	G (CH_2)
68.81	L (CH)
127.79	Arene
127.82	Arene
129.99	Arene
133.58	Arene
133.61	Arene
135.28	Arene
136.07	Arene
167.00	G (CO)
171.65	G (CO)
173.23	L (CO)

HRMS (ESI)

Calc. Mass
444.16 amu

Calc. $[M+Na^+]^+$
467.15 amu

Found $[M+Na^+]^+$
467.14973 amu

Composition
$C_{23}H_{28}O_7Si$

GGL-Si

Bn-GGL-Si (10.3 g, 19.3 mmol) was dissolved in 190 mL ethyl acetate in a Schlenk flask to prepare a 0.1 M solution. Pd/C (1.03 g, 10% by mass) was added, and two balloons of H_2 (g) were passed through the flask. A third balloon was attached to serve as a source of excess H_2 (g). The reaction was stirred at RT overnight. The solution was then filtered over a thick pad of celite and concentrated to provide the pure product, 7.3 g yield (85%).

Bn-GGGL-Si

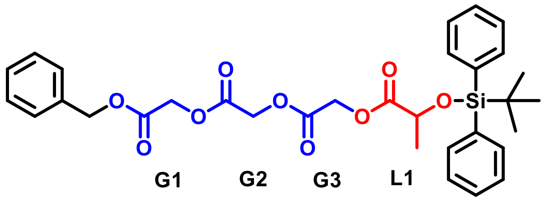

^{1}H-NMR (500 MHz, $CDCl_3$)

δ (ppm)	Mult. (J)	Int.	Assignment
1.10	s	9	TBDPS - tBu
1.43	d (6.5)	3	L1 (CH_3)
4.38	q (6.5)	1	L1 (CH)
4.53	d (16)	1	G
4.73	d (16)	1	G
4.77	dd (16)	4	G
4.79	s	2	G1
4.81	dd	2	G
5.20	dd	2	Bn
7.37	m	11	TBDPS – o, p + Bn
7.65	m	4	TBDPS - m

^{13}C-NMR (400 MHz, $CDCl_3$)

δ (ppm) + Assignment	
19.38	TBDPS (C)
21.40	TBDPS (CH_3)
60.32	G (CH_2)
60.81	G (CH_2)
61.34	G (CH_2)
67.49	Bn (CH_2)
68.81	L (CH)
127.79	Arene
127.82	Arene
128.59	Arene
128.79	Arene
128.83	Arene
130.00	Arene
133.58	Arene
133.61	Arene
135.28	Arene
136.07	Arene
166.70	G (CO)
166.96	G (CO)
166.97	G (CO)
173.11	L (CO)

HRMS (ESI)

Calc. Mass
N/A

Calc. $[M-H]^-$
N/A

Found
N/A

Composition
N/A

Bn-GGGL-Si

Bn-G (1.91 g, 11.5 mmol and **GGL-Si** (4.64 g, 10.4 mmol) were dissolved in 104 mL DCM. DPTS (0.612 g, 2.1 mmol) was added and allowed to dissolve before the addition of DCC (2.37 g, 11.5 mmol). The reaction was stoppered and allowed to stir at RT overnight. The solution was filtered, concentrated *in vacuo*, and purified by column chromatography using 5-10% ethyl acetate in hexanes. Product eluted in fractions 4-9 (250 mL fractions), 3.31 g, 59%.

GGGL-Si

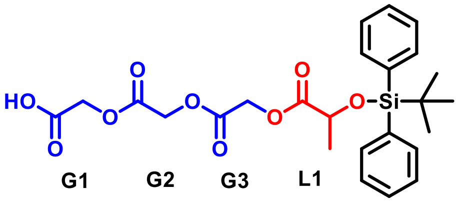

^{1}H-NMR (400 MHz, CDCl$_3$)

δ (ppm)	Mult. (J)	Int.	Assignment
1.09	s	9	TBDPS - tBu
1.41	d (6.5)	3	L1 (CH$_3$)
4.38	q (6.5)	1	L1 (CH)
4.53	d (16)	1	G
4.73	d (16)	1	G
4.77	dd (16)	4	G
4.79	s	2	G1
4.81	dd	2	G
7.37	m	6	TBDPS – o, p
7.65	m	4	TBDPS - m

^{13}C-NMR (400 MHz, CDCl$_3$)

δ (ppm) + Assignment	
19.38	TBDPS (C)
26.95	TBDPS (CH$_3$)
60.63	G (CH$_2$)
60.72	G (CH$_2$)
60.76	G (CH$_2$)
68.82	L (CH)
127.79	Arene
130.00	Arene
133.58	Arene
133.61	Arene
135.28	Arene
136.07	Arene
166.63	G (CO)
167.03	G (CO)
171.24	G (CO)
173.12	L (CO)

HRMS (ESI)

Calc. Mass
502.17 amu

Calc. [M-H]$^-$
501.16 amu

Found
[M-H]$^-$
501.15657 amu

Composition
$C_{25}H_{30}O_9Si$

GGGL-Si

Bn-GGGL-Si (3.31 g, 5.59 mmol) was dissolved in 55 mL ethyl acetate in a Schlenk flask to prepare a 0.1 M solution. Pd/C (0.330 g, 10% by mass) was added, and two balloons of H_2 (g) were passed through the flask. A third balloon was attached to serve as a source of excess H_2 (g). The reaction was stirred at RT overnight. The solution was then filtered through a thick pad of celite and concentrated to provide the pure product, 2.60 g yield (93%).

Bn-LGGGL-Si

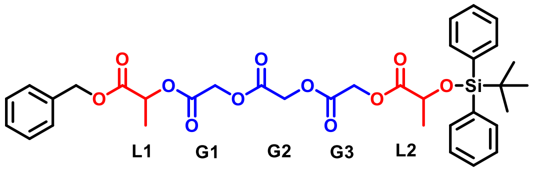

^{1}H-NMR (400 MHz, $CDCl_3$)

δ (ppm)	Mult. (J)	Int.	Assignment
1.09	s	9	TBDPS - tBu
1.41	d (6.5)	3	L2 (CH_3)
1.56	d (6.5)	3	L1 (CH_3)
4.38	q (6.5)	1	L2 (CH)
4.63	d (16)	1	G3
4.70	dd (16)	1	G3
4.79	dd (16)	4	G1, G2
5.18	d	2	Bn
5.26	m	2	L1 , L2 (CH)
7.37	m	11	TBDPS – o, p + Bn
7.65	m	4	TBDPS - m

^{13}C-NMR (400 MHz, $CDCl_3$)

δ (ppm) + Assignment	
16.94	L (CH_3)
19.38	TBDPS (C)
21.40	L (CH_3)
26.95	TBDPS (CH_3)
60.33	G (CH_2)
60.77	G (CH_2)
61.09	G (CH_2)
67.43	L (CH)
68.82	L (CH)
69.75	Bn (CH_2)
127.78	Arene
127.83	Arene
128.34	Arene
128.67	Arene
129.99	Arene
133.14	Arene
133.61	Arene
135.28	Arene
135.90	Arene
166.53	G (CO)
166.62	G (CO)
166.96	G (CO)
169.89	L (CO)
173.12	L (CO)

HRMS (ESI)

Calc. Mass
664.23 amu

Calc. $[M+NH_4]^+$
682.26 amu

Found
$[M+NH_4]^+$
682.26891 amu

Composition
$C_{35}H_{40}O_{11}Si$

Bn-LGGGL-Si

Bn-L (1.02 g, 5.69 mmol) and **GGGL-Si** (2.37 g, 4.01 mmol) were dissolved in 50 mL DCM. DPTS (0.305 g, 1.04 mmol) was added and allowed to dissolve before the addition of DCC (1.17 g, 5.17 mmol). The reaction was stoppered and allowed to stir at RT overnight. The solution was filtered, concentrated *in vacuo*, and purified by column chromatography using 10% ethyl acetate in hexanes. Product eluted in fractions 10-18 (250 mL fractions). 2.90 g yield (84%).

LGGGL-Si

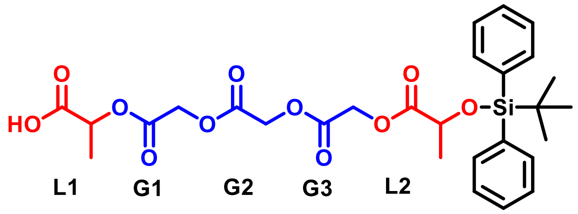

^{1}H-NMR (400 MHz, $CDCl_3$)

δ (ppm)	Mult. (J)	Int.	Assignment
1.09	s	9	TBDPS - tBu
1.41	d (6.5)	3	L2 (CH_3)
1.56	d (6.5)	3	L1 (CH_3)
4.38	q (6.5)	1	L2 (CH)
4.63	d (16)	1	G3
4.70	dd (16)	1	G3
4.79	dd (16)	4	G1, G2
5.26	m	2	L1 , L2 (CH)
7.37	m	6	TBDPS – o, p
7.65	m	4	TBDPS - m

^{13}C-NMR (400 MHz, $CDCl_3$)

δ (ppm)	+ Assignment
16.94	L (CH_3)
19.38	TBDPS (C)
21.40	L (CH_3)
26.95	TBDPS (CH_3)
60.33	G (CH_2)
60.77	G (CH_2)
61.09	G (CH_2)
67.43	L (CH)
68.82	L (CH)
127.78	Arene
129.99	Arene
133.61	Arene
135.28	Arene
166.53	G (CO)
166.62	G (CO)
166.96	G (CO)
169.89	L (CO)
173.12	L (CO)

HRMS (ESI)

Calc. Mass
574.19 amu

Calc. $[M+NH_4]^+$
592.22 amu

Found
$[M+NH_4]^+$
592.21976 amu

Composition
$C_{28}H_{34}O_{11}Si$

LGGGL-Si

Bn-LGGGL-Si (2.90 g, 4.36 mmol) was dissolved in 45 mL ethyl acetate in a Schlenk flask to prepare a 0.1 M solution. Pd/C (0.290 g, 10% by mass) was added, and two balloons of H_2 (g) were passed through the flask. A third balloon was attached to serve as a source of excess H_2 (g). The reaction was stirred at RT overnight. The solution was then filtered over a thick pad of celite and concentrated to provide the pure product, 2.33 g yield (Quantitative Yield).

Bn-SyLMLGGGL-Si

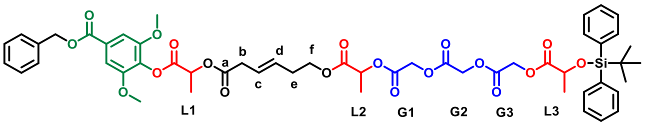

^{1}H-NMR (400 MHz, $CDCl_3$)

δ (ppm)	Mult. (J)	Int.	Assignment
1.09	s	9	TBDPS (tBu)
1.41	d (6.4)	3	L3 (CH_3)
1.48	d (6.4)	3	L2
1.68	d (6.4)	3	L1 (CH_3)
2.38	q (6.8)	2	**e**
3.13	m	2	**b**
3.85	s	6	Sy (CH_3)
4.15	m	2	**f**
4.37	q (6.4)	1	L3 (CH)
4.50	d (16)	1	G3
4.63	d (16)	1	G3
4.70	m	4	G1, G2
5.12	q (6.4)	1	L2 (CH)
5.37	s	2	Bn (CH_2)
5.45	q (6.4)	1	L1 (CH)
5.60	m	2	**d** , **e**
7.40	m	13	Sy + TBDPS o,p + Bn
7.65	m	4	TBDPS meta

^{13}C-NMR (400 MHz, $CDCl_3$)

δ (ppm) + Assignment			
16.80	L (CH_3)	127.69	Arene
17.16	L (CH_3)	128.36	Arene
19.23	TBDPS (C)	128.66	Arene
21.30	L (CH_3)	129.46	Arene
26.80	TBDPS (CH_3)	129.85	Arene
31.90	**e**	132.13	**d**
37.67	**b**	132.96	Arene
56.44	Sy (CH_3)	133.40	Arene
60.33	G (CH_2)	135.75	Arene
60.78	G (CH_2)	135.92	Arene
61.08	G (CH_2)	152.05	Arene
64.52	L (CH)	165.91	Sy (CO)
67.06	**b**	166.52	G (CO)
68.39	L (CH)	166.63	G (CO)
68.60	L (CH)	166.97	G (CO)
69.48	**f**	168.12	M (CO)
106.48	Arene	169.90	L (CO)
124.53	**c**	170.86	L (CO)
127.63	Arene	173.12	L (CO)

HRMS (ESI)

Calc. Mass
1028.35 amu

Calc Mass
$[M+H^{+}]^{+}$
1029.2379
amu

Found
1029.35679
amu

Composition
$C_{53}H_{60}O_{19}Si$

Bn-SyLMLGGGL-Si

Bn-SyLM (0.725 g, 1.53 mmol) and **LGGGL-Si** (0.966 g, 1.68 mmol) were dissolved in 16 mL DCM. DPTS (0.090 g, 0.31 mmol) was added and allowed to dissolve before the addition of DCC (0.378 g, 1.68 mmol). The reaction was stoppered and allowed to stir at RT overnight. The solution was filtered, concentrated *in vacuo*, and purified by column chromatography using 10% ethyl acetate in hexanes. Product eluted in fractions 10-18 (250 mL fractions), 0.947 g yield, 60%.

SyLMLGGGL-Si

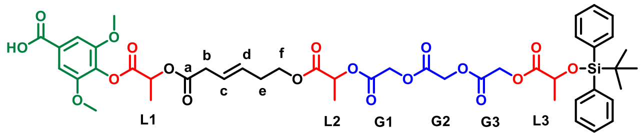

^{1}H-NMR (400 MHz, $CDCl_3$)

δ (ppm)	Mult. (J)	Int.	Assignment
1.09	s	9	TBDPS (tBu)
1.41	d (6.4)	3	L3 (CH_3)
1.48	d (6.4)	3	L2
1.68	d (6.4)	3	L1 (CH_3)
2.38	q (6.8)	2	**e**
3.13	m	2	**b**
3.85	s	6	Sy (CH_3)
4.15	m	2	**f**
4.37	q (6.4)	1	L3 (CH)
4.50	d (16)	1	G3
4.63	d (16)	1	G3
4.70	m	4	G1, G2
5.12	q (6.4)	1	L2 (CH)
5.45	q (6.4)	1	L1 (CH)
5.60	m	2	**d** , **e**
7.40	m	8	Sy + TBDPS o,p
7.65	m	4	TBDPS meta

^{13}C-NMR (400 MHz, $CDCl_3$)

δ (ppm) + Assignment			
16.80	L (CH_3)	127.69	Arene
17.16	L (CH_3)	129.46	Arene
19.23	TBDPS (C)	129.85	Arene
21.30	L (CH_3)	132.13	**d**
26.80	TBDPS (CH_3)	132.96	Arene
31.90	**e**	133.40	Arene
37.67	**b**	135.75	Arene
56.44	Sy (CH_3)	135.92	Arene
60.33	G (CH_2)	152.05	Arene
60.78	G (CH_2)	165.91	Sy (CO)
61.08	G (CH_2)	166.52	G (CO)
64.52	L (CH)	166.63	G (CO)
67.06	**b**	166.97	G (CO)
68.39	L (CH)	168.12	M (CO)
68.60	L (CH)	169.90	L (CO)
69.48	**f**	170.86	L (CO)
106.48	Arene	173.12	L (CO)
124.53	**c**		
127.63	Arene		

HRMS (ESI)
Calc. Mass 938.30 amu
Calc Mass $[M+H^{+}]^{+}$ 939.31 amu
Found 939.31042 amu
Composition $C_{46}H_{54}O_{19}Si$

SyLMLGGGL-Si

A 0.60 M solution of **Bn-SyLMLGGGL-Si** (0.947 g, 0.92 mmol) was prepared in DCM. A 0.60 M solution of palladium (II) acetate (0.0093 g, 0.041 mmol), triethylamine (16 μL, 0.0124 mmol), and triethylsilane (205 μL, 1.29 mmol) was prepared and allowed to stir for 30 min. The solution of **Bn-SyLMLGGGL-Si** was then added dropwise over the course of five min. The reaction was allowed to stir at RT overnight. The solution was quenched with 10 mL saturated aqueous ammonium chloride solution and the organic layer was extracted 3x with DCM. The organics were dried with magnesium sulfate, filtered, and concentrated *in vacuo* to yield the crude product as a yellow oil. The product was purified by column chromatography using 10% ethyl acetate in hexanes to yield pure product as a white solid (0.332 g, 38%).

SyLMLGGGL

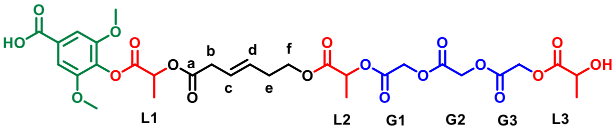

¹H-NMR (400 MHz, $CDCl_3$)

δ (ppm)	Mult. (J)	Int.	Assignment
1.41	m	6	L2, L3 (CH_3)
1.68	d (6.4)	3	L1 (CH_3)
2.38	q (6.8)	2	**e**
3.17	m	2	**b**
3.88	s	6	Sy (CH_3)
4.15	m	2	**f**
4.41	q (6.4)	1	L3 (CH)
4.80	m	6	G1, G2, G3
5.12	q (6.4)	1	L2 (CH)
5.45	q (6.4)	1	L1 (CH)
5.60	m	2	**d** , **e**
7.37	s	2	Sy

¹³C-NMR (400 MHz, $CDCl_3$)

δ (ppm) + Assignment

δ (ppm)	Assignment	δ (ppm)	Assignment
16.80	L (CH_3)	129.46	Arene
17.16	L (CH_3)	132.13	**d**
19.23	TBDPS (C)	152.33	Arene
		165.91	Sy (CO)
21.30	L (CH_3)	166.52	G (CO)
26.80	TBDPS (CH_3)	166.54	G (CO)
		166.76	G (CO)
31.90	**e**	168.21	M (CO)
37.67	**b**	169.90	L (CO)
56.44	Sy (CH_3)	170.90	L (CO)
		175.11	L (CO)
60.33	G (CH_2)		
60.78	G (CH_2)		
61.08	G (CH_2)		
64.52	L (CH)		
67.06	**b**		
68.39	L (CH)		
68.60	L (CH)		
69.48	**f**		
107.12	Arene		
124.53	**c**		
127.63	Arene		

HRMS (ESI)

Calc. Mass
700.19 amu

Calc Mass
$[M+H^+]^+$
701.197 amu

Found
701.19355amu

Composition
$C_{30}H_{36}O_{19}$

SyLMLGGGL

SyLMLGGGL-Si (0.332 g, 0.331 mmol) was dissolved in 3.3 mL THF to prepare a 0.1 M solution. The flask was cooled to 0 °C. TBAF (0.50 mL as a 1.0 M solution in THF, 0.50 mmol) was added to a vial and acetic acid (35 µL, 0.60 mmol) was added. The vial was vortexed briefly and this solution was added steadily to the solution of starting material. The reaction was warmed to RT over the course of 1 h and the reaction was quenched with 5 mL brine. The organics were extracted 3x with ethyl acetate, were dried with magnesium sulfate, filtered, and concentrated *in vacuo* to provide the crude product as a yellow oil. The product was purified by column chromatography (25% ethyl acetate in hexanes increased gradually to 90% ethyl acetate in hexanes). The product was a white solid, 0.151 g, 65%.

Cyc-SyLMLGGGL

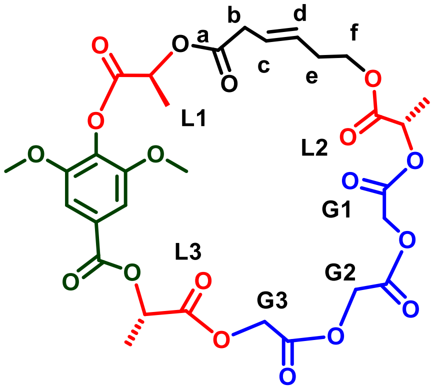

^{1}H-NMR (400 MHz, $CDCl_3$)

δ (ppm)	Mult. (J)	Int.	Assignment
1.39	d (6.4)	3	L (CH_3)
1.68	m	6	L (CH_3)
2.35	q (6.8)	2	**e**
3.17	m	2	**b**
3.86	s	6	Sy (CH_3)
4.15	m	2	**f**
4.80	m	6	G1, G2, G3
5.10	q (6.4)	1	L2 (CH)
5.45	q (6.4)	1	L1 (CH)
5.50	q (6.4)	1	L3 (CH)
5.60	m	2	**d** , **e**
7.36	s	2	Sy

^{13}C-NMR (400 MHz, $CDCl_3$)

δ (ppm) + Assignment			
16.80	L (CH_3)	129.46	Arene
17.16	L (CH_3)	132.13	**d**
19.23	TBDPS (C)	152.33	Arene
21.30	L (CH_3)	165.91	Sy (CO)
26.80	TBDPS (CH_3)	166.52	G (CO)
31.90	**e**	166.54	G (CO)
37.67	**b**	166.76	G (CO)
56.44	Sy (CH_3)	168.21	M (CO)
60.33	G (CH_2)	169.90	L (CO)
60.78	G (CH_2)	170.90	L (CO)
61.08	G (CH_2)	175.11	L (CO)
64.52	L (CH)		
67.06	**b**		
68.39	L (CH)		
68.60	L (CH)		
69.48	**f**		
107.12	Arene		
124.53	**c**		
127.63	Arene		

HRMS (ESI)

Calc. Mass
682.17 amu

Calc Mass $[M+H^+]^+$
683.18 amu

Found
683.18207 amu

Composition
$C_{30}H_{34}O_{18}$

Cyc-SyLMLGGGL

SyLM(L_3G_2) (0.113 g, 0.16 mmol) was dissolved in 2.5 mL dichloroethane and injected to a solution of DCC (0.066 g, 0.32 mmol) and DPTS (0.023 g, 0.08 mmol) in 2.5 mL dichloroethane at 60 °C over a span of 16 hrs. The solution was allowed to stir for an additional 24 hrs before being filtered and concentrated to obtain the crude product. A column loaded with 15% ethyl acetate in hexanes was used to purify the product (0.070 g, 64%), a white solid.

Polymerizations to prepare LGLGL, LGGGL-2.5, LGGGL-5, LGGGL-10, and LGGGL-20

Each monomer was dissolved in chloroform to prepare a 100 mg/mL solution. Each solution was pipetted using a micropipettor into a dram vial to prepare five 1,500 µL solution mixtures according to Table 3. The solutions were concentrated *in vacuo* to produce the solid mixtures ready for polymerization.

Table 3. Preparation of Errormer Mixtures.

Polymer	Volume of Base Sequence Solution (µL)	Volume of Errormer Solution (µL)	Error Mol %
LGLGL	1500	0	0
LGGGL-2.5	1462	37	2.5
LGGGL-5	1425	75	5
LGGGL-10	1350	150	10
LGGGL-20	1200	300	20

The polymerizations were performed with dry DCM obtained from a solvent system. A stock solution of Grubbs II was prepared and the appropriate volume was pipetted into each vial such that the reaction concentration was 0.7 M and 1.50 mol% catalyst was used. The vials were purged with nitrogen and sealed. Within 20 min, both solutions became very viscous. The reactions were left to react for 2 hrs before quenching with 0.05 mL of ethyl vinyl ether. The solutions were then concentrated *in vacuo* and the contents of the vials were placed in a vacuum chamber overnight. NMR spectra and SEC traces were collected on the following day. The polymers were reprecipitated in 500 mL cold methanol and allowed to stir for a half hour before filtering.

Solution Casting of Thick Polymer Films

The polymers were dissolved in methylene chloride to make 100 mg/mL solutions using a 100-1000 uL micropipettor. On the bottom of flat differential scanning calorimetry pans, 28 uL of this solution was cast onto each (with a 10-200 uL micropipettor), very carefully to create a convex droplet that covered the entire surface. The best films were prepared by first coating the perimeter of the slide and then filling in the middle. The solution was allowed to dry on the slides for 3 hrs before being placed in a vacuum chamber. After 2 days, those films that contained bubbles were removed from the glass slides using a razor blade and re-dissolved to prepare a 100 mg/mL solution. Films used for the hydrolysis study contained no bubbles, tears, or noticeable defects. The films were tan and transparent.

Film thicknesses were measured on representative films cut through the center using optical profilometry. A Bruker Contour Elite I optical profilometer was used. Samples were sliced to create a step indicative of film thickness and then analyzed.

Hydrolysis Study

Polymer films, removed from glass slides, were placed in dram vials followed by the addition of 2 mL of 10x phosphate buffer solution, pH = 7.4. The vials were capped and placed in an incubator set at 37 ℃. The films were placed on a rotating platform with a slow speed of 8 rpm to promote gentle mixing and to prevent localized concentration of acidic monomer around the films. The pH of the buffer solution was monitored over time and showed no distinguishable change. When timepoints were collected, the appropriate films were removed from the incubator, removed from the buffer solution, and blotted dry with a paper towel. Photographs were taken of each film at this point. The films were then rinsed with deionized water, blotted dry again and placed in new vials. Liquid N_2 was poured over the films and the films were lyophilized for several hrs. A full film was used for SEC analysis (~3 mg) and DSC analysis on weeks 2, 4, 6, 8, and 10.

5.0 Prospectus

As researchers develop methods to prepare SCPs on scales conducive to establishing sequence/bulk property relationships and identify monomer systems whose properties are dramatically affected by sequence, the field of sequence control can necessarily evolve to investigate the degrees to which synthetic demands can be lowered while retaining a property response. For copolymers like those discussed within this thesis, i.e. bioresorbable PLGA-like copolymers, the meaning of "scalable" is undeniably different to a synthetic chemist versus a researcher in applied biological engineering, and, therefore, laborious step-wise synthesis must be truncated for these sequenced copolymers to realize true application.

When sequence tolerance is established, it is most likely that application-level scalability will be accomplished by catalyst development to controllably polymerize simple monomers and/or semi-sequencing methodologies. Indeed, researchers interested in developing coordination-insertion catalysts have made strides in preparing stereo-sequenced PLAs, including isotactic (SSSS), syndiotactic (RSRS), heterotactic (RRSS), and a continuum between any one of these and atactic linkages.[34, 50-56, 151, 154, 196, 197] Currently, we are actively investigating the polymerization of an LG cyclic dimer, methyl glycolide, using catalysts such as these. The combination of the large-scale synthesis of methyl glycolide paired with regioselective ring-opening polymerization has yet to be realized, and with the former finally realized we are hopeful that copolymers of varying monomer alternation may be prepared with molecular weight control.

As mentioned previously, the development of polymerization techniques that require fewer synthetic steps to monomer as well as tunable sequence outcomes can be realized through semi-sequencing. Our group is currently investigating flow chemistry as an effective technique in this effort, in which key monomer spacings may be altered by adjustments in various flow rates. As this synthetic methodology evolves, the effects of broader long-range monomer sequencing will be studied while securing an elevated degree of scalability in the preparation of sequenced copolyesters.

Appendix A: Experimental Spectra and Supporting Data for Chapter 2

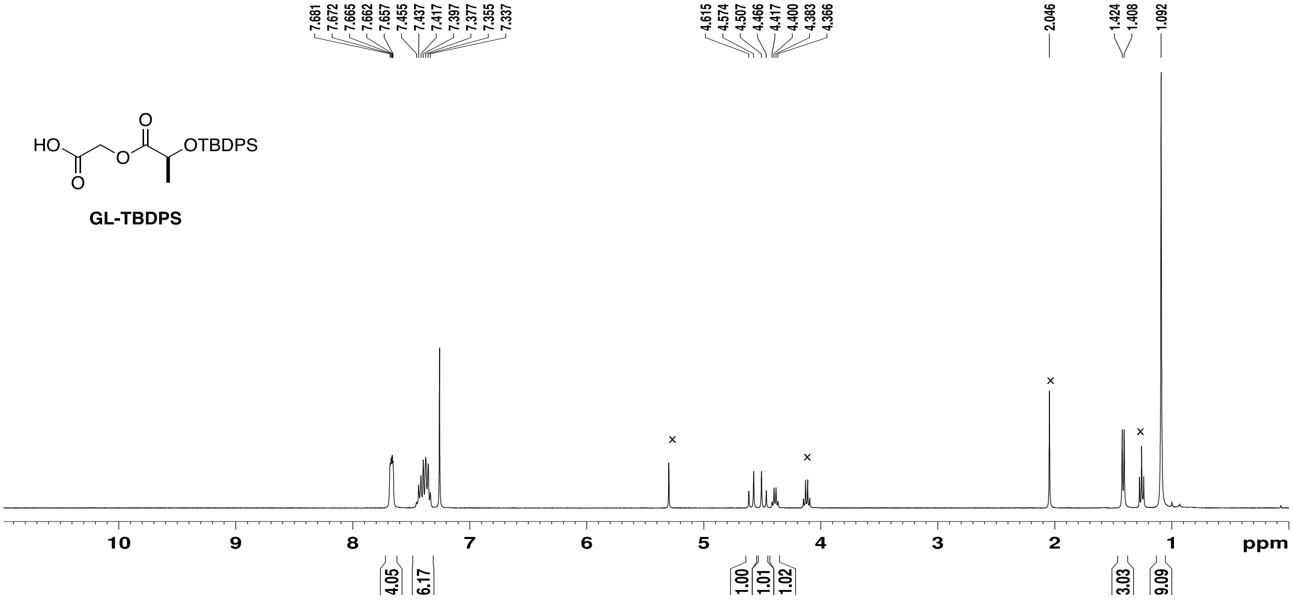

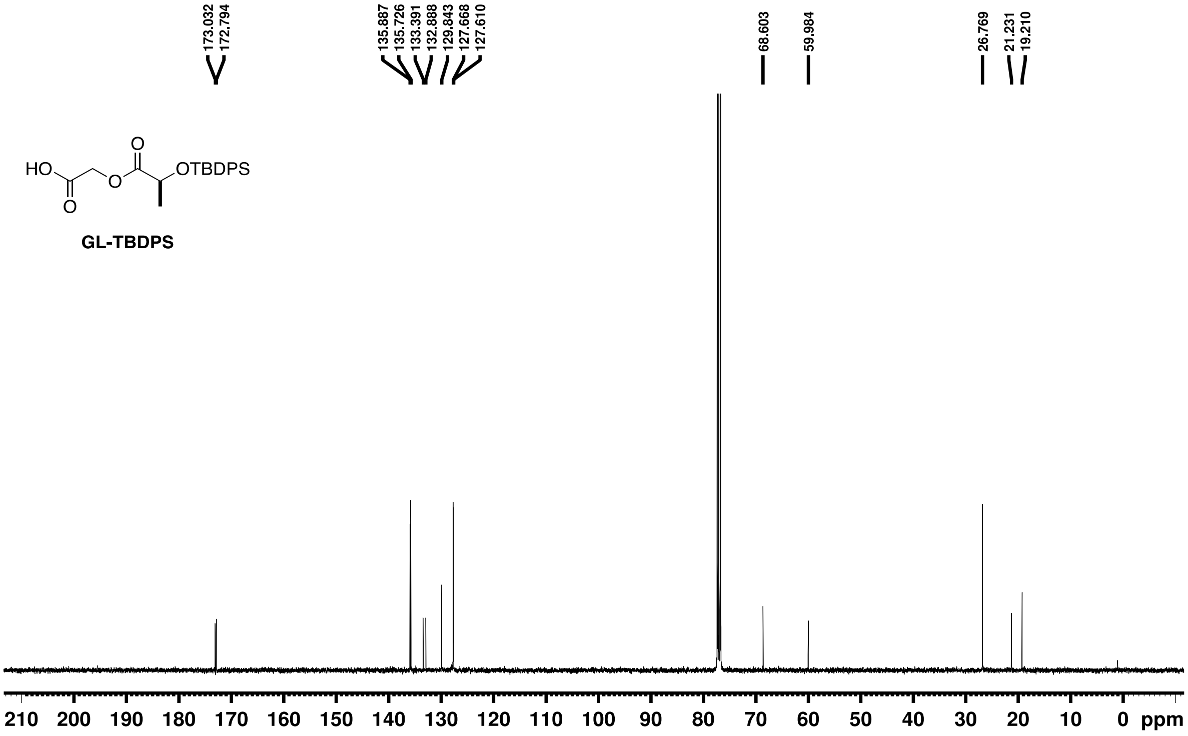

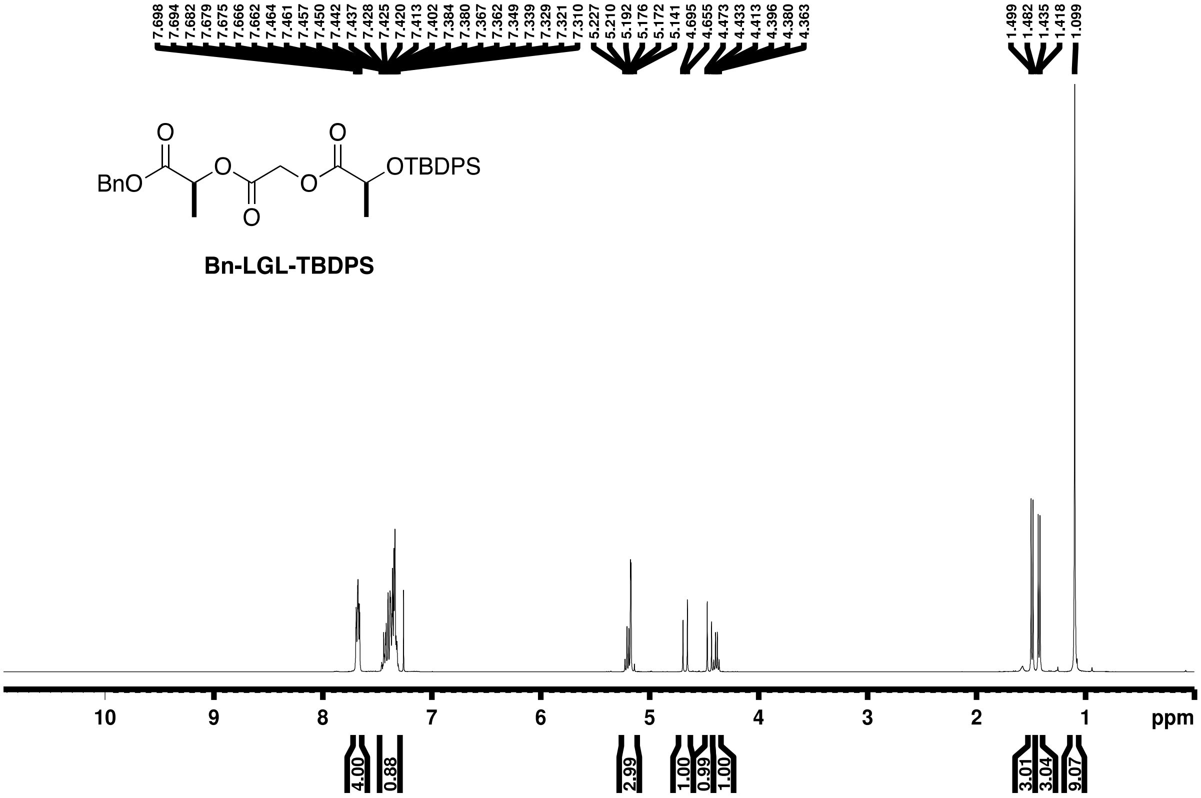

Bn-LGL-TBDPS

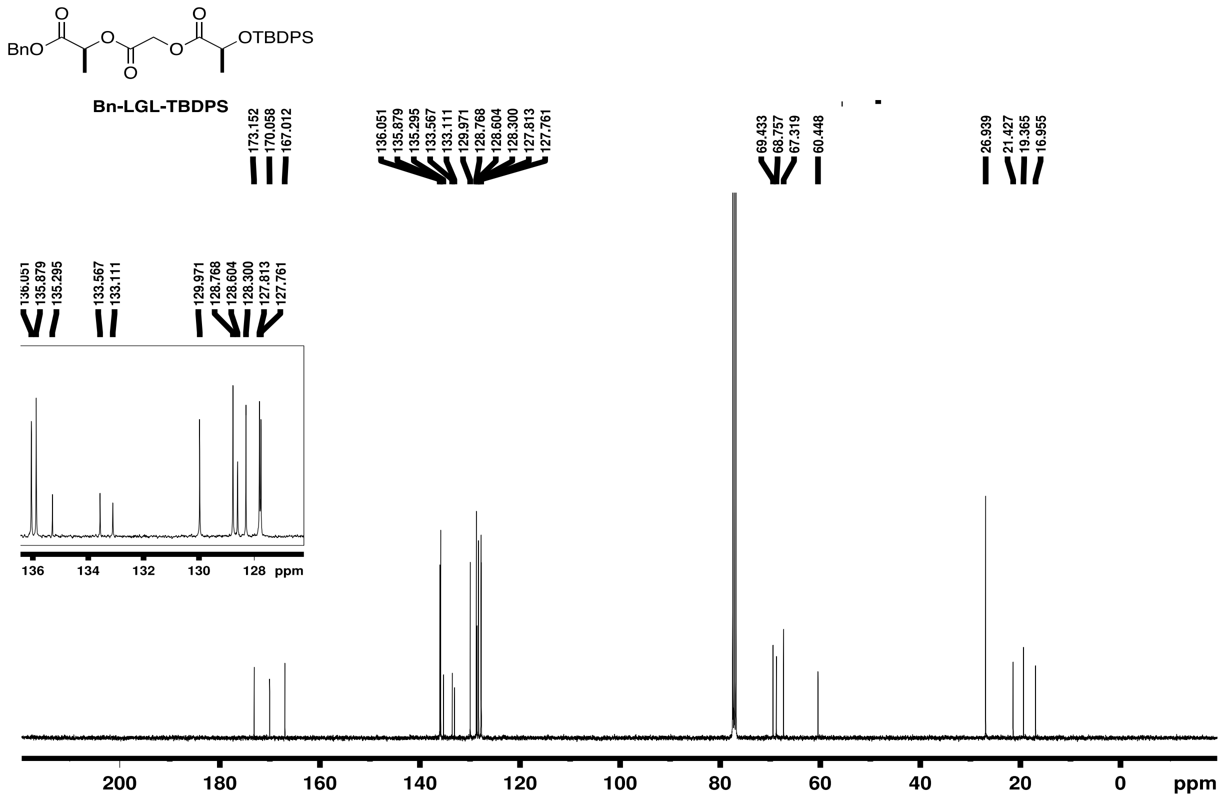

Bn-LGL-TBDPS

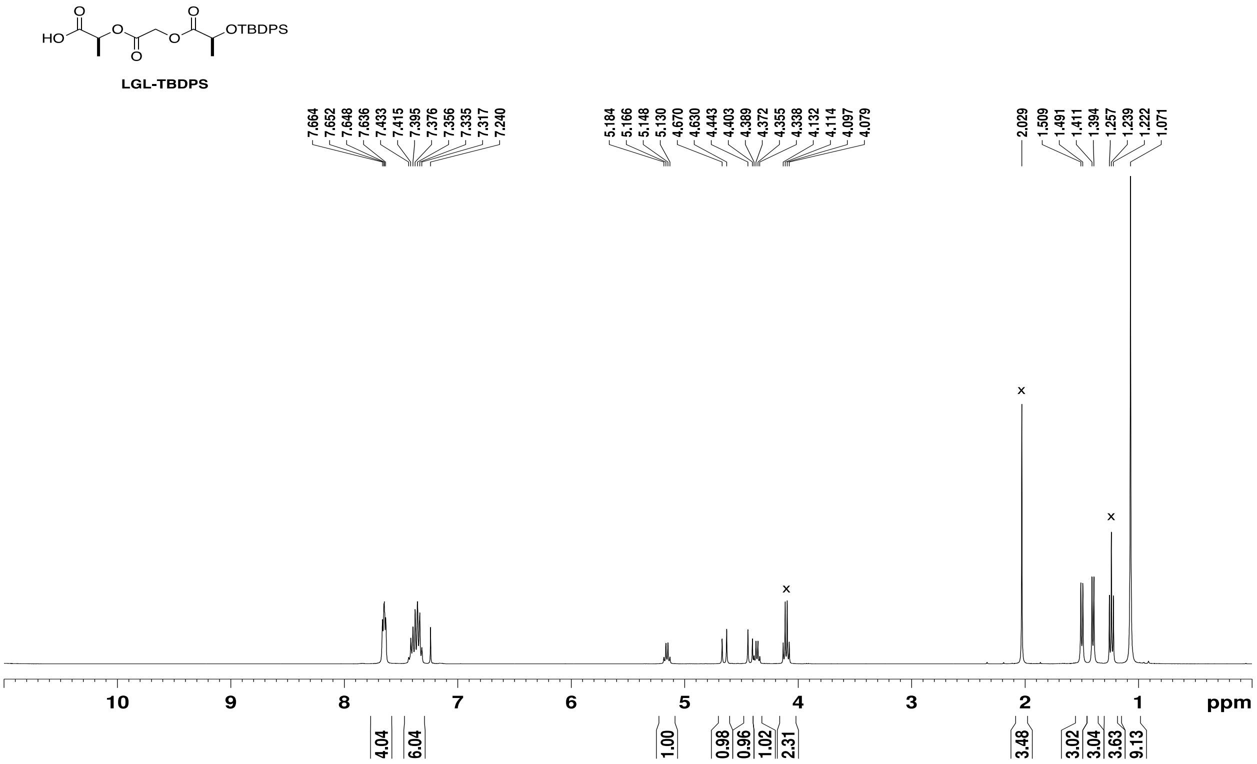
HO
O
O
O
O
O
OTBDPS
LGL-TBDPS
7.664
7.652
7.648
7.636
7.433
7.415
7.395
7.376
7.356
7.335
7.317
7.240
5.184
5.166
5.148
5.130
4.670
4.630
4.443
4.403
4.389
4.372
4.355
4.338
4.132
4.114
4.097
4.079
2.029
1.509
1.491
1.411
1.394
1.257
1.239
1.222
1.071
x
x
x
10
9
8
7
6
5
4
3
2
1
ppm
4.04
6.04
1.00
0.98
0.96
1.02
2.31
3.48
3.02
3.04
3.63
9.13

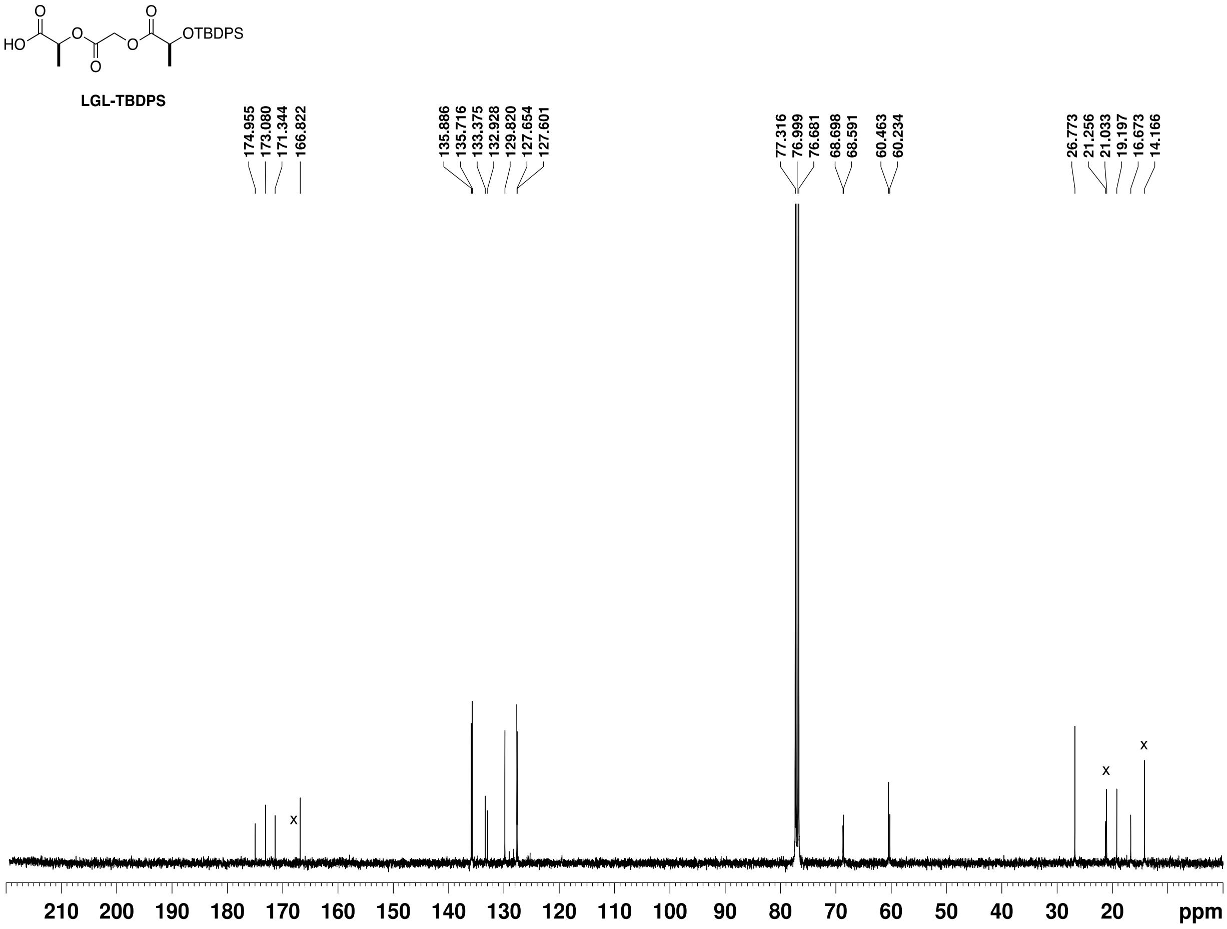
HO
O
O
O
O
O
OTBDPS
LGL-TBDPS
174.955
173.080
171.344
166.822
135.886
135.716
133.375
132.928
129.820
127.654
127.601
77.316
76.999
76.681
68.698
68.591
60.463
60.234
26.773
21.256
21.033
19.197
16.673
14.166
x
x
x
210
200
190
180
170
160
150
140
130
120
110
100
90
80
70
60
50
40
30
20
ppm

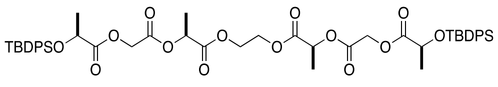
TBDPSO
OTBDPS
O

Eg-(LGL-TBDPS)$_2$

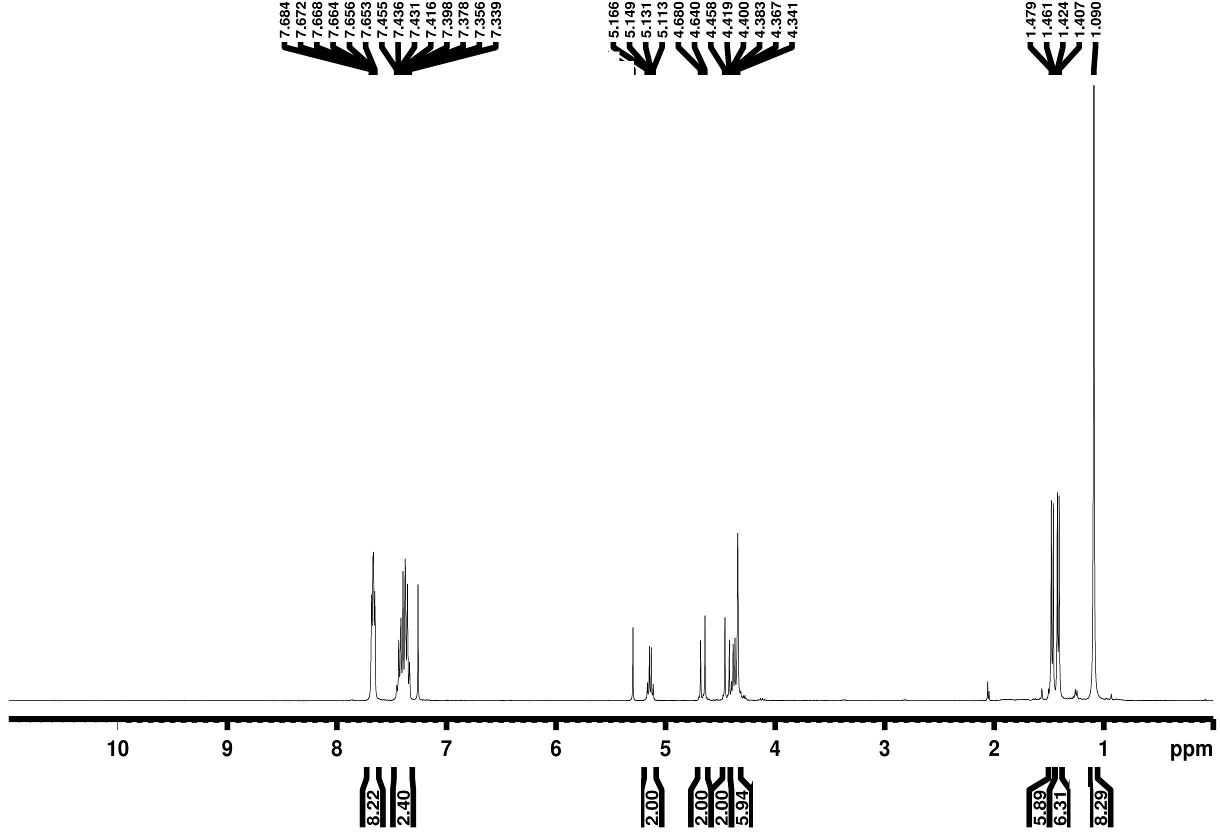

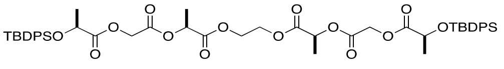
TBDPSO
OTBDPS
O

Eg-(LGL-TBDPS)$_2$

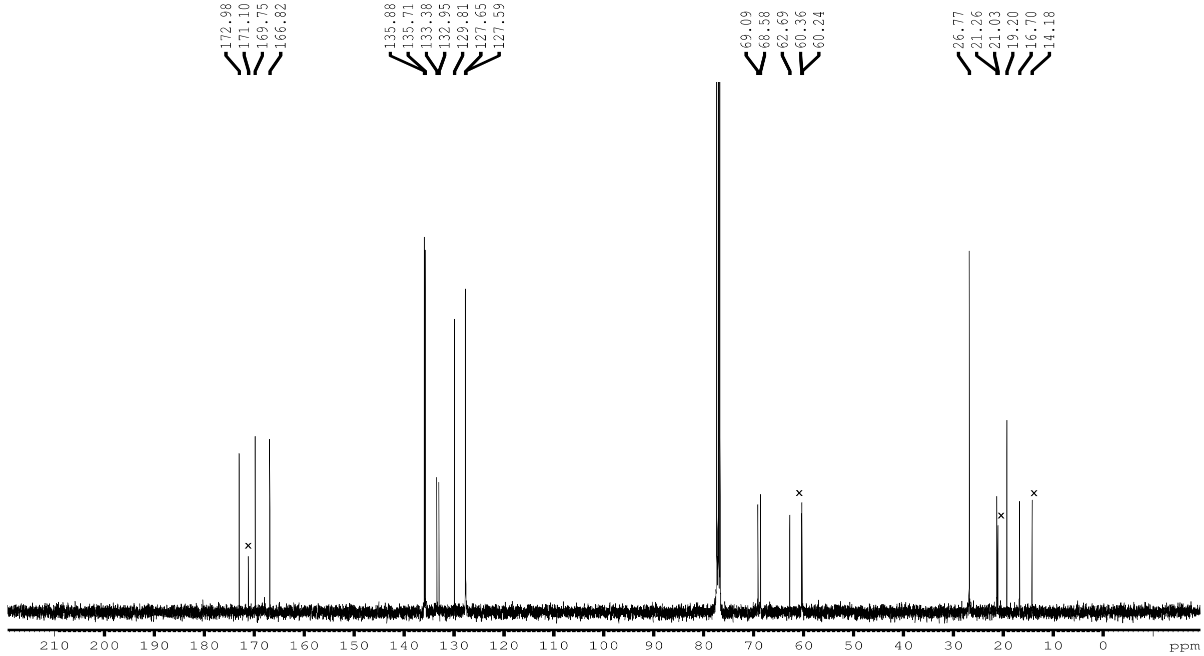

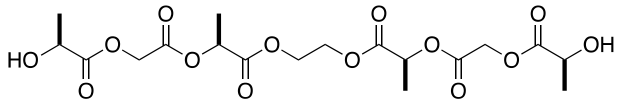

Eg-(LGL)$_2$

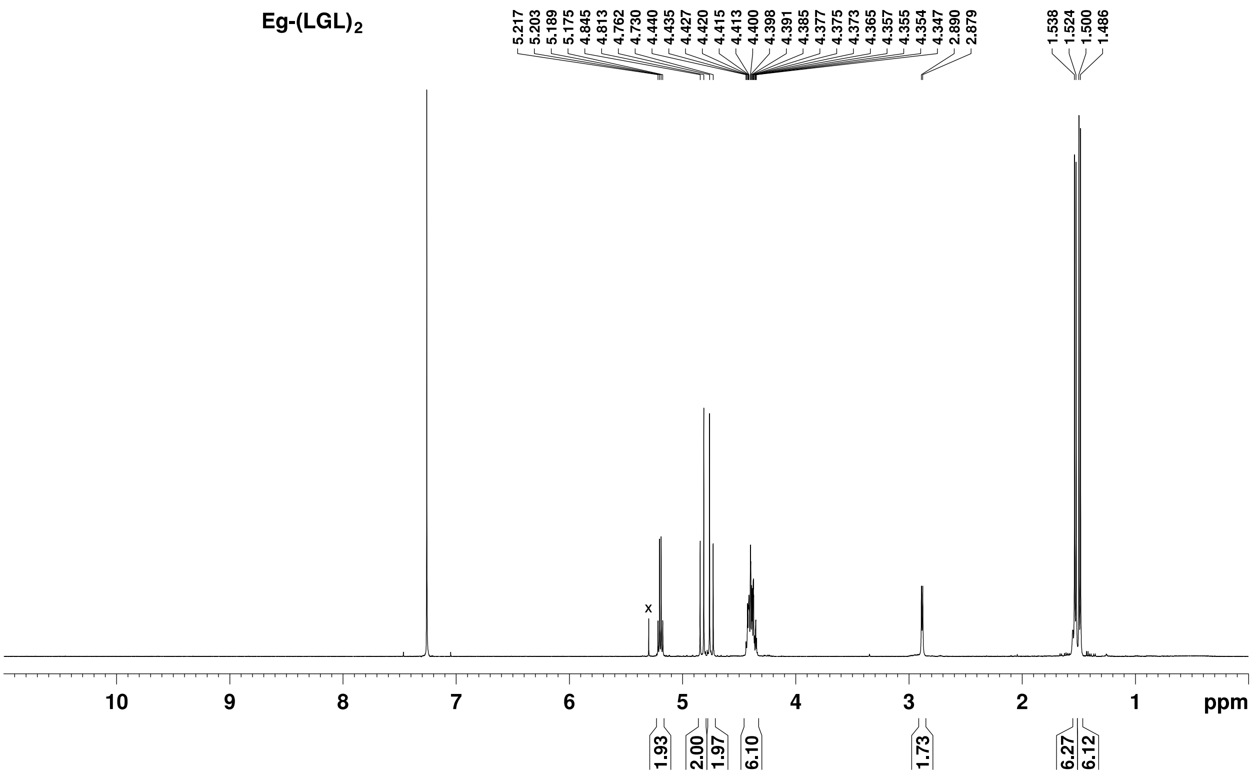
5.217
5.203
5.189
5.175
4.845
4.813
4.762
4.730
4.440
4.435
4.427
4.420
4.415
4.413
4.400
4.398
4.391
4.385
4.377
4.375
4.373
4.365
4.357
4.355
4.354
4.347
2.890
2.879
1.538
1.524
1.500
1.486
x
10
9
8
7
6
5
4
3
2
1
ppm
1.93
2.00
1.97
6.10
1.73
6.27
6.12

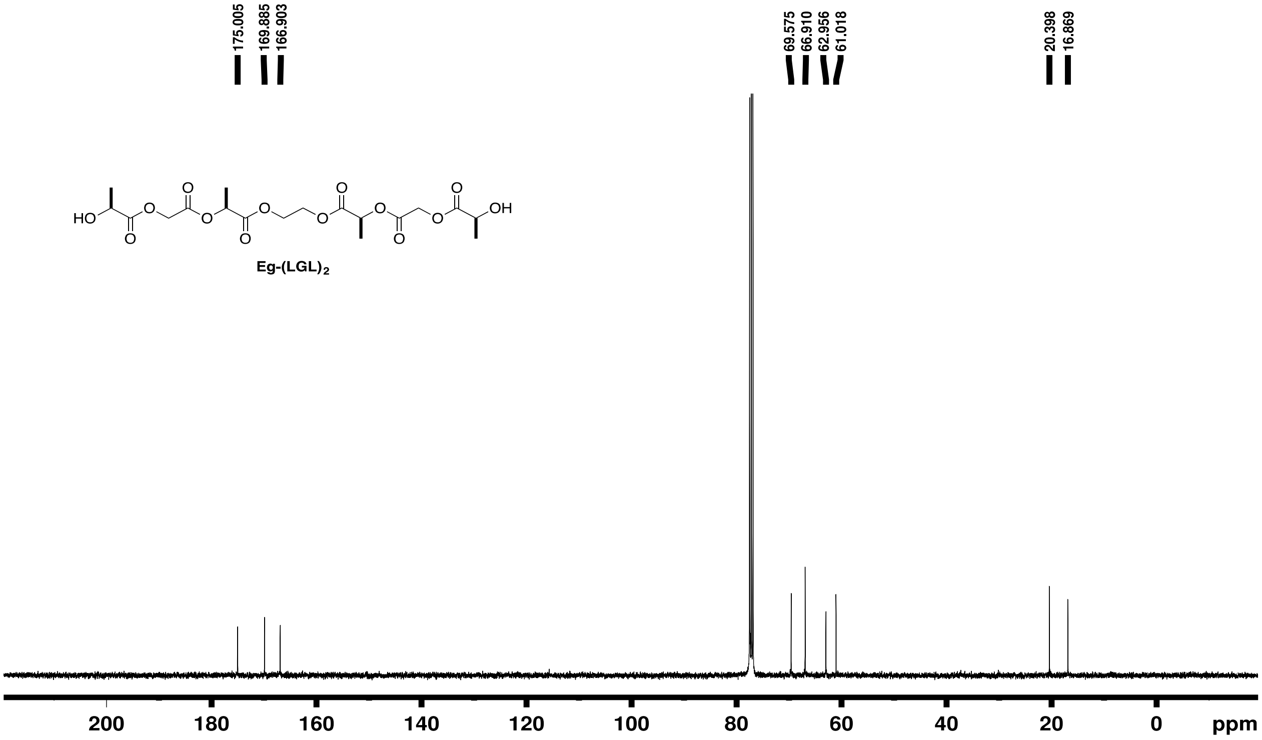
175.005
169.885
166.903
69.575
66.910
62.956
61.018
20.398
16.869
Eg-(LGL)2
200
180
160
140
120
100
80
60
40
20
0
ppm

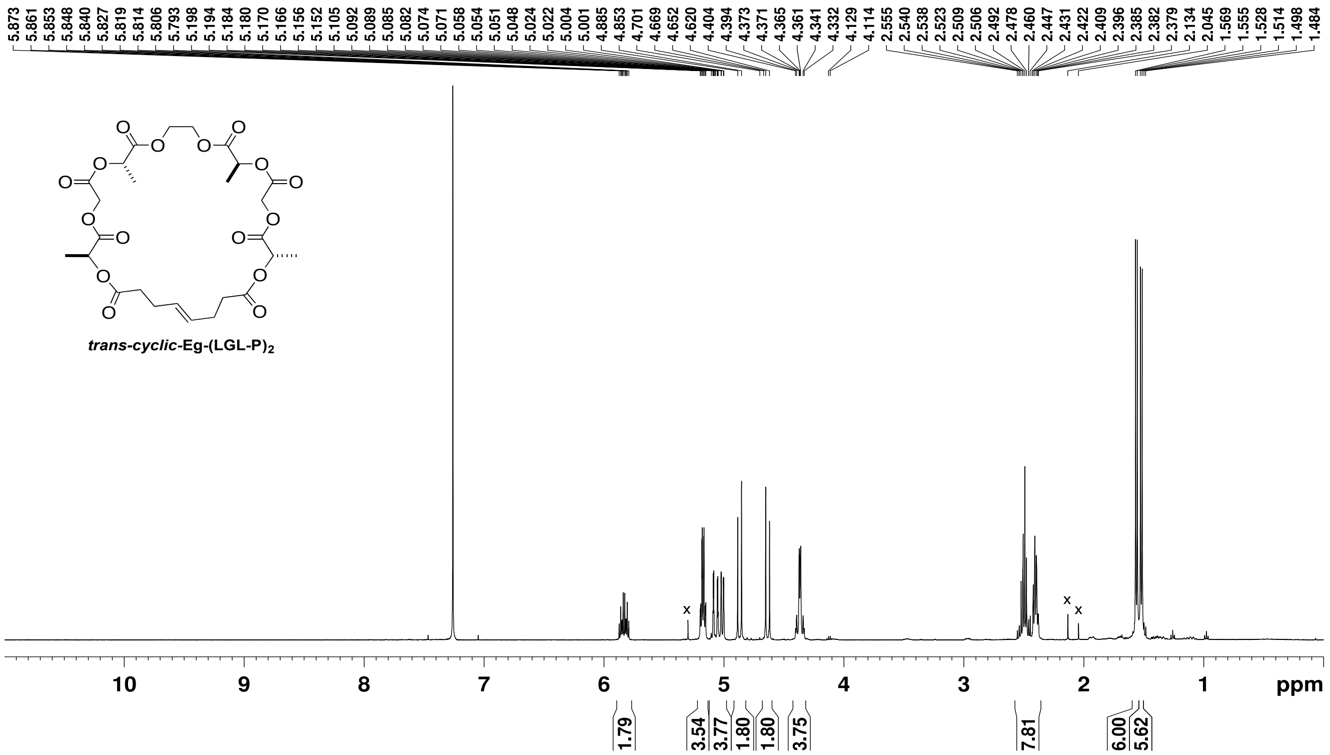
5.873
5.861
5.853
5.848
5.840
5.827
5.819
5.814
5.806
5.793
5.198
5.194
5.184
5.180
5.170
5.166
5.156
5.152
5.105
5.092
5.089
5.085
5.082
5.074
5.071
5.058
5.054
5.051
5.048
5.024
5.022
5.004
5.001
4.885
4.853
4.701
4.669
4.652
4.620
4.404
4.394
4.373
4.371
4.365
4.361
4.341
4.332
4.129
4.114
2.555
2.540
2.538
2.523
2.509
2.506
2.492
2.478
2.460
2.447
2.431
2.422
2.409
2.396
2.385
2.382
2.379
2.134
2.045
1.569
1.555
1.528
1.514
1.498
1.484
trans-cyclic-Eg-(LGL-P)2
x
x
x
10
9
8
7
6
5
4
3
2
1
ppm
1.79
3.54
3.77
1.80
1.80
3.75
7.81
6.00
5.62

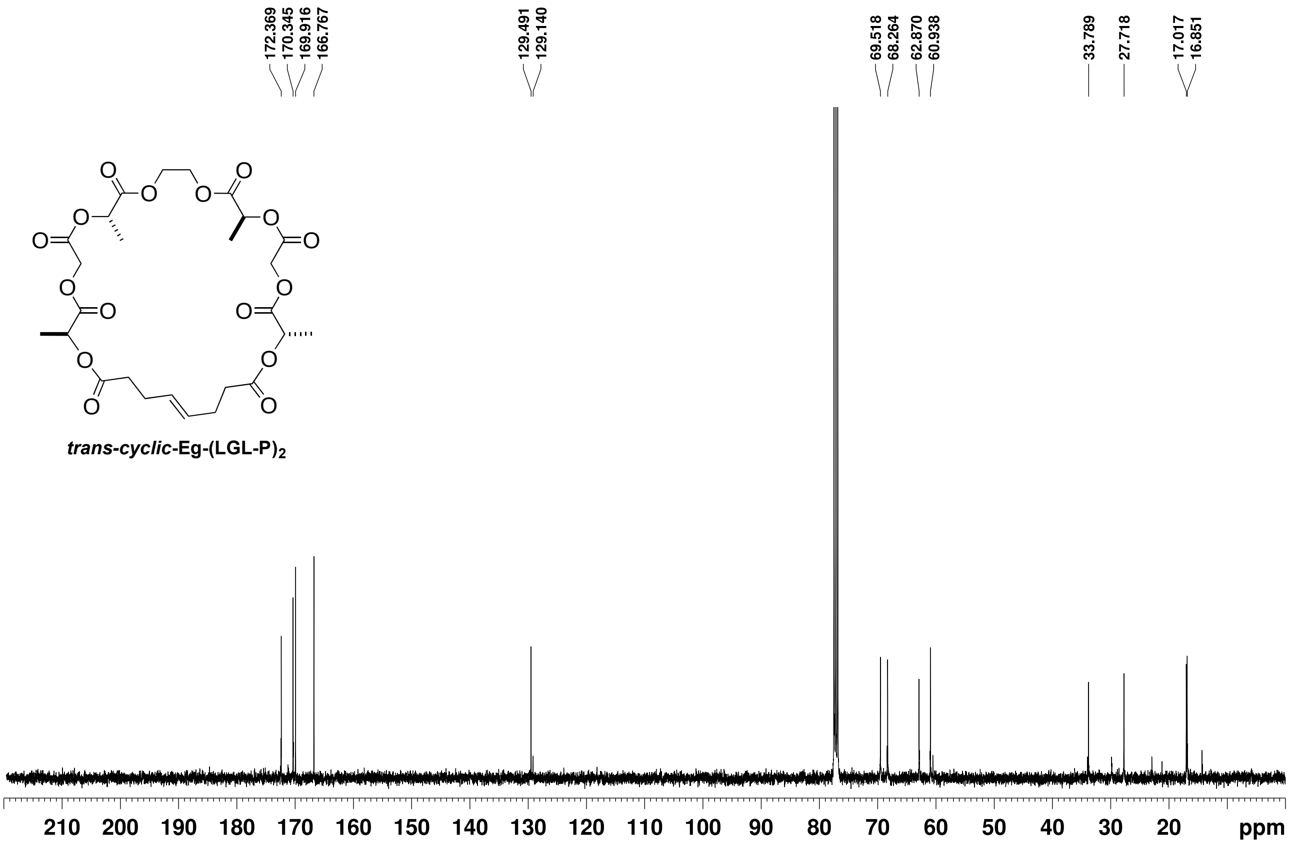
172.369
170.345
169.916
166.767
129.491
129.140
69.518
68.264
62.870
60.938
33.789
27.718
17.017
16.851
trans-cyclic-Eg-(LGL-P)2
210
200
190
180
170
160
150
140
130
120
110
100
90
80
70
60
50
40
30
20
ppm

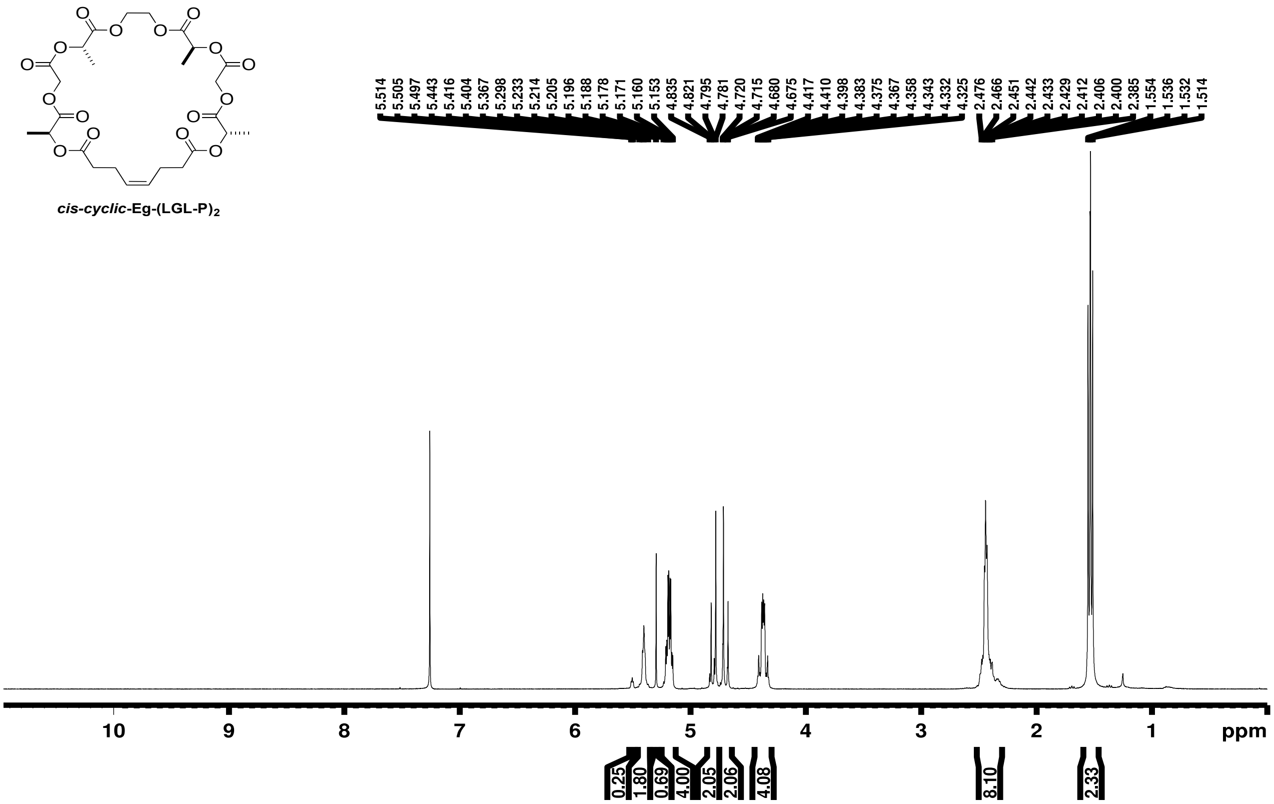
cis-cyclic-Eg-(LGL-P)$_2$

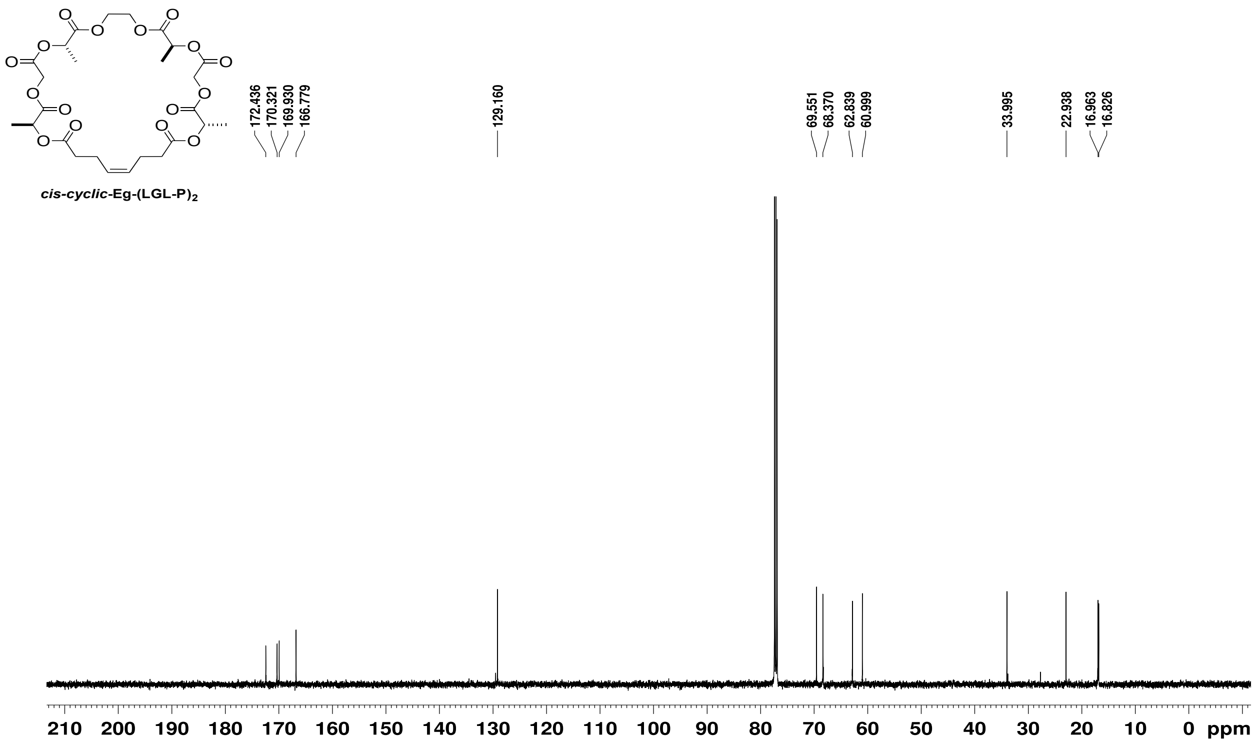
cis-cyclic-Eg-(LGL-P)$_2$

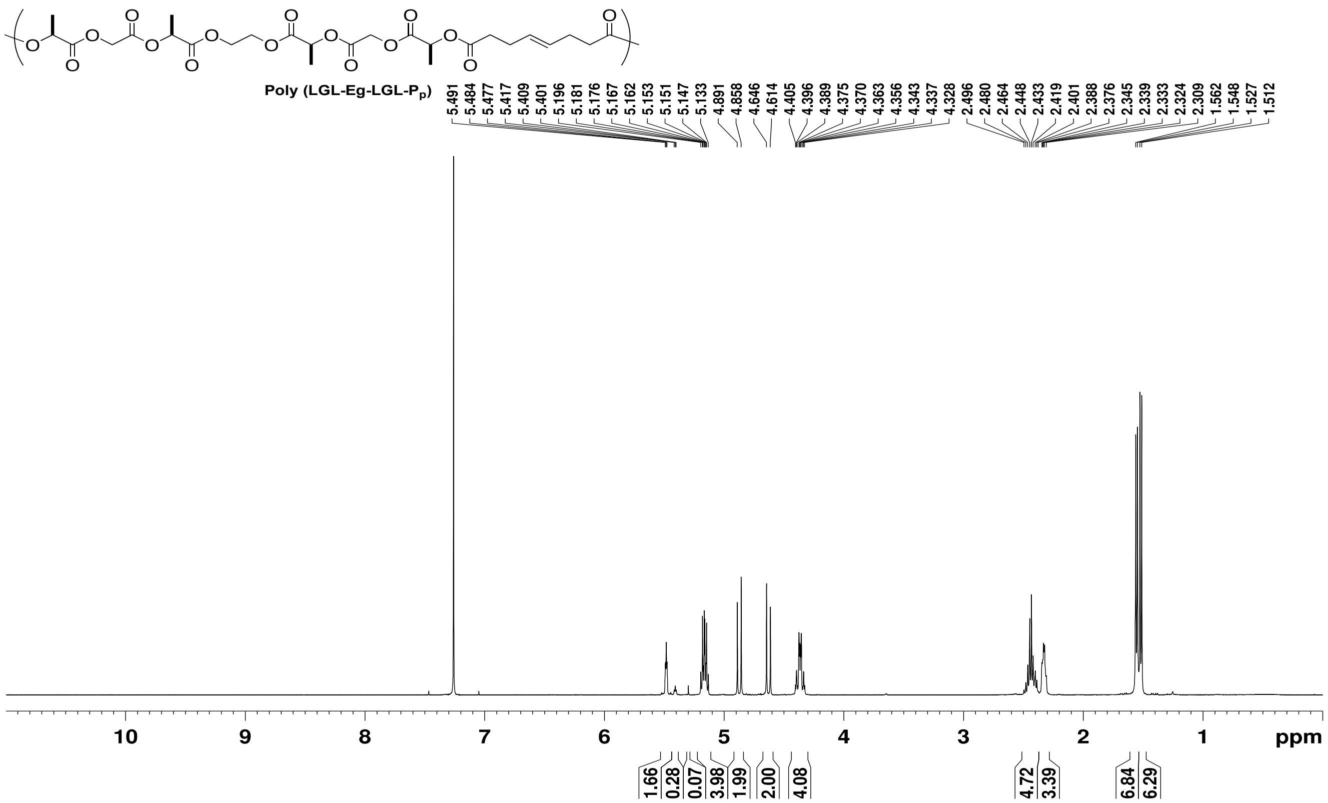
Poly (LGL-Eg-LGL-P$_p$)
5.491
5.484
5.477
5.417
5.409
5.401
5.196
5.181
5.176
5.167
5.162
5.153
5.151
5.147
5.133
4.891
4.858
4.646
4.614
4.405
4.396
4.389
4.375
4.370
4.363
4.356
4.343
4.337
4.328
2.496
2.480
2.464
2.448
2.433
2.419
2.401
2.388
2.376
2.345
2.339
2.333
2.324
2.309
1.562
1.548
1.527
1.512
10
9
8
7
6
5
4
3
2
1
ppm
1.66
0.28
0.07
3.98
1.99
2.00
4.08
4.72
3.39
6.84
6.29

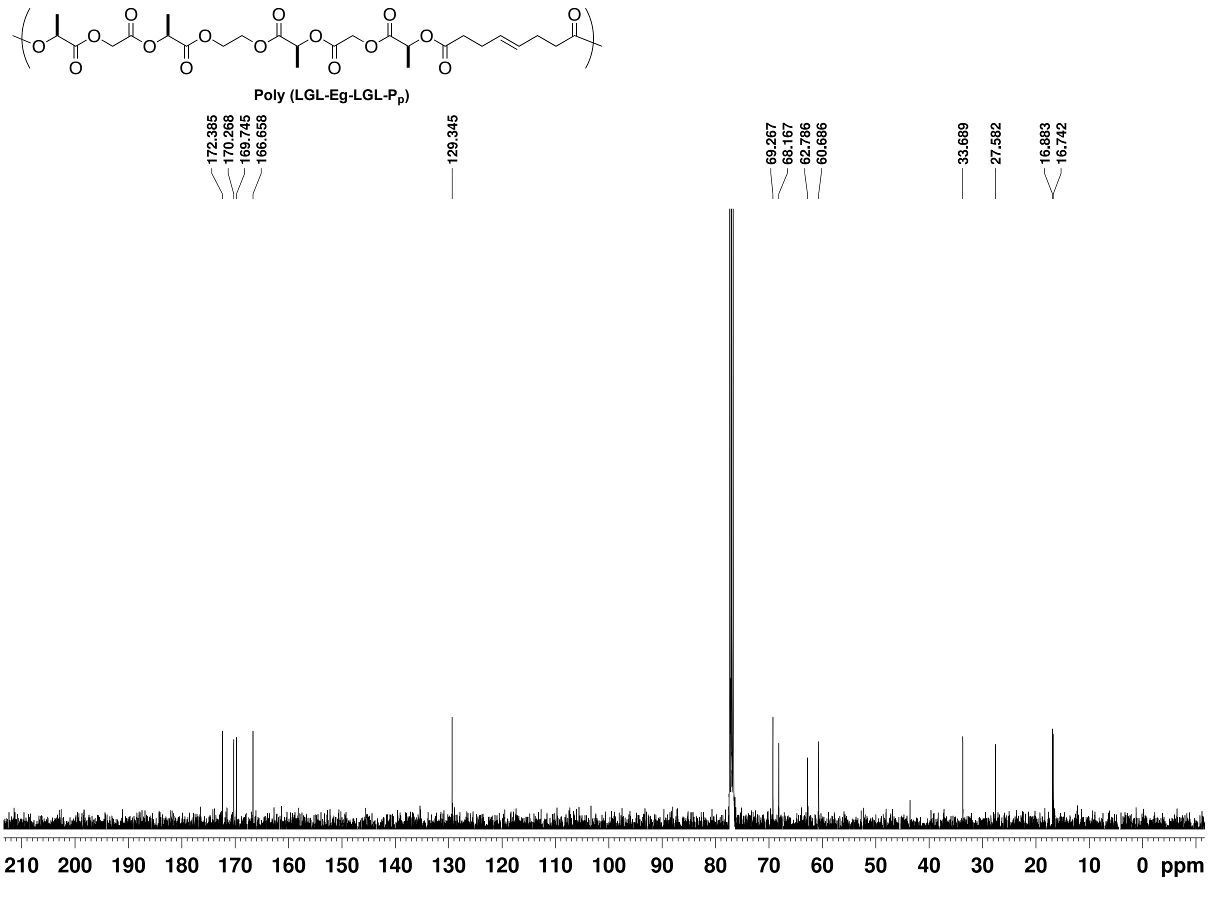
Poly (LGL-Eg-LGL-P$_p$)
172.385
170.268
169.745
166.658
129.345
69.267
68.167
62.786
60.686
33.689
27.582
16.883
16.742
210
200
190
180
170
160
150
140
130
120
110
100
90
80
70
60
50
40
30
20
10
0
ppm

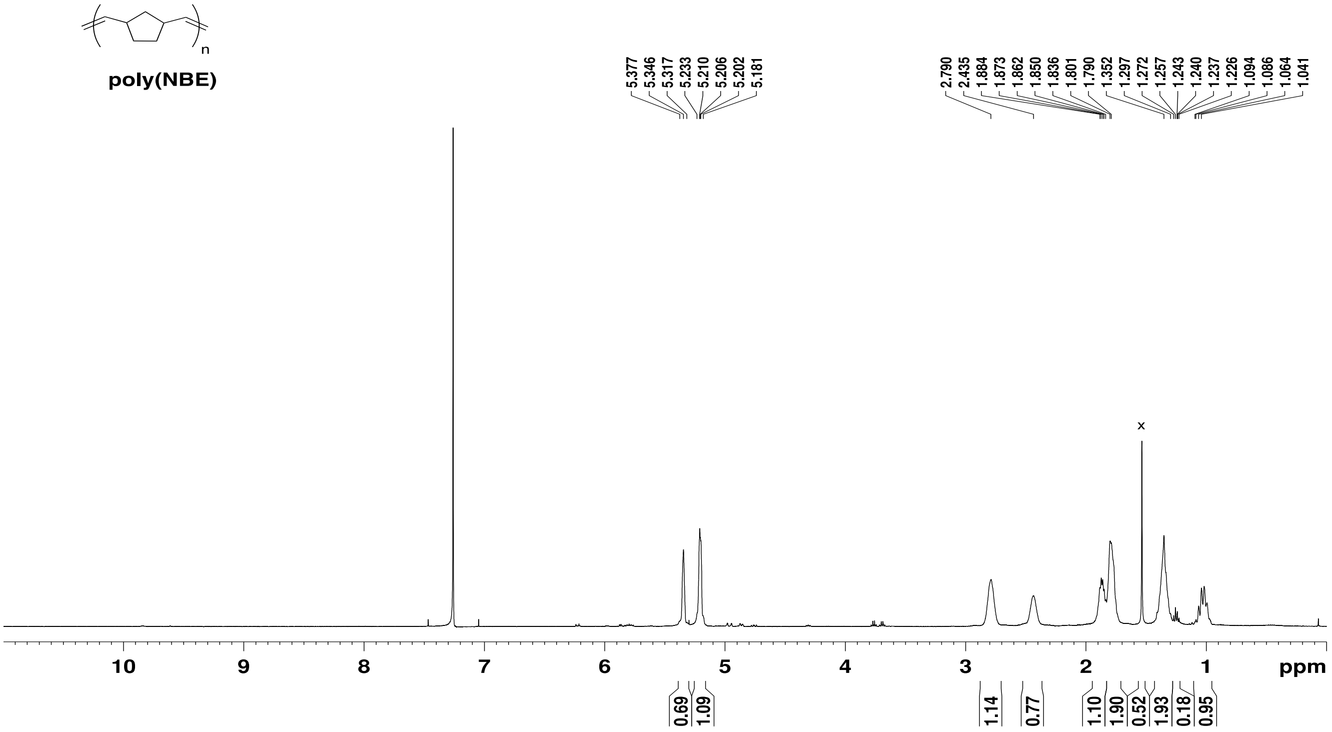
poly(NBE)
n
5.377
5.346
5.317
5.233
5.210
5.206
5.202
5.181
2.790
2.435
1.884
1.873
1.862
1.850
1.836
1.801
1.790
1.352
1.297
1.272
1.257
1.243
1.240
1.237
1.226
1.094
1.086
1.064
1.041
×
10
9
8
7
6
5
4
3
2
1
ppm
0.69
1.09
1.14
0.77
1.10
1.90
0.52
1.93
0.18
0.95

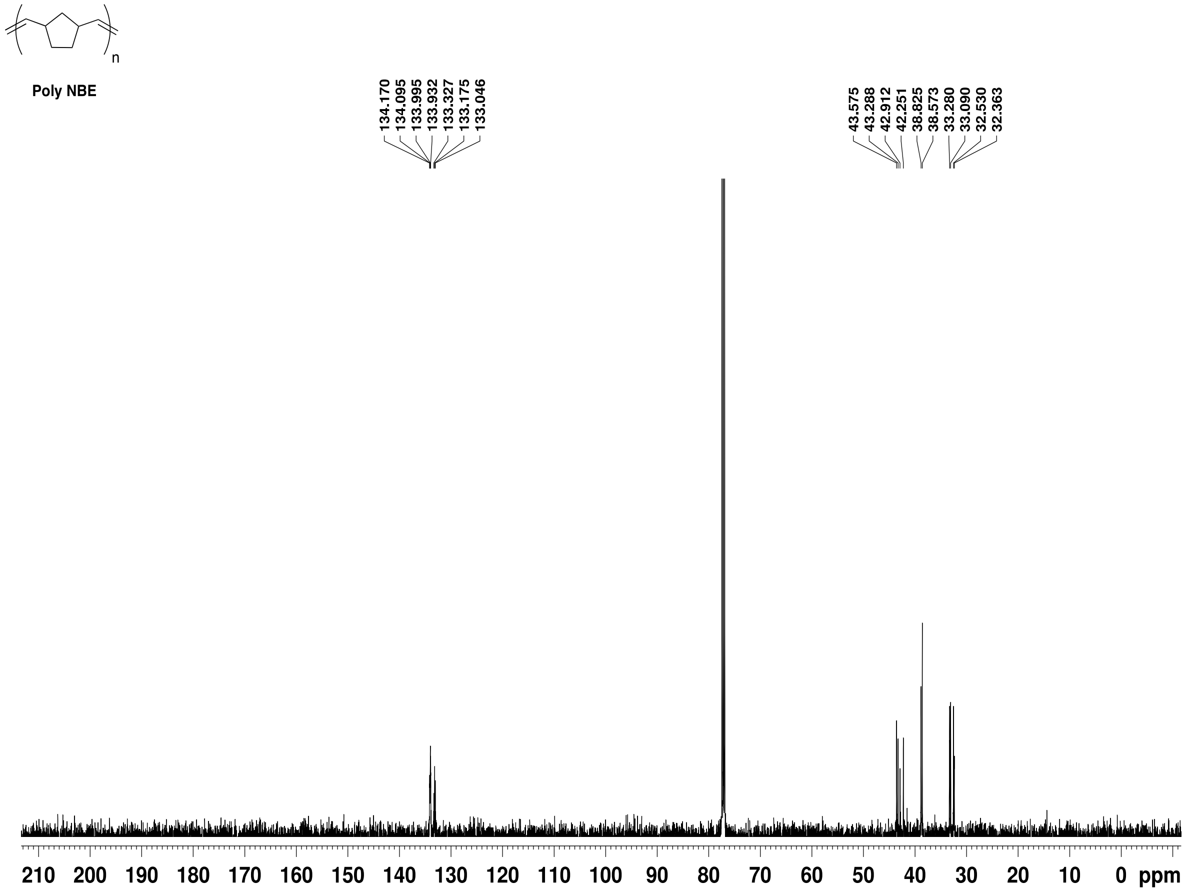
Poly NBE
n
134.170
134.095
133.995
133.932
133.327
133.175
133.046
43.575
43.288
42.912
42.251
38.825
38.573
33.280
33.090
32.530
32.363
210
200
190
180
170
160
150
140
130
120
110
100
90
80
70
60
50
40
30
20
10
0
ppm

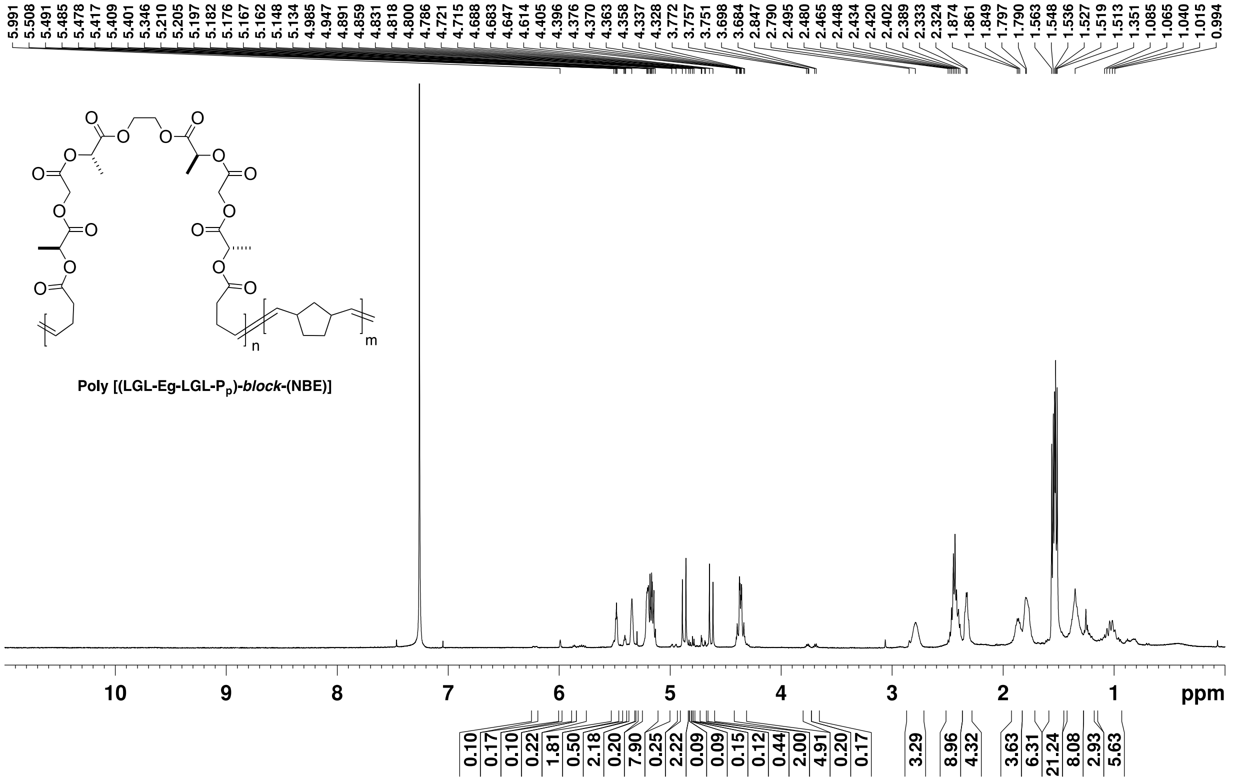
5.991
5.508
5.491
5.485
5.478
5.417
5.409
5.401
5.346
5.210
5.205
5.197
5.182
5.176
5.167
5.162
5.148
5.134
4.985
4.947
4.891
4.859
4.831
4.818
4.800
4.786
4.721
4.715
4.688
4.683
4.647
4.614
4.405
4.396
4.376
4.370
4.363
4.358
4.337
4.328
3.772
3.757
3.751
3.698
3.684
2.847
2.790
2.495
2.480
2.465
2.448
2.434
2.420
2.402
2.389
2.333
2.324
1.874
1.861
1.849
1.797
1.790
1.563
1.548
1.536
1.527
1.519
1.513
1.351
1.085
1.065
1.040
1.015
0.994
O
n
m
Poly [(LGL-Eg-LGL-P$_p$)-*block*-(NBE)]
10
9
8
7
6
5
4
3
2
1
ppm
0.10
0.17
0.10
0.22
1.81
0.50
2.18
0.20
7.90
0.25
2.22
0.09
0.09
0.15
0.12
0.44
2.00
4.91
0.20
0.17
3.29
8.96
4.32
3.63
6.31
21.24
8.08
2.93
5.63

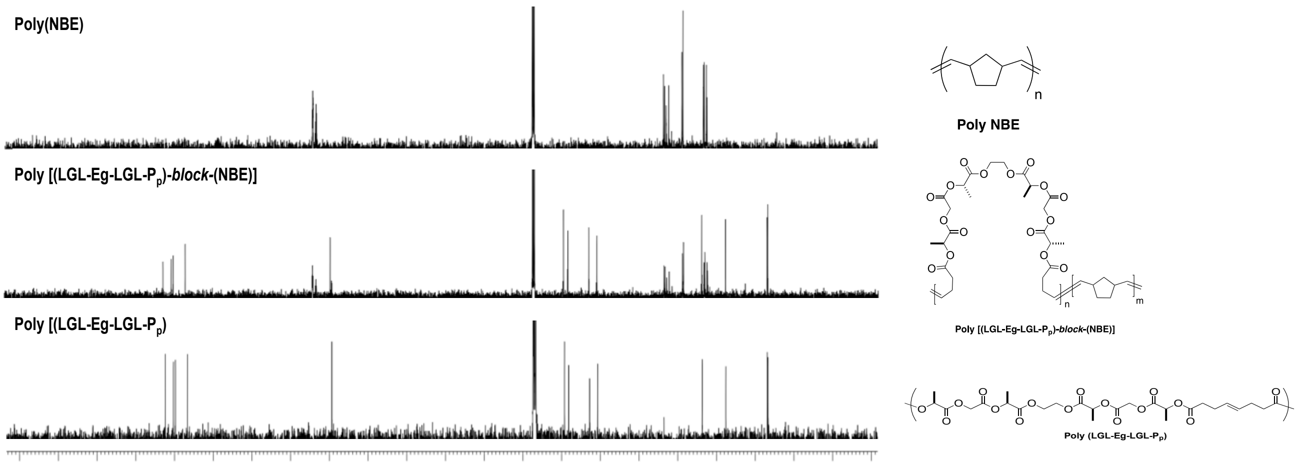
Poly(NBE)
Poly [(LGL-Eg-LGL-P$_p$)-*block*-(NBE)]
Poly [(LGL-Eg-LGL-P$_p$)
210
200
190
180
170
160
150
140
130
120
110
100
90
80
70
60
50
40
30
20
10
0 ppm
n
Poly NBE
O
n
m
Poly [(LGL-Eg-LGL-P$_p$)-*block*-(NBE)]
Poly (LGL-Eg-LGL-P$_p$)

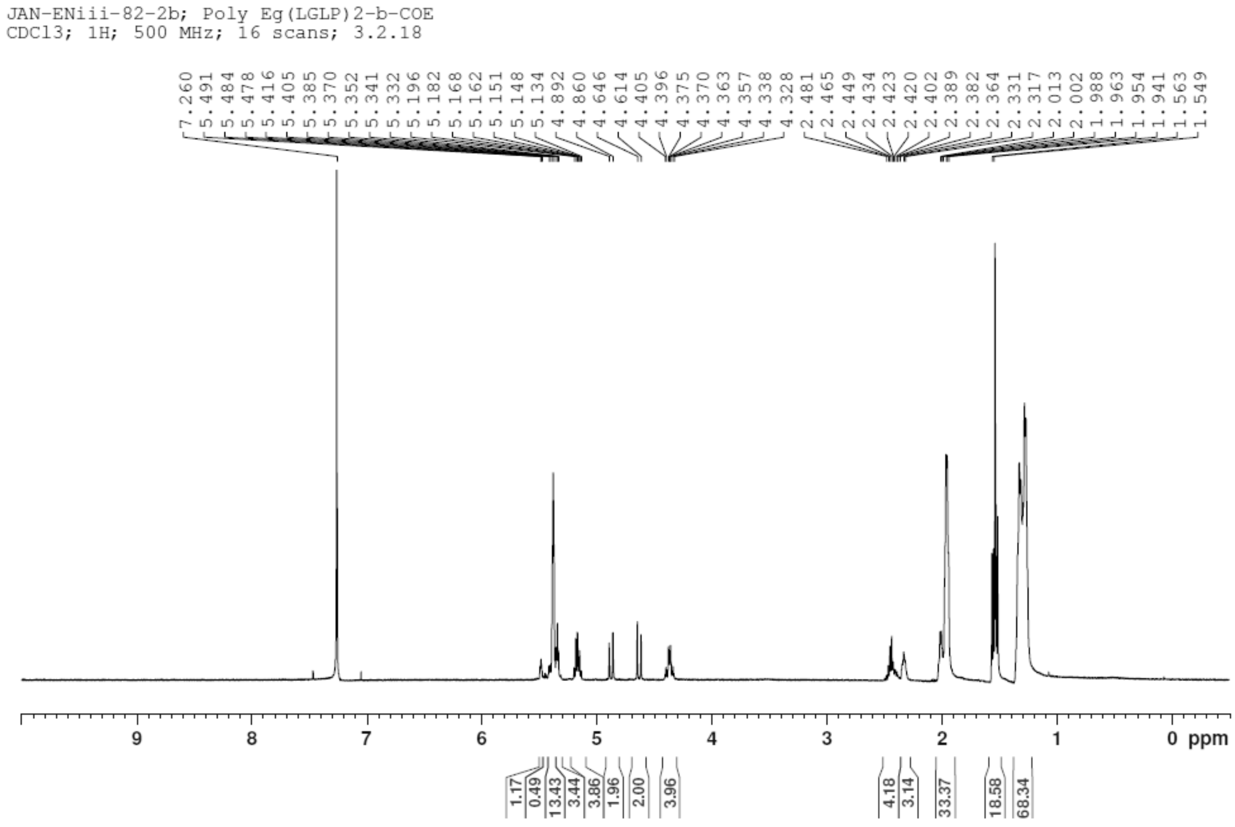
JAN-ENiii-82-2b; Poly Eg(LGLP)2-b-COE
CDCl3; 1H; 500 MHz; 16 scans; 3.2.18
7.260
5.491
5.484
5.478
5.416
5.405
5.385
5.370
5.352
5.341
5.332
5.196
5.182
5.168
5.162
5.151
5.148
5.134
4.892
4.860
4.646
4.614
4.405
4.396
4.375
4.370
4.363
4.357
4.338
4.328
2.481
2.465
2.449
2.434
2.423
2.420
2.402
2.389
2.382
2.364
2.331
2.317
2.013
2.002
1.988
1.963
1.954
1.941
1.563
1.549
9
8
7
6
5
4
3
2
1
0 ppm
1.17
0.49
13.43
3.44
3.86
1.96
2.00
3.96
4.18
3.14
33.37
18.58
68.34

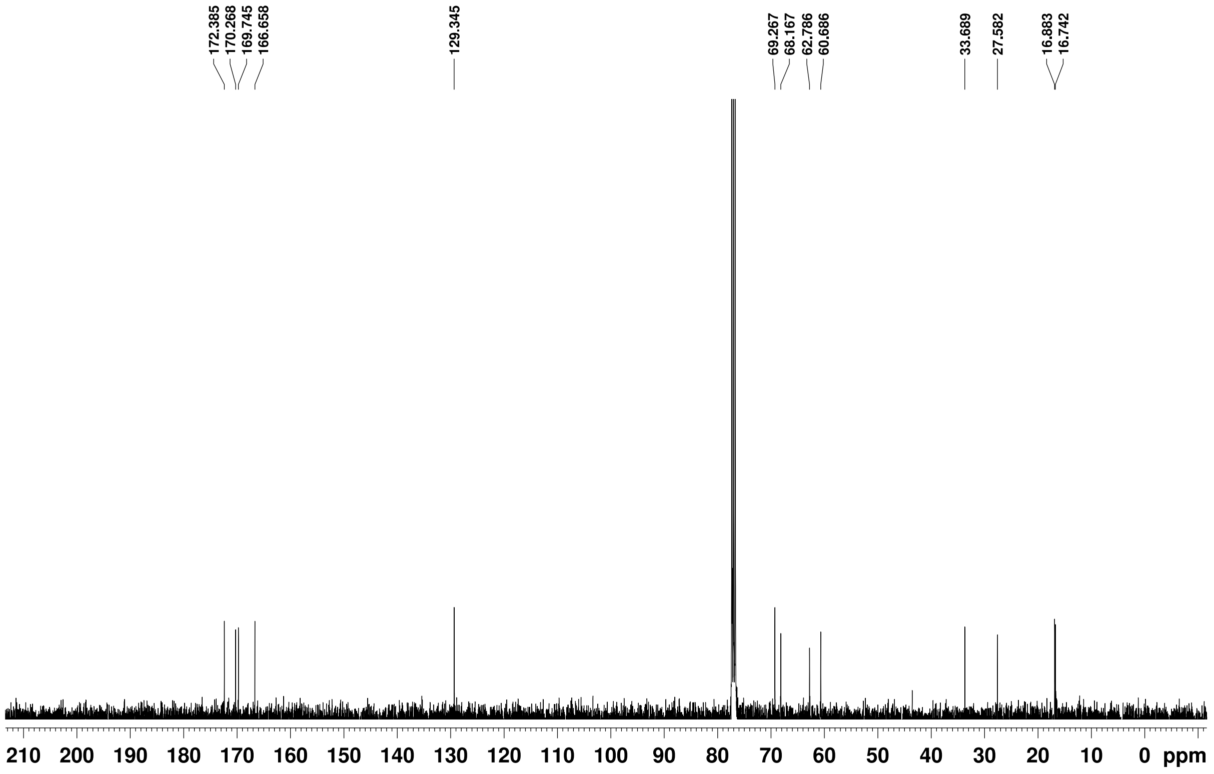
172.385
170.268
169.745
166.658
129.345
69.267
68.167
62.786
60.686
33.689
27.582
16.883
16.742
210
200
190
180
170
160
150
140
130
120
110
100
90
80
70
60
50
40
30
20
10
0 ppm

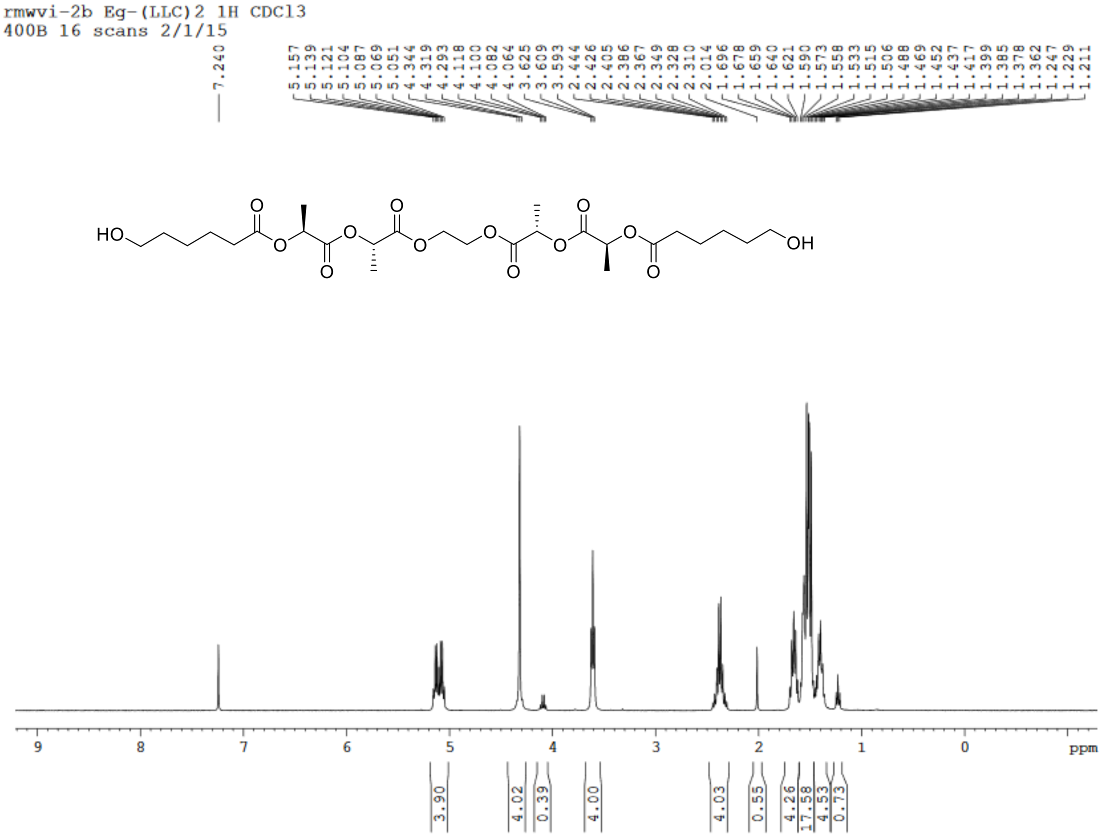
rmwvi-2b Eg-(LLC)2 1H CDCl3
400B 16 scans 2/1/15
7.240
5.157
5.139
5.121
5.104
5.087
5.069
5.051
4.344
4.319
4.293
4.118
4.100
4.082
4.064
3.625
3.609
3.593
2.444
2.426
2.405
2.386
2.367
2.349
2.328
2.310
2.014
1.696
1.678
1.659
1.640
1.621
1.590
1.573
1.558
1.533
1.515
1.506
1.488
1.469
1.452
1.437
1.417
1.399
1.385
1.378
1.362
1.247
1.229
1.211
HO
O
O
O
O
O
O
O
O
O
O
O
OH
9
8
7
6
5
4
3
2
1
0
ppm
3.90
4.02
0.39
4.00
4.03
0.55
4.26
17.58
4.53
0.73

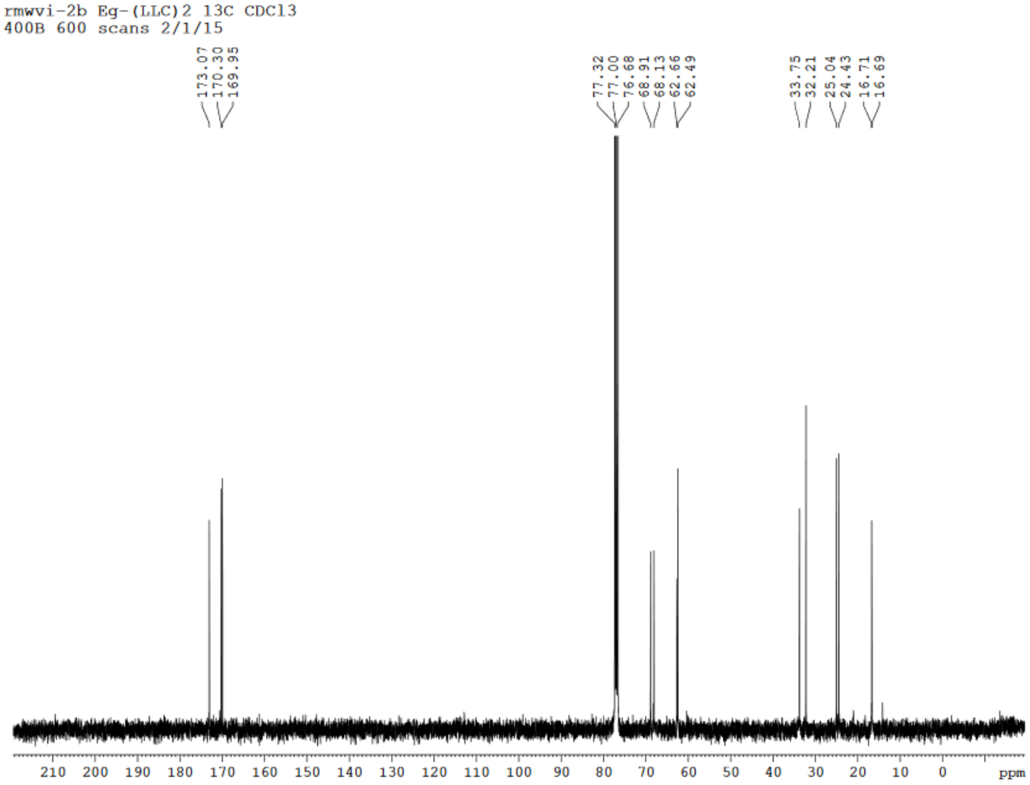
rmwvi-2b Eg-(LLC)2 13C CDCl3
400B 600 scans 2/1/15
173.07
170.30
169.95
77.32
77.00
76.68
68.91
68.13
62.66
62.49
33.75
32.21
25.04
24.43
16.71
16.69
210
200
190
180
170
160
150
140
130
120
110
100
90
80
70
60
50
40
30
20
10
0
ppm

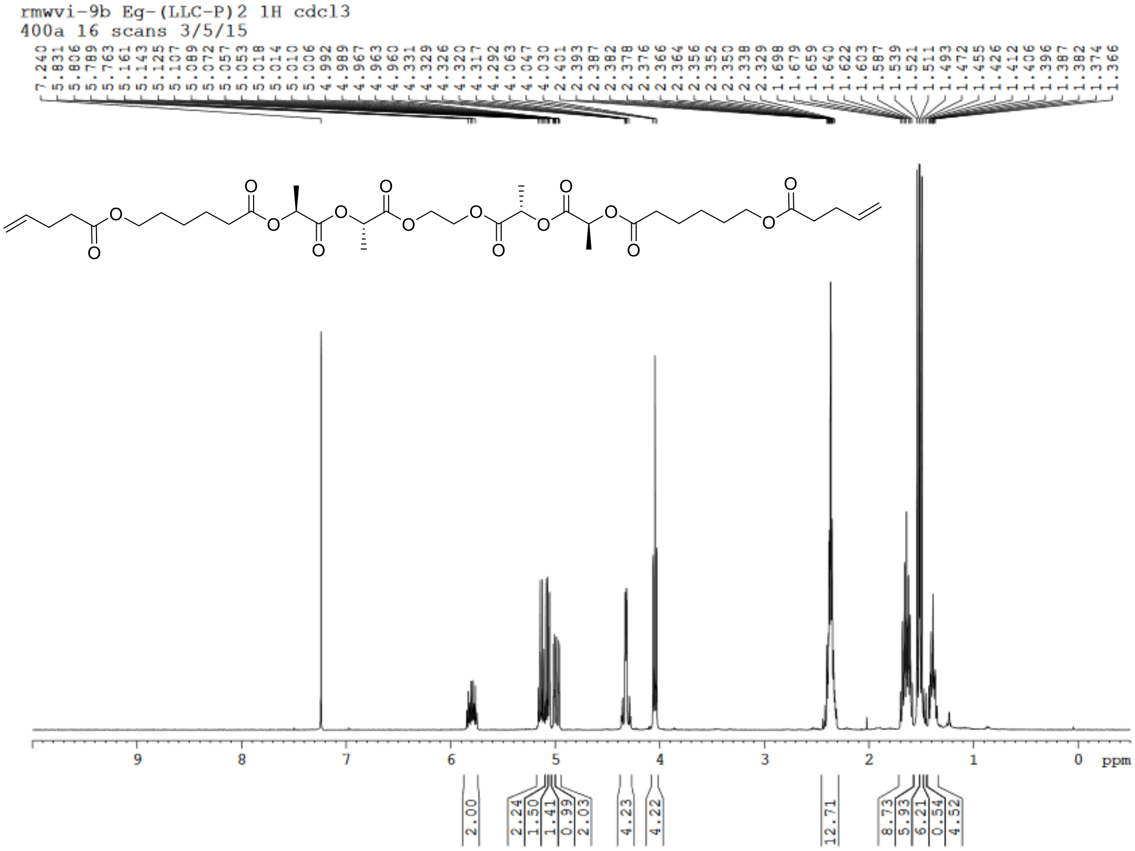
rmwvi-9b Eg-(LLC-P)2 1H cdcl3
400a 16 scans 3/5/15
7.240
5.831
5.806
5.789
5.763
5.161
5.143
5.125
5.107
5.089
5.072
5.057
5.053
5.018
5.014
5.010
5.006
4.992
4.989
4.967
4.963
4.960
4.331
4.329
4.326
4.320
4.317
4.292
4.063
4.047
4.030
2.401
2.393
2.387
2.382
2.378
2.376
2.366
2.364
2.356
2.352
2.350
2.338
2.329
1.698
1.679
1.659
1.640
1.622
1.603
1.587
1.539
1.521
1.511
1.493
1.472
1.455
1.426
1.412
1.406
1.396
1.387
1.382
1.374
1.366
9
8
7
6
5
4
3
2
1
0
ppm
2.00
2.24
1.50
1.41
0.99
2.03
4.23
4.22
12.71
8.73
5.93
6.21
0.54
4.52

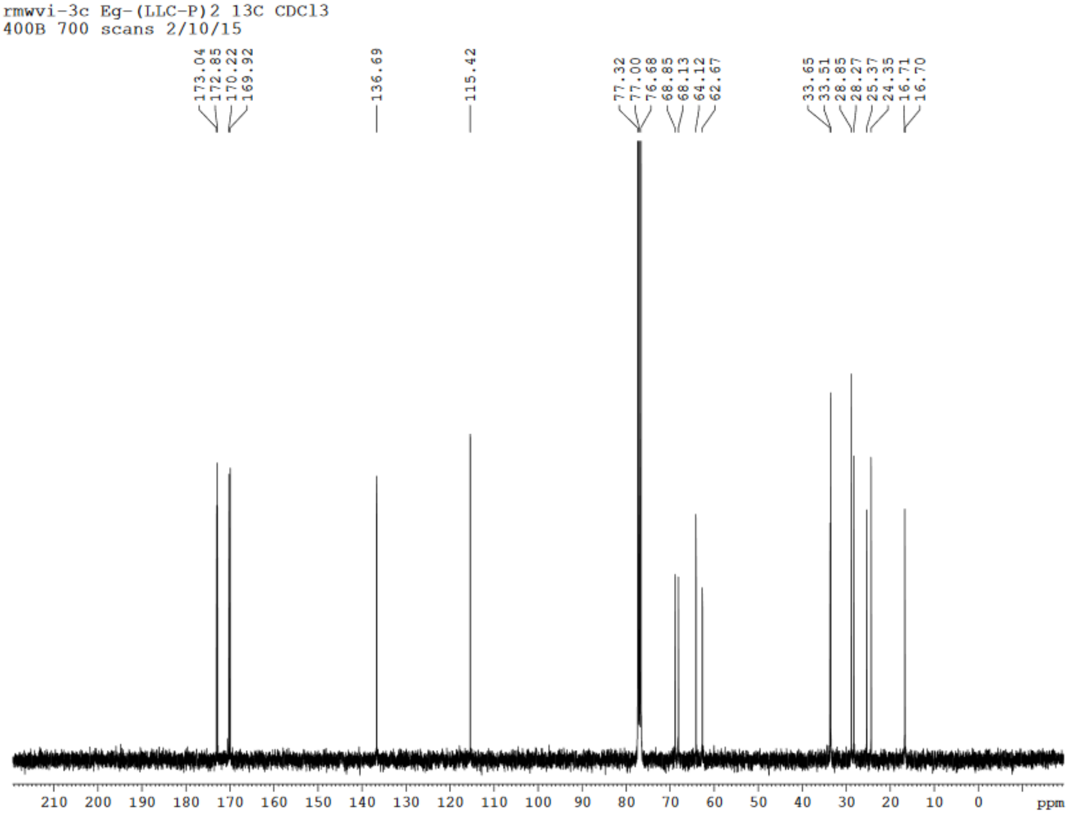
rmwvi-3c Eg-(LLC-P)2 13C CDCl3
400B 700 scans 2/10/15
173.04
172.85
170.22
169.92
136.69
115.42
77.32
77.00
76.68
68.85
68.13
64.12
62.67
33.65
33.51
28.85
28.27
25.37
24.35
16.71
16.70
210
200
190
180
170
160
150
140
130
120
110
100
90
80
70
60
50
40
30
20
10
0
ppm

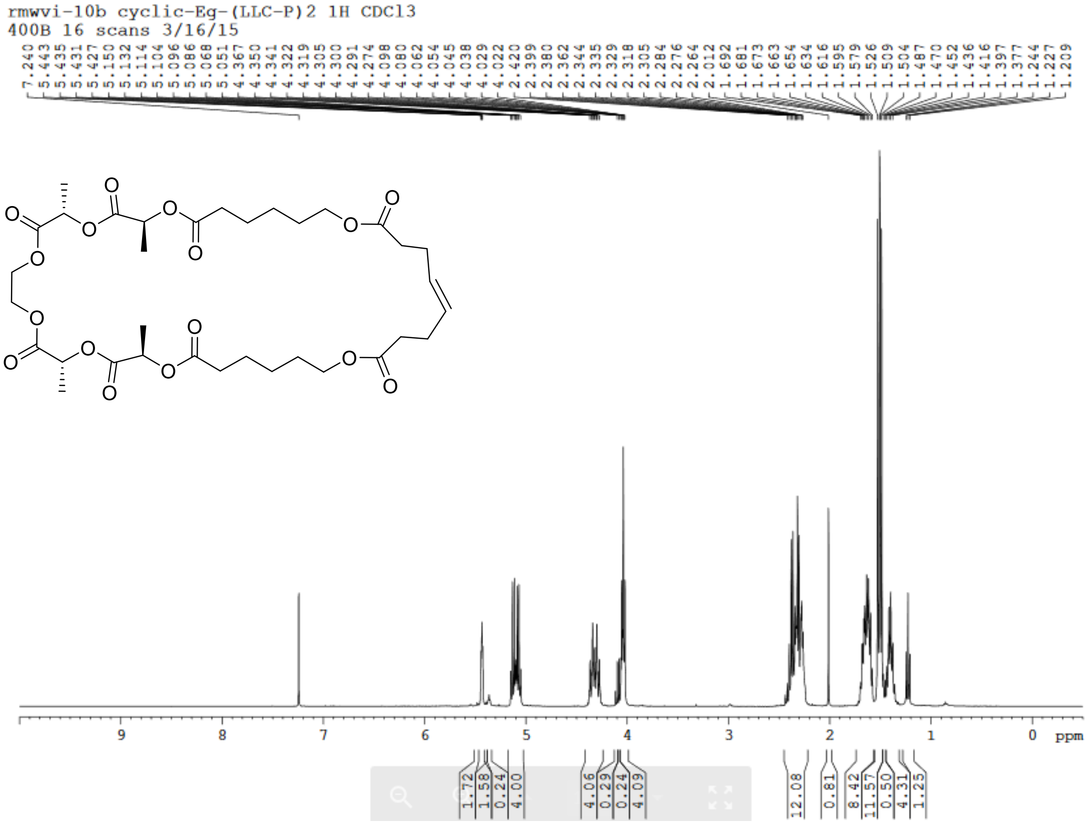
rmwvi-10b cyclic-Eg-(LLC-P)2 1H CDCl3
400B 16 scans 3/16/15
7.240 5.443 5.435 5.431 5.427 5.150 5.132 5.114 5.104 5.096 5.086 5.068 5.051 4.367 4.350 4.341 4.322 4.319 4.305 4.300 4.291 4.274 4.098 4.080 4.062 4.054 4.045 4.038 4.029 4.022 2.420 2.399 2.380 2.362 2.344 2.335 2.329 2.318 2.305 2.284 2.276 2.264 2.012 1.692 1.681 1.673 1.663 1.654 1.634 1.616 1.595 1.579 1.526 1.509 1.504 1.487 1.470 1.452 1.436 1.416 1.397 1.377 1.244 1.227 1.209
O
O
O
O
O
O
O
O
O
O
O
O
O
O
O
O
9
8
7
6
5
4
3
2
1
0
ppm
1.72
1.58
0.24
4.00
4.06
0.29
0.24
4.09
12.08
0.81
8.42
11.57
0.50
4.31
1.25

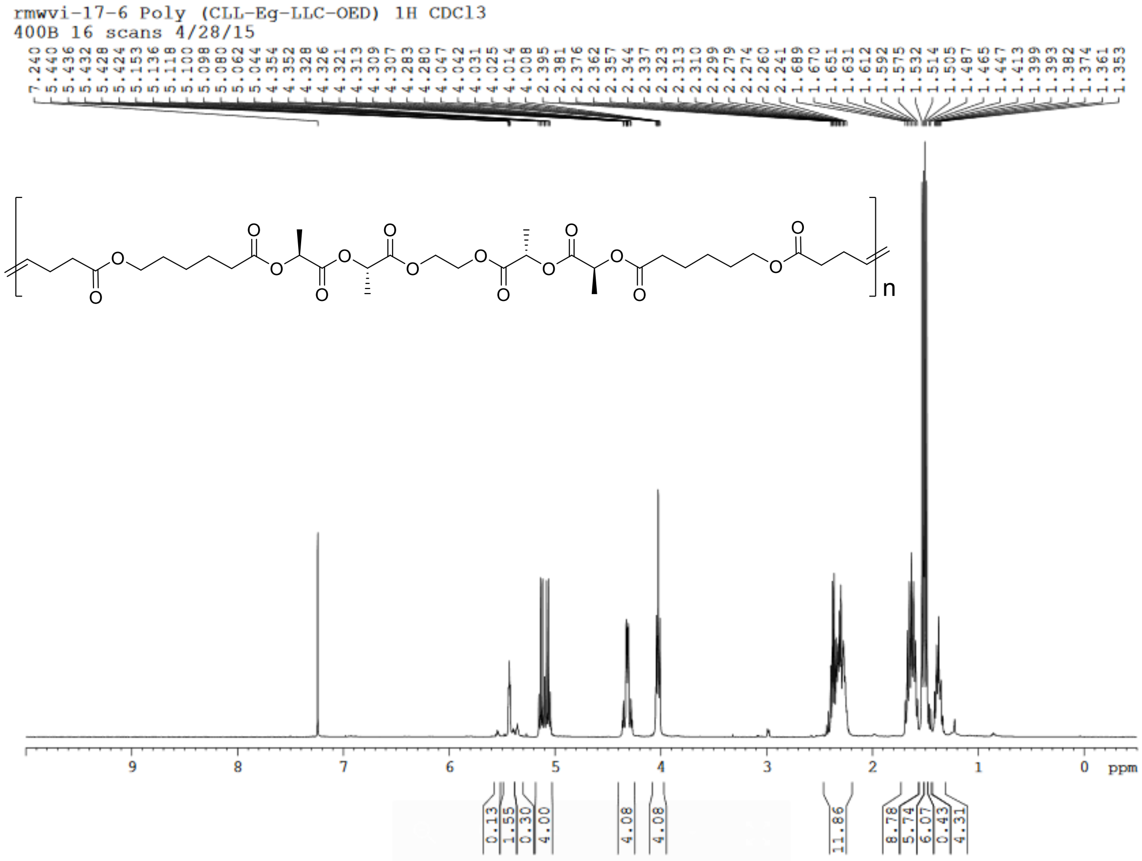
rmwvi-17-6 Poly (CLL-Eg-LLC-OED) 1H CDCl3
400B 16 scans 4/28/15
7.240 5.440 5.436 5.432 5.428 5.424 5.153 5.136 5.118 5.100 5.098 5.080 5.062 5.044 4.354 4.352 4.328 4.326 4.321 4.313 4.309 4.307 4.283 4.280 4.047 4.042 4.031 4.025 4.014 4.008 2.395 2.381 2.376 2.362 2.357 2.344 2.337 2.323 2.313 2.310 2.299 2.279 2.274 2.260 2.241 1.689 1.670 1.651 1.631 1.612 1.592 1.575 1.532 1.514 1.505 1.487 1.465 1.447 1.413 1.399 1.393 1.382 1.374 1.361 1.353
O
O
O
O
O
O
O
O
O
O
O
O
O
O
O
O
n
9
8
7
6
5
4
3
2
1
0
ppm
0.13
1.55
0.30
4.00
4.08
4.08
11.86
8.78
5.74
6.07
0.43
4.31

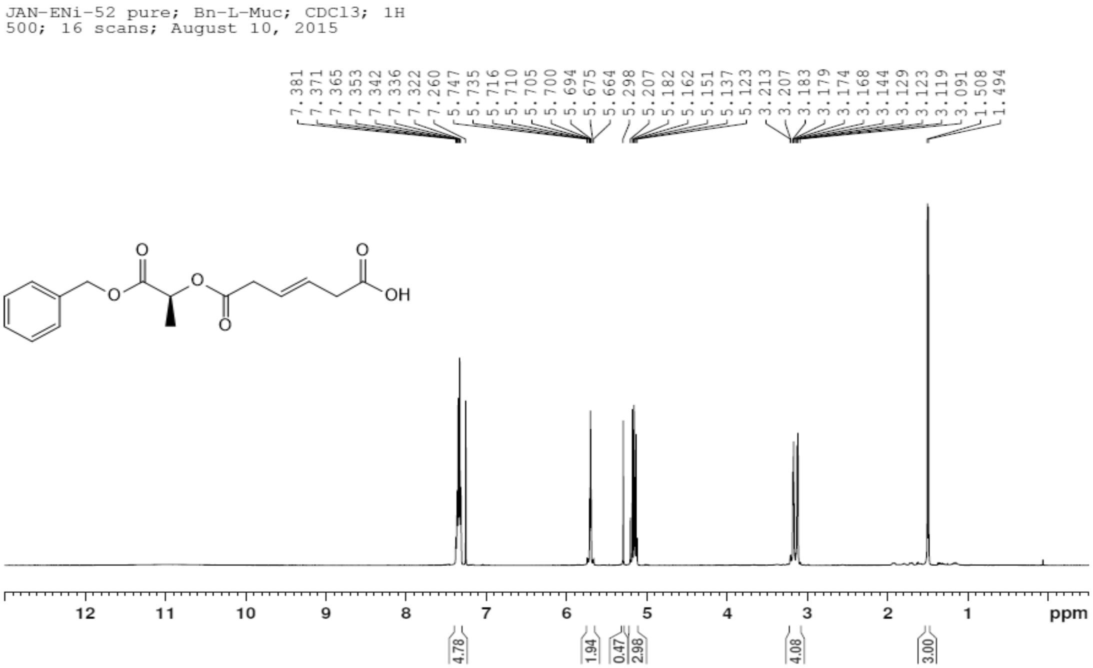
JAN-ENi-52 pure; Bn-L-Muc; CDCl3; 1H
500; 16 scans; August 10, 2015
7.381
7.371
7.365
7.353
7.342
7.336
7.322
7.260
5.747
5.735
5.716
5.710
5.705
5.700
5.694
5.675
5.664
5.298
5.207
5.182
5.162
5.151
5.137
5.123
3.213
3.207
3.183
3.179
3.174
3.168
3.144
3.129
3.123
3.119
3.091
1.508
1.494
O
O
O
O
O
O
OH
12
11
10
9
8
7
6
5
4
3
2
1
ppm
4.78
1.94
0.47
2.98
4.08
3.00

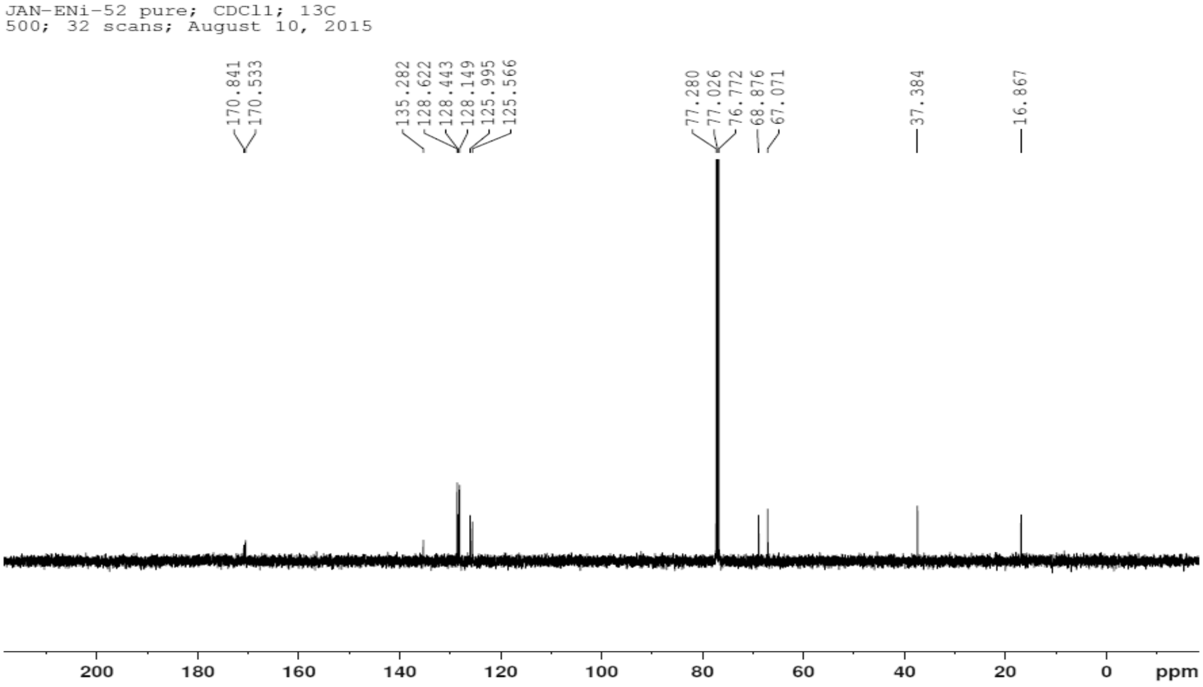
JAN-ENi-52 pure; CDCl1; 13C
500; 32 scans; August 10, 2015
170.841
170.533
135.282
128.622
128.443
128.149
125.995
125.566
77.280
77.026
76.772
68.876
67.071
37.384
16.867
200
180
160
140
120
100
80
60
40
20
0
ppm

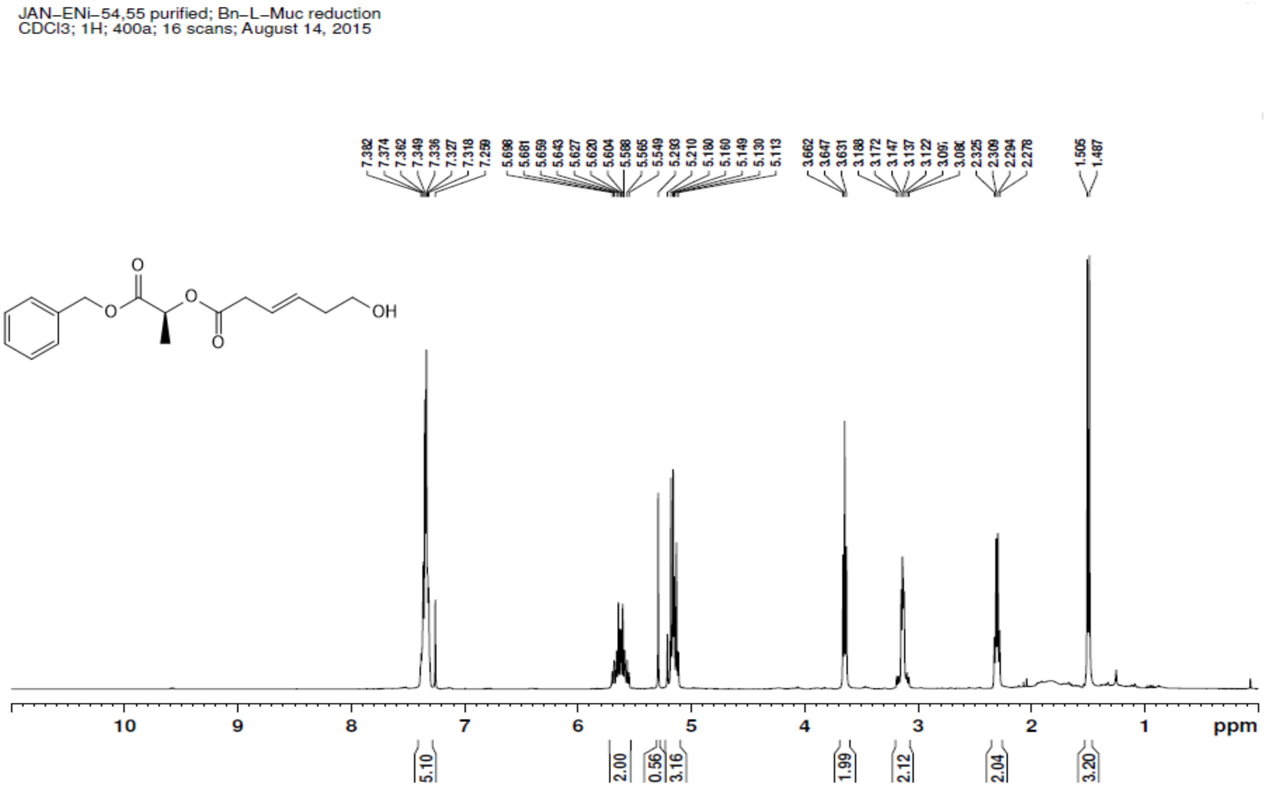
JAN–ENi–54,55 purified; Bn–L–Muc reduction
CDCl3; 1H; 400a; 16 scans; August 14, 2015

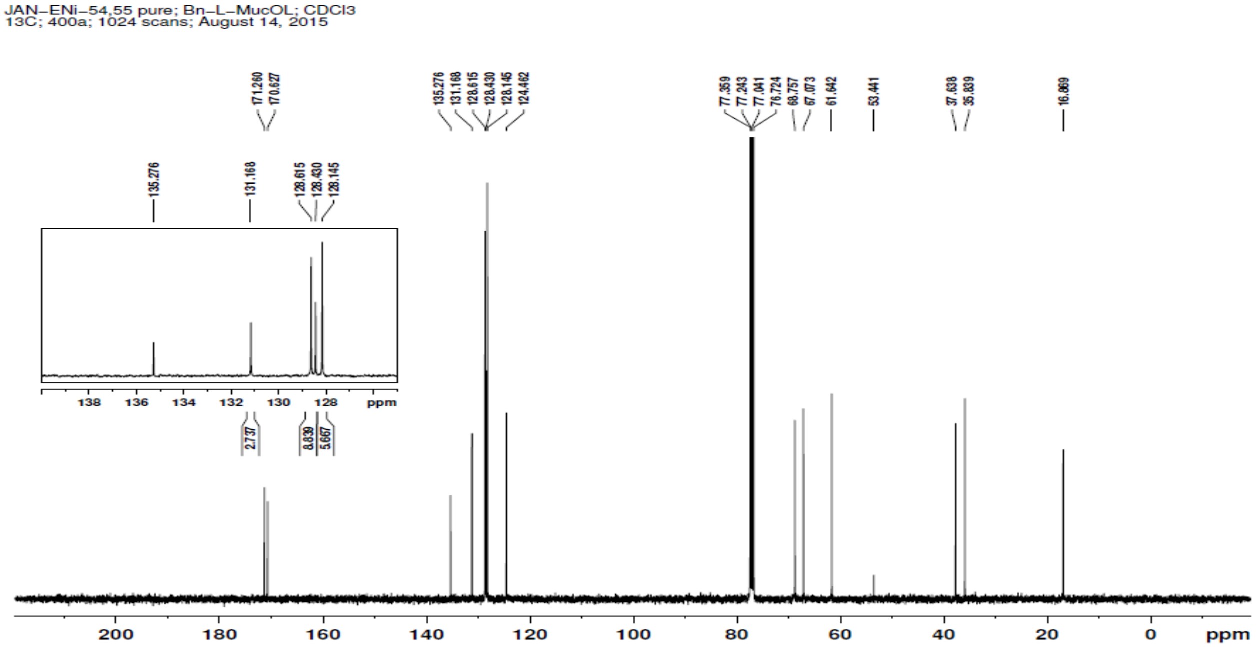
JAN–ENi–54,55 pure; Bn–L–MucOL; CDCl3
13C; 400a; 1024 scans; August 14, 2015

JAN-ENi-67 pure; Bn-LGL; CDCl3; 1H
400a; 16 scans; September 18, 2015

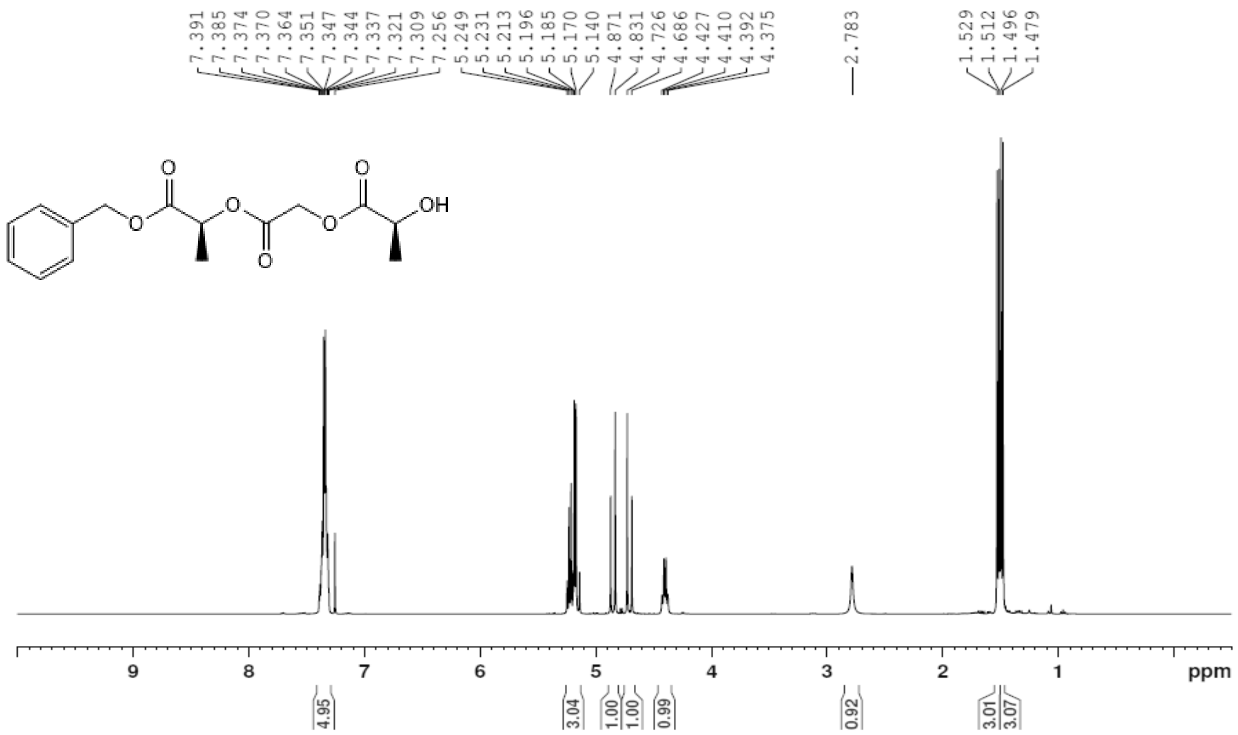

JAN-ENii-11; Bn-LGL; 13C; CDCl3; 400 MHz
16 scans; May 6, 2016

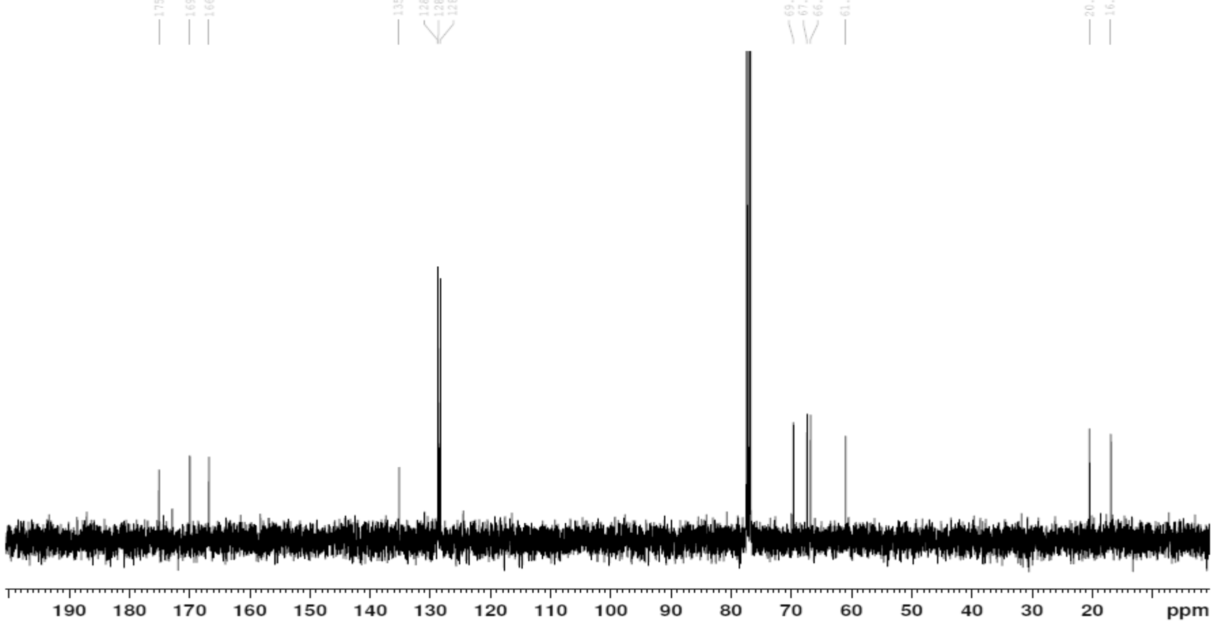

JAN-ENi-67 pure; Bn-LGLGL-Si; CDCl3; 1H
400a; 16 scans; September 18, 2015

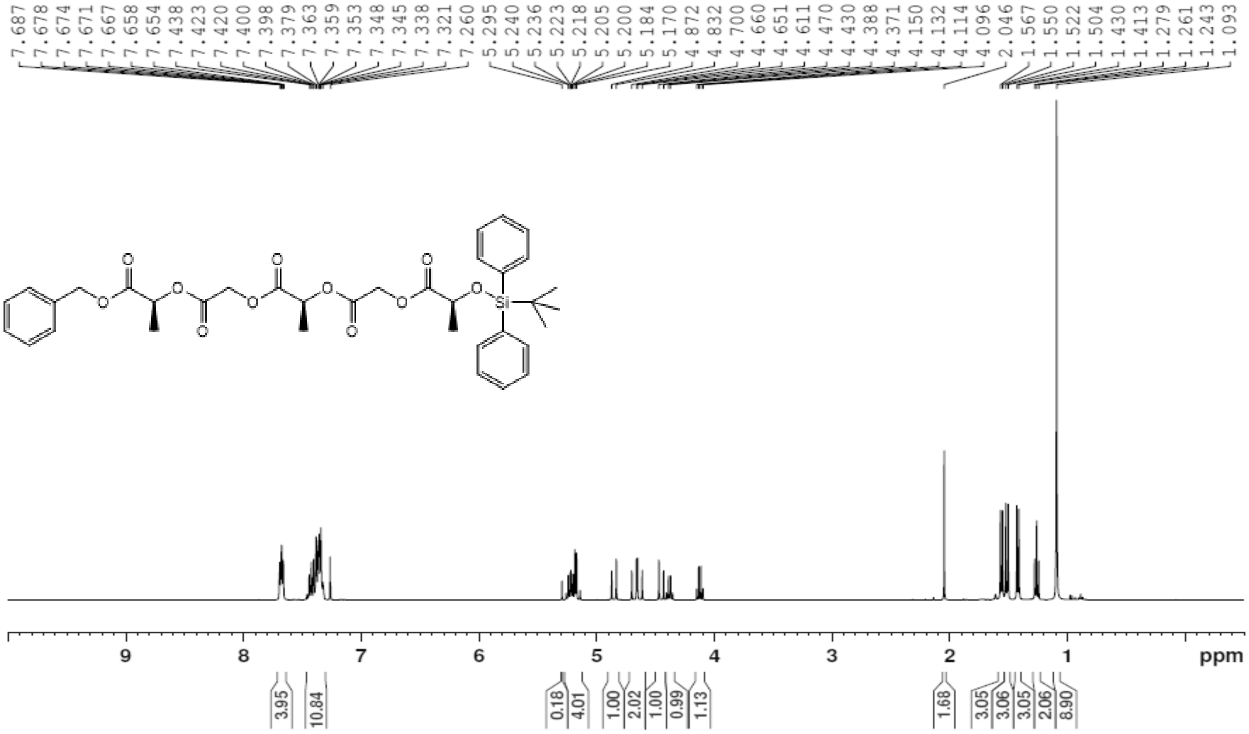

JAN-ENi-67 pure; Bn-LGLGL-Si; CDCl3; 13C
400a; 1024 scans; September 18, 2015

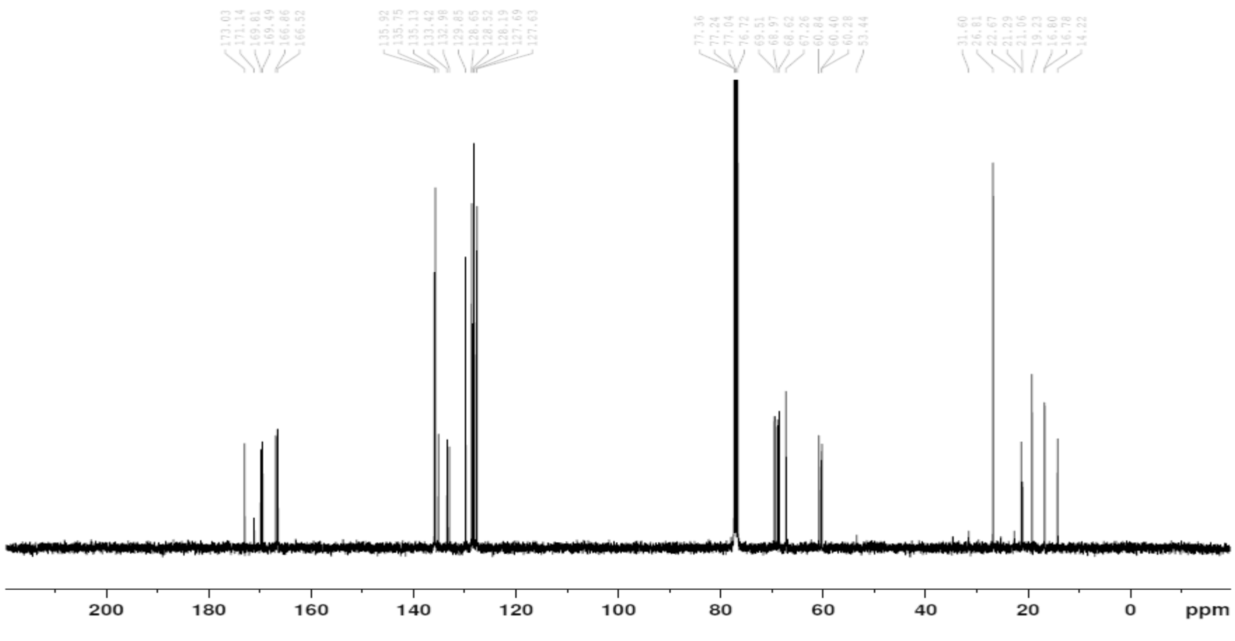

JAN-ENi-68 pure vac; Bn-LGLGL; CDCl3; 1H
400a; 16 scans; September 22, 2015

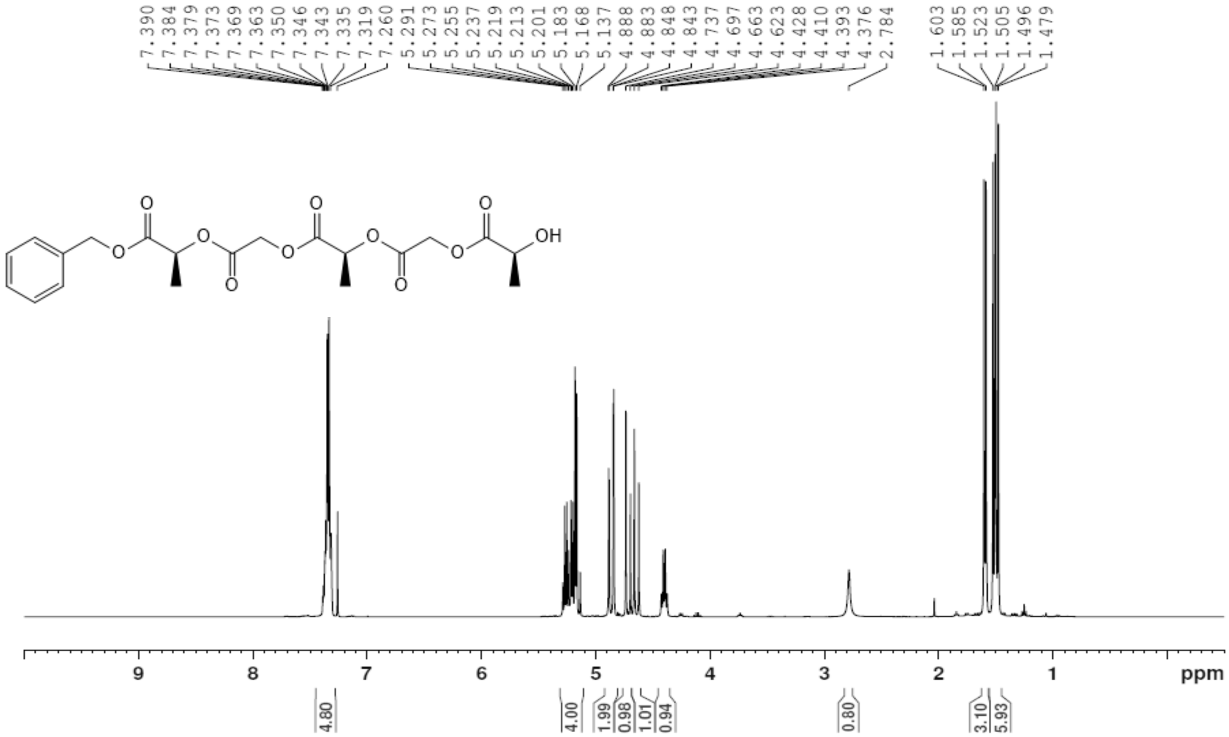

JAN-ENi-68; Bn-LGLGL; CDCl3; 13C
400a; 16 scans; September 22, 2015

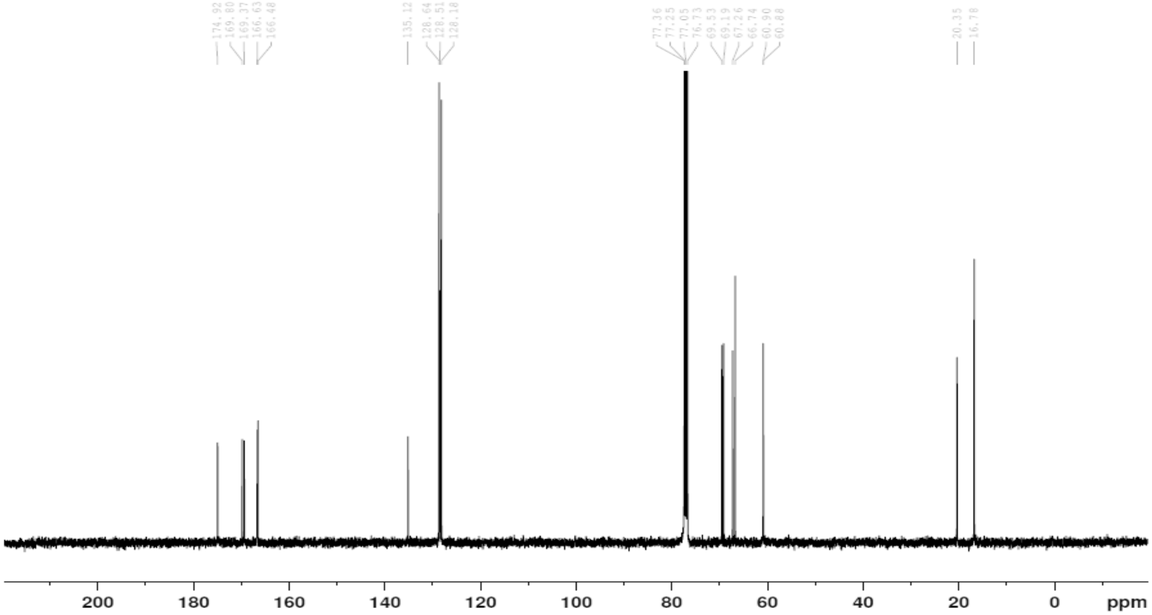

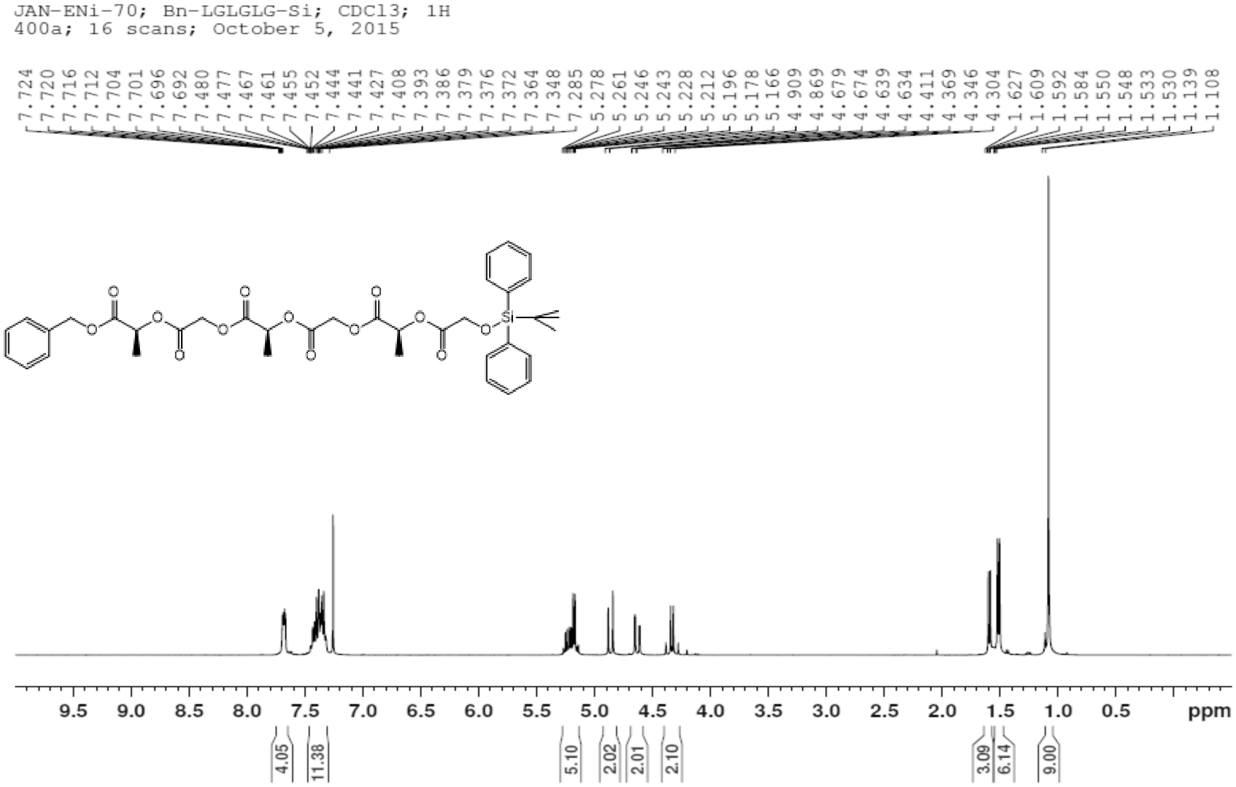

JAN-ENi-70; Bn-LGLGLG-Si; CDCl3; 1H
400a; 16 scans; October 5, 2015
7.724
7.720
7.716
7.712
7.704
7.701
7.696
7.692
7.480
7.477
7.467
7.461
7.455
7.452
7.444
7.441
7.427
7.408
7.393
7.386
7.379
7.376
7.372
7.364
7.348
7.285
5.278
5.261
5.246
5.243
5.228
5.212
5.196
5.178
5.166
4.909
4.869
4.679
4.674
4.639
4.634
4.411
4.369
4.346
4.304
1.627
1.609
1.592
1.584
1.550
1.548
1.533
1.530
1.139
1.108
O
O
O
O
O
O
O
O
O
O
O
O
O
Si
9.5
9.0
8.5
8.0
7.5
7.0
6.5
6.0
5.5
5.0
4.5
4.0
3.5
3.0
2.5
2.0
1.5
1.0
0.5
ppm
4.05
11.38
5.10
2.02
2.01
2.10
3.09
6.14
9.00

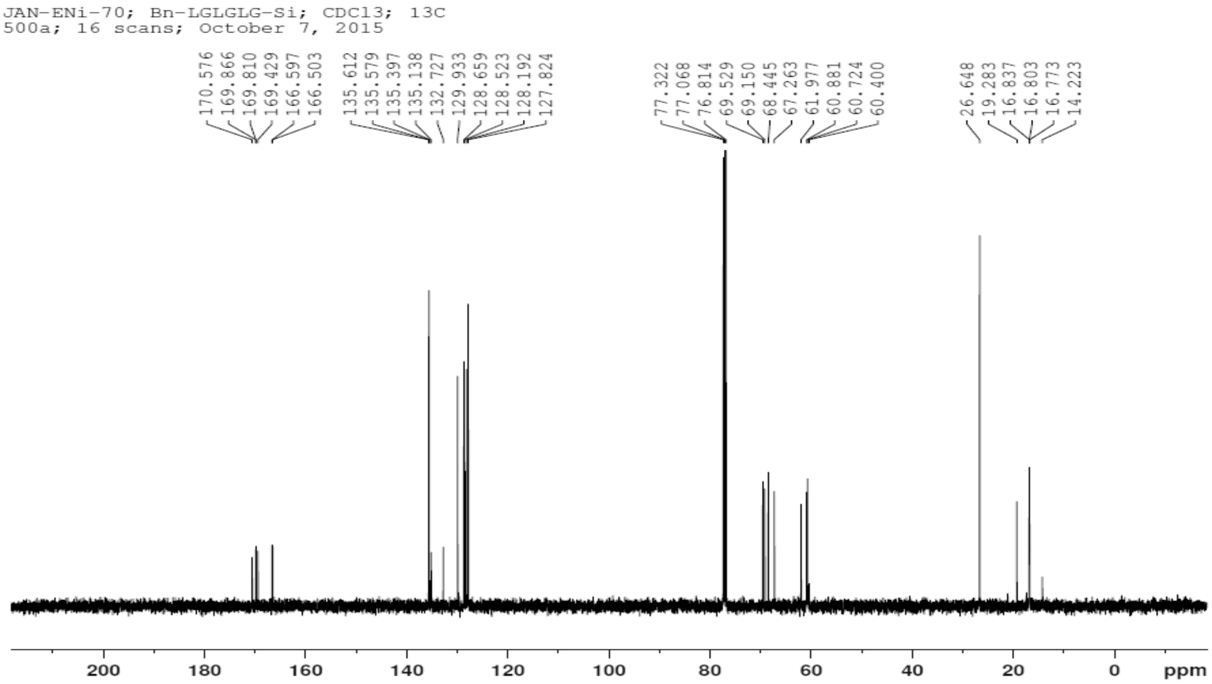

JAN-ENi-70; Bn-LGLGLG-Si; CDCl3; 13C
500a; 16 scans; October 7, 2015
170.576
169.866
169.810
169.429
166.597
166.503
135.612
135.579
135.397
135.138
132.727
129.933
128.659
128.523
128.192
127.824
77.322
77.068
76.814
69.529
69.150
68.445
67.263
61.977
60.881
60.724
60.400
26.648
19.283
16.837
16.803
16.773
14.223
200
180
160
140
120
100
80
60
40
20
0
ppm

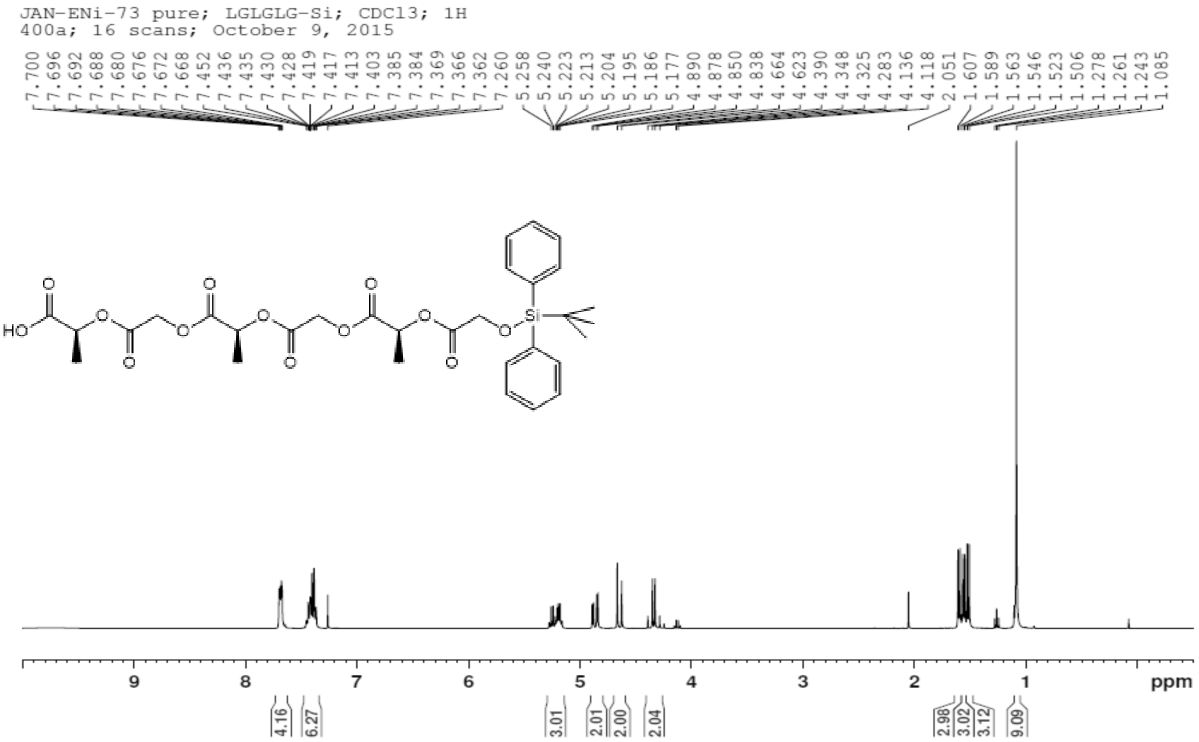
JAN-ENi-73 pure; LGLGLG-Si; CDCl3; 1H
400a; 16 scans; October 9, 2015
7.700 7.696 7.692 7.688 7.680 7.676 7.672 7.668 7.452 7.436 7.435 7.430 7.428 7.419 7.417 7.413 7.403 7.385 7.384 7.369 7.366 7.362 7.260 5.258 5.240 5.223 5.213 5.204 5.195 5.186 5.177 4.890 4.878 4.850 4.838 4.664 4.623 4.390 4.348 4.325 4.283 4.136 4.118 2.051 1.607 1.589 1.563 1.546 1.523 1.506 1.278 1.261 1.243 1.085
HO
O
Si
9
8
7
6
5
4
3
2
1
ppm
4.16
6.27
3.01
2.01
2.00
2.04
2.98
3.02
3.12
9.09

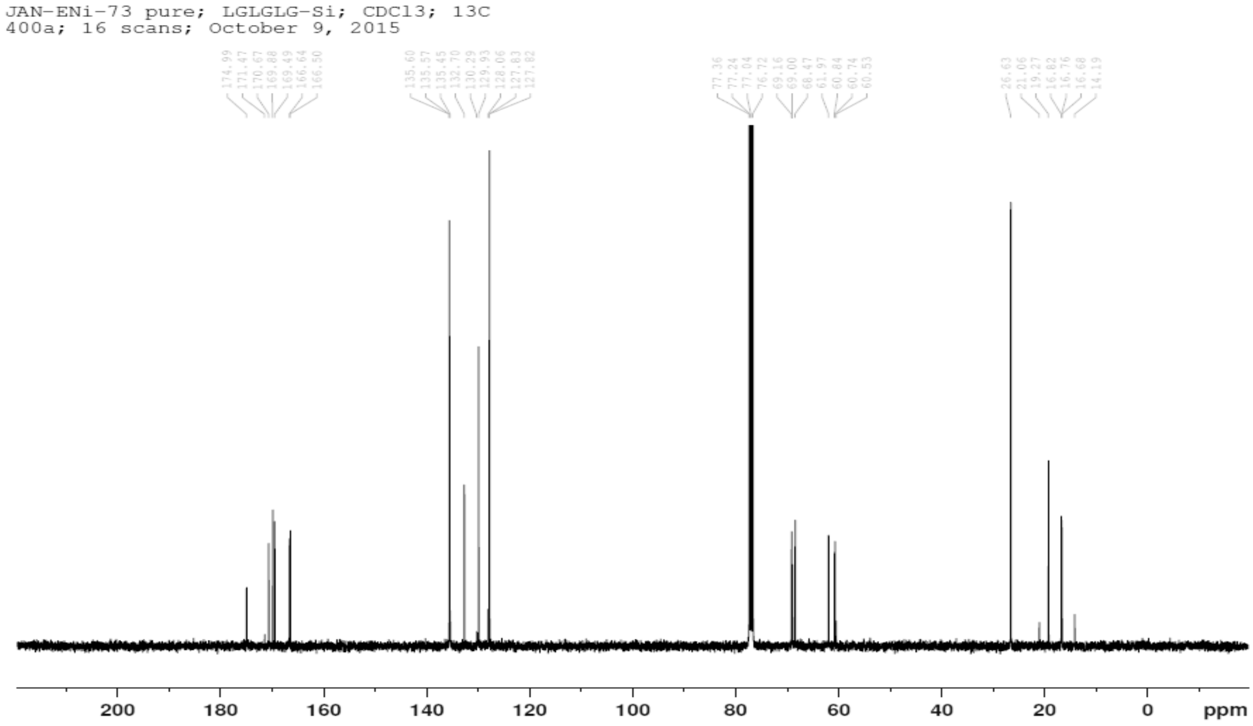
JAN-ENi-73 pure; LGLGLG-Si; CDCl3; 13C
400a; 16 scans; October 9, 2015
174.99 171.47 170.67 169.88 169.49 166.64 166.50
135.60 135.57 135.45 132.70 130.29 129.93 128.06 127.83 127.82
77.36 77.24 77.04 76.72 69.16 69.00 68.47 61.97 60.84 60.74 60.53
26.63 21.06 19.27 16.82 16.76 16.68 14.19
200
180
160
140
120
100
80
60
40
20
0
ppm

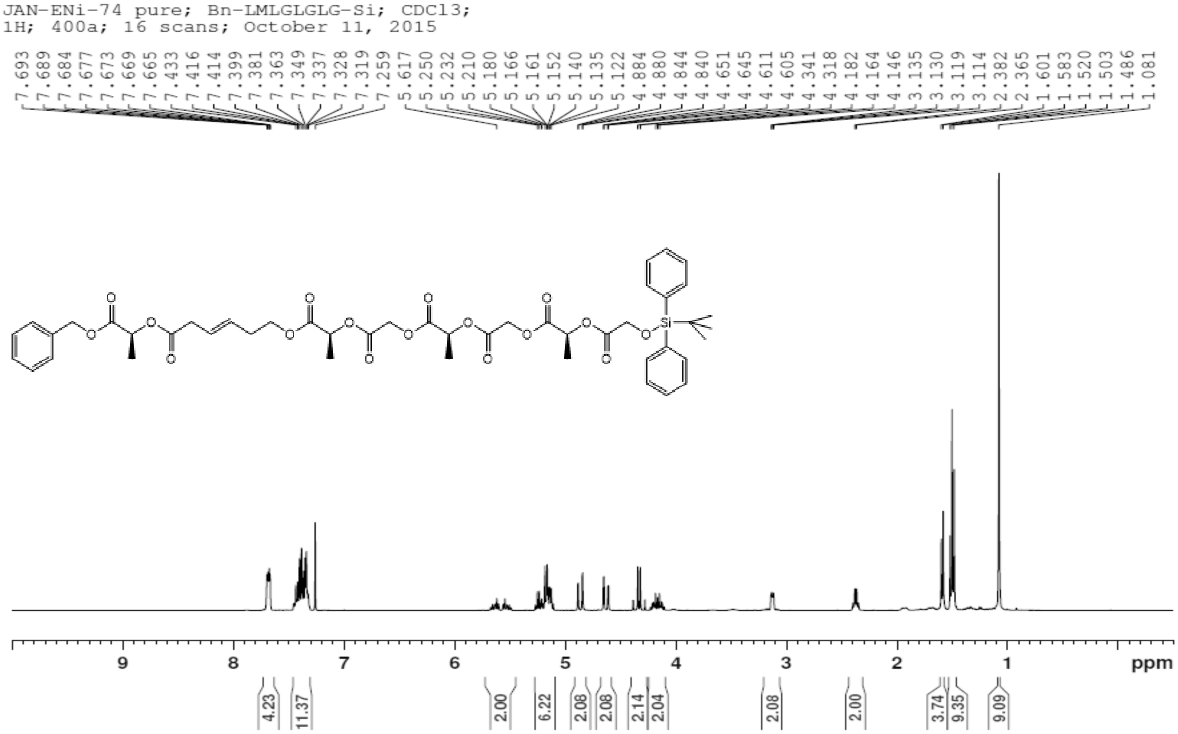
JAN-ENi-74 pure; Bn-LMLGLGLG-Si; CDCl3;
1H; 400a; 16 scans; October 11, 2015
7.693
7.689
7.684
7.677
7.673
7.669
7.665
7.433
7.416
7.414
7.399
7.381
7.363
7.349
7.337
7.328
7.319
7.259
5.617
5.250
5.232
5.210
5.180
5.166
5.161
5.152
5.140
5.135
5.122
4.884
4.880
4.844
4.840
4.651
4.645
4.611
4.605
4.341
4.318
4.182
4.164
4.146
3.135
3.130
3.119
3.114
2.382
2.365
1.601
1.583
1.520
1.503
1.486
1.081
Si
9
8
7
6
5
4
3
2
1
ppm
4.23
11.37
2.00
6.22
2.08
2.08
2.14
2.04
2.08
2.00
3.74
9.35
9.09

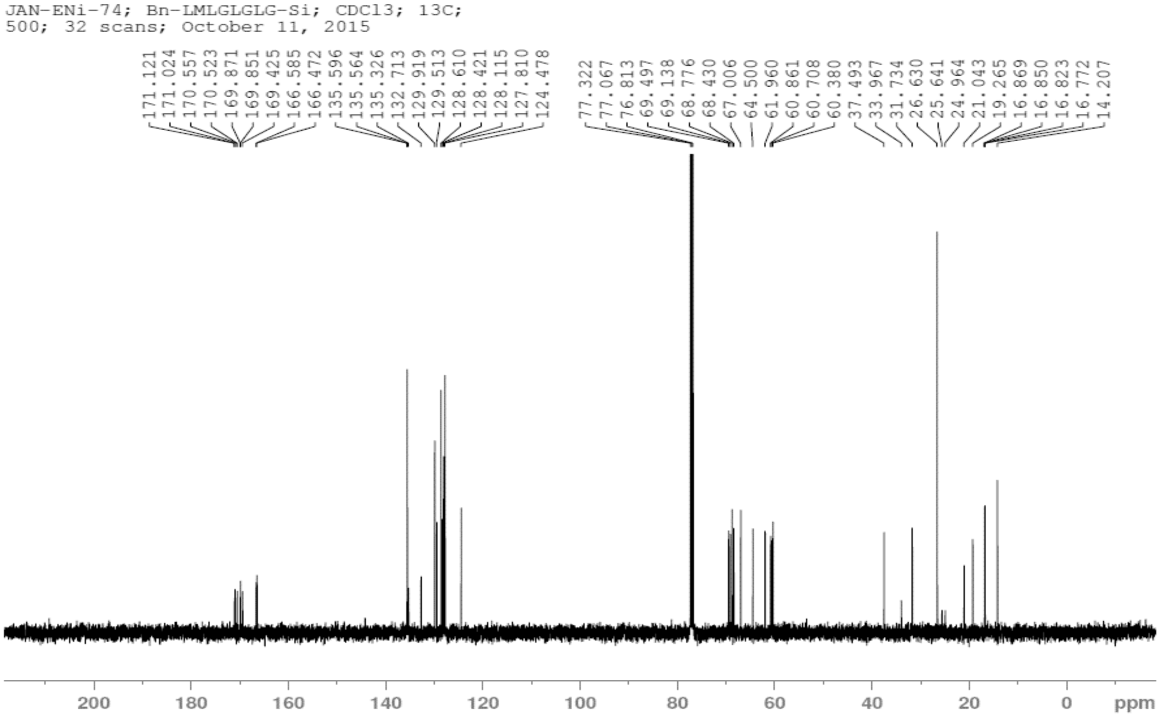
JAN-ENi-74; Bn-LMLGLGLG-Si; CDCl3; 13C;
500; 32 scans; October 11, 2015
171.121
171.024
170.557
170.523
169.871
169.851
169.425
166.585
166.472
135.596
135.564
135.326
132.713
129.919
129.513
128.610
128.421
128.115
127.810
124.478
77.322
77.067
76.813
69.497
69.138
68.776
68.430
67.006
64.500
61.960
60.861
60.708
60.380
37.493
33.967
31.734
26.630
25.641
24.964
21.043
19.265
16.869
16.850
16.823
16.772
14.207
200
180
160
140
120
100
80
60
40
20
0
ppm

JAN-ENi-74; LMLGLGLG-Si; CDCl3; 1H; 400a
16 scans; October 13, 2015

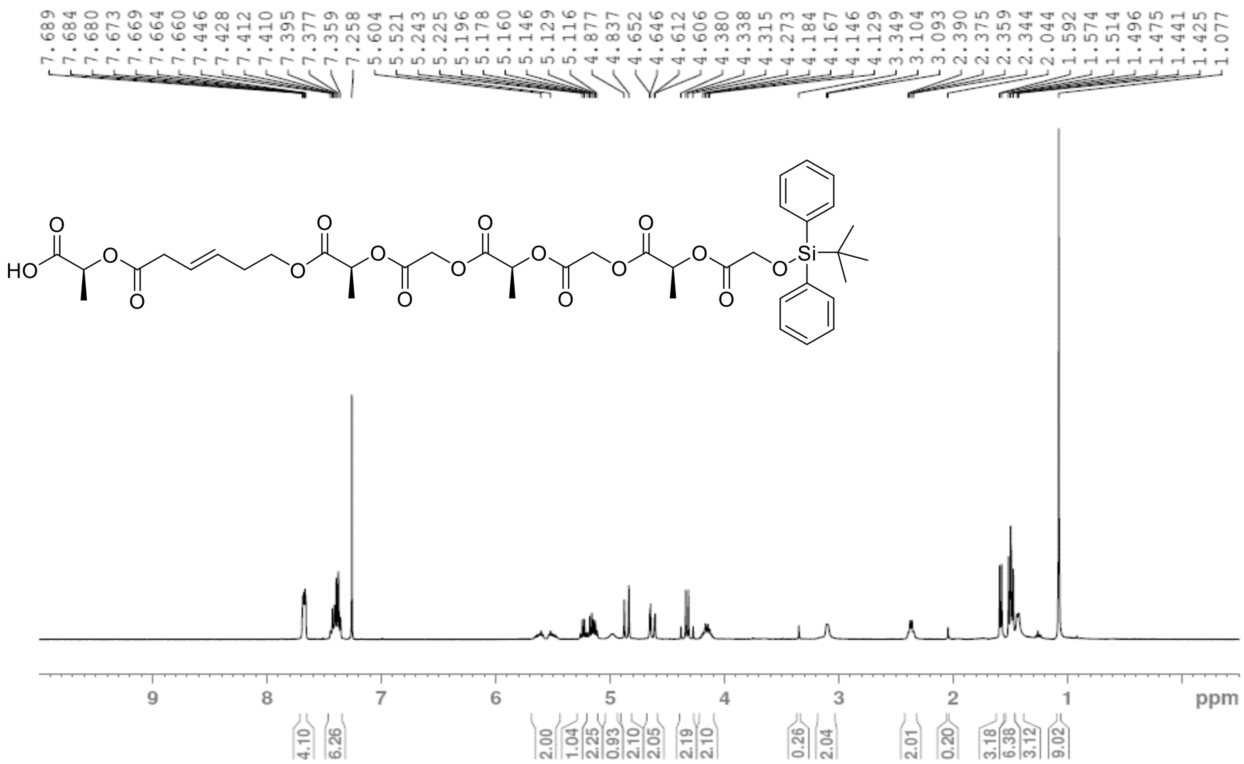

JAN-ENi-75; LMLGLGLG-Si; CDCl3; 13C
500; 32 scans; October 14, 2015

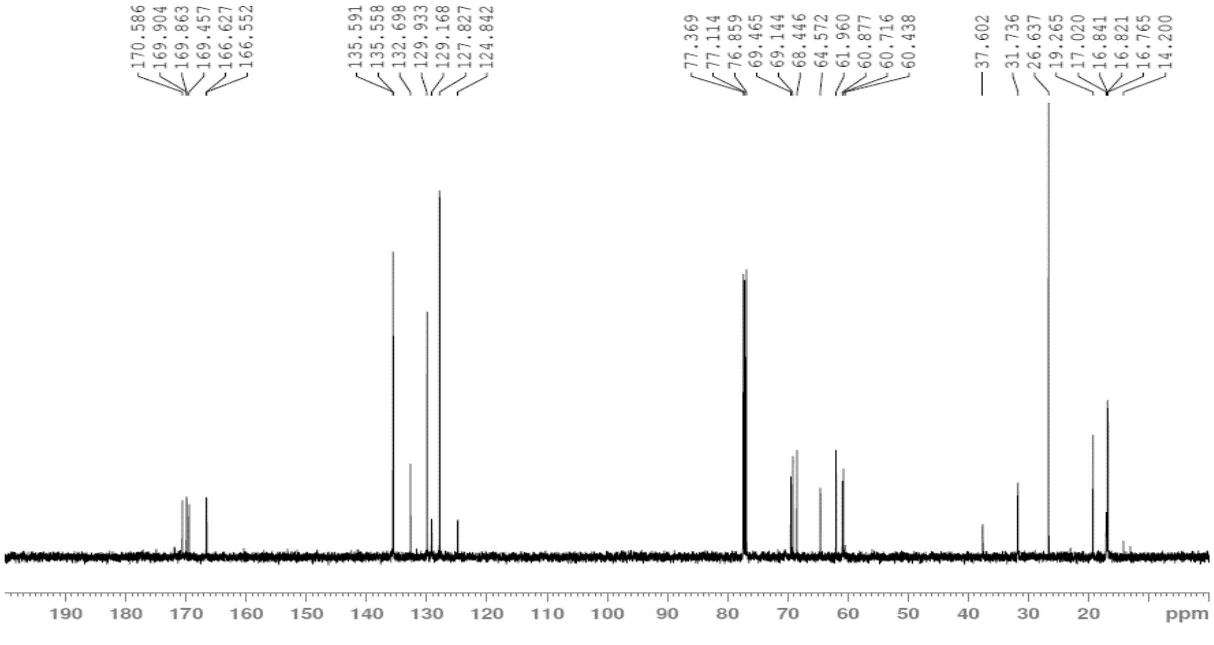

JAN-ENi-80; cyc-LMLGLGLG; CDCl3; 500; 1H
16 scans; October 23, 2015

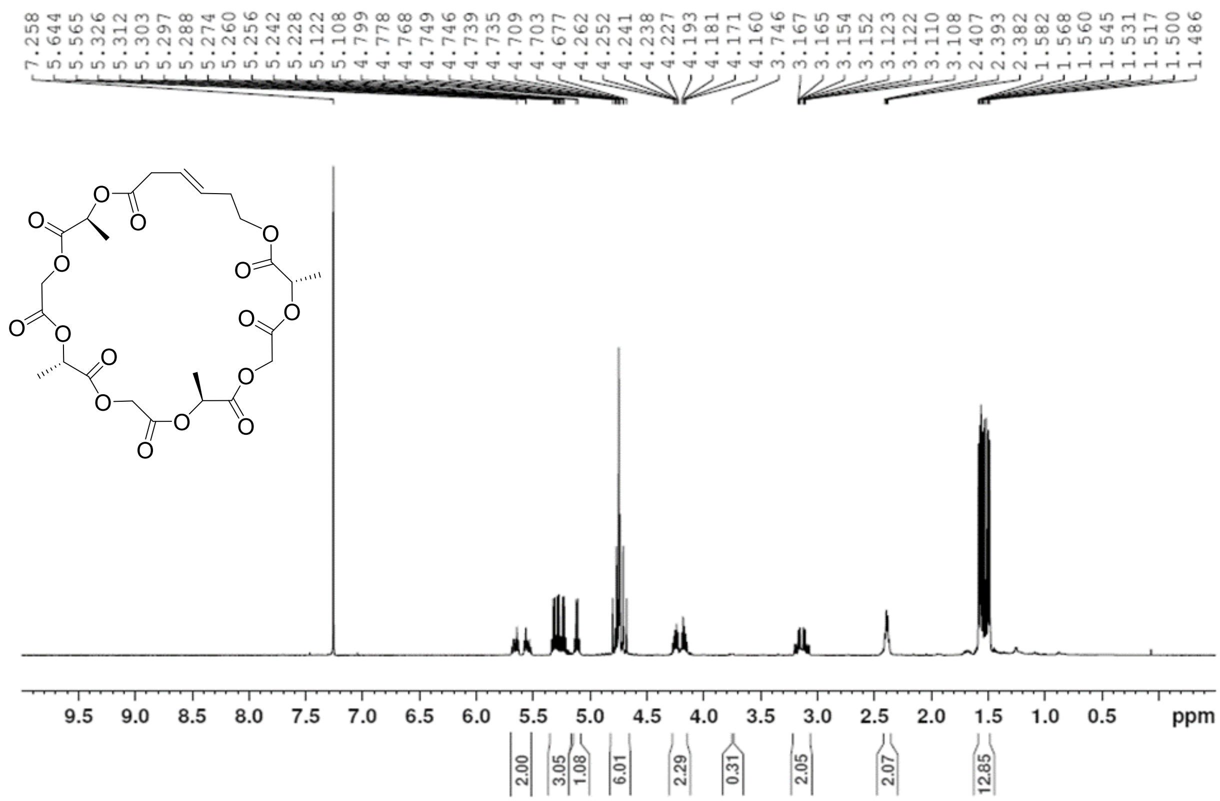

JAN-ENii-4; cyc-LMLGLGLG; CDCl3; 13C
500 MHz; 32 scans; February 19, 2016

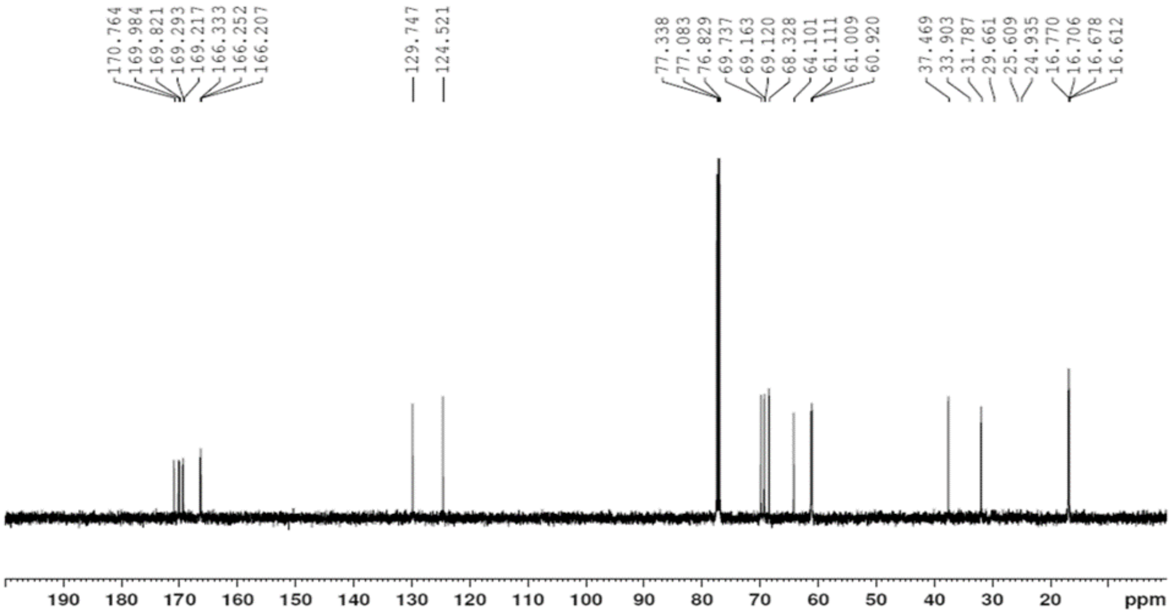

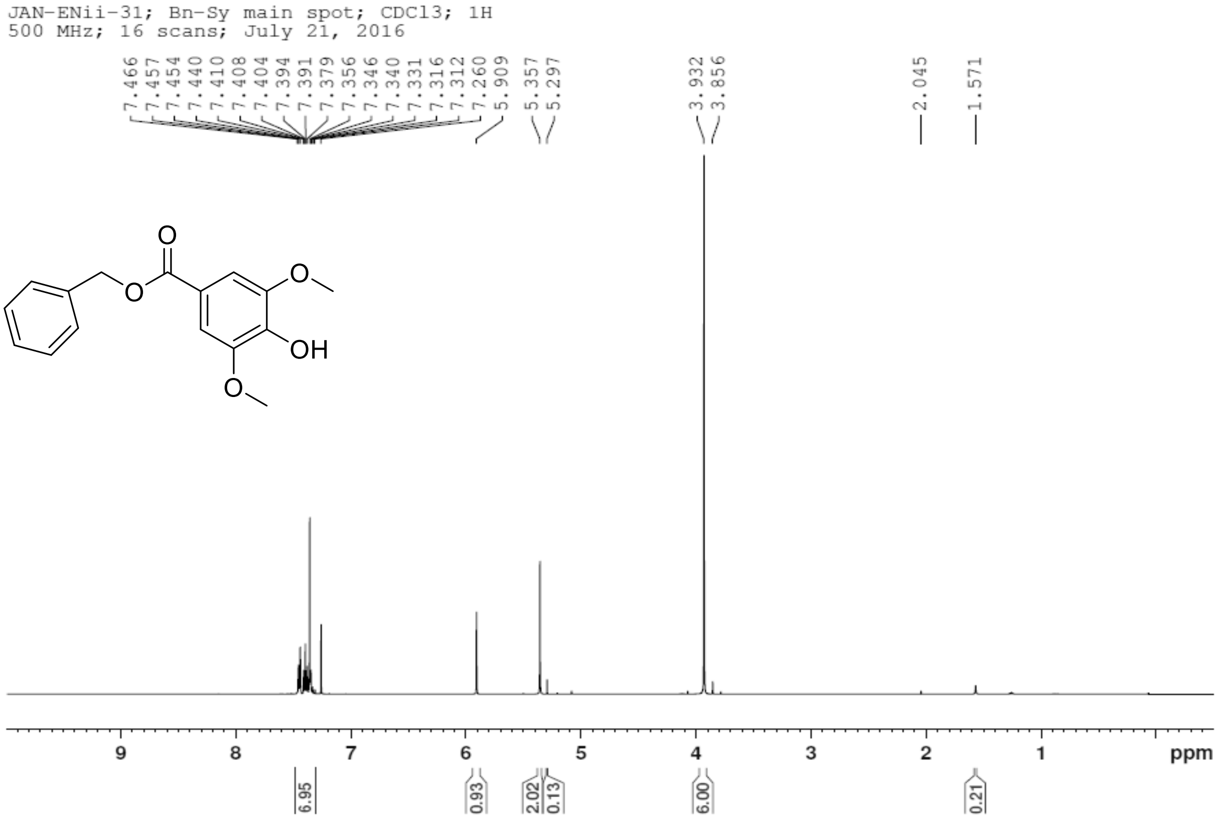
JAN-ENii-31; Bn-Sy main spot; CDCl3; 1H
500 MHz; 16 scans; July 21, 2016
7.466
7.457
7.454
7.440
7.410
7.408
7.404
7.394
7.391
7.379
7.356
7.346
7.340
7.331
7.316
7.312
7.260
5.909
5.357
5.297
3.932
3.856
2.045
1.571
O
O
O
OH
O
9
8
7
6
5
4
3
2
1
ppm
6.95
0.93
2.02
0.13
6.00
0.21

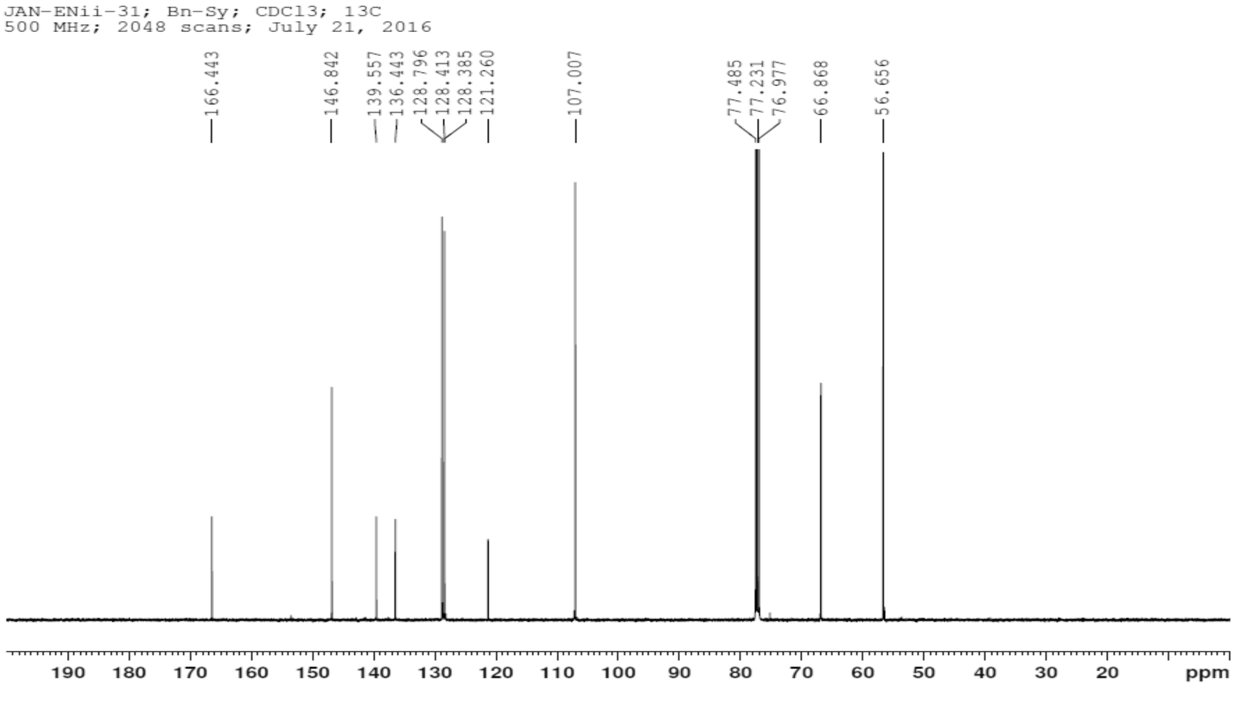
JAN-ENii-31; Bn-Sy; CDCl3; 13C
500 MHz; 2048 scans; July 21, 2016
166.443
146.842
139.557
136.443
128.796
128.413
128.385
121.260
107.007
77.485
77.231
76.977
66.868
56.656
190
180
170
160
150
140
130
120
110
100
90
80
70
60
50
40
30
20
ppm

JAN-ENii-44; Bn-LM-Si; CDCl3; 1H
400 MHz; 16 scans; August 30, 2016

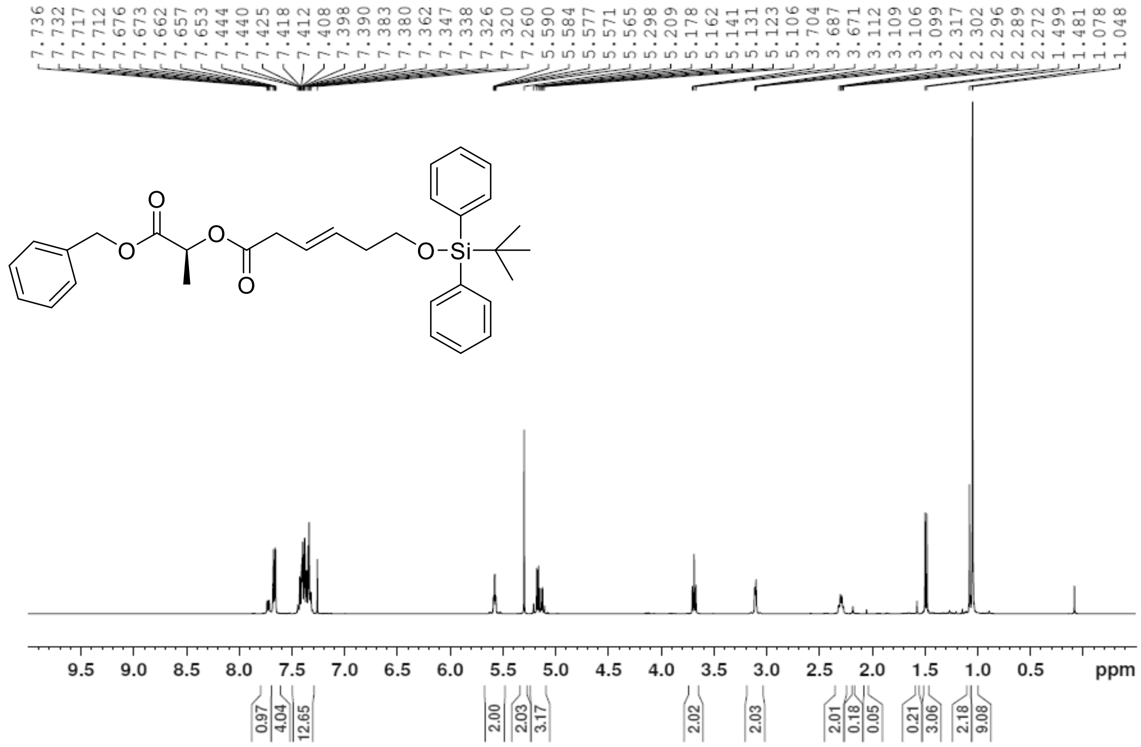

JAN-ENii-44; Bn-LM-Si; CDCl3; 1H
400 MHz; 16 scans; August 30, 2016

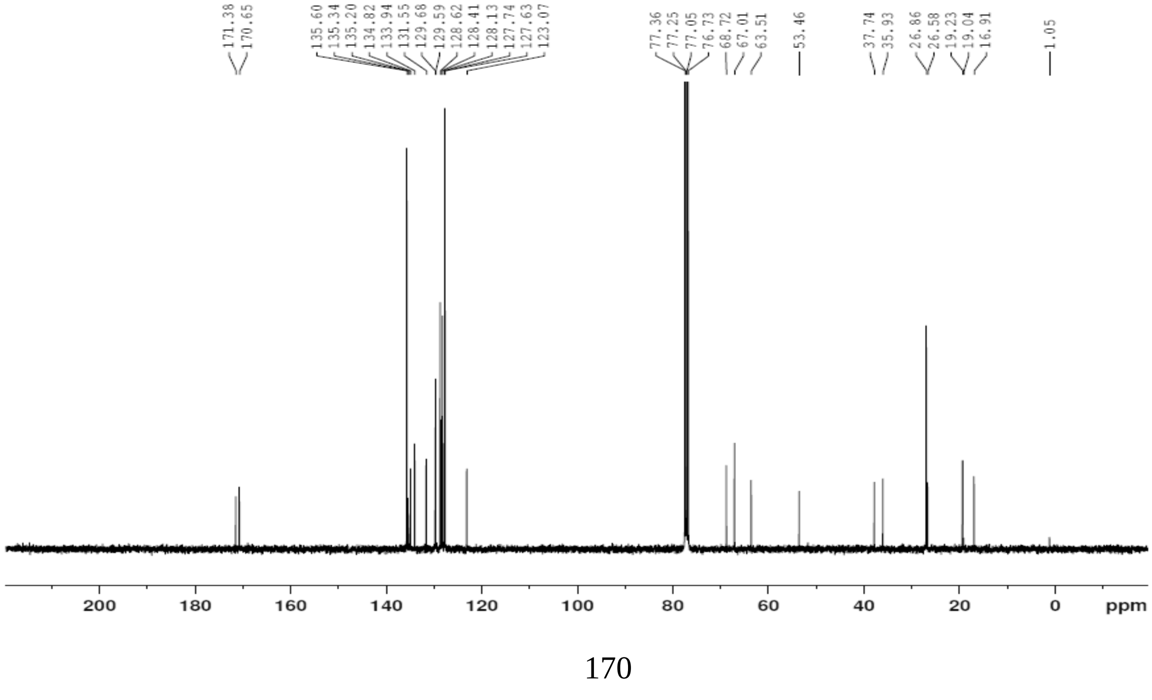

JAN-ENii-46; LM-Si; CDCl3; 1H; 400 MHz
16 scans; August 31, 2016

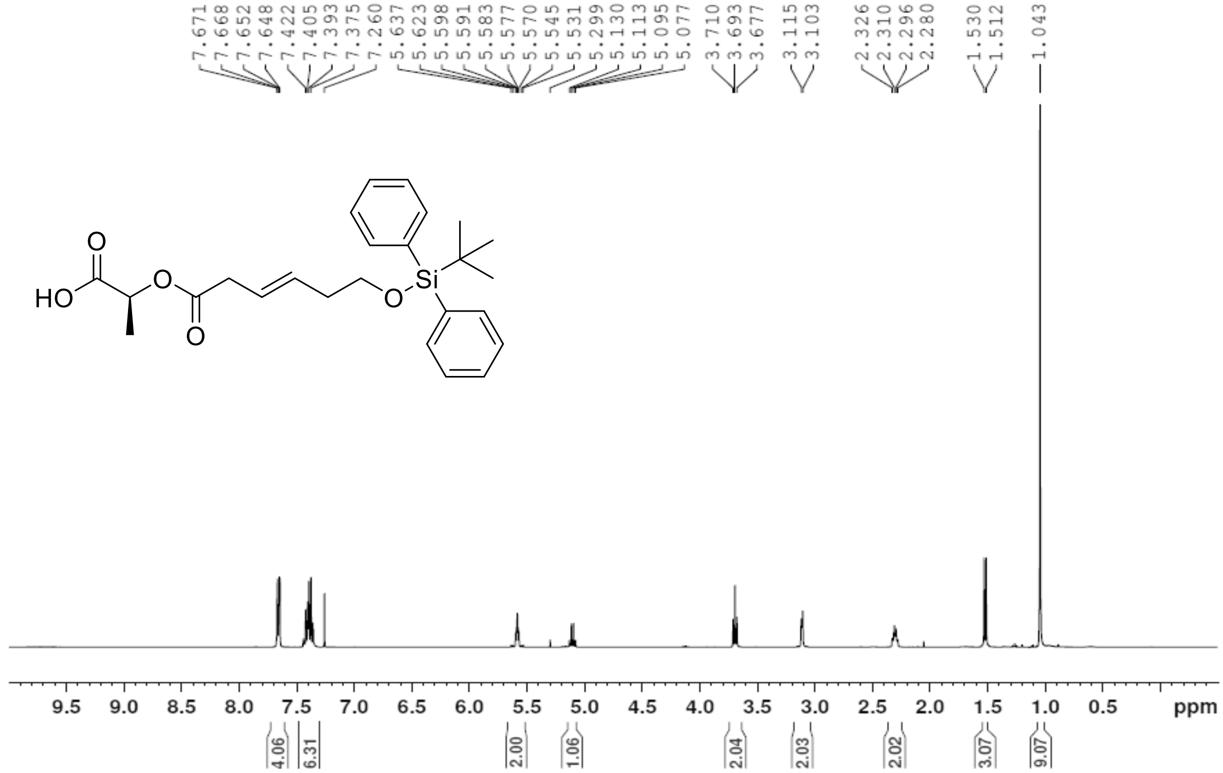

JAN-ENii-46; LM-Si; CDCl3; 13C; 400 MHz
1024 scans; August 31, 2016

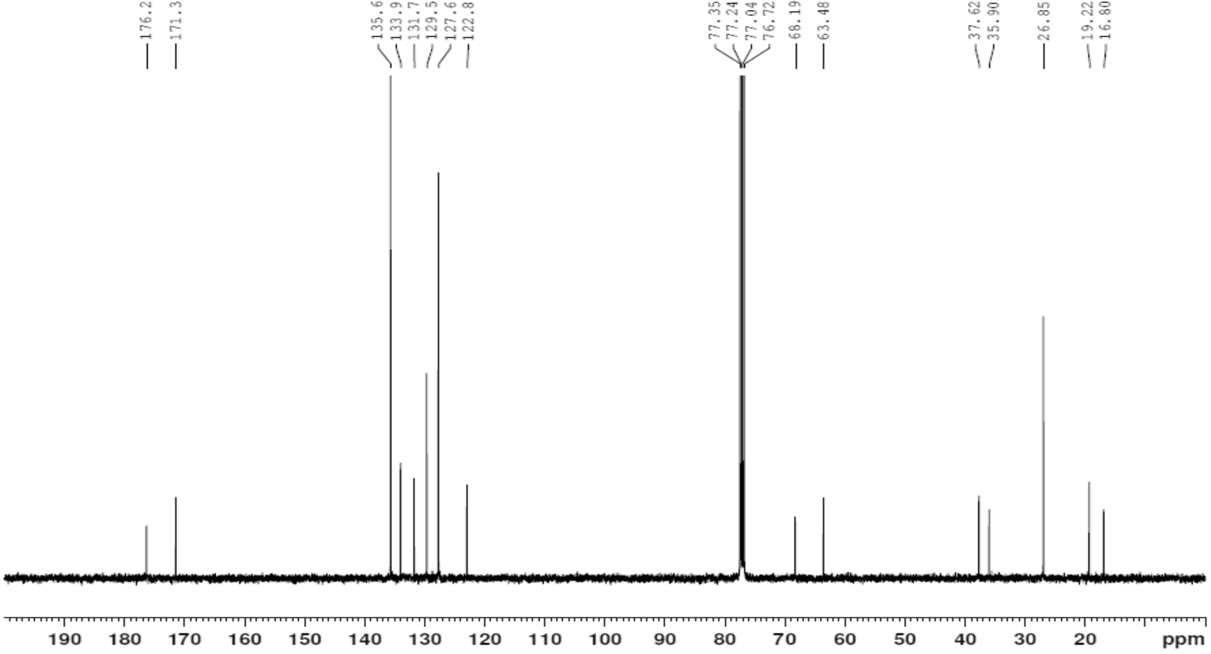

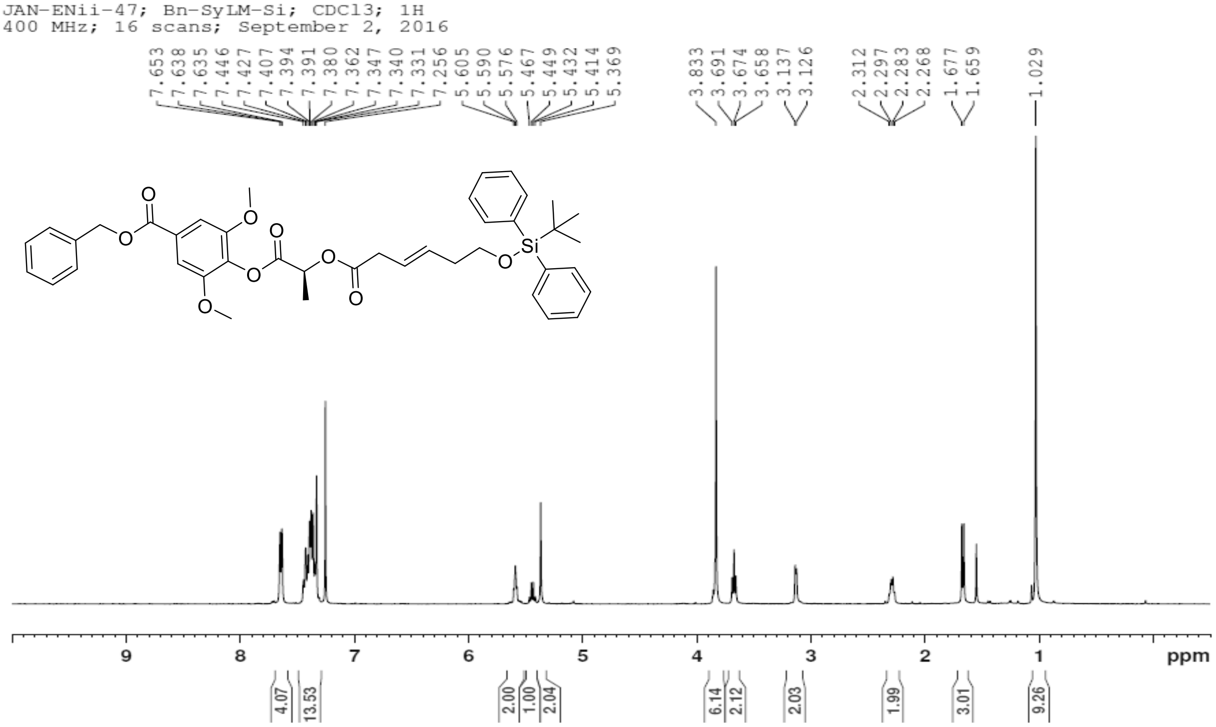
JAN-ENii-47; Bn-SyLM-Si; CDCl3; 1H
400 MHz; 16 scans; September 2, 2016
7.653
7.638
7.635
7.446
7.427
7.407
7.394
7.391
7.380
7.362
7.347
7.340
7.331
7.256
5.605
5.590
5.576
5.467
5.449
5.432
5.414
5.369
3.833
3.691
3.674
3.658
3.137
3.126
2.312
2.297
2.283
2.268
1.677
1.659
1.029
O
O
O
O
O
O
O
O
O
Si
9
8
7
6
5
4
3
2
1
ppm
4.07
13.53
2.00
1.00
2.04
6.14
2.12
2.03
1.99
3.01
9.26

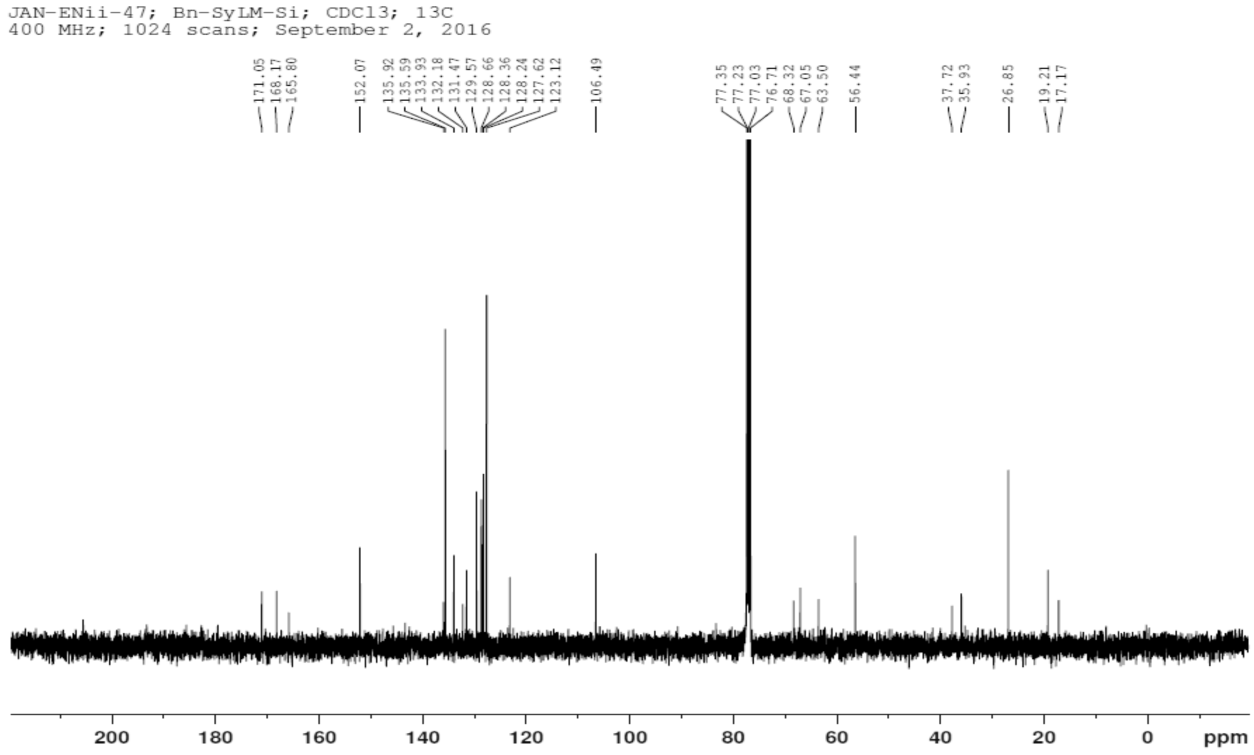
JAN-ENii-47; Bn-SyLM-Si; CDCl3; 13C
400 MHz; 1024 scans; September 2, 2016
171.05
168.17
165.80
152.07
135.92
135.59
133.93
132.18
131.47
129.57
128.66
128.36
128.24
127.62
123.12
106.49
77.35
77.23
77.03
76.71
68.32
67.05
63.50
56.44
37.72
35.93
26.85
19.21
17.17
200
180
160
140
120
100
80
60
40
20
0
ppm

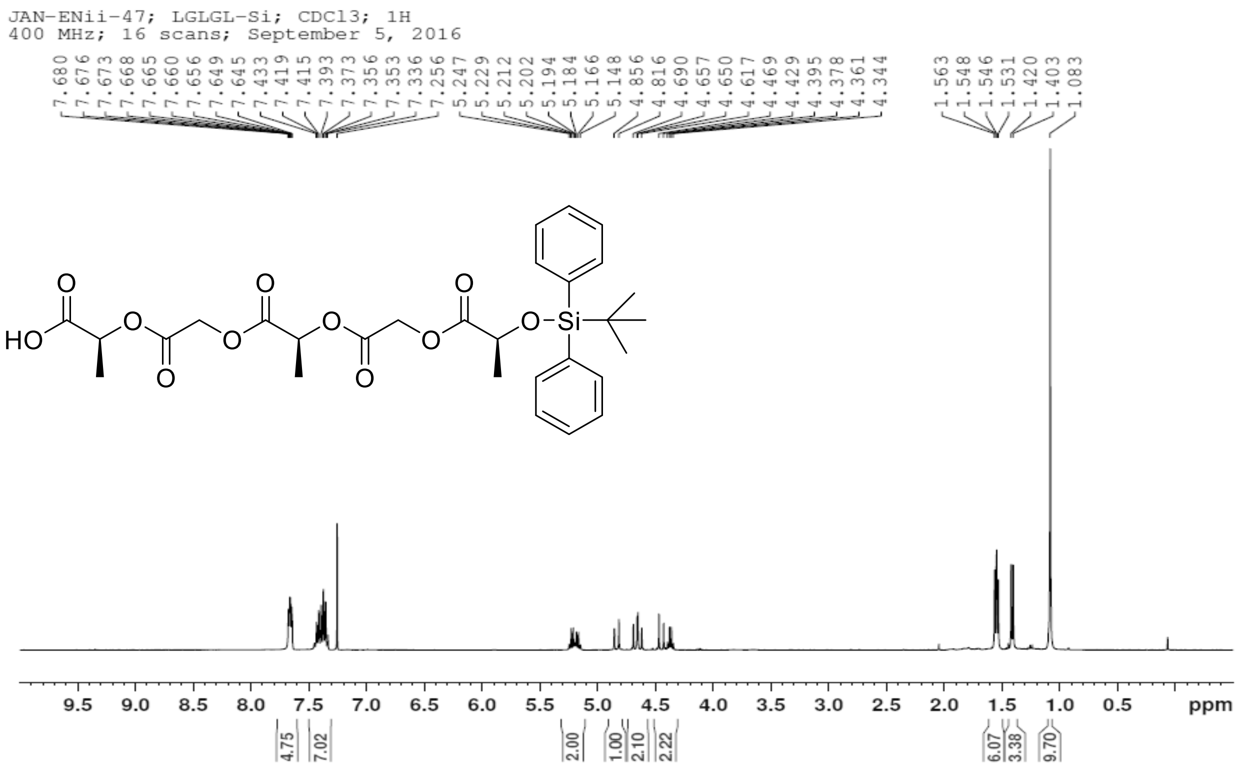
JAN-ENii-47; LGLGL-Si; CDCl3; 1H
400 MHz; 16 scans; September 5, 2016
7.680 7.676 7.673 7.668 7.665 7.660 7.656 7.649 7.645 7.433 7.419 7.415 7.393 7.373 7.356 7.353 7.336 7.256 5.247 5.229 5.212 5.202 5.194 5.184 5.166 5.148 4.856 4.816 4.690 4.657 4.650 4.617 4.469 4.429 4.395 4.378 4.361 4.344 1.563 1.548 1.546 1.531 1.420 1.403 1.083
HO
O
Si
9.5 9.0 8.5 8.0 7.5 7.0 6.5 6.0 5.5 5.0 4.5 4.0 3.5 3.0 2.5 2.0 1.5 1.0 0.5 ppm
4.75 7.02 2.00 1.00 2.10 2.22 6.07 3.38 9.70

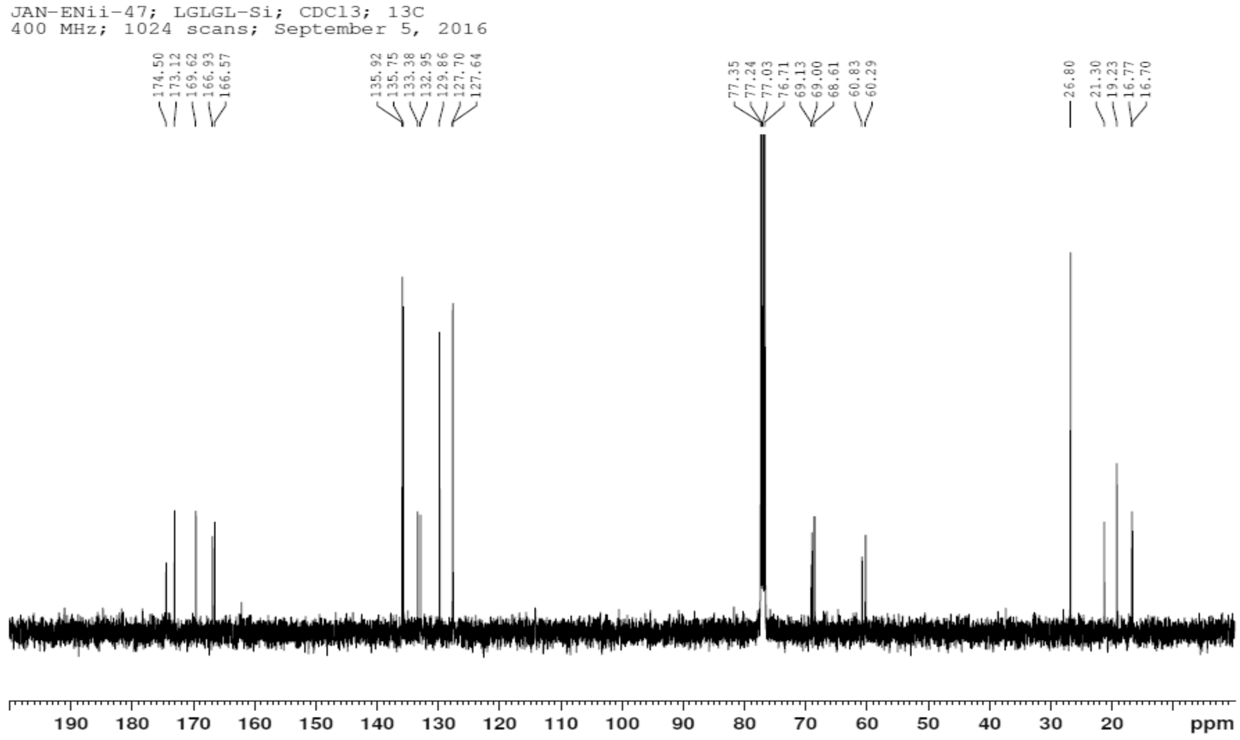
JAN-ENii-47; LGLGL-Si; CDCl3; 13C
400 MHz; 1024 scans; September 5, 2016
174.50 173.12 169.62 166.93 166.57 135.92 135.75 133.38 132.95 129.86 127.70 127.64 77.35 77.24 77.03 76.71 69.13 69.00 68.61 60.83 60.29 26.80 21.30 19.23 16.77 16.70
190 180 170 160 150 140 130 120 110 100 90 80 70 60 50 40 30 20 ppm

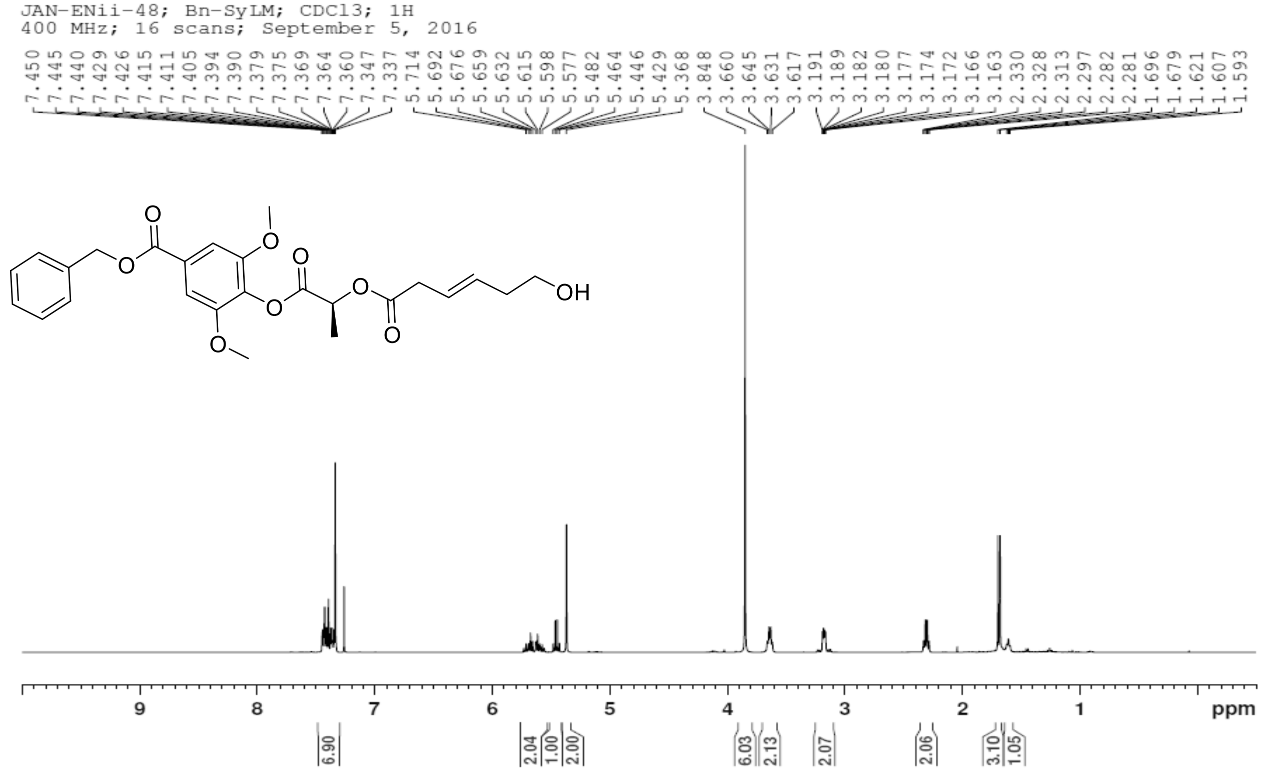
JAN-ENii-48; Bn-SyLM; CDCl3; 1H
400 MHz; 16 scans; September 5, 2016

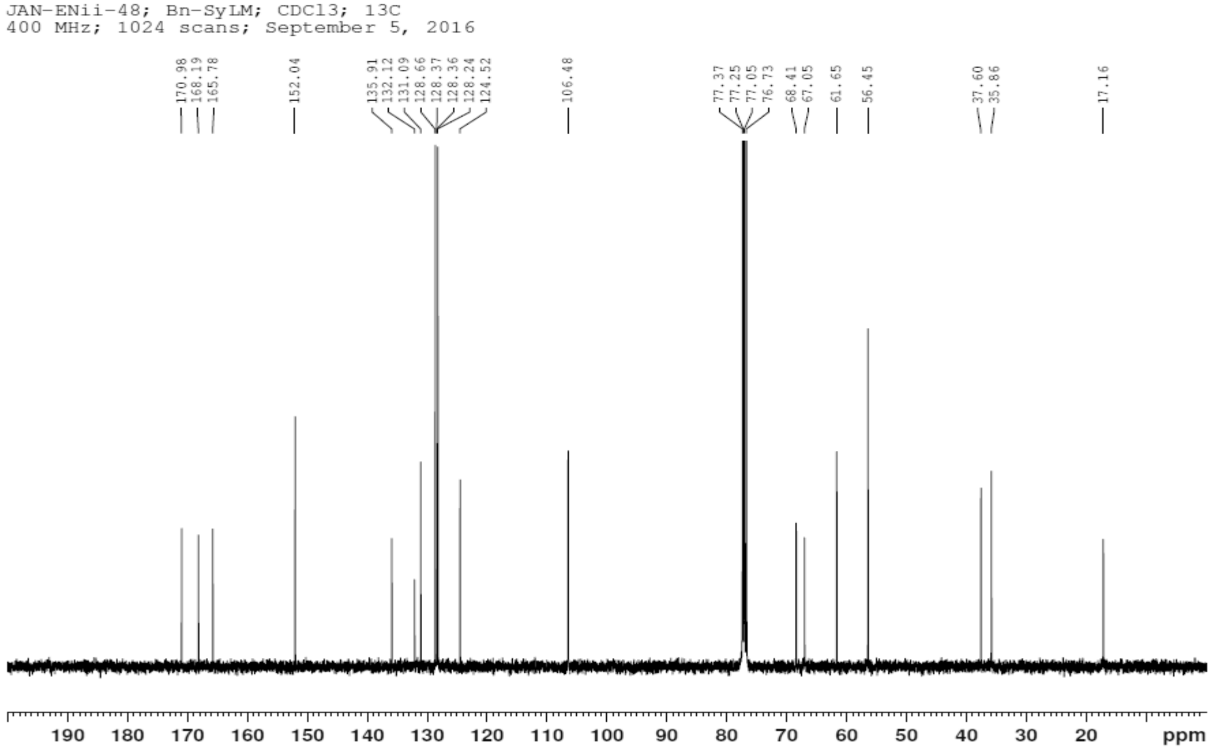
JAN-ENii-48; Bn-SyLM; CDCl3; 13C
400 MHz; 1024 scans; September 5, 2016

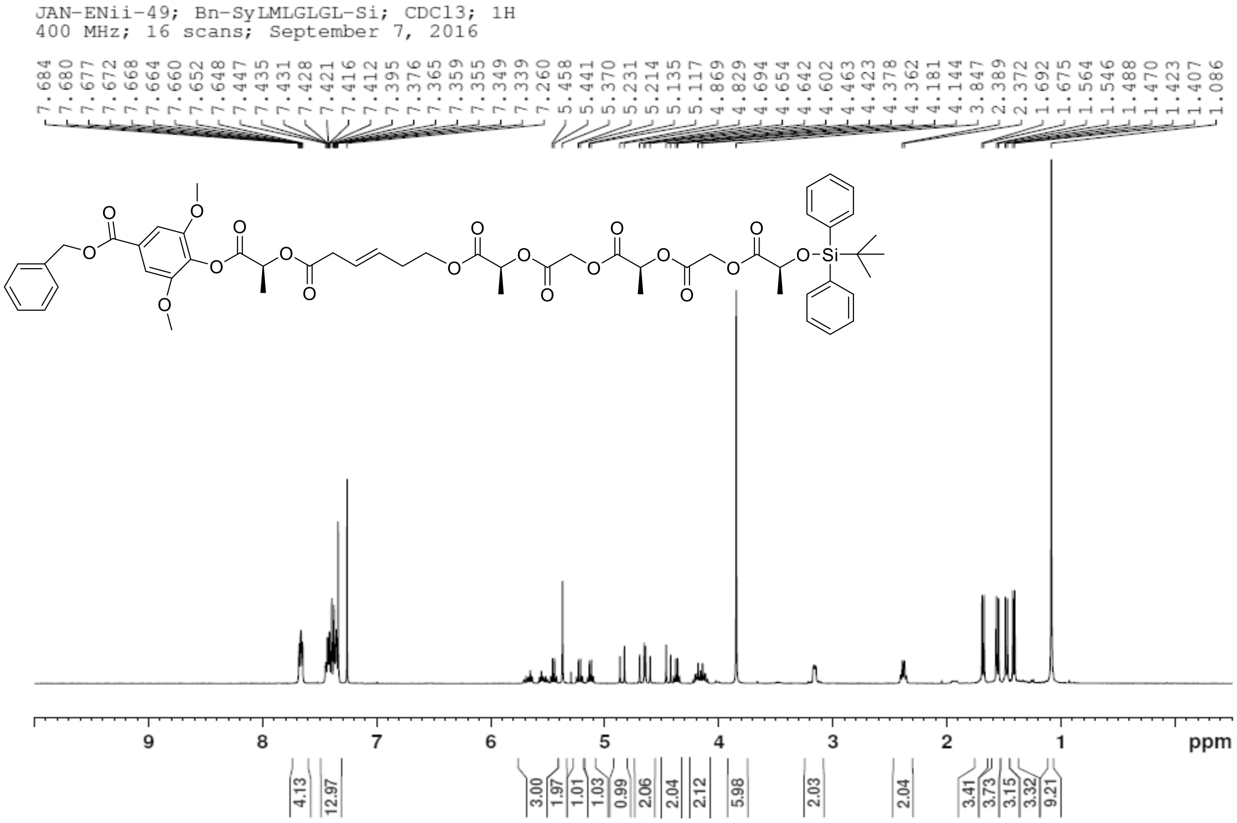
JAN-ENii-49; Bn-SyLMLGLGL-Si; CDCl3; 1H
400 MHz; 16 scans; September 7, 2016
7.684 7.680 7.677 7.672 7.668 7.664 7.660 7.652 7.648 7.447 7.435 7.431 7.428 7.421 7.416 7.412 7.395 7.376 7.365 7.359 7.355 7.349 7.339 7.260 5.458 5.441 5.370 5.231 5.214 5.135 5.117 4.869 4.829 4.694 4.654 4.642 4.602 4.463 4.423 4.378 4.362 4.181 4.144 3.847 2.389 2.372 1.692 1.675 1.564 1.546 1.488 1.470 1.423 1.407 1.086
O
O
O
O
O
O
O
O
O
O
O
O
O
O
O
O
O
O
Si
9
8
7
6
5
4
3
2
1
ppm
4.13
12.97
3.00
1.97
1.01
1.03
0.99
2.06
2.04
2.12
5.98
2.03
2.04
3.41
3.73
3.15
3.32
9.21

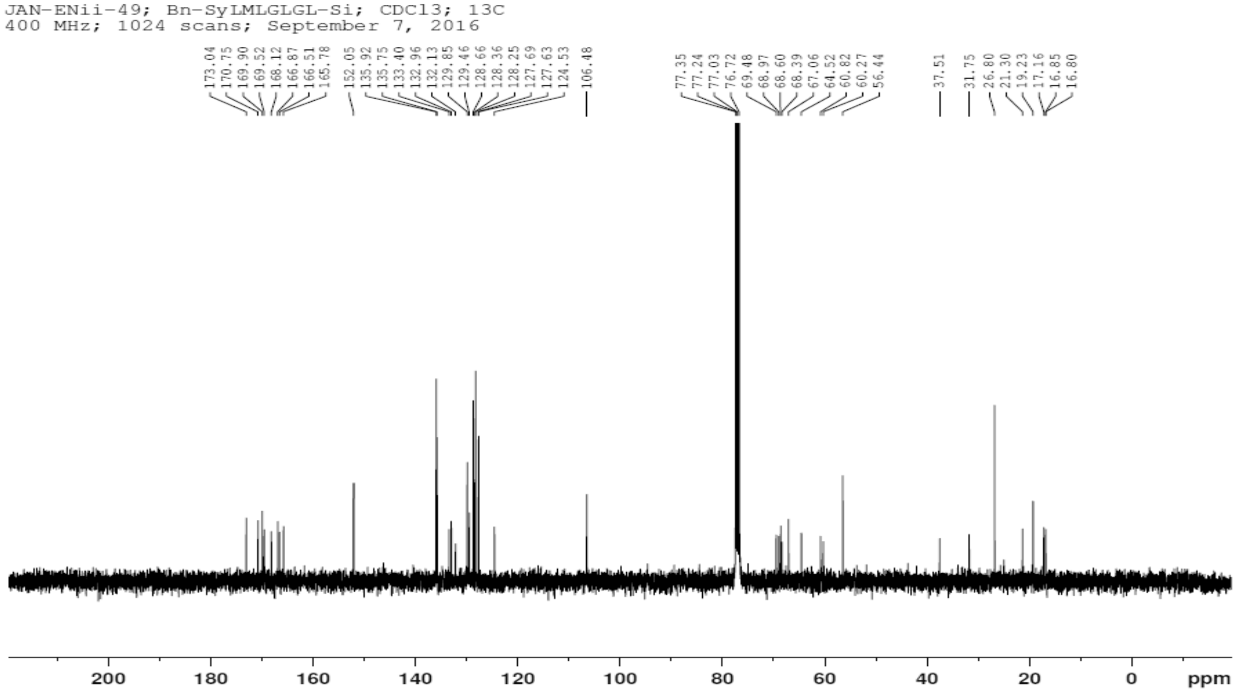
JAN-ENii-49; Bn-SyLMLGLGL-Si; CDCl3; 13C
400 MHz; 1024 scans; September 7, 2016
173.04 170.75 169.90 169.52 168.12 166.87 166.51 165.78 152.05 135.92 135.75 133.40 132.96 132.13 129.85 129.46 128.66 128.36 128.25 127.69 127.63 124.53 106.48 77.35 77.24 77.03 76.72 69.48 68.97 68.60 68.39 67.06 64.52 60.82 60.27 56.44 37.51 31.75 26.80 21.30 19.23 17.16 16.85 16.80
200
180
160
140
120
100
80
60
40
20
0
ppm

JAN-ENii-50; SyLMLGLGL-Si; CDCl3; 1H
400 MHz; 16 scans; September 7, 2016

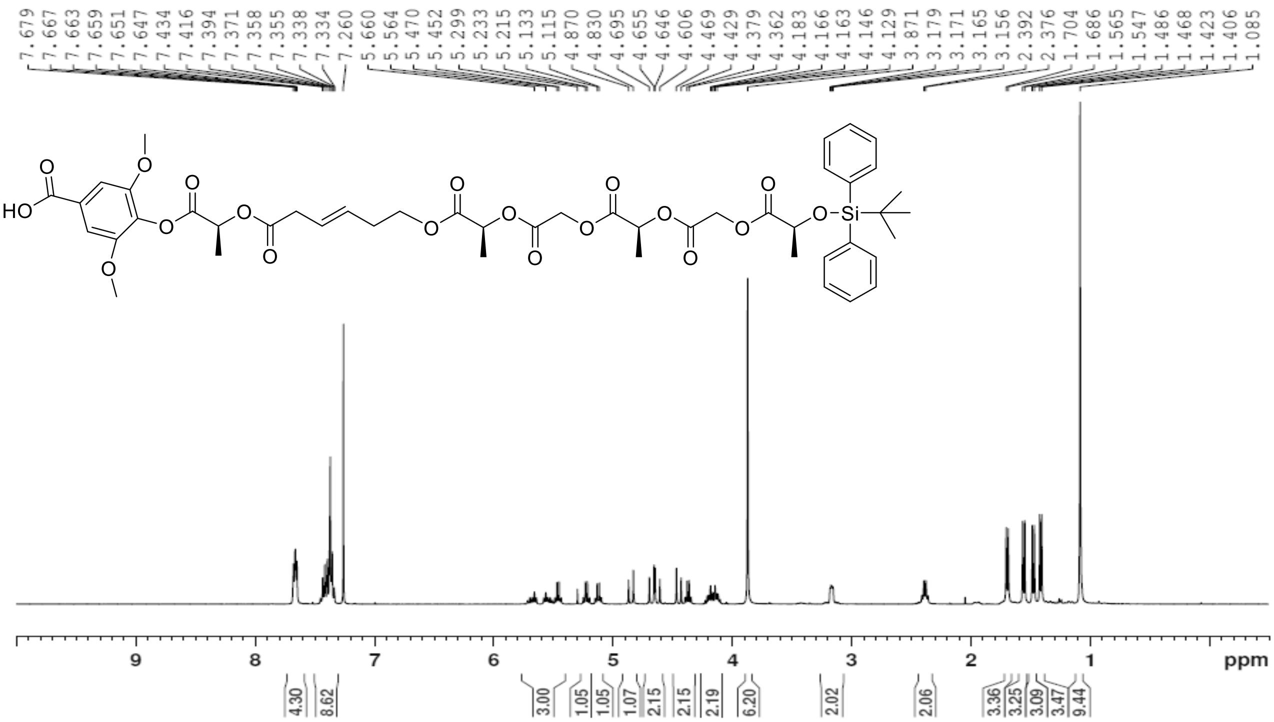

JAN-ENii-50; SyLMLGLGL-Si; CDCl3; 13C
400 MHz; 1024 scans; September 7, 2016

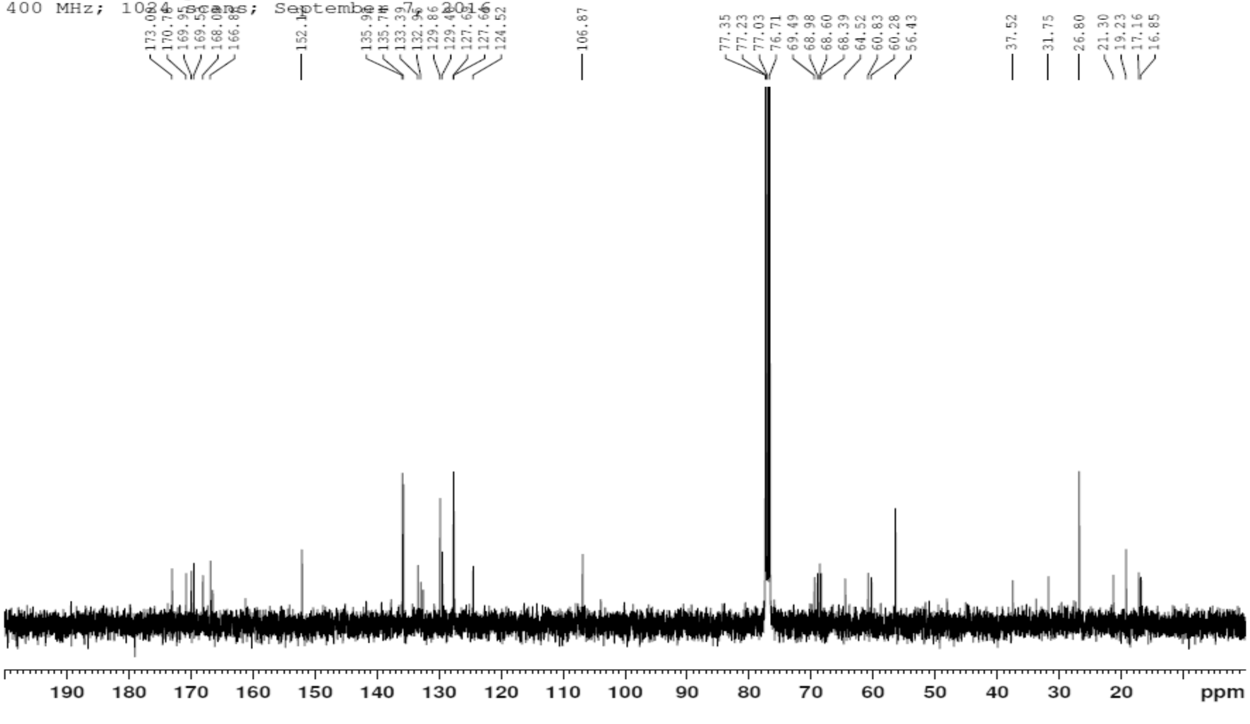

JAN-ENii-51; SyLMLGLGL; CDCl3; 1H
400 MHz; 16 scans; September 7, 2016

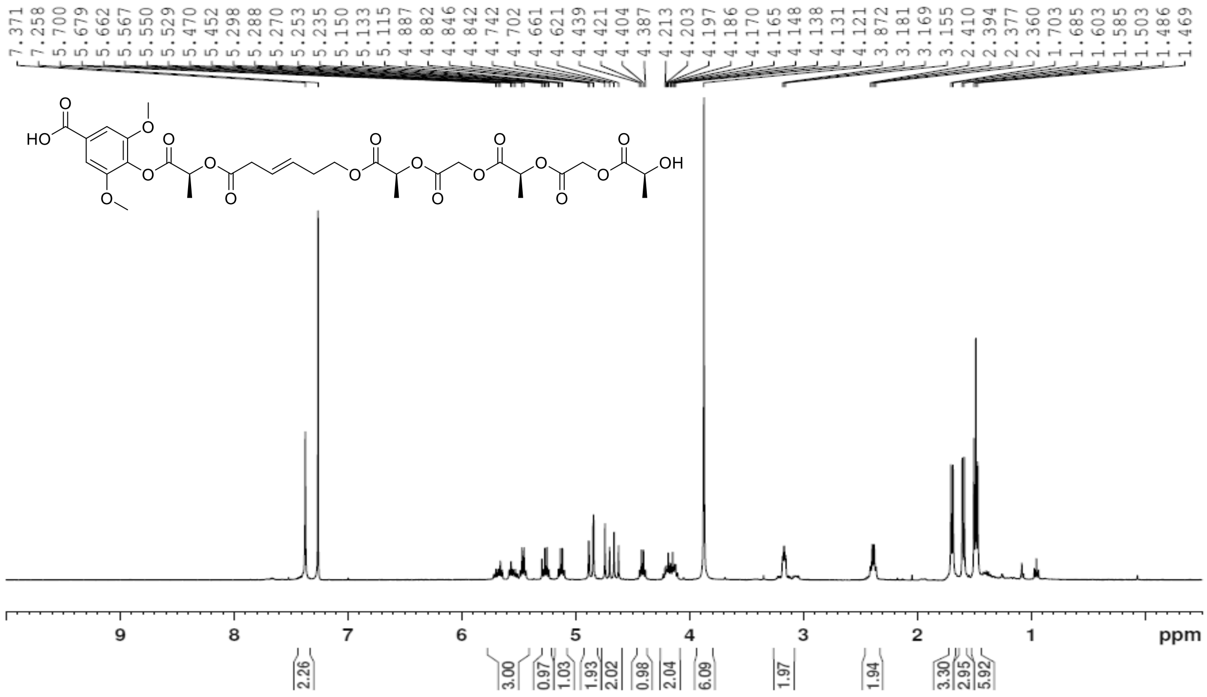

JAN-ENii-51; SyLMLGLGL; CDCl3; 13C
400 MHz; 1024 scans; September 7, 2016

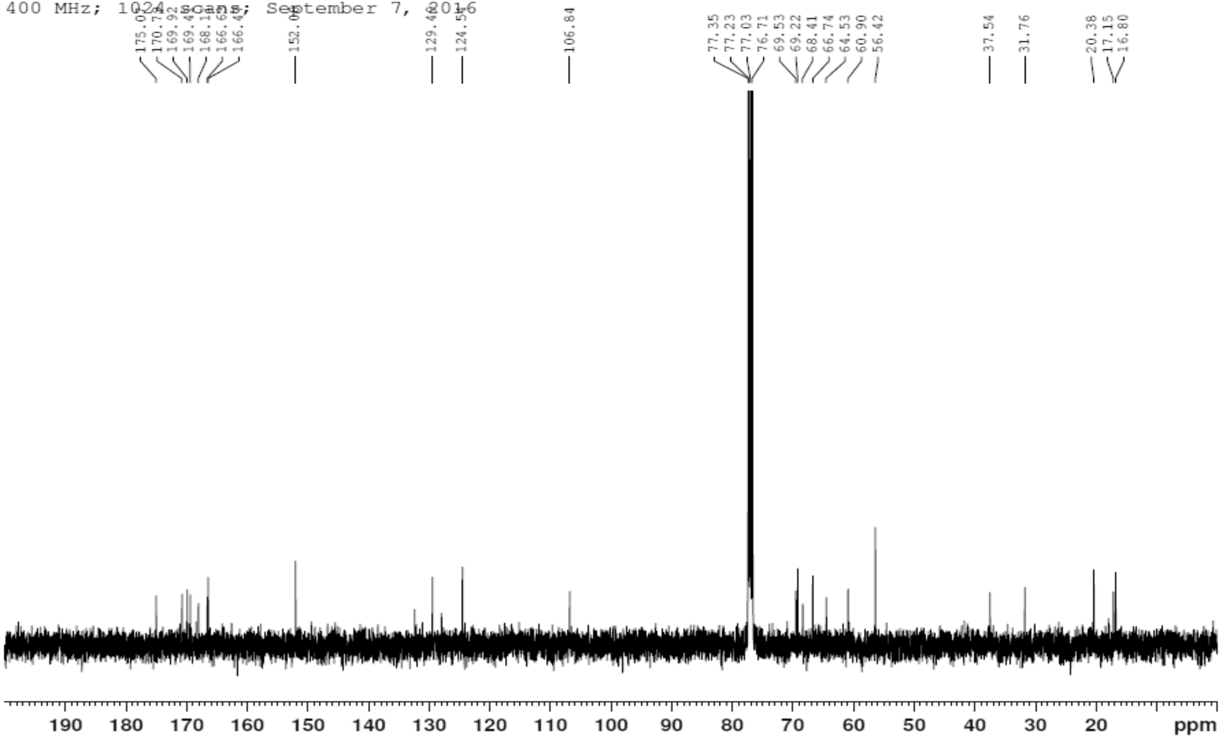

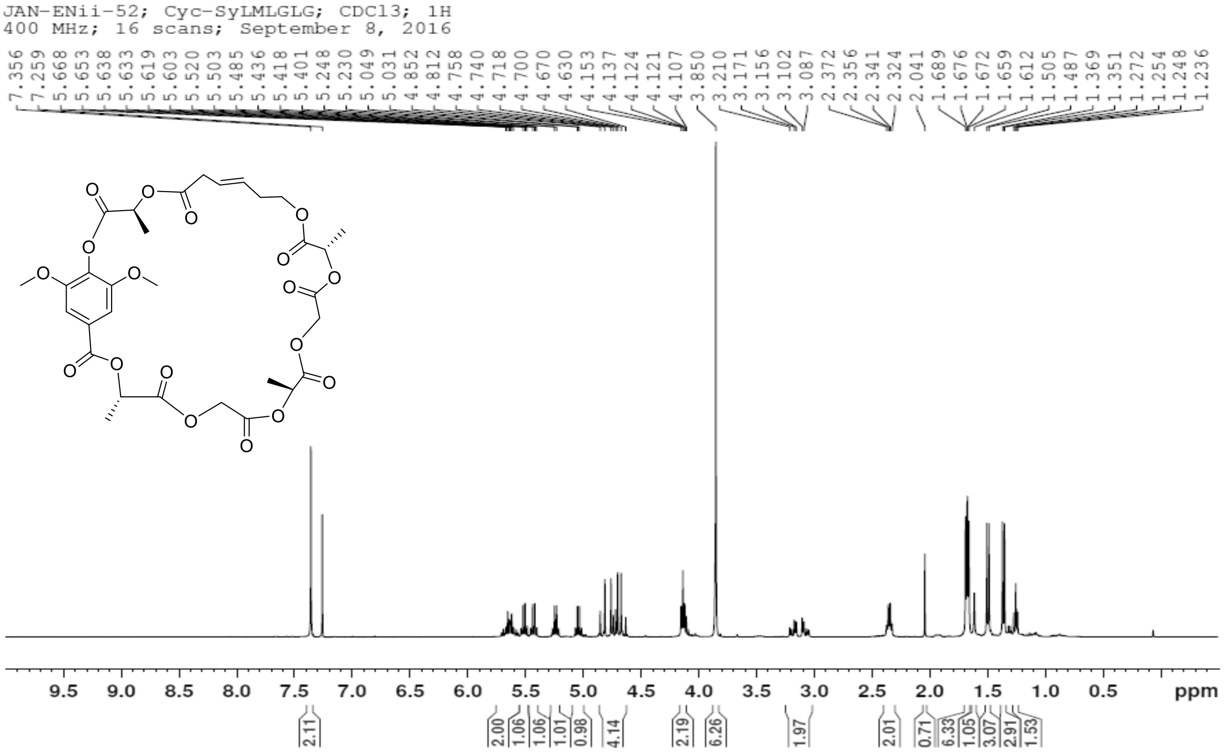
JAN-ENii-52; Cyc-SyLMLGLG; CDCl3; 1H
400 MHz; 16 scans; September 8, 2016
7.356
7.259
5.668
5.653
5.638
5.633
5.619
5.603
5.520
5.503
5.485
5.436
5.418
5.401
5.248
5.230
5.049
5.031
4.852
4.812
4.758
4.740
4.718
4.700
4.670
4.630
4.153
4.137
4.124
4.121
4.107
3.850
3.210
3.171
3.156
3.102
3.087
2.372
2.356
2.341
2.324
2.041
1.689
1.676
1.672
1.659
1.612
1.505
1.487
1.369
1.351
1.272
1.254
1.248
1.236
9.5
9.0
8.5
8.0
7.5
7.0
6.5
6.0
5.5
5.0
4.5
4.0
3.5
3.0
2.5
2.0
1.5
1.0
0.5
ppm
2.11
2.00
1.06
1.06
1.01
0.98
4.14
2.19
6.26
1.97
2.01
0.71
6.33
1.05
3.07
2.91
1.53

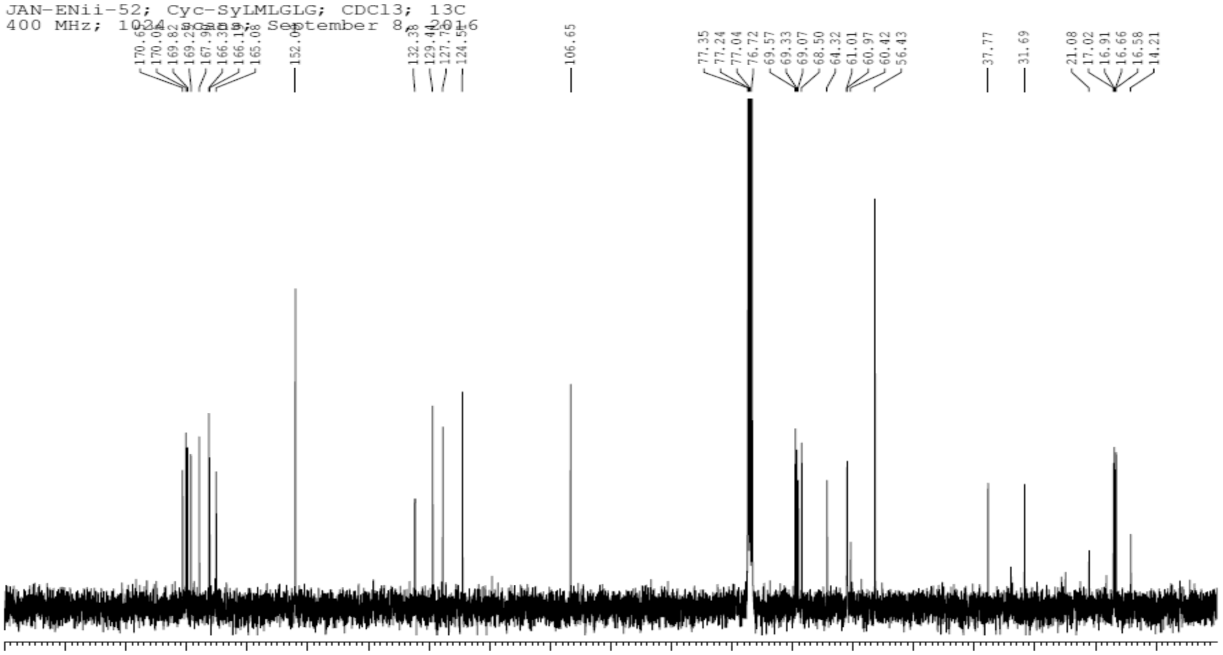
JAN-ENii-52; Cyc-SyLMLGLG; CDCl3; 13C
400 MHz; 1024 scans; September 8, 2016
170.6
170.0
169.82
169.2
167.9
166.3
166.1
165.08
152.0
132.38
129.4
127.7
124.5
106.65
77.35
77.24
77.04
76.72
69.57
69.33
69.07
68.50
64.32
61.01
60.97
60.42
56.43
37.77
31.69
21.08
17.02
16.91
16.66
16.58
14.21
190
180
170
160
150
140
130
120
110
100
90
80
70
60
50
40
30
20
ppm

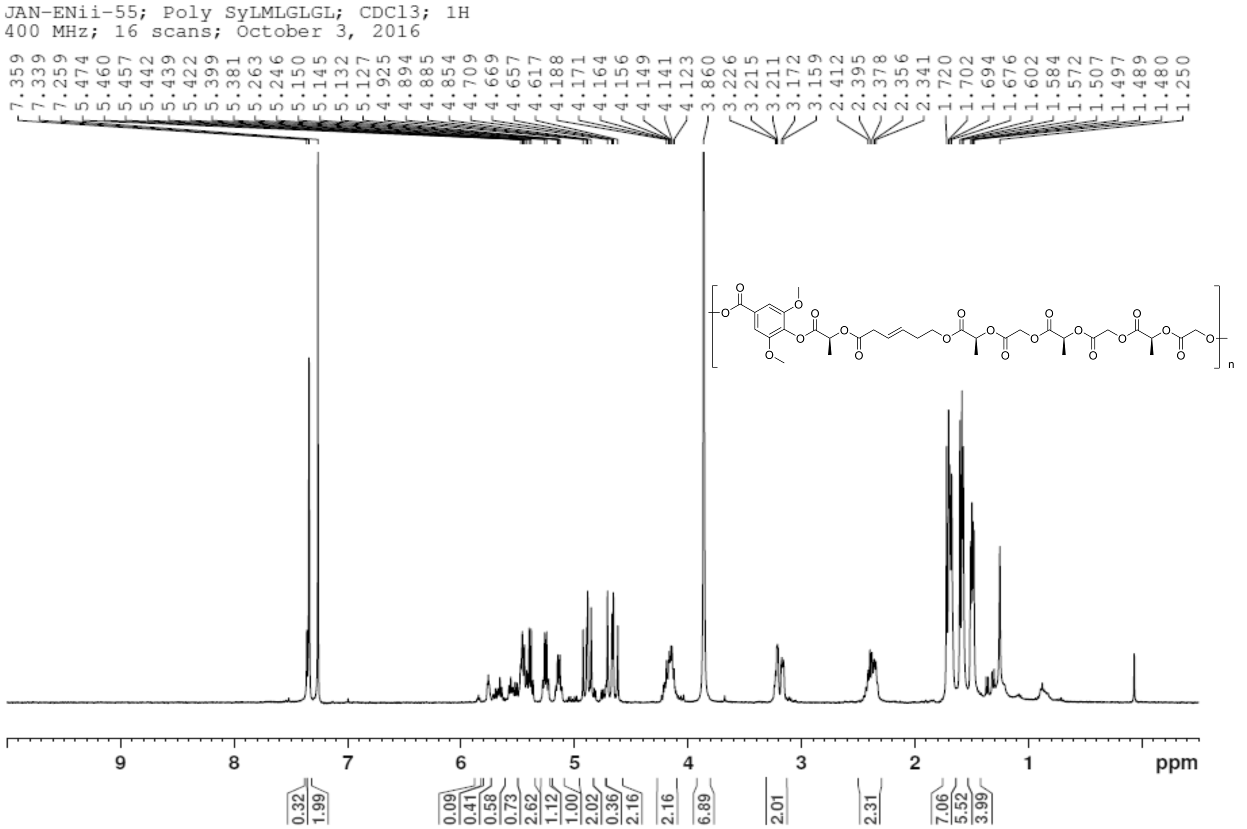
JAN-ENii-55; Poly SyLMLGLGL; CDCl3; 1H
400 MHz; 16 scans; October 3, 2016
7.359
7.339
7.259
5.474
5.460
5.457
5.442
5.439
5.422
5.399
5.381
5.263
5.246
5.150
5.145
5.132
5.127
4.925
4.894
4.885
4.854
4.709
4.669
4.657
4.617
4.188
4.171
4.164
4.156
4.149
4.141
4.123
3.860
3.226
3.215
3.211
3.172
3.159
2.412
2.395
2.378
2.356
2.341
1.720
1.702
1.694
1.676
1.602
1.584
1.572
1.507
1.497
1.489
1.480
1.250
n
9
8
7
6
5
4
3
2
1
ppm
0.32
1.99
0.09
0.41
0.58
0.73
2.62
1.12
1.00
2.02
0.36
2.16
2.16
6.89
2.01
2.31
7.06
5.52
3.99

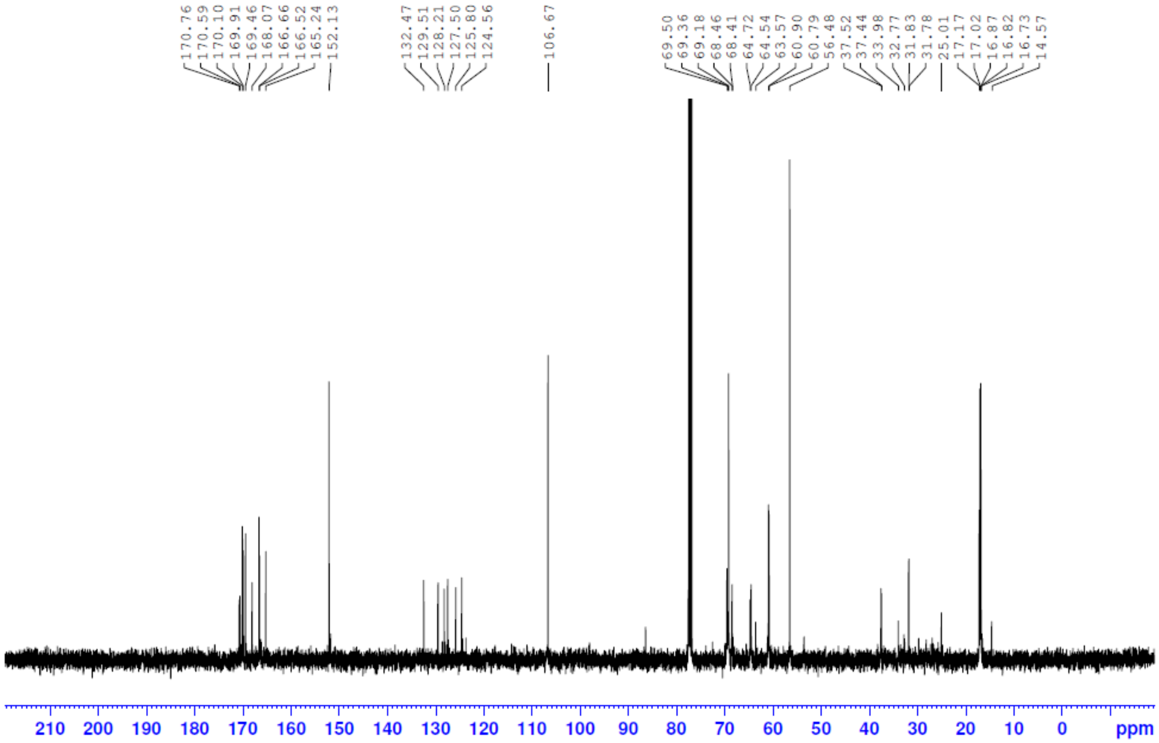
170.76
170.59
170.10
169.91
169.46
168.07
166.66
166.52
165.24
152.13
132.47
129.51
128.21
127.50
125.80
124.56
106.67
69.50
69.36
69.18
68.46
68.41
64.72
64.54
63.57
60.90
60.79
56.48
37.52
37.44
33.98
32.77
31.83
31.78
25.01
17.17
17.02
16.87
16.82
16.73
14.57
210
200
190
180
170
160
150
140
130
120
110
100
90
80
70
60
50
40
30
20
10
0
ppm

```
C:\Xcalibur\data\Meyer\73150ESIP                    2/10/2015 3:03:45 PM          rmwvi-36

73150ESIP#61-97 RT: 0.27-0.43 AV: 37
I: FTMS + p ESI Full ms [200.00-2000.00]
m/z=  743.00000-744.00000
    m/z     |  Intensity    |Relative|Theo. Mass | Delta  |   Composition
            |               |        |           | (ppm)  |
  743.34834 | 2579499008.0  | 100.00 | 743.34846 |  -0.16 |C36 H55 O16
```

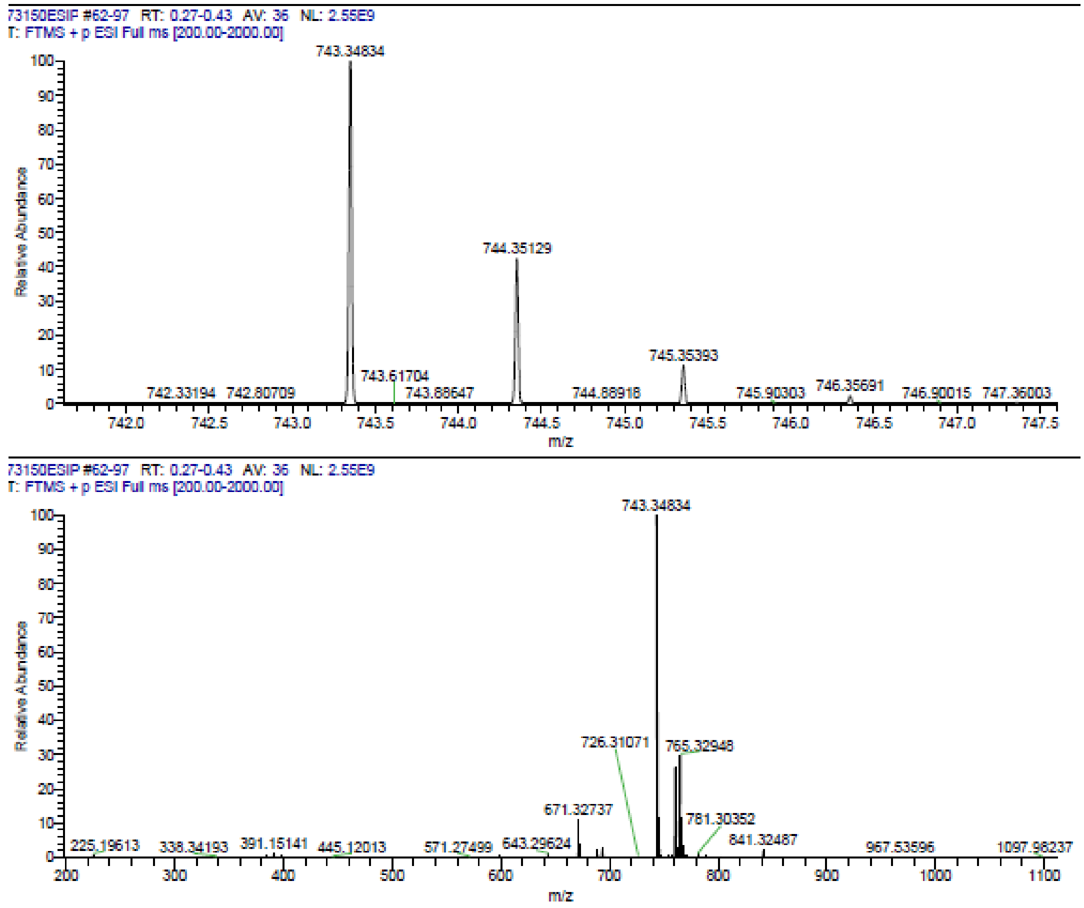

Mass spectrum of **Trans-Eg(LLCM)$_2$**.

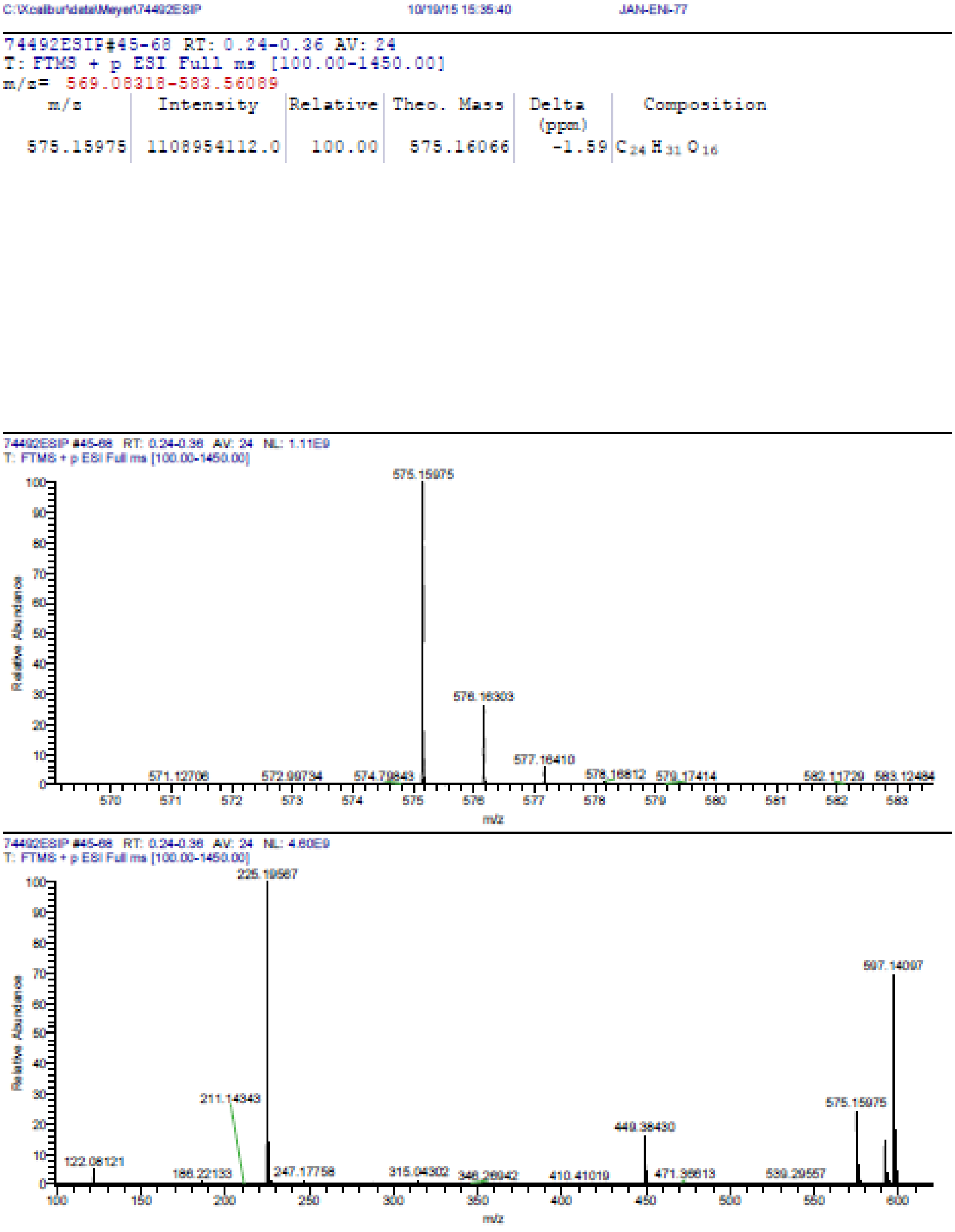

```
C:\Xcalibur\data\Meyer\74492ESIP                10/19/15 15:35:40          JAN-ENI-77

74492ESIP#45-68 RT: 0.24-0.36 AV: 24
T: FTMS + p ESI Full ms [100.00-1450.00]
m/z= 569.08318-583.56089
    m/z    |  Intensity   |Relative|Theo. Mass | Delta  |  Composition
           |              |        |           | (ppm)  |
 575.15975 | 1108954112.0 | 100.00 | 575.16066 |  -1.59 |C 24 H 31 O 16
```

Mass spectrum of **Cyc-LMLGLGLG**.

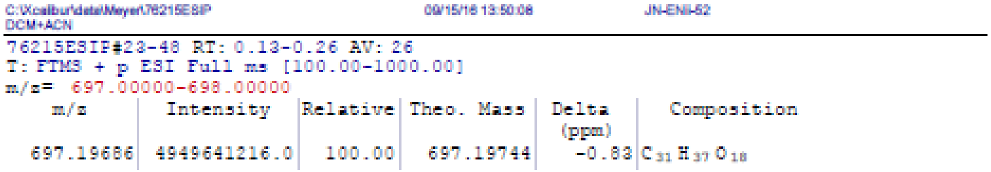

```
C:\Xcalibur\data\Meyer\76215ESIP                09/15/16 13:50:08           JN-ENI-52
DCM+ACN
76215ESIP#23-48 RT: 0.13-0.26 AV: 26
T: FTMS + p ESI Full ms [100.00-1000.00]
m/z= 697.00000-698.00000
    m/z    |    Intensity    |Relative|Theo. Mass |  Delta  |   Composition
           |                 |        |           |  (ppm)  |
 697.19686 | 4949641216.0    | 100.00 | 697.19744 |  -0.83  |C 31 H 37 O 18
```

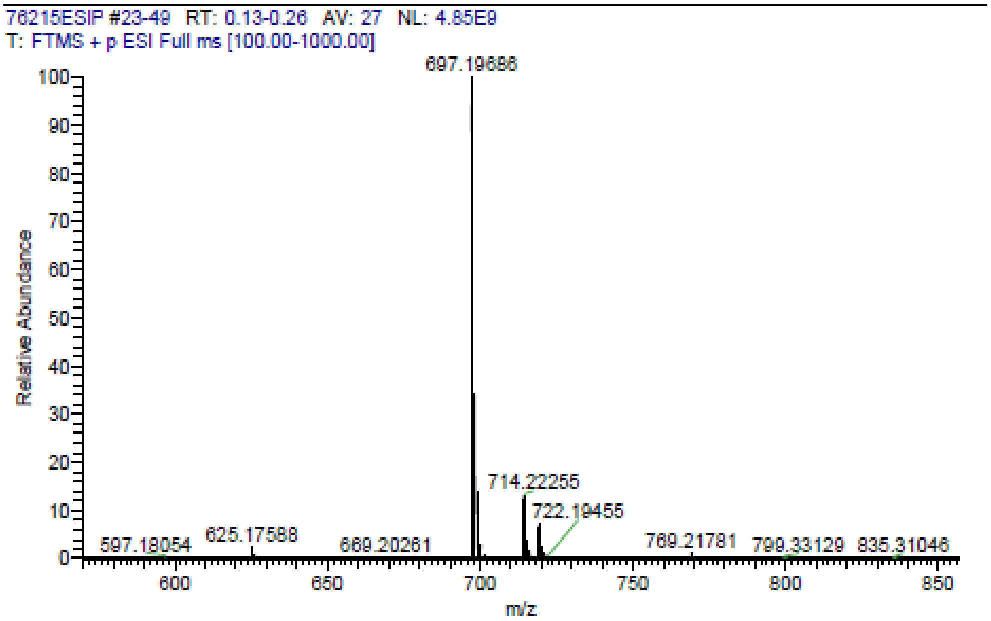

Mass spectrum of **Cyc-SyLMLGLGL**.

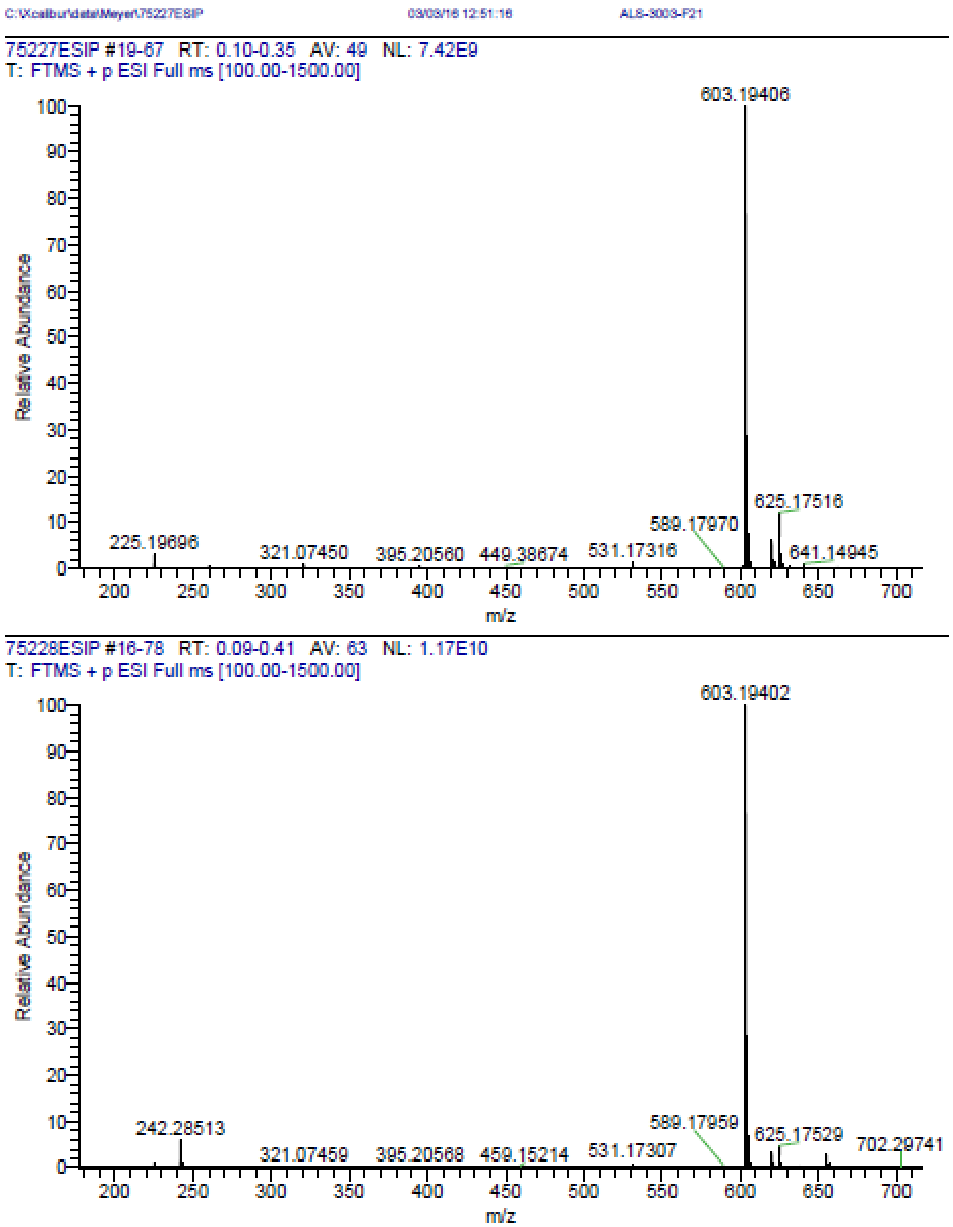

Mass spectrum of ***Cis*-Eg(LGLM)₂**.

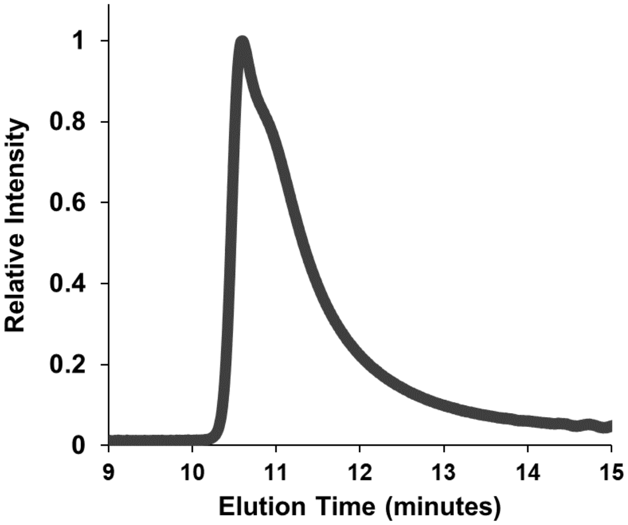

Figure 31. SEC trace of Poly SyLMLGLGL. M_n = 36, M_w = 44, Đ = 1.2, relative to polystyrene standards.

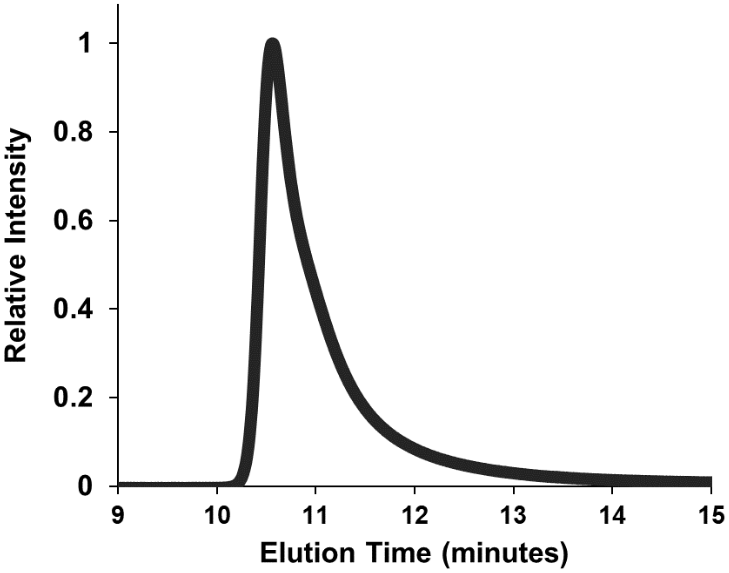

Figure 32. SEC trace of Poly SyLMLGLGL. M_n = 44, M_w = 51 , Đ = 1.2, relative to polystyrene standards.

Appendix B: Experimental Spectra and Supporting Data for Chapter 3

Scanning Electron Microscopy Imaging

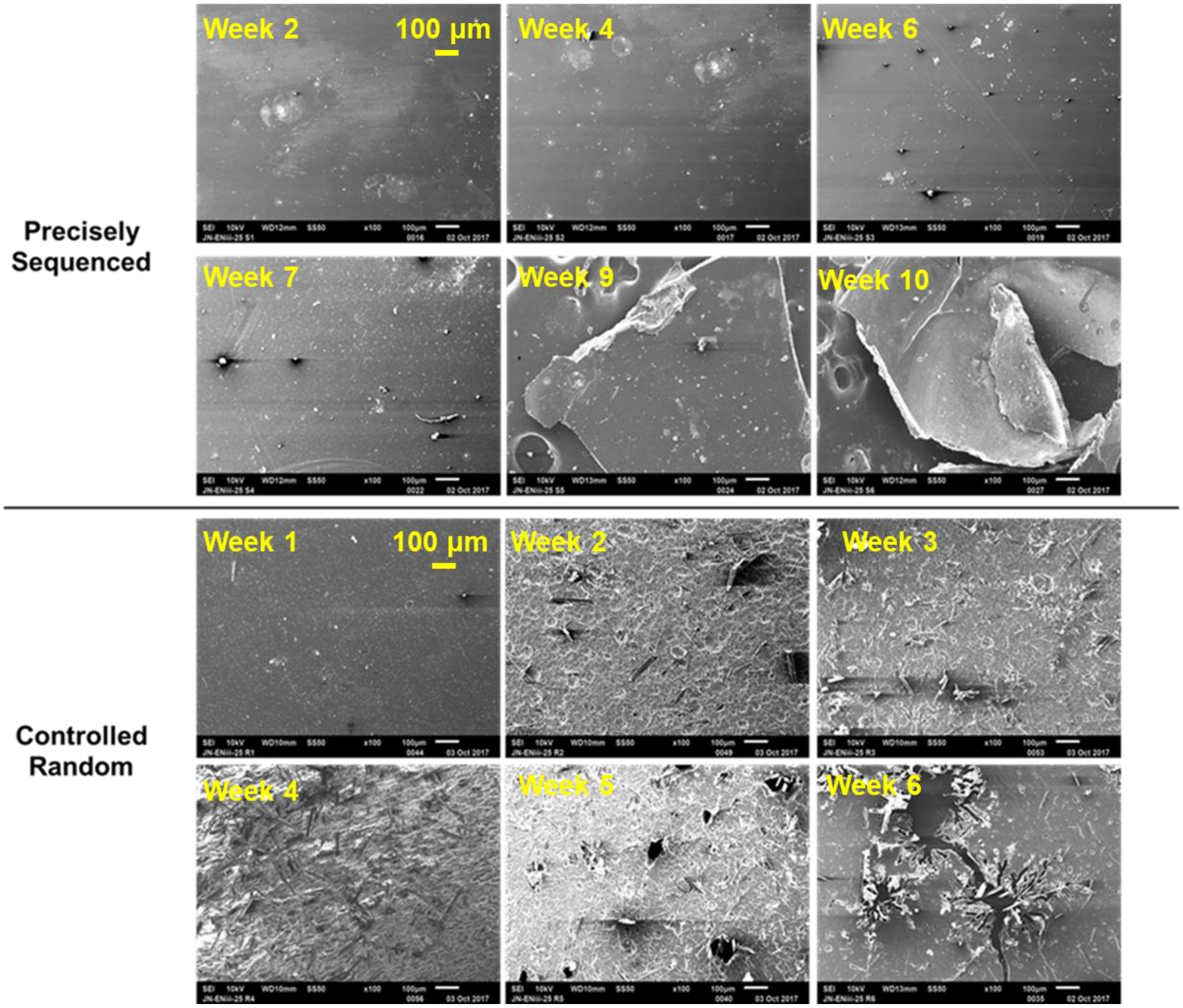
Precisely Sequenced
Week 2
100 µm
Week 4
Week 6
Week 7
Week 9
Week 10
Controlled Random
Week 1
100 µm
Week 2
Week 3
Week 4
Week 5
Week 6

Figure 33. Low magnification (100x) images of Poly SyLM(LGLGL) and Poly SyLM(L_3G_2) at the six time points over the course of hydrolysis.

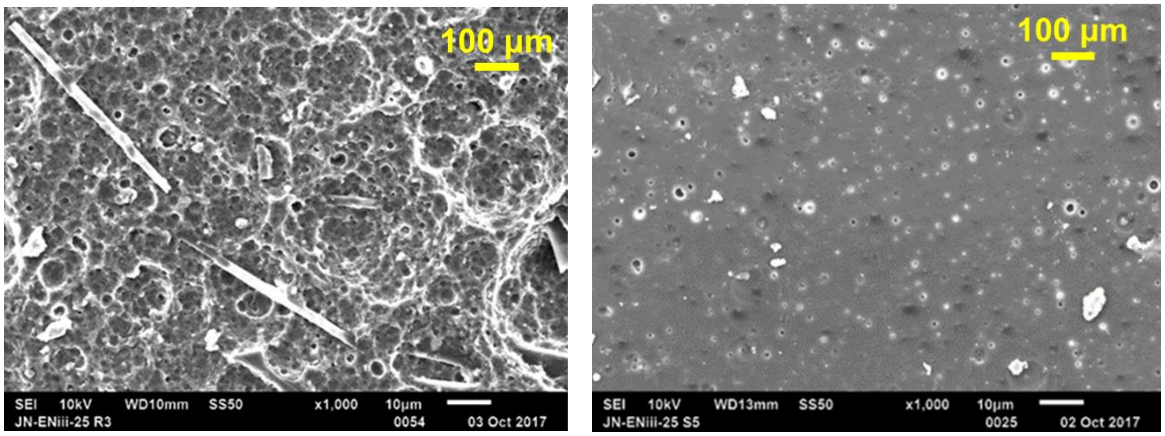
100 µm
SEI 10kV WD10mm SS50 x1,000 10µm
JN-ENiii-25 R3 0054 03 Oct 2017
100 µm
SEI 10kV WD13mm SS50 x1,000 10µm
JN-ENiii-25 S5 0025 02 Oct 2017

Figure 34. High magnification (1000x) of Poly SyLM(L_3G_2) (left) after three weeks of hydrolysis and Poly SyLM(LGLGL) (right) after five weeks of hydrolysis.

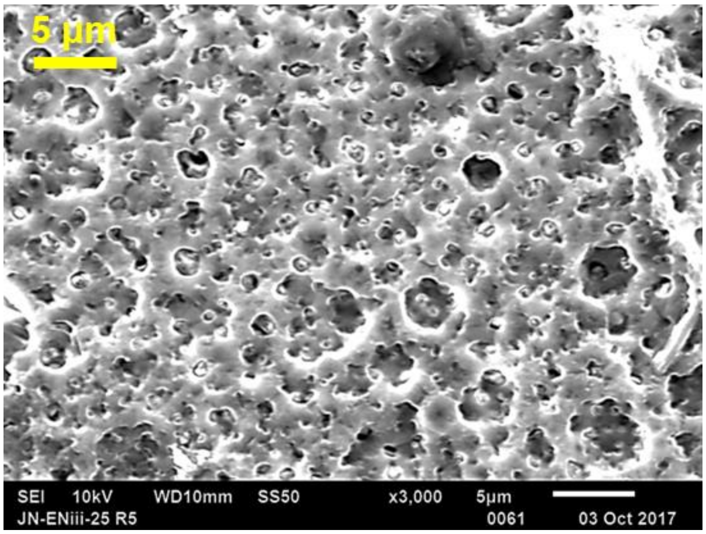
5 µm
SEI 10kV WD10mm SS50 x3,000 5µm
JN-ENiii-25 R5 0061 03 Oct 2017

Figure 35. High magnification (3000x) of the porous structure developed within Poly SyLM(L_3G_2) at Week 5 of hydrolysis.

Experimental Spectra

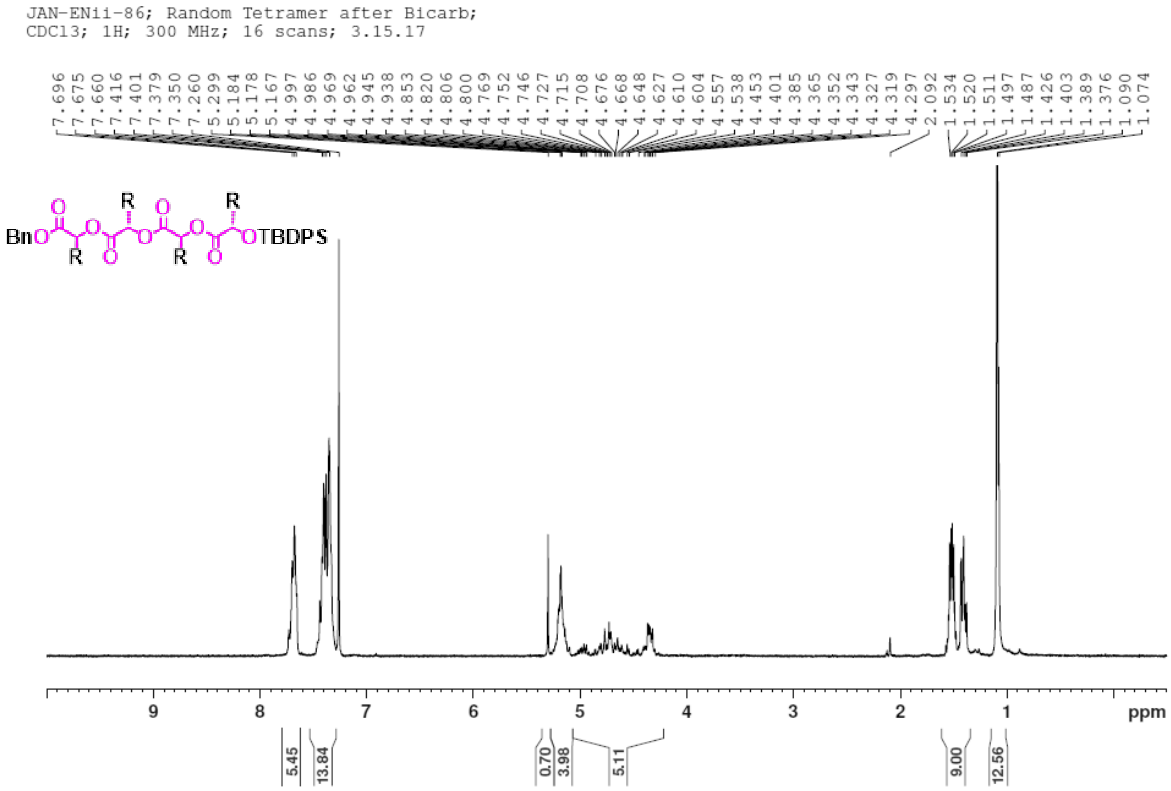

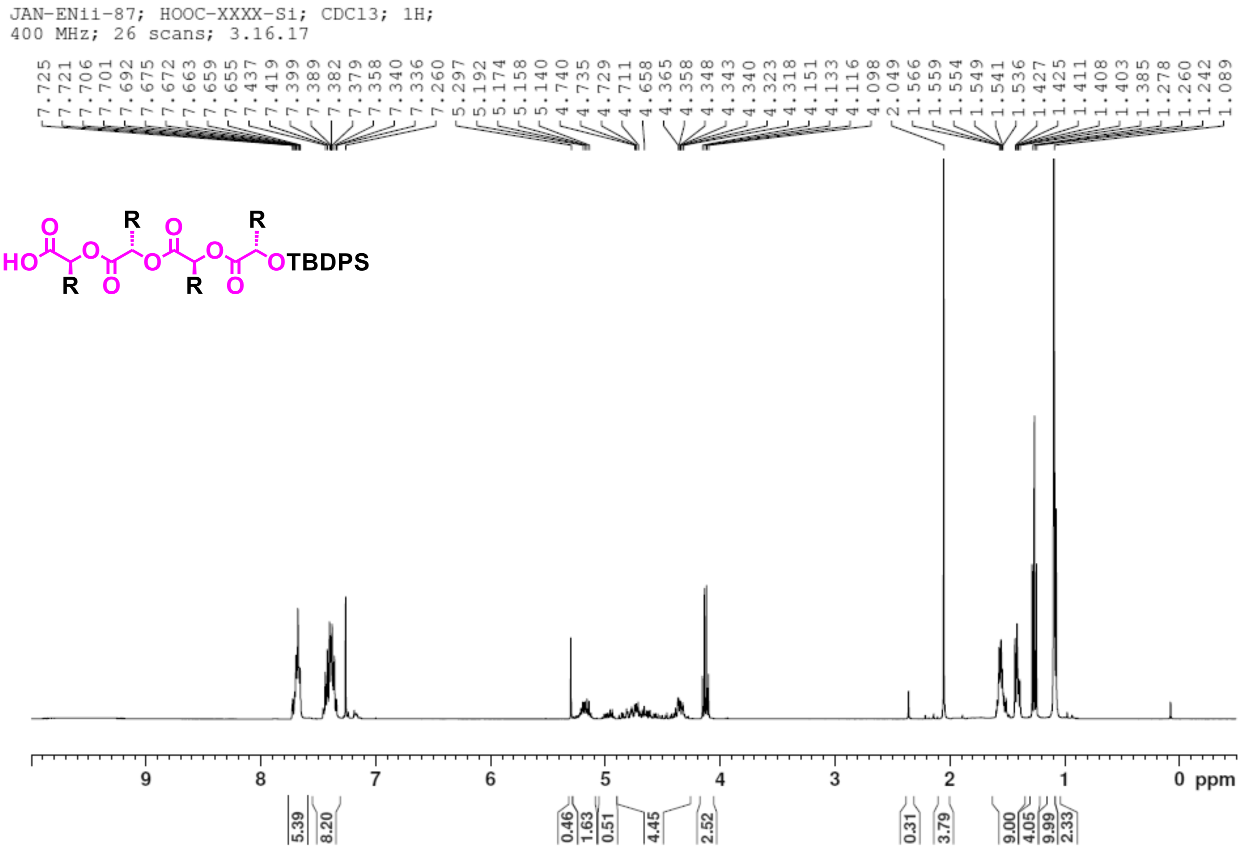
JAN-ENii-87; HOOC-XXXX-Si; CDCl3; 1H;
400 MHz; 26 scans; 3.16.17
7.725
7.721
7.706
7.701
7.692
7.675
7.672
7.663
7.659
7.655
7.437
7.419
7.399
7.389
7.382
7.379
7.358
7.340
7.336
7.260
5.297
5.192
5.174
5.158
5.140
4.740
4.735
4.729
4.711
4.658
4.365
4.358
4.348
4.343
4.340
4.323
4.318
4.151
4.133
4.116
4.098
2.049
1.566
1.559
1.554
1.549
1.541
1.536
1.427
1.425
1.411
1.408
1.403
1.385
1.278
1.260
1.242
1.089
HO
O
R
OTBDPS
9
8
7
6
5
4
3
2
1
0 ppm
5.39
8.20
0.46
1.63
0.51
4.45
2.52
0.31
3.79
9.00
4.05
9.99
2.33

JAN-ENii-87; Bn-LLLGG random; CDCl3; 1H
400 MHz; 16 scans; 3.20.17

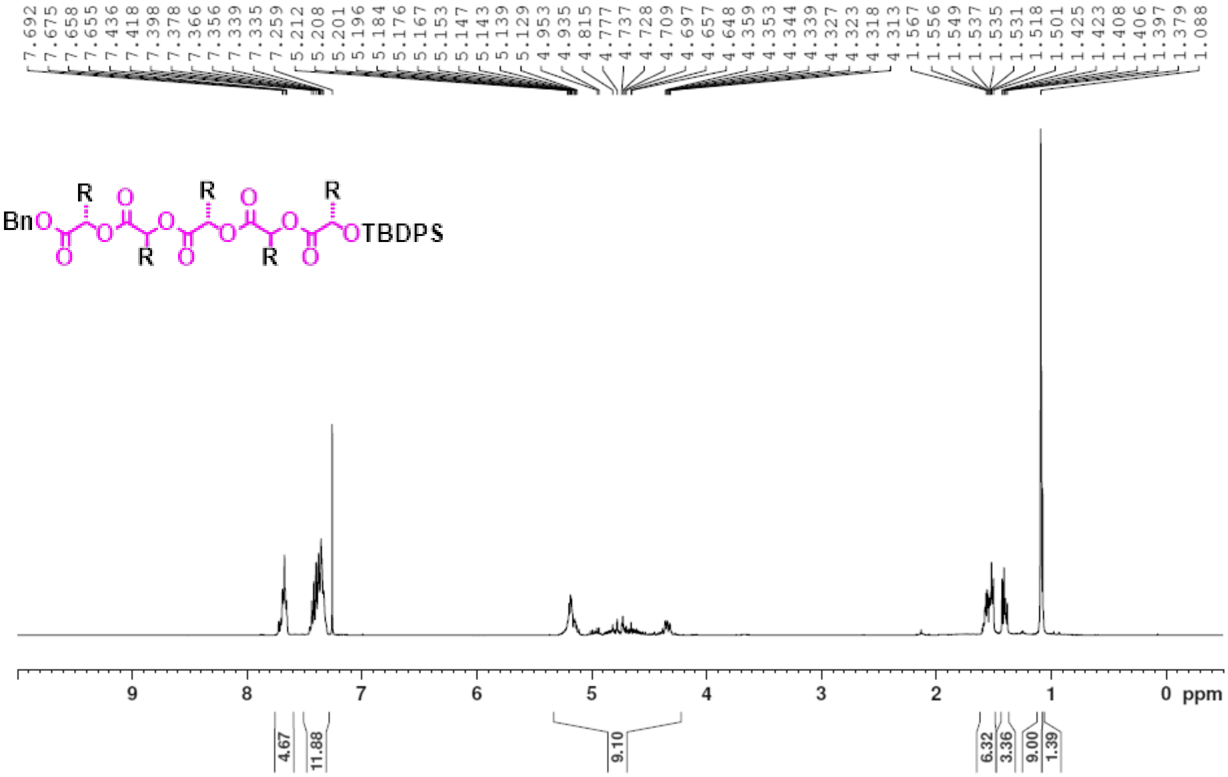

JAN-ENii-87; Bn-LLLGG-Si random; CDCl3; 13C
400 MHz; 16 scans; 3.21.17

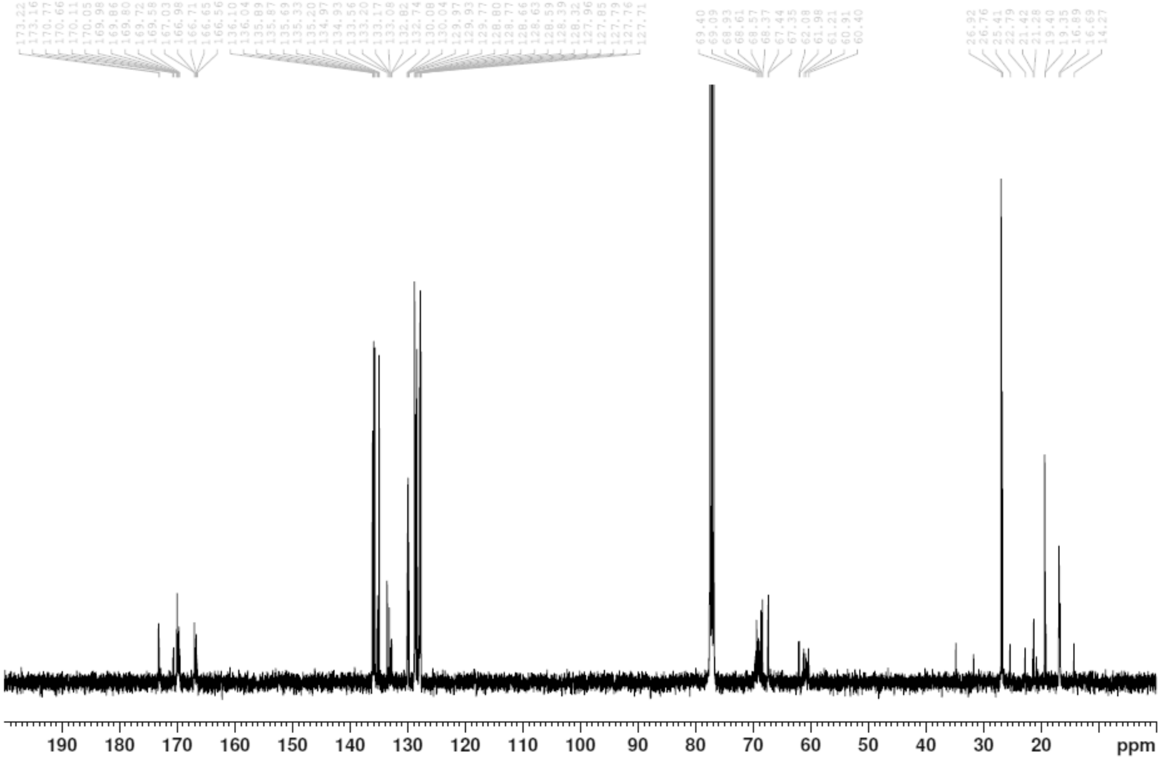

JAN-ENii-95; LLLGG-Si random; CDCl3; 1H
400 MHz; 16 scans; 3.30.17

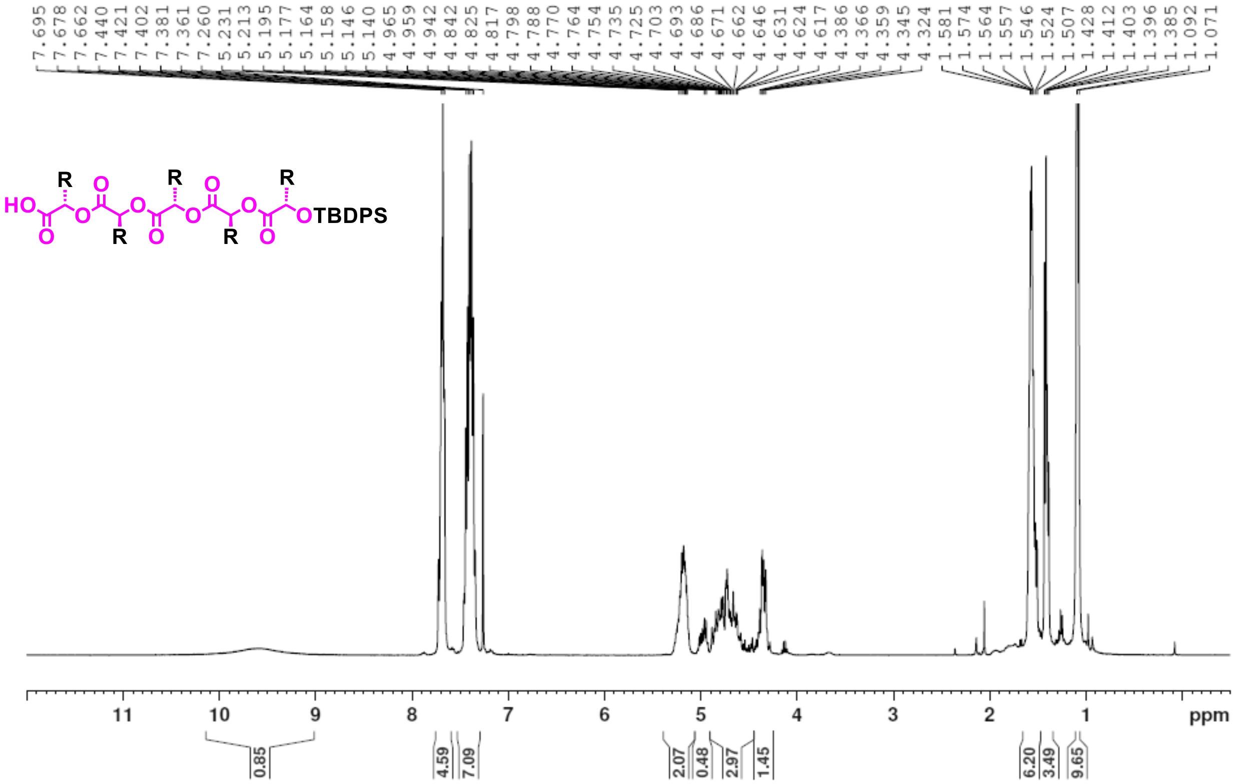

JAN-ENii-95; LLLGG-Si random; CDCl3; 13C
400 MHz; 16 scans; 3.30.17

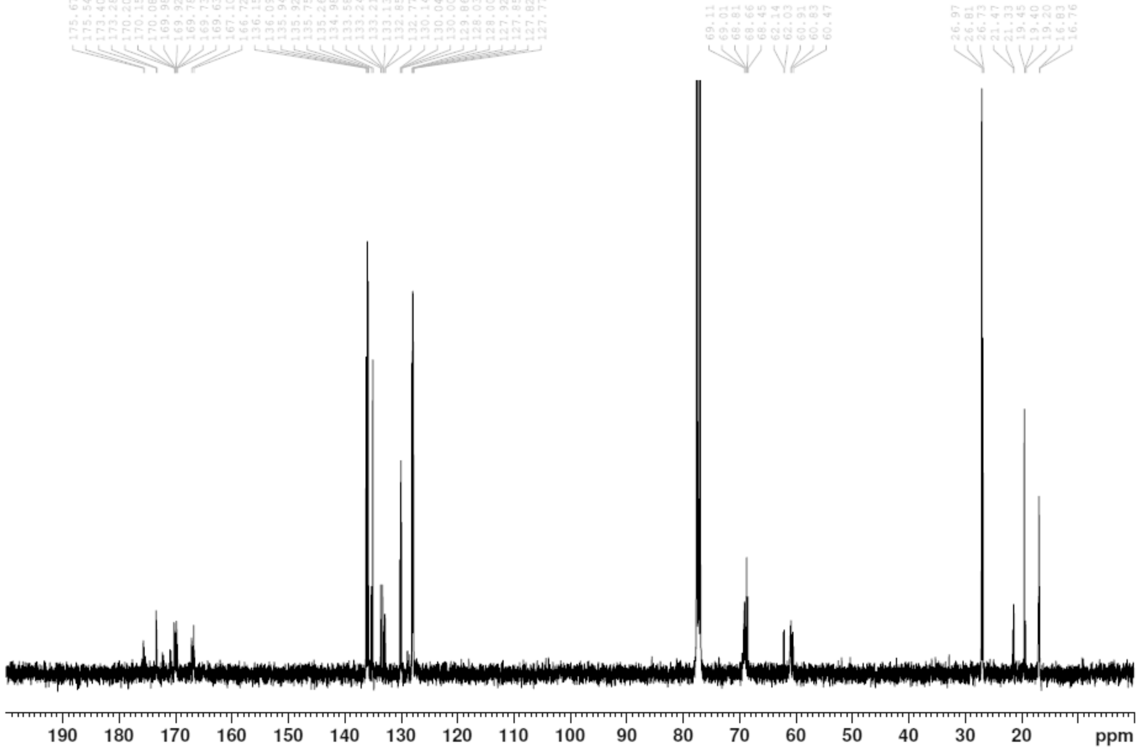

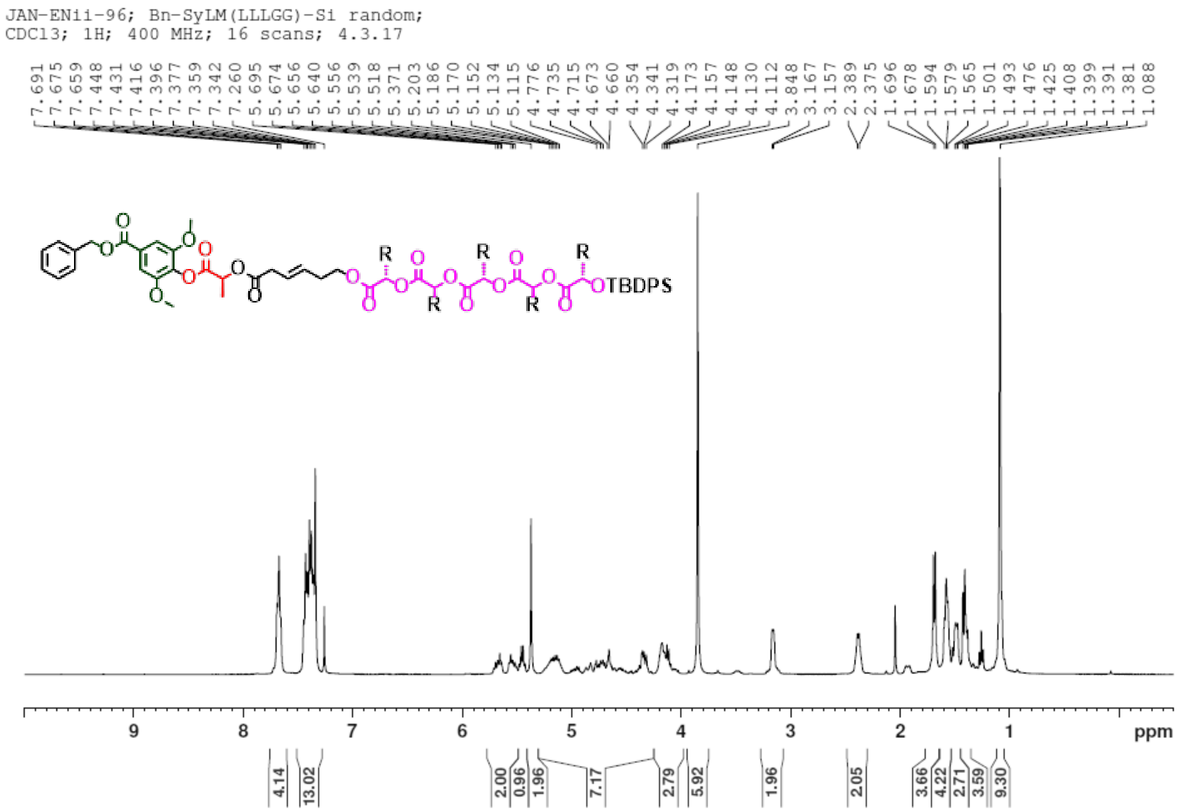
JAN-ENii-96; Bn-SyLM(LLLGG)-Si random;
CDCl3; 1H; 400 MHz; 16 scans; 4.3.17
7.691
7.675
7.659
7.448
7.431
7.416
7.396
7.377
7.359
7.342
7.260
5.695
5.674
5.656
5.640
5.556
5.539
5.518
5.371
5.203
5.186
5.170
5.152
5.134
5.115
4.776
4.735
4.715
4.673
4.660
4.354
4.341
4.319
4.173
4.157
4.148
4.130
4.112
3.848
3.167
3.157
2.389
2.375
1.696
1.678
1.594
1.579
1.565
1.501
1.493
1.476
1.425
1.408
1.399
1.391
1.381
1.088
R
O
OTBDPS
9
8
7
6
5
4
3
2
1
ppm
4.14
13.02
2.00
0.96
1.96
7.17
2.79
5.92
1.96
2.05
3.66
4.22
2.71
3.59
9.30

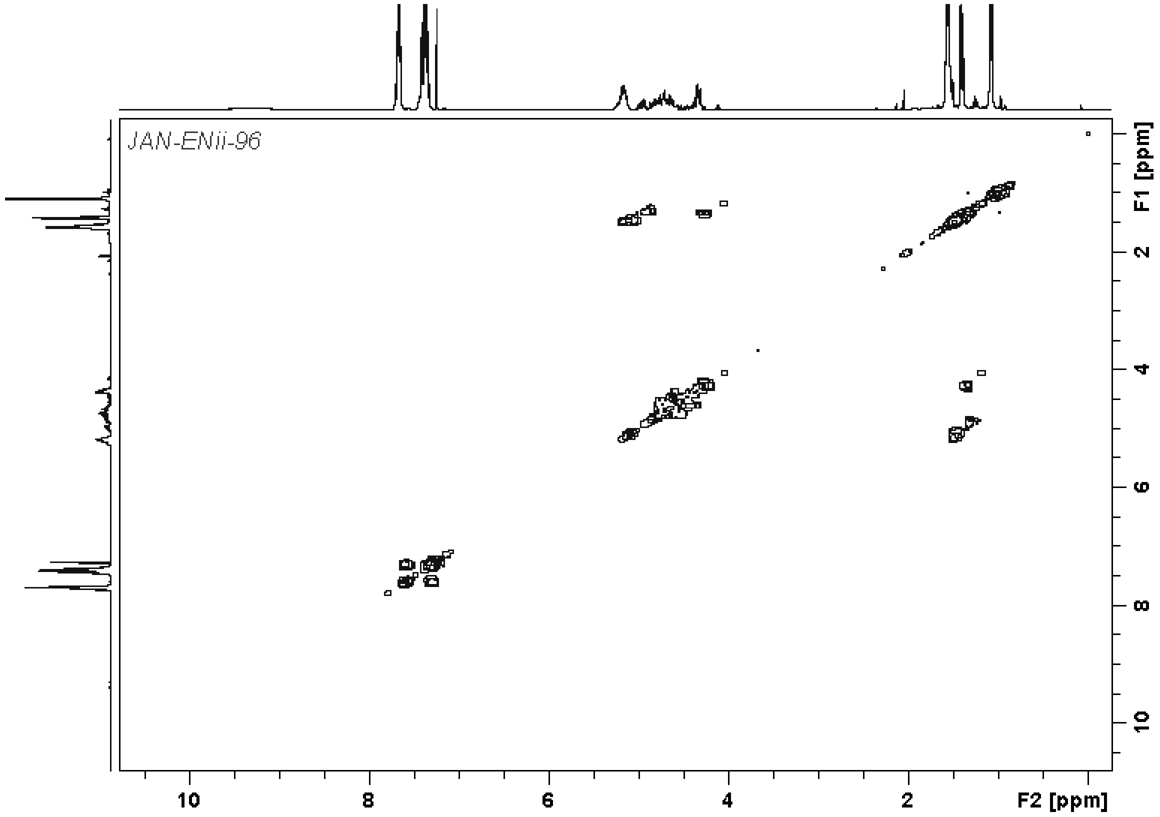

JAN-ENii-96; Bn-SyLM(LLLGG)-Si random;
CDCl3; 13C; 400 MHz; 16 scans; 4.3.17

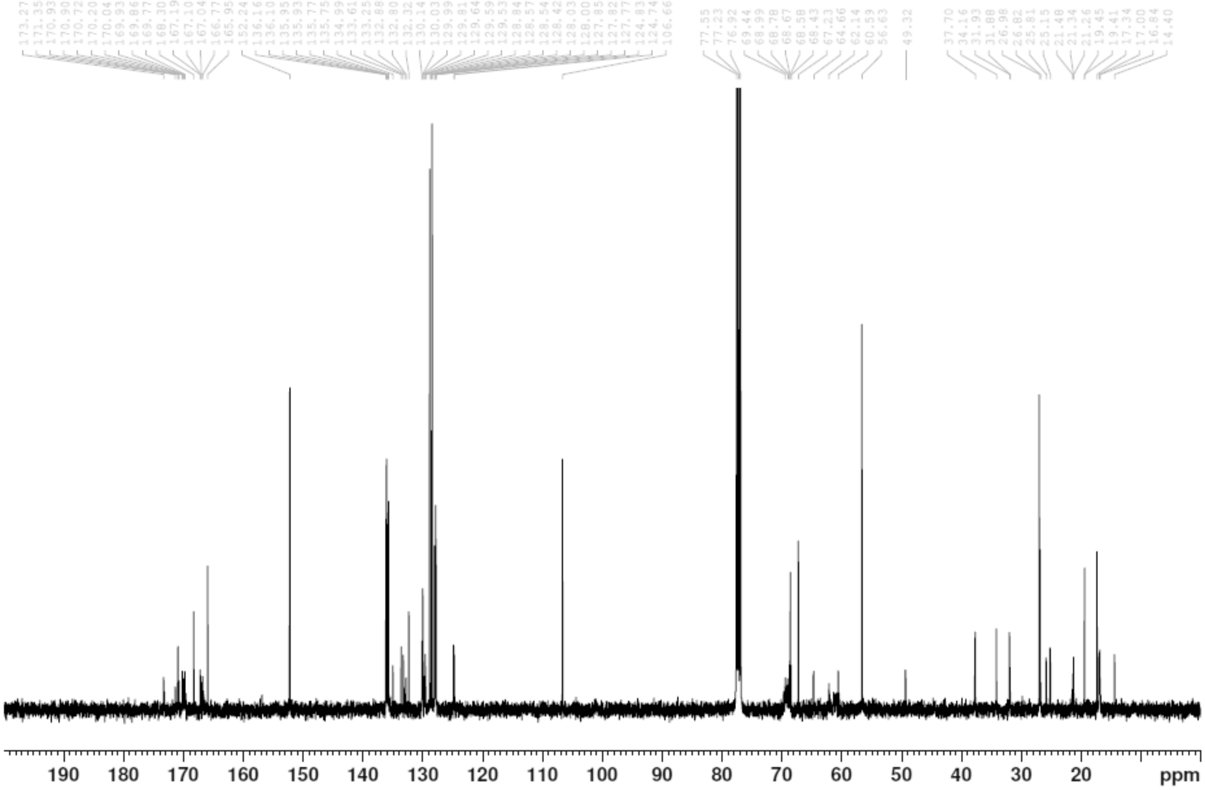

JAN-ENii-97; SyLM(LLLGG)-Si random; CDCl3
1H; 400 MHz; 16 scans; 4.5.17

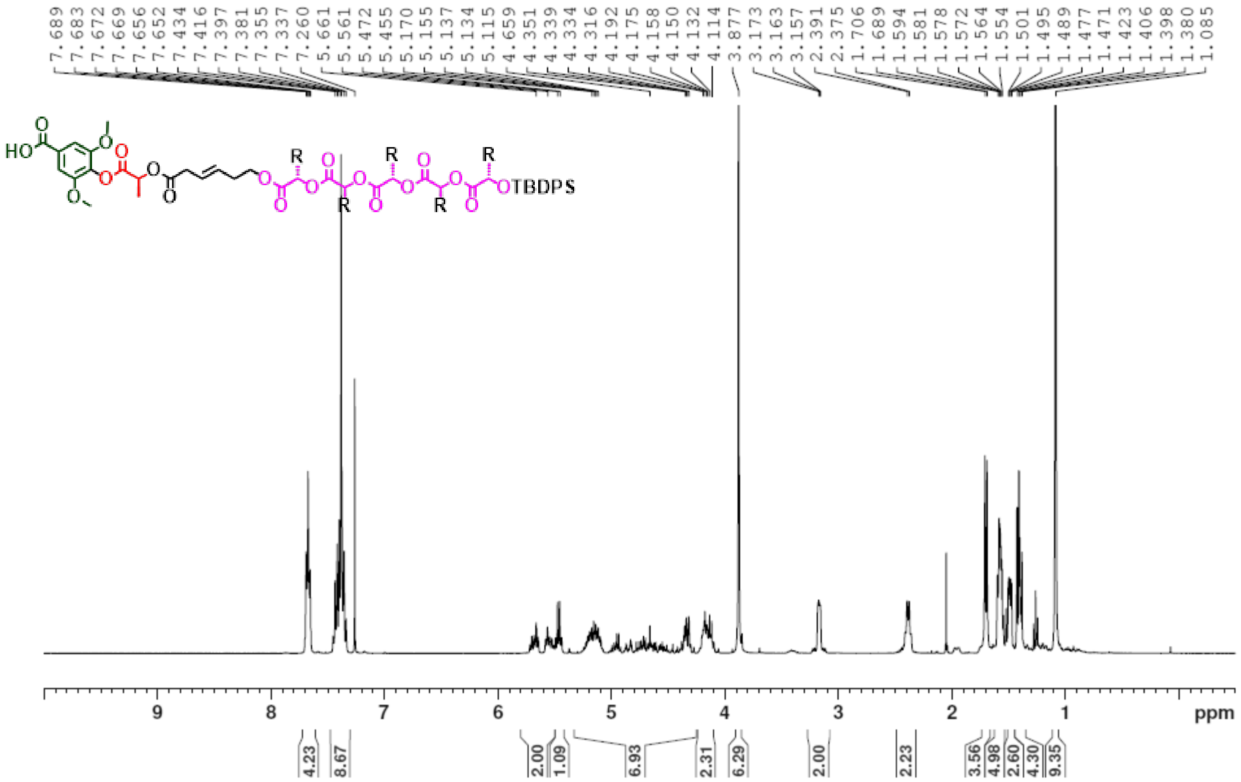

JAN-ENii-97; SyLM(LLLGG)-Si random; CDCl3
13C; 400 MHz; 16 scans; 4.5.17

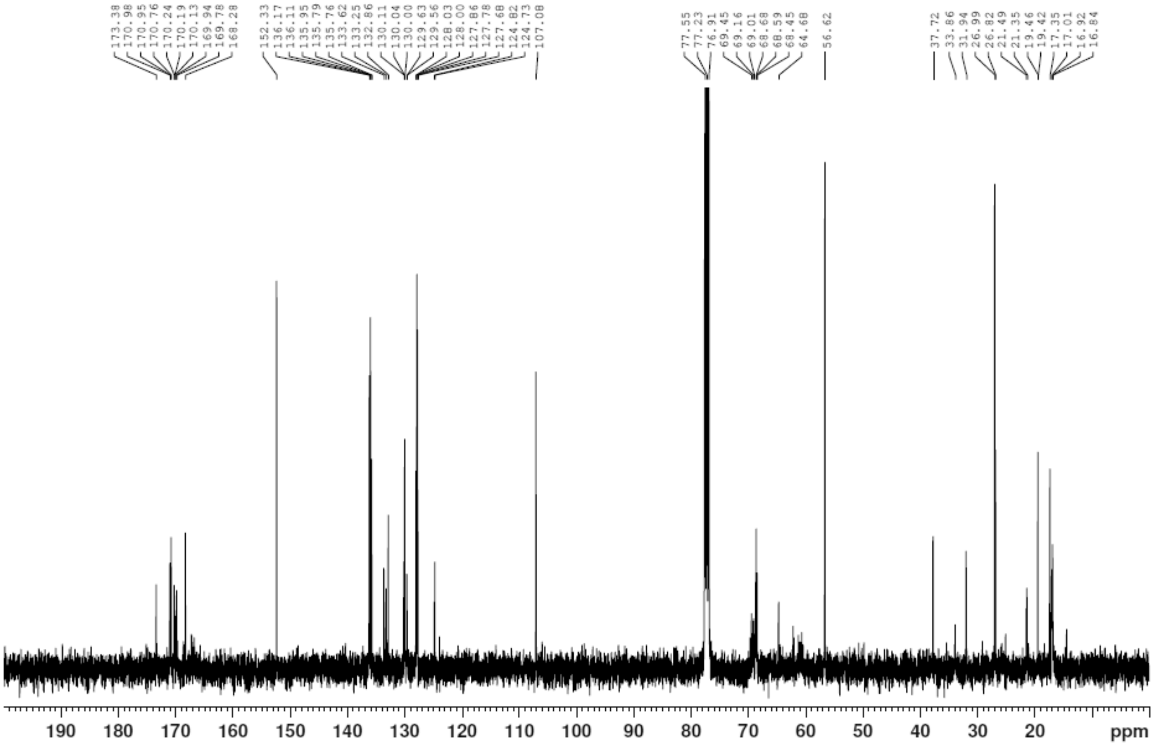

JAN-ENii-98; SyLM(LLLGG) random; CDCl3;
1H; 400 MHz; 16 scans; 4.6.17

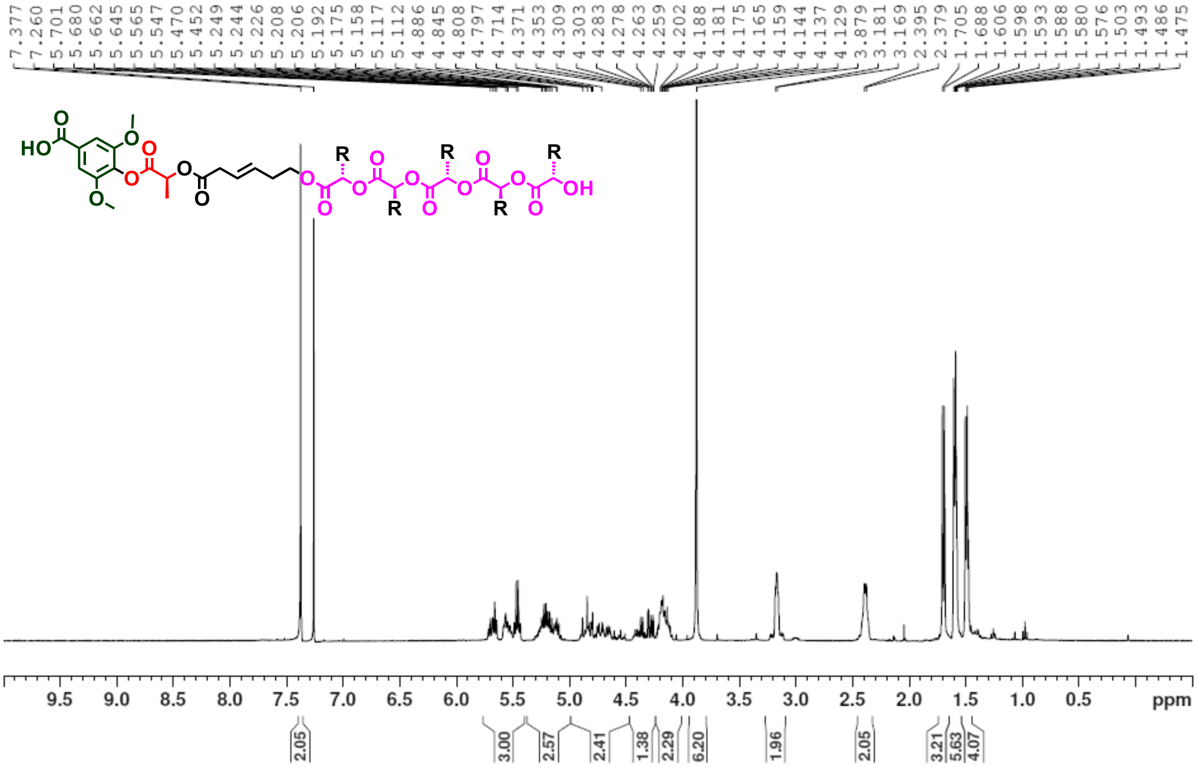

JAN-ENii-98; SyLM(LLLGG) random; CDCl3;
13C; 400 MHz; 16 scans; 4.6.17

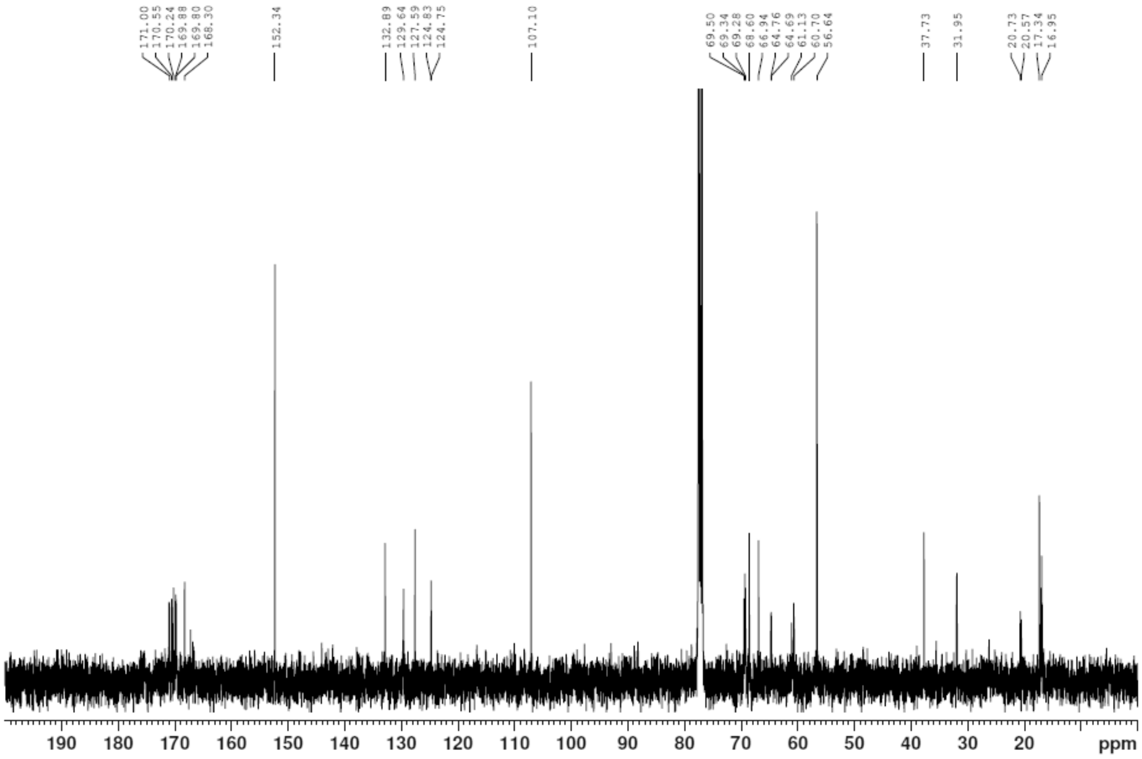

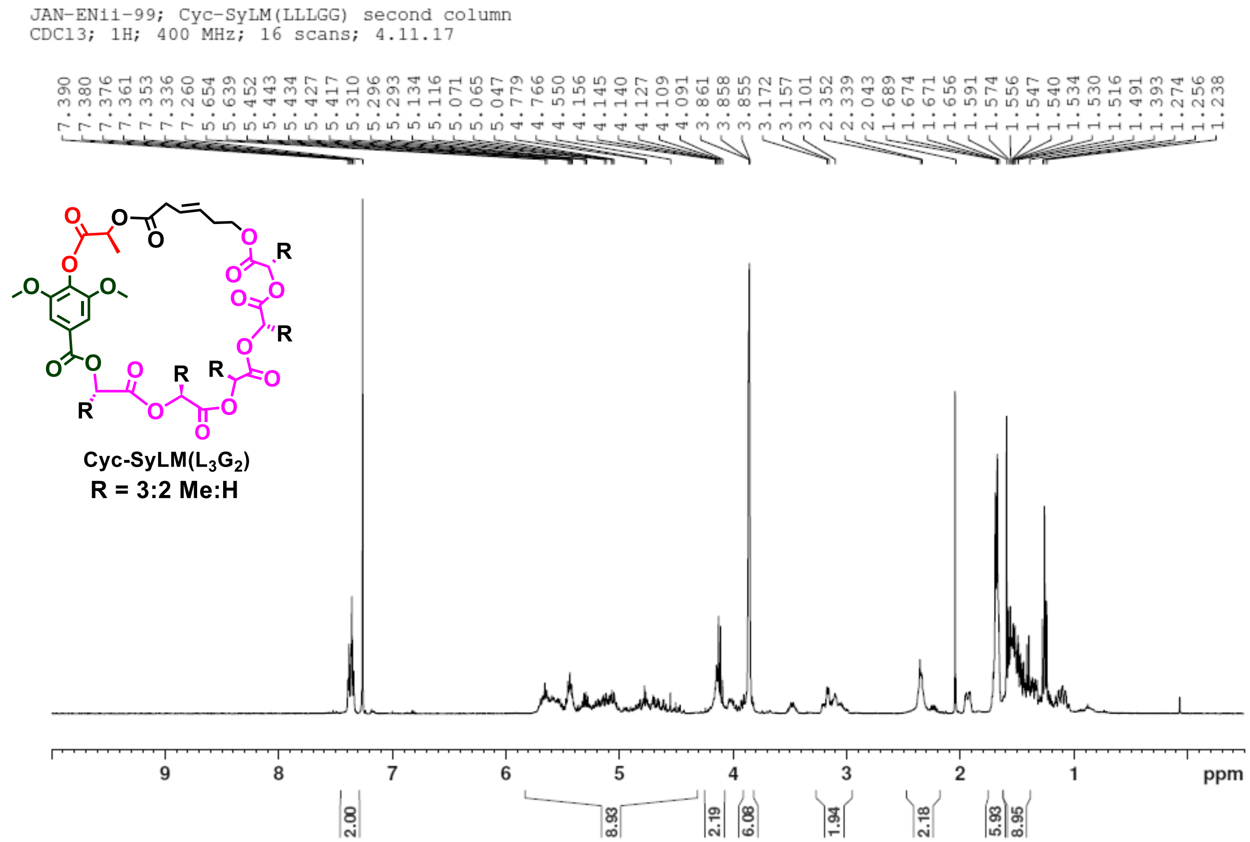

Cyc-SyLM(L_3G_2)
R = 3:2 Me:H

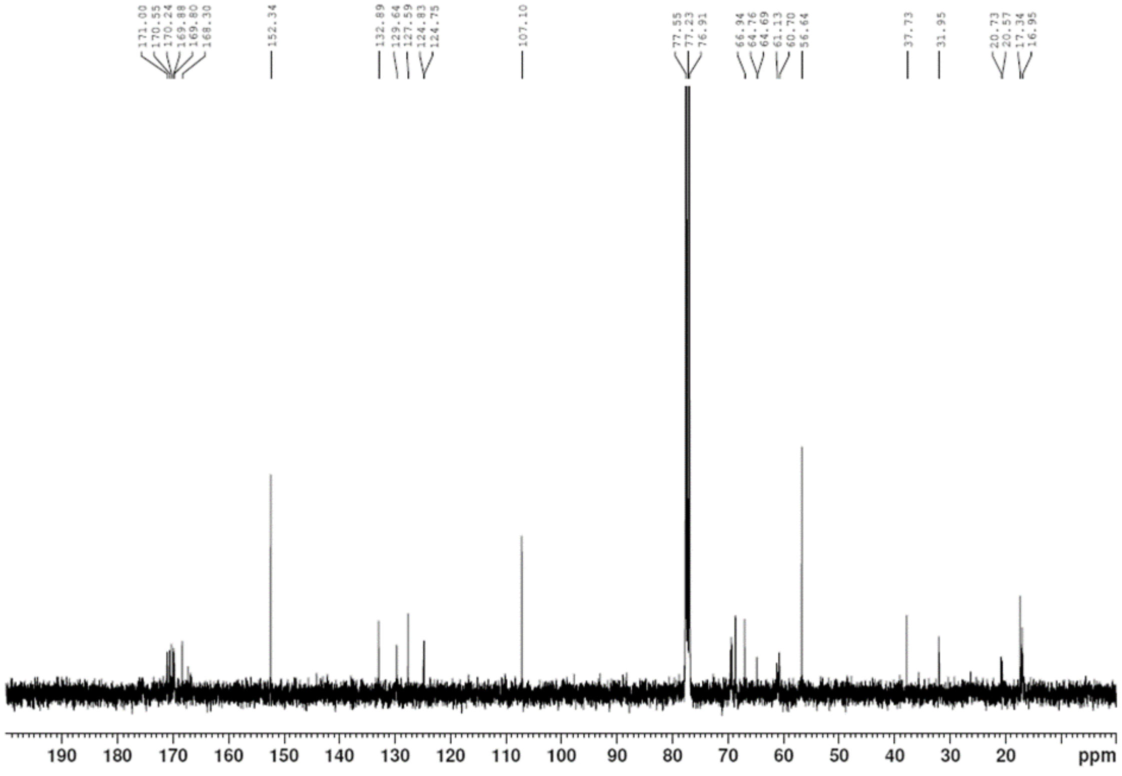

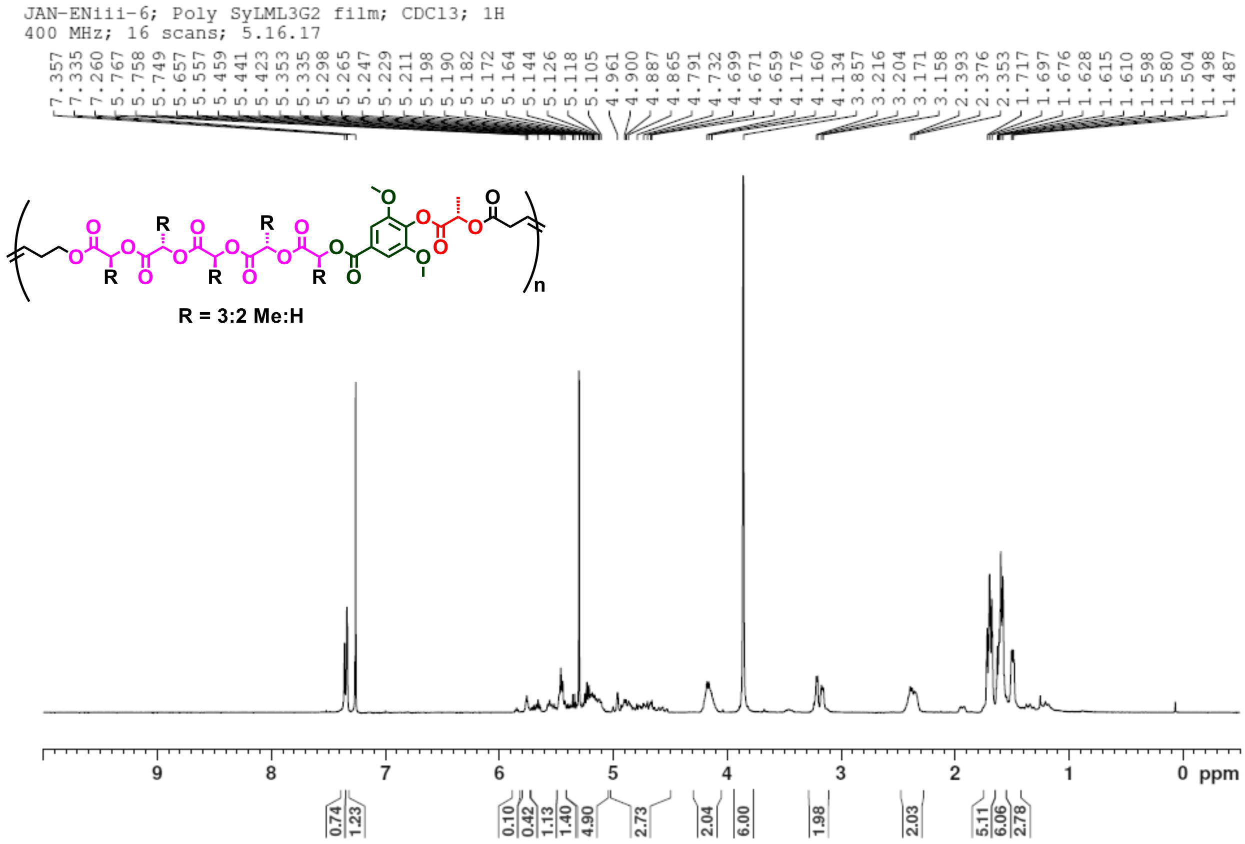
JAN-ENiii-6; Poly SyLML3G2 film; CDCl3; 1H
400 MHz; 16 scans; 5.16.17
7.357
7.335
7.260
5.767
5.758
5.749
5.657
5.557
5.459
5.441
5.423
5.353
5.335
5.298
5.265
5.247
5.229
5.211
5.198
5.190
5.182
5.172
5.164
5.144
5.126
5.118
5.105
4.961
4.900
4.887
4.865
4.791
4.732
4.699
4.671
4.659
4.176
4.160
4.134
3.857
3.216
3.204
3.171
3.158
2.393
2.376
2.353
1.717
1.697
1.676
1.628
1.615
1.610
1.598
1.580
1.504
1.498
1.487
O
R
O
R
O
R
O
R
O
O
O
O
O
O
O
O
O
O
O
O
n
R = 3:2 Me:H
9
8
7
6
5
4
3
2
1
0 ppm
0.74
1.23
0.10
0.42
1.13
1.40
4.90
2.73
2.04
6.00
1.98
2.03
5.11
6.06
2.78

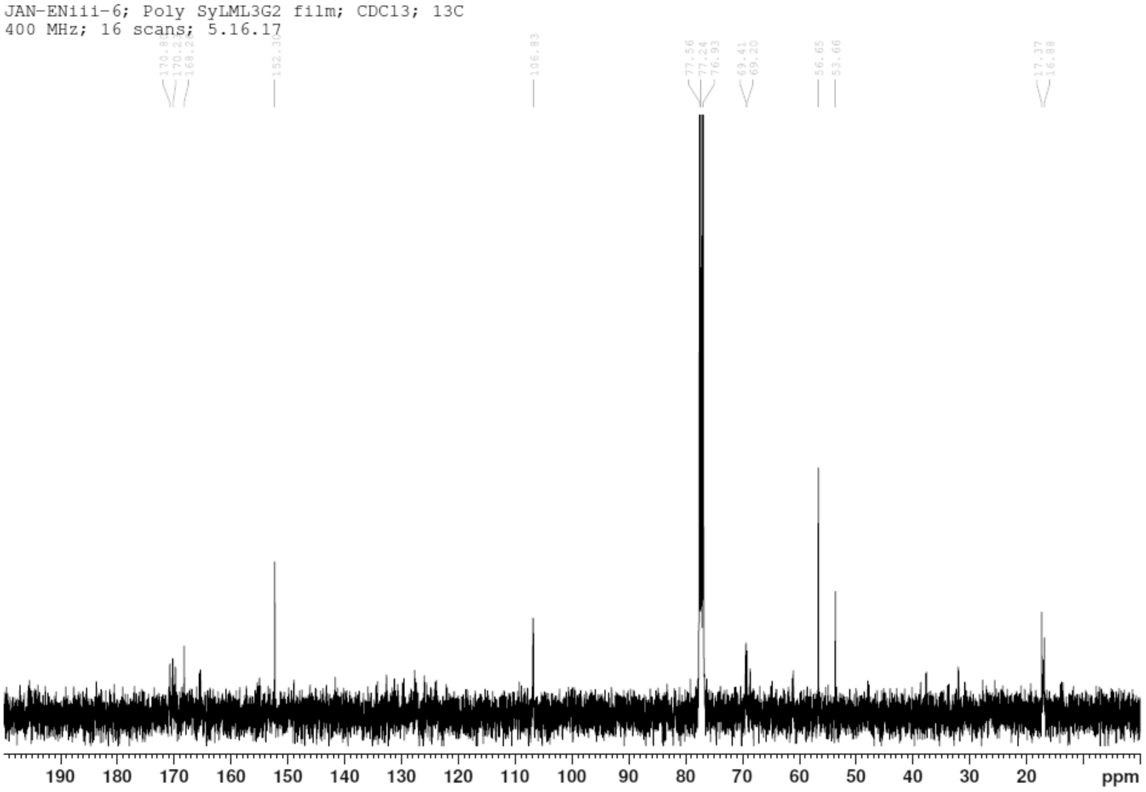
JAN-ENiii-6; Poly SyLML3G2 film; CDCl3; 13C
400 MHz; 16 scans; 5.16.17
170.80
170.23
168.26
152.30
106.83
77.56
77.24
76.93
69.41
69.20
56.65
53.66
17.37
16.88
190
180
170
160
150
140
130
120
110
100
90
80
70
60
50
40
30
20
ppm

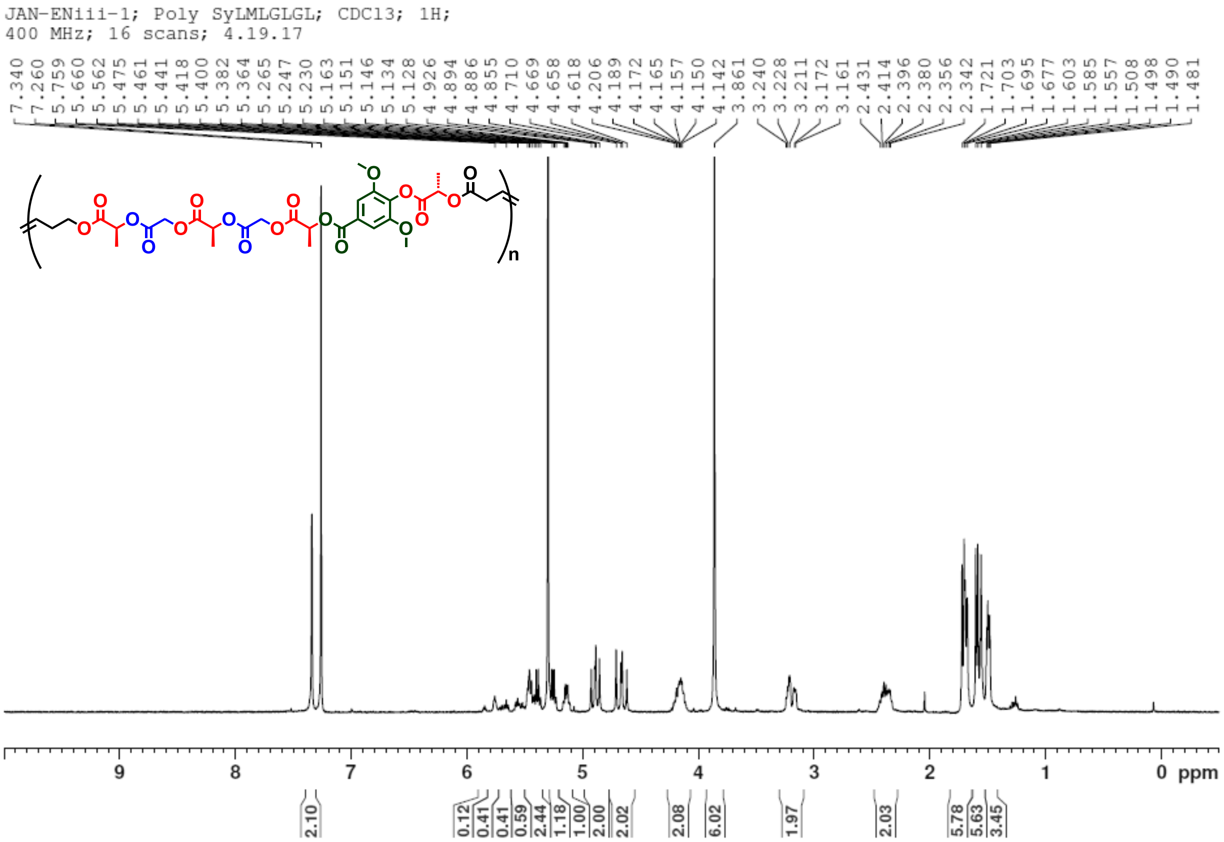
JAN-ENiii-1; Poly SyLMLGLGL; CDCl3; 1H;
400 MHz; 16 scans; 4.19.17
7.340
7.260
5.759
5.660
5.562
5.475
5.461
5.441
5.418
5.400
5.382
5.364
5.265
5.247
5.230
5.163
5.151
5.146
5.134
5.128
4.926
4.894
4.886
4.855
4.710
4.669
4.658
4.618
4.206
4.189
4.172
4.165
4.157
4.150
4.142
3.861
3.240
3.228
3.211
3.172
3.161
2.431
2.414
2.396
2.380
2.356
2.342
1.721
1.703
1.695
1.677
1.603
1.585
1.557
1.508
1.498
1.490
1.481
n
9
8
7
6
5
4
3
2
1
0 ppm
2.10
0.12
0.41
0.41
0.59
2.44
1.18
1.00
2.00
2.02
2.08
6.02
1.97
2.03
5.78
5.63
3.45

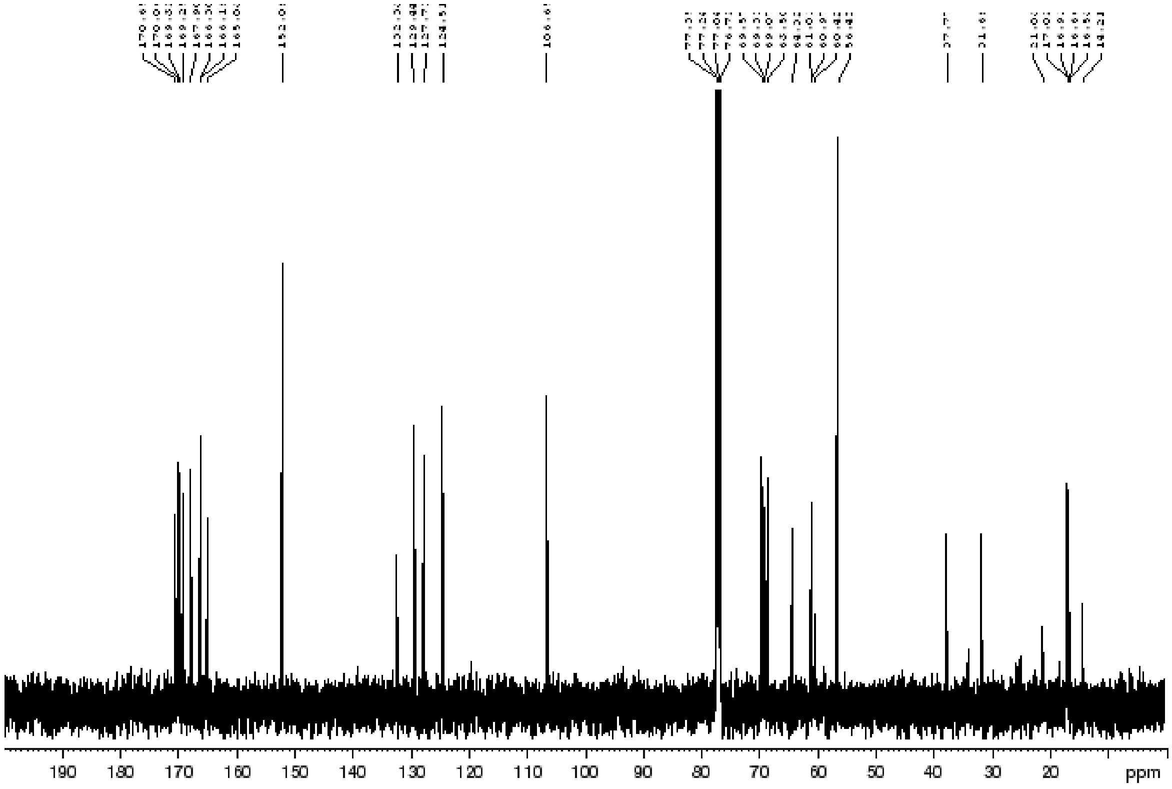
190
180
170
160
150
140
130
120
110
100
90
80
70
60
50
40
30
20
ppm

The following ^1H NMR spectra were collected on lyophilized samples at the given time point during the hydrolysis study (Where S = Sequenced, R = Controlled Random, and the number corresponds to the time point, e.g. S1 = the first sequenced sample collected at Week 2 during hydrolysis and R1 = the first random sample collected at Week 1 during hydrolysis).

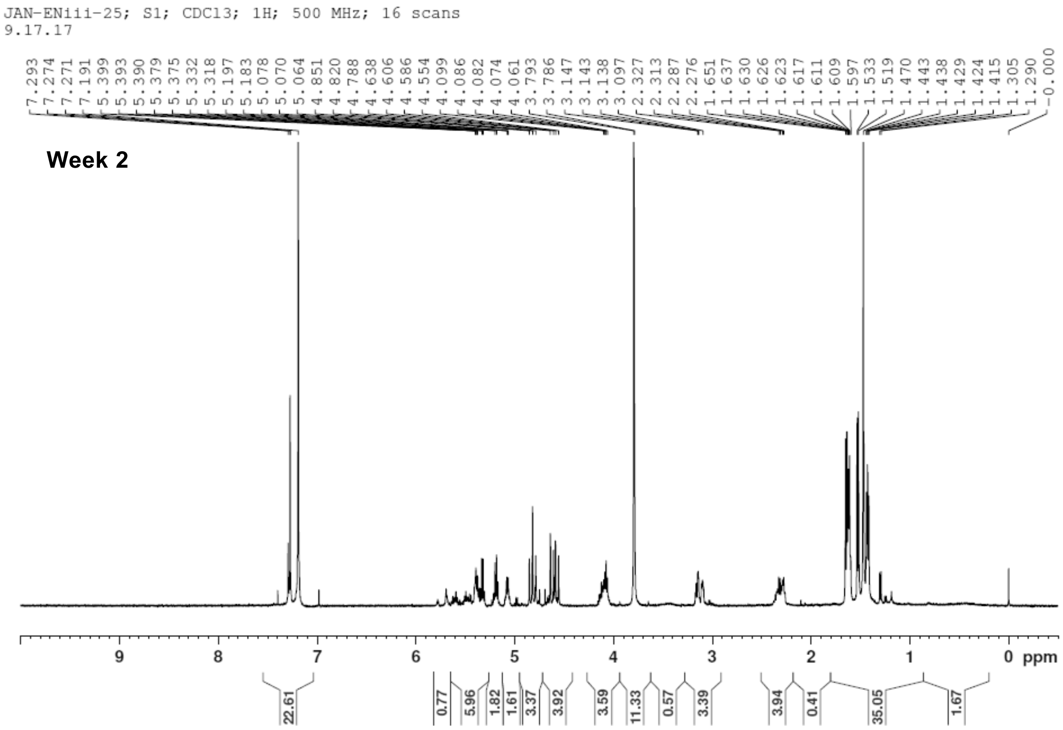

JAN-ENiii-25; S2; CDCl3; 1H: 500 MHz
16 scans; 9.17.17

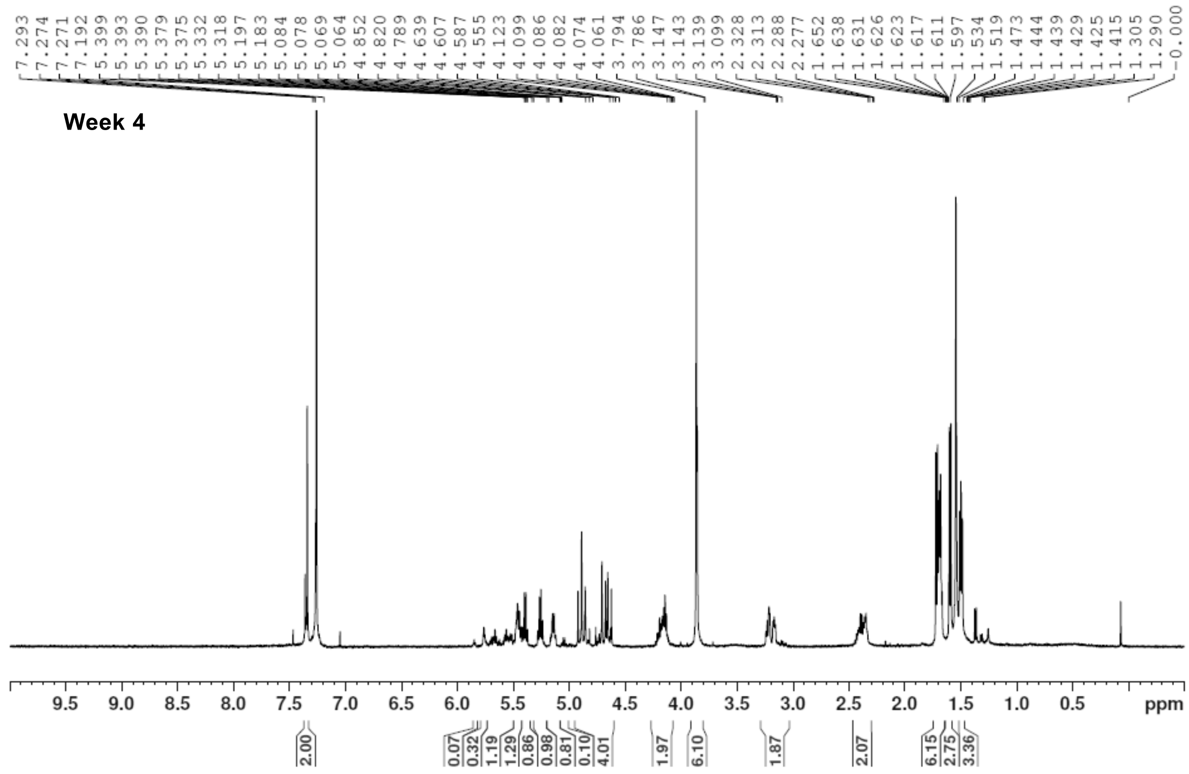

JAN-ENiii-25; S3; CDCl3; 1H; 500 MHz; 16 scans; 9.17.17

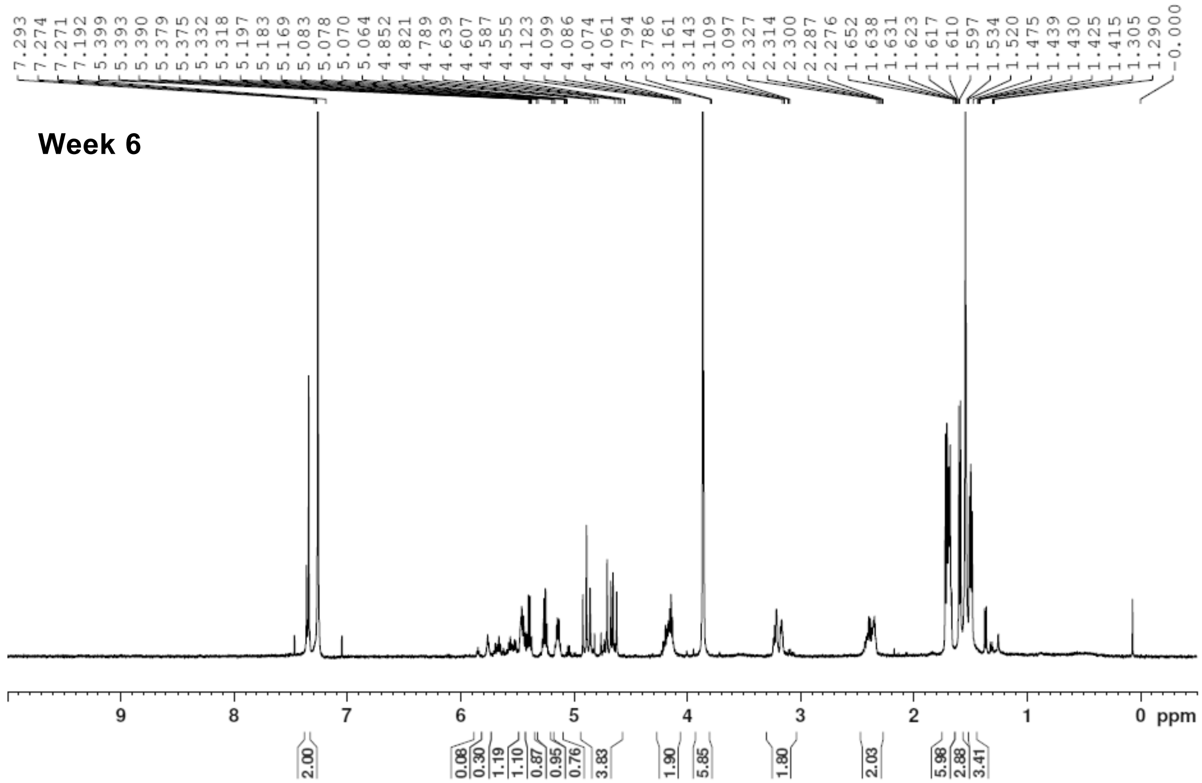

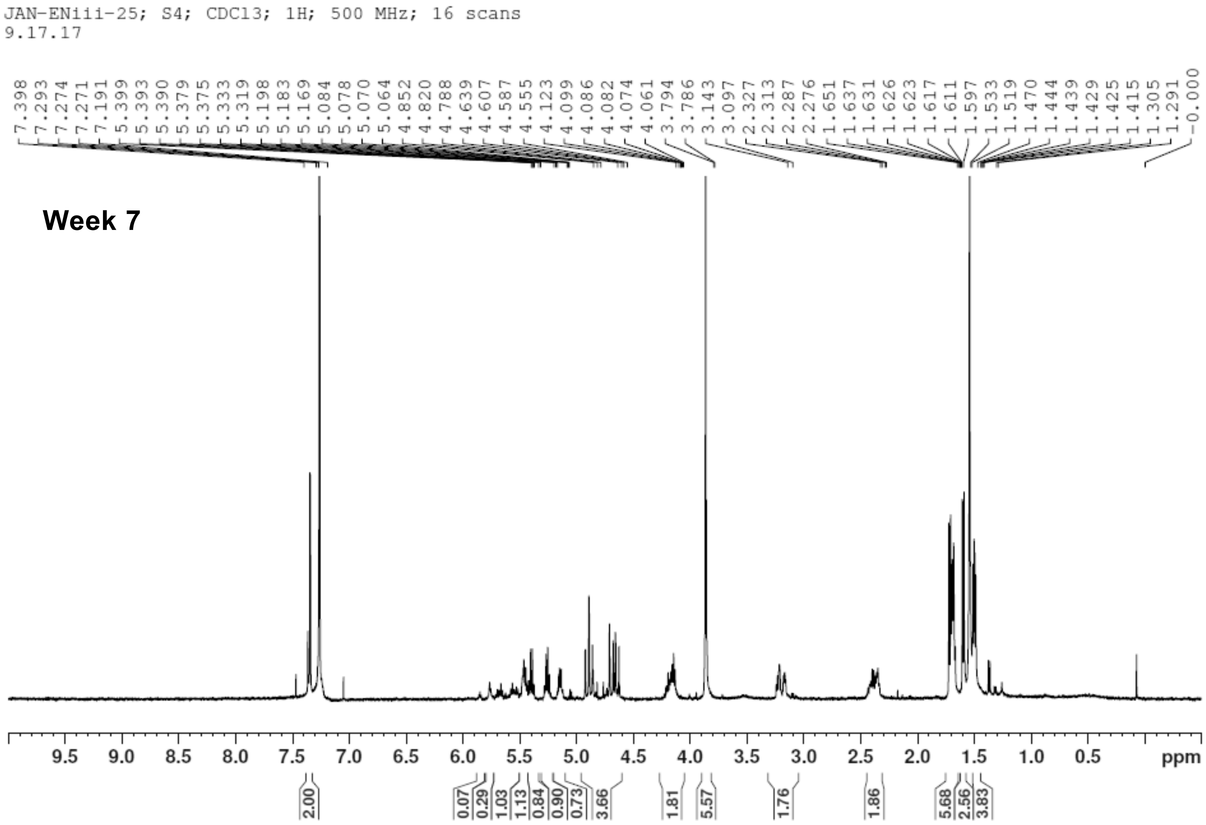
JAN-ENiii-25; S4; CDCl3; 1H; 500 MHz; 16 scans
9.17.17
7.398
7.293
7.274
7.271
7.191
5.399
5.393
5.390
5.379
5.375
5.333
5.319
5.198
5.183
5.169
5.084
5.078
5.070
5.064
4.852
4.820
4.788
4.639
4.607
4.587
4.555
4.123
4.099
4.086
4.082
4.074
4.061
3.794
3.786
3.143
3.097
2.327
2.313
2.287
2.276
1.651
1.637
1.631
1.626
1.623
1.617
1.611
1.597
1.533
1.519
1.470
1.444
1.439
1.429
1.425
1.415
1.305
1.291
-0.000
9.5
9.0
8.5
8.0
7.5
7.0
6.5
6.0
5.5
5.0
4.5
4.0
3.5
3.0
2.5
2.0
1.5
1.0
0.5
ppm
2.00
0.07
0.29
1.03
1.13
0.84
0.90
0.73
3.66
1.81
5.57
1.76
1.86
5.68
2.56
3.83

Week 7

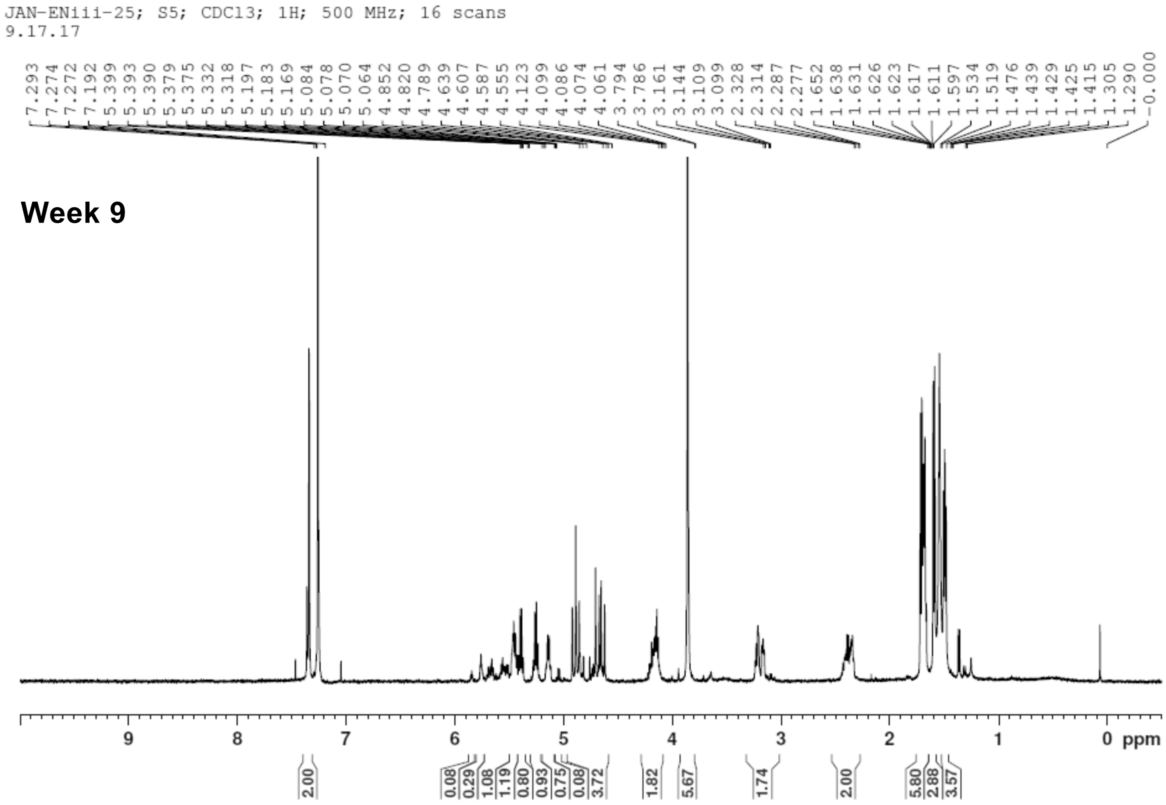
JAN-ENiii-25; S5; CDCl3; 1H; 500 MHz; 16 scans
9.17.17
7.293
7.274
7.272
7.192
5.399
5.393
5.390
5.379
5.375
5.332
5.318
5.197
5.183
5.169
5.084
5.078
5.070
5.064
4.852
4.820
4.789
4.639
4.607
4.587
4.555
4.123
4.099
4.086
4.074
4.061
3.794
3.786
3.161
3.144
3.109
3.099
2.328
2.314
2.287
2.277
1.652
1.638
1.631
1.626
1.623
1.617
1.611
1.597
1.534
1.519
1.476
1.439
1.429
1.425
1.415
1.305
1.290
-0.000
9
8
7
6
5
4
3
2
1
0 ppm
2.00
0.08
0.29
1.08
1.19
0.80
0.93
0.75
0.08
3.72
1.82
5.67
1.74
2.00
5.80
2.88
3.57

Week 9

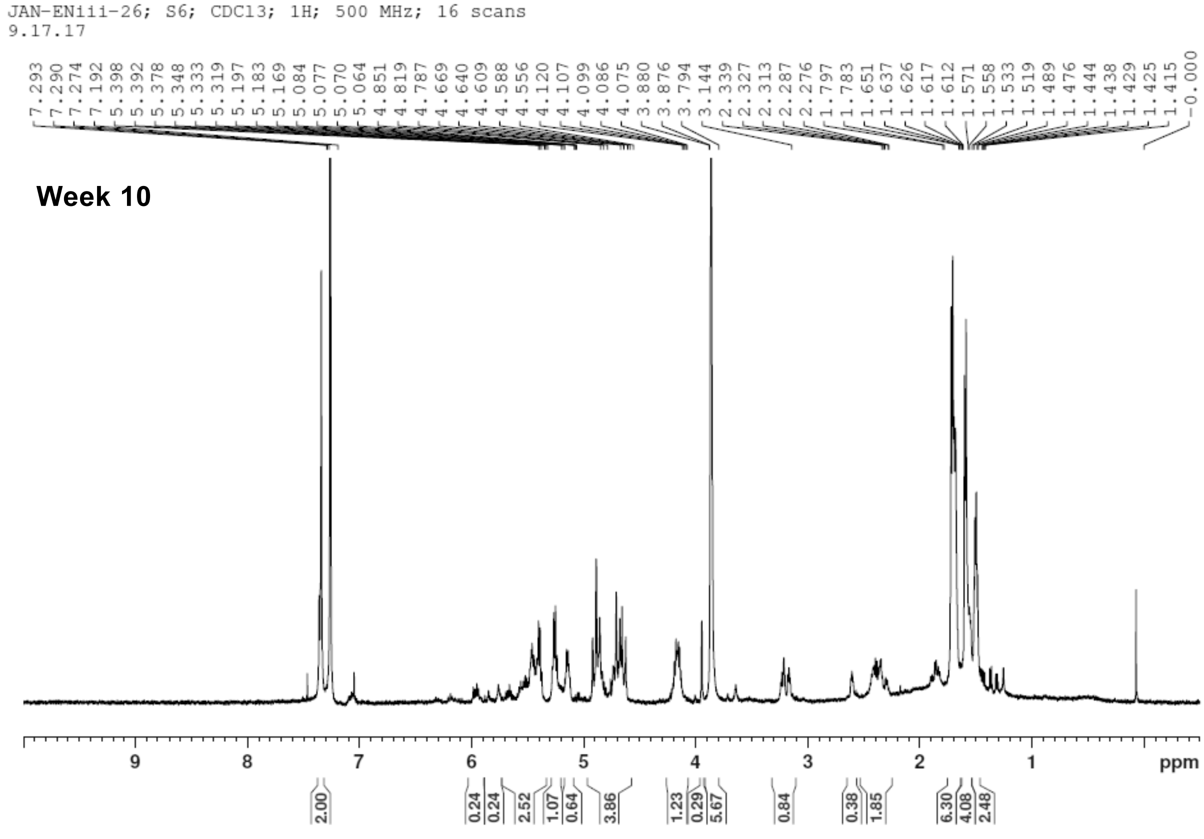
JAN-ENiii-26; S6; CDCl3; 1H; 500 MHz; 16 scans
9.17.17
7.293 7.290 7.274 7.192 5.398 5.392 5.378 5.348 5.333 5.319 5.197 5.183 5.169 5.084 5.077 5.070 5.064 4.851 4.819 4.787 4.669 4.640 4.609 4.588 4.556 4.120 4.107 4.099 4.086 4.075 3.880 3.876 3.794 3.144 2.339 2.327 2.313 2.287 2.276 1.797 1.783 1.651 1.637 1.626 1.617 1.612 1.571 1.558 1.533 1.519 1.489 1.476 1.444 1.438 1.429 1.425 1.415 -0.000
Week 10
9
8
7
6
5
4
3
2
1
ppm
2.00
0.24
0.24
2.52
1.07
0.64
3.86
1.23
0.29
5.67
0.84
0.38
1.85
6.30
4.08
2.48

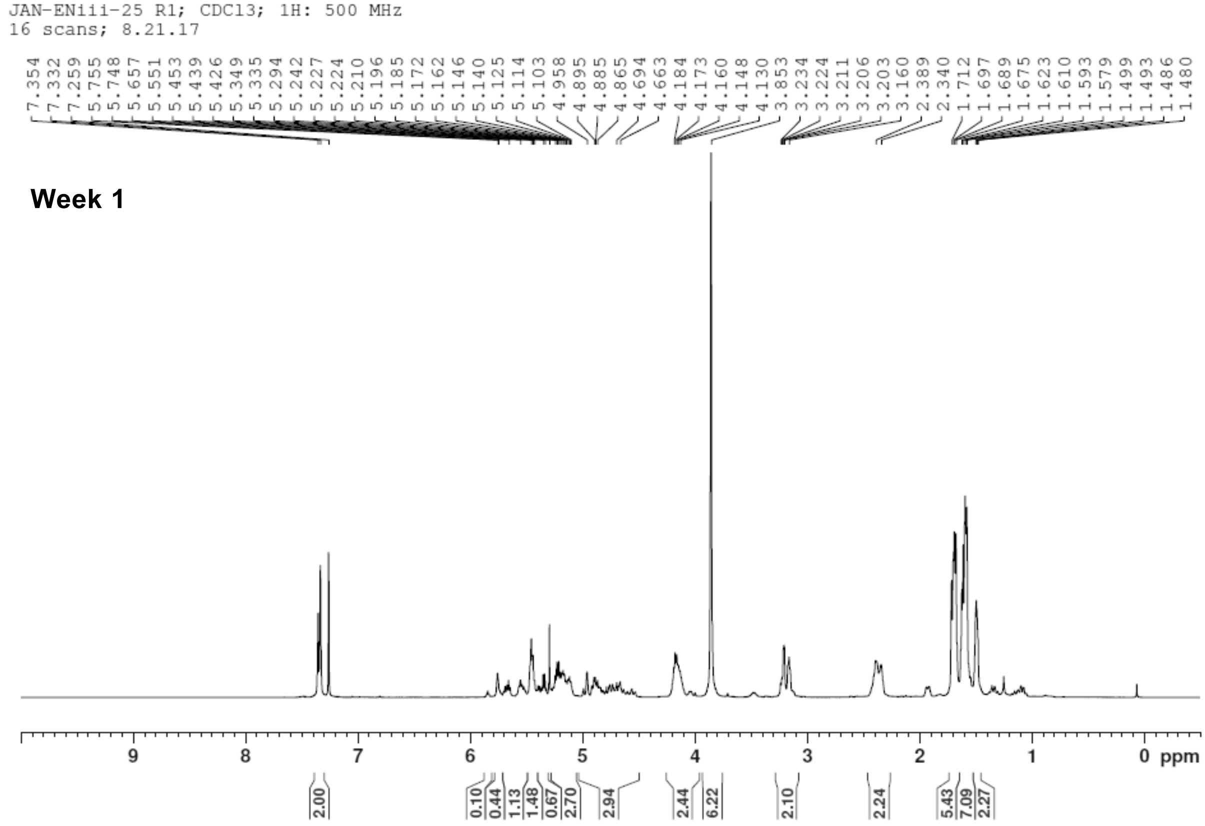
JAN-ENiii-25 R1; CDCl3; 1H: 500 MHz
16 scans; 8.21.17
7.354 7.332 7.259 7.255 5.748 5.657 5.551 5.453 5.439 5.426 5.349 5.335 5.294 5.242 5.227 5.224 5.210 5.196 5.185 5.172 5.162 5.146 5.140 5.125 5.114 5.103 4.958 4.895 4.885 4.865 4.694 4.663 4.184 4.173 4.160 4.148 4.130 3.853 3.234 3.224 3.211 3.206 3.203 3.160 2.389 2.340 1.712 1.697 1.689 1.675 1.623 1.610 1.593 1.579 1.499 1.493 1.486 1.480
Week 1
9
8
7
6
5
4
3
2
1
0 ppm
2.00
0.10
0.44
1.13
1.48
0.67
2.70
2.94
2.44
6.22
2.10
2.24
5.43
7.09
2.27

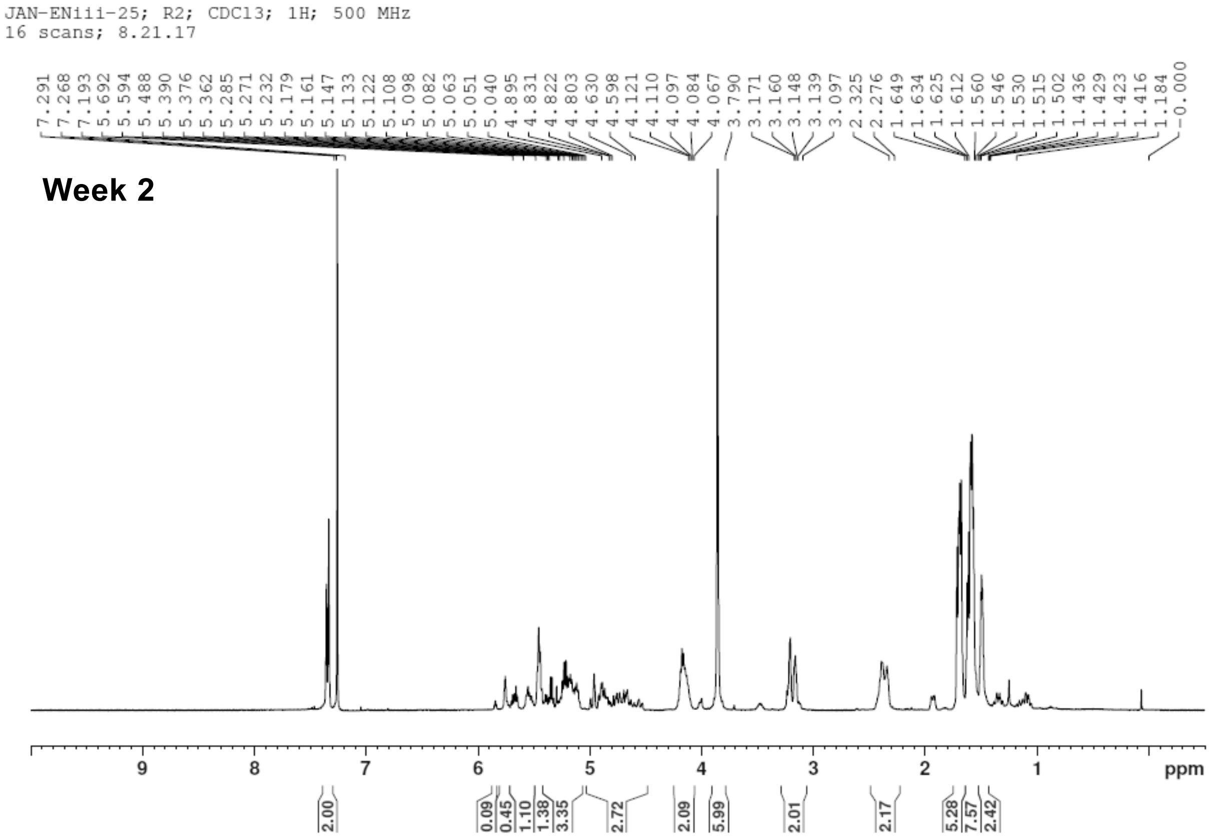
JAN-ENiii-25; R2; CDCl3; 1H; 500 MHz
16 scans; 8.21.17
7.291
7.268
7.193
5.692
5.594
5.488
5.390
5.376
5.362
5.285
5.271
5.232
5.179
5.161
5.147
5.133
5.122
5.108
5.098
5.082
5.063
5.051
5.040
4.895
4.831
4.822
4.803
4.630
4.598
4.121
4.110
4.097
4.084
4.067
3.790
3.171
3.160
3.148
3.139
3.097
2.325
2.276
1.649
1.634
1.625
1.612
1.560
1.546
1.530
1.515
1.502
1.436
1.429
1.423
1.416
1.184
-0.000
Week 2
9
8
7
6
5
4
3
2
1
ppm
2.00
0.09
0.45
1.10
1.38
3.35
2.72
2.09
5.99
2.01
2.17
5.28
7.57
2.42

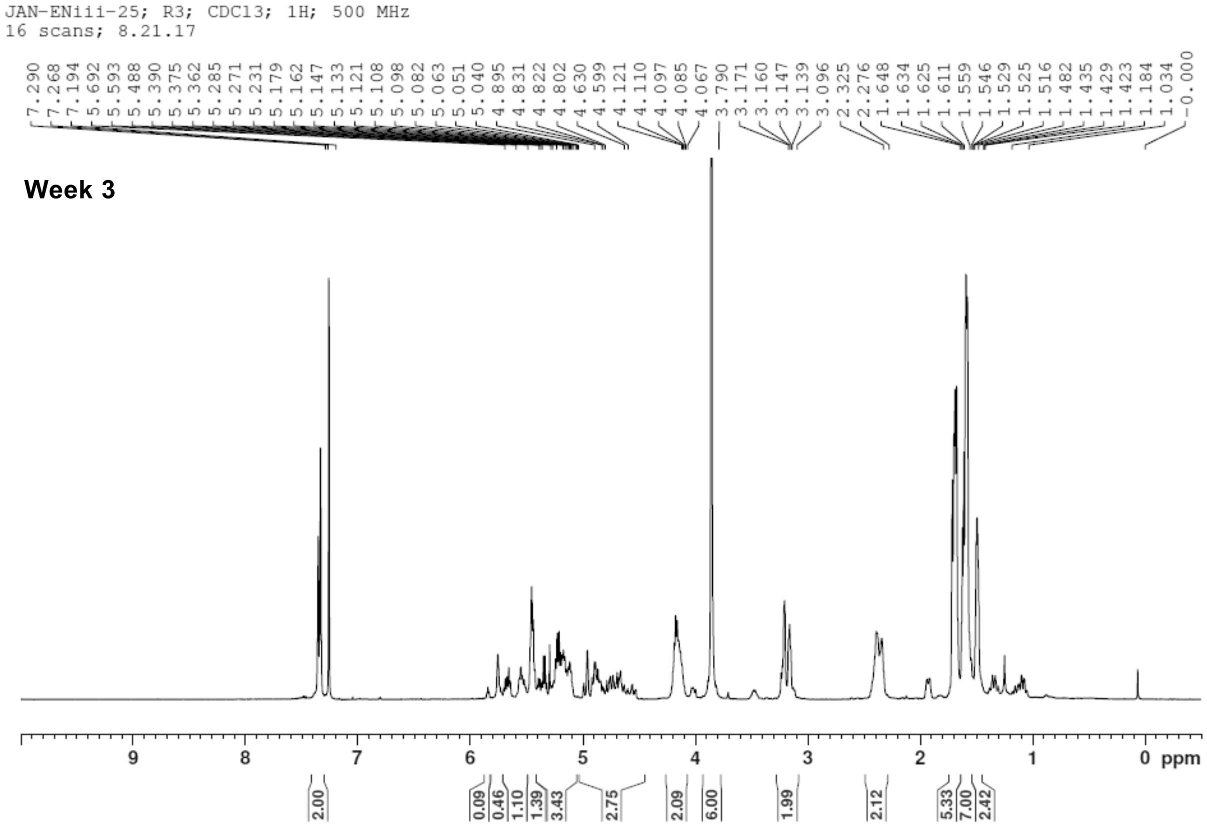
JAN-ENiii-25; R3; CDCl3; 1H; 500 MHz
16 scans; 8.21.17
7.290
7.268
7.194
5.692
5.593
5.488
5.390
5.375
5.362
5.285
5.271
5.231
5.179
5.162
5.147
5.133
5.121
5.108
5.098
5.082
5.063
5.051
5.040
4.895
4.831
4.822
4.802
4.630
4.599
4.121
4.110
4.097
4.085
4.067
3.790
3.171
3.160
3.147
3.139
3.096
2.325
2.276
1.648
1.634
1.625
1.611
1.559
1.546
1.529
1.525
1.516
1.482
1.435
1.429
1.423
1.184
1.034
-0.000
Week 3
9
8
7
6
5
4
3
2
1
0 ppm
2.00
0.09
0.46
1.10
1.39
3.43
2.75
2.09
6.00
1.99
2.12
5.33
7.00
2.42

JAN-ENiii-25; R4; CDCl3; 1H: 500 MHz
16 scans; 8.21.17

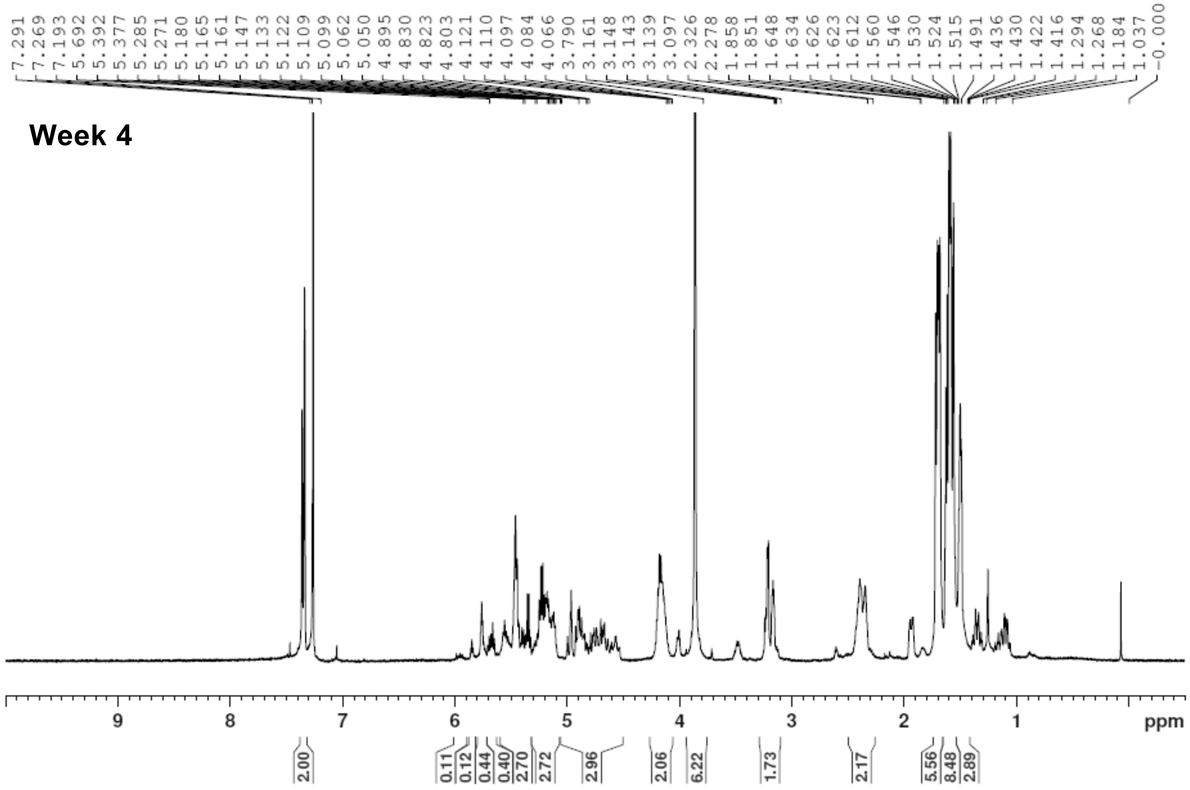

JAN-ENiii-25; R5; CDCl3; 1H; 500 MHz
16 scans; 8.21.17

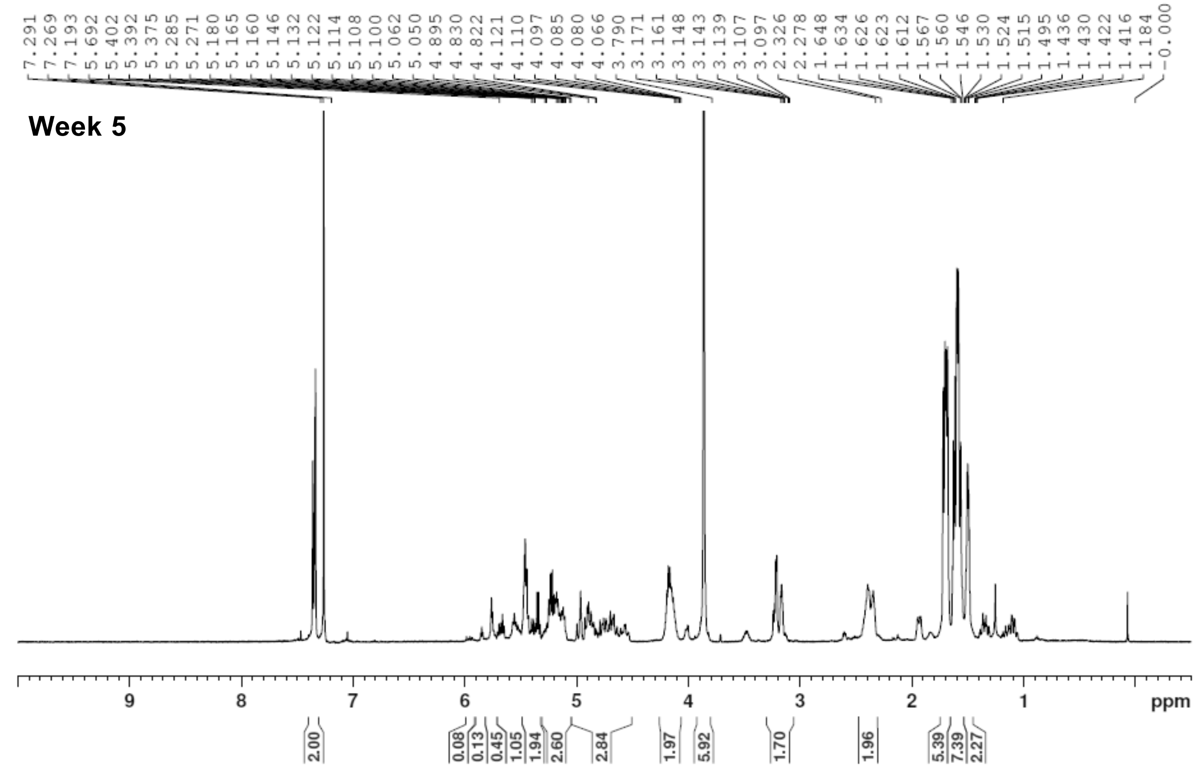

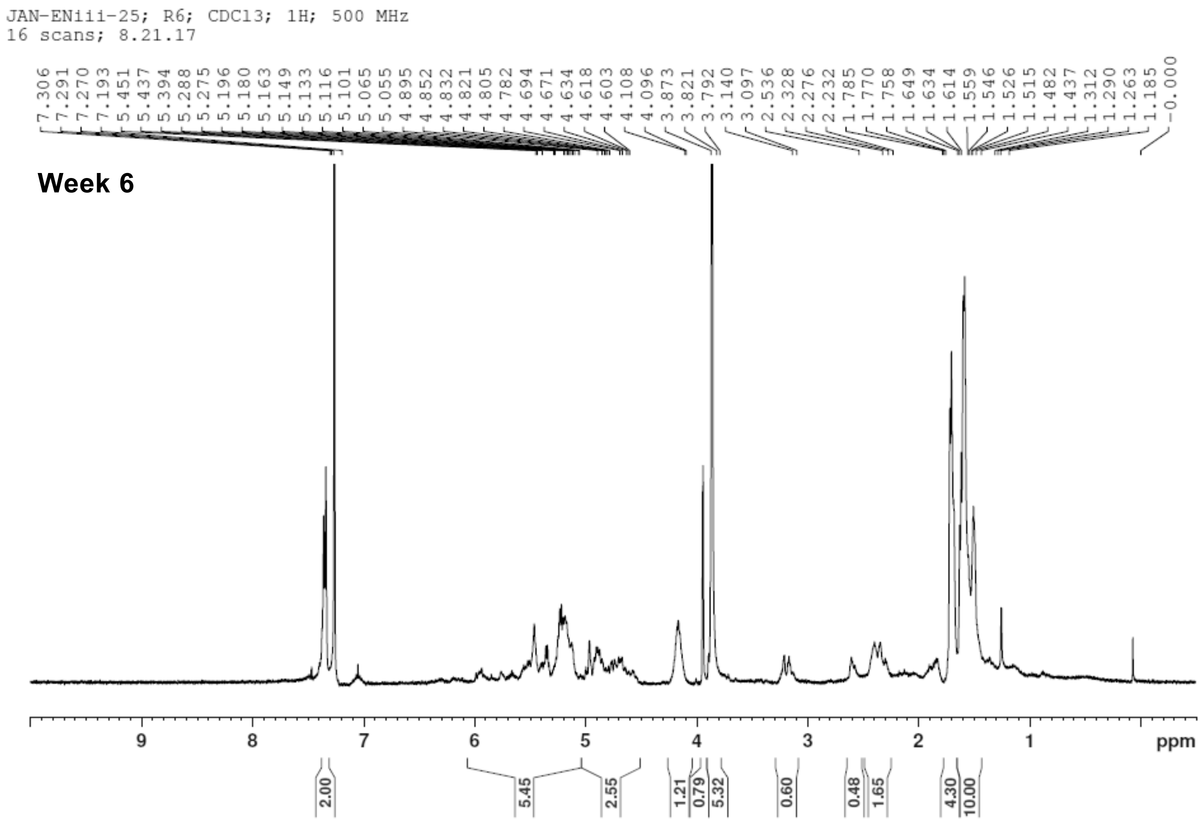
JAN-ENiii-25; R6; CDCl3; 1H; 500 MHz
16 scans; 8.21.17
Week 6
7.306
7.291
7.270
7.193
5.451
5.437
5.394
5.288
5.275
5.196
5.180
5.163
5.149
5.133
5.116
5.101
5.065
5.055
4.895
4.852
4.832
4.821
4.805
4.782
4.694
4.671
4.634
4.618
4.603
4.108
4.096
3.873
3.821
3.792
3.140
3.097
2.536
2.328
2.276
2.232
1.785
1.770
1.758
1.649
1.634
1.614
1.559
1.546
1.526
1.515
1.482
1.437
1.312
1.290
1.263
1.185
-0.000
9
8
7
6
5
4
3
2
1
ppm
2.00
5.45
2.55
1.21
0.79
5.32
0.60
0.48
1.65
4.30
10.00

Initial DSC Thermograms

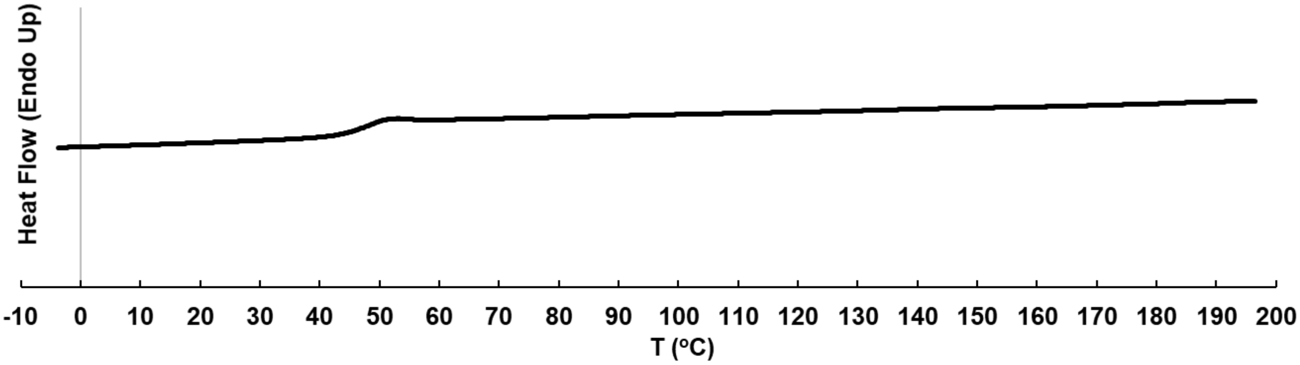

Poly SyLM(L_3G_2)

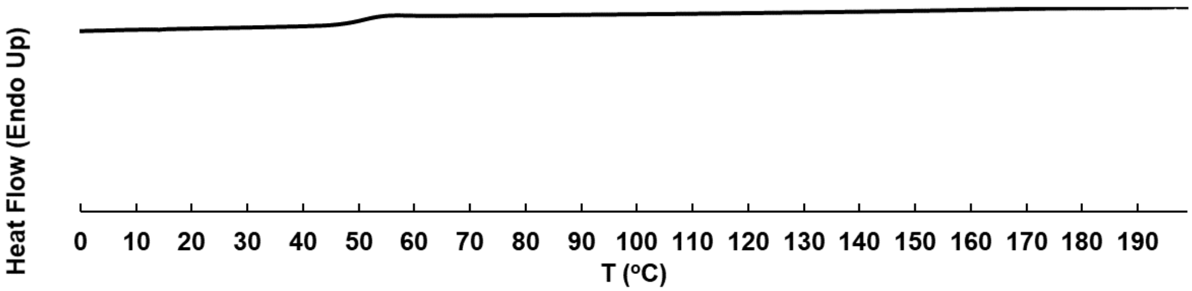

Poly SyLM(LGLGL)

Representative SEC Traces Over the Course of Hydrolysis

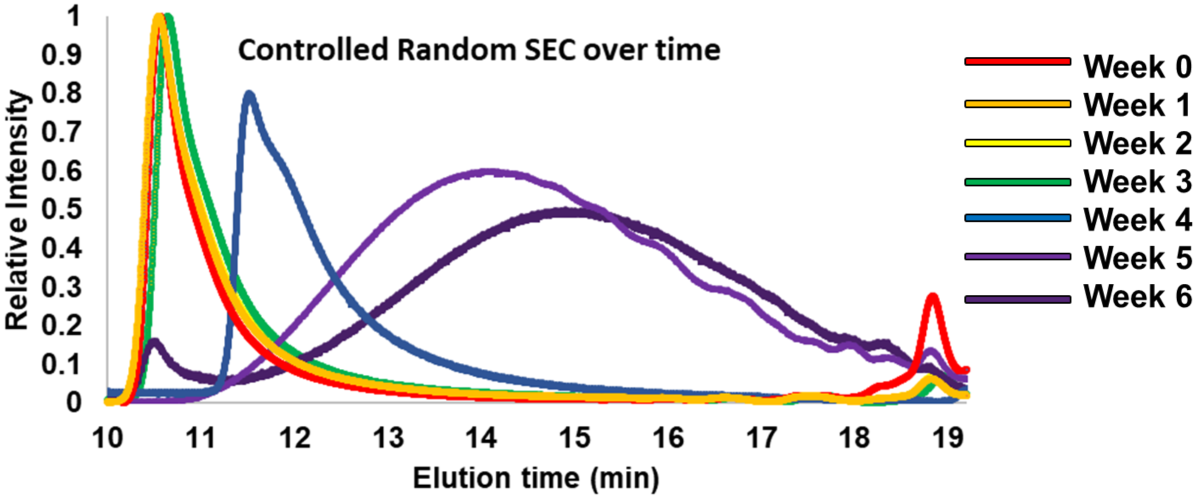

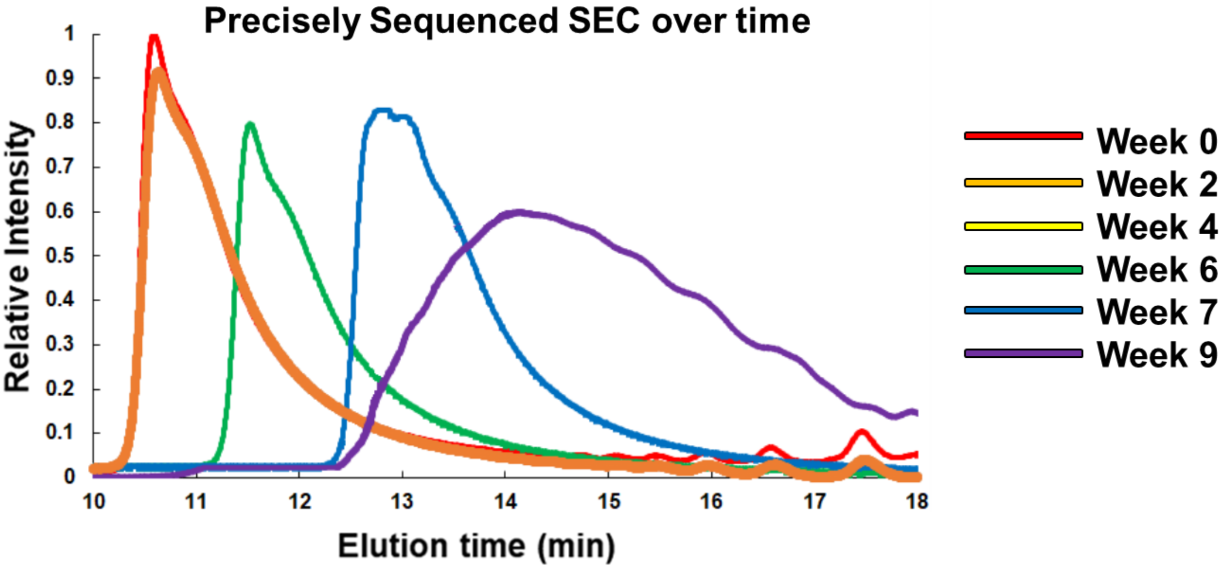

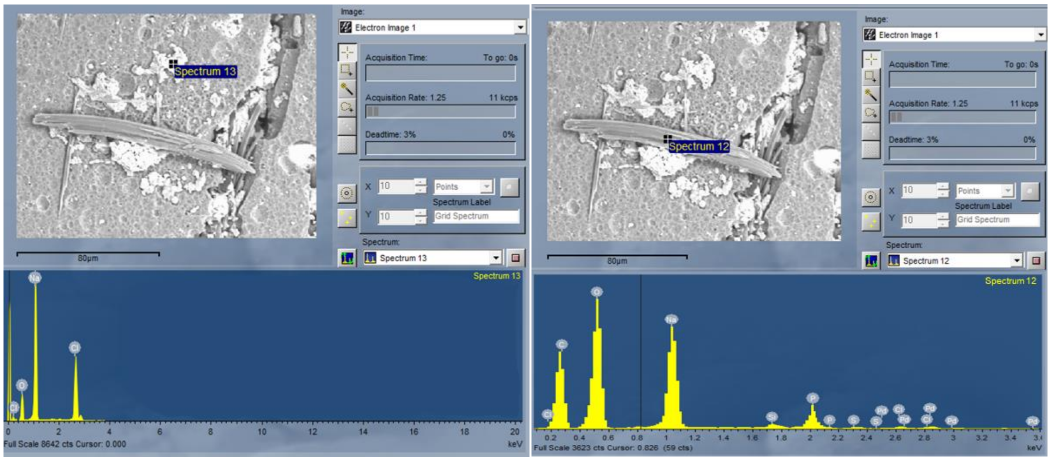

Image: Electron Image 1

Acquisition Time: To go: 0s

Acquisition Rate: 1.25 11 kcps

Deadtime: 3% 0%

X 10 Points

Y 10

Spectrum Label: Grid Spectrum

Spectrum: Spectrum 13

Full Scale 8642 cts Cursor: 0.000

Image: Electron Image 1

Acquisition Time: To go: 0s

Acquisition Rate: 1.25 11 kcps

Deadtime: 3% 0%

X 10 Points

Y 10

Spectrum Label: Grid Spectrum

Spectrum: Spectrum 12

Full Scale 3623 cts Cursor: 0.826 (59 cts)

Spectrum 13
80µm
Spectrum 13
Na
Cl
O
Cl
0
2
4
6
8
10
12
14
16
18
20
keV
Spectrum 12
80µm
Spectrum 12
C
O
Na
Cl
Si
P
P
S
S
Pd
Cl
Pd
Pd
Cl
Pd
Pd
0.2
0.4
0.6
0.8
1
1.2
1.4
1.6
1.8
2
2.2
2.4
2.6
2.8
3
3.2
3.4
keV

Figure 36. EDX characterization of residual buffer salt crystals on the degraded films.

Appendix C: Experimental Spectra and Supporting Data for Chapter 4

Scanning Electron Microscopy Imaging

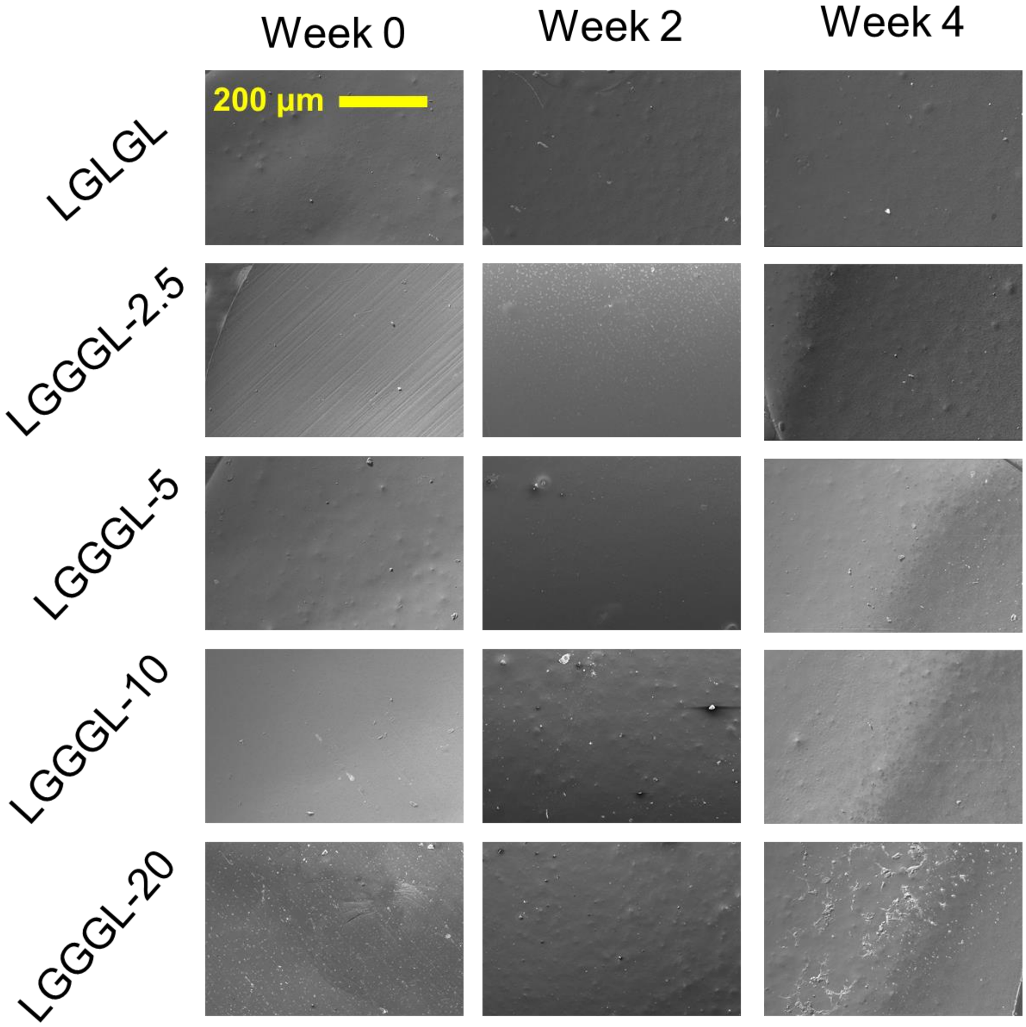
Week 0
Week 2
Week 4
200 µm
LGLGL
LGGGL-2.5
LGGGL-5
LGGGL-10
LGGGL-20

Figure 37. Scanning electron microscopy images (100x) of the films over the course of hydrolysis.

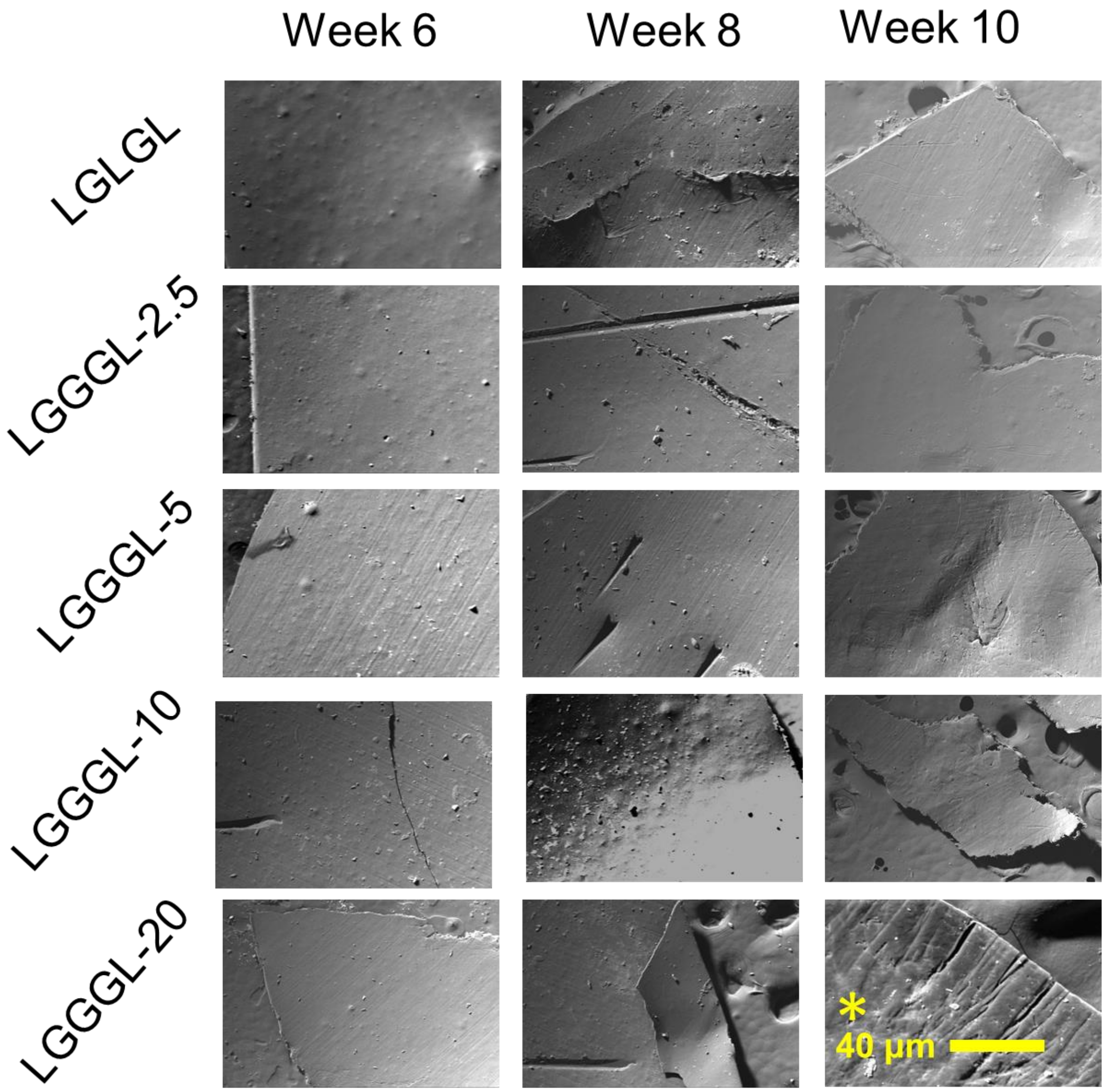
Week 6
Week 8
Week 10
LGLGL
LGGGL-2.5
LGGGL-5
LGGGL-10
LGGGL-20
*
40 µm

Figure 38. Scanning electron microscopy images (100x) of the films over the course of hydrolysis.

The detailed synthesis of **Cyc-SyLMLGLGL** was previously reported.[188]

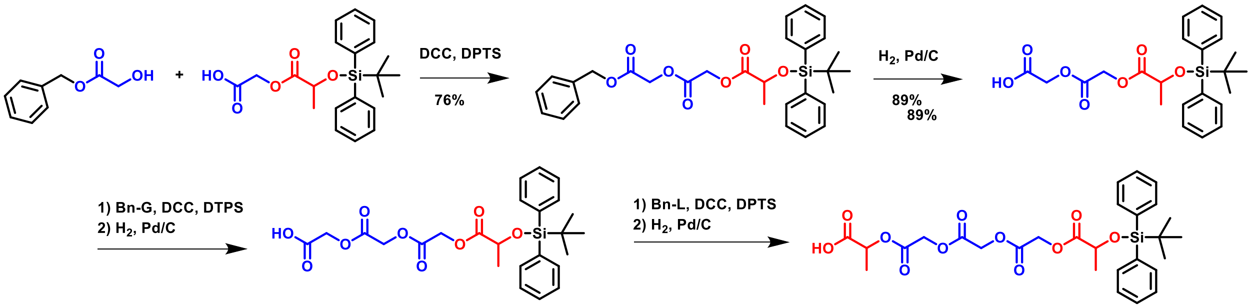
DCC, DPTS
76%
H2, Pd/C
89%
89%
1) Bn-G, DCC, DTPS
2) H2, Pd/C
1) Bn-L, DCC, DPTS
2) H2, Pd/C

Scheme 9. Synthetic steps toward LGGGL-Si.

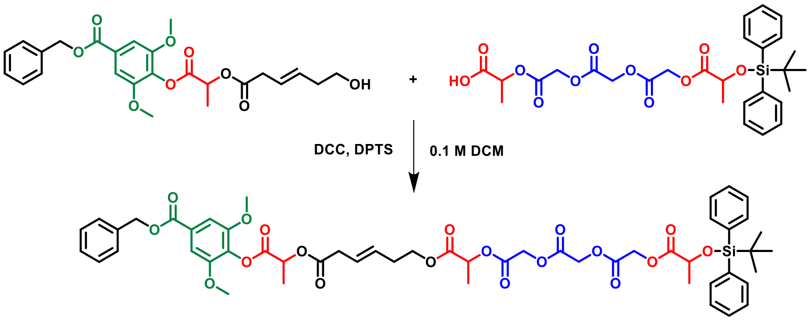
DCC, DPTS
0.1 M DCM

Scheme 10. Steglich esterification to Bn-SyLMLGGGL-Si.

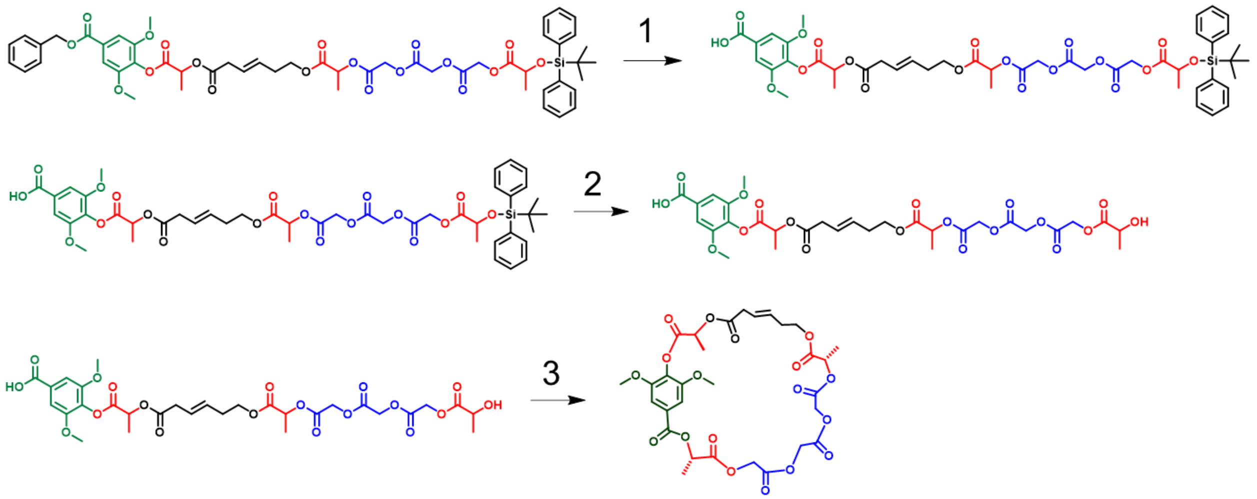

1:SiEt$_3$H, NEt$_3$, PdOAc, 0.3 M DCM70%

2:TBAF, AcOH, 0.1 M THF50%

3:DCC, DPTS, 0.03 M, 16 hr. addition of SM, 60°C,65%

Scheme 11. Benzyl and silyl deprotections to yield SyLMLGGGL and subsequent macrolactonization reaction to prepare Cyc-SyLMLGGGL.

Experimental Spectra

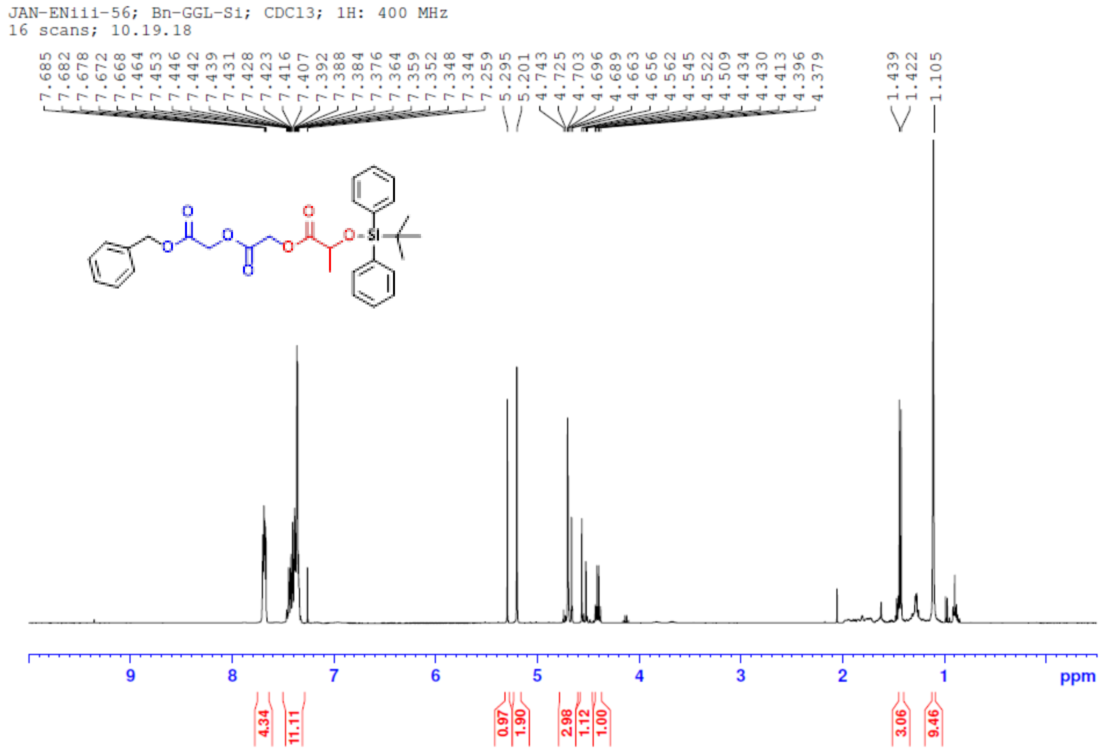

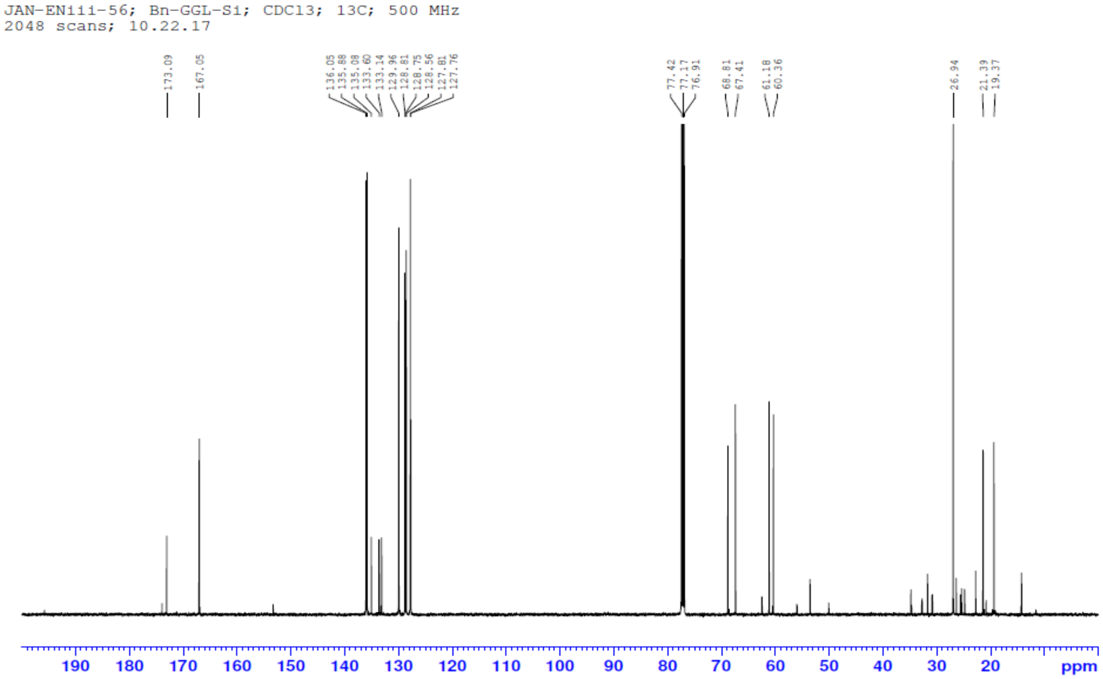

JAN-ENiii-56ii; GGL-Si; CDCl3; 1H: 500 MHz
16 scans; 10.23.17

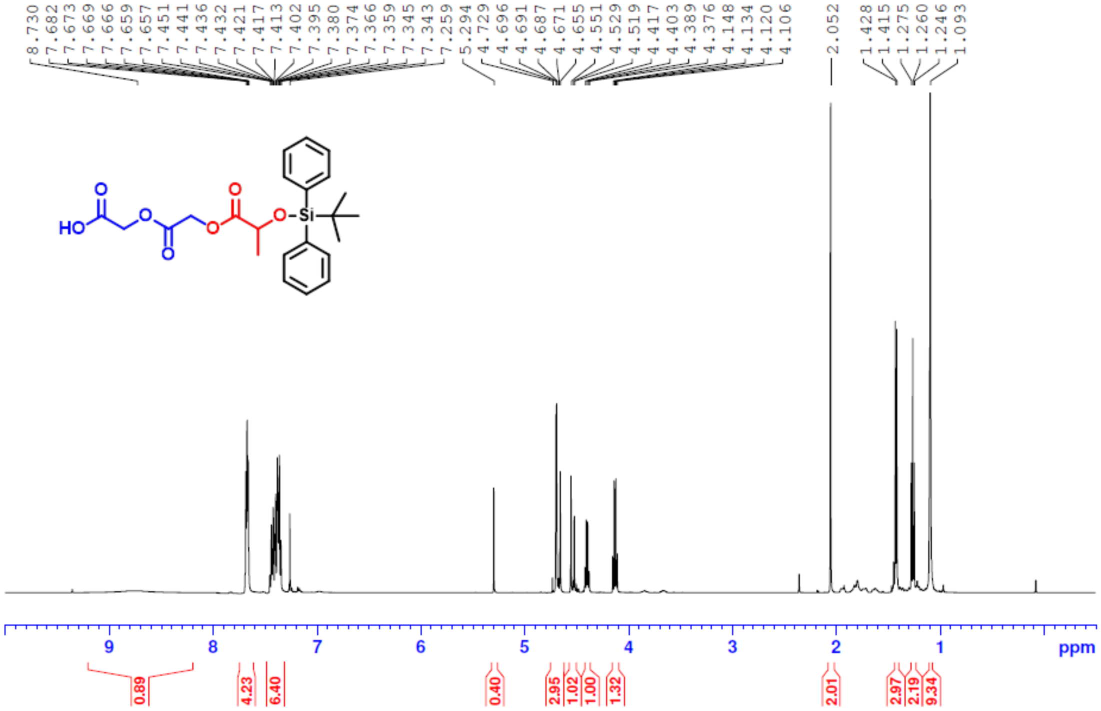

JAN-ENiii-56ii; GGL-Si; CDCl3; 13C: 500 MHz
16 scans; 10.23.17

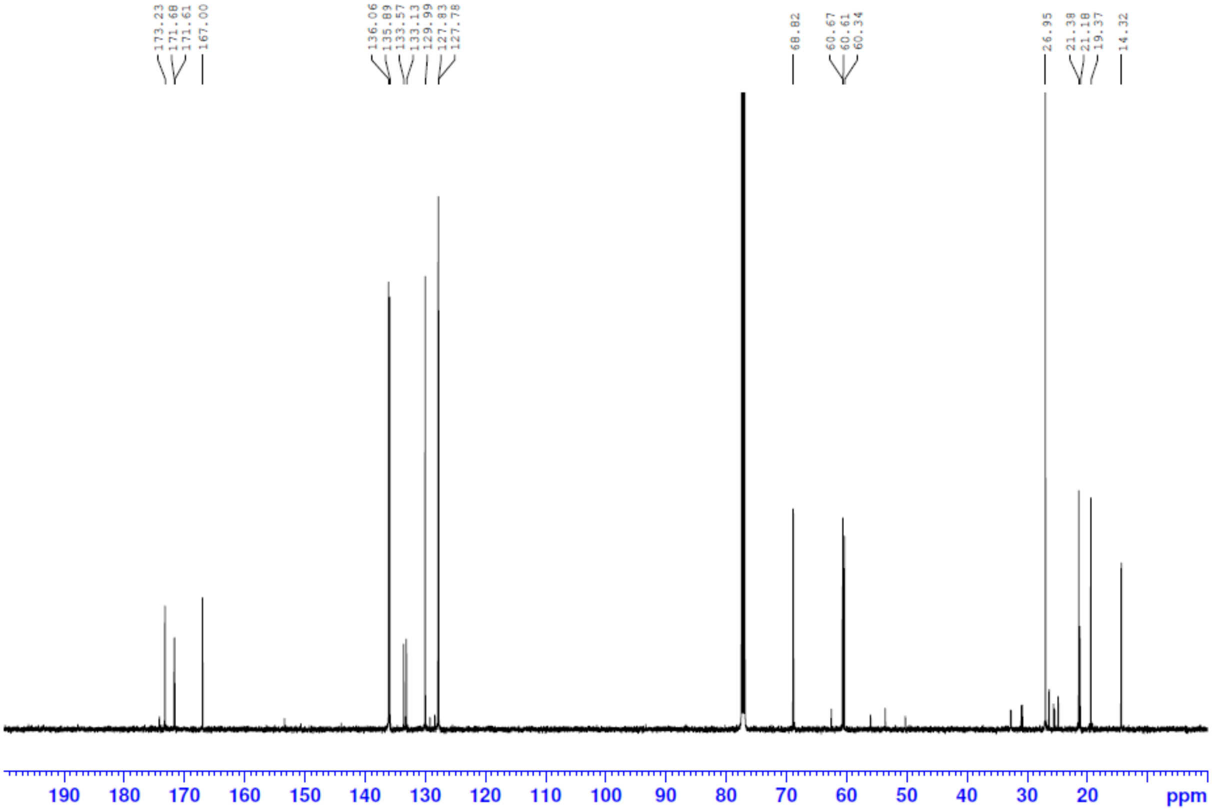

JAN-ENiii-57; Bn-GGGL-Si; CDCl3; 1H; 500 MHz
16 scans; 10.24.17

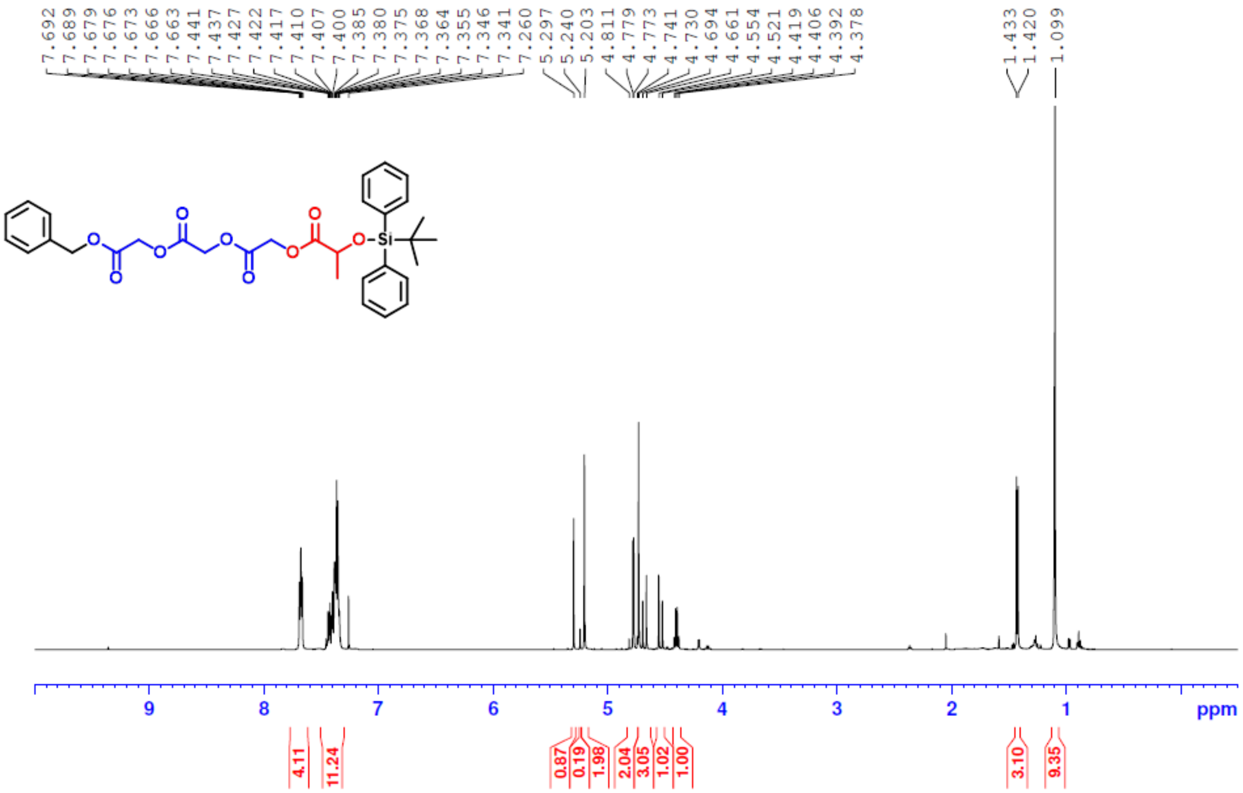

JAN-ENiii-57; Bn-GGGL-Si; CDCl3; 13C;
500 MHz; 2048 scans; 10.24.17

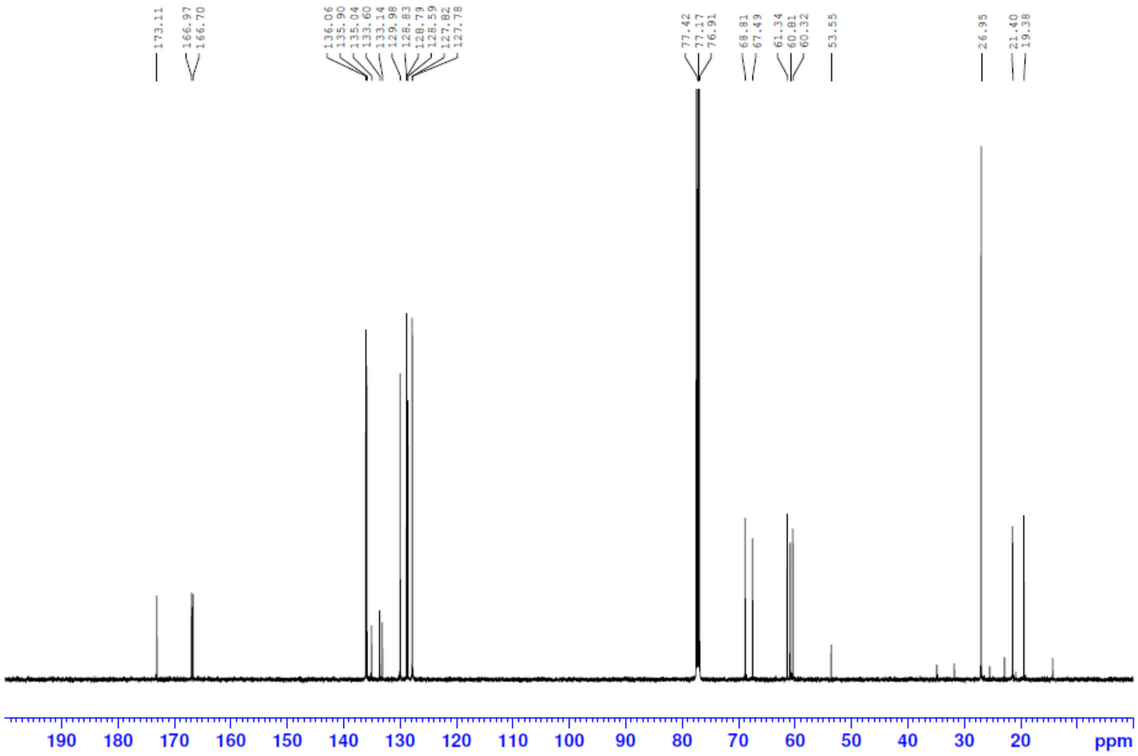

JAN-ENiii-58; GGGL-Si; CDCl3; 1H; 500 MHz
16 scans; 10.25.17

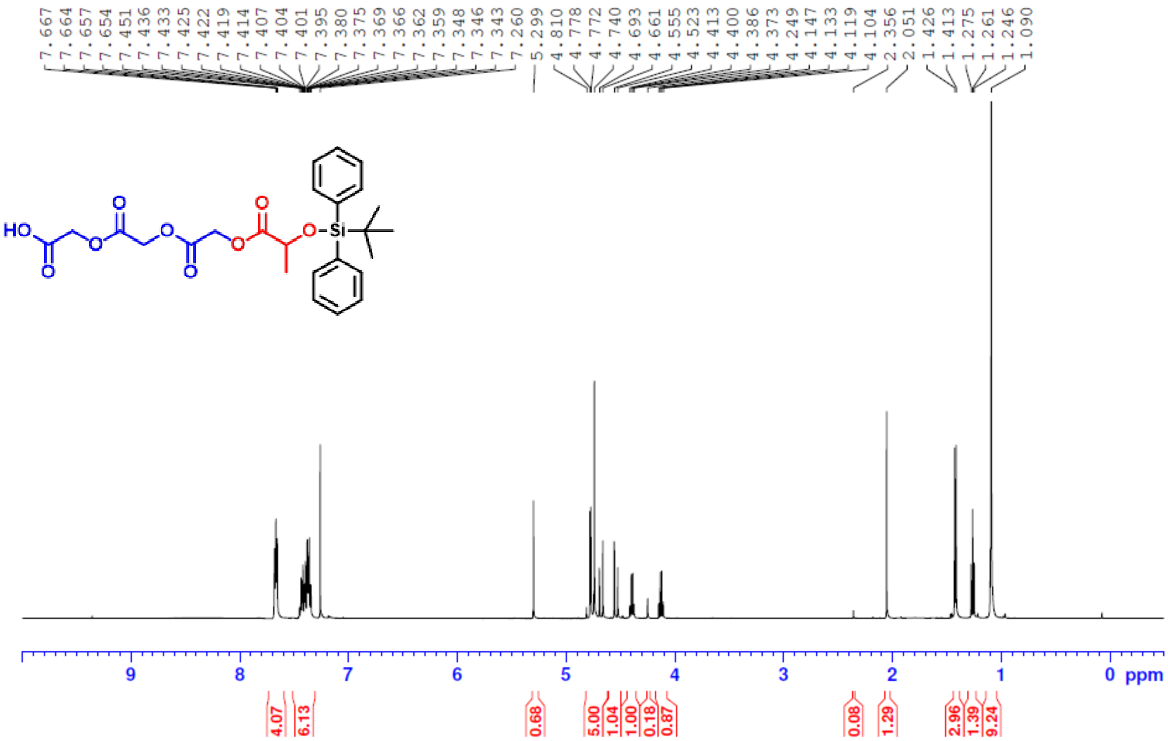

JAN-ENiii-58; GGGL-Si; CDCl3; 13C; 500 MHz
2048 scans; 10.25.17

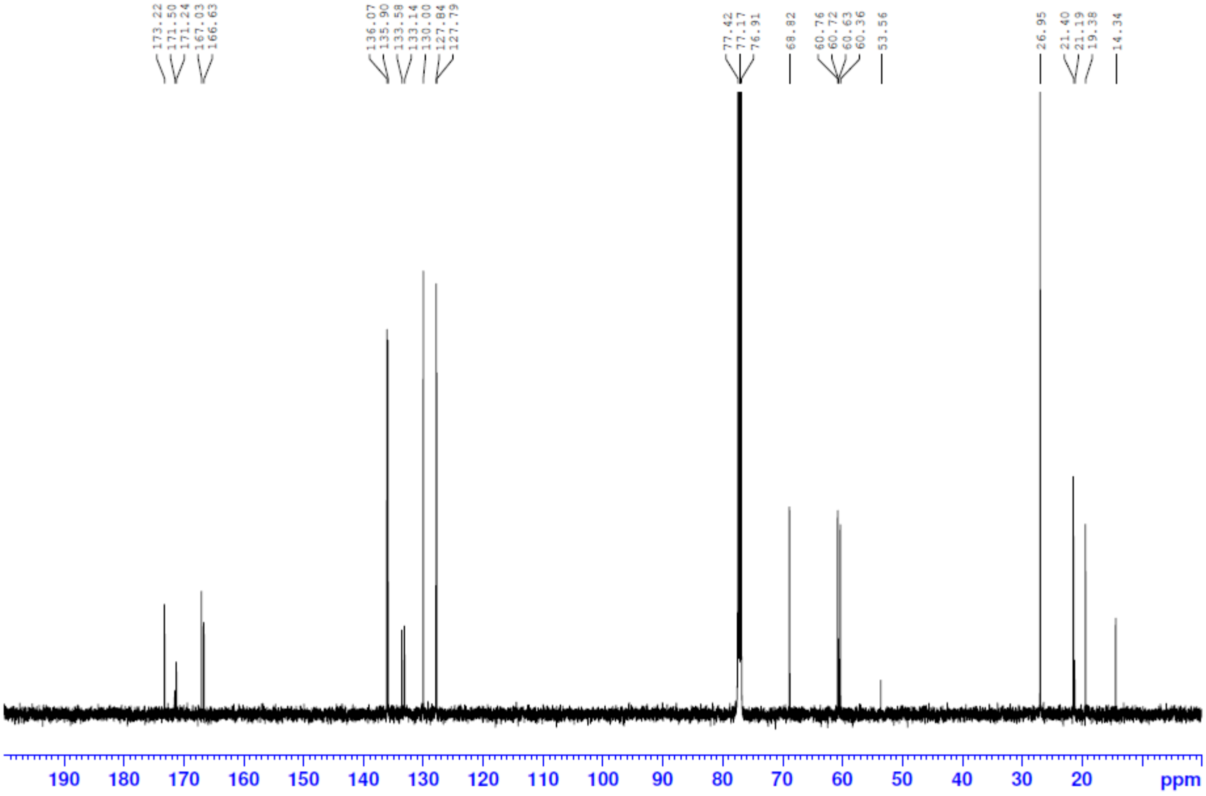

JAN-ENiii-59; Bn-LGGGL-Si; CDCl3; 1H; 500MHz
16 scans; 10.27.17

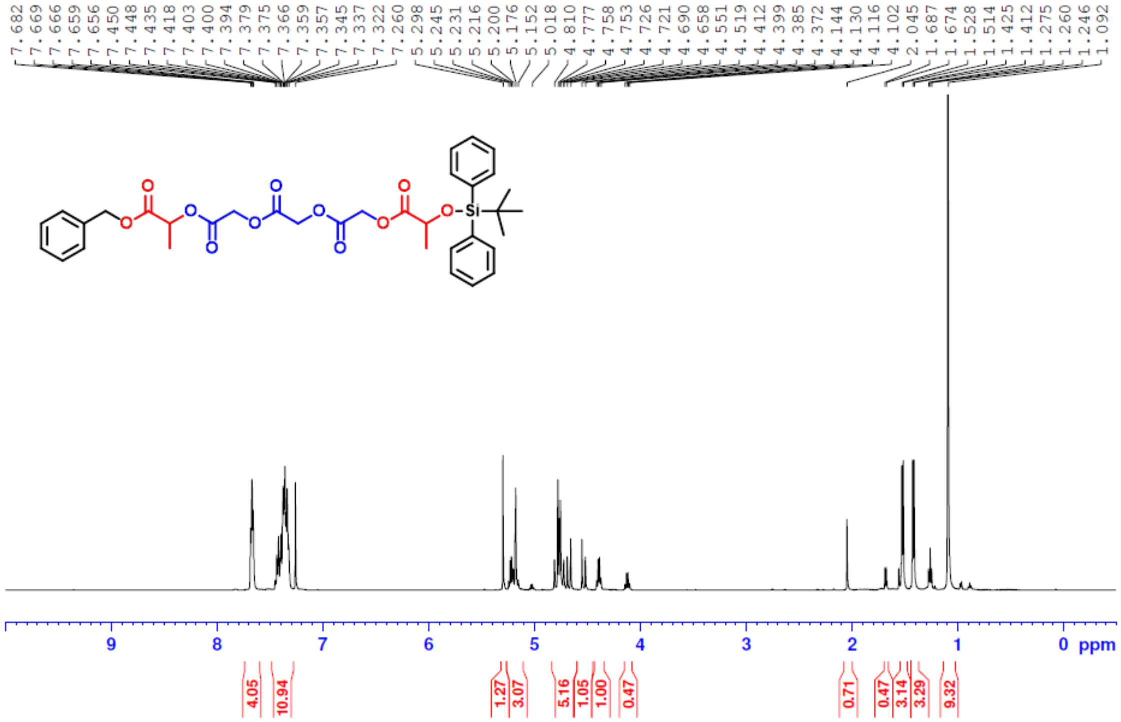

JAN-ENiii-59; Bn-LGGGL-Si; CDCl3; 13C;
500MHz; 2048 scans; 10.27.17

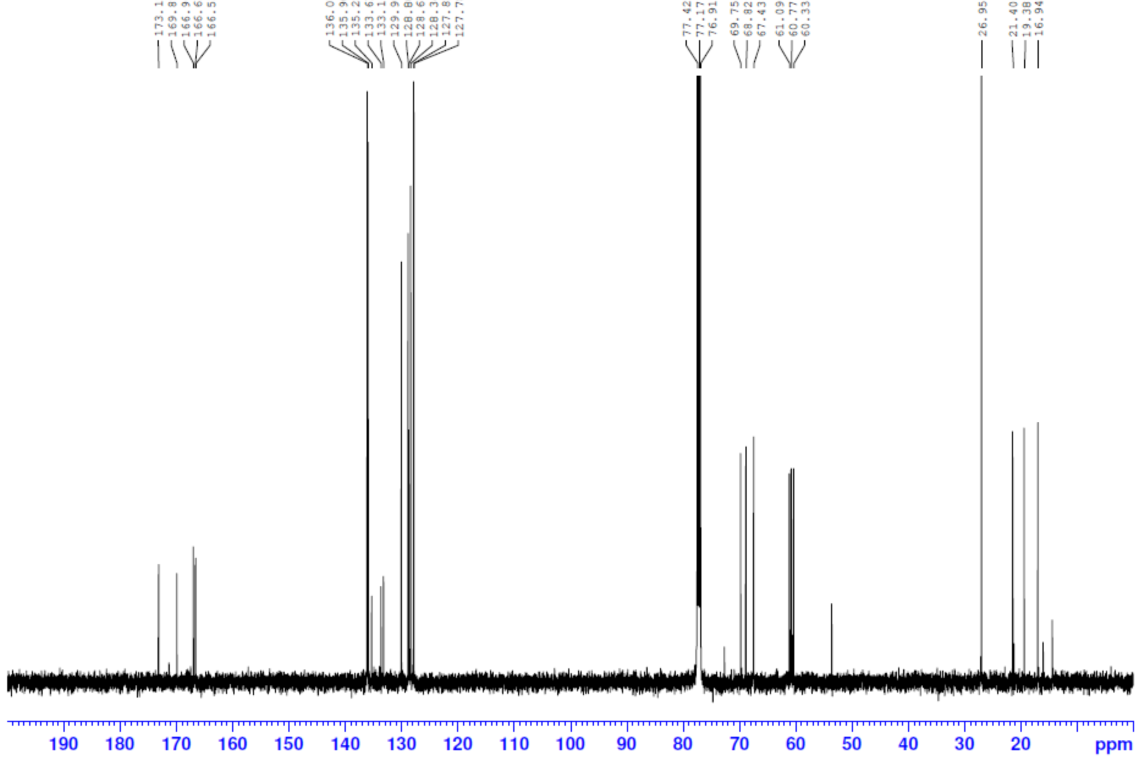

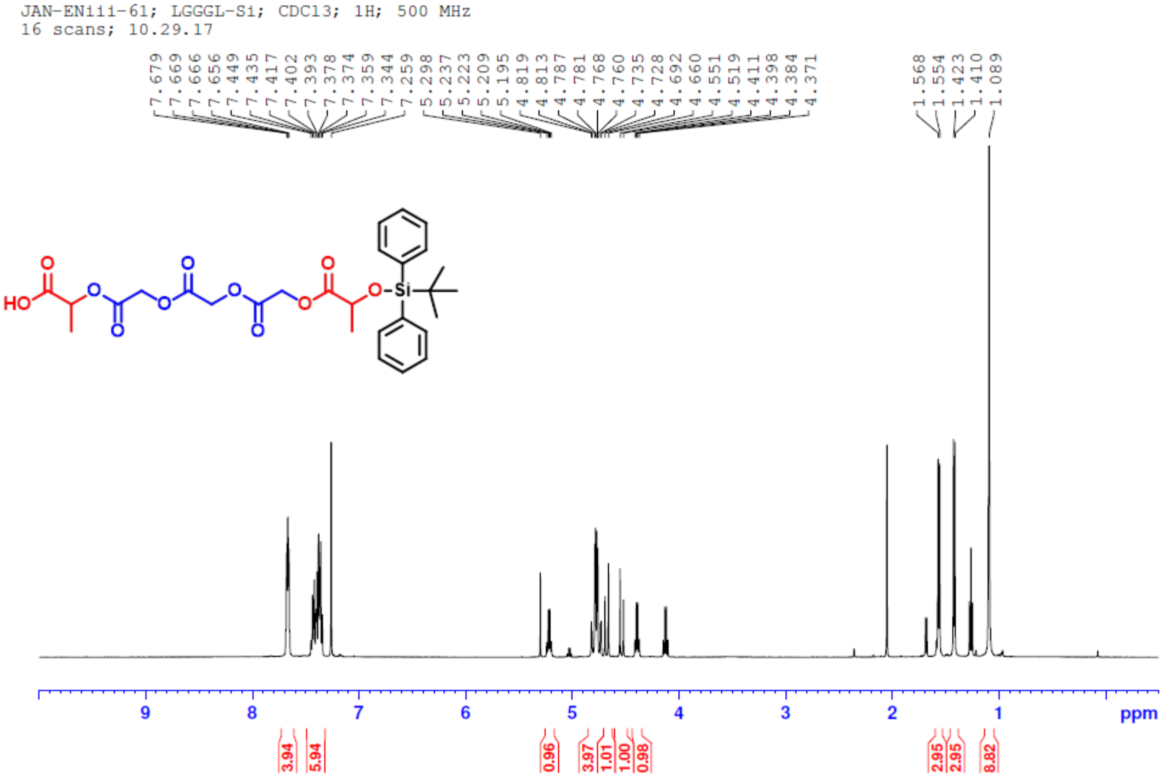
JAN-ENiii-61; LGGGL-Si; CDCl3; 1H; 500 MHz
16 scans; 10.29.17
7.679
7.669
7.666
7.656
7.449
7.435
7.417
7.402
7.393
7.378
7.374
7.359
7.344
7.259
5.298
5.237
5.223
5.209
5.195
4.819
4.813
4.787
4.781
4.768
4.760
4.735
4.728
4.692
4.660
4.551
4.519
4.411
4.398
4.384
4.371
1.568
1.554
1.423
1.410
1.089
HO
O
Si
9
8
7
6
5
4
3
2
1
ppm
3.94
5.94
0.96
3.97
1.01
1.00
0.98
2.95
2.95
8.82

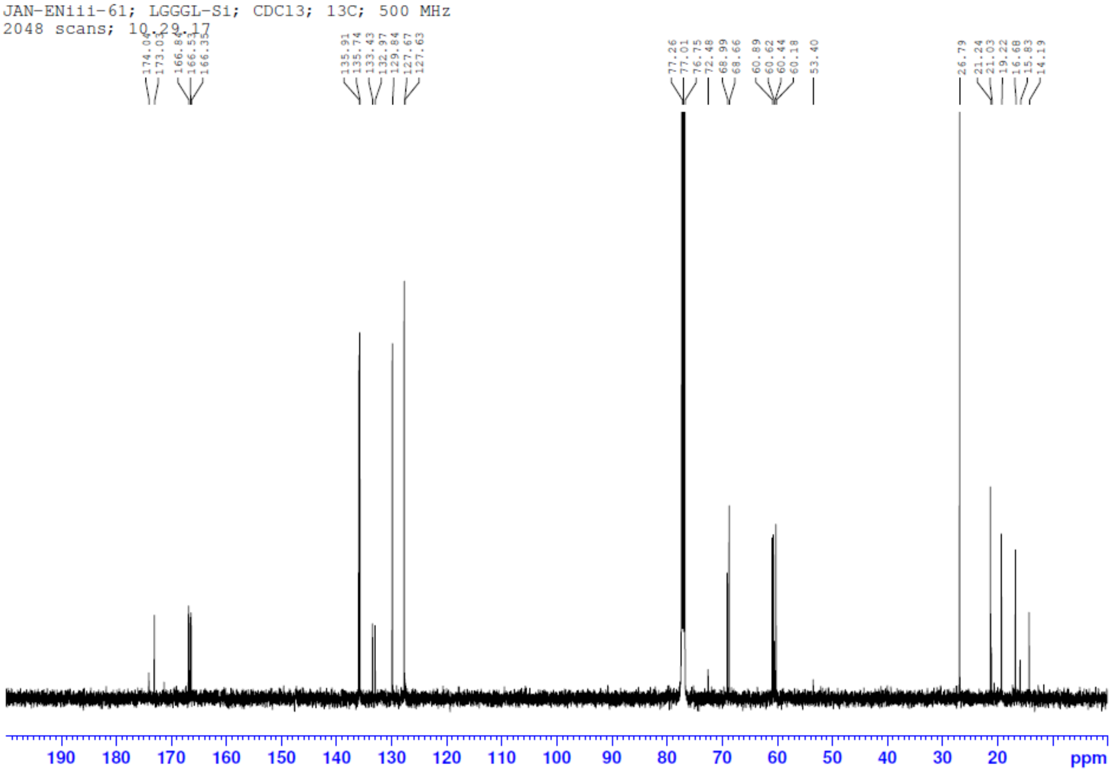
JAN-ENiii-61; LGGGL-Si; CDCl3; 13C; 500 MHz
2048 scans; 10.29.17
174.04
173.03
166.84
166.53
166.35
135.91
135.74
133.43
132.97
129.84
127.67
127.63
77.26
77.01
76.75
72.48
68.99
68.66
60.89
60.62
60.44
60.18
53.40
26.79
21.24
21.03
19.22
16.68
15.83
14.19
190
180
170
160
150
140
130
120
110
100
90
80
70
60
50
40
30
20
ppm

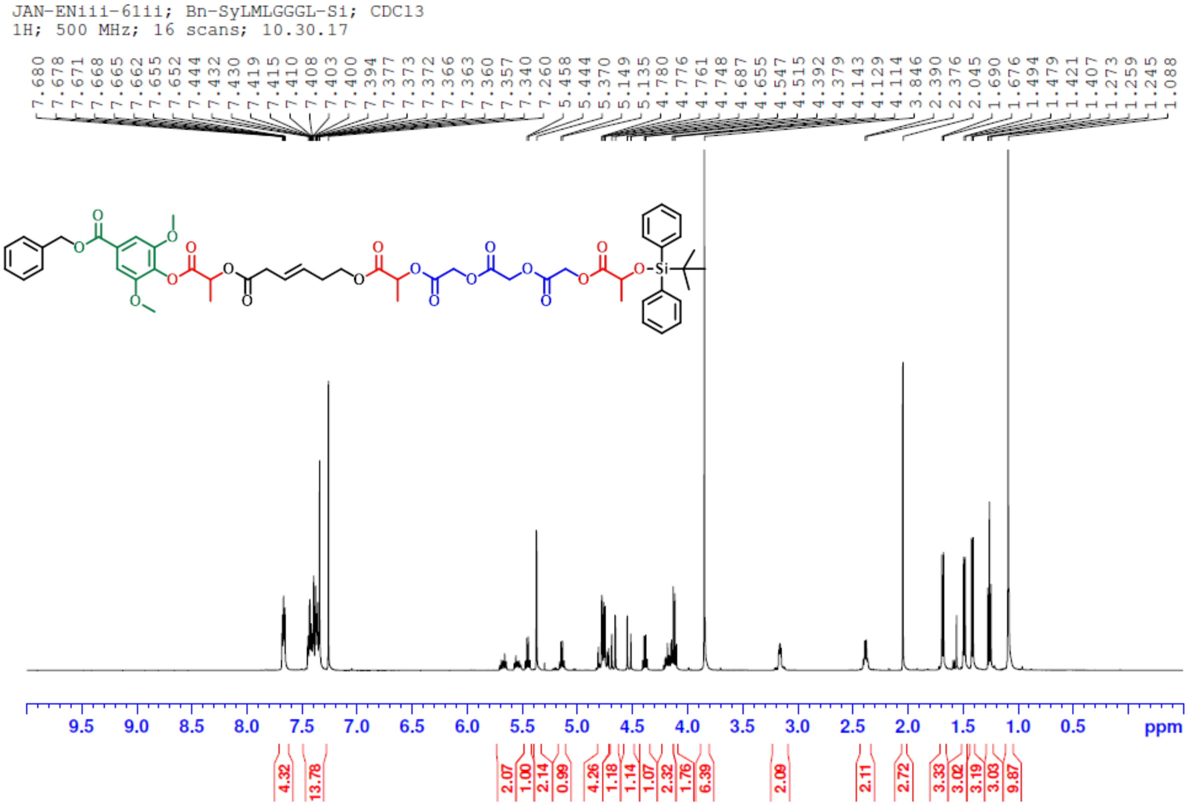
JAN-ENiii-61iii; Bn-SyLMLGGGL-Si; CDCl3
1H; 500 MHz; 16 scans; 10.30.17
7.680 7.678 7.671 7.668 7.665 7.662 7.655 7.652 7.444 7.432 7.430 7.419 7.415 7.410 7.408 7.403 7.400 7.394 7.377 7.373 7.372 7.366 7.363 7.360 7.357 7.340 7.260 5.458 5.444 5.370 5.149 5.135 4.780 4.776 4.761 4.748 4.687 4.655 4.547 4.515 4.392 4.379 4.143 4.129 4.114 3.846 2.390 2.376 2.045 1.690 1.676 1.494 1.479 1.421 1.407 1.273 1.259 1.245 1.088
O
Si
9.5 9.0 8.5 8.0 7.5 7.0 6.5 6.0 5.5 5.0 4.5 4.0 3.5 3.0 2.5 2.0 1.5 1.0 0.5 ppm
4.32 13.78 2.07 1.00 2.14 0.99 4.26 1.18 1.14 1.07 2.32 1.76 6.39 2.09 2.11 2.72 3.33 3.02 3.19 3.03 9.87

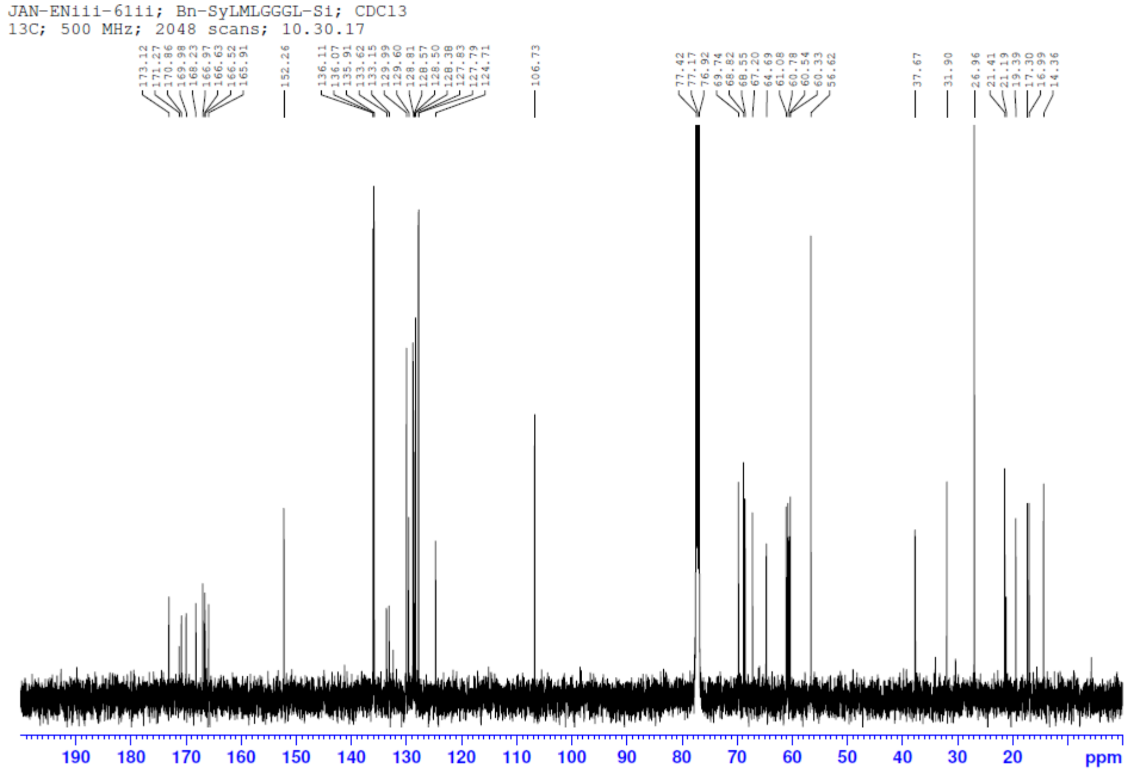
JAN-ENiii-61iii; Bn-SyLMLGGGL-Si; CDCl3
13C; 500 MHz; 2048 scans; 10.30.17
173.12 171.27 170.86 169.98 168.23 166.97 166.63 166.52 165.91 152.26 136.11 136.07 135.91 133.62 133.15 129.99 129.60 128.81 128.57 128.50 128.38 127.83 127.79 124.71 106.73 77.42 77.17 76.92 69.74 68.82 68.55 67.20 64.69 61.08 60.78 60.54 60.33 56.62 37.67 31.90 26.96 21.41 21.19 19.39 17.30 16.99 14.36
190 180 170 160 150 140 130 120 110 100 90 80 70 60 50 40 30 20 ppm

JAN-ENiii-62; SyLMLGGGL-Si; CDCl3; 1H;
500 MHz; 16 scans; 10.31.17

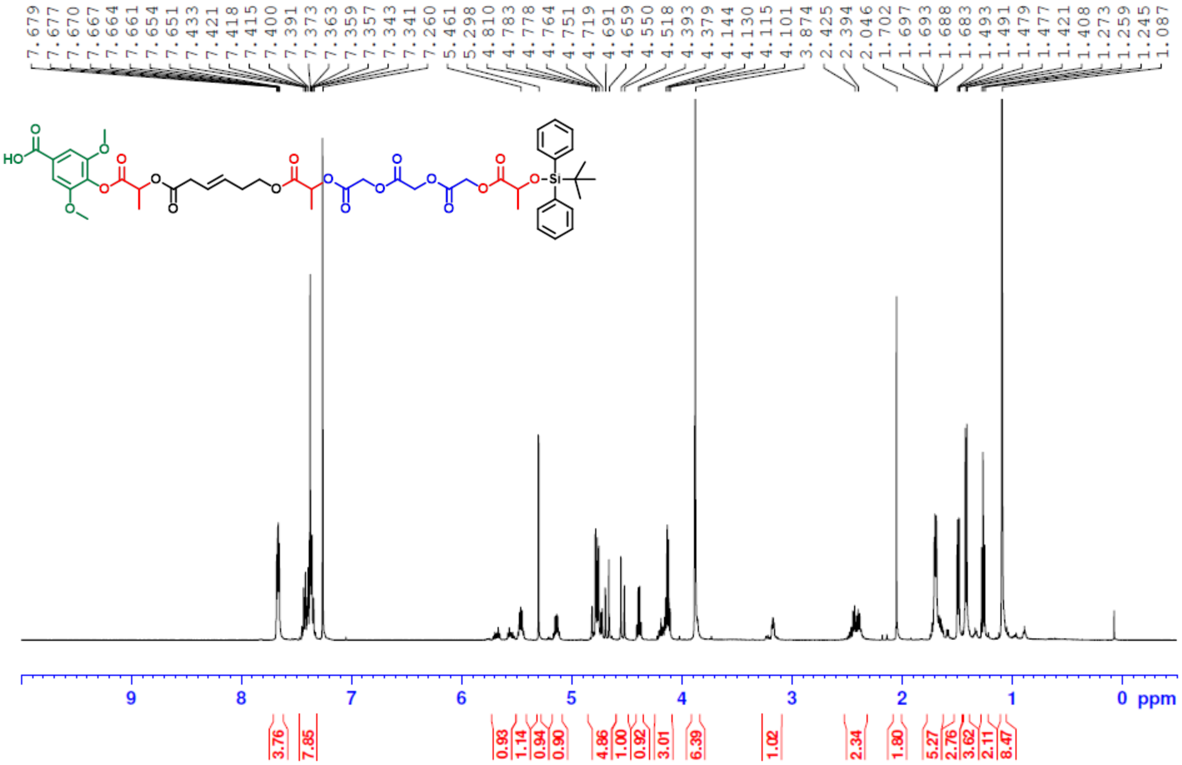

JAN-ENiii-62; SyLMLGGGL-Si; CDCl3; 13C:
500 MHz; 2048 scans; 11.3.17

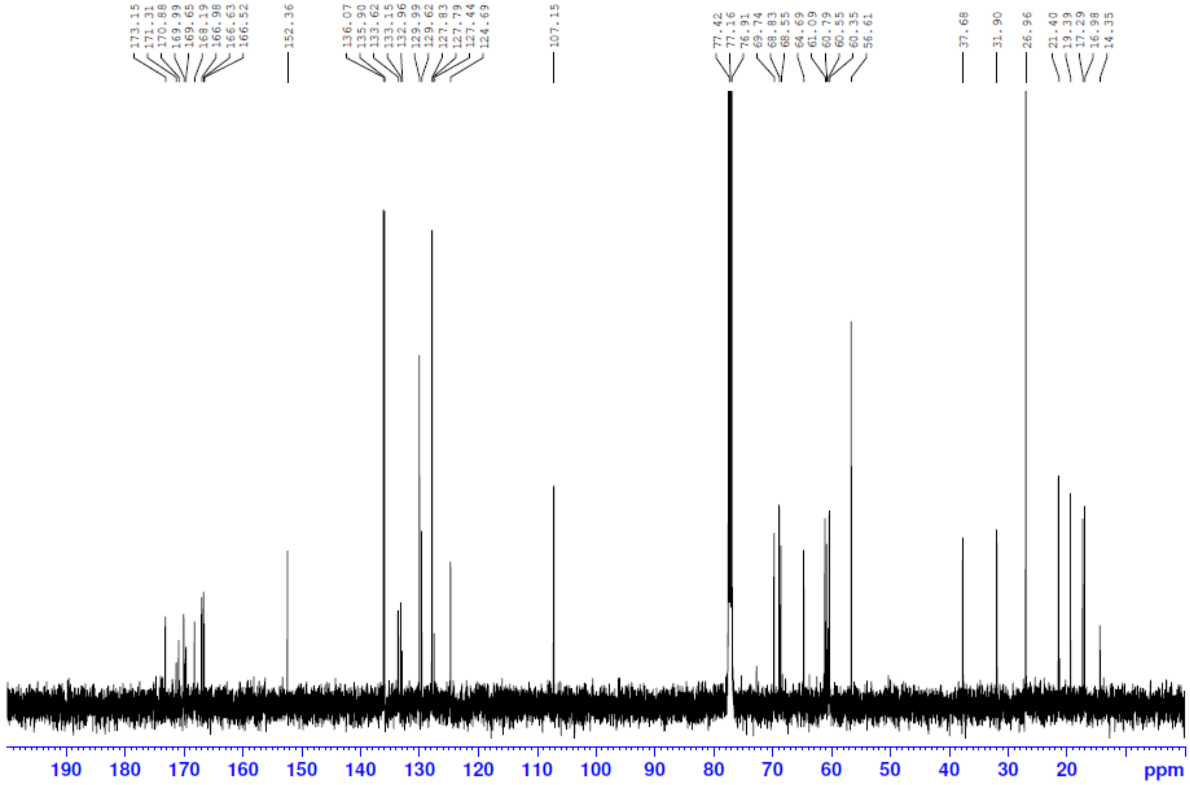

JAN-ENiii-63; SyLMLGGGL; CDCl3; 1H: 500 MHz
16 scans; 11.6.17

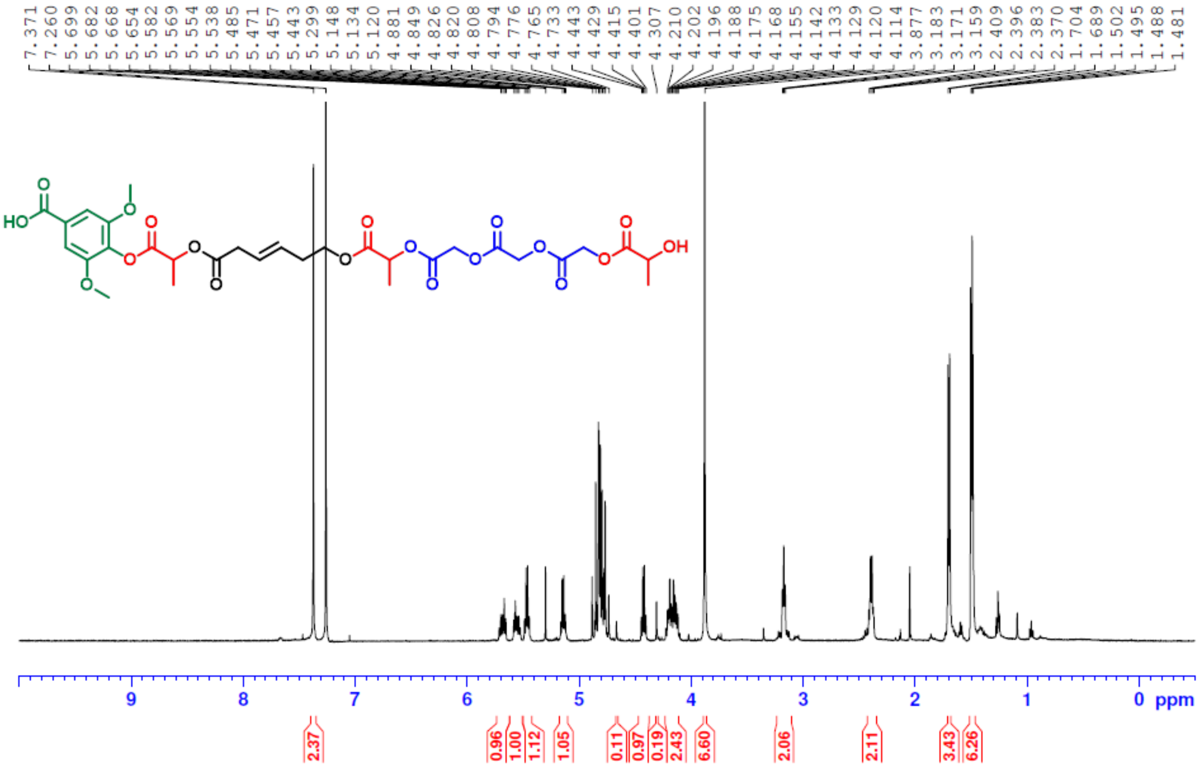

JAN-ENiii-63; SyLMLGGGL; CDCl3; 13C:
500 MHz; 4096 scans; 11.6.17

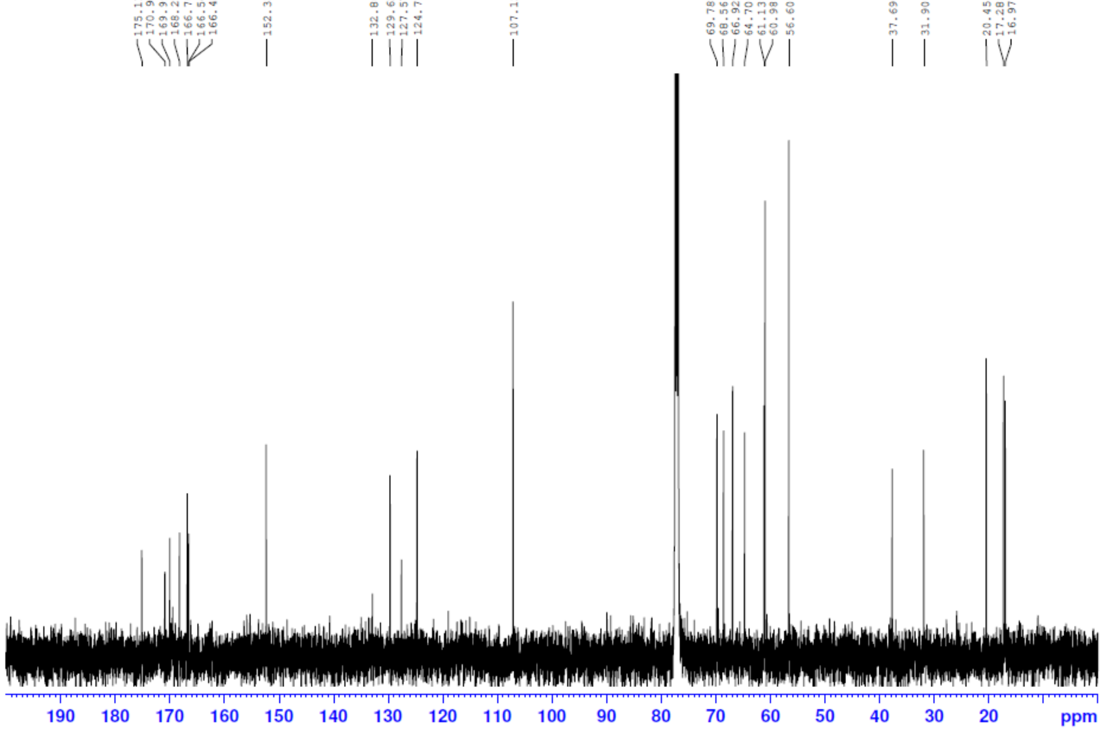

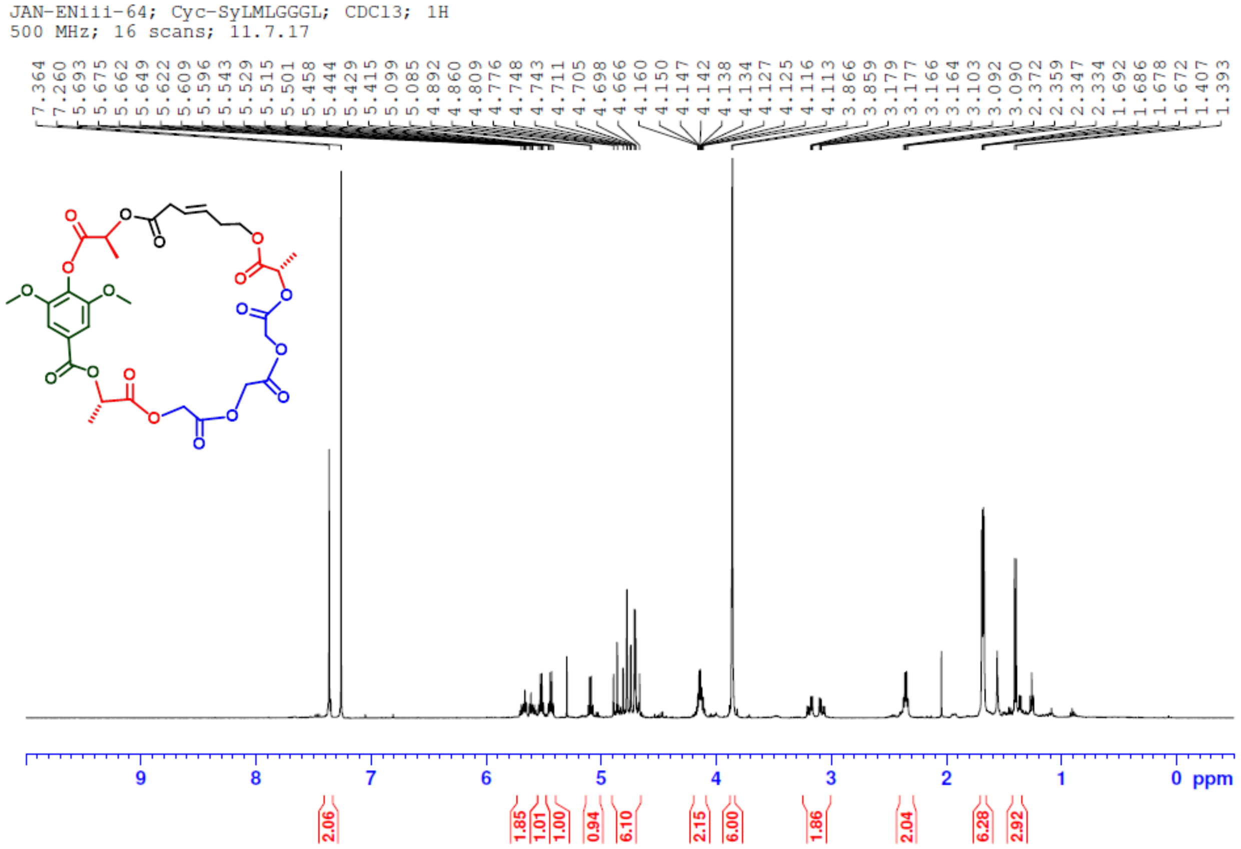
JAN-ENiii-64; Cyc-SyLMLGGGL; CDCl3; 1H
500 MHz; 16 scans; 11.7.17
7.364 7.260 5.693 5.675 5.662 5.649 5.622 5.609 5.596 5.543 5.529 5.515 5.501 5.458 5.444 5.429 5.415 5.099 5.085 4.892 4.860 4.809 4.776 4.748 4.743 4.711 4.705 4.698 4.666 4.160 4.150 4.147 4.142 4.138 4.134 4.127 4.125 4.116 4.113 3.866 3.859 3.179 3.177 3.166 3.164 3.103 3.092 3.090 2.372 2.359 2.347 2.334 1.692 1.686 1.678 1.672 1.407 1.393
9 8 7 6 5 4 3 2 1 0 ppm
2.06 1.85 1.01 1.00 0.94 6.10 2.15 6.00 1.86 2.04 6.28 2.92

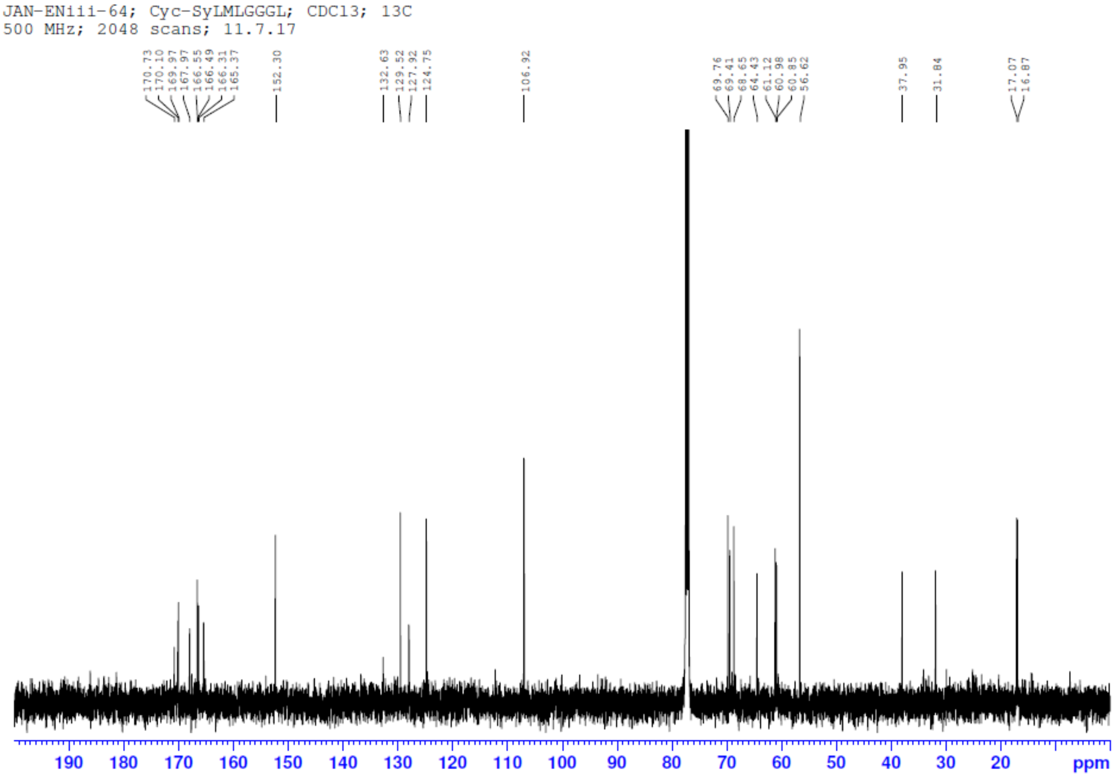
JAN-ENiii-64; Cyc-SyLMLGGGL; CDCl3; 13C
500 MHz; 2048 scans; 11.7.17
170.73 170.10 169.97 167.97 166.55 166.49 166.31 165.37 152.30 132.63 129.52 127.92 124.75 106.92 69.76 69.41 68.65 64.43 61.12 60.98 60.85 56.62 37.95 31.84 17.07 16.87
190 180 170 160 150 140 130 120 110 100 90 80 70 60 50 40 30 20 ppm

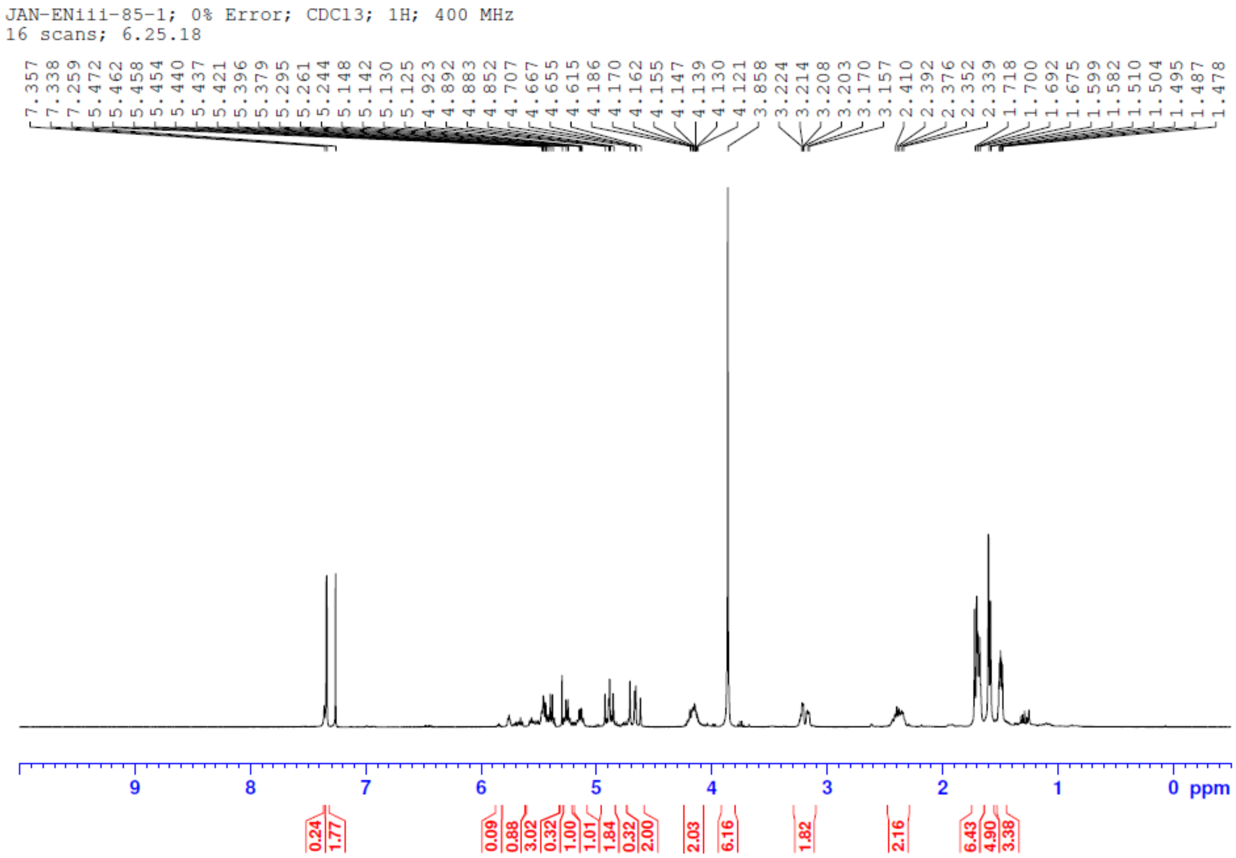
JAN-ENiii-85-1; 0% Error; CDCl3; 1H; 400 MHz
16 scans; 6.25.18
7.357
7.338
7.259
5.472
5.462
5.458
5.454
5.440
5.437
5.421
5.396
5.379
5.295
5.261
5.244
5.148
5.142
5.130
5.125
4.923
4.892
4.883
4.852
4.707
4.667
4.655
4.615
4.186
4.170
4.162
4.155
4.147
4.139
4.130
4.121
3.858
3.224
3.214
3.208
3.203
3.170
3.157
2.410
2.392
2.376
2.352
2.339
1.718
1.700
1.692
1.675
1.599
1.582
1.510
1.504
1.495
1.487
1.478
9
8
7
6
5
4
3
2
1
0 ppm
0.24
1.77
0.09
0.88
3.02
0.32
1.00
1.01
1.84
0.32
2.00
2.03
6.16
1.82
2.16
6.43
4.90
3.38

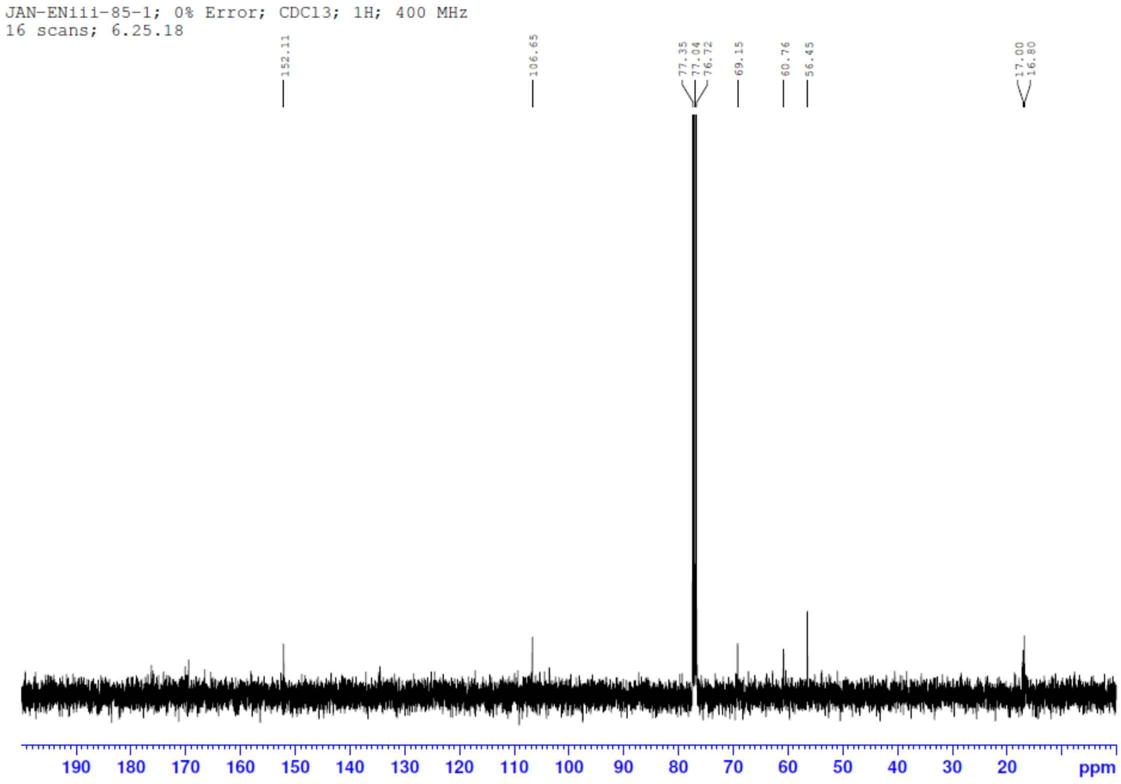
JAN-ENiii-85-1; 0% Error; CDCl3; 1H; 400 MHz
16 scans; 6.25.18
152.11
106.65
77.35
77.04
76.72
69.15
60.76
56.45
17.00
16.80
190
180
170
160
150
140
130
120
110
100
90
80
70
60
50
40
30
20
ppm

JAN-ENiii-85; 2.5% Error; CDCl3; 1H; 400 MHz
16 scans; 6.25.18

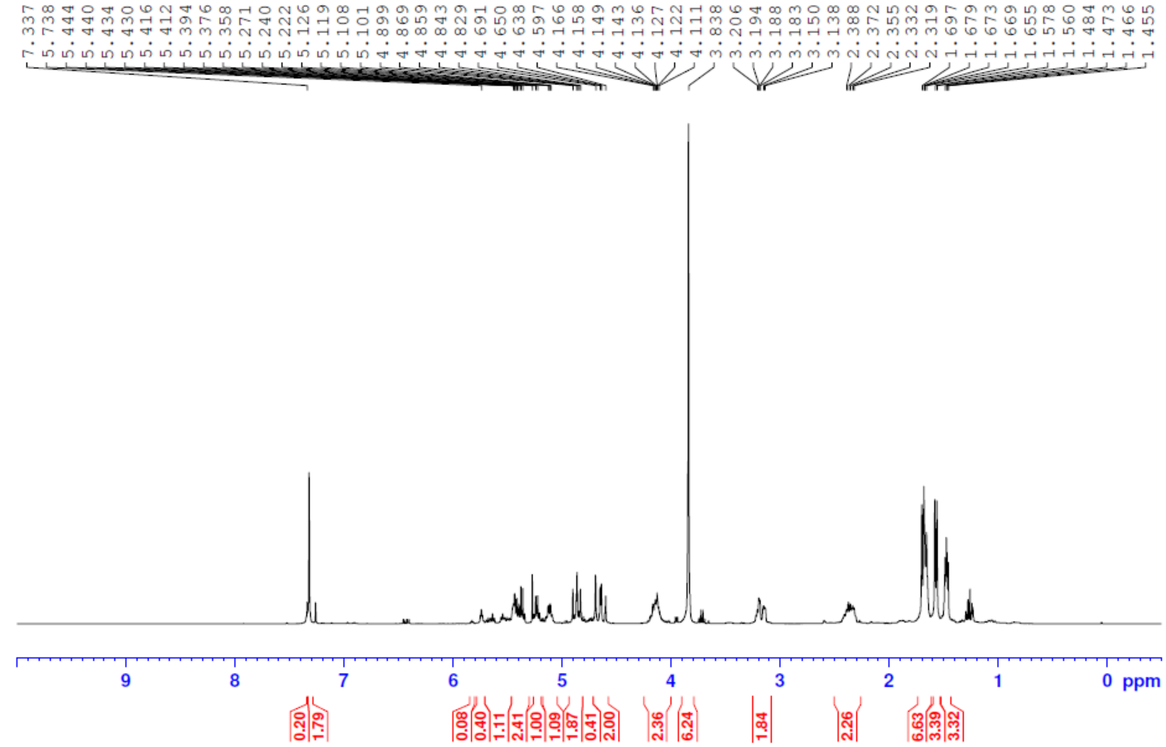

JAN-ENiii-85; 2.5% Error; CDCl3; 13C; 400 MHz
128 scans; 6.25.18

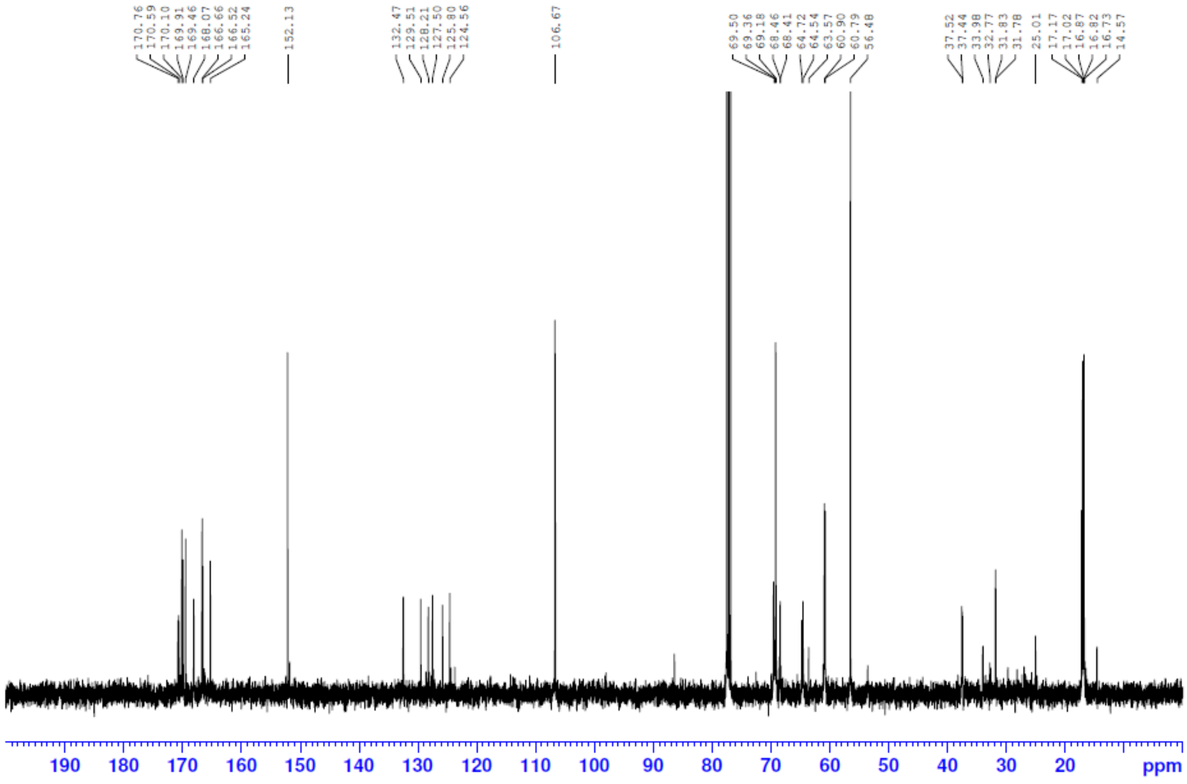

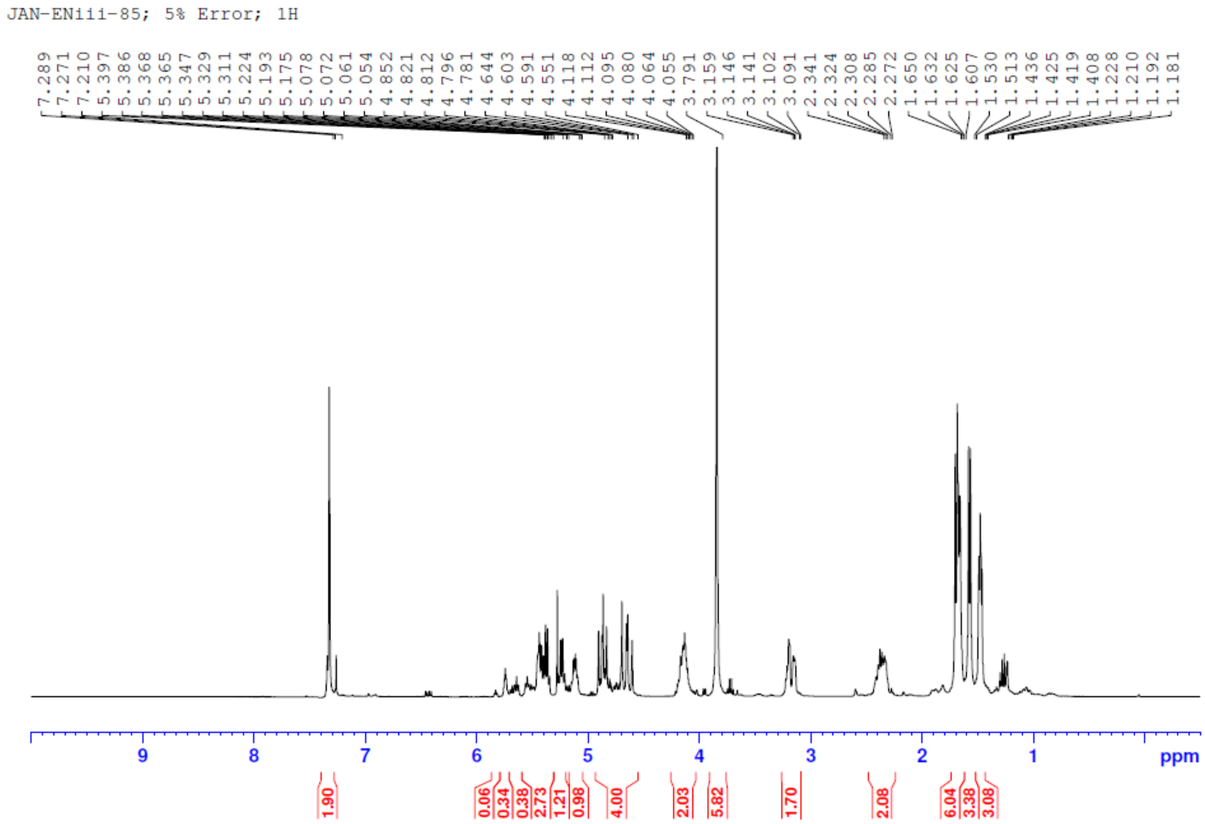
JAN-ENiii-85; 5% Error; 1H
7.289
7.271
7.210
5.397
5.386
5.368
5.365
5.347
5.329
5.311
5.224
5.193
5.175
5.078
5.072
5.061
5.054
4.852
4.821
4.812
4.796
4.781
4.644
4.603
4.591
4.551
4.118
4.112
4.095
4.080
4.064
4.055
3.791
3.159
3.146
3.141
3.102
3.091
2.341
2.324
2.308
2.285
2.272
1.650
1.632
1.625
1.607
1.530
1.513
1.436
1.425
1.419
1.408
1.228
1.210
1.192
1.181
9
8
7
6
5
4
3
2
1
ppm
1.90
0.06
0.34
0.38
2.73
1.21
0.98
4.00
2.03
5.82
1.70
2.08
6.04
3.38
3.08

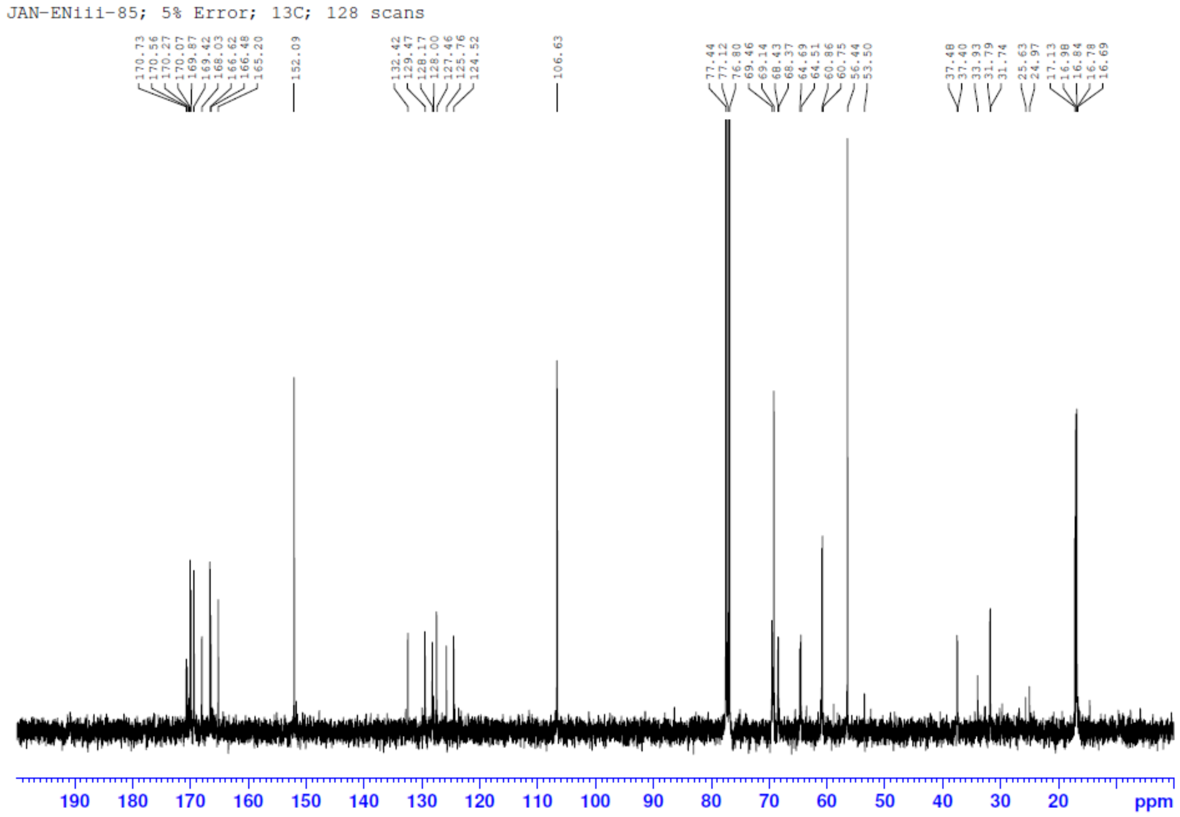
JAN-ENiii-85; 5% Error; 13C; 128 scans
170.73
170.56
170.27
170.07
169.87
169.42
168.03
166.62
166.48
165.20
152.09
132.42
129.47
128.17
128.00
127.46
125.76
124.52
106.63
77.44
77.12
76.80
69.46
69.14
68.43
68.37
64.69
64.51
60.86
60.75
56.44
53.50
37.48
37.40
33.93
31.79
31.74
25.63
24.97
17.13
16.98
16.84
16.78
16.69
190
180
170
160
150
140
130
120
110
100
90
80
70
60
50
40
30
20
ppm

JAN-ENiii-85; 10% Error; 1H

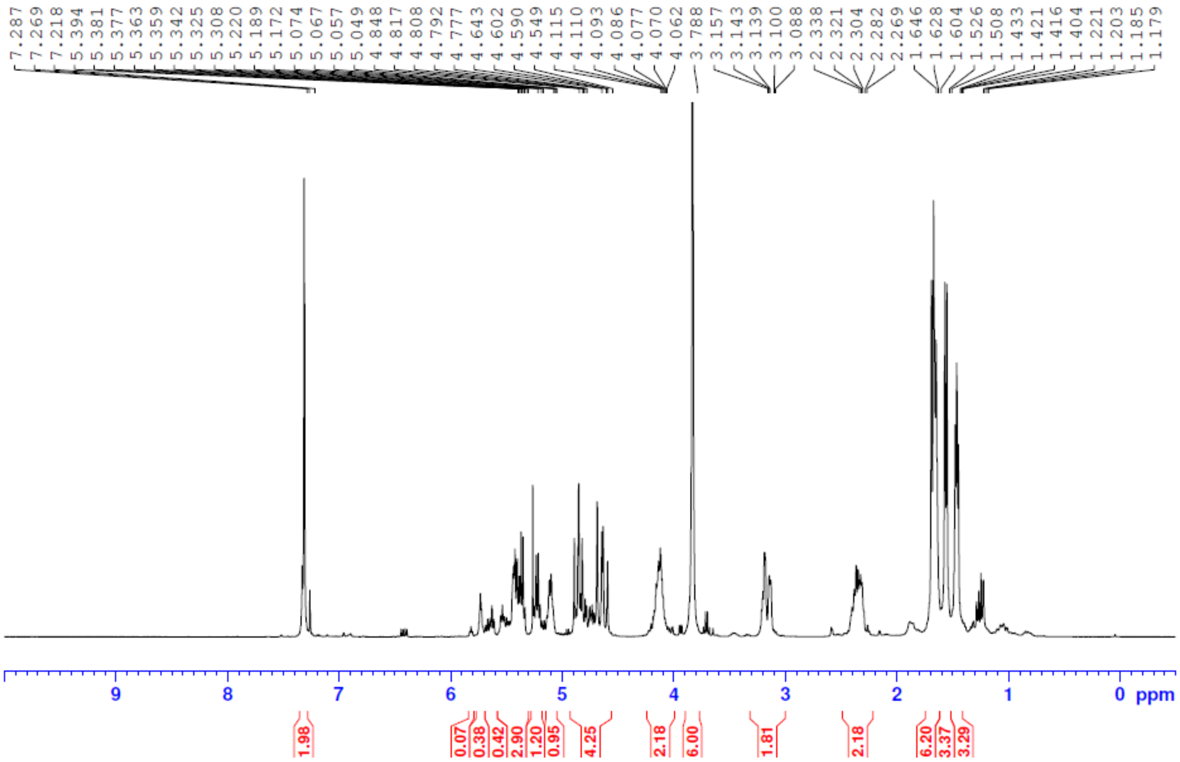

JAN-ENiii-85; 10% Error; 13C; 128 scans

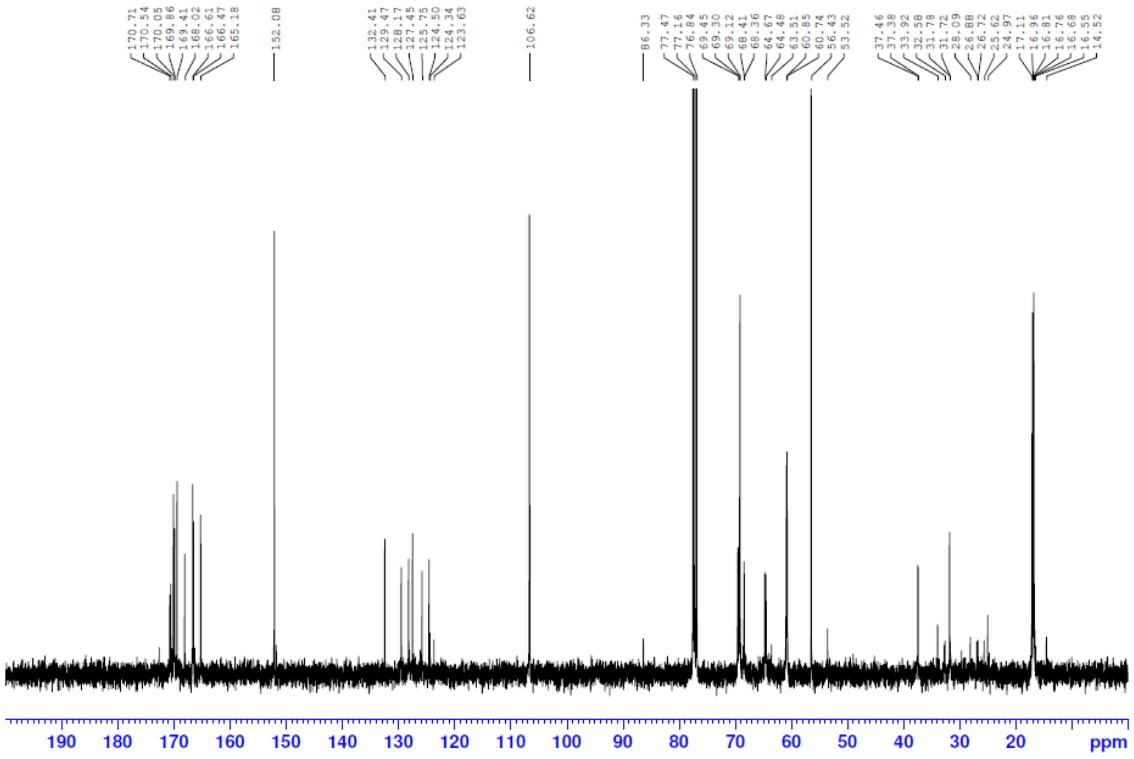

JAN-ENiii-85; 20% Error; 1H

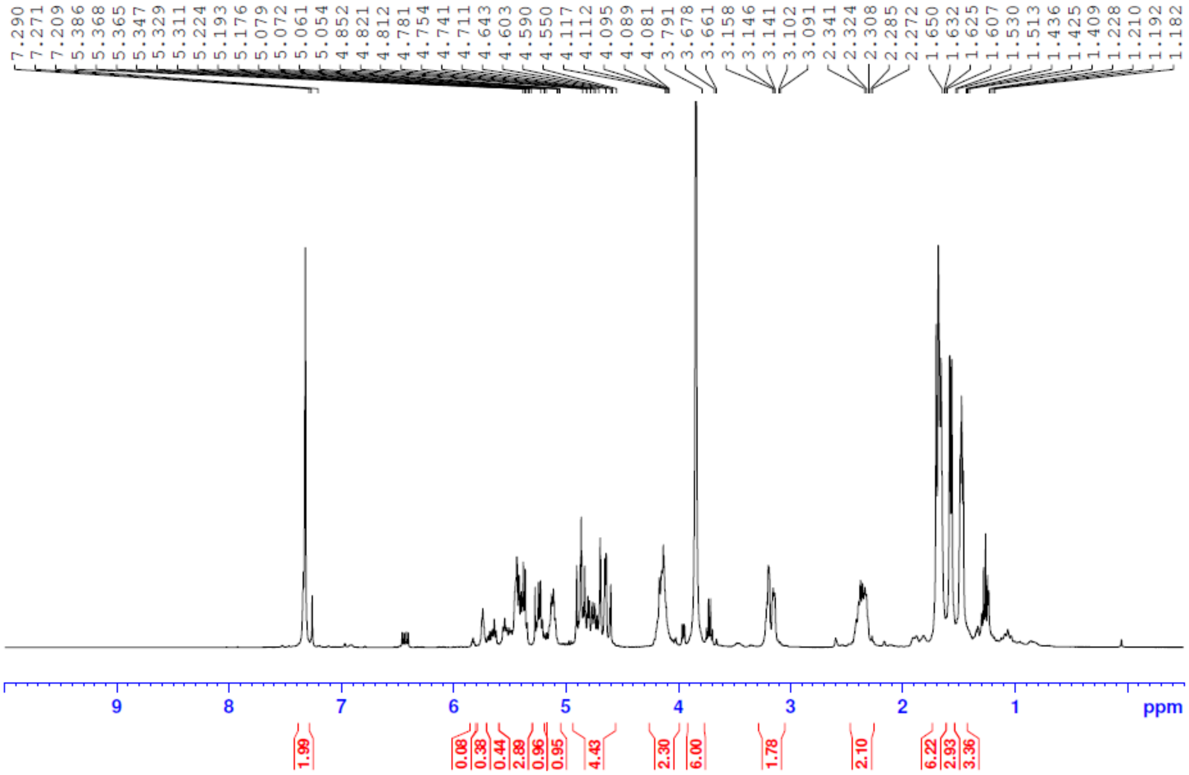

JAN-ENiii-85; 20% Error; 13C; 128 scans

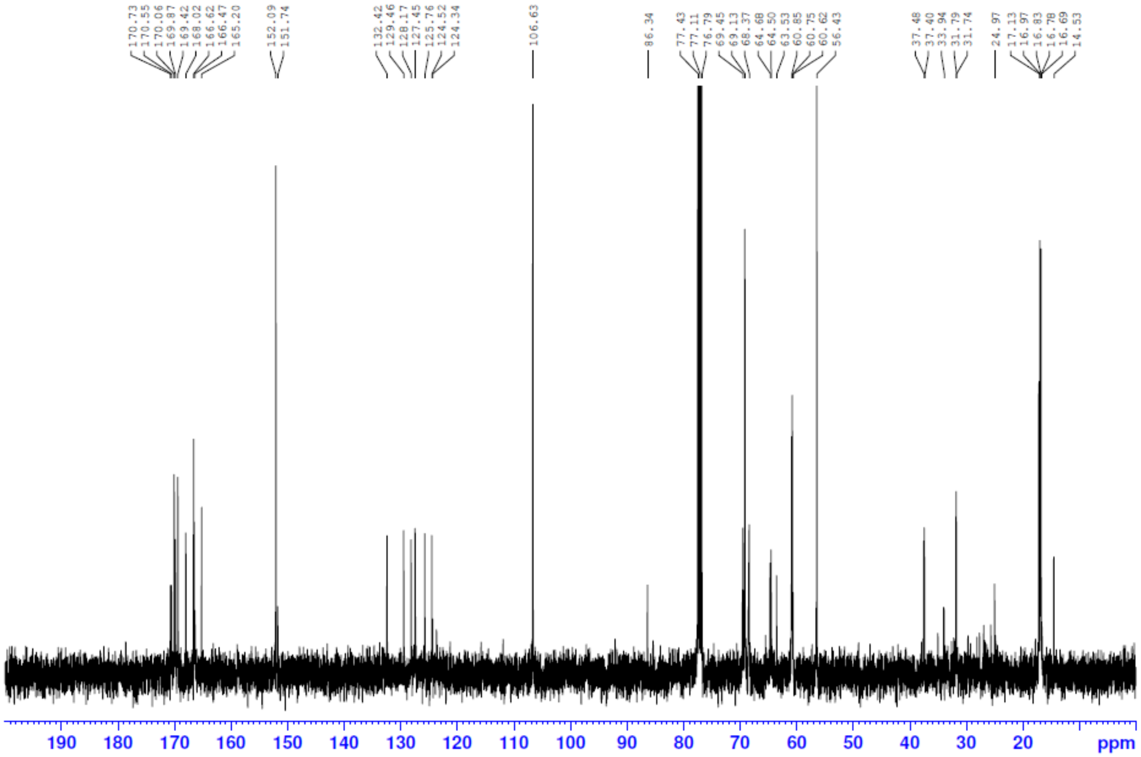

6.0 Bibliography

1. Batycky, R. P.; Hanes, J.; Langer, R.; Edwards, D. A., A Theoretical Model of Erosion and Macromolecular Drug Release from Biodegrading Microspheres. *Journal of Pharmaceutical Sciences* **1997,** *86* (12), 1464-1477.

2. Lu, L.; Garcia, C. A.; Mikos, A. G., In vitro degradation of thin poly(DL-lactic-co-glycolic acid) films. *Journal of Biomedical Materials Research* **1999,** *46* (2), 236-244.

3. Jain, R. A., The manufacturing techniques of various drug loaded biodegradable poly(lactide-co-glycolide) (PLGA) devices. *Biomaterials* **2000,** *21* (23), 2475-2490.

4. Darestani, M.; Akbar Entezami, A.; Mobedi, H.; Abtahi, M., *Degradation of Poly(D,L-lactide-co-glycolide) 50:50 Implant in Aqueous Medium*. 2005; Vol. 14.

5. Makadia, H. K.; Siegel, S. J., Poly Lactic-co-Glycolic Acid (PLGA) as Biodegradable Controlled Drug Delivery Carrier. *Polymers* **2011,** *3* (3), 1377-1397.

6. Pan, Z.; Ding, J., Poly(lactide-co-glycolide) porous scaffolds for tissue engineering and regenerative medicine. *Interface Focus* **2012,** *2* (3), 366-377.

7. Gentile, P.; Chiono, V.; Carmagnola, I.; Hatton, V. P., An Overview of Poly(lactic-co-glycolic) Acid (PLGA)-Based Biomaterials for Bone Tissue Engineering. *International Journal of Molecular Sciences* **2014,** *15* (3).

8. Shirazi, R. N.; Aldabbagh, F.; Erxleben, A.; Rochev, Y.; McHugh, P., Nanomechanical properties of poly(lactic-co-glycolic) acid film during degradation. *Acta Biomaterialia* **2014,** *10* (11), 4695-4703.

9. PLGA: a unique polymer for drug delivery. *Therapeutic Delivery* **2015,** *6* (1), 41-58.

10. Shibata, A.; Machida, M.; Kondo, N.; Terakawa, M., Biodegradability of poly(lactic-co-glycolic acid) and poly(l-lactic acid) after deep-ultraviolet femtosecond and nanosecond laser irradiation. *Applied Physics A* **2017,** *123* (6), 438.

11. Swisher, J. H. N., Jamie A.; Washington, Michael A.; Meyer, Tara Y., Properties and Applications of Sequence-Controlled Polymers. In *Sequence-Controlled Polymers*, Lutz, J.-F., Ed. Wiley: 2017.

12. Lutz, J.-F., Sequence-controlled polymerizations: the next Holy Grail in polymer science? *Polymer Chemistry* **2010,** *1* (1), 55-62.

13. Badi, N.; Lutz, J.-F., Sequence control in polymer synthesis. *Chemical Society Reviews* **2009,** *38* (12), 3383-3390.

14. Lutz, J.-F., Defining the Field of Sequence-Controlled Polymers. *Macromolecular Rapid Communications* **2017,** *38* (24), 1700582-n/a.

15. Lutz, J.-F.; Ouchi, M.; Sawamoto, M.; Meyer, T. Y., *Sequence-Controlled Polymers: Synthesis, Self-Assembly, and Properties*. American Chemical Society: 2014; Vol. 1170, p 0.

16. Cavallo, G.; Al Ouahabi, A.; Oswald, L.; Charles, L.; Lutz, J.-F., Orthogonal Synthesis of “Easy-to-Read” Information-Containing Polymers Using Phosphoramidite and Radical Coupling Steps. *Journal of the American Chemical Society* **2016,** *138* (30), 9417-9420.

17. Lutz, J.-F.; Lehn, J.-M.; Meijer, E. W.; Matyjaszewski, K., From precision polymers to complex materials and systems. *Nature Reviews Materials* **2016,** *1*, 16024.

18. Rosales, A. M.; Segalman, R. A.; Zuckermann, R. N., Polypeptoids: a model system to study the effect of monomer sequence on polymer properties and self-assembly. *Soft Matter* **2013,** *9* (35), 8400-8414.

19. Sun, J.; Teran, A. A.; Liao, X.; Balsara, N. P.; Zuckermann, R. N., Crystallization in Sequence-Defined Peptoid Diblock Copolymers Induced by Microphase Separation. *Journal of the American Chemical Society* **2014,** *136* (5), 2070-2077.

20. van Zoelen, W.; Buss, H. G.; Ellebracht, N. C.; Lynd, N. A.; Fischer, D. A.; Finlay, J.; Hill, S.; Callow, M. E.; Callow, J. A.; Kramer, E. J.; Zuckermann, R. N.; Segalman, R. A., Sequence of Hydrophobic and Hydrophilic Residues in Amphiphilic Polymer Coatings Affects Surface Structure and Marine Antifouling/Fouling Release Properties. *ACS Macro Letters* **2014,** *3* (4), 364-368.

21. Knight, A. S.; Zhou, E. Y.; Francis, M. B.; Zuckermann, R. N., Sequence Programmable Peptoid Polymers for Diverse Materials Applications. *Advanced Materials* **2015,** *27* (38), 5665-5691.

22. Chen, C.-L.; Zuckermann, R. N.; DeYoreo, J. J., Surface-Directed Assembly of Sequence-Defined Synthetic Polymers into Networks of Hexagonally Patterned Nanoribbons with Controlled Functionalities. *ACS Nano* **2016,** *10* (5), 5314-5320.

23. Murnen, H. K.; Khokhlov, A. R.; Khalatur, P. G.; Segalman, R. A.; Zuckermann, R. N., Impact of Hydrophobic Sequence Patterning on the Coil-to-Globule Transition of Protein-like Polymers. *Macromolecules* **2012,** *45* (12), 5229-5236.

24. van Zoelen, W.; Zuckermann, R. N.; Segalman, R. A., Tunable Surface Properties from Sequence-Specific Polypeptoid–Polystyrene Block Copolymer Thin Films. *Macromolecules* **2012,** *45* (17), 7072-7082.

25. Jiang, Y.; Golder, M. R.; Nguyen, H. V. T.; Wang, Y.; Zhong, M.; Barnes, J. C.; Ehrlich, D. J. C.; Johnson, J. A., Iterative Exponential Growth Synthesis and Assembly of Uniform Diblock Copolymers. *Journal of the American Chemical Society* **2016,** *138* (30), 9369-9372.

26. MacLeod, M. J.; Johnson, J. A., Block co-polyMOFs: assembly of polymer-polyMOF hybrids via iterative exponential growth and "click" chemistry. *Polymer Chemistry* **2017,** *8* (31), 4488-4493.

27. Lutz, J.-F.; Pakula, T.; Matyjaszewski, K., Synthesis and Properties of Copolymers with Tailored Sequence Distribution by Controlled/Living Radical Polymerization. In *Advances in Controlled/Living Radical Polymerization*, American Chemical Society: 2003; Vol. 854, pp 268-282.

28. Baeten, E.; Haven, J. J.; Junkers, T., RAFT multiblock reactor telescoping: from monomers to tetrablock copolymers in a continuous multistage reactor cascade. *Polymer Chemistry* **2017,** *8* (25), 3815-3824.

29. Fu, C.; Huang, Z.; Hawker, C. J.; Moad, G.; Xu, J.; Boyer, C., RAFT-mediated, visible light-initiated single unit monomer insertion and its application in the synthesis of sequence-defined polymers. *Polymer Chemistry* **2017,** *8* (32), 4637-4643.

30. Qian, W.; Song, T.; Ye, M.; Xu, P.; Lu, G.; Huang, X., PAA-g-PLA amphiphilic graft copolymer: synthesis, self-assembly, and drug loading ability. *Polymer Chemistry* **2017,** *8* (28), 4098-4107.

31. Satoh, K.; Hashimoto, H.; Kumagai, S.; Aoshima, H.; Uchiyama, M.; Ishibashi, R.; Fujiki, Y.; Kamigaito, M., One-shot controlled/living copolymerization for various comonomer sequence distributions via dual radical and cationic active species from RAFT terminals. *Polymer Chemistry* **2017,** *8* (34), 5002-5011.

32. Xue, L.; Xiong, X.; Chen, K.; Luan, Y.; Chen, G.; Chen, H., Modular synthesis of glycopolymers with well-defined sugar units in the side chain via Ugi reaction and click chemistry: hetero vs. homo. *Polymer Chemistry* **2016,** *7* (25), 4263-4271.

33. Deng, X.-X.; Li, L.; Li, Z.-L.; Lv, A.; Du, F.-S.; Li, Z.-C., Sequence Regulated Poly(ester-amide)s Based on Passerini Reaction. *ACS Macro Letters* **2012,** *1* (11), 1300-1303.

34. Tabata, Y.; Abe, H., Synthesis and Properties of Alternating Copolymers of 3-Hydroxybutyrate and Lactate Units with Different Stereocompositions. *Macromolecules* **2014,** *47* (21), 7354-7361.

35. Li, J.; Rothstein, S. N.; Little, S. R.; Edenborn, H. M.; Meyer, T. Y., The Effect of Monomer Order on the Hydrolysis of Biodegradable Poly(lactic-co-glycolic acid) Repeating Sequence Copolymers. *Journal of the American Chemical Society* **2012,** *134* (39), 16352-16359.

36. Washington, M. A.; Swiner, D. J.; Bell, K. R.; Fedorchak, M. V.; Little, S. R.; Meyer, T. Y., The impact of monomer sequence and stereochemistry on the swelling and erosion of biodegradable poly(lactic-co-glycolic acid) matrices. *Biomaterials* **2017,** *117*, 66-76.

37. Washington, M. A.; Balmert, S. C.; Fedorchak, M. V.; Little, S. R.; Watkins, S. C.; Meyer, T. Y., Monomer sequence in PLGA microparticles: Effects on acidic microclimates and in vivo inflammatory response. *Acta Biomaterialia* **2018,** *65*, 259-271.

38. Shi, X.; Wang, Y.; Ren, L.; Gong, Y.; Wang, D.-A., Enhancing Alendronate Release from a Novel PLGA/Hydroxyapatite Microspheric System for Bone Repairing Applications. *Pharmaceutical Research* **2009,** *26* (2), 422-430.

39. Tritto, I.; Marestin, C.; Boggioni, L.; Sacchi, M. C.; Brintzinger, H.-H.; Ferro, D. R., Stereoregular and Stereoirregular Alternating Ethylene−Norbornene Copolymers. *Macromolecules* **2001,** *34* (17), 5770-5777.

40. De Rosa, C.; Auriemma, F.; Villani, M.; Ruiz de Ballesteros, O.; Di Girolamo, R.; Tarallo, O.; Malafronte, A., Mechanical Properties and Stress-Induced Phase Transformations of Metallocene Isotactic Poly(1-butene): The Influence of Stereodefects. *Macromolecules* **2014,** *47* (3), 1053-1064.

41. Gourari, A.; Bendaoud, M.; Lacabanne, C.; Boyer, R. F., Influence of tacticity on Tβ, Tg, and TLL in poly(methyl methacrylate)s by the method of thermally stimulated current (TSC). *Journal of Polymer Science: Polymer Physics Edition* **1985,** *23* (5), 889-916.

42. Huang, C.-L.; Chen, Y.-C.; Hsiao, T.-J.; Tsai, J.-C.; Wang, C., Effect of Tacticity on Viscoelastic Properties of Polystyrene. *Macromolecules* **2011,** *44* (15), 6155-6161.

43. Chen, K.; Harris, K.; Vyazovkin, S., Tacticity as a Factor Contributing to the Thermal Stability of Polystyrene. *Macromolecular Chemistry and Physics* **2007,** *208* (23), 2525-2532.

44. Kaminsky, W.; Arndt, M., Metallocenes for polymer catalysis. In *Polymer Synthesis/Polymer Catalysis*, Springer Berlin Heidelberg: Berlin, Heidelberg, 1997; pp 143-187.

45. Coates, G. W., Precise Control of Polyolefin Stereochemistry Using Single-Site Metal Catalysts. *Chemical Reviews* **2000,** *100* (4), 1223-1252.

46. Resconi, L.; Cavallo, L.; Fait, A.; Piemontesi, F., Selectivity in Propene Polymerization with Metallocene Catalysts. *Chemical Reviews* **2000,** *100* (4), 1253-1346.

47. Brintzinger, H. H.; Fischer, D.; Mülhaupt, R.; Rieger, B.; Waymouth, R. M., Stereospecific Olefin Polymerization with Chiral Metallocene Catalysts. *Angewandte Chemie International Edition in English* **1995,** *34* (11), 1143-1170.

48. Angermund, K.; Fink, G.; Jensen, V. R.; Kleinschmidt, R., Toward Quantitative Prediction of Stereospecificity of Metallocene-Based Catalysts for α-Olefin Polymerization. *Chemical Reviews* **2000,** *100* (4), 1457-1470.

49. Södergård, A.; Stolt, M., Properties of lactic acid based polymers and their correlation with composition. *Progress in Polymer Science* **2002,** *27* (6), 1123-1163.

50. Stanford, M. J.; Dove, A. P., Stereocontrolled ring-opening polymerisation of lactide. *Chemical Society Reviews* **2010,** *39* (2), 486-494.

51. Chile, L.-E.; Mehrkhodavandi, P.; Hatzikiriakos, S. G., A Comparison of the Rheological and Mechanical Properties of Isotactic, Syndiotactic, and Heterotactic Poly(lactide). *Macromolecules* **2016,** *49* (3), 909-919.

52. Ovitt, T. M.; Coates, G. W., Stereoselective Ring-Opening Polymerization of meso-Lactide: Synthesis of Syndiotactic Poly(lactic acid). *Journal of the American Chemical Society* **1999,** *121* (16), 4072-4073.

53. Cheng, M.; Attygalle, A. B.; Lobkovsky, E. B.; Coates, G. W., Single-Site Catalysts for Ring-Opening Polymerization: Synthesis of Heterotactic Poly(lactic acid) from rac-Lactide. *Journal of the American Chemical Society* **1999,** *121* (49), 11583-11584.

54. Spassky, N.; Wisniewski, M.; Pluta, C.; Le Borgne, A., Highly stereoelective polymerization of rac-(D,L)-lactide with a chiral schiff's base/aluminium alkoxide initiator. *Macromolecular Chemistry and Physics* **1996,** *197* (9), 2627-2637.

55. Ovitt, T. M.; Coates, G. W., Stereoselective ring-opening polymerization of rac-lactide with a single-site, racemic aluminum alkoxide catalyst: Synthesis of stereoblock poly(lactic acid). *Journal of Polymer Science Part A: Polymer Chemistry* **2000,** *38* (S1), 4686-4692.

56. Nomura, N.; Hasegawa, J.; Ishii, R., A Direct Function Relationship between Isotacticity and Melting Temperature of Multiblock Stereocopolymer Poly(rac-lactide). *Macromolecules* **2009,** *42* (13), 4907-4909.

57. Eastwood, E. A.; Dadmun, M. D., Multiblock Copolymers in the Compatibilization of Polystyrene and Poly(methyl methacrylate) Blends: Role of Polymer Architecture. *Macromolecules* **2002,** *35* (13), 5069-5077.

58. Lyatskaya, Y.; Gersappe, D.; Gross, N. A.; Balazs, A. C., Designing Compatibilizers To Reduce Interfacial Tension in Polymer Blends. *The Journal of Physical Chemistry* **1996,** *100* (5), 1449-1458.

59. Galvin, M. E., Effect of sequence distribution on miscibility in polymer blends. *Macromolecules* **1991,** *24* (23), 6354-6356.

60. Winey, K. I.; Berba, M. L.; Galvin, M. E., Ternary Phase Diagrams of Poly(styrene-co-methyl methacrylate), Poly(methyl methacrylate), and Polystyrene: Monomer Sequence Distribution Effect and Encapsulation. *Macromolecules* **1996,** *29* (8), 2868-2877.

61. Colquhoun, H. M.; Dudman, C. C.; Blundell, D. J.; Bunn, A.; Mackenzie, P. D.; McGrail, P. T.; Nield, E.; Rose, J. B.; Williams, D. J., An aromatic polyether in which sequence-randomization leads to induction of crystallinity: x-ray structure of the crystalline phase [-OArCOArArCOAr-]n (Ar = 1,4-phenylene). *Macromolecules* **1993,** *26* (1), 107-111.

62. Lim, K. J.; Cross, P.; Mills, P.; Colquhoun, H. M., Controlled variation of monomer sequence distribution in the synthesis of aromatic poly(ether ketone)s. *High Performance Polymers* **2016,** *28* (8), 984-992.

63. Choe, E.-W.; Borzo, M., Synthesis and randomization of well-defined sequence, wholly aromatic copolyester/esteramides. *Journal of Applied Polymer Science* **1994,** *53* (5), 621-632.

64. Kricheldorf, H. R.; Eggerstedt, S., New Polymer Syntheses. 100. Multiblock Copolyesters by Combined Macrocyclic Polymerization and Silicon-Mediated Polycondensation. *Macromolecules* **1998,** *31* (19), 6403-6408.

65. Kang, E.-C.; Kaneko, T.; Shiino, D.; Akashi, M., Novel functional polymers: Poly(dimethyl siloxane)–polyamide multiblock copolymers. XI. The effects of sequence regularity on the thermal and mechanical properties. *Journal of Polymer Science Part A: Polymer Chemistry* **2003,** *41* (6), 841-852.

66. RANA, D.; MOUNACH, H.; HALARY, J. L.; MONNERIE, L., Differences in mechanical behavior between alternating and random styrene-methyl methacrylate copolymers. *Journal of Materials Science* **2005,** *40* (4), 943-953.

67. Kang, T. E.; Choi, J.; Cho, H.-H.; Yoon, S. C.; Kim, B. J., Donor-Acceptor Random versus Alternating Copolymers for Efficient Polymer Solar Cells: Importance of Optimal Composition in Random Copolymers. *Macromolecules (Washington, DC, U. S.)* **2016,** *49* (6), 2096-2105.

68. Heo, H.; Kim, H.; Lee, D.; Jang, S.; Ban, L.; Lim, B.; Lee, J.; Lee, Y., Regioregular D1-A-D2-A Terpolymer with Controlled Thieno[3,4-b]thiophene Orientation for High-Efficiency Polymer Solar Cells Processed with Nonhalogenated Solvents. *Macromolecules* **2016,** *49* (9), 3328-3335.

69. Schmidt, B. V. K. J.; Fechler, N.; Falkenhagen, J.; Lutz, J.-F., Controlled folding of synthetic polymer chains through the formation of positionable covalent bridges. *Nat Chem* **2011,** *3* (3), 234-238.

70. Luo, M.; Brown, J. R.; Remy, R. A.; Scott, D. M.; Mackay, M. E.; Hall, L. M.; Epps, T. H., Determination of Interfacial Mixing in Tapered Block Polymer Thin Films: Experimental and Theoretical Investigations. *Macromolecules* **2016,** *49* (14), 5213-5222.

71. Cole, J. P.; Hanlon, A. M.; Rodriguez, K. J.; Berda, E. B., Protein-like structure and activity in synthetic polymers. *Journal of Polymer Science Part A: Polymer Chemistry* **2017,** *55* (2), 191-206.

72. Crapster, J. A.; Guzei, I. A.; Blackwell, H. E., A Peptoid Ribbon Secondary Structure. *Angewandte Chemie (International ed. in English)* **2013,** *52* (19), 5079-5084.

73. Hebert, M. L.; Shah, D. S.; Blake, P.; Turner, J. P.; Servoss, S. L., Tunable peptoid microspheres: effects of side chain chemistry and sequence. *Organic & Biomolecular Chemistry* **2013,** *11* (27), 4459-4464.

74. McDaniel, J. R.; Weitzhandler, I.; Prevost, S.; Vargo, K. B.; Appavou, M.-S.; Hammer, D. A.; Gradzielski, M.; Chilkoti, A., Noncanonical Self-Assembly of Highly Asymmetric Genetically Encoded Polypeptide Amphiphiles into Cylindrical Micelles. *Nano Letters* **2014,** *14* (11), 6590-6598.

75. Shin, H.-M.; Kang, C.-M.; Yoon, M.-H.; Seo, J., Peptoid helicity modulation: precise control of peptoid secondary structures via position-specific placement of chiral monomers. *Chemical Communications* **2014,** *50* (34), 4465-4468.

76. Chen, Y.; Liu, T.; Xu, G.; Zhang, J.; Zhai, X.; Yuan, J.; Tan, Y., Aggregation behavior of X-shaped branched block copolymers at the air/water interface: effect of block sequence and temperature. *Colloid and Polymer Science* **2015,** *293* (1), 97-107.

77. Xu, X.; Shan, G.; Pan, P., Amphiphilic quasi-block copolymers and their self-assembled nanoparticles via thermally induced interfacial absorption in miniemulsion polymerization. *RSC Advances* **2015,** *5* (62), 50118-50125.

78. Stals, P. J. M.; Cheng, C.-Y.; van Beek, L.; Wauters, A. C.; Palmans, A. R. A.; Han, S.; Meijer, E. W., Surface water retardation around single-chain polymeric nanoparticles: critical for catalytic function? *Chemical Science* **2016,** *7* (3), 2011-2015.

79. Zhu, Z.; Cardin, C. J.; Gan, Y.; Murray, C. A.; White, A. J. P.; Williams, D. J.; Colquhoun, H. M., Conformational Modulation of Sequence Recognition in Synthetic Macromolecules. *Journal of the American Chemical Society* **2011,** *133* (48), 19442-19447.

80. Yoshimatsu, K.; Lesel, B. K.; Yonamine, Y.; Beierle, J. M.; Shea, K. J.; Hoshino, Y., Temperature-Responsive “Catch-and-Release” of Proteins using Multifunctional Polymer Nanoparticles. *Angewandte Chemie (International ed. in English)* **2012,** *51* (10), 2405-2408.

81. Romulus, J.; Weck, M., Single-Chain Polymer Self-Assembly Using Complementary Hydrogen Bonding Units. *Macromolecular Rapid Communications* **2013,** *34* (19), 1518-1523.

82. Mahon, C. S.; Fulton, D. A., Mimicking nature with synthetic macromolecules capable of recognition. *Nat Chem* **2014,** *6* (8), 665-672.

83. Trigg, E. B.; Tiegs, B. J.; Coates, G. W.; Winey, K. I., High Morphological Order in a Nearly Precise Acid-Containing Polymer and Ionomer. *ACS Macro Letters* **2017,** *6* (9), 947-951.

84. Seitz, M. E.; Chan, C. D.; Opper, K. L.; Baughman, T. W.; Wagener, K. B.; Winey, K. I., Nanoscale Morphology in Precisely Sequenced Poly(ethylene-co-acrylic acid) Zinc Ionomers. *Journal of the American Chemical Society* **2010,** *132* (23), 8165-8174.

85. Middleton, L. R.; Trigg, E. B.; Schwartz, E.; Opper, K. L.; Baughman, T. W.; Wagener, K. B.; Winey, K. I., Role of Periodicity and Acid Chemistry on the Morphological Evolution and Strength in Precise Polyethylenes. *Macromolecules* **2016,** *49* (21), 8209-8218.

86. Baughman, T. W.; Chan, C. D.; Winey, K. I.; Wagener, K. B., Synthesis and Morphology of Well-Defined Poly(ethylene-co-acrylic acid) Copolymers. *Macromolecules* **2007,** *40* (18), 6564-6571.

87. Li, X.-F.; Paoloni, F. P. V.; Weiber, E. A.; Jiang, Z.-H.; Jannasch, P., Fully Aromatic Ionomers with Precisely Sequenced Sulfonated Moieties for Enhanced Proton Conductivity. *Macromolecules* **2012,** *45* (3), 1447-1459.

88. Leng, C.; Buss, H. G.; Segalman, R. A.; Chen, Z., Surface Structure and Hydration of Sequence-Specific Amphiphilic Polypeptoids for Antifouling/Fouling Release Applications. *Langmuir* **2015,** *31* (34), 9306-9311.

89. Swisher, J. H.; Nowalk, J. A.; Washington, M. A.; Meyer, T. Y., Properties and Applications of Sequence-Controlled Polymers. In *Sequence-Controlled Polymers*, Wiley-VCH Verlag GmbH & Co. KGaA: 2018; pp 435-478.

90. Amonoo, J. A.; Li, A.; Purdum, G. E.; Sykes, M. E.; Huang, B.; Palermo, E. F.; McNeil, A. J.; Shtein, M.; Loo, Y.-L.; Green, P. F., An all-conjugated gradient copolymer approach for morphological control of polymer solar cells. *Journal of Materials Chemistry A* **2015,** *3* (40), 20174-20184.

91. Klumperman, B., Statistical, Alternating and Gradient Copolymers. In *Macromolecular Engineering*, Wiley-VCH Verlag GmbH & Co. KGaA: 2007; pp 813-838.

92. Hosono, N.; Gillissen, M. A. J.; Li, Y.; Sheiko, S. S.; Palmans, A. R. A.; Meijer, E. W., Orthogonal Self-Assembly in Folding Block Copolymers. *Journal of the American Chemical Society* **2013,** *135* (1), 501-510.

93. Grate, J. W.; Mo, K.-F.; Daily, M. D., Triazine-Based Sequence-Defined Polymers with Side-Chain Diversity and Backbone–Backbone Interaction Motifs. *Angewandte Chemie International Edition* **2016,** *55* (12), 3925-3930.

94. Lee, H.; Hoshino, Y.; Wada, Y.; Arata, Y.; Maruyama, A.; Miura, Y., Minimization of Synthetic Polymer Ligands for Specific Recognition and Neutralization of a Toxic Peptide. *Journal of the American Chemical Society* **2015,** *137* (34), 10878-10881.

95. Lutz, J.-F.; Ouchi, M.; Liu, D. R.; Sawamoto, M., Sequence-Controlled Polymers. *Science* **2013,** *341* (6146).

96. Tsai, C.-H.; Fortney, A.; Qiu, Y.; Gil, R. R.; Yaron, D.; Kowalewski, T.; Noonan, K. J. T., Conjugated Polymers with Repeated Sequences of Group 16 Heterocycles Synthesized through Catalyst-Transfer Polycondensation. *J. Am. Chem. Soc.* **2016,** *138* (21), 6798-6804.

97. Zhang, S.; Bauer, N. E.; Kanal, I. Y.; You, W.; Hutchison, G. R.; Meyer, T. Y., Sequence Effects in Donor–Acceptor Oligomeric Semiconductors Comprising Benzothiadiazole and Phenylenevinylene Monomers. *Macromolecules* **2017,** *50* (1), 151-161.

98. Bischof, A. M.; Zhang, S.; Meyer, T. Y.; Lear, B. J., Quantitative Assessment of the Connection between Steric Hindrance and Electronic Coupling in 2,5-Bis(alkoxy)benzene-Based Mixed-Valence Dimers. *The Journal of Physical Chemistry C* **2014,** *118* (24), 12693-12699.

99. Sun, J.; Stone, G. M.; Balsara, N. P.; Zuckermann, R. N., Structure–Conductivity Relationship for Peptoid-Based PEO–Mimetic Polymer Electrolytes. *Macromolecules* **2012,** *45* (12), 5151-5156.

100. Aitken, B. S.; Wieruszewski, P. M.; Graham, K. R.; Reynolds, J. R.; Wagener, K. B., Control of Charge-Carrier Mobility via In-Chain Spacer Length Variation in Sequenced Triarylamine Functionalized Polyolefins. *ACS Macro Letters* **2012,** *1* (2), 324-327.

101. Anderson, J. M.; Shive, M. S., Biodegradation and biocompatibility of PLA and PLGA microspheres. *Advanced Drug Delivery Reviews* **1997,** *28* (1), 5-24.

102. Xue, Z.; Mayer, M. F., Entropy-driven ring-opening olefin metathesis polymerizations of macrocycles. *Soft Matter* **2009,** *5* (23), 4600-4611.

103. Gautrot, J. E.; Zhu, X. X., High molecular weight bile acid and ricinoleic acid-based copolyesters via entropy-driven ring-opening metathesis polymerisation. *Chem. Commun.* **2008,** (14), 1674-1676.

104. Peng, Y.; Decatur, J.; Meier, M. A. R.; Gross, R. A., Ring-Opening Metathesis Polymerization of a Naturally Derived Macrocyclic Glycolipid. *Macromolecules* **2013,** *46* (9), 3293-3300.

105. Strandman, S.; Gautrot, J. E.; Zhu, X. X., Recent advances in entropy-driven ring-opening polymerizations. *Polymer Chemistry* **2011,** *2* (Copyright (C) 2012 American Chemical Society (ACS). All Rights Reserved.), 791-799.

106. Martinez, H.; Ren, N.; Matta, M. E.; Hillmyer, M. A., Ring-opening metathesis polymerization of 8-membered cyclic olefins. *Polymer Chemistry* **2014,** *5* (11), 3507-3532.

107. Zhang, J.; Matta, M. E.; Hillmyer, M. A., Synthesis of Sequence-Specific Vinyl Copolymers by Regioselective ROMP of Multiply Substituted Cyclooctenes. *ACS Macro Letters* **2012,** *1* (12), 1383-1387.

108. Martinez, H.; Miró, P.; Charbonneau, P.; Hillmyer, M. A.; Cramer, C. J., Selectivity in Ring-Opening Metathesis Polymerization of Z-Cyclooctenes Catalyzed by a Second-generation Grubbs Catalyst. *ACS Catalysis* **2012,** *2* (12), 2547-2556.

109. Kobayashi, S.; Pitet, L. M.; Hillmyer, M. A., Regio- and Stereoselective Ring-Opening Metathesis Polymerization of 3-Substituted Cyclooctenes. *J. Am. Chem. Soc.* **2011,** *133* (15), 5794-5797.

110. Gautrot, J. E.; Zhu, X. X., Main-Chain Bile Acid Based Degradable Elastomers Synthesized by Entropy-Driven Ring-Opening Metathesis Polymerization. *Angewandte Chemie* **2006,** *118* (41), 7026-7028.

111. Zhang, J.; Li, G.; Sampson, N. S., Incorporation of Large Cycloalkene Rings into Alternating Copolymers Allows Control of Glass Transition and Hydrophobicity. *ACS Macro Letters* **2018,** *7* (9), 1068-1072.

112. Swisher, J. H.; Nowalk, J. A.; Meyer, T. Y., Property impact of common linker segments in sequence-controlled polyesters. *Polymer Chemistry* **2018**.

113. Weiss, R. M.; Short, A. L.; Meyer, T. Y., Sequence-Controlled Copolymers Prepared via Entropy-Driven Ring-Opening Metathesis Polymerization. *ACS Macro Lett.* **2015,** *4* (9), 1039-1043.

114. Short, A. L.; Fang, C.; Nowalk, J. A.; Weiss, R. M.; Liu, P.; Meyer, T. Y., Cis-Selective Metathesis to Enhance the Living Character of Ring-Opening Polymerization: An Approach to Sequenced Copolymers. *ACS Macro Letters* **2018**, 858-862.

115. Hodge, P., Entropically Driven Ring-Opening Polymerization of Strainless Organic Macrocycles. *Chem. Rev.* **2014,** *114* (4), 2278-2312.

116. Hodge, P.; Kamau, S. D., Entropically Driven Ring-Opening-Metathesis Polymerization of Macrocyclic Olefins with 21–84 Ring Atoms. *Angewandte Chemie International Edition* **2003,** *42* (21), 2412-2414.

117. Tastard, C. Y.; Hodge, P.; Ben-Haida, A.; Dobinson, M., Entropically driven ring-opening metathesis polymerization (ED-ROMP) of macrocyclic olefin-containing oligoamides. *Reactive and Functional Polymers* **2006,** *66* (1), 93-107.

118. Deng, L.-L.; Guo, L.-X.; Lin, B.-P.; Zhang, X.-Q.; Sun, Y.; Yang, H., An entropy-driven ring-opening metathesis polymerization approach towards main-chain liquid crystalline polymers. *Polymer Chemistry* **2016,** *7* (33), 5265-5272.

119. Chatterjee, A. K.; Choi, T.-L.; Sanders, D. P.; Grubbs, R. H., A General Model for Selectivity in Olefin Cross Metathesis. *Journal of the American Chemical Society* **2003,** *125* (37), 11360-11370.

120. Nguyen, H. T. H.; Short, G. N.; Qi, P.; Miller, S. A., Copolymerization of lactones and bioaromatics via concurrent ring-opening polymerization/polycondensation. *Green Chemistry* **2017**.

121. Keitz, B. K.; Endo, K.; Patel, P. R.; Herbert, M. B.; Grubbs, R. H., Improved Ruthenium Catalysts for Z-Selective Olefin Metathesis. *J. Am. Chem. Soc.* **2011,** *134* (1), 693-699.

122. Fandrick, K. R.; Savoie, J.; Yee, N.; Song, J. J.; Senanayake, C. H., Challenges and Opportunities for Scaling the Ring-Closing Metathesis Reaction in the Pharmaceutical Industry. In *Olefin Metathesis*, John Wiley & Sons, Inc.: 2014; pp 349-365.

123. Ahmed, S. R.; Bullock, S. E.; Cresce, A. V.; Kofinas, P., Polydispersity control in ring opening metathesis polymerization of amphiphilic norbornene diblock copolymers. *Polymer* **2003,** *44* (17), 4943-4948.

124. Liu, Z.; Rainier, J. D., Regioselective Ring-Opening/Cross-Metathesis Reactions of Norbornene Derivatives with Electron-Rich Olefins. *Organic Letters* **2005,** *7* (1), 131-133.

125. Schwab, P.; Grubbs, R. H.; Ziller, J. W., Synthesis and Applications of RuCl2(CHR')(PR3)2: The Influence of the Alkylidene Moiety on Metathesis Activity. *J. Am. Chem. Soc.* **1996,** *118* (1), 100-110.

126. Maynard, H. D.; Okada, S. Y.; Grubbs, R. H., Synthesis of Norbornenyl Polymers with Bioactive Oligopeptides by Ring-Opening Metathesis Polymerization. *Macromolecules* **2000,** *33* (17), 6239-6248.

127. Sutthasupa, S.; Shiotsuki, M.; Matsuoka, H.; Masuda, T.; Sanda, F., Ring-Opening Metathesis Block Copolymerization of Amino Acid Functionalized Norbornene Monomers. Effects of Solvent and pH on Micelle Formation. *Macromolecules* **2010,** *43* (4), 1815-1822.

128. Floros, G.; Saragas, N.; Paraskevopoulou, P.; Psaroudakis, N.; Koinis, S.; Pitsikalis, M.; Hadjichristidis, N.; Mertis, K., Ring Opening Metathesis Polymerization of Norbornene and Derivatives by the Triply Bonded Ditungsten Complex Na[W2(μ-Cl)3Cl4(THF)2]·(THF)3. *Polymers* **2012,** *4* (4), 1657-1673.

129. Gringolts, M. L.; Denisova, Y. I.; Shandryuk, G. A.; Krentsel, L. B.; Litmanovich, A. D.; Finkelshtein, E. S.; Kudryavtsev, Y. V., Synthesis of norbornene-cyclooctene copolymers by the cross-metathesis of polynorbornene with polyoctenamer. *RSC Advances* **2015,** *5* (1), 316-319.

130. Patel, P. R.; Kiser, R. C.; Lu, Y. Y.; Fong, E.; Ho, W. C.; Tirrell, D. A.; Grubbs, R. H., Synthesis and Cell Adhesive Properties of Linear and Cyclic RGD Functionalized Polynorbornene Thin Films. *Biomacromolecules* **2012,** *13* (8), 2546-2553.

131. Maynard, H. D.; Okada, S. Y.; Grubbs, R. H., Inhibition of Cell Adhesion to Fibronectin by Oligopeptide-Substituted Polynorbornenes. *J. Am. Chem. Soc.* **2001,** *123* (7), 1275-1279.

132. Boden, E. P.; Keck, G. E., Proton-transfer steps in Steglich esterification: a very practical new method for macrolactonization. *The Journal of Organic Chemistry* **1985,** *50* (13), 2394-2395.

133. Coleman, R. S.; Shah, J. A., Chemoselective Cleavage of Benzyl Ethers, Esters, and Carbamates in the Presence of Other Easily Reducible Groups. *Synthesis* **1999,** *1999* (S 01), 1399-1400.

134. Zhang, J.; Matta, M. E.; Martinez, H.; Hillmyer, M. A., Precision Vinyl Acetate/Ethylene (VAE) Copolymers by ROMP of Acetoxy-Substituted Cyclic Alkenes. *Macromolecules* **2013,** *46* (7), 2535-2543.

135. Gutekunst, W. R.; Hawker, C. J., A General Approach to Sequence-Controlled Polymers Using Macrocyclic Ring Opening Metathesis Polymerization. *Journal of the American Chemical Society* **2015,** *137* (25), 8038-8041.

136. Chang, A. B.; Miyake, G. M.; Grubbs, R. H., Sequence-Controlled Polymers by Ruthenium-Mediated Ring-Opening Metathesis Polymerization. In *Sequence-Controlled Polymers: Synthesis, Self-Assembly, and Properties*, American Chemical Society: 2014; Vol. 1170, pp 161-188.

137. Farrell, W. S.; Beers, K. L., Ring-Opening Metathesis Polymerization of Butyl-Substituted trans-Cyclooctenes. *ACS Macro Letters* **2017,** *6* (8), 791-795.

138. Parker, K. A.; Sampson, N. S., Precision Synthesis of Alternating Copolymers via Ring-Opening Polymerization of 1-Substituted Cyclobutenes. *Accounts of Chemical Research* **2016,** *49* (3), 408-417.

139. Stayshich, R. M.; Meyer, T. Y., New Insights into Poly(lactic-co-glycolic acid) Microstructure: Using Repeating Sequence Copolymers To Decipher Complex NMR and Thermal Behavior. *Journal of the American Chemical Society* **2010,** *132* (31), 10920-10934.

140. Weiss, R. M.; Li, J.; Liu, H. H.; Washington, M. A.; Giesen, J. A.; Grayson, S. M.; Meyer, T. Y., Determining Sequence Fidelity in Repeating Sequence Poly(lactic-co-glycolic acid)s. *Macromolecules* **2017,** *50* (2), 550-560.

141. Ohno, K.; Tsujii, Y.; Miyamoto, T.; Fukuda, T.; Goto, M.; Kobayashi, K.; Akaike, T., Synthesis of a Well-Defined Glycopolymer by Nitroxide-Controlled Free Radical Polymerization. *Macromolecules* **1998,** *31* (4), 1064-1069.

142. Lu, H.; Cheng, J., Hexamethyldisilazane-Mediated Controlled Polymerization of α-Amino Acid N-Carboxyanhydrides. *Journal of the American Chemical Society* **2007,** *129* (46), 14114-14115.

143. Habraken, G. J. M.; Peeters, M.; Dietz, C. H. J. T.; Koning, C. E.; Heise, A., How controlled and versatile is N-carboxy anhydride (NCA) polymerization at 0 [degree]C? Effect of temperature on homo-, block- and graft (co)polymerization. *Polymer Chemistry* **2010,** *1* (4), 514-524.

144. Fujita, Y.; Koga, K.; Kim, H.-K.; Wang, X.-S.; Sudo, A.; Nishida, H.; Endo, T., Phosgene-free synthesis of N-carboxyanhydrides of α-amino acids based on

bisarylcarbonates as starting compounds. *Journal of Polymer Science Part A: Polymer Chemistry* **2007,** *45* (22), 5365-5370.

145. Habraken, G. J. M.; Wilsens, K. H. R. M.; Koning, C. E.; Heise, A., Optimization of N-carboxyanhydride (NCA) polymerization by variation of reaction temperature and pressure. *Polymer Chemistry* **2011,** *2* (6), 1322-1330.

146. Sullivan, B.; Sill, K. N., Large-scale synthesis of α-amino acid-N-carboxyanhydrides AU - Semple, J. Edward. *Synthetic Communications* **2017,** *47* (1), 53-61.

147. Kricheldorf, H. R., *Alpha-Aminoacid-N-Carboxy-Anhydrides and Related Heterocycles*. Universitat Hamburg: Hamburg, Germany, 1987.

148. Masutani, K.; Kimura, Y., Chapter 1 PLA Synthesis. From the Monomer to the Polymer. In *Poly(lactic acid) Science and Technology: Processing, Properties, Additives and Applications*, The Royal Society of Chemistry: 2015; pp 1-36.

149. Schneiderman, D. K.; Hillmyer, M. A., Aliphatic Polyester Block Polymer Design. *Macromolecules* **2016,** *49* (7), 2419-2428.

150. Kim, Y.; Verkade, J. G., Living Polymerization of Lactide Using Titanium Alkoxide Catalysts. **2005,** *224* (1), 105-118.

151. Lin, B.; Waymouth, R. M., Urea Anions: Simple, Fast, and Selective Catalysts for Ring-Opening Polymerizations. *Journal of the American Chemical Society* **2017,** *139* (4), 1645-1652.

152. Manzini, B.; Hodge, P.; Ben-Haida, A., Entropically-driven ring-opening polymerization of macrocyclic esters with up to 84-membered rings catalysed by polymer-supported Candida antarctica lipase B. *Polymer Chemistry* **2010,** *1* (3), 339-346.

153. Amador, A. G.; Watts, A.; Neitzel, A. E.; Hillmyer, M. A., Entropically Driven Macrolide Polymerizations for the Synthesis of Aliphatic Polyester Copolymers Using Titanium Isopropoxide. *Macromolecules* **2019,** *52* (6), 2371-2383.

154. Nomura, N.; Ishii, R.; Akakura, M.; Aoi, K., Stereoselective Ring-Opening Polymerization of Racemic Lactide Using Aluminum-Achiral Ligand Complexes: Exploration of a Chain-End Control Mechanism. *Journal of the American Chemical Society* **2002,** *124* (21), 5938-5939.

155. Dong, C.-M.; Qiu, K.-Y.; Gu, Z.-W.; Feng, X.-D., Synthesis of star-shaped poly(d,l-lactic acid-alt-glycolic acid) with multifunctional initiator and SnOct2 catalyst. *Polymer* **2001,** *42* (16), 6891-6896.

156. Weiss, R. M.; Short, A. L.; Meyer, T. Y., Sequence-Controlled Copolymers Prepared via Entropy-Driven Ring-Opening Metathesis Polymerization. *ACS Macro Letters* **2015,** *4* (9), 1039-1043.

157. Tsuchiya, K.; Ishii, T.; Masunaga, H.; Numata, K., Spider dragline silk composite films doped with linear and telechelic polyalanine: Effect of polyalanine on the structure and mechanical properties. *Scientific Reports* **2018,** *8* (1), 3654.

158. Rising, A.; Johansson, J., Toward spinning artificial spider silk. *Nature Chemical Biology* **2015,** *11*, 309.

159. Heim, M.; Keerl, D.; Scheibel, T., Spider Silk: From Soluble Protein to Extraordinary Fiber. **2009,** *48* (20), 3584-3596.

160. Li, G.; Sampson, N. S., Alternating Ring-Opening Metathesis Polymerization (AROMP) of Hydrophobic and Hydrophilic Monomers Provides Oligomers with Side-Chain Sequence Control. *Macromolecules* **2018**.

161. Simocko, C.; Young, T. C.; Wagener, K. B., ADMET Polymers Containing Precisely Spaced Pendant Boronic Acids and Esters. *Macromolecules* **2015,** *48* (16), 5470-5473.

162. Rojas, G.; Wagener, K. B., Precisely and Irregularly Sequenced Ethylene/1-Hexene Copolymers: A Synthesis and Thermal Study. *Macromolecules* **2009,** *42* (6), 1934-1947.

163. Cole, J. P.; Lessard, J. J.; Rodriguez, K. J.; Hanlon, A. M.; Reville, E. K.; Mancinelli, J. P.; Berda, E. B., Single-chain nanoparticles containing sequence-defined segments: using primary structure control to promote secondary and tertiary structures in synthetic protein mimics. *Polymer Chemistry* **2017,** *8* (38), 5829-5835.

164. Soejima, T.; Satoh, K.; Kamigaito, M., Sequence-regulated vinyl copolymers with acid and base monomer units via atom transfer radical addition and alternating radical copolymerization. *Polymer Chemistry* **2016,** *7* (29), 4833-4841.

165. Soejima, T.; Satoh, K.; Kamigaito, M., Main-Chain and Side-Chain Sequence-Regulated Vinyl Copolymers by Iterative Atom Transfer Radical Additions and 1:1 or 2:1 Alternating Radical Copolymerization. *J. Am. Chem. Soc.* **2016,** *138* (3), 944-954.

166. Lu, X.; Watts, E.; Jia, F.; Tan, X.; Zhang, K., Polycondensation of Polymer Brushes via DNA Hybridization. *Journal of the American Chemical Society* **2014,** *136* (29), 10214-10217.

167. Sigle, J. L.; Clough, A.; Zhou, J.; White, J. L., Controlling Macroscopic Properties by Tailoring Nanoscopic Interfaces in Tapered Copolymers. *Macromolecules* **2015,** *48* (16), 5714-5722.

168. O'Connor, K. S.; Watts, A.; Vaidya, T.; LaPointe, A. M.; Hillmyer, M. A.; Coates, G. W., Controlled Chain Walking for the Synthesis of Thermoplastic Polyolefin Elastomers: Synthesis, Structure, and Properties. *Macromolecules* **2016,** *49* (18), 6743-6751.

169. Tang, D.; Chen, Z.; Correa-Netto, F.; Macosko, C. W.; Hillmyer, M. A.; Zhang, G., Poly(urea ester): A family of biodegradable polymers with high melting temperatures. *Journal of Polymer Science Part A: Polymer Chemistry* **2016,** *54* (24), 3795-3799.

170. Zhang, J.; Landry, M. P.; Barone, P. W.; Kim, J.-H.; Lin, S.; Ulissi, Z. W.; Lin, D.; Mu, B.; Boghossian, A. A.; Hilmer, A. J.; Rwei, A.; Hinckley, A. C.; Kruss, S.; Shandell, M. A.; Nair, N.; Blake, S.; Sen, F.; Sen, S.; Croy, R. G.; Li, D.; Yum, K.; Ahn, J.-H.; Jin, H.; Heller, D. A.; Essigmann, J. M.; Blankschtein, D.; Strano, M. S., Molecular recognition using corona phase complexes made of synthetic polymers adsorbed on carbon nanotubes. *Nat Nano* **2013,** *8* (12), 959-968.

171. Lavilla, C.; Byrne, M.; Heise, A., Block-Sequence-Specific Polypeptides from α-Amino Acid N-Carboxyanhydrides: Synthesis and Influence on Polypeptide Properties. *Macromolecules* **2016,** *49* (8), 2942-2947.

172. Bergman, J. A.; Cochran, E. W.; Heinen, J. M., Role of the segment distribution in the microphase separation of acrylic diblock and triblock terpolymers. *Polymer* **2014,** *55* (16), 4206-4215.

173. Wada, Y.; Lee, H.; Hoshino, Y.; Kotani, S.; Shea, K. J.; Miura, Y., Design of multi-functional linear polymers that capture and neutralize a toxic peptide: a comparison with cross-linked nanoparticles. *Journal of Materials Chemistry B* **2015,** *3* (8), 1706-1711.

174. Robinson, D. B.; Buffleben, G. M.; Langham, M. E.; Zuckermann, R. N., Stabilization of nanoparticles under biological assembly conditions using peptoids. *Peptide Science* **2011,** *96* (5), 669-678.

175. Pesko, D. M.; Webb, M. A.; Jung, Y.; Zheng, Q.; Miller, T. F.; Coates, G. W.; Balsara, N. P., Universal Relationship between Conductivity and Solvation-Site Connectivity in Ether-Based Polymer Electrolytes. *Macromolecules* **2016,** *49* (14), 5244-5255.

176. Luo, S.; Stevens, K. A.; Park, J. S.; Moon, J. D.; Liu, Q.; Freeman, B. D.; Guo, R., Highly CO2-Selective Gas Separation Membranes Based on Segmented Copolymers of Poly(Ethylene oxide) Reinforced with Pentiptycene-Containing Polyimide Hard Segments. *ACS Appl. Mater. Interfaces* **2016,** *8* (3), 2306-2317.

177. Panganiban, B.; Qiao, B.; Jiang, T.; DelRe, C.; Obadia, M. M.; Nguyen, T. D.; Smith, A. A. A.; Hall, A.; Sit, I.; Crosby, M. G.; Dennis, P. B.; Drockenmuller, E.; Olvera de la Cruz, M.; Xu, T., Random heteropolymers preserve protein function in foreign environments. **2018,** *359* (6381), 1239-1243.

178. Howard, J. B.; Ekiz, S.; Cuellar De Lucio, A. J.; Thompson, B. C., Investigation of Random Copolymer Analogues of a Semi-Random Conjugated Polymer Incorporating Thieno[3,4-b]pyrazine. *Macromolecules* **2016,** *49* (17), 6360-6367.

179. Singh, N.; Tureau, M. S.; Epps, I. I. I. T. H., Manipulating ordering transitions in interfacially modified block copolymers. *Soft Matter* **2009,** *5* (23), 4757-4762.

180. Versteegen, R. M.; Sijbesma, R. P.; Meijer, E. W., Synthesis and Characterization of Segmented Copoly(ether urea)s with Uniform Hard Segments. *Macromolecules* **2005,** *38* (8), 3176-3184.

181. Lambert, S.; Wagner, M., Environmental performance of bio-based and biodegradable plastics: the road ahead. *Chemical Society Reviews* **2017,** *46* (22), 6855-6871.

182. Brannigan, R. P.; Dove, A. P., Synthesis, properties and biomedical applications of hydrolytically degradable materials based on aliphatic polyesters and polycarbonates. *Biomaterials Science* **2017,** *5* (1), 9-21.

183. Lambert, S.; Wagner, M., Environmental performance of bio-based and biodegradable plastics: the road ahead. *Chemical Society Reviews* **2017**.

184. Laycock, B.; Nikolić, M.; Colwell, J. M.; Gauthier, E.; Halley, P.; Bottle, S.; George, G., Lifetime prediction of biodegradable polymers. *Progress in Polymer Science* **2017,** *71* (Supplement C), 144-189.

185. Weiss, R. M.; Jones, E. M.; Shafer, D. E.; Stayshich, R. M.; Meyer, T. Y., Synthesis of repeating sequence copolymers of lactic, glycolic, and caprolactic acids. *Journal of Polymer Science Part A: Polymer Chemistry* **2011,** *49* (8), 1847-1855.

186. Thorn-Csányi, E.; Ruhland, K., Quantitative description of the metathesis polymerization/depolymerization equilibrium in the 1,4-polybutadiene system, 3. Influence of the solvent. *Macromol. Chem. Phys.* **1999,** *200* (12), 2606-2611.

187. Pepels, M. P. F.; Souljé, P.; Peters, R.; Duchateau, R., Theoretical and Experimental Approach to Accurately Predict the Complex Molecular Weight Distribution in the Polymerization of Strainless Cyclic Esters. *Macromolecules* **2014,** *47* (16), 5542-5550.

188. Nowalk, J. A.; Fang, C.; Short, A. L.; Weiss, R. M.; Swisher, J. H.; Liu, P.; Meyer, T. Y., Sequence-Controlled Polymers Through Entropy-Driven Ring-Opening Metathesis Polymerization: Theory, Molecular Weight Control, and Monomer Design. *Journal of the American Chemical Society* **2019**.

189. Short, G. N.; Nguyen, H. T. H.; Scheurle, P. I.; Miller, S. A., Aromatic polyesters from biosuccinic acid. *Polymer Chemistry* **2018,** *9* (30), 4113-4119.

190. Gleadall, A.; Pan, J.; Kruft, M.-A.; Kellomäki, M., Degradation mechanisms of bioresorbable polyesters. Part 1. Effects of random scission, end scission and autocatalysis. *Acta Biomaterialia* **2014,** *10* (5), 2223-2232.

191. Pan, P.; Zhu, B.; Inoue, Y., Enthalpy Relaxation and Embrittlement of Poly(l-lactide) during Physical Aging. *Macromolecules* **2007,** *40* (26), 9664-9671.

192. Ho, Y. K.; Doshi, P.; Yeoh, H. K.; Ngoh, G. C., Modeling chain-end scission using the Fixed Pivot technique. *Chemical Engineering Science* **2014,** *116,* 601-610.

193. *Sequence-Controlled Polymers*. Wiley-VCH Verlag GmbH & Co. KGaA: 2017.

194. George, K. L.; Horne, W. S., Foldamer Tertiary Structure through Sequence-Guided Protein Backbone Alteration. *Accounts of Chemical Research* **2018,** *51* (5), 1220-1228.

195. Pahnke, K.; Brandt, J.; Gryn'ova, G.; Lin, C. Y.; Altintas, O.; Schmidt, F. G.; Lederer, A.; Coote, M. L.; Barner-Kowollik, C., Entropy-Driven Selectivity for Chain Scission: Where Macromolecules Cleave. *Angewandte Chemie International Edition* **2016,** *55* (4), 1514-1518.

196. Chamberlain, B. M.; Cheng, M.; Moore, D. R.; Ovitt, T. M.; Lobkovsky, E. B.; Coates, G. W., Polymerization of Lactide with Zinc and Magnesium β-Diiminate Complexes: Stereocontrol and Mechanism. *Journal of the American Chemical Society* **2001,** *123* (14), 3229-3238.

197. Thomas, C. M., Stereocontrolled ring-opening polymerization of cyclic esters: synthesis of new polyester microstructures. *Chemical Society Reviews* **2010,** *39* (1), 165-173.